(12) INTERNATIONAL APPLICATION PUBLISHED UNDER THE PATENT COOPERATION TREATY (PCT)

(19) World Intellectual Property Organization
International Bureau

(43) International Publication Date
30 October 2014 (30.10.2014)

WIPO | PCT

(10) International Publication Number
WO 2014/174470 A1

(51) International Patent Classification:
C12N 5/0735 (2010.01) *C12N 5/074* (2010.01)

(21) International Application Number:
PCT/IB2014/060954

(22) International Filing Date:
23 April 2014 (23.04.2014)

(25) Filing Language: English

(26) Publication Language: English

(30) Priority Data:
61/814,920 23 April 2013 (23.04.2013) US
61/878,769 17 September 2013 (17.09.2013) US
61/932,935 29 January 2014 (29.01.2014) US

(71) Applicant: **YEDA RESEARCH AND DEVELOPMENT CO. LTD.** [IL/IL]; at the Weizmann Institute of Science, P.O. Box 95, 7610002 Rehovot (IL).

(72) Inventors: **HANNA, Yaqub**; 106 Rothschild Boulevard, Apt. 14, 6527106 Tel-Aviv (IL). **NOVERSHTERN, Noa**; c/o Yeda Research and Development Co. Ltd., at the Weizmann Institute of Science, P.O. Box 95, 7610002 Rehovot (IL). **RAIS, Yoach**; c/o Yeda Research and Development Co. Ltd., at the Weizmann Institute of Science, P.O. Box 95, 7610002 Rehovot (IL).

(74) Agents: **G.E. EHRLICH (1995) LTD.** et al.; 11 Menachem Begin Road, 5268104 Ramat Gan (IL).

(81) Designated States *(unless otherwise indicated, for every kind of national protection available)*: AE, AG, AL, AM, AO, AT, AU, AZ, BA, BB, BG, BH, BN, BR, BW, BY, BZ, CA, CH, CL, CN, CO, CR, CU, CZ, DE, DK, DM, DO, DZ, EC, EE, EG, ES, FI, GB, GD, GE, GH, GM, GT, HN, HR, HU, ID, IL, IN, IR, IS, JP, KE, KG, KN, KP, KR, KZ, LA, LC, LK, LR, LS, LT, LU, LY, MA, MD, ME, MG, MK, MN, MW, MX, MY, MZ, NA, NG, NI, NO, NZ, OM, PA, PE, PG, PH, PL, PT, QA, RO, RS, RU, RW, SA, SC, SD, SE, SG, SK, SL, SM, ST, SV, SY, TH, TJ, TM, TN, TR, TT, TZ, UA, UG, US, UZ, VC, VN, ZA, ZM, ZW.

(84) Designated States *(unless otherwise indicated, for every kind of regional protection available)*: ARIPO (BW, GH, GM, KE, LR, LS, MW, MZ, NA, RW, SD, SL, SZ, TZ, UG, ZM, ZW), Eurasian (AM, AZ, BY, KG, KZ, RU, TJ, TM), European (AL, AT, BE, BG, CH, CY, CZ, DE, DK, EE, ES, FI, FR, GB, GR, HR, HU, IE, IS, IT, LT, LU, LV, MC, MK, MT, NL, NO, PL, PT, RO, RS, SE, SI, SK, SM, TR), OAPI (BF, BJ, CF, CG, CI, CM, GA, GN, GQ, GW, KM, ML, MR, NE, SN, TD, TG).

Declarations under Rule 4.17:

— *of inventorship (Rule 4.17(iv))*

Published:

— *with international search report (Art. 21(3))*

— *before the expiration of the time limit for amending the claims and to be republished in the event of receipt of amendments (Rule 48.2(h))*

— *with sequence listing part of description (Rule 5.2(a))*

(54) Title: ISOLATED NAIVE PLURIPOTENT STEM CELLS AND METHODS OF GENERATING SAME

(57) Abstract: Provided is an isolated human naive pluripotent stem cell (PSC), wherein: (i) when the naive PSC is a female PSC, then said naive female PSC has two unmethylated alleles of an X-inactive specific transcript (XIST) gene; and (ii) when said naive PSC is a male PSC, then said naive male PSC has an unmethylated allele of said XIST gene. Also provided is a culture medium which comprises an ERK1/2 inhibitor, a GSK3beta inhibitor, a p38 inhibitor, a JNK inhibitor, a STAT3 activator and at least one agent selected from the group consisting of: bFGF, TGFbeta 1, a PKC inhibitor, a ROCK inhibitor and a NOTCH inhibitor; or at least agent selected from the group consisting of: a TGFR inhibitor, a FGFR inhibitor, a PKC inhibitor, a ROCK inhibitor and a NOTCH inhibitor.

WO 2014/174470 A1

ISOLATED NAIVE PLURIPOTENT STEM CELLS AND METHODS OF GENERATING SAME

RELATED APPLICATIONS

This application claims the benefit of priority under 35 USC §119(e) of U.S. Provisional Patent Application Nos. 61/932,935 filed on January 29, 2014, 61/878,769 filed on September 17, 2013 and 61/814,920 filed on April 23, 2013.

This application is also related to co-filed, co-pending and co-assigned U.S. Patent Application entitled "ISOLATED NAIVE PLURIPOTENT STEM CELLS AND METHODS OF GENERATING SAME" (Attorney Docket No. 58870) by Yaqub HANNA, Noa NOVERSHTERN and Yoach RAIS.

The contents of the above applications are incorporated herein by reference in their entirety.

FIELD AND BACKGROUND OF THE INVENTION

The present invention, in some embodiments thereof, relates to isolated naive pluripotent stem cell, novel culture medium which can be used to generate same and methods of generating and culturing same and, more particularly, but not exclusively, to methods of improving dedifferentiation of somatic cells for generation of induced pluripotent stem cells.

ESC-like cells, termed induced pluripotent (iPS) cells can be generated from somatic cells by ectopic expression of different transcription factors, originally Oct4, Sox2, Klf4 and c-Myc (Takahashi and Yamanaka, 2006), that share all defining features with naive mouse ESCs (Takahashi and Yamanaka, 2006; Hanna et al., 2009a). The reprogramming process typically requires extensive cell proliferation of a period of at least one week, after which a certain fraction of the cell progeny successfully converts into ES-like state in an unpredictable pattern and with different time latencies (Hanna et al., 2009b). Great progress has been achieved in identifying additional and alternative transcriptional factors and small molecules that can substitute some of the exogenous factor or boost reprogramming efficiency when combined with Oct4, Sox2, Klf4 and c-Myc (OSKM) (Orkin and Hochedlinger, 2011). A variety of enzymes and chromatin remodelers have been identified to cooperate with the reprogramming factors in

facilitating the required early and late chromatin changes leading to authentic iPSC reprogramming in a fraction of donor cell progeny (e.g., Wdr5, Utx, Tet2) (Ang et al., 2011; Mansour et al., 2012; Onder et al., 2012).

Despite of these advances, the reprogramming efficiency of somatic cells remains to be low, even in the most optimized reprogramming recipes used (up to 0.1-20%) (Hanna et al., 2010b). Further, per a starting individual somatic epigenome challenged with the overexpression of reprogramming factors, the outcome is highly stochastic, and the majority of cells assume different levels of reprogramming (Hanna et al., 2009b). The latter has allowed the isolation of a variety of intermediate populations identified by surface markers that can be further challenged and perturbed to generate iPSCs in a random manner (Polo et al., 2012). Biological systems - based approaches for modeling the nature of stochastic elements and progression of reprogramming have revealed that while somatic cell reprogramming involves thousands of molecular changes, as few as one rate limiting event may adequately recapitulate the experimentally observed kinetics by clonal cell monitoring (Hanna et al., 2009b). The identity of such stochastic rate limiting element(s) remains to be defined.

Further, the fact that only fully reprogrammed ES-like cells have been derived via cell fusion or nuclear transfer reprogramming approaches with no evidence for partially reprogrammed cells, suggests that reprogramming by nuclear transfer or cell fusion may follow a more synchronized and deterministic pattern, in comparison to OSKM induced reprogramming (Hanna et al., 2010b). The above raises the hypothesis of whether it is feasible to devise deterministic direct iPSC reprogramming approaches, and whether additional genetic manipulations together with transcription factor transduction may enable synchronized and *deterministic in vitro* reprogramming.

Embryonic stem cells (ESCs) were first isolated from mouse embryos by explanting the inner cell mass (ICM) of developing embryos *in vitro* in the presence of the leukemia inhibitory factor (LIF) cytokine and mouse embryonic feeder (MEF) cells (Hanna et al., 2010a; Takahashi and Yamanaka, 2006). Mouse ESCs recapitulate molecular signatures of the nascent ICM and are, therefore, termed as “naive pluripotent cells” (Hanna, 2010; Hanna et al., 2010a; 2009a; Takahashi and Yamanaka, 2006). This includes expression of Oct4, Nanog and Klf pluripotency genes, lack of epiblast and somatic early lineage specific markers, and maintenance of a pre X-inactivation

state with both X chromosomes active in female cells. Further, the cells retain a non-restricted developmental potential as they can robustly differentiate into all cell types *in vitro* and, upon injection into the mouse blastocyst, they efficiently contribute to the three germ layers and to the germ-line of chimeric animals (Hanna et al., 2010a; 2009b). Finally, the high growth rate and open chromatin confirmation of mouse ES cells, has rendered these cells as one of the most valuable tools for mouse genetics by allowing efficient gene specific targeting via homologous recombination (Hanna et al., 2010a; Orkin and Hochedlinger, 2011).

Recently, a dramatically different type of pluripotent cells, termed EpiSCs, were derived by explanting the post-implantation epiblast in growth conditions supplemented with FGF2 [also known as "basic fibroblast growth factor (bFGF)"] and Activin (Ang et al., 2011; Mansour et al., 2012; Onder et al., 2012; Tesar et al., 2007). Although EpiSCs are pluripotent, they have a restricted developmental potential in comparison to ESCs and therefore are termed as *"primed pluripotent cells"*. EpiSCs are highly inefficient in generating animal chimeras, have already undergone X chromosome inactivation, and demonstrate heterogeneous expression of early lineage-commitment markers (Hanna et al., 2009a; 2010a). Hanna Y., et al. (2009a) have recently defined the relationships between the two distinct types of pluripotent states. Whereas naive murine pluripotent cells can differentiate into a primed EpiSC-like state *in vitro* by promoting Activin and FGF2 signaling, EpiSCs can epigenetically revert back to ESC-like naive pluripotency by defined signaling stimuli.

Remarkably, ESCs derived from humans nearly share several defining features with EpiSC cells, rather than with mouse ESCs. In contrast to mouse ESCs, the maintenance of human ES cells requires FGF2 and Activin (rather than LIF/Stat3 signaling), they are highly sensitive to passaging as single cells, display heterogeneous expression of epiblast and lineage commitment markers, and utilize the proximal enhancer element to drive the expression of Oct4 in the post-implantation Epiblast (rather than the distal Oct4 enhancer active in the ICM) (Hanna et al., 2009a; 2009b). Thus, the molecular and biological similarities of human ESCs with mouse epiblast EpiSCs suggest that human ESCs correspond to the primed pluripotent state rather than the naive state of mouse ESCs and that this could be the underlying reason for the biological properties of conventional human ESCs that impede their use for disease

related research (Hanna et al., 2010b; Polo et al., 2012). This includes laborious culture conditions, low gene targeting efficiencies by homologous recombination and the dramatic heterogeneity in differentiation propensity among different human ESC and iPSC lines (Hanna et al., 2009b; 2010a).

The fact that conventional/primed human ESCs are derived from the ICM has mistakenly suggested that the primed state is the only or "default" state of pluripotency that can be isolated in humans (Hanna et al., 2010a). However, revisiting this concept was provoked following the work of the present inventors on defining the *in vitro* stability and identity of pluripotent state in relatively "non-permissive" mouse strains for naive ES derivation (yielded exclusively EpiSC-like pluripotent cells until recently) (Hanna et al., 2009a). Mouse naive ESC cells can be derived from Non-obese diabetogenic (NOD) mice blastocysts only if additional signaling molecules or transcription factors are exogenously provided together with LIF cytokine (e.g. Naive NOD ESC and iPSCs could be propagated in PD0325901/CHIR99021/LIF or Kenopaullone/CHIR99021/LIF or constitutive expression of Klf4/Lif and c-Myc/LIF conditions) (Hanna et al., 2009a). In the absence of these additional factors (or in LIF only conditions), the naive state, even if isolated from the mouse ICM, is masked by *in vitro* acquisition of pluripotent state that is nearly indistinguishable from EpiSC cells in a process that probably imitates *in vivo* differentiation during normal early development (Hanna et al., 2009a). These findings allowed the generation of fully pluripotent naive ES and iPS cells from previously considered "non-permissive' strains. Experiments in NOD mice have raised the question whether appropriate conditions that allow derivation of naive or mouse ESC-like stem cell in humans have not been devised yet and that stabilization of a naive human pluripotent state requires additional undefined factors (similar or different from those applied to NOD mouse and rat ESCs/iPSCs) (Hanna et al., 2009a). Further support for the possibility that explanted blastocysts differentiate *in vitro* into a primed state was generated by close monitoring of X chromosome dynamics in human female ESC lines derived *in vitro* and demonstrated that the cells undergo X chromosome inactivation as a part of an *in vitro* adaptation process following this derivation, and this can be accelerated by high oxygen concentrations, and attenuated partially by addition of LIF or specific types of feeder cells that provide undefined signals (Lengner et al., 2010; Okamoto et al., 2011;

Tomoda et al., 2012). These results indicated that XaXa (X-active, X-active, based on absence of XIST bodies) naive cells might be present in the human ICM, and that *in vitro* captured conventional human ESCs poorly reflect their ICM counterparts (Okamoto et al., 2011).

These observations have raised the possibility that appropriate conditions may have not been devised to allow isolation of naive stem cells from a range of species that have yielded thus far primed or EpiSC-like cells, possibly including humans (Hanna et al., 2009a). Indeed in a follow-up work evidence was provided for the possibility to derive alternative human pluripotent cell states that more extensively share defining features with murine ESCs. As previously shown (Hanna et al., 2010b), a screening approach was taken that involved introducing reprogramming factors and/or small molecules that support the naive pluripotent state led to *in vitro* stabilization of a novel pluripotent cell state that shares several defining features with murine ESCs (Hanna et al., 2010b). The propagation in LIF cytokine and ERK1/2 inhibitor PD0325901 and GSK3b inhibitor CHIR99021 (abbreviated as 2i supplemented conditions – two small molecule inhibitors of ERK1/2 signaling and GSK3β to promote WNT signaling, abbreviated as "PD/CH" or "2i" conditions) together with over-expression of OCT4/KLF4 or KLF2/KLF4 induced conversion of conventional human ES and iPS cells to what was then mistakenly referred as human naive pluripotent state reminiscent of that of mouse ESCs (Hanna et al., 2010b). These previously described naive human ESCs were pluripotent by several available criteria including embryonic body differentiation and *in vivo* teratoma formation. Importantly, they were epigenetically and molecularly distinct from conventional "primed" human ESCs/iPSCs. "Naive" hPSCs generated by Hanna et al., 2010b exhibited XIST methylation on both X alleles, high single cell cloning efficiency and showed a gene expression pattern that resembled that of naive mouse ES cells (lack of MHC class I expression, and clustered with murine naive ESCs in cross-species unbiased gene clustering for 9773 expressed orthologue genes) (Hanna et al., 2010b). Nevertheless, a major limitations and unsolved questions remain that cast doubt on the true pluripotency of previously published/established lines and their stability. Only transgene dependent naive ESC/iPSCs could be maintained for over 18 passages. Forskolin enabled replacement of exogenous factors together with 2i/LIF, but only for no more than 19 passages and the cultures retained high

differentiation propensity (Hanna et al., 2010b). XIST was completely methylated in the previously referred naive human ESC/iPSCs and the cells lacked any XIST transcription (Hanna et al., 2010b), which is inconsistent with *in vivo* results on human blastocysts that clearly show XIST transcription (without forming XIST bodies, *i.e.*, XIST coated X chromosomes) (Okamoto et al., 2011). Collectively, these findings suggest that the isolated cells thus far do not reflect authentic features of human ICM, and retain a compromised pluripotency and enhanced propensity for differentiation. Substantial published data generated by many different groups highlight the rationale behind the concept that genetically unmodified pluripotent naive human stem cells have not been adequately isolated so far, and that the conditions allowing expansion of such cells and their molecular properties (if they indeed are proven to exist) are not known (De Los Angeles et al., 2012; Hanna et al., 2010b).

Additional background art includes Xu Y., et al., 2013 (Journal of Biological Chemistry, 288: 9767-9778); Luo M., et al., 2013 (Stem Cells. Mar 26. doi: 10.1002/stem.1374. [Epub ahead of print]); International Application No. PCT/US08/04516 ("Reprogramming of Somatic Cells", Jaenisch; Rudolf; et al).

SUMMARY OF THE INVENTION

According to an aspect of some embodiments of the present invention there is provided an isolated (e.g., primate e.g., human) naive pluripotent stem cell (PSC), comprising:

an unmethylated X-inactive specific transcript (XIST) gene, wherein:

(i) when the naive PSC is a female PSC, then the naive female PSC has two unmethylated alleles of the XIST gene; and

(ii) when the naive PSC is a male PSC, then the naive male PSC has an unmethylated allele of the XIST gene;

and/or

an expression level of transcription factor E3 (TFE3) is characterized by a nucleus to cytoplasm expression ratio which is equal to or higher than 1 as determined by an immunostaining assay.

According to some embodiments of the invention, the isolated primate (e.g., human) naive PSC of some embodiments of the invention, being in a pluripotent state,

wherein when the isolated naive PSC is incubated in the presence of an agent selected from the group consisting of Bone morphogenetic protein 4 (BMP4), JNK inhibitor, and P38 inhibitor, the naive PSC remains in the pluripotent state, and maintains a pluripotent phenotype.

According to some embodiments of the invention, the primate (e.g., human) naive PSC is characterized by reduced methylation of CpG islands as compared to a level of methylation of the CpG islands in a primate (e.g., human) primed PSC.

According to an aspect of some embodiments of the present invention there is provided an isolated population of naive PSCs comprising at least 10% of the isolated primate (e.g., human) naive PSC cells of some embodiments of the invention.

According to an aspect of some embodiments of the present invention there is provided a cell culture comprising the isolated naive PSC of some embodiments of the invention, or the isolated population of naive PSCs of some embodiments of the invention and a culture medium.

According to some embodiments of the invention, the culture medium is capable of maintaining the naive PSC in an undifferentiated and pluripotent state for at least 10 passages.

According to an aspect of some embodiments of the present invention there is provided a culture medium comprising an ERK1/2 inhibitor, a GSK3β inhibitor, a p38 inhibitor, a JNK inhibitor, a STAT3 activator and at least one agent selected from the group consisting of: basic fibroblast growth factor (bFGF), transforming growth factor beta 1 (TGFβ1), a protein kinase C (PKC) inhibitor, a ROCK inhibitor and a NOTCH inhibitor.

According to an aspect of some embodiments of the present invention there is provided a culture medium comprising an ERK1/2 inhibitor, a GSK3β inhibitor, a p38 inhibitor, a JNK inhibitor, a STAT3 activator and at least one agent selected from the group consisting of: a transforming growth factor receptor (TGFR) inhibitor, a fibroblast growth factor receptor (FGFR) inhibitor, a protein kinase C (PKC) inhibitor, a ROCK inhibitor and a NOTCH inhibitor.

According to some embodiments of the invention the STAT3 activator is selected from the group consisting of leukemia inhibitory factor (LIF) and interleukin 6 (IL6).

According to some embodiments of the invention the culture medium further comprising at least one additional agent selected from the group consisting of: insulin-like growth factor 1 (IGF1), insulin-like growth factor II (IGFII), a bone morphogenetic protein (BMP) signaling inhibitor, a Sonic Hedgehog pathway (SHH) inhibitor, an ERK5 inhibitor, Forskolin, Kenpaullone, BayK8644, Bix1294, and stem cell factor (SCF).

According to some embodiments of the invention the culture medium further comprising at least one additional agent selected from the group consisting of: insulin-like growth factor 1 (IGF1), insulin-like growth factor II (IGFII), bone morphogenetic protein 4 (BMP4), a Sonic Hedgehog pathway (SHH) inhibitor, an ERK5 inhibitor, Forskolin, Kenpaullone, BayK8644, Bix1294, and stem cell factor (SCF).

According to some embodiments of the invention, the STAT3 activator comprises the LIF, and wherein the at least one agent comprises the PKC inhibitor.

According to some embodiments of the invention, the STAT3 activator comprises the LIF, and wherein the at least one agent comprises the TGFβ1 and the protein kinase C inhibitor.

According to some embodiments of the invention, the culture medium further comprises an FGFR inhibitor.

According to some embodiments of the invention, the culture medium further comprises TGFR inhibitor.

According to some embodiments of the invention, the STAT3 activator comprises the LIF and wherein the at least one agent comprises the TGFβ1 and the protein kinase C inhibitor.

According to some embodiments of the invention, the culture medium further comprises an FGFR inhibitor.

According to some embodiments of the invention, the STAT3 activator comprises the LIF, and wherein the at least one agent comprises the bFGF and the TGFβ1.

According to some embodiments of the invention, the culture medium further comprises a ROCK inhibitor.

According to some embodiments of the invention, the culture medium further comprises a protein kinase C inhibitor.

According to some embodiments of the invention, the STAT3 activator comprises the LIF and wherein the at least one agent comprises the bFGF, the ROCK inhibitor, a bone morphogenetic protein (BMP) inhibitor, the NOTCH inhibitor, and a transforming growth factor receptor (TGFR) inhibitor.

According to some embodiments of the invention, the culture medium further comprises a Sonic Hedgehog pathway (SHH) inhibitor.

According to some embodiments of the invention, the STAT3 activator comprises the LIF and wherein the at least one agent comprises the NOTCH inhibitor, and a fibroblast growth factor receptor (FGFR) inhibitor.

According to some embodiments of the invention, the culture medium further comprises an agent selected from the group consisting of insulin-like growth factor II (IGFII), stem cell factor (SCF) and transforming growth factor beta 1 (TGFβ1).

According to an aspect of some embodiments of the present invention there is provided a culture medium comprising leukemia inhibitor factor (LIF), an ERK1/2 inhibitor, a GSK3b inhibitor, a p38 inhibitor, a JNK inhibitor, and a protein kinase C inhibitor.

According to some embodiments of the invention, the culture medium of some embodiments of the invention further comprises an FGFR inhibitor.

According to some embodiments of the invention, the culture medium of some embodiments of the invention further comprises a TGFR inhibitor.

According to an aspect of some embodiments of the present invention there is provided a culture medium comprising leukemia inhibitor factor (LIF), an ERK1/2 inhibitor, a GSK3b inhibitor, a p38 inhibitor, a JNK inhibitor, TGFβ1 and a protein kinase C inhibitor.

According to some embodiments of the invention, the culture medium of some embodiments of the invention further comprises a FGFR inhibitor.

According to an aspect of some embodiments of the present invention there is provided a culture medium comprising leukemia inhibitor factor (LIF), an ERK1/2 inhibitor, a GSK3b inhibitor, a p38 inhibitor, a JNK inhibitor, basic fibroblast growth factor (bFGF) and transforming growth factor-beta 1 (TGFβ1).

According to some embodiments of the invention, the culture medium of some embodiments of the invention further comprises a ROCK inhibitor.

According to some embodiments of the invention, the culture medium of some embodiments of the invention further comprises a protein kinase C inhibitor.

According to some embodiments of the invention, the culture medium of some embodiments of the invention further comprising a factor selected from the group consisting of: bone morphogenetic protein 4 (BMP4), IGF1, IGFII, Forskolin, FGFR inhibitor, TGFR inhibitor, Kenpaullone, BayK8644, Bix1294, and stem cell factor (SCF).

According to some embodiments of the invention, the culture medium of some embodiments of the invention further comprising BMP type I receptors (ALK2,3,6) inhibitor.

According to some embodiments of the invention, the culture medium of some embodiments of the invention further comprises ascorbic Acid.

According to some embodiments of the invention, the culture medium of some embodiments of the invention further comprises oleic Acid.

According to some embodiments of the invention, the culture medium of some embodiments of the invention further comprises Linoleic Acid.

According to some embodiments of the invention, the culture medium of some embodiments of the invention further comprises Pipecolic Acid.

According to some embodiments of the invention, the culture medium of some embodiments of the invention being devoid of animal serum.

According to some embodiments of the invention, the culture medium of some embodiments of the invention further comprises serum replacement.

According to an aspect of some embodiments of the present invention there is provided a cell culture comprising cells and the culture medium of some embodiments of the invention.

According to some embodiments of the invention, the culture medium is capable of maintaining naive pluripotent stem cell in an undifferentiated state for at least 2 passages.

According to an aspect of some embodiments of the present invention there is provided a method of generating a naive pluripotent stem cell (PSC), comprising incubating a non-naive PSC cell under conditions which allow generation of the naive PSC from the non-naive PSC, wherein:

(i) when the naive PSC is a female PSC, then the naive female PSC has two unmethylated alleles of an X-inactive specific transcript (XIST) gene; and

(ii) when the naive PSC is a male PSC, then the naive male PSC has an unmethylated allele of the XIST gene,

and/or

an expression level of transcription factor E3 (TFE3) in the naive PSC is characterized by a nucleus to cytoplasm expression ratio which is equal to or higher than 1 as determined by an immunostaining assay,

thereby generating the naive PSC.

According to some embodiments of the invention, the PSC is a primate PSC.

According to some embodiments of the invention, the PSC is a human PSC.

According to some embodiments of the invention, the conditions comprise the culture medium of some embodiments of the invention.

According to some embodiments of the invention, the conditions comprise hypoxia.

According to some embodiments of the invention, the conditions comprise a culture medium comprising an ERK1/2 inhibitor, a GSK3β inhibitor, a p38 inhibitor, a JNK inhibitor, a STAT3 activator and at least one agent selected from the group consisting of: basic fibroblast growth factor (bFGF), transforming growth factor beta 1 (TGFβ1), a protein kinase C (PKC) inhibitor, a ROCK inhibitor and a NOTCH inhibitor, wherein the STAT3 activator is selected from the group consisting of leukemia inhibitory factor (LIF) and interleukin 6 (IL6).

According to some embodiments of the invention, the conditions comprise a culture medium comprising an ERK1/2 inhibitor, a GSK3β inhibitor, a p38 inhibitor, a JNK inhibitor, a STAT3 activator and at least one agent selected from the group consisting of: a transforming growth factor receptor (TGFR) inhibitor, a fibroblast growth factor receptor (FGFR) inhibitor, a protein kinase C (PKC) inhibitor, a ROCK inhibitor and a NOTCH inhibitor, wherein the STAT3 activator is selected from the group consisting of leukemia inhibitory factor (LIF) and interleukin 6 (IL6).

According to some embodiments of the invention, the conditions comprise a culture medium which further comprises at least one additional agent selected from the group consisting of: insulin-like growth factor 1 (IGF1), insulin-like growth factor II

(IGFII), a bone morphogenetic protein (BMP) signaling inhibitor, a Sonic Hedgehog pathway (SHH) inhibitor, an ERK5 inhibitor, Forskolin, Kenpaullone, BayK8644, Bix1294, and stem cell factor (SCF).

According to some embodiments of the invention, the conditions comprise a culture medium which further comprises at least one additional agent selected from the group consisting of: insulin-like growth factor 1 (IGF1), insulin-like growth factor II (IGFII), bone morphogenetic protein 4 (BMP4), a Sonic Hedgehog pathway (SHH) inhibitor, an ERK5 inhibitor, Forskolin, Kenpaullone, BayK8644, Bix1294, and stem cell factor (SCF).

According to some embodiments of the invention, the conditions include a culture medium which comprises leukemia inhibitor factor (LIF), an ERK1/2 inhibitor, a GSK3b inhibitor, a p38 inhibitor, a JNK inhibitor, and a protein kinase C inhibitor.

According to some embodiments of the invention, the conditions include a culture medium which comprises leukemia inhibitor factor (LIF), an ERK1/2 inhibitor, a GSK3b inhibitor, a p38 inhibitor, and a JNK inhibitor.

According to some embodiments of the invention, the conditions include a culture medium which comprises leukemia inhibitor factor (LIF), an ERK1/2 inhibitor, a GSK3b inhibitor, a p38 inhibitor, a JNK inhibitor, and a BMP inhibitor.

According to some embodiments of the invention, the culture medium further comprises FGFR inhibitor.

According to some embodiments of the invention, the culture medium further comprises TGFR inhibitor.

According to some embodiments of the invention, the conditions include a culture medium which comprises leukemia inhibitor factor (LIF), an ERK1/2 inhibitor, a GSK3b inhibitor, a p38 inhibitor, a JNK inhibitor, TGFβ1 and a protein kinase C inhibitor.

According to some embodiments of the invention, the culture medium further comprises FGFRi.

According to some embodiments of the invention, the conditions include a culture medium which comprises leukemia inhibitor factor (LIF), an ERK1/2 inhibitor, a GSK3b inhibitor, a p38 inhibitor, a JNK inhibitor, basic fibroblast growth factor (bFGF) and transforming growth factor-beta 1 (TGFβ1).

According to some embodiments of the invention, the culture medium further comprises a ROCK inhibitor.

According to some embodiments of the invention, the culture medium further comprises a protein kinase C inhibitor.

According to some embodiments of the invention, the culture medium further comprises a factor selected from the group consisting of: bone morphogenetic protein 4 (BMP4), IGF1, IGFII, Forskolin, FGFR inhibitor, TGFR inhibitor, Kenpaullone, BayK8644, Bix1294, and stem cell factor (SCF).

According to some embodiments of the invention, the culture medium further comprises an ascorbic acid.

According to some embodiments of the invention, the culture medium further comprises an oleic Acid.

According to some embodiments of the invention, the culture medium further comprises a Linoleic Acid.

According to some embodiments of the invention, the culture medium further comprises a Pipecolic Acid.

According to some embodiments of the invention, the culture medium being devoid of animal serum.

According to some embodiments of the invention, the culture medium further comprises serum replacement.

According to some embodiments of the invention, the culture medium further comprises an MBD3 inhibitor.

According to some embodiments of the invention, the culture medium further comprises a chromodomain helicase DNA binding protein 4 (CHD4) inhibitor.

According to some embodiments of the invention, the culture medium further comprises P66 alpha coiled-coil domain.

According to some embodiments of the invention, the non-naive PSC is selected from the group consisting of a primed PSC, a blastocyst, an induced pluripotent stem cell (iPSC) and a somatic cell.

According to some embodiments of the invention, wherein when the non-naive PSC comprises a somatic cell then the method further comprising subjecting the somatic cell to de-differentiation conditions, to thereby obtain an induced pluripotent stem cell.

According to some embodiments of the invention, the de-differentiation conditions comprise expressing within the somatic cell at least two growth factors selected from the group consisting of Oct4, Sox2, Klf4 and c-Myc.

According to an aspect of some embodiments of the present invention there is provided a method of improving generation of induced pluripotent stem cells (iPSCs) from a somatic cell, comprising:

(a) expressing within the somatic cell at least two growth factors selected from the group consisting of Oct4, Sox2, Klf4 and c-Myc; and

(b) inhibiting Mbd3 expression and/or activity in the somatic cell,

thereby improving generation of the iPSCs from a somatic cell.

According to some embodiments of the invention, inhibiting Mbd3 activity is performed by inhibiting binding of the Mbd3 to the nucleosome remodeling and deacetylase (NuRD) complex.

According to some embodiments of the invention, inhibiting the binding of the Mbd3 to the NuRD complex is performed using a chromodomain helicase DNA binding protein 4 (CHD4) inhibitor.

According to some embodiments of the invention, inhibiting the binding of the Mbd3 to the NuRD complex is performed using a P66 alpha coiled-coil domain.

According to some embodiments of the invention, inhibiting the Mbd3 expression is performed using a protein kinase C (PKC) inhibitor.

According to some embodiments of the invention, the method further comprising exogenously expressing embryonic stem (ES) cell expressed Ras (ERAS) coding sequence or activating endogenous expression of the ERAS in the somatic cell.

According to some embodiments of the invention, expressing is effected for at least 48 hours such that the inhibiting the Mbd3 is effected to 10-30% of a level of the Mbd3 prior to the expressing.

According to some embodiments of the invention, expressing is effected for about 48 hours and the inhibiting is effected after the about 48 hours.

According to some embodiments of the invention, the iPSC is a murine iPSC.

According to some embodiments of the invention, the method of some embodiments of the invention, further comprising culturing the murine iPSC in a medium which comprises LIF, an ERK1/2 inhibitor, and a GSK3b inhibitor.

According to some embodiments of the invention, wherein when the iPSC is a primate (e.g., human) iPSC, the method further comprises: (c) culturing the primate (e.g., human) iPSC in a culture medium which comprises LIF, an ERK1/2 inhibitor, a GSK3b inhibitor, a P38 inhibitor, a JNK inhibitor, basic fibroblast growth factor (bFGF) and transforming growth factor-beta 1 (TGFβ1).

According to some embodiments of the invention, the medium further comprises a ROCK inhibitor.

According to some embodiments of the invention, wherein step (c) is performed following about 48 hours from the expressing of step (a).

According to some embodiments of the invention, expressing is performed using DNA transfection of the growth factors.

According to some embodiments of the invention, expressing is performed using RNA transfection of the growth factors.

According to some embodiments of the invention, expressing is performed using protein transfection of the growth factors.

According to some embodiments of the invention, the PSC is selected from the group consisting of embryonic stem cell (ESC), induced pluripotent stem cells (iPSCs), and embryonic germ cell (EGC).

According to some embodiments of the invention, the naive PSC expresses XIST.

According to some embodiments of the invention, the naive PSC is devoid of XIST bodies.

According to some embodiments of the invention, the naive ESC is capable of X-inactivation when induced to differentiate.

According to some embodiments of the invention, the naive PSC is capable to differentiate into the endodermal, mesodermal and ectodermal embryonic germ layers.

According to some embodiments of the invention, the naive PSC is capable of being maintained in the undifferentiated and pluripotent state for more than 20 passages in culture.

According to some embodiments of the invention, the naive PSC expresses a lower level of MHC class I as compared to a primed PSC under identical detection assay conditions, and wherein the primed PSC exhibits one methylated and one unmethylated

allele of XIST, expresses XIST, exhibits XIST bodies and exhibits a H3K27me3/polycomb focus.

According to some embodiments of the invention, the naive PSC is characterized by at least 10 % more RNA polymerase II pausing on chromosomes as compared to a primed PSC under identical assay conditions, and wherein the primed PSC exhibits one methylated and one unmethylated allele of XIST, expresses XIST, exhibits XIST bodies and exhibits a H3K27me3/polycomb focus.

According to some embodiments of the invention, the isolated naive PSC has an inhibited p38 pathway as compared to a primed PSC.

According to some embodiments of the invention, the isolated naive PSC has an inhibited JNK pathway as compared to a primed PSC.

According to some embodiments of the invention, the isolated naive PSC has an inhibited ROCK pathway as compared to a primed PSC.

According to an aspect of some embodiments of the present invention there is provided a method of generating a naive pluripotent stem cell (PSC), comprising incubating a non-naive PSC cell under conditions which allow generation of the naive PSC from the non-naive PSC, the naive PSC comprising:

an unmethylated X-inactive specific transcript (XIST) gene, wherein:

(i) when the naive PSC is a female PSC, then the naive female PSC has two unmethylated alleles of the XIST gene; and

(ii) when the naive PSC is a male PSC, then the naive male PSC has an unmethylated allele of the XIST gene,

and/or

an expression level of transcription factor E3 (TFE3) characterized by a nucleus to cytoplasm expression ratio which is equal to or higher than 1 as determined by an immunostaining assay.

wherein the conditions which comprise a culture medium which comprises KO-DMEM, N2 supplement (Gibco), Albumax I, LIF, ERK1/2 inhibitor, GSK3b inhibitor, p38 inhibitor, JNK inhibitor and a protein kinase C inhibitor,

thereby generating the naive PSC.

According to some embodiments of the invention, the culture medium further comprises FGFR inhibitor.

According to some embodiments of the invention, the culture medium further comprises TGFR inhibitor.

According to an aspect of some embodiments of the present invention there is provided a method of generating a naive pluripotent stem cell (PSC), comprising incubating a non-naive PSC cell under conditions which allow generation of the naive PSC from the non-naive PSC, the naive PSC comprising:

an unmethylated X-inactive specific transcript (XIST) gene, wherein:

(i) when the naive PSC is a female PSC, then the naive female PSC has two unmethylated alleles of the XIST gene; and

(ii) when the naive PSC is a male PSC, then the naive male PSC has an unmethylated allele of the XIST gene,

and/or

an expression level of transcription factor E3 (TFE3) characterized by a nucleus to cytoplasm expression ratio which is equal to or higher than 1 as determined by an immunostaining assay.

wherein the conditions which comprise a culture medium which comprises KO-DMEM, N2 supplement (Gibco), Albumax I (Invitrogen), LIF, TGFβ1, ERK1/2 inhibitor, GSK3b inhibitor, p38 inhibitor, JNK inhibitor and a protein kinase C inhibitor,

thereby generating the naive PSC.

According to some embodiments of the invention, the culture medium further comprises FGFRi.

According to an aspect of some embodiments of the present invention there is provided a method of generating a naive pluripotent stem cell (PSC), comprising incubating a non-naive PSC cell under conditions which allow generation of the naive PSC from the non-naive PSC, the naive PSC comprising:

an unmethylated X-inactive specific transcript (XIST) gene, wherein:

(i) when the naive PSC is a female PSC, then the naive female PSC has two unmethylated alleles of the XIST gene; and

(ii) when the naive PSC is a male PSC, then the naive male PSC has an unmethylated allele of the XIST gene,

and/or

an expression level of transcription factor E3 (TFE3) characterized by a nucleus to cytoplasm expression ratio which is equal to or higher than 1 as determined by an immunostaining assay.

wherein the conditions which comprise a culture medium which comprises KO-DMEM, N2 supplement (Gibco), Albumax I (Invitrogen), LIF, bFGF, TGFβ1, ERK1/2 inhibitor, GSK3b inhibitor, p38 inhibitor, and JNK inhibitor,

thereby generating the naive PSC.

According to an aspect of some embodiments of the present invention there is provided a method of generating a naive pluripotent stem cell (PSC), comprising incubating a non-naive PSC cell under conditions which allow generation of the naive PSC from the non-naive PSC, the naive PSC comprising:

an unmethylated X-inactive specific transcript (XIST) gene, wherein:

(i) when the naive PSC is a female PSC, then the naive female PSC has two unmethylated alleles of the XIST gene; and

(ii) when the naive PSC is a male PSC, then the naive male PSC has an unmethylated allele of the XIST gene,

and/or

an expression level of transcription factor E3 (TFE3) characterized by a nucleus to cytoplasm expression ratio which is equal to or higher than 1 as determined by an immunostaining assay.

wherein the conditions which comprise a culture medium which comprises KO-DMEM, N2 supplement (Gibco), defined lipid concentrate (Gibco), LIF, bFGF, TGFβ1, ERK1/2 inhibitor, GSK3b inhibitor, p38 inhibitor, JNK inhibitor, and an MBD3 inhibitor,

thereby generating the naive PSC.

According to an aspect of some embodiments of the present invention there is provided an isolated naive pluripotent stem cell obtainable by the method of some embodiments of the invention.

According to some embodiments of the invention, the naive pluripotent stem cell comprising:

an unmethylated X-inactive specific transcript (XIST) gene, wherein:

(i) when the naive PSC is a female PSC, then the naive female PSC has two unmethylated alleles of the XIST gene; and

(ii) when the naive PSC is a male PSC, then the naive male PSC has an unmethylated allele of the XIST gene,

and/or

an expression level of transcription factor E3 (TFE3) characterized by a nucleus to cytoplasm expression ratio which is equal to or higher than 1 as determined by an immunostaining assay.

According to an aspect of some embodiments of the invention, there is provided a method of generating differentiated cells, comprising subjecting the naive pluripotent stem cells generated according to some embodiments of the invention, or the isolated naive pluripotent stem cells of some embodiments of the invention to differentiation conditions, thereby generating differentiated cells.

According to an aspect of some embodiments of the invention, there is provided a method of generating a primordial germ cell, comprising culturing a primate (e.g., human) naive pluripotent stem cell in a culture medium selected capable of inducing the primate naive pluripotent stem cells into primordial germ cell, wherein the culture medium comprises a Rho kinase (ROCK) inhibitor and bone morphogenetic protein 4 (BMP4), thereby generating the primordial germ cell.

According to some embodiments of the invention, the primate naive pluripotent stem cell comprises:

an unmethylated X-inactive specific transcript (XIST) gene, wherein:

(i) when the naive PSC is a female PSC, then the naive female PSC has two unmethylated alleles of the XIST gene; and

(ii) when the naive PSC is a male PSC, then the naive male PSC has an unmethylated allele of the XIST gene,

and/or

an expression level of transcription factor E3 (TFE3) characterized by a nucleus to cytoplasm expression ratio which is equal to or higher than 1 as determined by an immunostaining assay.

According to some embodiments of the invention, the primordial germ cell is characterized by CD61 (intergrin beta 3) expression pattern.

According to some embodiments of the invention, the primordial germ cell is characterized by $CD61^+/SSEA4^+$ expression pattern.

According to some embodiments of the invention, the culture medium used by the method of generating primordial germ cell further comprises at least one agent selected from the group consisting of: leukemia inhibitory factor (LIF), Stem Cell Factor (SCF) and Epidermal Growth Factor (EGF).

According to an aspect of some embodiments of the invention, there is provided an isolated population of primate primordial germ cells comprising primate primordial germ cells generated according to the method of some embodiments of the invention.

According to some embodiments of the invention, the isolated population of primate primordial germ cells comprising at least 50% of primordial germ cells characterized by $CD61^+/SSEA4^+$ expression pattern.

According to an aspect of some embodiments of the invention, there is provided a method of treating a subject in need thereof, comprising administering the primordial germ cells of some embodiments of the invention to a gonad tissue of the subject, thereby treating the subject in need thereof.

According to some embodiments of the invention, the subject suffers from infertility.

According to an aspect of some embodiments of the invention, there is provided a kit comprising the primate primordial germ cells of some embodiments of the invention and a medicament for treating infertility.

According to an aspect of some embodiments of the invention, there is provided a method of generating a chimeric animal, comprising introducing the isolated naive primate (e.g., human) PSC of some embodiments of the invention, or the primordial germ cells of some embodiments of the invention into a pre-implantation embryo of a host animal, thereby generating the chimeric animal.

According to some embodiments of the invention, the method further comprising allowing said pre-implantation embryo to grow *ex vivo* or *in vivo*.

According to some embodiments of the invention, the introducing is performed *in vivo*.

According to some embodiments of the invention, the introducing is performed *in vitro* or *ex vivo*.

According to some embodiments of the invention, the pre-implantation embryo comprises at least 4 cells.

According to some embodiments of the invention, the pre-implantation embryo comprises no more than 128 cells.

According to some embodiments of the invention, the host animal is a mouse.

According to some embodiments of the invention, the isolated naïve PSC or the primordial germ cell is allogeneic to the host animal.

According to some embodiments of the invention, the isolated naïve PSC or the primordial germ cell is xenogeneic to the host animal.

Unless otherwise defined, all technical and/or scientific terms used herein have the same meaning as commonly understood by one of ordinary skill in the art to which the invention pertains. Although methods and materials similar or equivalent to those described herein can be used in the practice or testing of embodiments of the invention, exemplary methods and/or materials are described below. In case of conflict, the patent specification, including definitions, will control. In addition, the materials, methods, and examples are illustrative only and are not intended to be necessarily limiting.

BRIEF DESCRIPTION OF THE DRAWINGS

Some embodiments of the invention are herein described, by way of example only, with reference to the accompanying drawings. With specific reference now to the drawings in detail, it is stressed that the particulars shown are by way of example and for purposes of illustrative discussion of embodiments of the invention. In this regard, the description taken with the drawings makes apparent to those skilled in the art how embodiments of the invention may be practiced.

In the drawings:

FIGs. 1A-N show that Mbd3 inhibition boosts epigenetic reversion of mouse primed pluripotent cells to naive pluripotency. FIGs. 1A-B: An siRNA screen for factors that can boost epigenetic reversion of primed EpiSCs into naive ESCs. Nanog-GFP mouse EpiSCs were used for the screening, and Nanog-GFP reactivation is used as a specific marker for naive pluripotency formation after expansion in 2i/LIF conditions. FIG. 1A: Schematic illustration depicting the siRNA screen. FIG. 1B: A histogram depicting percentage of Nanog-GFP expressing cells as a result of inhibition with the

tested siRNAs. Note that Mbd3 inhibition led to a dramatic increased in EpiSC reprogramming into naive ESCs. FIGs. 1C-G: $Mbd3^{+/+}$ and $Mbd3^{flox/-}$ EpiSCs were tested for reversion into naive cells in 2i/LIF. FIG. 1C: Schematic illustration of the reversion assay from EpiSCs into Naive ES-like colonies. FIGs. 1D-G: Microscopy photographs depicting formation of naive ES-like colonies from $Mbd3^{+/+}$ EpiSCs (FIG. 1D) or $Mbd3^{flox/-}$ EpiSCs (FIG. 1E). Note the dramatically increased reprogramming efficiency in Mbd3 depleted cells. FIGs. 1F-G: $Mbd3^{flox/-}$ $Rosa26\text{-}CreER^{+/-}$ $Nanog\text{-}GFP^{+/-}$ cells are shown under phase microscopy (FIG. 1F) and fluorescence microscopy (FIG. 1G). Note the homogenous reactivation of Nanog-GFP marker (FIG. 1G). FIG. 1H: Single cell cloning efficiency and quantification for EpiSC reprogramming efficiency into naive ESCs from different mutant lines. Notably, pBRY-Mbd3 rescue constructs stably expressed in the indicated lines, reduced reprogramming efficiency back to those observed in $Mbd3^{+/+}$ WT cells. Shown is a histogram depicting average percentage of $Nanog\text{-}GFP^{+}$ cells following the reversion of the various mutant lines towards naive cells in 2i/LIF conditions. FIGs. 1I-J are Western blot analyses indicating Mbd3 expression levels in different mutant ES lines. $Mbd3^{flox/-}$ cells had over 80% reduction in Mbd3 expression levels in comparison to $Mbd3^{+/+}$ cells. $Mbd3^{-/-}$ cells has complete absence of Mbd3 protein. FIGs. 1K-L are photographs of Agouti colored chimeras obtained from reprogrammed EpiSCs following Mbd3 depletion. Shown are two examples of chimeric mice generated after microinjection of reverted cells into naive pluripotency. The agouti coat color originates from the injected cells, while black coat color originates from the host mouse. These results indicated that the reverted cells are functionally pluripotent as naive cells and can give rise to differentiated cells upon differentiation *in vivo*. FIG. 1M is a schematic illustration depicting generation of chimeras for the purpose of isolating day E8.5 PGCs. $Mbd3^{flox/-}$ and $Mbd3^{+/+}$ ESC lines (with or without Mbd3 overexpression pBRY-Mbd3 rescue allele, as indicated) were targeted with Oct4-GFP reporter and injected into host chimeras. FIG. 1N – a histogram depicting evaluation of generation of naive ES-like cells from PGCs. Day E8.5 primordial germ cells (PGCs) were sorted into naive conditions [N2B27 and 2i/LIF/SCF (Stem Cell Factor, 10 ng/ml)/bFGF (basic fibroblast growth factor, 8 ng/ml)] and evaluated for efficiency to generate ES-like embryonic germ cells (EG cells). Mbd3 depleted PGCs convert *ex vivo* into naive ES-like cells with efficiency nearing 100%.

FIGs. 1O-T are images depicting confocal immunostaining analysis for temporal Mbd3 expression in developing mouse embryos. FIG. 1O – zygote stage; FIG. 1P – 2 cell stage; FIG. 1Q – 8 cell stage; FIG. 1R – Morula stage; FIG. 1S – Blastocyst at embryonic day 3.25; FIG. 1T – Blastocyst at embryonic day 3.75. Arrows indicate polar body. Note the reduction in Mbd3 expression after fertilization, and how it gets re-expressed at the late blastocyst stage. Right panels represent enlargement of the highlighted dashed areas.

FIGs. 2A-O show derivation of ESCs from $Mbd3^{-/-}$ blastocysts. FIG. 2A – a schematic illustration of generation of naive mouse ESCs. $Mbd3^{+/-}$ heterozygous mice were mated, and ESCs were derived from blastocysts in naive defined 2i/LIF conditions. $Mbd3^{-/-}$ ESCs were obtained at expected Mendelian ratio. FIGs. 2B-C are images of the $Mbd3^{-/-}$ ES cells initial colony at day 9 (FIG. 2B) and of the naive $Mbd3^{-/-}$ ESCs established and imaged at passage 4 (FIG. 2C), showing ES like morphology. FIGs. 2D-E – Images of MBD3 wild type (+/+) and depleted (-/-) ESCs stained for alkaline phosphatase (AP) pluripotent stem cells marker. Note the significant AP staining in the $MBD3^{-/-}$ ESCs demonstrating they normally express stem cell markers. FIGs. 2F-G – images of immuno-staining for Oct4 of $MBD3^{+/-}$ (heterozygotes) (FIG. 2F) and $MBD3^{-/-}$ (depleted) (FIG. 2G). These results indicate that Mbd3 is dispensable for establishing pluripotency *in vivo* and *in vitro*, and that Mbd3 depleted ES cells are indistinguishable from wild type ES and iPS cells. FIGs. 2H-O are Western blot analyses for pluripotency markers of MBD3 wild type (+/+) or depleted (-/-) ESCs. FIG. 2H – Mbd3; FIG. 2I – Gapdh; FIG. 2J – Sox2; FIG. 2K – Sall4; FIG. 2L – Klf4; FIG. 2M – Mi2β; FIG. 2N – Klf5; FIG. 2O – c-Myc.

FIGs. 3A-G depict genetically engineered systems for deterministic reprogramming in mouse cells. FIG. 3A – The present inventors have established a reprogrammable mouse $Mbd3^{+/+}$ and $Mbd3^{flox/-}$ iPSC lines carrying (1) an Oct4-GFP reporter, (2) mCherry constitutively expressed marker, (3) m2RtTa and (4) a TetO inducible OKSM polycistronic cassette. These lines were injected into host blastocysts, and their differentiated derivatives were re-isolated *in vitro.* Subsequently, reprogramming efficiency and progression can be analyzed following DOX induction. This exact system allows 6 day 100% reprogramming as shown in FIGs. 4A-O. Further, this transgenic system allows non-restricted derivation of homogenous somatic cells,

which will be harvested every 24 hours during the 7-day course of iPSC completion following DOX treatment. FIGs. 3B-D – photographs of isolated $Mbd3^{flox/-}$ ESCs at phase contrast (FIG. 3B), and fluorescence microscopy. FIG. 3C – staining for mCherry expression (red); FIG. 3D – staining for Oct4-GFP expression (green). FIGs. 3E-F - Western blot analyses using anti-Mbd3 (FIG. 3E) and anti Hsp90 (FIG. 3F) staining. Show is Mbd3 expression in $Mbd3^{-/-}$ ESCs/iPSCs, with or without addition of pBRY-Mbd3 rescue transgene (recovery clones). FIG. 3G - Southern blot analysis showing correct gene targeting of the Rosa26 locus with Cre-ER knock in construct introduced into $Mbd3^{flox/-}$ ESCs. Altogether, the results show genetically engineered systems for deterministic reprogramming in mouse cells.

FIGs. 4A-P show deterministic and synchronized reprogramming of mouse fibroblasts into iPSCs following Mbd3 depletion. FIG. 4A - Mbd3 WT and depleted (flox/- or -/-) cells were directly infected with lentiviruses expressing a polycistronic OKSM cassette, and expanded in mouse naive 2i/LIF conditions. Reprogramming efficiency was evaluated by measuring percentage of $Oct4\text{-}GFP^{+}$ cells, and it was noted that of > 95% $Oct4\text{-}GFP^{+}$ levels was observed in Mbd3 depleted cells. FIG. 4B - Secondary reprogrammable fibroblasts, carrying an Oct4-GFP reporter and a mCherry constitutively expressed marker, were single cell sorted and subjected to DOX reprogramming. Reprogramming efficiency at day 10 was calculated by dividing the number of Oct4-GFP+ wells by mCherry+ wells (mCherry was used to normalize for plating efficiency). The 2i/LIF conditions were applied starting from day 2. Please note that in Mbd3 depleted samples (flox/- or -/-) all mcherry+ clones became $Oct4\text{-}GFP^{+}$ cells (indicated as green). Only $Mbd3^{+/+}$ samples had mCherry+ clonal populations that did not turn on the specific pluripotency marker Oct4-GFP (and thus indicated as red colored boxes). FIGs. 4C-E depict immunostaining analyses of the $Mbd3^{+/+}$ iPSC (FIG. 4C), the $Mbd3^{flox/-}$ iPSC (FIG. 4D) or the $Mbd3^{-/-}$ iPSC (FIG. 4E) clones for the Oct4 (left), Nanog (middle) or Alkaline Phosphatase (AP) (right) pluripotency markers. Note that iPSCs obtained following Mbd3 depletion normally express all pluripotency markers tested as in wild type $Mbd3^{+/+}$ cells. FIGs. 4F-G are photographs of Agouti coat colored chimera (FIG. 4F) and germ-line transmission from $Mbd3^{flox/-}$ iPSCs derived (FIG. 4G). This indicates that Mbd3 depleted iPSCs can give rise to adult chimeric animals following injection into host mice, and are pluripotent. FIGs. 4H-I are images

depicting live imaging of reprogramming of $Mbd3^{+/+}$ (FIG. 4H) and $Mdb3^{flox/-}$ (FIG. 4I) cells, after plating 50 cells per well. Note the dramatically increased ES-like colony formation in $Mbd3^{flox/-}$ cells. FIGs. 4J-O are images depicting immunofluorescence of $Mdb3^{+/+}$ (FIGs. 4J, 4K and 4L) or $Mdb3^{flox/-}$ (FIGs. 4M, 4N and 4O) cells stained for mCherry (FIGs. 4J and 4M), Oct4-GFP (FIGs. 4K and 4N) and mCherry Oct4-GFP (FIGs. 4L and 4O). By day 6 mCherry+ and Oct4-GFP+ nearly >90% co-localize in $Mbd3^{flox/-}$ cells, and not in WT cells. FIG. 4P – A graph indicating cumulative Oct4-GFP^{+} colony formation nearing 99% in $Mbd3^{flox/-}$ cells (red graph) by day 6 based on live imaging follow-up. Note the narrow window of synchronized Oct4-GFP activation at days 4-5 (red line and blue bar).

FIGs. 4Q-R depict radically efficient and synchronized iPSC reprogramming to pluripotency. FIG. 4Q – A graph indicating cumulative Oct4-GFP+ colonies for $Mbd3^{flox/-}$ (red plot) and $Mbd3^{+/+}$ (blue plot) based on live imaging follow-up. Statistics of Oct4-GFP activation were calculated from all segmented colonies. Note the narrow window of synchronized Oct4-GFP activation at days 4-5. FIG. 4R - A graph indicating the average fraction of Oct4-GFP+ cells within single colonies measured with live imaging follow-up. Approximately 85% of cells within individual $Mbd3^{flox/-}$ clonal population became Oct4-GFP^{+} cells by day 6. Plot values indicate the mean and error bars indicate standard deviation calculated over 4 replicates (wells) in each sample and time point.

FIGs. 5A-F show comparative analysis of Mbd3 depleted somatic cell properties during reprogramming. FIG. 5A – A histogram depicting the results of RT-PCR analysis demonstrating relative transgene induction levels in different somatic cells (from BU-V19-OSKM transgenic reprogrammable systems) in the presence or absence of DOX as indicated. Results are presented with +/- s.d. (standard deviation) of 3 replicates per sample. Transgene induction level was not altered in Mbd3 depleted MEF or B cells on DOX for 8 days. FIGs. 5B-C - Western blot analysis using anti heat shock protein 90 (Hsp90) (FIG. 5B) and anti-Mbd3 (FIG. 5C) antibodies, validating Mbd3 protein reduction in NGFP1 knockdown (KD) cells. FIG. 5D – A histogram depicting the results of RT-PCR analysis demonstrating relative transgene induction levels in different somatic cells (from NGFP1 transgenic reprogrammable systems) in the presence or absence of DOX as indicated. Results are presented with +/- s.d. of 3

replicates per sample. Transgene induction level was not altered in Mbd3 depleted MEF (mouse embryonic fibroblasts) or B cells on DOX for 8 days. FIG. 5E is a histogram depicting the results of a flow cytometry based detection of apoptosis in wild type and Mbd3 depleted MEFs and B cells following DOX induction. The results indicate that apoptosis levels were similar upon transgene induction in both cell samples. Overall, the results presented in FIGs. 5A-E exclude changes or defects in transgene induction or proliferation as underlying causes for enhanced reprogramming in Mbd3 depleted somatic cells. FIG. 5F – A similar growth kinetics was observed in $Mbd3^{+/+}$ and $Mbd3^{flox/-}$ MEFs upon DOX mediated transgene induction. One representative experiment is shown out of 2 performed. Overall, the results presented in FIGs. 5A-E exclude changes in transgene induction or proliferation as predominant causes for enhanced reprogramming in Mbd3 depleted somatic cells.

FIGs. 6A-B show that Mbd3 deletion renders deterministic and complete reprogramming of multiple adult somatic cell types. Indicated somatic cells from NGFP1-control (FIG. 6A), NGFP1-$Mbd3^{KD}$ [knockdown (KD)] (FIG. 6B) adult chimeras were isolated and subjected to single cell reprogramming and evaluation of Nanog-GFP expression after 8 days of DOX. "EpiSC" – Epiblast stem cells; "NPC" – Neural precursors; "HSC" – Hematopoietic Stem Cell; "CMP" – Common Myeloid progenitor; "Monocytes" – blood cells macrophages; "Pro-B lymphocytes"; "Mature B" – mature B lymphocytes; "Mature T" – mature T cells. Near 100% efficiency was obtained from all $Mbd3^{flox/-}$ (Mbd3-depleted) somatic cell types tested. Average of 2-3 independent experiments per each cell type is shown.

FIG. 7 shows that Mbd3 depleted cells are completely reprogrammed and transcriptionally indistinguishable from ESCs/iPSCs by 8 days of DOX induction. Gene expression analysis was conducted on the indicated genetically matched mouse samples. $Mbd3^{flox/-}$, but not $Mbd3^{+/+}$, MEFs clustered differently from donor somatic MEFs only after 4 days of OKSM (DOX) induction. By day 8, flox/- cells were transcriptionally indistinguishable from established ESCs and iPSCs line. $Mbd3^{+/+}$ population even after 11 days of longer reprogramming did not cluster with pluripotent ESCs-iPSC lines. These findings support complete reprogramming in donor somatic cells following OSKM overexpression together with Mbd3 inhibition.

FIGs. 8A-Q show deterministic and synchronized reprogramming following Mbd3 depletion in mouse and human cells. FIGs. 8A-D – Images of $Mbd3^{flox/-}$ (FIGs. 8A and 8C) and $Mbd3^{+/+}$ cells at day 8 (FIGs. 8A and 8B) or at passage 2 (FIGs. 8C and 8D). Note that colonies obtained following $Mbd3^{flox/-}$ somatic cell reprogramming have ESC-like morphology and become GFP homogenous for Nanog expression at passage 1. In WT cells, most colonies are not fully reprogrammed and do not have ES-like morphology. FIG. 8E – A histogram depicting quantification of Nanog-GFP positive cells. By quantifying amount of Nanog-GFP positive cells at time of detection (day 8 for Mbd3-KD cells), it is notable that >99% of cells within each clonal population at day 8 in Mbd3KD cells are positive. For other reprogramming combinations shown, when a clonal population becomes positive (above 0.5% threshold set), a minority of cells turns on Nanog-GFP, indicating that only a fraction of the clone successfully reprogrammed. These findings support deterministic and synchronized completion of reprogramming by inhibition of Mbd3 expression and function in naive pluripotency promoting growth conditions. FIGs. 8F-K show flow cytometry analyses of a partially reprogrammed cell clone containing OSKM transgenes, without reactivation of the Oct4-GFP reporter following treatment with: FIG. 8F – untreated; FIG. 8G – scrambled siRNA day 20; FIG. 8H – untreated day 20; FIG. 8I – 5-aza + TSA Day 20; FIG. 8J – Mbd3 siRNA Day 5; FIG. 8K – Mbd3 siRNA Day 6. Mbd3 knockdown resulted in complete and rapid completion of reprogramming. 4-Aza and TSA treatment, previously reported to promote reprogramming, only activates a fraction of the cells. These results demonstrate that Mbd3 elimination potently opens the gateway of reprogramming to pluripotency. FIG. 8L - $Mbd3^{flox/-}$ human ES cells were generated by genetic engineering with TALE nuclease effectors. Targeting strategy for a floxed conditional allele is shown. FIGs. 8M-N – Western blot analyses of correctly targeted $MBD3^{flox/-}$ clone, based on southern blot verification, using anti-MBD3 antibody (FIG. 8M) or anti-HSP90 antibody (FIG. 8N). Note the over 90% reduction in MBD3 protein expression levels (comparable reduction to that seen in mouse flox/- cells FIGs. 1I-J. FIG. 8O – $MBD3^{+/+}$ and $MBD3^{flox/-}$ iPSCs carrying DOX inducible OKSM transgene were labeled with constitutively expressed mCherry and targeted with an OCT4-GFP knock-in allele. *In vitro* differentiated fibroblasts from the latter lines were reprogrammed as indicated in the scheme. 98-100% of human $Mbd3^{flox/-}$ fibroblasts

become GFP+ IPSCs after 8 days of transgene induction. These results demonstrate a similar effect in mouse and human reprogramming for Mbd3 inhibition. Error bars indicate s.d. of 2 biological replicates. * Indicates significant *P* value <0.01 in comparison to $MBD3^{+/+}$ samples (n=2). FIGs. 8P-Q – Images of $MBD3^{flox/-}$ cells in WIS-NHSM medium. MBD depleted human pluripotent stem cells have a dramatic round mouse-ESC like morphology and grow homogenously. These results indicate that Mbd3 inhibition might further improve WIS-NHSM naive growth conditions (described herein).

FIGs. 8R-S Alleviating Mbd3 expression facilitates transition to ground state pluripotency in mouse and human cells. FIG. 8R - Spearman correlation matrix between the indicated genetically matched mouse samples, measured over gene expression levels of all 16,620 expressed genes. The matrix is clustered with Hierarchical clustering producing the dendrogram shown. Note that after 4 days of OKSM (DOX) induction, $Mbd3^{flox/-}$ MEFs, but not $Mbd3^{+/+}$ MEFs, were more similar to established ESC and iPSC lines, than to the original somatic MEFs. By day 8, $Mbd3^{flox/-}$ cells are transcriptionally indistinguishable from ESCs and iPSCs. $Mbd3^{+/+}$ population did not cluster with ESCs and iPSCs even after 11 days of OKSM induction. FIG. 8S - Monoclonal lines established from $Mbd3^{+/+}$ and $^{flox/-}$ secondary cells and reprogrammed in 2i-LIF + DOX. Fraction of pre-iPS clones that did not reactivate Oct4 or Nanog GFP markers (either SSEA1 positive or negative) is shown. GFP negative clones could not be established from Mbd3 depleted cells, as they all became fully reprogrammed already by day 10.

FIG. 9 is schematic presentation of evolutionary analysis of the NuRD complex and other associated proteins. The present inventors assigned orthologs for many human proteins that are either known to be part of the NuRD complex (or are related to these proteins), from 15 representative metazoan species (mouse - M.musculus, platypus - O.anatinus, zebra finch - T.guttata, chicken – G.gallus, frog – X. tropicalis, zebrafish – D.rerio, pufferfish - T.nigroviridis, lancelet - B.floridae, sea urchin - S.purpuratus, mosquito - A.gambiae, fruit fly -D. melanogaster, honeybee - A.mellifera, beetle - T.castaneum, sea anemone - N. vectensis, trichoplax - T. adhaerens), and the yeast S.cerevisiae, as an outgroup. The last metazoan in this list – T. adhaerens, represents a basal group of metazoan, and is used to study the origins of animal multicellularity.

Proteins that have an ortholog in T. adhaerens were likely to be present in the basal multicellular animals, while proteins that appear in yeast precede animal multicellularity. The analysis indicates that Mbd3 and other NuRD components are conserved in all multi-cellular organisms, and thus inhibition of Mbd3 function may potentially promote direct reprogramming in many (or even all) multicellular organisms. The color scale indicates degree of homology, i.e., percentage of sequence similarity between proteins.

FIGs. 10A-P demonstrate that siRNA inhibition of MBD3 promotes human iPSC reprogramming by OSKM. FIG. 10A – A schematic illustration depicting secondary human reprogrammable fibroblasts carrying DOX inducible OSKM transgenes, being subjected to the depicted reprogramming protocol with DOX. FIGs. 10B-C – Western blot analyses using anti MBD3 antibody (FIG. 10B) or anti-Hsp90 antibody (FIG. 10C) of cells treated with MBD3 siRNA, with a control siRNA, or remained untreated. Note the reduction of MBD3 in cells treated with MBD3 siRNA, but not in cells treated with the control siRNA or in untreated cells. FIG. 10D – In WIS-NHSM growth conditions, Knockdown of Mbd3 at days 2 and 4, but not with scrambled control siRNA, dramatically increased the formation of alkaline phosphatase+ iPSC clones. FIG. 10E - Schematic illustration of a single round reprogramming. Human fibroblasts are subject to treatment with MBD3 siRNA at 7 and 2 days prior to mRNA transfection with the OSKM and Lin28 factors. FIGs. 10F-O are images of the formed iPSCs. FIG. 10F – Day 7 iPS colony, passage 0; FIG. 10G – iPSCs at passage 3; FIGs. 10I-J – IPSCs (Passage 7) stained with Dapi (blue, nuclear staining) (FIG. 10I) and with OCT4 (red) (FIG. 10J); FIGs. 10L-M – IPSCs (Passage 10) stained with Dapi (blue, nuclear staining) (FIG. 10L) and with Nanog (red) (FIG. 10M); FIGs. 10N-O - IPSCs (Passage 10) stained with Dapi (blue, nuclear staining) (FIG. 10N) and with TRA1-60 (green) (FIG. 10O); FIGs. 10H, 10K and 10P – histological staining of cells differentiated from the iPSCs. *In vivo* Teratoma formation generated from P8 iPSCs showing differentiation into ectoderm (FIG. 10H), mesoderm (FIG. 10K) and ectoderm (FIG. 10P) embryonic germ layers. These results show that at day 7 MBD3 siRNA treatment of human fibroblasts allows generation of iPSCs in WIS-NHSM conditions, by single round of reprogramming with mRNA transfection with OSKM and Lin28 factors, and alleviates the need for many rounds of repeated mRNA

transfections. These results indicate that inhibition of MBD3 expression and/or function promotes iPSC formation by transient mRNA or other transient transfection protocols (with protein or cDNAs).

FIGs. 11A-P demonstrate mechanisms of Mbd3 function and influence on reprogramming to pluripotency. FIGs. 11A-H are immunoblot analyses using anti MBD3 antibody (FIGs. 11A-D) or anti-FLAG antibody (FIGs. 11E-11). Constructs encoding Flag-tagged OCT4 (FIGs. 11A and 11E), or KLF4 (FIGs. 11C and 11G) or SOX2 (FIGs. 11B and 11F) or HDAC1 (used as a positive control; FIGs. 11D and 11H) were transfected into HEK293T cells in combination with MBD3. The cell lysates were immunoprecipitated (IP) with an anti-Flag antibody (or anti-IgG as control), followed by an immunoblot analysis (IB). The expression levels in whole-cell lysates or IP extract were determined by IB anti-Flag (FIGs. 11E-H) or anti-Mbd3 (FIGs. 11A-D). This analysis demonstrates direct interaction of Mbd3 with OSK pluripotency factors. FIGs. 11I-P – are immunoblot analyses using anti MBD3 antibody (FIGs. 11I-L) or anti-FLAG antibody (FIGs. 11M-P). Reproducing the experiment in FIGs. 11A-H, but by overexpressing of Mbd2, instead of Mbd3. Constructs encoding Flag-tagged OCT4 (FIGs. 11I and 11M), or KLF4 (FIGs. 11K and 11O) or SOX2 (FIGs. 11J and 11N) or HDAC1 (used as a positive control; FIGs. 11L and 11P) were transfected into HEK293T cells in combination with MBD2. This analysis demonstrated lack of enriched or specific interaction for MBD2 with reprogramming factors OSK. These results indicate that Mbd3 directly interacts with reprogramming pluripotency factors, and thus by recruiting the NuRD complex, it inhibits their activity and prevents the reactivation of their downstream target genes.

FIGs. 12A-V demonstrate *in vitro* stabilization of transgene independent and long-term stable naive human pluripotent cells. FIG. 12A – A schematic illustration depicting the strategy used for calibrating conditions to isolate naive transgene independent iPSCs in the presence of ERK inhibition. The present inventors used C2 human iPSC line carrying DOX-inducible lentiviruses (TetO) encoding Oct4, Sox2, Klf4 and c-Myc. This cell line was targeted with TALE effector nuclease to insert a GFP-2A-Puro allele in the endogenous OCT4 locus. GFP+ C2 cells can be grown in 2i/LIF conditions but only with the presence of DOX, and approximately 60% of correctly targeted clones specifically expressed GFP. The present inventors screened for

addition of small molecule factors and cytokines that allow obtaining Oct4-GFP positive cells in the absence of DOX and presence of ERK inhibition. Two Pools of combined factors were used for the screen as indicated. Pool 1: ERKi, GSK3βI, LIF, BMP4, IGF, P38i. JNKi, Forskolin. Pool 2: FGFi, TGFi, Kenpaullone, Go6983, BayK8644, Bix1294, ROCKi and SCF. FIGs. 12B-C – microscopic images depicting phase contrast (FIG. 12B) and GFP fluorescence staining (green, FIG. 12C) of the C2 correctly targeted iPS clones used for the screen. FIG. 12D – A histogram depicting the percentage of Oct4-GFP$^+$ colonies on day 14 (s.d.m; n=3) in the presence of different combinations of factors as indicated. Cells were expanded in the DOX + 2iLIF as well as in various media such as DOX only (DOX is used to induce OSKM transgenic factors), 2i/LIF only, 16F (pools 1 and 2 combined); with the 16F medium with the following omitted (marked with "-") or added (marked with "+") factors: -2i/LIF, -pool1, -pool2, -TGFi/-FGFi, -TGFi/-FGFi + FGF2 (bFGF) and TGFβ1; with pool 2 with the following omitted factors: -TGFi, -FGFi; and pool 1 with FGF2 and TGFβ1. Note that the presence of 2i/LIF or pool1 is essential for maintaining DOX-independent OCT4-GFP+ cells. Also note, TGFi and FGFi negatively influence DOX-independent OCT4-GFP+ cells, and that addition of TGFβ1 and FGF2 positively support maintenance of DOX-independent OCT4-GFP+ cells in the context of 2i/LIF medium. FIG. 12E - A histogram depicting percentage of Oct4-GFP$^+$ colonies on day 20 relative to control cells in the presence of different combinations of factors as indicated. Cells were expanded in the 14F + bFGF/TGFβ1 medium which includes the 14 factors [which are the 16 factors of pools 1 and 2, yet without inhibitors of FGF and TGF pathways] and with TGFβ1 and bFGF. Next, from this medium combination (14F + bFGF/TGFβ1) the present inventors have eliminated the factors shown near the "X" axis, e.g., ERKi (shown as "-ERki" in FIG. 12E), etc., in order to determine the essential factors required for maintaining Oct4-GFP$^+$ cells in the absence of DOX. This analysis indicates that ERKi, CHIR, P38i, JNKi, LIF, bFGF and TGFB were essential components. Removing any of them resulted in significant deterioration and differentiation of C2 Oct4-GFP+ cells in the absence of DOX. FIG. 12F - A histogram depicting percentage of Oct4-GFP+ colonies on day 8 relative to control cells. For further optimizing naive growth conditions and substitute of Knockout serum replacement, Knockout serum replacement can be substitute only with using N2

supplement and either 1% albumax or 1% Defined fatty acid mix concentrate (FAA) (Invitrogen). FIG. 12G - Summary of essential elements calibrated to expand human naive pluripotent cells for long term and without exogenous transgenes. This media is termed WIS-NHSM (Weizmann Institute of Science- Naive Human Stem cell Medium). FIG. 12H – A histogram depicting percentage of Oct4-GFP+ colonies on day 8 relative to control cells grown under various conditions as indicated. Note that naive human iPSCs can be grown without feeder cells either on Matrigel coated plates or 0.2% gelatin + 1 ng/ml vitronectin coated plates (but not gelatin alone). FIG. 12I - Karyotype of transgene independent C1 naive pluripotent cell line in WIS-NHSM media. FIGs. 12J-K – images depicting phase contrast (FIG. 12J) or fluorescence (FIG. 12K) microscopy of C2 iPSC clones expanded in WIS-NHSM independent of DOX and shows homogenous Oct4-GFP expression. Note Oct4-GFP expression (green staining, FIG. 12K) demonstrating the cells are pluripotent. FIGs. 12L-N – images of morphological staining of teratoma formation from the C2 iPS clone line shown in FIGs. 12I-K. Note the differentiation into cells of the mesoderm (FIG. 12L), endoderm (FIG. 12M) and ectoderm (FIG. 12N) embryonic germ layers, demonstrating the pluripotency of the naive C2 iPSC cell line. FIGs. 12O-R are images depicting iPSCs that were derived from BJ fibroblasts. Human naive iPSCs can be directly formed from human BJ fibroblasts, following direct infection with an OKSM polycistronic cassette delivered by a lentivirus. FIG. 12O – phase contrast of iPSC colonies at day 6 DOX in WIS-NHSMP3 medium; FIG. 20P – phase contrast of BJ iPSC at passage 3; FIG. 12Q – fluorescent microscopy showing Nanog expression (green staining) of BJ fibroblasts derived iPS cells at passage 8. The inset shows DAPI staining (blue); FIG. 12R - fluorescent microscopy showing SSEA4 expression (red staining) of BJ iPSC cells at passage 13. The inset shows DAPI staining (blue); Altogether, FIGs. 12O-R show that the established BJ iPSC line expressed all pluripotency marker tested. FIG. 12S - Cells were expanded in the presence of bFGF/TGFβ and Pool1 factors, and the essential factors required for maintaining OCT4-GFP+ cells in the absence of DOX were determined by screening for loss of GFP upon withdrawal of these components (green font). One out of three independent replicate experiments is shown. * t-test P value < 0.01 (between indicated samples marked by connecting lines). Error bars indicate s.d.m (n=4). FIG. 12T - Summary of essential elements calibrated to expand human naive

pluripotent cells for long term and without exogenous transgenes. This optimized media is termed WIS-NHSM (Weizmann Institute of Science- Naive human Stem cell Medium). FIG. 12U - Components of optimized WIS-NHSM conditions. FIG. 12V - Representative large-field view of OCT4-GFP+ hiPSC colonies grown in WIS-NHSM media.

FIGs. 13A-W demonstrate the derivation of human naive iPSCs and ESCs from already established primed/conventional ESCs lines or blastocysts. FIG. 13A – A schematic illustration depicting epigenetic reversion of primed/conventional human ESCs to ground state naive state, and without genetic modifications. Primed already established cell line H1, H9, BGO1, WIBR2, WIBR3 hESCs and C1, C2 iPSCs were plated on gelatin/vitronectin-coated plates and grown in WISNHSM conditions. Within 5 days, many cells differentiate, but round dome colonies emerge. After trypsinization and passaging, homogenous naive ESC/iPSC lines can be established. FIGs. 13B-E are microscopic phase contrast images. FIG. 13B – Primed BG01 hESC; FIG. 13C –naive BGO1 cell line at passage 2; FIG. 13D – BGO1 cell line on day 5 in the WIS-NHSM medium; FIG. 13E – BGO1 cell line at passage 31. FIGs. 13F-J are microscopic images demonstrating expression of pluripotent markers by naive BGO1, as a representative example. FIGs. 13F – naive BG01 hESC stained with Hoechst (left panel, blue nuclear staining) Nanog (middle panel, green staining) and a merged image of Hoechst and Nanog (right panel). FIG. 13G – naive BG01 hESC at passage 41 (46 XY) stained with Hoechst (left panel, blue nuclear staining), SSEA3 (middle panel, red staining) and a merged image of Hoechst and SSEA3 (right panel). FIG. 13H - naive BG01 hESC at passage 41 (46 XY) stained with Hoechst (left panel, blue nuclear staining), SSEA4 (middle panel, red staining) and a merged image of Hoechst and SSEA4 (right panel). FIG. 24I - naive BG01 hESC at passage 41 (46 XY) stained with Hoechst (left panel, blue nuclear staining), TRA1-60 (second from left panel, red staining), a merged image of Hoechst and TRA1-60 (third from left panel) and alkaline phosphatase (AP) staining (pink-purple staining, right panel). FIG. 13J - naive BG01 hESC at passage 41 (46 XY) stained with Hoechst (left panel, blue nuclear staining), Oct4 (second from left panel, red staining), TRA1-81 (third from left panel) and a merged image of TRA-81 and Oct4 staining (right panel). The results presented in FIGs. 13F-J demonstrate that the naive pluripotent stem cells (PSCs) express all known human pluripotent markers, and retain a

normal 46XY male karyotype after many passages in the absence of exogenous transgenes. All naive lines described here in show no signs of deterioration, crisis or decay with expansion (for over 70 passages thus far). FIGs. 13K-M are images depicting morphological staining of teratomas formed from the naive PSCs. Shown are cells of the mesoderm (FIG. 13K), ectoderm (FIG. 13L) and endoderm (FIG. 13M) embryonic germ layers, demonstrating that the naive PSCs are pluripotent as shown by their ability to generate differentiated teratomas *in vivo*. FIG. 13N – a schematic illustration depicting generation of a human naive PSC from a blastocyst. A Human ICM-blastocyst was plated on feeder cells in WIS-NHSM conditions. At day 6-8, the original outgrowth was trypsinized, and naive pluripotent cell lines were established in WIS-NHSM conditions on gelatin/vitronectin coated plates independent of feeders (representative images at P3 of established lines is shown). FIG. 13O – Images depicting phase contrast microscopy of a naive PSC at passages 0 (day 6) and 3, formed from a human blastocyst that was cultured in WIS-NHSM medium. FIG. 13P – images of a fluorescence microscopy showing a naive WIS1 hESC stained with Hoechst (upper panel, blue staining), nanog (second from top panel, green staining), SSEA4 (third from top panel, red staining), and a merged image of the Hoechst, Nanog and SSEA4 (bottom panel). FIG. 13Q - images of a fluorescence microscopy showing a naive WIS1 hESC stained with Hoechst (upper panel, blue staining), OCT4 (green staining, middle panel), and a merged image of Hoechst and OCT4 (bottom panel). FIG. 13R - images of a fluorescence microscopy showing a naive WIS1 hESC stained with Hoechst (upper panel, blue staining), SSEA3 (green staining, middle panel), and a merged image of Hoechst and SSEA3 (bottom panel). FIGs. 13S-U – images depicting morphological staining of teratomas formed from the naive WIS1 hESC line. Shown are cells of the endoderm (FIG. 13S), mesoderm (FIG. 13T), and ectoderm (FIG. 13U) embryonic germ layers. The results shown in FIGs. 13P-U demonstrate that the naive WIS1 hESC line is pluripotent based on pluripotency marker expression (FIGs. 13P-R) and teratoma differentiation *in vivo* (FIGs. 13S-U). FIG. 13V - Naive hiPSCs can be directly formed from human BJ fibroblasts, following reprogramming with mRNA transfection in WIS-NHSM conditions. Note distinct domed colony emerging 10 days after factor transduction. FIG. 13W - Naïve hiPSCs can be directly formed from human BJ fibroblasts in WIS-NHSM conditions.

FIGs. 14A-D are images (phase contrast microscopy) depicting the morphology of genetically matched naive and primed human pluripotent cell lines. FIGs. 14A-B - Representative images showing distinct morphology for embryo-derived naive hESCs in WIS-NHSM conditions (Marked as "WIS1 hESC", "WIS2 hESC", "LIS1 hESC" and "LIS2 hESC" grown on feeder cells (FIG. 14B) or without feeder cells (FIG. 14A). FIGs. 14C-D - Representative images showing distinct morphology for conventional/primed pluripotent cells lines (FIG. 14C), versus genetically matched naive hESCs and hiPSCs grown in WIS-NHSM conditions (FIG. 14D). Naive cells display a more domed morphology and with a less distinct cell-cell boundary. P indicates the passage number. For naive cells, P indicates number of passages already achieved in naive WIS-NHSM conditions. For primed cells, P includes number of passages already achieved in naive WIS-NHSM conditions (6 passages) and in primed conditions.

FIGs. 15A-M demonstrate signaling state and karyotype of human naive iPSCs and ESCs. Western blot analyses of primed or naive human pluripotent cells (Passage 25) (WIBR3 hESC) using antibodies directed against total and phosphorylated forms of distinct signaling adaptors. FIG. 15A – pERK1/2 42,44; FIG. 15B – Total ERK1/2; FIG. 15C – HSP90; FIG. 15D – Total p38; FIG. 15E – pP38 180,182; FIG. 15F – HSP90. FIG. 15G – pSTAT3 705; FIG. 15H – Total STAT3; FIG. 15I - pβCatenin 33,37; FIG. 15J - βCatenin; FIG. 15K – pJNK1,2; FIG. 15L – JNK; FIG. 15M – HSP90. Note that human WIBR3 naive hESCs that are grown in WIS-NHSM conditions show specific blocked and reduced activity for ERK1, P38 and JNK in naive pluripotency. Consistent with the essence of LIF in WIS-NHSM phosphorylated STAT3 levels accumulate in naive hESCs. Samples were loaded in triplicates for demonstrating consistency. Similar results were obtained when analyzing naive and primed C1 hiPSCs, WIS2 hESCs (not shown). FIGs. 15H-I are karyotypes of different naive human ESCs and iPSCs.

FIGs. 15N-S demonstrate karyotype and clonal stability of human naive pluripotent cells. Shown are representative karyotype analysis results indicating normal karyotypes of different naive hESC and hiPSCs. FIG. 15N – C1 naive hiPSC; FIG. 15O – WIS1 naive hESC; FIG. 15P – WIBR3 naive hESC; FIG. 15Q – BG01 naive hESC; FIG. 15R – LIS1 naive hESC; FIG. 15S – LIS2 naive hESC. The passage number (p) at

which cells were harvested for karyotyping is indicated. These data indicate that naive hESCs and hiPSCs can be established from both sexes, and maintain a normal karyotype without a dramatic tendency to acquire chromosomal abnormalities.

FIGs. 15T-U - Immunostaining for pluripotency markers on individually subcloned lines (labeled 1-4) from naive hESC lines WIBR3 (FIG. 15T) and BGO1 (FIG. 15UO). Note that both naive hESC lines express OCT4, nanog, Tra-1-60, Tra-1-81 and SSEA4.

FIGs. 16A-H are images depicting immunostaining analyses for pluripotency markers on naive WIBER3 hESCs. FIG. 16A – Hoechst (blue staining, left panel), TRA1-80 (green staining, middle panel), and a merged image (right panel); FIG. 16B - Hoechst (blue staining, left panel), TRA1-80 (green staining, middle panel), and a merged image (right panel); FIG. 16C - Hoechst (blue staining, left panel), KLF4 (red staining, middle panel), and a merged image (right panel); FIG. 16D - Hoechst (blue staining, left panel), KLF4 (red staining, middle panel), and a merged image (right panel); FIG. 16E - Hoechst (blue staining, left panel), SSEA1 (middle panel), and a merged image (right panel); FIG. 16F - Hoechst (blue staining, upper panel), TRA1-60 (green staining, second panel), Nanog (red staining, third panel), and a merged image (bottom panel); FIG. 16G - Hoechst (blue staining, upper panel), E-cadherin (green staining, second panel), Oct4 (red staining, third panel), and a merged image (bottom panel); FIG. 16H - Hoechst (blue staining, upper panel), SSEA4 (green staining, second panel), OCT4 (red staining, third panel), and a merged image (bottom panel); The immunostaining results show that the naive hESC line exhibits positive staining for all known human pluripotency markers tested. Notably, SSEA1, which is specific for mouse and not human pluripotent cells, is not expressed in human naive ESCs and iPSCs (FIG. 16E, middle panel).

FIGs. 17A-H are images depicting immunostaining analyses for pluripotency markers on naive C1 hiPSC. FIG. 17A – Hoechst (blue staining, left panel), TRA1-80 (green staining, middle panel), and a merged image (right panel); FIG. 17B - Hoechst (blue staining, left panel), TRA1-80 (green staining, middle panel), and a merged image (right panel); FIG. 17C - Hoechst (blue staining, left panel), KLF4 (red staining, middle panel), and a merged image (right panel); FIG. 17D - Hoechst (blue staining, left panel), Nanog (red staining, middle panel), and a merged image (right panel); FIG. 17E

- Hoechst (blue staining, left panel), SSEA1 (middle panel), and a merged image (right panel); FIG. 17F - Hoechst (blue staining, upper panel), TRA1-60 (green staining, second panel), Nanog (red staining, third panel), and a merged image (bottom panel); FIG. 17G - Hoechst (blue staining, upper panel), E-cadherin (green staining, second panel), Oct4 (red staining, third panel), and a merged image (bottom panel); FIG. 17H - Hoechst (blue staining, upper panel), SSEA4 (green staining, second panel), OCT4 (red staining, third panel), and a merged image (bottom panel); The immunostaining results show that the naive C1 hiPSC line exhibits positive staining for all known human pluripotency markers tested. Notably, SSEA1, which is specific for mouse and not human pluripotent cells, is not expressed in human naive iPSCs and ESCs (FIG. 17E, middle panel).

FIGs. 18A-F are images depicting immunostaining analyses for pluripotency markers on naive C2 hiPSC (FIGs. 18A-F). FIG. 18A –Hoechst (blue staining, upper panel), KLF4 (red staining, second panel), and a merged image (bottom panel); FIG. 18B - Hoechst (blue staining, upper panel), TRA1-81 (yellow staining, second panel), and a merged image (bottom panel); FIG. 18C – Alkaline phosphatase (AP; upper panel), Hoechst (blue staining, second panel), SSEA1 (third panel), and a merged image (bottom panel); FIG. 18D - Hoechst (blue staining, upper panel), TRA1-60 (yellow staining, second panel), Nanog (red staining, third panel), and a merged image (bottom panel); FIG. 18E - Hoechst (blue staining, upper panel), E-cadherin (green staining, second panel), Oct4 (red staining, third panel), and a merged image (bottom panel); FIG. 18F – Hoechst (blue staining, upper panel), SSEA4 (green staining, second panel), Oct4 (red staining, third panel), and a merged image (bottom panel); The immunostaining results show that the naive C2 hiPSC line exhibits positive staining for all known human pluripotency markers tested. Notably, SSEA1, which is specific for mouse and not human pluripotent cells, is not expressed in human naive iPSCs and ESCs (FIG. 18C, third panel from the top).

FIGs. 19A-I are images demonstrating the *in vitro* differentiation potential of human naive ESCs and iPSCs. Shown are images for day 6 EB structures from the indicated cell lines (defined by name and passage number). Images indicate differentiated embryonic body structures. FIG. 19A – Naive WIBR3 EBs (Passage 21); FIG. 19B – Naive H1 EBs (Passage 51); FIG. 19C – Naive BG01 EBs (Passage 41);

FIG. 19D – Naive C1 EBs (Passage 21); FIG. 19E - Naive C2 EBs (Passage 27); FIG. 19F – Naive WIS1 EBs (passage 13); FIG. 19G – Naive WIS2 EBs (passage 21); FIG. 19H – Naive LIS1 EBs (passage 17); FIG. 19I - Naive LIS2 EBs (passage 11). These results demonstrate that human naive iPSCs and ESCs can differentiate into Embryoid Bodies (EBs) *in vitro*.

FIGs. 19J-O - qRT-PCR analysis for expression of lineage differentiation markers (FIG. 19J – BRACHYURY; FIG. 19K - SOX17; FIG. 19L - PAX6; FIG. 19M – AFP; FIG. 19N – SOX1) and a pluripotency marker (FIG. 19O – OCT4). EBs were generated from the following cell lines: WIBR3 ESC, H1 ESC, BG01 ESC, C1 iPSC, C2 iPSC, WIS1 ESC, WIS2 ESC, LIS1 ESC and LIS2 ESC. All cell lines tested showed marked upregulation of lineage commitment genes and down regulation of OCT4 pluripotency marker, consistent with lineage differentiation. Relative qRT-PCR expression levels were normalized to levels expressed in naive pluripotent cells prior to differentiation.

FIGs. 20A-L are images demonstrating the *in vivo* differentiation potential of human naive ESCs and iPSCs. Human naive iPSCs and ESCs expanded in WIS-NHSM conditions for the indicated number of passages. The cells were harvested and injected in immune-deficient mice subcutaneously, and examined for teratoma formation. FIG. 20A – Naive WIBR3 hESC (Passage 9); FIG. 20B – Naive WIBR3 hESC (passage 22); FIG. 20C – Naive WIBR3 hESC (passage 40); FIG. 20D – Naive H1 hESC (Passage 22); FIG. 20E - Naive BG01 hESC (passage 38); FIG. 20F – Naive H9 hESC (passage 20); FIG. 20G – Naive WIBR1 hESC (passage 21); FIG. 20H - Naive C2 hiPSC (passage 41); FIG. 20I – Naive C1 hiPSC (passage 51); FIG. 20J – Naive BJ1 hiPSC (passage 25); FIG. 20K – Naive LIS1 hESC (Passage 9); FIG. 20L – Naive LIS2 hESC (passage 9). All tested lines gave rise to well differentiated mature teratomas with cells from the three germ lineages: endoderm, mesoderm and ectoderm. "P" indicates passage number in WIS-NHSM conditions at which cells were harvested and injected.

FIGs. 20M-T - Individual subcloned naive lines from WIBR3 (FIGs. 20M-P) and BGO1 (FIGs. 20Q-T) hESC lines (sub clones numbered 1-4) were also found pluripotent with competency to form mature teratomas.

FIGs. 21A-L demonstrate distinct signaling dependence and response for human naive ESCs/iPSCs that resembles murine ESCs/iPSCs. Shown are histograms depicting

colony formation of pluripotent cell lines in various media. Cell populations were equally divided and plated on gelatin/vitronectin coated plates in the indicated growth medium in which these cell lines are normally maintained (mouse naive cells in a medium containing 2i/LIF, naive hESCs/iPSCs in a WIS-NHSM medium, mouse EpiSCs and human primed ESCS/iPSCs in a KSR/bFGF/TGFβ medium). 36 hours later the wells were supplemented with the indicated inhibitors or growth factors. After 14 days (2 passages), wells were analyzed for Oct4-GFP pluripotency marker expression by FACS, to determine the relative percentage of pluripotent colonies. Pluripotent cell frequency was normalized to an internal control, as indicated by "Growth medium" only on the far left column (For naive cells growth medium was WIS-NHSM, and for primed cells was conventional KSR/bFGF/TGFβ containing medium as specified in methods). When components already included in WIS-NHSM were supplemented, this yielded a 2-fold increase in their relative concentration. Normalized percentages lower than 50% are defined as "sensitive" to the presence of the supplemented inhibitor. FIG. 21A – Naive 129 mESC; FIG. 21B – Primed 129 mEpiSC; FIG. 21C – Naive WIBR3 hESC; FIG. 21D – Primed/conventional WIBR3 hESC; FIG. 21E – Naive C1 hiPSC; FIG. 21F – Primed/conventional C1 hiPSC; FIG. 21G – naive C1 hESC; FIG. 21H – primed C1 hESC; FIG. 21I – Naive WIS1 hESC; FIG. 21J – Primed WIS1 hESC; FIG. 21K – LIS1 hESC; FIG. 21L – primed LIS1 hESC. Note that human naive ESCs remain pluripotent in the presence of different ERK, GSK3β and RAF inhibitors. Human naive pluripotent cells do not differentiate in response to BMP4 (up to 5-10 ng/ml BMP4) or forskolin supplementation. Primed human ESCs/iPSCs differentiated upon ERK, GSK3b, RAF inhibition, or stimulation with BMP4 or forskolin. Importantly, naive human ESCs/iPSCs are unique from any previously reported naive pluripotent lines, in that they rely on LIF and bFGF/TGFβ signaling (together with presence of multiple ERK, p38 and JNK inhibitors).

FIGs. 22A-K demonstrate unique signaling requirement and response for naive hESCs/iPSCs. Naive hESCs/iPSCs grown in WIS-NHSM conditions supplemented with 5 ng/ml BMP4 remain pluripotent, and can differentiate into teratomas *in vivo*. Shown are images of morphological staining the teratomas formed by the naive PSCs. FIGs. 22A-C – Naive H1 hESC [Passage 32 with BMP4 (5 ng/ml]; FIGs. 22D-F – Naive C1 hiPSC [Passage 25 with BMP4 (5 ng/ml)]; FIG. 22G – Naive H1

constitutively active Stat 3 (expanded under "naive conditions" WIS-NHSM conditions without LIF). FIG. 22H - Naive WIS1–Stat3-CA (expanded in naive WIS-NHSM conditions without LIF). Note differentiation into endoderm (FIGs. 22A, 22D, 22G (left panel) and 22H (left panel)), mesoderm (FIGs. 22B, 22E, 22G (middle panel), and 22H (middle panel)) and ectoderm (FIGs. 22C, 22F, 22G (right panel) and 22H (right panel)) embryonic germ layers. FIGs. 22I-K are immunofluorescence images depicting expression of pluripotent markers in naive hESCs/iPSCs carrying a constitutively activate Stat3 mutant. FIG. 22I - Hoechst (blue staining, upper panel), Nanog (green staining, second panel), SSEA4 (red staining, third panel), and a merged image (bottom panel); FIG. 22J - Hoechst (blue staining, upper panel), Oct4 (green staining, second panel), and a merged image (bottom panel); FIG. 22K - Hoechst (blue staining, upper panel), SSEA3 (green staining, second panel), and a merged image (bottom panel). The results show that the naive hESCs/iPSCs carrying a constitutively activate Stat3 mutant remain pluripotent in the absence of exogenous LIF from WIS-NHSM media, based on teratoma formation and immunostaining for pluripotency markers. These results show that naive hESCs/iPSCs described herein share defining features with rodent naive PSCs in their dependence on LIF/Stat3 signaling to remain pluripotent in WIS-NHSM conditions, and tolerance for exogenous BMP4 cytokine, at least at low levels of BMP4 up to 5 ng/ml – 10 ng/ml as tested herein.

FIGs. 23A-D demonstrate that female Naive hESCs/iPSCs retain a unique pre-X inactivation state in WIS-NHSM conditions. FIGs. 23A – Shown are bisulfite sequencing analyses of six CpG sites in single clones of an XIST promoter amplicon (lower panels). Note that in naive cells both alleles are demethylated, while in primed cells one of the alleles becomes silenced. Methylation of Oct4 locus CpG are shown as controls (upper panels). FIG. 23B – A histogram depicting quantification of an RT-PCR analysis of the XIST transcript in various naive and somatic cells. Note the low expression levels of XIST in naive hESCs/iPSCs, in comparison to female differentiated fibroblast cells that upregulate XIST expression. FIGs. 23C-D – Immuno-fluorescence analysis showing presence of H3K27me3/polycomb bodies. FIG. 23C – Naive WIBR3 hESC; FIG. 23D – Differentiated cells from naive WIBR3 hESC. Note the trace numbers of cells that were found to have H3K27me3/polycomb bodies in nuclei of naive cells (FIG. 23C) as compared to the significant presence of H3K27me3/polycomb

bodies in the differentiated cells therefrom. Thus, upon differentiation the numbers of H3K27me3/polycomb bodies dramatically increase, indicating that female human naive cells are capable to initiate X chromosome inactivation following differentiation. The results indicate that the X chromosome in female naive iPSCs/hESCs grown in WIS-NHSM conditions is in a pre-activated state resembling that described in human ICM.

FIGs. 24A-C demonstrate that the naive human ESCs/iPSCs exhibit a distinct transcriptional program. FIG. 24A - Hierarchical clustering of differentially expressed genes on different conventional/primed and naive hESC/hiPSC lines as indicated. Note how all naive hESCs/iPSCs clustered independently from all primed samples. Note how naive WIBR3 hESCs, when transferred again (re-primed) into conventional primed growth conditions, cluster with all other primed samples indicating that these states are interconvertable by growth conditions. FIGs. 24B-C - Histograms of surface expression of MHC class I using FACS analysis on the indicated naive and primed cell lines. FIG. 24B – WIBR3 hESC; FIG. 24C – C1 hiPSC. 293HEK cells were used as a control for differentiated cells (that typically express high MHC class I levels). Median Fluorescence Intensity (MFI) values are indicated. This shows that naive cells express no/low levels of MHC class I, while primed cells express medium and higher levels of MHC class I. No stain curves for each cell line are also included to have accurate controls for the MHC class I stained samples.

FIGs. 25A-M demonstrate presence of a unique Oct4 enhancer utilization in naive hESCs/hiPSCs. FIG. 25A – A histogram depicting evaluation of human Oct4 distal enhancer and proximal enhancer reporter gene activity in the indicated pluripotent cell lines. Baseline activity was analyzed by transfecting with an empty vector. Predominant utilization of distal enhancer is clearly evident in hESCs/iPSCs grown in naive WIS-NHSM conditions. FIGs. 25B-M – flow cytometry analyses of WIBR3 hESCs that were stably transfected with either: 1) Oct4-GFP-2A reporter that marks all types of pluripotent cells [naive and primed; (FIGs. 25C, 25E, 25G)]; 2) deltaDE-Oct4-GFP-2A-Puro that is typically more active in primed pluripotent cells [based on data in mice (FIGs. 25I, 25K and 25M)]; 3) DeltaPE-OCT4GFP-2A-Puro that is typically more active in naive pluripotent cells [FIGs. 25H, 25J and 25L) or non-transfected WIBR3 hESCs [FIGs. 25B, 25D and 25F]. FIGs. 25B-C and 25H-I – cells grown under naive WIS-NHSM growth conditions. FIGs. 25D-E and 25J-K– cells grown in a

conventional/primed bFGF/TGFβ medium. FIGs. 25F-G and 25L-M – cells grown in a differentiation medium; cells were subjected to flow cytometry analyses after 21 days in a differentiation medium, when the cells were differentiated into fibroblasts. These analyses show that detaPE-Oct4-GFP reporter is more active in naive WIS-NHSM conditions (FIG. 25H), relative to primed/conventional conditions (FIG. 25J), or to cells differentiated into fibroblasts (FIG. 25L). On the other hand, delatDE-OCT4-GFP reporter is active in primed/conventional conditions (FIG. 25K) rather than in naive conditions (FIG. 25I) or in cells differentiated into fibroblasts (FIG. 25M). These results indicate that the naive hESCs/iPSCs according to some embodiments of the invention retain a unique epigenetic stability and configuration. MFI = Median fluorescence intensity.

FIGs. 26A-K depict cross species mouse-human chimeric embryos. FIGs. 26A-C - shown are images demonstrating that naive human iPSCs can contribute to mouse development *in vivo*. Human naive C2 iPSCs were constitutively labeled with GFP and BCL-2 overexpression vector. Cells were aggregated with developing mouse embryo morulas, and 24 hours GFP cells were viable in developing early mouse embryos. These results indicate that human naive cells grown in WIS-NHSM conditions can contribute to cross-species chimeric organisms. FIGs. 26D-K show how GFP labeled human naive iPSCs can be injected into E2.5 mouse morulas, and remain integrated in blastocysts at E3.5. FIG. 26D – loading of human naive GFP+ (positive) iPSCs; FIG. 26E – injection of the cells shown in FIG. 26D into mouse morula; FIGs. 26F-H show the injected cells into the mouse morula at the day of injection (Inj.) under bright field (FIG. 26F), EGFP (Enhanced Green Fluorescent Protein) (FIG. 26G) and a merged image (FIG. 26H). FIGs. 26I-K show the injected cells into the mouse morula at one day after injection. FIG. 26I – bright field; FIG. 26J - EGFP; FIG. 26K – Merged image.

FIG. 27 depicts the nucleic acid sequence of the XIST amplicon (SEQ ID NO:70) formed using bisulfite sequencing according to some embodiments of the invention, with the CpG islands highlighted in yellow. Note that in the shown amplicon there are six CpG islands.

FIGs. 28A-C depict nuclear/cytoplasm ratio in the expression level of transcripts in naive human ESCs. FIGs. 28A-B - Naive and primed hESCs were double immunostained for TFE3 and OCT4. Cells were counter-stained for DAPI (nuclear

staining). Representative confocal images are shown for primed LIS2 hESC line and naive LIS2 hESC line. Insets are enlargements of the dashed boxes. Predominant nuclear localization was observed in naive hESCs but not in cells grown under primed conditions. FIG. 28C - Quantitative unbiased imaging analysis for preferential nuclear localization was conducted on randomly selected 200 cells from independent image frames per sample. Box and whisker plots of nuclear/cytoplasmic TFE3 ratios in naive and primed mouse and human ESCs are shown. Naive hESCs showed distributions similar to those in naive mESCs, and the nuclear enrichment was lost in primed human and mouse ESCs * t-test P values $< 1 \times 10^{-100}$.

FIGs. 29A-D depict epigenetic configuration of human naive pluripotency. FIGs. 29A-B are immunostaining analyses for OCT4 and DNMT3B [DNA (cytosine-5-)-methyltransferase 3 beta] in human naive (FIG. 29B) and primed (FIG. 29A) cells. Human naive cells down-regulate DNMT3B protein expression, but not OCT4 protein expression. FIGs. 29C-D are histograms of the change in methylation between primed and naive samples in human and mouse. The histograms depict the distribution of the per-CpG difference in methylation, calculated for all CpGs residing in CpG rich regions (>4% CpG content) and having a coverage of ≥10x in both samples. For clarity, only CpGs with a non-zero change in methylation are included in the histogram. The distribution is left-skewed, indicating a general reduction in methylation in the naive samples.

FIGs. 30A-I depict DNA methylation changes in human naive pluripotency. FIGs. 30A-C are Western blot analyses for DNMT3A (FIG. 30A), DNMT3B (FIG. 30B) and HSP90 (FIG. 30C) levels in human primed and naive ESCs/iPSCs. Note the significant downregulation of the expression levels of DNMT3A (FIG. 30A), DNMT3B (FIG. 30B) in the naive human PSCs as compared to primed PSCs. FIG. 30D - Histogram of the change in methylation between primed WIBR3 cells and naive LIS2 cells. The histogram depicts the distribution of the per-CpG difference in methylation, calculated for all CpGs residing in CpG rich regions (>4% CpG content) and having a coverage of ≥10x in both samples. For clarity, only CpGs with a non-zero change in methylation are included in the histogram. The bar-plot on the right counts the number of CpGs in which this difference exceeds two standard-deviations, and the naive sample has lower methylation (blue) or the primed sample has lower methylation (green). The

dotted line indicates the expected number of CpGs with a difference that exceeds two standard deviation assuming a normal distribution. FIG. 30E - The same analysis as in FIG. 30D above was applied to the two samples, this time considering all CpGs having a coverage of ≥10x in both samples, regardless of the region's CpG content. FIG. 30F - Composition of naive WIS-NHSM medium that is devoid of FGF2 and TGFB cytokines, and instead retains PKCi, FGFRi and TGFRi. The medium includes: LIF (20 ng/ml), ERK1/2i (PD0325901 1 μM), GSK3βi (CHIR99021 3 μM), JNKi (SP600125 10 μM), P38i (BIRB796 2 μM), FGFRi (PD173074 0.2 μM), TGFβ1 (8 ng/ml) +/- ROCKi (Y27632 2 μM). FIG. 30G - Human naive iPSCs and ESCs expanded for 8 days under these conditions (with the medium having the composition as described in FIG. 30F above) show dramatic reduction in total methylated cytosine levels (mdC), as determined by LC-MS quantitative analysis and normalized to dG abundance levels. FIG. 30H - Human and mouse naive and primed cells were expanded in the presence or absence of inhibitors for DNA methylation (5d-AZA) or EED polycomb component (DzNEP). Only naive cells retain their pluripotency after passaging in the presence of these inhibitors. Pluripotency measurement was conducted by following Oct4-GFP specific reporter levels. FIG. 30I - Relative methylation of FMR1 promoter region in naive and primed human iPSCs derived from Fragile X male patient fibroblasts. Naive human Fragile X iPSCs show predominant loss of methylation at FMR1 promoter in Fragile X patients. * t-test P value <0.05.

FIGs. 31A-E depict numerical description of direct iPSC reprogramming following Mbd3 depletion. FIG. 31A - Secondary NGFP1-control ($Mbd3^{+/+}$), Nanog over expression ($NGFP1\text{-}Nanog^{OE}$) and Mbd3 depleted ($NGFP1\text{-}Mbd3^{KD}$) Pre-B cells were subjected to DOX reprogramming and measured weekly using FACS (for monoclonal wells), and also with daily polyclonal Nanog-GFP follow-up in the first 8 days of reprogramming. FIGs. 31B-C - Cumulative percentage of Nanog-GFP+ wells versus time on DOX, measured for various clonal B-cell-derived populations. NGFP1-control, $NGFP1\text{-}Nanog^{OE}$ and $NGFP1\text{-}Mbd3^{KD}$ latencies show distinctly different cumulative distributions. One representative experiment is shown out of 2 performed. FIG. 31B – days on DOX; FIG. 31C – Cell divisions on DOX. FIGs. 31D-E - Fitting of NGFP1-control (FIG. 31D) and $NGFP1\text{-}Mbd3^{KD}$ (FIG. 31E) reprogramming latencies (measured in days) to a deterministic step function model, using adjusted R^2 (see details

in methods) statistics for goodness of fit. NGFP1-Mbd3^{KD} is tightly fitted to a deterministic step function model (R^2>0.9) in comparison to NGFP1-control (R^2=0.55).

FIGs. 32A-H depict mechanisms for Mbd3 inhibitory effect on OSKM during reprogramming to pluripotency. FIGs. 32A-B - Constructs encoding Flag-tagged OCT4, c-MYC, KLF4, SOX2, NANOG or HDAC1 (used as a positive control) were transfected into HEK293T cells in combination with Mbd3. The cell lysates were immunoprecipitated (IP) with an anti-Flag antibody (or anti-IgG as control), followed by an immunoblot analysis (IB). The expression levels in whole-cell lysates or IP extract were determined by IB with anti-Flag (FIG. 32B) or anti-Mbd3 (FIG. 32A). This analysis demonstrates direct interaction of Mbd3 with OSKM pluripotency factors, but not with Nanog. Hdac1 was used as appositive control. FIG. 32C - Functional enrichment of Mbd3 direct targets as was measured in somatic MEFs before and after OSKM induction. FIG. 32D - Functional enrichment of Mi2β (Chd4) direct targets as was measured in somatic MEFs before and after OSKM induction. Color levels indicate enrichment *P*-values (calculated using Fisher exact test) that pass FDR threshold of 0.0001%. White indicates enrichments falling below that threshold. FIG. 32E - Distribution of gene expression fold-change relative to MEF of Mbd3$^{+/+}$ samples (blue) and Mbd3$^{flox/-}$ samples (red) throughout reprogramming (0, 4 days, 8 days, 11 days and iPSC/ESC). Box plot centers indicate the median value, and box edges indicate the 25th and 75th percentiles. *P*-values of distribution differences indicated in the graph were estimated with paired sample t-test. This analysis was calculated with all identified binding targets of Mbd3 (1400 genes) from Mbd3$^{+/+}$ cells following OSKM induction. Results show general activation of Mbd3 targets throughout the reprogramming process and specifically accelerated activation of Mbd3 targets in the Mbd3$^{flox/-}$ samples. FIG. 32F - Distribution of histone marks and Oct4 binding levels in z-score values at day 4 after OSKM (DOX) induction. This analysis was done over all identified binding targets of Mbd3 (1400 genes) from Mbd3$^{+/+}$ samples. Box plot centers indicate the median value, and box edges indicate the 25th and 75th percentiles. P-values of distribution differences indicated in the graph were estimated with paired sample t-test. Results show a significant induction of H3K27ac and H3K4me3 while reduction of H3K27me3 in Mbd3$^{flox/-}$ sample, compared to Mbd3$^{+/+}$, as well as induction of Oct4 binding in Mbd3$^{flox/-}$ samples. FIG. 32G - Reprogramming efficiency of Mbd3$^{flox/-}$ MEFs after

infection with lentiviruses encoding wild-type and different mutant Mbd3 inserts as indicated in the panel. Error bars indicate s.d. of biological triplicates. * Indicates significant *P* value <0.001 in comparison to uninfected control sample. FIG. 32H - Scheme depicting mechanistic model for inducing pluripotency in somatic cells.

FIGs. 33A-G - depict Knockdown screen for epigenetic repressors in EpiSCs. FIG. 33A- Knockdown efficiency of the indicated siRNA pools in EpiSCs measured by qRT-PCR. Expression values for each gene were normalized to those measured in control siRNA. Error bars indicated s.d. * indicates student t test *p* Value < 0.05. FIGs. 33B-C - Phase images of $Mbd3^{+/+}$ (FIG. 33B) and $Mbd3^{flox/-}$ (FIG. 33C) EpiSC lines in this study. The cell lines had typical flat morphology when expanded on gelatin/vitronectin or Matrigel coated plates (feeder free conditions). FIGs. 33D-E - Oct4 Immunostaining on EpiSC lines. $Mbd3^{+/+}$EpiSC (FIG. 33D), $Mbd3^{flox/-}$EpiSC (FIG. 33E); FIGs. 33F-G - EpiSC lines were pluripotent as evident by their ability to form mature differentiated teratomas upon microinjection subcutaneously in immune-deficient mice. $Mbd3^{+/+}$EpiSC (FIG. 33F), $Mbd3^{flox/-}$EpiSC (FIG. 33G).

FIGs. 34A-C depict derivation of ESCs from $Mbd3^{-/-}$ blastocysts. FIG. 34A-B – Histograms depicting RT-PCR analyses for Oct4 and trophoblast marker expression of $Mbd3^{+/+}$ (FIG. 34A) and $Mbd3^{-/-}$ (FIG. 34B) ESCs expanded either in FBS/LIF or 2i/LIF conditions. Only $Mbd3^{-/-}$ ESCs and only in serum conditions upregulate trophoblast differentiation markers. Stringent serum free 2i/LIF conditions maintain $Mbd3^{-/-}$ ESCs indistinguishably from $Mbd3^{+/+}$ ESCs. Error bars indicate s.d. of biological triplicate samples. FIG. 34C - Agouti chimera derived following blastocyst microinjection with $Mbd3^{-/-}$ ESC line carrying rescue expression transgene for Mbd3.

FIGs. 35A-C depict transcriptional expression of Mbd3 during pre-implantation development. FIGs. 35A-B - RT-PCR analyses demonstrating the expression of Mbd3 (FIG. 35B) and Nanog (FIGs. 35A) during early mouse development, presented as a relative quantification column scheme. Error bars indicate s.d. of biological triplicates. Mbd3 transcript is detected at low levels in oocytes while Mbd3 protein is readily detected by immunostaining in oocytes and zygotes (FIGs. 36A-D and FIGs. 1O-T), consistent with maternal inheritance. Mbd3 transcription becomes increased towards the end of pre-implantation development at the morula and blastocyst stages, consistent with re-expression of Mbd3 protein in late blastocyst stage (FIGs. 1O-T). FIG. 35C -

Relative transcriptional levels of MBD3 in human pre-implantation embryos based on available repository transcriptional measurements in early human developing embryos [intranet (dot) cmrb (dot) eu/Human_embryos/home.html], and showing a similar trend to that measured in mouse embryos. These data show that Mbd3 transcription is increased at late stages of pre-implantation development, consistent with protein immunostaining data showing prominent expression at late blastocyst stage (FIGs. 1O-T).

FIGs. 36A-J depict immunostaining analysis for Mbd3. FIGs. 36A-D - Immunostaining for Mbd3 in mouse oocytes, indicating maternal inheritance of Mbd3. FIGs. 36E-H - Immunostaining for Mbd3 and lineage markers in E5.5 post-implantation epiblast, indicating prominent expression as seen in late-blastocyst stage (FIGs. 1O-T). FIGs. 36I-J- Immunostaining analysis for Mbd3, showing prominent nuclear expression in pluripotent cells expanded in defined naive and primed growth conditions. These results exclude perturbation for nuclear localization of Mbd3 protein in naive 2i/LIF conditions.

FIGs. 37A-C depict comparative analysis of Mbd3 depleted somatic cell properties during reprogramming. FIG. 37A - Reprogramming efficiency following infection with indicated MEF lines with moloney retroviruses encoding individual factors. FIG. 37B - Reprogramming efficiency following infection with indicated MEF lines with polycistronic OKSM encoding lentivirus. FIG. 37C - $Mbd3^{flox/-}$ MEFs were infected with polycistronic OKSM vector in LIF containing ES medium with or without the indicated exogenous supplements. * Indicates student t-test p value <0.01 relative to $Mbd3^{+/+}$ control. Reprogramming efficiency was evaluated by Oct4-GFP levels on day 9 following transduction without cell splitting during the process.

FIGs. 38A-B show that Mbd3 depletion renders deterministic and radically efficient reprogramming of multiple adult somatic cell types. FIG. 38A - $Mbd3^{+/+}$, $Mbd3^{-/-}$ and $Mbd3^{flox/-}$ MEFs, adult tail tip derived fibroblast (TTF) and neural precursor cells (NPC) were tested for iPSC formation in 2i/LIF with or without OKSM lentiviral transduction. This analysis indicates that OKSM is essential for iPS formation, and that Mbd3 depletion alone is not sufficient to reprogram any of these cells types to pluripotency (even after 30 days of follow up). FIG. 38B - Reprogramming efficiency of MEFs following transduction with the indicated combinations of reprogramming

factors at day 10. Polycistronic lentiviral vectors were used for OSK and OSKM combinations. Error bars indicate s.d. of replicate samples.

FIGs. 39A-D depict teratoma formation by $Mbd3^{-/-}$ iPSCs. FIGs. 39A-C - Randomly selected $Mbd3^{-/-}$ iPSC clones (clones 1, 2, and 3) were expanded and injected subcutaneously in immunodeficient mice. All lines generated teratomas containing differentiated cells from the three germ lineages (mesoderm, endoderm and ectoderm). These results are consistent with results obtained from $Mbd3^{-/-}$ ESCs (Kaji et al. development 2007). The latter cells (without reconstitution of Mbd3 expression) have restricted developmental potential when it comes to formation of high-contribution chimeras, but can for differentiated teratomas (Kaji et al. development 2007). Further, note that $Mbd3^{flox/-}$ somatic cells also reprogram with 100% efficiency, and adult chimeras can be obtained with germ-line transmission without exogenous overexpression of Mbd3. From the technical perspectives, Mbd3 small molecule inhibitors will hopefully be discovered in the future, as they will allow easier regulation of Mbd3 expression and activity without genetic manipulations during reprogramming and differentiation. FIG. 39D - $Mbd3^{-/-}$ iPSCs can retain normal karyotype (40) after expansion in 2i/LIF defined conditions. P indicates passage number.

FIGs. 40A-E depict time-lapse live microscopic imaging and tracking of cell reprogramming. Schematic representation of the main steps of automated segmentation protocol. This protocol was used to automatically analyze time-lapse full well mosaic data, measured for two fluorescent wavelengths. The main protocol steps include: filtering plate margins, applying adaptive detection for each channel and time point, isolating dense colonies using specific morphological filter, clustering using low-pass-filter (LPF) and connected components clustering, extracting colony information and Oct4-GFP activation information per colony and conducting statistical analysis over all time-points information (see methods).

FIGs. 41A-D depict time evolution of mCherry and Oct4-GFP reactivation in full well mosaic (FIG. 41A) and 3 representative single $Mbd3^{flox/-}$ colonies (FIGs. 41B-D) out of approximately 100 colonies tracked.

FIGs. 42A-E - Time-lapse live imaging of deterministic iPSC reprogramming. FIGs. 42A-C - Full well mosaic images of mCherry (FIG. 42A), Oct4-GFP (FIG. 42B) and combined channels (FIG. 42C) at day 6 following DOX in 2i/LIF 5% pO_2

conditions. ES-like mCherry+ colonies are abundant and co-localize with Oct4-GFP signal in Mbd3$^{flox/-}$ cells. FIG. 42D - Cumulative distribution of Oct4-GFP+ colonies (red graph) and density function of Oct4-GFP+ activation (blue bar plot) for Mbd3$^{flox/-}$, statistics were analyzed from all detected colonies (approximately 100 segmented colonies per well). Results show a very narrow window of synchronized Oct4-GFP activation around day 4.5, more than 50% of the colonies reactivated Oct4-GFP at 0.5 day interval. One representative experiment is shown out of 4 performed. FIG. 42E - Box-plot graph showing the distribution of intra-colony progeny Oct4-GFP activation (which is the ratios of Oct4-GFP+ & mCherry+ pixels out of all mCherry+ pixels within each segmented colony), as a function of time after induction, Box plot centers indicate the median values, and box edges indicate the 25th and 75th percentiles. Statistics were calculated from 100 segmented colonies (all detected colonies). At day 6, 95% of Mbd3$^{flox/-}$ colonies have more than 85% Oct4-GFP positive progeny cells.

FIGs. 43A-B depict radically enhanced Oct4-GFP reactivation and iPSC formation. Flow cytometry measurements of Oct4-GFP reactivation dynamics in 2i/LIF following DOX (OSKM) induction in Mbd3$^{flox/-}$ (FIG. 43B) or Mbd3$^{+/+}$ (FIG. 43A) cells. Mbd3$^{flox/-}$ secondary cells synchronously and rapidly reactivate Oct4-GFP by day 7 in the entire donor cell population. Importantly, wells at the indicated time points were harvested for analysis without prior passaging and splitting during the reprogramming course. 1 out of 3 independent experiments is shown. (FSC – forward scatter). Note the dramatic reactivation of Oct4-GFP occurring in the narrow time window at days 4-5, as also seen in microscopic time-lapse live imaging measurements.

FIGs. 44A-B depict characterization of the effect for Mbd3 expression reconstitution during deterministic reprogramming of somatic cells to pluripotency. FIG. 44A - Scheme demonstrates experimental strategy for defining the temporal ability of Mbd3 during reprogramming to inhibit iPS formation. FIG. 44B - Secondary OSKM reprogrammable Mbd3$^{flox/-}$ MEFs were tested for their amenability to reprogramming following over-expression of Mbd3, Mbd2 or empty FUW lentiviruses at different time points during reprogramming. Mbd2 or mock-vector transfection, did not result in a decrease in iPSC reprogramming efficiency. Introducing Mbd3 drastically reduced iPSC formation when delivered before day 5 in reprogramming. 1 out of 2 representative experiments is shown. Average of duplicates is shown per condition.

Error bars indicate s.d.

FIGs. 45A-B depict gene expression analysis during iPSC reprogramming following Mbd3 depletion. FIG. 45A- Gene expression was measured in donor fibroblasts before and after DOX induction and compared to established pluripotent iPSCs and ESC lines. Clustering of full gene signature (16,620 genes) by hierarchical clustering using Spearman correlation as a distance metric and average linkage. Results show that $Mbd3^{flox/-}$, but not $Mbd3^{+/+}$, MEFs clustered differently from donor somatic MEFs only after 4 days of OKSM (DOX) induction. By day 8, $Mbd3^{flox/-}$ cells were transcriptionally indistinguishable from established ESCs and iPSCs line. $Mbd3^{+/+}$ population cluster with $Mbd3^{flox/-}$ 4 day cells even after 11 days of longer reprogramming, and did not cluster with pluripotent ESCs-iPSC lines. FIG. 45B - Clustering of the full gene expression signature (16,620 genes) by principle component analysis (PCA) that detects the principle components with the largest variation in the data. Plotted principle components explain more than 80% of data variation. Samples in each colored ellipse show similar dynamics, where $Mbd3^{flox/-}$ 8 day cells are transcriptionally indistinguishable from established ESC and iPSC lines. (KO= $Mbd3^{-/-}$, HET=$Mbd3^{flox/-}$, WT=$Mbd3^{+/+}$).

FIGs. 46A-E depict gene expression pattern changes during iPSC reprogramming. Single gene expression progression describes the extent to which each gene reaches its expression value in iPSC. These values were quantified using the following transformation

$$\hat{X}_j(t) = \max\left(\frac{X_j(t) - X_j(MEF_Mbd3^{+/+})}{\overline{X}_j(IPS) - \overline{X}_j(MEF)}, 0\right)$$

This transformation represents a distance from MEF expression values (set to 0) towards iPS values (set to 1). Selected group of pluripotency related genes or selected targets of Mbd3, are plotted in different time points after DOX induction. Red bars represent progression of gene expression in $Mbd3^{flox/-}$ and blue bars represent progression of gene expression in $Mbd3^{+/+}$. FIG. 46A - Absence of initial transcription of bona fide pluripotency genes can be seen in MEF samples (both $Mbd3^{flox/-}$ and $Mbd3^{+/+}$). FIG. 46B - Fast induction of multiple pluripotency related genes including Sall4, Lin28a, Utf1 and Nanog can be seen 4 days after OSKM induction in $Mbd3^{flox/-}$, but not $Mbd3^{+/+}$. FIG. 46C - These genes reach their levels observed in iPS/ES cells

(around 1) by day 8, in $Mbd3^{flox/-}$ but in most cases not in $Mbd3^{+/+}$. FIGs. 46D-E - Single cell qRT-PCR analysis for detection of pluripotency gene markers. Analysis was conducted on $Mbd3^{+/+}$ (FIG. 46D) and $Mbd3^{flox/-}$ (FIG. 46E) MEFs before (day 0) and 6 days after DOX induction. Genes that were expressed above detection level are marked in green (and undetected are marked in red). Only in $Mbd3^{flox/-}$ samples and only after DOX, 12/12 analyzed cells showed reactivation of all pluripotency markers tested. It is noted that endogenous Sox2 reactivation by RT-PCR is robust in 2i/LIF+DOX in WT cells, indicating that it does not stringently reflect authentic pluripotency reactivation.

FIGs. 47A-B depict clustering of all histone marks values, as measured over differentially expressed genes. Chromatin IP-Seq (IP= Immunoprecipitation) was performed in donor fibroblasts before and after DOX induction and compared to chromatin ChIP-Seq from established pluripotent iPSCs and ESC lines. Gene profiles of H3K4me3, H3K27me3 and H3K27ac were extracted and normalized to z-score. For the current analysis the value of each gene and each histone mark was chosen as the max value of the appropriate z-score profile. Clustering was carried out on concatenate vectors including all histone marks (H3K4me3, H3K27me3 and H3K27ac) for each gene. FIG. 47A - Hierarchical clustering of H3K4me3, H3K27me3 and H3K27ac focusing on the top 1323 genes whose gene expression differentiated between wild type MEF and ESC samples (see methods). Hierarchical clustering was calculated using Spearman correlation as a distance metric and average linkage. Results show that by day 8 $Mbd3^{flox/-}$, but not $Mbd3^{+/+}$, were epigenetically similar to established ESCs and iPSCs line. FIG. 47B - Spearman correlation between the vectors described above (1323 genes with all histone marks.). Here too, $Mbd3^{flox/-}$, but not $Mbd3^{+/+}$, MEFs clustered differently from donor somatic MEFs only after 4 days of OKSM (DOX) induction. By day 8, $Mbd3^{flox/-}$ cells show epigenetic signature that strongly correlates with established ESCs and iPSCs line. $Mbd3^{+/+}$ population does not show strong correlation with pluripotent ESCs-iPSC lines even after 8 days of reprogramming.

FIGs. 48A-C depict clustering of each histone mark separately. Hierarchical clustering of H3K27me3 (FIG. 48A), H3K27ac (FIG. 48B) and H3K4me3 (FIG. 48C) z-score values focusing on the top 1323 genes whose gene expression differentiated between wild type MEF and ES samples (see methods). Hierarchical clustering was calculated using Spearman correlation as a distance metric and average linkage. Results

show that even when considering each histone mark separately, by day 8 $Mbd3^{flox/-}$, but not $Mbd3^{+/+}$, were epigenetically similar to established ESC and iPSC lines.

FIGs. 49A-B depict changes in DNA methylation level during deterministic reprogramming. FIG. 49A - Average level of DNA methylation drops after 8 days of OSKM (DOX) induction in $Mbd3^{flox/-}$ cells, but not in $Mbd3^{+/+}$ ones. Genome-wide methylation levels were assayed using reduced representation bisulfite sequencing (RRBS, see methods). Methylation level was calculated separately for each CpG dinucleotide and then averaged across all CpGs that were covered by 5 or more distinct sequencing reads (34,522 CpG sites in total). The average methylation level of low-passage $Mbd3^{+/+}$ iPSCs (calculated across the same set of CpGs) is provided as a dashed line for reference. FIG. 49B - The same analysis of average methylation was repeated as in (a). However only the 18,749 CpGs (out of 34,522) that reside in CpG rich areas (i.e. CpG abundance > 4%) were used.

FIGs. 50A-C depict deterministic and synchronized iPSC reprogramming following Mbd3 depletion in 2i/LIF conditions. FIG. 50A - Representative examples of partially reprogrammed (Pre-iPSC lines) generated from secondary $Mbd3^{+/+}$ MEFs and expanded in 2i/LIF + DOX conditions. Note the lack of Oct4-GFP expression in mCherry+ pre-iPSC lines. Subcloned Oct4-GFP+/mCherry+ iPSC line is shown as a positive control (bottom panel row). FIG. 50B - Previously described (Mikkelsen, T. S. *et al. Nature* 454, 49–55, 2008) partially reprogrammed (intermediate pre-iPS) cell lines BIV1, MCV6 and MCV8 were subjected to 2 rounds of transfection with either control (scrambled) or Mbd3 siRNA and expanded in 2i/LIF conditions. Mbd3 depletion resulted in dramatic conversion of the majority of cells into pluripotent iPSCs. Error bars indicate s.d. of biological replicates. FIG. 50C - Adult chimera generated from rescued BIV1 iPSCs as evident by agouti coat color contribution.

FIG. 51 depicts enhancing cell fusion based reprogramming by Mbd3 depletion in 2i/LIF conditions. Inhibiting Mbd3 expression promotes robust reprogramming to pluripotency via cell fusion reprogramming assay between somatic MEFs and ESCs. $Mbd3^{+/+}$ and $Mbd3^{-/-}$ ESCs (that do not carry Oct4-GFP reporter) were made transgenic with a construct encoding constitutive CAAGS promoter driven Hygromycin resistance cassette. Their ability to reprogram wild type of Mbd3 depleted ($Mbd3^{flox/-}$) MEFs (carrying Oc4-GFP reporter and constitutive Puromycin resistance cassette) via PEG

mediated cell fusion was evaluated. PEG cells fusion was conducted and cells were incubated in Puromycin + Hygromycin to select for double resistant colonies. Reactivation of Oct4-GFP transgenes in reprogrammed MEFs in 2i/LIF condition was used to quantify cell fusion reprogramming efficiency. The results clearly indicate that depleting Mbd3 and donor and recipient cells results in radical acceleration of reprogramming somatic cells to Nanog+ pluripotency in 2i/Lif. For each of the panels, one out of 2 independently performed experiments is shown. * indicates student t-test *P* value <0.01. Error bars indicate s.d.

FIGs. 52A-C demonstrate TALE nuclease based targeting of MBD3 locus in human pluripotent cells. FIG. 52A - Schematic overview depicting the targeting strategy for generating of conditional knockout allele of MBD3 that allows excision of Exon 2 following Cre recombinase transfection. Southern blot probes are shown as black lines, exons as blue boxes. Digestion sites for *Nhe1* and *HindIII* are indicated. FIGs. 52B-C - Southern blot analyses following targeting of human WIBR3 hESC lines with the 5' probe (FIG. 52B) and with the 3' probe (FIG. 52C). Targeting efficiency was high and allowed isolation of clones where both alleles were correctly modified following a single round of targeting. Southern blot analysis indicates correct 5' and 3' targeting of both Mbd3 alleles in WIBR3 hESC clones #33 and #37. Clone #37 showing hypomorphic expression of MBD3 protein (FIGs. 8M-N) was selected for further experimental follow up and analysis.

FIGs. 53A-E demonstrate that depleting Mbd3 expression facilitates human iPSC formation from *in vitro* differentiated fibroblasts. FIG. 53A - $MBD3^{+/+}$ and $MBD3^{flox/-}$ iPSCs carrying DOX inducible OKSM transgene were labeled with constitutively expressed mCherry and targeted with an OCT4-GFP knock-in allele [54] (Hockemeyer, D. *et al. Nat Biotechnol* 29, 731–734, 2011). I*n vitro* differentiated fibroblasts from the latter lines were reprogrammed as indicated in the scheme. >95% of human $Mbd3^{flox/-}$ fibroblasts became NANOG/TRA1-60+ IPSCs after 8 days of transgene induction. Error bars indicate s.d. of biological replicates. * Indicates significant *P* value <0.001 in comparison to $MBD3^{+/+}$ samples. FIG. 53B - Normal karyotype of $Mbd3^{flox/-}$ iPSC clone maintained in WIS-NHSM growth conditions. FIG. 53C-E - Pluripotency of randomly selected iPSC clones (1, 2, and 3) as evident by

teratoma formation and generation of differentiated cells form three germ lineages (mesoderm, endoderm and ectoderm).

FIGs. 54A-G demonstrate that siRNA inhibition of MBD3 promotes human iPSC reprogramming by OSKM. FIGs. 54A-B - MBD3 siRNA treatment of human primary fibroblasts allows generation of iPSCs by only two rounds of reprogramming with mRNA transfection with OSKM and LIN28 factors, (STEMGENT) and alleviates the need for many rounds of repeated mRNA transfections with pluripotency factors. Note the number of nanog+/SSEA4+ colonies at day 8 in cells treated with MBD3 siRNA, but not in cells treated with the control siRNA (FIG. 54B). FIG. 54C - Representative human iPSC clones (1 and 2) are shown at different time points and passages (P indicates passage number; day 7 and passage 11). FIGs. 54D-F - Pluripotency of randomly selected clones (1 and 2) is shown by specific staining for OCT4 and SSEA4 pluripotency markers (FIG. 54D) and teratoma formation (FIGs. 54E and 54F). FIG. 54G – Human naive cells were injected subcutaneously into SCID immune-deficient mice and formed after 4-8 weeks well differentiated teratoma tumors with differentiation into the three lineages [(endoderm (left), ectoderm (middle) and mesoderm (right)]. This indicates the cells are functionally pluripotent. These results indicate that inhibition of MBD3 expression and/or function promotes iPSC formation by transient mRNA or other transient transfection protocols for iPSC reprogramming.

FIGs. 55A-D depict reprogramming kinetics following Mbd3 depletion. FIG. 55A - Cumulative percentage of GFP+ wells versus time (in days), measured by FACS. Two replicates of NGFP1-control and NGFP1-Mbd3^{KD} measured daily over 10 days. Results show fast Nanog-GFP activation of >95% of NGFP1-Mbd3^{KD} cells between day 4 and 6. FIG. 55B - NGFP1-Mbd3^{KD} pre-B cells reprogramming measured by FACS and Mbd3$^{flox/-}$ MEFs reprogramming measured by microscopy live imaging show similar kinetics. Graph values indicate the mean and error bars indicate standard deviation calculated over 4 MEF replicates and 2 B-cell replicates. FIGs. 55C-D - NGFP1-control (FIG. 55C) and NGFP1-Mbd3^{KD} (FIG. 55D) reprogramming latencies (measured in days), fitted to multiple tandem rate limiting step models. FIG. 55C (middle) – Fitting plot of NGFP1-Mbd3$^{+/+}$ to multi-phase process with two exponential transitions and single intermediate state. FIG. 55D (middle) - Fitting plot of NGFP1-Mbd3^{KD} to single exponential transition with no intermediate states. Fitting was done

using both nonlinear regression with adjusted R^2 statistic and weighted nonlinear fit by chi^2 minimization (see details in methods). Note that NGFP1-$Mbd3^{+/+}$ fits poorly to a single transition process and best fits to a process with 1-2 intermediates phases (FIGs. 56A-F, 57A-D). NGFP1-$Mbd3^{KD}$ on the other hand, fits optimally to single exponential transition with no intermediate states (adj R^2=0.992). The reprogramming rate as calculated from the transition rate of the model fit is indicated at the bottom of the panels. Note that the rates are scaled differently due to differences in measurements of polyclonal and monoclonal assays (see methods).

FIGs. 56A-F depict statistical analysis using Gaussian distribution. NGFP1-control and NGFP1-$Mbd3^{KD}$ reprogramming latencies were fit to Gaussian distribution. FIGs. 56A-B - Goodness of fit plots for fitting of NGFP1-$Mbd3^{+/+}$ (FIG. 56A) and NGFP1-$Mbd3^{KD}$ (FIG. 56B) to Gaussian distribution. FIG. 56C-D – Graphs showing 12-fold reduction in average reprogramming time (FIG. 56C), and 80-fold reduction in $Mbd3^{KD}$ standard deviation (FIG. 56D). FIGs. 56E-F – Graphs showing synchronized transformation from somatic state to iPS after 6 cell cycles (FIG. 56E) with variability (standard deviation) less than half cell cycle (FIG. 56F). Error bars represent 95% confidence intervals for the parameters, as estimated by maximum likelihood.

FIGs. 57A-E depict quantification of iPSC reprogramming after integrating cell cycle variability. The variability observed in the reprogramming latency measurements was quantified and further compared to the inherent cell cycle variability. FIG. 57A - The coefficient of variation (CV=std/mean) of each sample ($Mbd3^{KD}$ and $Mbd3^{+/+}$, dark red and blue colors) was compared with the coefficient of variation of the cell cycle measured for that sample (light red and blue colors). The graph shows that while the coefficient of variation in the $Mbd3^{+/+}$ sample is 0.5, the $Mbd3^{KD}$ coefficient of variation is reduced to 0.09, tightly proximal to the cell cycle estimated coefficient of variation (0.08). Error bars represent 95% confidence intervals for the coefficient of variation, as estimated by maximum likelihood and calculated by propagation of error (see methods). FIG. 57B - Using a *Brownian motion* (BM) model, the present inventors have estimated the dynamic variability for each sample (see methods). This variability is the ratio of the *Brownian motion* standard deviation (σ) divided by the *Brownian motion* drift parameter (ν), where $\sigma/\nu > 1$ corresponds with a high variability dynamics. The present inventors show that while the dynamic variability in the $Mbd3^{+/+}$ sample is $\sigma/\nu > 5$, the

$Mbd3^{KD}$ and cell cycle measurements show both a dynamic variation of $\sigma/\nu \approx 0.5$. Error bars represent 95% confidence intervals for the coefficient of variation, as estimated by maximum likelihood and calculated by propagation of error (see methods). FIG. 57C - Illustration of the *first passage time* model. In this *Brownian motion* (BM) model, the present inventors assume that reprogramming time depends on the first time in which some master regulator (i.e. Nanog or Oct4) transient from their low inactive state to high expression state by passing a fixed expression threshold. FIGs. 57D-E – The present inventors have then fitted the cell cycle time distribution (see methods) to the observed reprogramming latency. By this method the present inventors show a perfect fit (R^2=0.999) between the $Mbd3^{KD}$ dynamic and cell cycle model (FIG. 57E), but not in the control $Mbd3^{+/+}$ dynamics (R^2=0.73) (FIG. 57D).

FIGs. 58A-D depict modeling of a multiple rate-limiting process in the context of iPSC reprogramming. NGFP1-$Mbd3^{+/+}$ and NGFP1-$Mbd3^{KD}$ reprogramming latencies were fit to multiple tandem rate limiting step models. Each experimental dataset was tested against models with 1 to 5 exponential transitions. Fitting was done with nonlinear regression and adjusted R^2 statistic (see methods). FIG. 58A - Fitting of NGFP1-$Mbd3^{+/+}$ to single exponential transition with no intermediate states. Note that NGFP1-$Mbd3^{+/+}$ fit poorly (adj R^2=0.94) to a single transition process. FIG. 58B - Fitting of NGFP1-$Mbd3^{+/+}$ to multi-phase process with two exponential transitions and single intermediate state. Note that NGFP1-$Mbd3^{+/+}$ fit reasonably (adj R^2=0.996) to two exponential transitions process. FIG. 58C - Fitting of NGFP1-$Mbd3^{+/+}$ to multi-phase process with three exponential transitions and two intermediate states. Note that NGFP1-$Mbd3^{+/+}$ fit optimally (adj R^2=0.998) to three exponential transitions process. FIG. 58D - adjusted R^2 values obtained with the different models for NGFP1-$Mbd3^{+/+}$ (blue) and NGFP1-$Mbd3^{KD}$ (red), indicating that the best fit model for NGFP1-$Mbd3^{KD}$ is a single exponential transition with no intermediate states, and the best fit model for NGFP1-$Mbd3^{+/+}$ is a multi-phase process with three exponential transitions and two intermediate states.

FIGs. 59A-G depict modeling of a multiple rate-limiting process in the context of iPSC reprogramming. The fitting results were validated using a second fitting procedure based on weighted nonlinear fit by chi^2 minimization (see methods). For each model the graphical goodness of fit is given in the left panels (FIGs. 59A, C, E), and the

observational errors (residuals) are given in the right panels (FIGs. 59B, D, F). FIGs. 59A-B – Fitting of NGFP1-Mbd3$^{+/+}$ to single exponential transition with no intermediate states. FIGs. 59C-D - Fitting of NGFP1-Mbd3$^{+/+}$ to multi-phase process with two exponential transitions and single intermediate state. FIGs. 59E-F – Fitting of NGFP1-Mbd3$^{+/+}$ to multi-phase process with three exponential transitions and two intermediate states. FIG. 59G – Chi^2 values obtained with the different models for NGFP1-Mbd3$^{+/+}$ (blue) and NGFP1-Mbd3^{KD} (red), indicating that the best fit model for NGFP1-Mbd3^{KD} is a single exponential transition with no intermediate states, and the best fit model for NGFP1-Mbd3$^{+/+}$ is multi-phase process with three exponential transitions and two intermediate states.

FIGs. 60A-C depict direct interaction of Mbd3/NuRD with OSKM pluripotency factors during reprogramming. FIG. 60A - Over-expression of Flag-tagged Mbd3 simultaneously with Oct4, Sox2, Klf4, c-Myc or Nanog in HEK293 cells was followed by Co-immunoprecipitation (co-IP) assay. Immunoblot analysis (IB) using antibodies against Oct4, Sox2, Klf4, c-Myc and Nanog showed specific binding between Mbd3 and the pluripotent factors except Nanog. FIG. 60B - A knock in targeting strategy in murine V6.5 ESCs with a targeting construct generating endogenously labeled Flag-tagged Oct4 allele. This line shows specific co-IP for Mbd3 with Oct4 in 2i/LIF conditions. Co-IP with Nanog is shown as a positive control. FIG. 60C - Co-IP assay of Chd4 (Mi2b), the core subunit of the NuRD complex, in secondary Mbd3$^{+/+}$ fibroblasts 3 days after Dox induction and applying 2i/LIF conditions. Co-IP for NuRD component, Chd4, followed by IB analysis indicated specific pull-down of other Mbd3/NuRD components (Mbd3 and Mta2) and OSKM reprogramming factors.

FIGs. 61A-C demonstrate that Mbd3 binds pluripotent proteins in ESC but not Mbd2. FIG. 61A – The present inventors established an ESC line carrying recovery of Flag-tagged Mbd3 transgene inserted in Mbd3$^{-/-}$ ESC line. Co- immunoprecipitation using flag beads followed by western blot shows that Mbd3 strongly binds the Mi2b and Mta2 members of the NuRD complex, but not Mbd2. Moreover, Mbd3 interacts with Sall4 pluripotency reprogramming factor in ESCs. FIGs. 61B-C - A control ESC line shows that Mta2, a member of the NuRD complex, binds either Mbd3 or Mbd2 (FIG. 61B). But, pull down of Mbd2 does not show any interaction with Mbd3 (FIG. 61C). These assays recapitulate observation in many other cell lines where Mbd2 and Mbd3

form mutually exclusive complexes (Le Guezennec, X. et al. Mol. Cell. Biol. 26, 843–851, 2006; Aguilera, C. et al. Nature 469, 231–235, 2011).

FIGs. 62A-C demonstrate that MBD domain of Mbd3 is critical for direct interaction with OSKM reprogramming factors. Deletion mutations in the MBD site of Mbd3 was designed in order to find the binding region of Mbd3. Flag-tagged mutation constructs were co-transfected with Oct4, Sox2, Klf4 and c-Myc in HEK 293T cells for 48 hours followed by Co-immunoprecipitation with anti-flag beads and immunoblot against Oct4, Klf4, Sox2 and c-Myc. This analysis showed loss of binding and interaction between Mbd3 and OSKM when deletion covering 25-49 amino acid region of Mbd3 were used (as schematically shown in FIG. 62C).

FIG. 63 depicts motif enrichment analysis for Mbd3 binding following reprogramming. Top motifs abundant among Mbd3 binding regions following OSKM induction. Shown are the sequence logos of selected motifs, along with associated factors, the *Z* score and the *P* values. The motifs were inferred using SeqPos software in Cistrome package (see methods).

FIGs. 64A-H depict the effect of Mbd3 depletion on targets common to OSKM and Mi2b. FIGs. 64A-D - Profiles of Mi2b (Chd4) binding read densities at day 4 for $Mbd3^{+/+}$ (blue) and $Mbd3^{flox/-}$ (red) samples. The profiles describe read density normalized to z-score between 1Kb upstream and downstream to TSS. Each plot includes genes that have been characterized previously (Sridharan, R., et al., Cell 36: 364-77, 2009) to be binding targets of one of the OSKM factors (Oct4, Sox2, Klf4 and c-Myc), the z-score profile is averaged over all genes included in the factor binding target set. FIGs. show a reduction in Mi2b binding to OSKM targets upon Mbd3 depletion. FIGs. 64E-F - Western blot indicating protein depletion efficiency upon siRNA transfection of either Mbd3 or Chd4 targeting siRNA pools. FIGs. 64G-H - Reprogramming efficiency of $Mbd3^{+/+}$ secondary MEFS, following knockdown of Mbd3 or Chd4 (as depicted in scheme). Error bars indicate s.d. * Indicates student t-test p value < 0.01.

FIGs. 65A-E depict the effect of Mbd3 depletion on OSKM target genes. FIGs. 65A-B - Box plot centers indicate the median value, and box edges indicate the 25^{th} and 75^{th} percentiles. P-values of distribution differences indicated in the graph (in each panel) were estimated with paired sample t-test. FIG. 65A - Distribution of gene

expression fold-change relative to MEF of $Mbd3^{+/+}$ samples (blue) and $Mbd3^{flox/-}$ samples (red) throughout reprogramming (0, 4 days, 8 days and iPS/ES) as described in FIG. 32F, but here calculated over 2928 genes that were previously found to be bound by at least one of the following factors in OSKM induced MEFs or ESCs: Oct4, Sox2, Klf4, c-Myc and Nanog (Sridharan, R., et al. Cell, 36:364-77, 2009) and are upregulated during reprogramming of wild type cells. FIG. 65B - Distribution of histone marks and Oct4 binding levels in z-score values at day 4 after OSKM (DOX) induction, calculated from the same set of 2928 genes described above. Results show enhanced transcription activation of OSKM targets in the $Mbd3^{flox/-}$ samples, and a significant induction of H3K27ac and H3K4me3 while reduction of H3K27me3 in $Mbd3^{flox/-}$ sample, compared to $Mbd3^{+/+}$, as well as mild induction of Oct4 binding in $Mbd3^{flox/-}$ samples. FIGs. 65C-E - Profiles of H3K27me3 (FIG. 65C), H3K27ac (FIG. 65D) and H3K4me3 (FIG. 65E) read densities at day 4, are plotted for four representative OSKM target genes (Sall4, Klf5, Prdm14 and Tbx3). The profiles describe read density normalized to z-score between 1 Kb upstream to TSS and TES. $Mbd3^{flox/-}$ profiles of H3K27ac and H3K4me3 (red area) are significantly increased (>3 Std), and H3K27me3 significantly reduced, in comparison to $Mbd3^{+/+}$ sample (blue area).

FIGs. 66A-F depict the effect of Mbd3 depletion on OSKM and Mbd3. Box plot centers indicate the median value, and box edges indicate the 25^{th} and 75^{th} percentiles. P-values of distribution differences indicated in the graph were estimated with paired sample t-test. FIG. 66A - Same as in FIG. 65A, but calculated over genes that are bound by both OSKM and Mbd3 targets (n=320 genes) FIG. 66B - Same as in 65B but calculated over genes that are bound by Mbd3 and are upregulated during reprogramming (differentially expressed gene signature described in methods). Results here show similar trends to what was described in FIGs. 65A-B. FIGs. 66C-F - Distribution of histone marks and Oct4 binding levels in z-score values in Mbd3 depleted ($Mbd3^{flox/-}$) or wild type ($Mbd3^{+/+}$) cells. The results presented in FIGs. 66C-F demonstrate that in the Mbd3 depleted samples, during reprogramming Mbd3 targets and/or OSKM targets acquire more open chromatin and get easily and fully reactivated.

FIGs. 67A-D demonstrate that pluripotency promoting epigenetic activators are essential for both deterministic and stochastic iPSC formation. FIG. 67A - Requirement for DOX mediated transgene induction during iPSC reprogramming form $Mbd3^{+/+}$ and

Mbd3 $^{flox/-}$ secondary MEFS. Percentage of Oct4-GFP colonies was quantified at final set time point on day 9. Similar time frame for minimal DOX induction was required for iPSC formation in both cell samples. FIGs. 67B-D - Specific knockdown of Utx [lysine (K)-specific demethylase 6A; KDM6A,Gene ID: 7403] and Wdr5 [WD repeat domain 5; Gene ID: 11091] epigenetic regulators that are required for iPSC formation (Mansour et al. 2012, Nature *488*, 409–413; Ang Y.-S. et al 2011, Cell 145, 183–197) significantly inhibited iPSC formation in both Mbd3$^{+/+}$ and Mbd3$^{flox/-}$ cells. * indicates *p* value <0.01 in comparison to control siRNA sample. One out of 2 independent experiments is shown. s.d. was based on measurements in duplicate identical samples.

FIGs. 68A-K demonstrate that naive human stem cells share defining epigenetic features with mouse ESCs. FIG. 68A-B - As representative examples, characterization for WIS1 (FIG. 68A) and WIS2 (FIG. 68B) naive hESCs is shown. The cells were taken at the indicated passage number (Passage 31 for WIS1, and Passage 27 for WIS2) and express all human pluripotent markers tested (*i.e.*, NANOG, TRA-1-60, OCT4, TRA-1-81, SSEA3, SOX2 and SSEA4), and do not express SSEA1. All naive lines described herein show no signs of deterioration, crisis or decay with expansion (for over 30-70 passages thus far tested). FIGs. 68C-H - The pluripotent capacity of the naive human cells WIS1 at passage 33 (FIGs. 68C, E and G) and WIS2 at passage 19 (FIGs. 68D, F, H) was evaluated by the ability to form teratomas with cells of all three embryonic germ layers. Representative hematoxylin and eosin staining of teratoma sections are shown. FIGs. 68C-D – differentiation into endoderm; FIGs. 68E-F – differentiation into mesoderm; FIGs. 68G-H – differentiation into ectoderm. FIGs. 68I-K - Representative confocal images obtained after double immunostaining for OCT4 and H3K27me3 on naive (FIG. 68I), primed (FIG. 68J) and differentiated samples (Embryoid bodies, obtained from naive cells; FIG. 68K). Naive female pluripotent cells nearly lack the formation of H3K27m3 foci that mark the inactive X allele (FIG. 68I, less than 2% of the cells exhibit the H3K27m3 foci). Primed cells, while they retain OCT4 pluripotency marker expression, H3K27me3 foci (one per nucleus) became clearly detectable in the majority of cells (FIG. 68J, left panel, arrowhead). Upon differentiation into somatic cells, the naive pluripotent cells lose OCT4 expression and acquire H3K27m3 nuclear foci (FIG. 68K). Average percentages of positive counted nuclei from 150-200 cells per sample are indicated.

FIGs. 69A-I depict global transcriptional profile of human naive pluripotency. FIG. 69A - Go categories significantly enriched for genes up-regulated in primed compared to naive human cell lines, with their (–log10) FDR-corrected *P*-value. The respective mouse fold-enrichment values for the categories that are also significant in mouse are indicated. FIG. 69B - Cross-species hierarchical clustering of naive and primed pluripotent cells from mice and humans. Gene expression in naive mESCs and naive hESCs/hiPSCs formed a distinct group apart from mEpiSCs and primed/conventional hESCs and hiPSCs. Mouse cells include "129" and "NOD"; all the rest are human cells. Correlation matrix of gene expression was clustered using Spearman correlation and average linkage. Color bar indicates correlation strength. FIGs. 69C-D - Gene expression across different naive samples is less noisy and more homogenous than across different primed samples. A box plot showing the median and quartiles of the distributions of the coefficients of variance (σ/μ) calculated for each of the homologous genes. The naive distributions are significantly smaller (single-tail t-test, p=0) than the primed ones. FIG. 69C – human naive versus human primed pluripotent stem cells; FIG. 69D – mouse naive versus mouse primed pluripotent stem cells. FIGs. 69E-F - Naive human (FIG. 69F) and primed human (FIG. 69E) hESCs were double immunostained for TFE3 and OCT4. Representative confocal images are shown for LIS2 hESC line. Insets are enlargements of the dashed boxes. Oct4 staining is localized to the nucleus in both states of cells (primed and naive). On the other hand, a predominant nuclear localization is shown for TFE3 in naive hESCs but not in primed conditions, demonstrating that TFE3 shuttles and changes between the states of the cells. FIG. 69G - Quantitative unbiased imaging analysis for preferential nuclear localization was conducted on randomly selected 200 cells from independent image frames per sample. Box and whisker plots of nuclear/cytoplasmic TFE3 ratios in naive and primed mouse and human ESCs are shown. Naive hESCs showed distributions similar to those in naive mESCs, and the nuclear enrichment was lost in primed human and mouse ESCs * t-test *P* values $< 1 \times 10^{-100}$. FIG. 69H –Transcriptional comparison of *in vitro* and *in vivo* isolated human pluripotent cells. Hierarchical clustering of the mean expression profile of differentially expressed genes between Naïve and Primed samples (FDR< 0.05), in the different groups [Naive (this study), Primed (this study), Belmonte's primed ESCs, and human ICMs (Belmonte and colleagues (Vassena, R. *et*

al. Waves of early transcriptional activation and pluripotency program initiation during human preimplantation development. *Development* 138, 3699–3709, 2011)], using Spearman correlation. Note that while primed ESC samples previously derived by Belmonte and colleagues cluster with the primed samples derived herein, human ICM samples cluster with the naïve samples expanded in WIS-NHSM conditions. FIG. 69I - Principal Component Analysis showing that human ICM samples are closer to Naïve than to Primed samples (along the 1st principal component axis). Primed samples are also more dispersed, showing higher variability and heterogeneity, and not as closely grouped as human Naïve and ICM samples are.

FIGs. 70A-J depict epigenetic configuration of human naive pluripotency. FIGs. 70A-B - Profiles of H3K27me3 chromatin mark of developmental genes in human (FIG. 70A) and mouse (FIG. 70B), naive (blue) and primed (red), represented as normalized read-density. Human profiles indicate average and s.d. (error-bars) calculated over 5 different cell lines (C1, LIS2, WIBR3, WIBR3-MBD3mut and BGO1). Average difference between plots is indicated alongside variance and P-values (calculated with paired-sample t-test). FIGs. 70C-D - Chromatin landscape of 5 pluripotent example genes. H3K27me3 and H3K4me3 marks are shown for naive (blue) and primed (red) cell lines, in both human (FIG. 70C) and mouse (FIG. 70D), showing high consistency between the organisms. FIGs. 70E-F - Same as in FIGs. 70C-D for 5 developmental genes. FIG. 70E – human; FIG. 70F – mouse; FIG. 70G - Representative relative transcript levels in human naive and primed WIBR3 cells. * t-test P value <0.01. Error bars indicate s.d. (n=3). FIG. 70H - Immunostaining for OCT4 (left panels) and DNMT3B (right panels) in human naive cells (lower panels) and primed cells (upper panels). Human naive cells down-regulate MBD3, but not OCT4, protein expression. FIGs. 70I-J - Histograms of the change in methylation between primed and naive samples in human (FIG. 70I) and mouse (FIG. 70J). The histograms depict the distribution of the per-CpG difference in methylation, calculated for all CpGs residing in CpG rich regions (>4% CpG content) and having a coverage of ≥10x in both samples. For clarity, only CpGs with a non-zero change in methylation are included in the histogram. The distribution is left-skewed, indicating a general reduction in methylation in the naive samples.

FIGs. 71A-G depict signaling and functional characteristics of human naive pluripotency. FIG. 71A - LIF/Stat3 is required for stabilization of the *in vitro* stability of naive hESC/hiPSCs in WIS-NHSM. Naive V6.5 NOD mESCs, naive WIS1 and H1 hESCs, and BJ naive hiPSCs were electroporated with mock a pBRY-CAGGS-flox-DsRedT4-IRES-Puro control plasmid, a plasmid encoding a dominant negative Stat3 Y705F mutant (Stat3-DN), or a plasmid Stat3-C constitutively active mutant (pBRY-Stat3-CA). Cells were passaged three times in the presence of puromycin selection. After 20 days, colonies positive for OCT4 pluripotency markers were counted and normalized to colonies from cells electroporated with empty vector. (n=3 for each condition and error bars indicate s.d.). * Student's t test *P* value <0.01. FIGs. 71B-C - Upper panels indicate schemes for gene targeting of OCT4 (FIG. 71C) and COL1A (FIG. 71B) loci. Tables indicate number and percentage of correctly targeted ES clones, as determined by both 5' and 3' southern blot validation strategies. FIG. 71D - Secondary iPSC reprogramming efficiency of wild-type and MBD3 depleted ($MBD3^{mut}$) cells when reprogramming in naive (blue scheme) or primed/conventional (red scheme) conditions. Error bars indicate s.d.m (n=3). * Indicates t-test P value <0.01. FIG. 71E - Relative transcript expression of FMR1 and NANOG genes in cells isolated from healthy or Fragile X patients. Error bars indicate s.d.m (n=3). FIGs. 71F-G – Targeting strategy by homologous recombination of *COL1A* locus in H9 ESCs. Correct targeting efficiency in different H9 naïve and primed pluripotent cell experimental replicates is shown. Correct targeting was scored after confirmation with both 5' and 3' southern blot analysis on extracted DNA from analyzed clones. **Indicates significant *P* value <0.02. **b**, as in **a,** but for *OCT4* locus. *Indicates significant *P* value <0.05.

FIGs. 72A-D demonstrate defining and optimizing conditions for capturing transgene independent human naive pluripotent iPSCs. FIG. 72A - qRT-PCT analysis for relative expression of endogenous OCT4 pluripotency marker and SOX1 neural markers. Relative values to those measured in primed/conventional 1.2 iPSC lines are shown. In the presence of DOX, the cells express the endogenous pluripotency OCT4 (consistent with previously described results and teratoma formation ability of these cells (Hanna, J. *et al. Proc. Natl. Acad. Sci. U.S.A.* 107, 9222–9227, 2010), however SOX1 is significantly upregulated, consistent with unstable pluripotency maintenance in

these conditions (Hanna, J. *et al. Proc. Natl. Acad. Sci. U.S.A.* 107, 9222–9227, 2010). WIS-NHSM conditions that were optimized in this study maintain OCT4 expression and do not acquire aberrant SOX1 upregulation. Error bars indicate s.d. one representative experiment is shown out of two performed. FIG. 72B - Genetically unmodified BJ1 naive hiPSC line generated by mRNA reprogramming approach, showed similar dependence to that observed to C1.2 naive hiPSC line (expanded without DOX), in WIS-NHSM conditions (FIG. 12S). These results exclude leakiness in C1 line as an independent parameter contributing to naive pluripotency in WIS-NHSM. This data is consistent with the ability to robustly generate naive genetically unmodified hESCs throughout the study in WIS-NHSM conditions. * student's t test *P* value <0.01 relative to control WIS-NHSM conditions. FIG. 72C - For further optimizing naive growth conditions, 1% Albumax can be substituted by using either 15% KSR (knockout serum replacement) or 1% chemically defined lipid concentrate (Invitrogen). 1% albumax was used in WIS-NHSM defined throughout the study and used for molecular analysis of naive cells. FIG. 72D - OCT4-GFP+ levels for naive pluripotent cells expanded in WIS-NHSM media on tissue culture plates coated with the indicated components. Naive hiPSCs can be grown without feeder cells either on matrigel coated plates, vitronectin coated plates or 0.2% gelatin + 1ng/ml vitronectin coated plates (but not gelatin alone). * student's t test *P* value <0.01 relative to control Gelatin + feeder cells (MEF) condition. One representative experiment is shown out of 3 performed.

FIGs. 73A-F depict immunostaining for pluripotency markers on newly embryo derived naive hESCs. FIGs. 73A-B - The LIS1 (FIG. 73B), LIS2 (FIG. 73A), WIS1, and WIS2 ESC lines established from human ICM in WIS-NHSM conditions were analyzed, and showed a strong uniform staining for all indicated human pluripotency markers (OCT4, NANOG, SSEA3, SSEA4, TRA1-60, TRA1-81 and Sox2). Notably, SSEA1, which is specific for mouse (both naive and primed stem cells) and not human pluripotent cells, is not expressed on naive hESCs. FIGs. 73C-F - Expression of KLF2 and ESRRB pluripotency factors in naive hESCs. FIG. 73C – naive LIS2 hESC; FIG. 73D – naive WIBR3 hESC; FIG. 73E – naive V6.5 mESC; FIG. 73F – primed mEpiSCs. Representative confocal double immunostaining images demonstrating expression of KLF2 and ESRRB pluripotency factors in naive human and mouse ESCs.

FIGs. 74A-D depict enhanced growth rate and single cell cloning efficiency of human naive pluripotent stem cells. FIG. 74A - Population doubling time of various mouse and human pluripotent stem cell lines. After plating each cell lines in replicates, cells were harvested at days 2,4 and 6 and there growth was normalized by counting cell number at each stage and calculating growth rate relative to the number of cells harvested and counted at day 2 (rather than number of plated cells to account for variability in survival after plating). Error bars represent s.d., and *P* values represent t-test of average from primed hESC/hiPSC lines to average of naive hESC/hiPSC lines. FIG. 74B - Single-cell cloning efficiency of different pluripotent stem cell lines as determined by the number of wells containing NANOG+ colonies 6 days after plating (with or without ROCK inhibitor as indicated in the figure). * indicates student's t-test *P* value <0.01 between the average of the compared groups. Error bars indicate s.d. These results highlight an enhanced single cell survival and cloning efficiency of naive pluripotent cells, in comparison to conventional hESCs/hiPSCs. FIG. 74C - Cross species differences in ERAS protein expression influence remaining growth properties differences between genetically unmodified human and mouse naive PSCs. Single-cell cloning efficiency of different pluripotent stem cell lines as determined by the number of wells containing Nanog+ colonies 6 days after plating (without using ROCK inhibitor as indicated in the figure). * indicates student's t-test *P* value <0.01 between the average of the compared groups. Error bars indicate s.d. These results highlight a relatively compromised single cell survival and cloning efficiency of Eras knockout naive mESCs, in comparison to conventional ESCs/iPSCs. Reconstitution of ERAS in naive hESCs rescues their relative deficiency in single cell colony formation assay. FIG. 74D - Mouse ESC derivation efficiency in 2i/LIF/MEF feeder conditions, from WT or Eras KO ICMs. Error bars indicate s.d.m. Student t-test P value is indicated.

FIGs. 75A-I depict predominant utilization of distal enhancer element in mouse and human naive pluripotency. FIG. 75A - Schematic illustration demonstrating the relative localization of the evolutionary conserved distal and proximal enhancer elements in the human OCT4 locus. Distal enhancer (DE) and proximal enhancer (PE) are highlighted in the human OCT4 locus, and were accordingly deleted in ΔPE and ΔDE reporter constructs used in this study. Insertion site of GFP-2A-Puromuycin resistance cassette by BAC recombineering is indicated. FIGs. 75B-E -WIS1 (FIGs.

75B and 75C) and LIS2 (also referred to as "LIS39" herein) (FIGs. 75D-E) naive hESCs were stably transfected with ΔPE-OCT4-GFP-2A reporter construct that marks naive pluripotency configuration. GFP expression was specifically detected by flow cytometry in naive pluripotent cells (FIGs. 75B and 75D), while their genetically matched primed cells generated after 10 days in primed/conventional hESC conditions did not show GFP expression (FIGs. 75C and 75E). FIGs. 75F-G - Similar results were obtained when the ΔPE reporter was inserted in naive murine V6.5 ESCs, that showed specific down regulation of GFP activity after transferring the cells to mEpiSC primed media (FIG. 75G). Therefore, the human ΔPE-Oct4-GFP-2A-PURO reporter showed similar specific activity in mESCs expanded in 2i/LIF, but not primed mEpiSCs (FIGs. 75F and G), further supporting the specificity of the reporter used and the similarity between mouse and human naive pluripotent configurations. FIGs. 75H-I - naive C1.2 hiPSC propagated in WIS-NHSM media showed specific expression of GFP marker (FIG. 75H), while C1 cells grown in previously described 2i/LIF + DOX conditions (to induced OSK transgenes) down regulate GFP activity and had a heterogeneous expression pattern (FIG. 75I). The latter is consistent with data in FIGs. 12A-C and 72A-D, indicating the previously described (Hanna, J. *et al. Proc. Natl. Acad. Sci. U.S.A.* **107,** 9222–9227, 2010) transgene dependent naive pluripotent cells are unstable relatively to the genetically unmodified and transgene independent cells described in this study.

FIGs. 76A-C demonstrate that female naive hESCs/hiPSCs retain a unique pre-X inactivation state in WIS-NHSM conditions. FIG. 76A - Confocal images obtained after double immunostaining for OCT4 and H3K27me3 on naive, primed and differentiated samples were analyzed and quantified for the fraction of cells with nuclear H3K27me3 foci that mark the inactive X allele. Average percentages of 150-200 individual cells counted per sample from at least ten independent frames are shown. Error bars indicate s.d. * indicates student's t-test *P* value <0.01 when comparing samples to naive pluripotent cells. Naive female pluripotent cells have very low H3K27m3 foci. In primed and differentiated cells, H3K27me3 foci (one per nucleus) became clearly detectable in the majority of cells. Male lines do not exhibit H3K27me3 foci/clouds in any of the states as expected. FIG. 76B - qRT-PCR analysis indicates no/low expression levels of XIST in naive hESCs/iPSCs, in comparison to female

differentiated fibroblast cells that upregulate XIST expression. Error bars indicate s.d.m (n=3) * indicate student's t-test *P* value < 0.01. FIG. 76C - H3K9m3 level [RPKM (read-per-kilo base-per-million reads)] distributions of all the genes in chromosome X. Distributions of H3K9me3 RPKM levels in chromosome X genes, measured in the different cell lines. Boxes – 25^{th} and 75^{th} percentiles, horizontal lines – median, crosses – outliers. RPKM were measured for each gene between 1 Kb upstream to TSS (Transcription Start Site) and TES (Transcription Ending Site). Shown are 4 human cell lines (WIBR3, C1, LIS2, WIS2). Blue – naive cell lines, Red – primed cell lines. Lines WIBR3, C1 and LIS2 are females and BGO1 is a male cell line. Distributions of H3K9me3 in female primed cells are significantly higher compared to their naive counterparts, while in male cells they are the same. P-values were calculated with 1-tail paired-sample t-test.

FIGs. 77A-B depict distinct transcriptome for human naive ESCs/iPSCs. FIG. 77A - Microarray transcriptional profile of selected pluripotency and lineage-specific marker genes, their mean expression ratio in primed hESCs and naive hESCs relative to the median of all samples. Values are shown in natural scale. Error bars represent SEM of each gene. Asterisks denote statistically significant differentially expressed genes in which the false discovery rate was <0.05 between the naive and primed groups of samples. Panel was generated by R software. FIG. 77B - qRT-PCR validation analysis for gene upregulated or down regulated in naive vs. primed human pluripotent cells. *Indicates student t-test P value <0.01 for comparisons between naive and primed samples. Error bars indicate s.d.m (n=3).

FIG. 78 depicts GO ontology analysis for genes down regulated in human naive pluripotency. GO ontology categories enriched for and down-regulated genes in naive pluripotency, checked and visualized using the online tool GOrilla. Color bar shows p-values, the FIG. shows only trees containing GO terms with p-values < 10-5, resulting in FDR corrected p-values < 0.05.

FIGs. 79A-D depict transcriptional comparison of *in vitro* and *in vivo* isolated human pluripotent cells. FIG. 79A - Hierarchical clustering of gene expression of genes differentially expressed between Naive and Primed samples, in human cell lines and in the human inner-cell-mass (ICM), using Spearman correlation. Note that while the ESC samples previously derived by Belmonte and colleagues cluster with the Primed

samples derived herein, the human ICM samples cluster with the Naive samples. FIG. 79B -Hierarchical clustering of the mean expression profile of all the genes in the different groups (Naive, Primed, Belmonte's ESCs, and ICM), using Spearman correlation. FIG. 79C – Hierarchical clustering of the mean expression profile of differentially expressed genes in all individual samples. FIG. 79D - Principal Component Analysis showing that human ICM samples are closer to Naive than to Primed samples (along the 1st principal component axis). Primed samples are also more dispersed, showing higher variability and heterogeneity, and not as closely grouped as Naive and ICM samples are.

FIGs. 80A-D depict distinct MHC class I and TFE3 protein cellular localization pattern in naive human pluripotent cells. Shown are representative confocal images of double immunostaining for OCT4 and TFE3 followed by fluorescence intensity profiling of the yellow-dashed box area. FIG. 80A – Naive mESC; FIG. 80B – Naive WIBR3 hESC; FIG. 80C – Primed mEpiSC; FIG. 80D – Primed WIBR3 hESC. This analysis demonstrated overlap between OCT4 nuclear expression with TFE3 in mouse and human pluripotent cells (naive and primed). These representative images reveal strict nuclear localization of TFE3 in naive pluripotency, while primed pluripotency is associated with increased cytoplasmic localization of TFE3 both in mice and human primed cell lines. Y-axis represents fluorescence intensity, profiling measured with Zen blue 2011 software. See Fig. 3e and Methods for systematic unbiased quantifications.

FIGs. 81A-D depict enhanced surface E-CADHERIN expression in human naive pluripotent cells. Representative confocal immunostaining images for the expression of E-CADHERIN and OCT4 on genetically matched naive (FIGs. 81A and 81C) and primed (FIGs. 81B and 81D) hESCs. The samples were processed simultaneously and analyzed under identical conditions. Insets represent enlargements of boxed areas. While E-CADHERIN is expressed in primed hESCs, its expression becomes homogenously distributed and more enhanced in humane naive hESCs expanded in WIS-NHSM conditions.

FIGs. 82A-B depict cross-species clustering of naive and primed pluripotency. FIG. 82A - Cross-species gene expression hierarchical clustering of all 9,803 orthologous genes represented on both mouse and human gene arrays used in this study, clustered using Pearson correlation. Naive mouse and human pluripotent cells formed a

distinct group apart from primed mEpiSCs and conventional/primed hESCs and hiPSCs. Heat map showing row-normalized expression levels (log-ratio) with red and green colors representing up and down regulated genes, respectively. Naive cells are labeled in blue, primed cells are labeled in red. Mouse samples were obtained from either 129 or NOD strains. This analysis strikingly confirms that pluripotent cells lines preferentially cluster based on naive and primed configuration, rather by the species of origin. FIG. 82B - Boxplot of gene-specific gene expression levels in Primed samples showing higher noise and heterogeneity than in Naive samples. This pattern is consistent with the genome-wide data in FIGs. 69A-G. Five out of nine genes are significantly more variable, tested by F-test of equality of variances).

FIGs. 83A-D depict global H3K27me3 and H3K4me3 deposition in naive and primed pluripotent cells. Profiles of H3K27me3 (FIGs. 83A-B) and H3K4me3 (FIGs. 83C-D) chromatin modifications of all RefSeq genes in human (n=43,463; FIGs. 83A and 83C) and mouse (n=30,480; FIGs. 83B and 83D), naive (blue) and primed (red), represented as normalized read-density. Human profiles indicate average and s.d. (error-bars) calculated over 5 different cell lines (C1, LIS2, WIBR3, WIBR3-MBD3^{mut} and BGO1). Average difference between plots is indicated alongside variance and P-values (calculated with paired-sample t-test).

FIGs. 84A-G depict gnome wide redistribution of H3K27me3 in human naive pluripotency. FIGs. 84A-B - Distribution of H3K27me3 peaks in different genomic components (promoter, gene-body and intergenic region), as a function of the peak density (represented as RPKM, read-per-kilobase-per-million-reads), in human cell lines (WIBR3, C1 and BGO1). In addition to a reduction in total number of peaks in naive conditions, the peaks distribute differently from primed, with lower number of peaks in promoters and gene bodies, compared to primed conditions. FIG. 84C - Western blot analysis for quantifying total H3K27me3 levels in naive and primed LIS2 hESC samples. Total levels of H3K27me3 were not significantly altered between naive and primed samples (similar to what was observed in mice). Similar results were seen in WIBR3 and C1 cell lines (data not shown). FIGs. 84D-E - Number of enhancers of class I (active transcription) and class II (poised) in naive (blue) vs. primed (red) human (FIG. 84D) and mouse (FIG. 84E). In human, numbers correspond to common enhancers in lines WIBR3 and C1. The number of reads was normalized by down-

sampling such that the number of reads in all human samples is identical, and so is the number of reads in all mouse samples. A dramatic decrease in class II enhancers can be seen in the naive cells in both human and mouse. FIGs. 84 F-G - Expression level distribution of genes associated with class I and class II enhancers, present in either naive cells only (blue) or in primed cells only (red) in human (FIG. 84F) or mouse (FIG. 84G) cells. Expression level distribution of all genes is presented as control. Boxes represent 25th and 75th quantiles, and whiskers represent min and max values that are not outliers. Analysis shows that Primed state specific class II enhancers continue to retain very low expression levels in both naive and primed states (despite the loss of H3K27me3 mark in naive pluripotency over their enhancer). P-values (t-test) indicate significant differences between distributions in naive and primed cells.

FIGs. 85A-C - Primed/conventional WIBR3 human ESCs were passaged in 12 different WIS-NHSM based conditions. FIG. 85A depicts the compositions of the different variations of the WIS-NHSM conditions used in this experiment, in addition to the basic medium of KO-DMEM, supplemented with 1% ALBUMAX, 50 microgram/ml (μg/ml) L-ascorbic acid, N2 supplement (Invitrogen) and additional 6.25 mg human insulin. Small molecules and cytokines were included as indicated in combinations of conditions 1-12. Cells were expanded on 0.2% Gelatin coated plates for 25 days (6 passages). FIG. 85B – A histogram depicting OCT4-GFP+ levels as evaluated by FACS analysis to measure the pluripotency maintenance in these conditions. Error bars indicate s.d. n=2. FIG. 85C – A histogram depicting the percentage of methylated cytosine. Genomic DNA was harvested and was subjected to quantification of methylated cytosine frequency by mass spectrometry. Error bars indicate s.d. n=2 replicates. Primed cells were used as a reference control sample.

FIGs. 86A-C depict the influence of MAPK signaling perturbation on human naive and primed pluripotent cells. FIG. 86A - qRT-PCR for expression of the indicated lineage commitment genes in different conditions. Supplementing primed hESCs with ERKi, GSK3βi (CHIR99021) or both (2i) results in upregulation of SOX1 neural marker, consistent with their tendency to differentiation upon ERK inhibition. FIG. 86B - naive WIS1 hESCs expanded in WIS-NHSM conditions, were expanded after omitting the indicated factors from WIS-NHSM conditions for 72 hours. qRT-PCR of lineage commitment genes is shown. The results indicate that TGFβ blocks the SOX1 inductive

effect induced by the presence of ERKi in the medium. FIG. 86C - qRT-PCR analysis for lineage commitment gene upregulation 72 hours after withdrawal of p38i and/or JNKi from WIS-NHSM conditions. These results indicate that the components in WIS-NHSM conditions cooperatively promote pluripotency stability and counter-balance and neutralize pro-differentiation effects induced by some of the ingredients. Error bars indicate s.d.m (n=3). Representative results of one out of three biological replicates experiments is shown. * indicates student's t-test *P* value <0.01.

FIGs. 87A-B depict signaling requirements for maintaining naive hESCs and hiPSCs. FIG. 87A - WIS1 and LIS1 naive hESCs were targeted with the ΔPE-OCT4-GFP reporter and analyzed for the ability to retain naive pluripotency in different conditions as indicated. OCT4-GFP+ levels detected by FACS from two experimental replicates were averaged. Error bars indicate s.d. The results indicate ERK inhibition is essential for maintaining hESCs in WIS-NHSM, and this effect can be achieved by using two different ERK inhibitor (PD 0325901 or PD184352). b, p38 inhibition is essential for maintaining hESCs in WIS-NHSM, and this effect can be achieved by using two different p38 kinase inhibitors (SB203580 or SB202190). FIG. 87B - Different hESCs and hiPSC line carrying OCT4-GFP or ΔPE-OCT4 GFP reporter were used to evaluate different conditions for their ability to maintain pluripotency and specifically naive pluripotency (by ΔPE-Construct). Only WIS-NHSM conditions enabled maintenance of all cell lines tested while activating both OCT4-GFP and ΔPE-OCT4-GFP reporter. * Indicates student t-test P values <0.01 between indicated compared samples/groups. Error bars indicate s.d.m between well replicates (n=3).

FIGs. 88A-J demonstrate different defined growth conditions which enable maintenance of mouse naive pluripotency. FIGs. 88A-G - V6.5 mESCs carrying the naive pluripotency specific ΔPE-Oct4-GFP reporter were maintained in distinct chemically defined growth conditions as indicated in the panel labels: FIG. 88A - N2B27 LIF; FIG. 88B - N2B27 ERKi/GSK3βi (2i)/LIF; FIG. 88C - N2B27 p38i/GSK3βi/LIF; FIG. 88D - N2B27 JNKi/GSK3βi/LIF; FIG. 88E - WIS-NHSM; FIG. 88F - WIS-NHSM without FGF2/TGFβ; FIG. 88G - mEpiSCs medium (with FGF2/TGFβ). The analysis indicates that naive GFP+ mESCs can be maintained in LIF, GSK3βi together with either ERK1/2i, p38i or JNKi. FIGs. 88H-J - Representative images of high-contribution chimeras generated after blastocyst microinjection of the

indicated lines. FIG. 88H - N2B27 p38i/GSK3βi/LIF; FIG. 88I - N2B27 JNKi/GSK3βi/LIF; FIG. 88J - WIS-NHSM. Agouti coat color indicates high-level chimera contribution.

FIGs. 89A-D depict competence of different mouse naive growth conditions in tetraploid embryo complementation assay. FIG. 89A -V6.5 naive mESCs were expanded in the indicated conditions for 12 passages, after which they were tested for tetraploid complementation assay to form all-ESC animals. The analysis indicates unrestricted developmental potential is equivalently obtained at the functional level when naive mESCs are expanded with either p38i, JNKi or ERK1/2i (together with supplementation of LIF and GSK3βi in all conditions). FIGs. 89B-C - Representative images of "all-ESC" agouti coat colored animals obtained. FIG. 89D - Competence of different mouse naïve growth conditions in tetraploid embryo complementation assay. V6.5 naïve mESCs were expanded in the indicated conditions for 12 passages, after which they were tested for tetraploid complementation assay to form all-ESC animals. The analysis indicates unrestricted developmental potential is equivalently obtained at the functional level when naïve mESCs are expanded with p38i, Jnki or Erk1/2i (together with supplementation of LIF and GSK3βi in all conditions).

FIG. 90 depicts LIF/STAT3 signaling dependence by naive hESCs/iPSCs. qRT-PCR levels of the indicated lineage commitment genes after subjecting naive WIS1 hESCs to LIF withdrawal and/or supplementation with JAK small molecule inhibitor (JAKi 0.6μM) for 72 hours. Averages of biological triplicates are indicated, as normalized levels to un-stimulated control. Error bars indicate s.d.m (n=3). Interfering with LIF/STAT3 signaling results in specific upregulation of lineage commitments genes in naive hESCs. * Indicates student t test P values <0.01 compared to control WIS-NHSM conditions. Error bars indicate s.d.

FIGs. 91A-C depict unique signaling requirement and response to BMP4 for naive hESCs/iPSCs. FIGs. 91A-B - qRT-PCR levels of the indicated commitment genes after subjecting naive (FIG. 91B) and primed (FIG. 91A) WIS1 hESCs to BMP4 for 72 hours. Averages of biological triplicates are indicated, as normalized levels to un-stimulated control. Error bars indicate s.d.m (n=3). Naive WIBR3 hESCs upregulated ID3 (inhibitor of DNA binding 3, dominant negative helix-loop-helix protein; Gene ID: 3399) in response to BMP4 (5-10 ng/ml bone morphogenetic protein 4), but not

trophoblast early markers CDX2 (caudal type homeobox 2; Gene ID: 1045) and HAND1 (heart and neural crest derivatives expressed 1; Gene ID: 9421). This is reminiscent of naive mESCs to BMP4 where it was shown to support and maintain their pluripotency by up regulating Id3 [Ying, Q.-L., et al. *Cell* 115, 281–292 (2003). BMP Induction of Id Proteins Suppresses Differentiation and Sustains Embryonic Stem Cell Self-Renewal in Collaboration with STAT3]. Primed WIBR3 hESCs upregulate trophoblast differentiation markers CDX2 and HAND1 in response to BMP4 and do not upregulate ID3. FIG. 91C - Global gene expression analysis indicates that naive WIS2, H9 and BGO1 expanded with the addition of BMP4 for 12 passages, retain a transcriptional program that clusters with naive hESCs and hiPSCs, rather than primed cells. Hierarchical clustering of genome-wide gene expression of human cell lines, using Euclidean distance. Naive hESC and hiPSCs either with or without BMP4 clustered separately from conventional/primed hESCs/hiPSCs, as shown by the dendrogram. Heat map showing row-normalized expression levels with red and green colors representing up and down regulated genes, respectively. Note the two left-most genetically identical samples that were used for Batch effect correction, allowing two different datasets to be united for further analysis (see online Methods). Collectively these findings indicate a unique tolerance for naive human pluripotent cells for BMP4 that does not compromise the maintenance of the naive pluripotent state.

FIGs. 92A-D depict reprogramming efficiency of $Mbd3^{+\backslash+}$ Secondary MEF after knockdown of Mbd3 (Mbd3 siRNA) or Chd4 (Chd4 siRNA). FIG. 92A - MEFs were subjected to reprogramming with STEMCCA-OKSM with DOX induction, and on day 3 the 2i/LIF medium was added. The indicated siRNAs were added on days 2, 4 and 6. FIGs. 92B-C - Western blot analyses indicating protein depletion efficiency on siRNA transfection of either Mbd3 (FIG. 92C) or Chd4 (FIG. 92B) targeting siRNA pools. FIG. 92D – A histogram depicting reprogramming efficiency. Reprogramming efficiency was measured by quantitation of the OCT4-GFP positive cells (assayed by FACS). Shown are Error bars indicate s.d. from average (n=3). Asterisks indicate Student's t-test P value < 0.01.

FIG. 93 shows that P66a-CC interrupts Mbd3 binding to Chd4. 293T cells were transfected with both with Flag-Mbd3 (WT) and P66a-CC (SEQ ID NO:71; GenBank Accession NO. NM_017660.3) or a control vector (mCherry), Mbd3 interacting proteins

were pulled down by immunoprecipitation (IP) using Flag-magnetic beads. The results indicate specific loss of Chd4 interaction with Mbd3 following the p66a-CC transfection.

FIGs. 94A-B depict the generation of a mCherry knock in reporter allele in Nanos3 locus of a naive human ESC (WIS1). FIG. 94A – A schematic illustration depicting genetic engineering via TALENs in WIS1 naive human ESCs to generate mCherry knock in reporter allele in Nanos3 locus. Scheme indicates targeting strategy. FIG. 94B - Southern blot analysis depicting correctly targeted allele (mut) in a number of WIS clones (2h, 4g, 8a, and 8e).

FIG. 95 illustrates the differentiation strategy of naive EIS1 NANOS3-cherry reporter human ESCs into primordial germ cell (PGC)-like cells (abbreviated as PGCLC). Shown are images of the cells/colonies during the differentiation process.

FIGs. 96A-I depict the process of differentiating human ESCs into primordial germ cell like cells. FIG. 96A – schematic illustration of the differentiation process. FIGs. 96B-I - FACS analyses for detecting PGCLC marker expression NANOS3-Cherry. FIG. 96B – naive ESCs; FIG. 96C – primed EpiLC; FIGs. 96D-F – cells were cultured in a PGC medium which included BMP4; FIGs. 96G-I – cells were cultured in a PGC medium which did not include BMP4. Shown are FACS results after 2 (FIGs. 96D and 96G), 4 (FIGs. 96E and 96H), and 6 (FIGs. 96F and 96I) days in the PGC medium. The FIGs. show specific induction of mCherry reporter at Day 2+4 and only when BMP4 is included in the differentiation medium (FIG. 96E). Note Naive ESCs do not express mCherry (FIG. 96B), neither EpiLC cells (FIG. 96C). One representative experiment is shown out of five performed. +/- indicates s.d. (n=5).

FIGs. 97A-H depict expression of PGC markers in human PGCLC cells. Shown are real-time PCR analyses for expression of different PGC markers during the induction protocol. FIG. 97A – TFAP2c (also known as AP2gamma; FIG. 97B – BLIMP1 (also known as PRDM1 – PR domain containing 1, with ZNF domain: Gene ID:639); FIG. 97C – PRDM14 (PR domain containing 14); FIG. 97D – STELLA (developmental pluripotency associated 3); FIG. 97E – DND1 (DND microRNA-mediated repression inhibitor 1); FIG. 97F – NANOS3 (nanos homolog 3); FIG. 97G – INTEGRIN B3 [integrin, beta 3 (platelet glycoprotein IIIa, antigen CD61)]; FIG. 97H - VASA; Results clearly show that PGCLC markers are induced in protocol applied on human naive

ESCs, including STELLA (FIG. 97D), INTEGRINB3 (FIG. 97G), BLIMP1 (FIG. 97B) and VASA (FIG. 97H).

FIGs. 98A-B depict FACS analyses of conventional/primed human ESCs that were subjected to the same induction protocol as described in Example 11 of the Examples section which follows, and in FIGs. 95-97 above. FIG. 98A – FACS analysis after 4 days in PGC medium. FIG. 98B – FACS analysis after subjecting the primed ESCs to epiblast medium (EpiLC medium) for 2 days, following by further 4 days in the PGC medium. Note the low nano-cherry percentage of cells in FIG. 98A (0.25%) and the slight increase of nanos-cherry positive cells in FIG. 98B (1.74%). These results show that conventional/primed human ESCs subjected to BMP4 including PGCLC induction protocol do not successfully turn on NANOS3 mCherry reporter. Results indicate the importance of using human naive pluripotent cells as a starting material for human PGCLC induction.

FIGs. 99A-G depict reprogramming of MBD3 knocked down human fibroblasts. FIG. 99A – Human BJ fibroblasts were infected with TRIPZ MBD3 shRNA lentiviruses (3.1, 3.2, 3.3 indicate three different hairpin constructs targeting MBD3). Shown is a histogram with quantification of real time PCR expression for MBD3 which was conducted after 72 hours with or without DOX induction. The results validate down-regulation of MBD3 in human fibroblasts in a DOX dependent manner. FIGs. 99B-G - Human adult dermal fibroblasts were infected with FUW-RtTA, TetO-OKSM, TetO-ERAS and Tripz-MBD3 shRNA lentiviral mix. The following DOX inducible MBD3 knockdown lentiviral clones were used: TRIPZ Human MBD3 shRNA Clone ID: V3THS_392206 (#1); V3THS_392209 (#2); V3THS_392210 (#3). First 3 days of reprogramming were in the presence of DMEM medium supplemented with 15% FBS (fetal bovine serum) + 50 microgram/ml Vitamin C + DOX (2 microgram/ml). After 3 days, NHSM conditions were applied (using the NHSM medium) with continued DOX induction. FIGs. 99B-C - Reprogramming of MBD3 knocked down human fibroblasts. Shown are the reprogrammed cells which express shMBD3-red fluorescent protein (RFP) in red fluorescence (FIG. 99B) or in bright filed (BF; FIG. 99C). FIGs. 99D-G - Reprogramming of MBD3 KD primary human fibroblasts with overexpression of OKSM and ERAS in NHSM conditions. Shown are the clonal populations with ES-like morphology appeared at days 5 (FIGs. 99D-E) and 11 (FIGs. 99F-G). Phase contrast

images are shown in FIGs. 99D and 99F. Red fluorescence images are shown in FIGs. 99E and 99G. MBD3 knocked-down clones that over express ERAS develop in 5 days, and were subjected for iPSC follow up analysis.

FIGs. 100A-T show staining for OCT4, SSEA4, TRA1-60 and TRA1-81 pluripotency markers on cells reprogramming in NHSM conditions following 10 days of OKSM, RtTa, ERAS and MBD3 shRNA DOX induction. FIGs. 100A-D – Cells were stained for DAPI (FIG. 100A), OCT4 (FIG. 100B), and SSEA4 (FIG. 100C). FIG. 100D – merged image. Note the co-expression of OCT4 and SSEA4. FIGs. 100E-I – Cells were stained for DAPI (FIG. 100E), OCT4 (FIG. 100F), SSEA4 (FIG. 100G). FIG. 100H – merged image showing co-expression of OCT4 and SSEA4. FIG. 100I – Staining for the MBD3-shRNA induction reporter. Note the co-localization of shMBD3 with cells expressing the OCT4 and SSEA4 pluripotency markers. FIGs. 100J-N - Cells were stained for DAPI (FIG. 100J), OCT4 (FIG. 100K), TRA1-60 (FIG. 100L). FIG. 100M – merged image showing co-expression of OCT4 and TRA1-60. FIG. 100N – Staining for the MBD3-shRNA induction reporter. Note the co-localization of shMBD3 with cells expressing the OCT4 and TRA1-60 pluripotency markers. FIGs. 100O-S - Cells were stained for DAPI (FIG. 100O), OCT4 (FIG. 100P), TRA1-81 (FIG. 100Q). FIG. 100R – merged image showing co-expression of OCT4 and TRA1-81. FIG. 100S – Staining for the MBD3-shRNA induction reporter. Note the co-localization of shMBD3 with cells expressing the OCT4 and TRA1-81 pluripotency markers. FIG. 100T – A histogram depicting quantification of the Nanog+/TRA1-60+ human iPSC colonies at day 10. Primary females adult dermal fibroblast cells (line #13) were transduced with RtTa, OSKM and ERAS vectors in WIS-NHSM conditions, with or without MBD3 knockdown via TRIPZ-MBD3 shRNAs 1+3 that were added to the reprogramming. iPSC colony numbers were counted at day 10 by staining for NANOG and TRA1-60 markers (FIG. 100T). Note the dramatic increase in iPSC formation from primary human somatic cells when MBD3 inhibition is introduced.

FIGs. 101A-B are Western blot analyses showing expression of MBD3 (FIG. 101B) and of HSP90 (FIG. 101A) in v6.5 mouse ES cells after different treatments. V6.5 mouse ES cells were expanded for 4 days in the indicated conditions and subjected to Western blot analysis for MBD3 protein expression. The conditions are indicated in the FIG. above the lanes. Following are the abbreviations and concentrations of the

indicated factors and agents. PBS = phosphate buffered saline; "LIF" = leukemia inhibitory factor, provided at a concentration of 20 nanograms/milliliter (ng/ml); KSR = knockout serum replacement; "2i/LIF" = small-molecule inhibitors CHIR99021 (CH, 3 μM- Axon Medchem) and PD0325901 (PD, 1 μM - TOCRIS), with 20 ng/ml LIF; "DMSO" = Dimethyl sulfoxide at a concentration of 0.1%; TGFRi (inhibitor of transforming growth factor receptor; SB431542 at 5 micromolar); PKC-i (inhibitor of protein kinase C; Go6983 at 5 micromolar). Note that significant depletion of MBD3 protein levels in cells treated with the PKC inhibitor (Go6983 5 microM) (PKCi). The results show that inhibition of PKC leads to down regulation in MBD3 expression in mouse embryonic stem cells.

FIG. 102 – A histogram depicting the effect of the various WIS-NHSM media that are specified in Table 3 (Example 13 of the Examples section which follows) on methylation of DNA (% of total methylated cytosine levels (5 mdC) normalized to dG.

FIG. 103 - A histogram depicting the effect of the various WIS-NHSM media that are specified in Table 3 (Example 13 of the Examples section which follows) on relative DNMT3L mRNA expression (normalized to primed cells).

FIG. 104 - A histogram depicting the effect of the various WIS-NHSM media that are specified in Table 3 (Example 13 of the Examples section which follows) on relative DNMT3B mRNA expression (normalized to primed cells).

FIG. 105- A histogram depicting the effect of the various WIS-NHSM media that are specified in Table 3 (Example 13 of the Examples section which follows) on % $OCT4^+$ WIBR3 cells after 9 passages on 0.2% gelatin plates.

FIGs. 106A-D - FACS analyses for anti human CD61 (integrin B3) expression in human naive ESCs (FIGs. 106A-B) and PGCLCs (day 4 after induction; FIGs. 106C-D) carrying the NANOs3 mCherry knock-in reporter. FIGs. 106A and 106C – control cells (not stained with the antibody); FIGs. 106B and 106D – Cells stained with anti-human CD61 (Alexa-647) antibody.

FIGs. 107A-B - FACS analyses for anti human SSEA4 (FIG. 107A) or CD61 (integrin β3; FIG. 107B) expression in human PGCLCs (day 2+4 after induction from human naive cells) carrying the NANOS3 mCherry knock-in reporter.

FIGs. 108A-C – Signaling and functional characteristics of human naïve pluripotency. FIG. 108A - Pluripotency maintenance by different pluripotent cell lines

cultivated in various media conditions. For defining Signaling characteristics of human and mouse pluripotent cells the present inventors tested pluripotency maintenance by different pluripotent cell lines cultivated in various media conditions. Cell populations were equally divided and plated on gelatin/vitronectin coated plates in the indicated growth medium in which these cell lines are normally maintained (mouse naïve cells – N2B27-2i/LIF, naïve hESCs/hiPSCs – WIS-NHSM, mEpiSCs and primed hESCs/hiPSCs – in KSR/bFGF/TGFβ conditions). 36 hours later the wells were supplemented with the indicated inhibitors or growth factors. After 14 days (2 passages), wells were analyzed by OCT4 immunostaining of direct detection of OCT4-GFP pluripotency reporter expression, to determine the relative percentage of undifferentiated pluripotent cells. Colony formation is normalized to an internal control, as indicated by "Growth medium" only on the far left column. When components already included in WIS-NHSM were supplemented, this yielded a 2-fold increase in their relative concentration. Normalized percentages lower than 50% are defined as "sensitive" to the presence of the supplemented inhibitor. FIG. 108B - LIF/Stat3 is required for stabilization of the *in vitro* stability of naïve hESC/hiPSCs in WIS-NHSM. Naïve V6.5 mESCs, naïve WIS1 and H1 hESCs, and BJ naïve hiPSCs were electroporated with mock a pBRY-CAGGS-flox-DsRedT4-IRES-Puro control plasmid, a plasmid encoding a dominant negative Stat3 Y705F mutant (Stat3-DN), or a plasmid encoding Stat3-CA constitutively active mutant (pBRY-Stat3-CA). Cells were passaged three times in the presence of puromycin selection. After 20 days, colonies positive for OCT4 pluripotency markers were counted and normalized to colonies from cells electroporated with empty vector. (n=3 for each condition and error bars indicate s.d.). FIG. 108C - Representative images showing human naive GFP labeled iPSC derived cell integration into different locations in the anterior part of an E10.5 mouse embryo. 1st column shows the whole embryo (z-stack interval is 30 um, 18 focal-planes total). The 2nd column shows a zoom in images focusing on the head region (white square R1) where the hiPSC-derived cells (GFP positive cells) are pointed out (arrowheads, z-stack interval is 20μm, 11 stacks total). 3rd column shows the posterior part of the embryo (yellow square R2) where no GFP positive cells were detected (z-stack interval is 20μm, 9 focal-planes total). Light-blue square in the first two images in the 2nd column represent the area shown in the insert at the corner of each image. (ov–optic vesicle, op–

optic pit, fba–first branchial arch, flb–forelimb bud, s–somite). Scale bar in all images is 50 μm.

FIGs. 109A-E – Chimerism with human naïve iPSCs derived cells following mouse morula microinjection. FIG. 109A - C1 human naïve iPSCs were targeted with constitutively CAGGS promoter driven EGFP into the human AAVS1 locus via ZFN utilization. Subsequently cells were microinjected into E2.5 mouse early morulas, and micro-manipulated embryos were allowed to recover and develop into blastocysts *in vitro* for additional 24 hours. Images show specific GFP+ human cell survival and integration in mouse pre-implantation embryos. FIG. 109B – A histogram depicting naive and primed GFP+ human iPSC survival *in vitro*, 24-36 hours after microinjection into mouse morulas. *Student t-test *P* value <0.01. Error bars indicate s.d. (n=3). Note that while the naive iPSCs survive in mouse blastocysts 24-36 hours post injection (almost 80% of the cells), only a minor fraction (less than 5%) of the primed PSC survive in the blastocyst. FIG. 109C – Representative confocal analysis following immunostaining for GFP (green) OCT4 (red) and CDX2 (magenta) was done 24 hours following mouse morula microinjections with GFP labeled naive hiPSCs. Note surviving GFP+ cells (white arrow) that specifically integrate and stain positive for OCT4, but not CDX2 (No co-localization between GFP and Cdx2 was not observed). Scale bar 10 μm. FIG. 109D - Subsequently, mouse blastocysts were implanted *in vivo* in mice and allowed to develop for additional 7 days in vivo (as indicated), before dissection and confocal analysis. Representative images showing robust integration of hiPSC derived cell integration into the neural folds of an E8.5 mouse embryo (upper panels). Notably, GFP was not detected in the control non-injected mouse embryos (n=3, lower panels). z-stack interval is 20 μm; 17 focal-planes total (nf–neural folds). Scale bar 50 μm. FIG. 109E - Naive hiPSC derived cells are integrated into different locations at the craniofacial region of an E10.5 mouse embryo. A sequence of different focal planes from 108C, showing multiple hiPSC derived cells integrated into different locations on the craniofacial region (arrowheads). First image in each row shows the maximum intensity projection of all z-stacks. The distance between the different focal planes appears on the upper right corner of each one. (ov–optic vesicle, op–optic pit, fba–first branchial arch). Scale bar 50 μm.

DESCRIPTION OF SPECIFIC EMBODIMENTS OF THE INVENTION

The present invention, in some embodiments thereof, relates to an isolated primate (e.g., human) naive pluripotent stem cell, novel culture medium which can be used to generate same and methods of generating and culturing same and, more particularly, but not exclusively, to methods of improving dedifferentiation of somatic cells for generation of induced pluripotent stem cells.

Before explaining at least one embodiment of the invention in detail, it is to be understood that the invention is not necessarily limited in its application to the details set forth in the following description or exemplified by the Examples. The invention is capable of other embodiments or of being practiced or carried out in various ways.

The present inventors have uncovered the conditions, which are required for isolating and generating a primate (e.g., human) naive pluripotent stem cell, and maintaining same in the naive state.

Thus, according to an aspect of some embodiments of the invention there is provided an isolated primate (e.g., human) naive pluripotent stem cell (PSC) comprising:

an unmethylated X-inactive specific transcript (XIST) gene, wherein:

(i) when the naive PSC is a female PSC, then the naive female PSC has two unmethylated alleles of the XIST gene; and

(ii) when the naive PSC is a male PSC, then the naive male PSC has an unmethylated allele of the XIST gene,

and/or

an expression level of transcription factor E3 (TFE3) characterized by a nucleus to cytoplasm expression ratio which is equal to or higher than 1 as determined by an immunostaining assay.

As used herein the phrase *"pluripotent stem cell (PSC)"* refers to an undifferentiated cell (e.g., a primate cell, a mammalian cell) capable of differentiating into all three embryonic germ cell layers, *i.e.,* to the mesoderm, ectoderm and endoderm embryonic germ layers.

According to some embodiments of the invention, the pluripotent stem cell is selected from the group consisting of embryonic stem cell (ESC), induced pluripotent stem cells (iPSCs), and embryonic germ cell (EGC).

According to some embodiments of the invention, the primate naive pluripotent stem cell is of homo sapiens (human), monkey, chimpanzee, Gorillas, Rhesus and/or Baboon.

The phrase *"naive pluripotent stem cell (PSC)"* refers to a cell capable of forming a PSC, and that exhibits a pre-X-inactivation state, and therefore is considered to be the origin of the PSC.

The pre-X-inactivation state according to some embodiments of the invention is characterized by presence of two unmethylated alleles of an X-inactive specific transcript (XIST) gene in the female cell, and presence an unmethylated allele of the XIST gene in a male cell.

The XIST gene is located on human Xq13.2 chromosome and has the sequence depicted in clone NC_000023.10 (73040486..73072588, complement, based on GenBank version GRCh37.p10. The XIST gene has a non-coding RNA which is provided in GenBank Accession NO. NR_001564.2 (SEQ ID NO:20).

According to some embodiments of the invention, presence of two unmethylated alleles of XIST gene in a female cell refers to having below about 20% of CpG methylated reads sequenced in the XIST promoter, e.g., below about 19%, below about 18%, below about 17%, below about 16%, below about 15%, below about 14%, below about 13%, below about 12%, below about 11%, below about 10%, below about 9%, below about 8%, below about 7%, below about 6%, below about 5%, below about 4%, below about 3%, below about 2%, below about 1%, e.g., 0% (e.g., complete absence) of CpG methylated reads sequenced in the XIST promoter.

According to some embodiments of the invention, presence of one unmethylated allele of XIST gene in a male cell refers to having below about 20% of CpG methylated reads sequenced in the XIST promoter, e.g., below about 19%, below about 18%, below about 17%, below about 16%, below about 15%, below about 14%, below about 13%, below about 12%, below about 11%, below about 10%, below about 9%, below about 8%, below about 7%, below about 6%, below about 5%, below about 4%, below about 3%, below about 2%, below about 1%, e.g., 0% of CpG methylated reads sequenced in the XIST promoter.

A non-limited example of the XIST promoter which includes CpG islands which can be either methylated or unmethylated is provided in the XIST promoter amplicon set forth by SEQ ID NO:70.

According to some embodiments of the invention, the human naive PSC is characterized by a reduced methylation of CpG islands as compared to a level of methylation of the CpG islands in a human primed PSC.

Thus, as shown in Figure 30G, human naive iPSCs and human naive ESCs are characterized by significantly low levels of total methylated cytosine out of the total guanine nucleotides in each cell (e.g., 1-2%, Figure 30G) as determined by Liquid Chromatography - Mass Spectrometry (LC-MS) quantitative analysis.

According to some embodiments of the invention, the human naive PSC is characterized by 0-3% of total methylated cytosine out of the total Guanine nucleotides in the naive PSC cell. For comparison, the primed PSC or a somatic cell has between 3.5%-5% of total methylated cytosine out of the total Guanine nucleotides in the primed PSC cell.

Thus, the naive pluripotent stem cell of some embodiments of the invention is in a naive state.

As used herein the phrase "naive state" refers to being in an undifferentiated state wherein both alleles of the X-inactive specific transcript (XIST) gene of the female cell are unmethylated, or wherein the XIST allele of the male cell is unmethylated.

It should be noted that the naive PSCs of some embodiments of the invention (which are in a pre-X inactivation and a naive state) can upon differentiation inactivate one of the X chromosome alleles and methylate one of the XIST genes.

According to some embodiments of the invention, the naive PSC maintains the naive state (as defined hereinabove) while being maintained (e.g., cultured) in the presence of ERK1/2 inhibitors (e.g., as exemplified here in below).

According to some embodiments of the invention, the naive PSC maintains the naive state (as defined hereinabove) while being maintained (e.g., cultured) in the absence of TGFβ signaling inhibition (e.g., in the absence of TGFβi).

According to some embodiments of the invention, the naive PSC maintains the naive state (as defined hereinabove) while being maintained (e.g., cultured) in the presence of TGFβ stimulation, e.g., in the presence of TGFβ1 and/or FGF2 stimulation.

According to some embodiments of the invention, the naive PSC maintains the naive state (as defined hereinabove) while being maintained (e.g., cultured) in the presence of ERK1/2 inhibitors and in the presence of TGFβ1 stimulation (e.g., by addition of TGFβ1) and/or FGF2 stimulation.

The phrase *"primed PSC" or "conventional PSC"* which are interchangeably used herein refers to a PSC which are known to date, e.g., human embryonic stem cells (hESC), human induced pluripotent stem cells (hiPSC), and human embryonic germ cells (hEGC), which are characterized by one methylated allele of XIST and one unmethylated allele of XIST in the female cell, and by one methylated allele in the male cell.

As used herein the term *"isolated"* refers to at least partially separated from the natural environment e.g., from the primate (e.g., mammalian) embryo or the primate (e.g., mammalian) body.

The phrase "embryonic stem cells" refers to embryonic cells which are capable of differentiating into cells of all three embryonic germ layers *(i.e.*, endoderm, ectoderm and mesoderm), or remaining in an undifferentiated state. The phrase "embryonic stem cells" may comprise cells which are obtained from the embryonic tissue formed after gestation (e.g., blastocyst) before implantation of the embryo (*i.e.*, a pre-implantation blastocyst), extended blastocyst cells (EBCs) which are obtained from a post-implantation/pre-gastrulation stage blastocyst (see WO2006/040763) and embryonic germ (EG) cells which are obtained from the genital tissue of a fetus any time during gestation, preferably before 10 weeks of gestation.

Induced pluripotent stem cells (iPS; embryonic-like stem cells), are cells obtained by de-differentiation of adult somatic cells which are endowed with pluripotency (*i.e.*, being capable of differentiating into the three embryonic germ cell layers, *i.e.,* endoderm, ectoderm and mesoderm). According to some embodiments of the invention, such cells are obtained from a differentiated tissue (e.g., a somatic tissue such as skin) and undergo de-differentiation by genetic manipulation which re-program the cell to acquire embryonic stem cells characteristics. According to some embodiments of the invention, the induced pluripotent stem cells are formed by inducing the expression of Oct-4, Sox2, Kfl4 and c-Myc in a somatic stem cell.

The embryonic stem cells of some embodiments of the invention can be obtained using well-known cell-culture methods. For example, human embryonic stem cells can be isolated from human blastocysts. Human blastocysts are typically obtained from human *in vivo* preimplantation embryos or from *in vitro* fertilized (IVF) embryos. Alternatively, a single cell human embryo can be expanded to the blastocyst stage. For the isolation of human ES cells the zona pellucida is removed from the blastocyst and the inner cell mass (ICM) is isolated by immunosurgery, in which the trophectoderm cells are lysed and removed from the intact ICM by gentle pipetting. The ICM is then plated in a tissue culture flask containing the appropriate medium which enables its outgrowth. Following 9 to 15 days, the ICM derived outgrowth is dissociated into clumps either by a mechanical dissociation or by an enzymatic degradation and the cells are then re-plated on a fresh tissue culture medium. Colonies demonstrating undifferentiated morphology are individually selected by micropipette, mechanically dissociated into clumps, and re-plated. Resulting ES cells are then routinely split every 4-7 days. For further details on methods of preparation human ES cells see Thomson et al., [U.S. Pat. No. 5,843,780; Science 282: 1145, 1998; Curr. Top. Dev. Biol. 38: 133, 1998; Proc. Natl. Acad. Sci. USA 92: 7844, 1995]; Bongso et al., [Hum Reprod 4: 706, 1989]; and Gardner et al., [Fertil. Steril. 69: 84, 1998].

Another method for preparing ES cells is described in Chung et al., Cell Stem Cell, Volume 2, Issue 2, 113-117, 7 February 2008. This method comprises removing a single cell from an embryo during an in vitro fertilization process. The embryo is not destroyed in this process.

It will be appreciated that commercially available stem cells can also be used according to some embodiments of the invention. Human ES cells can be purchased from the NIH human embryonic stem cells registry [Hypertext Transfer Protocol://grants (dot) nih (dot) gov/stem_cells/registry/current (dot) htm]. Non-limiting examples of commercially available embryonic stem cell lines are BG01, BG02, BG03, BG04, CY12, CY30, CY92, CY10, TE03, TE32, CHB-4, CHB-5, CHB-6, CHB-8, CHB-9, CHB-10, CHB-11, CHB-12, HUES 1, HUES 2, HUES 3, HUES 4, HUES 5, HUES 6, HUES 7, HUES 8, HUES 9, HUES 10, HUES 11, HUES 12, HUES 13, HUES 14, HUES 15, HUES 16, HUES 17, HUES 18, HUES 19, HUES 20, HUES 21, HUES 22, HUES 23, HUES 24, HUES 25, HUES 26, HUES 27, HUES 28, CyT49, RUES3,

WA01, UCSF4, NYUES1, NYUES2, NYUES3, NYUES4, NYUES5, NYUES6, NYUES7, UCLA 1, UCLA 2, UCLA 3, WA077 (H7), WA09 (H9), WA13 (H13), WA14 (H14), HUES 62, HUES 63, HUES 64, CT1, CT2, CT3, CT4, MA135, Eneavour-2, WIBR1, WIBR2, WIBR3, WIBR4, WIBR5, WIBR6, HUES 45, Shef 3, Shef 6, BJNhem19, BJNhem20, SA001, SA001.

In addition, ES cells can be obtained from other species as well, including mouse (Mills and Bradley, 2001), golden hamster [Doetschman et al., 1988, Dev Biol. 127: 224-7], rat [Iannaccone et al., 1994, Dev Biol. 163: 288-92] rabbit [Giles et al. 1993, Mol Reprod Dev. 36: 130-8; Graves & Moreadith, 1993, Mol Reprod Dev. 1993, 36: 424-33], several domestic animal species [Notarianni et al., 1991, J Reprod Fertil Suppl. 43: 255-60; Wheeler 1994, Reprod Fertil Dev. 6: 563-8; Mitalipova et al., 2001, Cloning. 3: 59-67] and non-human primate species (Rhesus monkey and marmoset) [Thomson et al., 1995, Proc Natl Acad Sci U S A. 92: 7844-8; Thomson et al., 1996, Biol Reprod. 55: 254-9].

Extended blastocyst cells (EBCs) can be obtained from a blastocyst of at least nine days post fertilization at a stage prior to gastrulation. Prior to culturing the blastocyst, the zona pellucida is digested [for example by Tyrode's acidic solution (Sigma Aldrich, St Louis, MO, USA)] so as to expose the inner cell mass. The blastocysts are then cultured as whole embryos for at least nine and no more than fourteen days post fertilization (*i.e.*, prior to the gastrulation event) *in vitro* using standard embryonic stem cell culturing methods.

EG cells are prepared from the primordial germ cells obtained from fetuses of about 8-11 weeks of gestation (in the case of a human fetus) using laboratory techniques known to anyone skilled in the arts. The genital ridges are dissociated and cut into small chunks which are thereafter disaggregated into cells by mechanical dissociation. The EG cells are then grown in tissue culture flasks with the appropriate medium. The cells are cultured with daily replacement of medium until a cell morphology consistent with EG cells is observed, typically after 7-30 days or 1-4 passages. For additional details on methods of preparation human EG cells see Shamblott et al., [Proc. Natl. Acad. Sci. USA 95: 13726, 1998] and U.S. Pat. No. 6,090,622.

Induced pluripotent stem cells (iPS) (embryonic-like stem cells) can be generated from somatic cells by genetic manipulation of somatic cells, e.g., by retroviral

transduction of somatic cells such as fibroblasts, hepatocytes, gastric epithelial cells with transcription factors such as Oct-3/4, Sox2, c-Myc, and KLF4 [Yamanaka S, Cell Stem Cell. 2007, 1(1):39-49; Aoi T, et al., Generation of Pluripotent Stem Cells from Adult Mouse Liver and Stomach Cells. Science. 2008 Feb 14. (Epub ahead of print); IH Park, Zhao R, West JA, et al. Reprogramming of human somatic cells to pluripotency with defined factors. Nature 2008;451:141-146; K Takahashi, Tanabe K, Ohnuki M, et al. Induction of pluripotent stem cells from adult human fibroblasts by defined factors. Cell 2007;131:861-872]. Other embryonic-like stem cells can be generated by nuclear transfer to oocytes, fusion with embryonic stem cells or nuclear transfer into zygotes if the recipient cells are arrested in mitosis.

Chromosome X inactivation is an early developmental process in mammalian females that transcriptionally silences one of the pair of X chromosomes, thus providing dosage equivalence between males and females. The process is regulated by several factors, including a region of chromosome X called the X inactivation center (XIC). The XIC comprises several non-coding and protein-coding genes, and XIST gene was the first non-coding gene identified within the XIC.

When XIST bodies are present, then XIST is exclusively expressed from the XIC of the inactive X chromosome, and is essential for the spread of X-inactivation.

The methylation status of the XIST gene can be determined by various methods such as bisulfite sequencing [Lengner Cell 141, 872–883 (2010); Hanna et al., Cell 143, 508–525 (2010), each of which is fully incorporated herein by reference in its entirety] of the promoter region of the XIST gene. The XIST promoter region can be amplified by the following PCR primers: Forward primer (used on bisulfite treated DNA): 5'-taa att tta aat taa tta aat tat (SEQ ID NO:22), and Reverse primer (used on bisulfite treated DNA): 5'- tgt ttt aga aag aat ttt aag tgt aga ga (SEQ ID NO:23). The amplicon region amplified by the above primers (203 bp covering human XIST transcription start site) is provided in SEQ ID NO:70. A representative result of such XIST bisulfite sequencing is shown in Figure 23A. The CpG islands in the XIST promoter amplicon are highlighted in yellow in Figure 27.

Following is a non-limiting description of a methylation specific PCR assay for the XIST gene. Bisulfite treatment of genomic DNA is performed with the EpiTect Bisulfite kit (Qiagen, Germany). Methylation-specific PCR (MS-PCR) utilizes this

sodium bisulfite treatment to distinguish methylated from unmethylated DNA. Purified, non-methylated and methylated human DNA standards (for negative and positive controls in methylation detection application) include the Human Methylated & Non-methylated DNA set (Zymo Research, USA). Each sample is analyzed in two independent MS-PCR reactions. PCR reactions included 25 µl PCR reaction mix which contained 2X PCR HotStart Premix buffer (Takara, Tokyo, Japan), 0.5 µM primer-M forward and 0.5 µM primer-M reverse in the PCR reaction amplifying the methylated imprint specifically or 0.5 µM primer-U forward and 0.5 µM primer-U reverse in the unmethylated PCR, and 2 µl of bisulfite-modified DNA. Primer pairs for methylation and unmethylation specific PCR for *XIST* gene include: Unmethylation forward 5'-TGTTTTTTTGTTTATTGGGGTTGTG (SEQ ID NO:21; M97168, 691–715), and Unmethylation reverse 5'-ACAACTAACCTAAACCAAATTATACA (SEQ ID NO:67; M97168, 944–970); Methylation forward 5'-TGTTTTTTTGTTTATCGGGGTCGCG (SEQ ID NO:68; M97168, 691–715) and Methylation reverse 5'-CGAATTATACGACAAATCTAAAATAACG (SEQ ID NO:69; M97168, 927–954) can be used as described elsewhere (Kawakami T, et al., Lancet. 2004 Jan 3; 363(9402):40-2. XIST unmethylated DNA fragments in male-derived plasma as a tumour marker for testicular cancer; which is fully incorporated herein by reference in its entirety), and with the following PCR conditions: The polymerase is activated at 95°C for 5 minutes. DNA is amplified in 35 cycles at 94°C, 60°C, 72°C for 45 seconds each, followed by a final extension at 72°C for 5 minutes. The resulting PCR fragments are 264 bp (base pairs) for the methylated allele (M) and 280 bp for the unmethylated allele (U). PCR products are separated on a 2% agarose gel, stained with ethidium bromide and visualized under UV illumination.

Additionally or alternatively, the methylation status of the XIST gene can be determined using Southern blot analyses using methylation-sensitive restriction enzymes and probes specific to the XIST gene (or CpG islands), essentially as described in Lengner Cell 141, 872–883 (2010); and Hanna et al., Cell 143, 508–525 (2010), each of which is fully incorporated herein by reference in its entirety. Following is a non-limiting description of a methylation assay which can be used to determine the methylation status of the XIST gene in a cell (TAKASHI SADO et al., DEVELOPMENTAL DYNAMICS 205: 421-434 (1996). Mosaic Methylation of Xist

Gene Before Chromosome Inactivation in Undifferentiated Female Mouse Embryonic Stem and Embryonic Germ Cells; which is fully incorporated herein by reference in its entirety). Genomic DNA is prepared from the cells using known methods (e.g., Sambrook et al., Molecular Cloning: A Laboratory Manual, Cold Springs Harbor Laboratory, New York (1989, 1992)). Briefly, 10 μg of DNA is digested with one of methylation sensitive enzymes (HpaII, CfoI, MZuI, SacII, and AuaI) in combination with EcoRI or EcoRI + PuuII according to the manufacturers' recommendation. Digestion is carried out overnight with 10-fold excess of each enzyme in reaction volume of 300 μl. Restricted DNA is purified by phenol extraction, precipitated with ethanol, electrophoresed on 1% or 2% agarose gel, blotted onto Hybond N + (Amersham, Buckinghamshire, UK), and probed by a cDNA fragment of Xist 5' portion (probe 1) or a genomic *Hpa*I-*Mlu*I fragment of the 5' upstream region (probe 2) labeled by random priming. Subsequent washes are carried out in accordance with the membrane manufacturer's recommendation.

Thus, the skilled in the art is capable of distinguishing between an unmethylated allele of XIST and a methylated allele of XIST, and thus can easily distinguish between a female cell having two unmethylated alleles of the XIST gene or a female cell having one methylated and one unmethylated allele of XIST. Similarly, the skilled in the art can easily distinguish between a male cell having a methylated XIST allele or a male cell having an unmethylated XIST allele.

As mentioned, the isolated primate (e.g., human) naive PSC is in an undifferentiated and pluripotent state (capable of differentiating into all three embryonic germ layers).

Primed human PSCs such as hiPSCs or hESCs are induced to differentiation upon incubation with bone morphogenetic protein 4 (BMP4), JNK inhibitor, and P38 inhibitor [Hanna et al., Cell 143, 508–525 (2010); De Los Angeles, et al., *Curr. Opin. Genet. Dev.* 22, 272–282 (2012)].

Contrary to the known primed PSC, the naive PSC of some embodiments of the invention is “resistant” to induction of differentiation by BMP4, JNK inhibitor, and/or P38 inhibitor. Thus, as shown in Figures 21(A-L) -22(A-H), incubation of the naive PSC with BMP4 or forskolin did not alter the undifferentiated and pluripotent state of the Naive PSCs.

According to some embodiments of the invention, when the isolated naive PSC is incubated in the presence of an agent selected from the group consisting of Bone morphogenetic protein 4 (BMP4), JNK inhibitor, and P38 inhibitor, the naive PSC remains in the pluripotent state.

According to some embodiments of the invention, the naive PSC has an inhibited p38 pathway as compared to a primed PSC. For example, p38 activity is inhibited in the naive PSC.

According to some embodiments of the invention, the level of p38 RNA and/or phosphorylated p38 protein in the naive PSC is less than about 30%, e.g., less than about 20%, e.g., less than about 5%, e.g., less than about 0.5%, e.g., less than about 0.1% as compared to the level of p38 RNA and/or phosphorylated p38 protein, respectively, in a non-naive PSC incubated and/or cultured under the same conditions, yet without being subject to p38 inhibition.

According to some embodiments of the invention, the naive PSC has an inhibited JNK pathway as compared to a primed PSC. For example, JNK activity is inhibited in the naive PSC.

According to some embodiments of the invention, the level of JNK RNA and/or phosphorylated JNK protein in the naive PSC is less than about 30%, e.g., less than about 20%, e.g., less than about 5%, e.g., less than about 0.5%, e.g., less than about 0.1% as compared to the level of JNK RNA and/or phosphorylated JNK protein, respectively, in a non-naive PSC incubated and/or cultured under the same conditions, yet without being subject to JNK inhibition.

According to some embodiments of the invention, the naive PSC has an inhibited ROCK pathway as compared to a primed PSC. For example, ROCK activity is inhibited in the naive PSC.

According to some embodiments of the invention, the level of ROCK RNA and/or phosphorylated ROCK protein in the naive PSC is less than about 30%, e.g., less than about 20%, e.g., less than about 5%, e.g., less than about 0.5%, e.g., less than about 0.1% as compared to the level of ROCK RNA and/or phosphorylated ROCK protein, respectively, in a non-naive PSC incubated and/or cultured under the same conditions, yet without being subject to ROCK inhibition.

Monitoring the differentiation state of pluripotent stem cells - During the culturing step the pluripotent stem cells are further monitored for their differentiation state. Cell differentiation can be determined upon examination of cell or tissue-specific markers which are known to be indicative of differentiation. For example, primate PSCs may express the stage-specific embryonic antigen (SSEA) 4, the tumour-rejecting antigen (TRA)-1-60 and TRA-1-81. Undifferentiated pluripotent stem cells highly express SSEA4, TRA-1-60 and TRA-1-81 markers and down regulate their expression upon differentiation.

Tissue/cell specific markers can be detected using immunological techniques well known in the art [Thomson JA et al., (1998). Science 282: 1145-7]. Examples include, but are not limited to, flow cytometry for membrane-bound markers, immunohistochemistry for extracellular and intracellular markers and enzymatic immunoassay, for secreted molecular markers.

Determination of PSC differentiation can also be effected via measurements of alkaline phosphatase activity. Undifferentiated human ES cells have alkaline phosphatase activity which can be detected by fixing the cells with 4% paraformaldehyde and developing with the Vector Red substrate kit according to manufacturer's instructions (Vector Laboratories, Burlingame, California, USA).

According to an aspect of some embodiments of the invention, there is provided an isolated population of naive PSCs comprising at least about 10%, at least about 12%, at least about 14%, at least about 16%, at least about 18%, at least about 20%, at least about 22%, at least about 24%, at least about 26%, at least about 28%, at least about 30%, at least about 32%, at least about 34%, at least about 36%, at least about 38%, at least about 40%, at least about 42%, at least about 44%, at least about 46%, at least about 48%, at least about 50%, at least about 55%, at least about 60%, at least about 65%, at least about 70%, at least about 75%, at least about 80%, at least about 85%, at least about 90%, at least about 95%, at least about 96%, at least about 97%, at least about 98%, at least about 99%, e.g., 100% of the isolated human naive PSC cells of some embodiments of the invention.

According to a specific embodiment of the invention the isolated population of cells is positive for one or more markers. Positive is also abbreviated by (+). Positive for a marker means that at least about 70%, 80%, 85%, 90%, 95%, or 100% of the cells

in the population present detectable levels of the marker (e.g., OCT4, NANOG, TRA1-81, TRA1-60, SSEA3, SSEA4) assayed by a method known to those of skill in the art [e.g., fluorescent activated cell sorter (FACS) analysis, immunofluorescence, immunohistochemistry, Western blot analysis]. Thus, for example, the cells stain positively with anti SSEA3 antibody as determined using FACS or stained positive by immunofluorescence or immunohistochemistry using the OCT4 antibody. The OCT4, NANOG, TRA1-81, TRA1-60, SSEA3, SSEA4-positive cells according to this embodiment, stain negatively to one or more markers, e.g., SSEA1. Negative is also abbreviated by (-). Negative for a marker means that no more than about 30%, no more than about 25%, no more than about 20%, no more than about 15%, no more than about 10%, no more than about 5%, no more than about 4%, no more than about 3%, no more than about 2%, no more than about 1%, of the cells in the population present detectable levels of the marker (e.g., SSEA1) assayed by a method known to those of skill in the art such as immunofluorescence or FACS. Such a marker presentation either of a single cell or an isolated population of cells is also referred to as a signature.

As shown in Figures 12F and 25B-M, the present inventors have shown a population of stem cells having about 99% of naive PSC.

According to some embodiments of the invention, the naive PSC expresses XIST.

Methods of detecting XIST expression are known in the art and include for example reverse transcriptase - polymerase chain reaction (RT-PCR) analysis using XIST specific PCR primers, e.g., the forward primer: 5'-AGGGAGCAGTTTGCCCTACT (SEQ ID NO:24), and the reverse primer: 5'-CACATGCAGCGTGGTATCTT (SEQ ID NO: 25), as shown in Figure 23B.

According to some embodiments of the invention, the naive PSC is devoid of XIST bodies.

As used herein the phrase "XIST bodies" refers to a XIST-coated inactive X chromosome.

Methods of detecting XIST bodies are known in the art and include for example RNA fluorescent *in situ* hybridization. RNA fluorescence *in situ* hybridization (FISH) is carried out as previously described [Hanna J., et al., *Cell* 143, 508–525]. Briefly, human pluripotent stem cells are harvested, MEF-depleted, and cytospun onto glass slides

before fixation. cDNA probes are generated to XIST exon 1 (GenBank Accession No. U80460: 61251–69449, SEQ ID NO:26) and exon 6 (GenBank Accession No. U80460: 75081–78658, SEQ ID NO:27) and labeled by nick translation (Roche) with Cy3- dUTP (Amersham), and Cot-1 DNA is labeled with fluorescein- 12-dUTP using the Prime-It Fluor Labeling Kit (Stratagene).

According to some embodiments of the invention, the naive PSC is devoid of an H3K27me3/polycomb focus.

As used herein the phrase "H3K27me3/polycomb focus" refers to nuclear focus obtained following immuno-staining that corresponds to condensed inactive X chromosome.

Methods of detecting H3K27me3/polycomb focus are known in the art and include for example, the use of immuno-fluorescence analysis using anti H3K27me3 antibodies (e.g., Rabbit anti H3K27me3, Millipore, CA, USA Catalogue number 07-449), as shown for example in Figures 23C-D.

According to some embodiments of the invention, the naive PSC has a low XIST expression level while being in the naive state, without inactivation of any of the X chromosomes and without presence of XIST bodies.

According to some embodiments of the invention, the naive PSC is capable of X-inactivation when induced to differentiate.

According to some embodiments of the invention, the naive PSC is capable of differentiation into the endodermal, mesodermal and ectodermal embryonic germ layers.

Methods of determining ability of stem cells to differentiate into the endodermal, mesodermal and ectodermal embryonic germ layers include for example generation of embryoid bodies (*in vitro*) or teratomas (*in vivo*) as shown in the Examples section which follows and in Figures such as 12L-N, 13K-M, 13S-U, 19A-I, and 20A-T.

As used herein the phrase "embryoid bodies" (EBs) refers to three dimensional multicellular aggregates of differentiated and undifferentiated cells derivatives of three embryonic germ layers.

Embryoid bodies are formed upon the removal of the naive PSCs from feeder layers or feeder cells-free culture systems. Naive PSCs removal can be performed using type IV Collagenase treatment or Trypsin for a limited time. Following dissociation

from the culturing surface, the cells are transferred to tissue culture plates containing a culture medium supplemented with serum and amino acids.

During the culturing period, EBs are further monitored for their differentiation state. Cell differentiation can be determined upon examination of cell or tissue-specific markers which are known to be indicative of differentiation. For example, EB-derived-differentiated cells may express the neurofilament 68 KD which is a characteristic marker of the ectoderm cell lineage.

The differentiation level of the EB cells can be monitored by following the loss of expression of Oct-4, and the increased expression level of other markers such as α-fetoprotein, NF-68 kDa, α-cardiac and albumin. Methods useful for monitoring the expression level of specific genes are well known in the art and include RT-PCR, semi-quantitative RT-PCR, Northern blot, RNA *in situ* hybridization, Western blot analysis and immunohistochemistry.

Teratomas: The pluripotent capacity of the naive PSCs of some embodiments of the invention can also be confirmed by injecting cells into SCID mice [Evans MJ and Kaufman M (1983). Pluripotential cells grown directly from normal mouse embryos. Cancer Surv. 2: 185-208], which upon injection form teratomas. Teratomas are fixed using 4 % paraformaldehyde and histologically examined for the three germ layers (*i.e.*, endoderm, mesoderm and ectoderm).

In addition to monitoring a differentiation state, the naive PSCs are often also being monitored for karyotype, in order to verify cytological euploidity, wherein all chromosomes are present and not detectably altered during culturing. Cultured naive PSCs can be karyotyped using a standard Giemsa staining and compared to published karyotypes of the corresponding species.

According to some embodiments of the invention, the naive PSC is capable of being maintained in the undifferentiated and pluripotent state, while maintaining the naive state (as defined above) for more than about 20 passages in culture, e.g., for at least about 25, about 30, about 35, about 40, about 45, about 50, about 55, about 60, about 65, about 70, about 75 and about 80 passages while in culture.

According to some embodiments of the invention, the naive PSC which is maintained in the undifferentiated, pluripotent and naive state (as defined above), expresses significantly lower levels SOX1 as compared to the level of expression present

in primed PSC (e.g., primed ESC) under identical SOX1 assay conditions, and wherein the primed PSC exhibits one methylated and one unmethylated allele of XIST (in a female cell) or one methylated allele of XIST (in a male cell); expresses XIST; exhibits XIST bodies; and exhibits a H3K27me3/polycomb focus.

According to some embodiments of the invention, the naive PSC expresses a lower level of MHC class I as compared to a primed PSC under identical detection assay conditions, and wherein the primed PSC exhibits one methylated and one unmethylated allele of XIST (in a female cell) or one methylated allele of XIST (in a male cell); expresses XIST; exhibits XIST bodies; and exhibits a H3K27me3/polycomb focus.

The level of MHC class I can be determined by various methods known in the art such as FACS analysis using specific antibodies to detect the surface expression of the MHC class I molecules (e.g., see Figures 24B and 24C), and using fluorescently labeled anti HLA-A,B,C antibody (BD Biosciences).

According to some embodiments of the invention, the naive PSC is characterized by at least about 10%, at least about 20%, at least about 30%, at least about 40%, at least about 50%, at least about 60%, at least about 70%, at least about 80%, at least about 90% more RNA polymerase II pausing on chromosomes as compared to a primed PSC under identical assay conditions, and wherein the primed PSC exhibits one methylated and one unmethylated allele of XIST (in a female cell) or one methylated allele of XIST (in a male cell); expresses XIST; exhibits XIST bodies; and exhibits a H3K27me3/polycomb focus.

According to some embodiments of the invention, the naive PSC exhibiting a pre-X inactivation status similar to the pre-X inactivation status of a human Inner cell mass (ICM).

According to an aspect of some embodiments of the invention, there is provided a cell culture comprising the isolated naive PSC of some embodiments of the invention, or the isolated population of naive PSCs of some embodiments of the invention and a culture medium.

According to some embodiments of the invention, the culture medium is capable of maintaining the naive PSC in an undifferentiated and pluripotent state for at least 10 passages.

The cell culture can be maintained *in vitro*, under culturing conditions, in which the cells are being passaged for extended periods of time (e.g., for at least 20 passages, e.g., at least about 30, 40, 50, 60, 70, 80, 90, 100 passages or more), while maintaining the cells in their naive pluripotent and undifferentiated state.

As used herein the phrase "culture medium" refers to a solid or a liquid substance used to support the growth of stem cells and maintain them in an undifferentiated state. Preferably, the phrase "culture medium" as used herein refers to a liquid substance capable of maintaining the stem cells in an undifferentiated state. The culture medium used by the present invention can be a water-based medium which includes a combination of substances such as salts, nutrients, minerals, vitamins, amino acids, nucleic acids, proteins such as cytokines, growth factors and hormones, all of which are needed for cell proliferation and are capable of maintaining the stem cells in an undifferentiated state. For example, a culture medium can be a synthetic tissue culture medium such as Ko-DMEM (Gibco-Invitrogen Corporation products, Grand Island, NY, USA), DMEM/F12 (Gibco-Invitrogen Corporation products, Grand Island, NY, USA), or DMEM/F12 (Biological Industries, Biet Haemek, Israel), supplemented with the necessary additives as is further described hereinunder. Preferably, all ingredients included in the culture medium of the present invention are substantially pure, with a tissue culture grade.

The present inventors have identified a novel culture medium which can be used to generate naive PSC and maintain them in a pluripotent and undifferentiated state. Thus, as shown in Figures 12A-G, 85A-C, 102, 103, 104, and 105, and Tables 3, 4, and 5 in the Examples section which follows, following laborious experimentations the present inventors have uncovered the factors needed for maintaining naive PSCs in the "naive state", as was evidenced by the expression of OCT4-GFP+ (positive) cells and percentage of total methylated cytosine (% 5mdC).

According an aspect of some embodiments of the invention, there is provided a culture medium comprising an ERK1/2 inhibitor, a GSK3β inhibitor, a p38 inhibitor, a JNK inhibitor, a STAT3 activator and at least one agent selected from the group consisting of: basic fibroblast growth factor (bFGF), transforming growth factor beta 1 (TGFβ1), a protein kinase C (PKC) inhibitor, a ROCK inhibitor and a NOTCH inhibitor.

According an aspect of some embodiments of the invention, there is provided a culture medium comprising an ERK1/2 inhibitor, a GSK3β inhibitor, a p38 inhibitor, a JNK inhibitor, a STAT3 activator and at least one agent selected from the group consisting of: a transforming growth factor receptor (TGFR) inhibitor, a fibroblast growth factor receptor (FGFR) inhibitor, a protein kinase C (PKC) inhibitor, a ROCK inhibitor and a NOTCH inhibitor.

As used herein the term "STAT3" refers to the signal transducer and activator of transcription 3 gene product (acute-phase response factor) (Gene ID 6774). In response to cytokines and growth factors, STAT family members are phosphorylated by the receptor associated kinases, and then form homo- or heterodimers that translocate to the cell nucleus where they act as transcription activators. Known STAT3 activators include, but are not limited to, interferon (IFN), epidermal growth factor (EGF), interleukin 5 (IL5), interleukin 6 (IL6), hepatocyte growth factor (HGF), leukemia inhibitory factor (LIF) and bone morphogenetic protein 2 (BMP2).

According to some embodiments of the invention, the STAT3 activator, which is used by the medium, cells and/or methods of some embodiments of the invention is selected from the group consisting of LIF, IL6 and EGF.

According to some embodiments of the invention, the STAT3 activator, which is used by the medium, cells and/or methods of some embodiments of the invention is selected from the group consisting of LIF, and IL6.

According to some embodiments of the invention, the STAT3 activator, which is used by the medium, cells and/or methods of some embodiments of the invention is LIF.

According to some embodiments of the invention, the culture medium further comprising at least one additional agent selected from the group consisting of: insulin-like growth factor 1 (IGF1), insulin-like growth factor II (IGFII), a bone morphogenetic protein (BMP) signaling inhibitor, a Sonic Hedgehog pathway (SHH) inhibitor, an ERK5 inhibitor, Forskolin, Kenpaullone, BayK8644, Bix1294, and stem cell factor (SCF).

According to some embodiments of the invention, the culture medium further comprising at least one additional agent selected from the group consisting of: insulin-like growth factor 1 (IGF1), insulin-like growth factor II (IGFII), bone morphogenetic

protein 4 (BMP4), a Sonic Hedgehog pathway (SHH) inhibitor, an ERK5 inhibitor, Forskolin, Kenpaullone, BayK8644, Bix1294, and stem cell factor (SCF).

According to some embodiments of the invention, the STAT3 activator comprises the LIF, and wherein the at least one agent comprises the PKC inhibitor.

According to some embodiments of the invention, the culture medium further comprising FGFR inhibitor.

According to some embodiments of the invention, the culture medium further comprising TGFR inhibitor.

According to some embodiments of the invention, the STAT3 activator comprises the LIF and wherein the at least one agent comprises the TGFβ1 and the protein kinase C inhibitor.

According to some embodiments of the invention, the culture medium further comprising an FGFR inhibitor.

According to some embodiments of the invention, the STAT3 activator comprises the LIF, and wherein the at least one agent comprises the bFGF and the TGFβ1.

According to some embodiments of the invention, the culture medium further comprising a ROCK inhibitor.

According to some embodiments of the invention, the culture medium further comprising a protein kinase C inhibitor.

According to some embodiments of the invention, the STAT3 activator comprises the LIF and wherein the at least one agent comprises the bFGF, the ROCK inhibitor, a bone morphogenetic protein (BMP) inhibitor, the NOTCH inhibitor, and a transforming growth factor receptor (TGFR) inhibitor.

According to some embodiments of the invention, the culture medium further comprising a Sonic Hedgehog pathway (SHH) inhibitor.

According to some embodiments of the invention, the STAT3 activator comprises the LIF and wherein the at least one agent comprises the NOTCH inhibitor, and a fibroblast growth factor receptor (FGFR) inhibitor.

According to some embodiments of the invention, the culture medium further comprises an agent selected from the group consisting of insulin-like growth factor II (IGFII), stem cell factor (SCF) and transforming growth factor beta 1 (TGFβ1).

According to some embodiments of the invention, the culture medium comprising leukemia inhibitor factor (LIF), an ERK1/2 inhibitor, a GSK3b inhibitor, a p38 inhibitor, a JNK inhibitor, and a protein kinase C inhibitor.

According to some embodiments of the invention, the culture medium further comprising a fibroblast growth factor receptor (FGFR) inhibitor (FGFRi).

According to some embodiments of the invention, the culture medium further comprising a transforming growth factor receptor inhibitor (TGFRi).

According to some embodiments of the invention, the culture medium which comprises leukemia inhibitor factor (LIF), an ERK1/2 inhibitor, a GSK3b inhibitor, a p38 inhibitor, a JNK inhibitor, and a protein kinase C inhibitor, further comprises a fibroblast growth factor receptor (FGFR) inhibitor (FGFRi).

According to some embodiments of the invention, the culture medium which comprises leukemia inhibitor factor (LIF), an ERK1/2 inhibitor, a GSK3b inhibitor, a p38 inhibitor, a JNK inhibitor, and a protein kinase C inhibitor, further comprises a transforming growth factor receptor inhibitor (TGFRi).

According to some embodiments of the invention, the culture medium which comprises leukemia inhibitor factor (LIF), an ERK1/2 inhibitor, a GSK3b inhibitor, a p38 inhibitor, a JNK inhibitor, and a protein kinase C inhibitor, further comprises a fibroblast growth factor receptor (FGFR) inhibitor (FGFRi) and a transforming growth factor receptor inhibitor (TGFRi).

According to some embodiments of the invention, the culture medium comprising leukemia inhibitor factor (LIF), an ERK1/2 inhibitor, a GSK3b inhibitor, a p38 inhibitor, a JNK inhibitor, TGFβ1 and a protein kinase C inhibitor.

According to some embodiments of the invention, medium which comprises leukemia inhibitor factor (LIF), an ERK1/2 inhibitor, a GSK3b inhibitor, a p38 inhibitor, a JNK inhibitor, TGFβ1 and a protein kinase C inhibitor further comprising FGFR inhibitor (FGFRi).

According to some embodiments of the invention, the culture medium comprising leukemia inhibitor factor (LIF), an ERK1/2 inhibitor, a GSK3b inhibitor, a p38 inhibitor, a JNK inhibitor, basic fibroblast growth factor (bFGF) and transforming growth factor-beta 1 (TGFβ1).

As used herein the term "leukemia inhibitor factor (LIF)" refers to a polypeptide which comprises the amino acid sequence as set forth by GenBank Accession No. NP_001244064.1 (SEQ ID NO:119), encoded by the nucleotide sequence set forth in GenBank Accession No. NM_001257135 (SEQ ID NO:30). Preferably, the LIF used by the method according to some embodiments of the invention is capable of supporting, along with other factors which are described herein, the undifferentiated growth of naive primate (e.g., human) PSCs, while maintaining their pluripotent capacity. LIF can be obtained from various manufacturers such as Millipore, Peprotech, and R&D systems.

According to some embodiments of the invention, LIF is provided at a concentration range from about 0.5 nanogram per milliliter (ng/ml) to about 1000 ng/ml, e.g., about 1-1000 ng/ml, e.g., about 1-900 ng/ml, e.g., about 1-800 ng/ml, e.g., about 1-700 ng/ml, e.g., about 1-600 ng/ml, e.g., about 1-500 ng/ml, e.g., about 1-400 ng/ml, e.g., about 1-300 ng/ml, e.g., about 1-200 ng/ml, e.g., about 1-100 ng/ml, e.g., about 1-50 ng/ml, e.g., about 2-50 ng/ml, e.g., about 4-50 ng/ml, e.g., about 5-50 ng/ml, e.g., about 10-50 ng/ml, e.g., about 10-40 ng/ml, e.g., about 10-30 ng/ml, e.g., about 20 ng/ml.

As used herein the term "interleukin 6 (IL6)" refers to a polypeptide which comprises the amino acid sequence set forth by GenBank Accession No. NP_000591.1 (SEQ ID NO: 120), which is encoded by the nucleic acid set forth by GenBank Accession No. NM_000600.3 (SEQ ID NO: 111). Preferably, the IL6 used by the method according to some embodiments of the invention is capable of supporting, along with other factors which are described herein, the undifferentiated growth of naive primate (e.g., human) PSCs, while maintaining their pluripotent capacity. IL6 can be obtained from various manufacturers such as Speed BioSystems, Millipore, Peprotech, and R&D systems.

According to some embodiments of the invention, IL6 is provided at a concentration range from about 0.1 ng/ml to about 100 ng/ml, e.g., about 0.1-90 ng/ml, e.g., about 0.1-80 ng/ml, e.g., about 0.1-70 ng/ml, e.g., about 0.1-50 ng/ml, e.g., about 0.1-40 ng/ml, e.g., about 0.1-30 ng/ml, e.g., about 0.1-20 ng/ml, e.g., about 0.1-10 ng/ml, e.g., about 0.1-8 ng/ml, e.g., about 0.1-7 ng/ml, e.g., about 0.1-6 ng/ml, e.g.,

about 0.1-5 ng/ml, e.g., about 0.1-4 ng/ml, e.g., about 0.1-3 ng/ml, e.g., about 0.1-4 ng/ml, e.g., about 0.5-4 ng/ml, e.g., about 0.5-4 ng/ml, e.g., about 3 ng/ml.

As used herein the phrase "TGFβ1" refers to an isoform beta-1 (β1) of the transforming growth factor beta (e.g., homo sapiens $TGF\beta_1$, GenBank Accession No. NP_000651; SEQ ID NO:28, which is encoded by the sequence depicted in GenBank Accession No. NM_000660.5; SEQ ID NO:31). TGFβ acts in inducing transformation and also acts as a negative autocrine growth factor. TGFβ1 isoform can be obtained from various commercial sources such as R&D Systems Minneapolis MN, USA.

According to some embodiments of the invention, TGFβ1 is provided at a concentration range from about 0.1 nanogram per milliliter (ng/ml) to about 500 ng/ml, e.g., about 0.1-400 ng/ml, e.g., about 0.1-300 ng/ml, e.g., about 0.1-200 ng/ml, e.g., about 0.1-100 ng/ml, e.g., about 0.1-50 ng/ml, e.g., about 0.1-30 ng/ml, e.g., about 0.1-20 ng/ml, e.g., about 0.1-10 ng/ml, e.g., about 0.1-8 ng/ml, e.g., about 0.1-7 ng/ml, e.g., about 0.1-6 ng/ml, e.g., about 0.1-5 ng/ml, e.g., about 0.1-4 ng/ml, e.g., about 0.1-3 ng/ml, e.g., about 0.1-2 ng/ml, e.g., about 0.5-2 ng/ml, e.g., about 0.5-1.5 ng/ml, e.g., about 1 ng/ml.

According to some embodiments of the invention, activators of TGF/ACTIVIN pathway including ACTIVIN A (also known as Inhibin beta A, INHBA, Gene ID: 3624; GenBank Accession No. NM_002192.2 (SEQ ID NO:123), which encodes GenBank Accession No. NP_002183.1; SEQ ID NO:117) can be used to replace TGFβ1.

According to some embodiments of the invention, the TGFβ1 cytokine can be replaced with recombinant Nodal and/or Activin.

The phrases "basic fibroblast growth factor (bFGF)" or "FGF2" which are interchangeably used herein refer to a polypeptide of the fibroblast growth factor (FGF) family, which bind heparin and possess broad mitogenic and angiogenic activities. The mRNA for the BFGF gene contains multiple polyadenylation sites, and is alternatively translated from non-AUG (CUG) and AUG initiation codons, resulting in five different isoforms with distinct properties. The CUG-initiated isoforms are localized in the nucleus and are responsible for the intracrine effect, whereas, the AUG-initiated form is mostly cytosolic and is responsible for the paracrine and autocrine effects of this FGF.

According to some embodiments of the invention, the bFGF used by the medium of some embodiments of the invention is provided in GenBank Accession No.

NP_001997 (SEQ ID NO:29). BFGF can be obtained from various manufacturers such as Peprotech, RnD systems, Millipore. According to some embodiments of the invention, the bFGF used by the medium of some embodiments of the invention is provided from R&D Systems (Catalog Number: 233-FB).

According to some embodiments of the invention, bFGF is provided at a concentration range from about 0.5 nanogram per milliliter (ng/ml) to about 500 ng/ml, e.g., about 1-500 ng/ml, e.g., about 1-400 ng/ml, e.g., about 1-300 ng/ml, e.g., about 1-200 ng/ml, e.g., about 1-100 ng/ml, e.g., about 1-80 ng/ml, e.g., about 1-70 ng/ml, e.g., about 1-70 ng/ml, e.g., about 1-60 ng/ml, e.g., about 1-50 ng/ml, e.g., about 1-40 ng/ml, e.g., about 1-30 ng/ml, e.g., about 1-20 ng/ml, e.g., about 2-20 ng/ml, e.g., about 2-10 ng/ml, e.g., about 3-10 ng/ml, e.g., about 4-10 ng/ml, e.g., about 8 ng/ml.

It will be appreciated that any of the proteinaceous factors used in the culture medium of some embodiments of the invention (e.g., the LIF, IL6, TGFβ1, or bFGF) can be recombinantly expressed or biochemically synthesized. In addition, naturally occurring proteinaceous factors such as bFGF and TGFβ can be purified from biological samples (e.g., from human serum, cell cultures) using methods well known in the art.

Biochemical synthesis of the proteinaceous factors of the present invention (e.g., the LIF, IL6, TGFβ1, or bFGF) can be performed using standard solid phase techniques. These methods include exclusive solid phase synthesis, partial solid phase synthesis methods, fragment condensation and classical solution synthesis.

Recombinant expression of the proteinaceous factors of the present invention (e.g., the LIF, IL6, TGFβ1, or bFGF) can be generated using recombinant techniques such as described by Bitter et al., (1987) Methods in Enzymol. 153:516-544, Studier et al. (1990) Methods in Enzymol. 185:60-89, Brisson et al. (1984) Nature 310:511-514, Takamatsu et al. (1987) EMBO J. 6:307-311, Coruzzi et al. (1984) EMBO J. 3:1671-1680, Brogli et al., (1984) Science 224:838-843, Gurley et al. (1986) Mol. Cell. Biol. 6:559-565 and Weissbach & Weissbach, 1988, Methods for Plant Molecular Biology, Academic Press, NY, Section VIII, pp 421-463.

For example, to generate the LIF, IL6, TGFβ1, or bFGF, a polynucleotide sequence encoding the LIF, IL6, TGFβ1, or bFGF [e.g., the polynucleotide set forth by SEQ ID NO: 30 (LIF, GenBank Accession No. NM_001257135), SEQ ID NO: 31 (TGFβ1, GenBank Accession NO. NM_000660), SEQ ID NO: 32 (BFGF, GenBank

Accession NO. NM_002006), SEQ ID NO:111 (IL6, GenBank Accession No. NM_000600.3)] is preferably ligated into a nucleic acid construct suitable for expression in a host cell [*i.e.*, a cell in which the polynucleotide encoding the polypeptide-of-choice (e.g., the LIF, IL6, TGFβ1, or bFGF) is expressed]. Preferably, to generate an LIF, IL6, TGFβ1, or bFGF with the amount and pattern of glycosylation as of the naturally occurring LIF, IL6, TGFβ1, or bFGF, the host cell employed is a eukaryotic host cell, more preferably a mammalian host cell such as human cell or CHO cell). Additional description of nucleic acid constructs (or expression vectors) which can be used to produce a polypeptide-of-interest (e.g., the proteinaceous factors described above) is provided hereinunder.

As used herein the term "ERK1" refers to the mitogen-activated protein kinase 3 (MAPK3) isoform 1 set forth by GenBank Accession No. NP_002737.2 (SEQ ID NO:33), the MAPK3 isoform 2 set forth by GenBank Accession No. NP_001035145.1 (SEQ ID NO:34), the MAPK3 isoform 3 set forth by GenBank Accession No. NP_001103361.1 (SEQ ID NO:35) and/or ERK1 set forth in GenBank Accession No. M84490 (SEQ ID NO:36) having the MAPK signaling activity.

As used herein the term "ERK2" refers to the mitogen-activated protein kinase 1 (MAPK1) set forth by GenBank Accession No. NP_002736.3 (SEQ ID NO:37) and/or GenBank Accession No. NP_620407.1 (SEQ ID NO:38) having the MAPK signaling activity.

As used herein the term "ERK1/2 inhibitor" refers to any molecule capable of inhibiting the activity of ERK1/2 as determined by Western blot protein detection of phosphorylated ERK1/2 proteins.

Non-limiting examples of ERK1/2 inhibitors include PD0325901 (AXONMEDCHEM - AXON 1408), PD98059 (AXONMEDCHEM - Axon 1223), and PD184352 (AXONMEDCHEM – AXON 1368); or even inhibitors of RAF (which is upstream of ERK) such as Sorafenib or SB (AXONMEDCHEM –AXON 1397).

According to some embodiments of the invention, PD0325901 is provided at a concentration range from about 0.01 microM (μM) to about 50 μM, e.g., between about 0.05-45 μM, e.g., between about 0.1-50 μM, e.g., between about 0.1-45 μM, e.g., between about 0.1-40 μM, e.g., between about 0.1-35 μM, e.g., between about 0.1-30 μM, e.g., between about 0.1-25 μM, e.g., between about 0.1-20 μM, e.g., between about

0.1-15 μM, e.g., between about 0.1-10 μM, e.g., between about 0.2-10 μM, e.g., between about 0.3-10 μM, e.g., between about 0.4-10 μM, e.g., between about 0.5-10 μM, e.g., between about 0.6-10 μM, e.g., between about 0.7-10 μM, e.g., between 0.8-10 μM, e.g., between 0.9-10 μM, e.g., between 0.9-9 μM, e.g., between 0.9-8 μM, e.g., between 0.9-7 μM, e.g., between 0.9-6 μM, e.g., between 0.8-5 μM, e.g., between 0.8-4 μM, e.g., between 0.8-3 μM, e.g., between 0.8-2 μM, e.g., between 0.8-1.5 μM, e.g., between 0.9-1.2 μM, e.g., about 1 μM.

According to some embodiments of the invention, PD98059 is provided at a concentration range from about 0.1 microM (μM) to about 70 μM, e.g., between about 0.1-65 μM, e.g., between about 0.1-55 μM, e.g., between about 0.1-50 μM, e.g., between about 0.1-45 μM, e.g., between about 0.1-40 μM, e.g., between about 0.1-35 μM, e.g., between about 0.1-30 μM, e.g., between about 0.1-25 μM, e.g., between about 0.1-20 μM, e.g., between about 0.1-15 μM, e.g., between about 2-20 μM, e.g., between about 5-15 μM, e.g., about 10 μM, e.g., between about 0.1-10 μM, e.g., between about 0.2-10 μM, e.g., between about 0.3-10 μM, e.g., between about 0.4-10 μM, e.g., between about 0.5-10 μM, e.g., between about 0.6-10 μM, e.g., between about 0.7-10 μM, e.g., between 0.8-10 μM, e.g., between 0.9-10 μM, e.g., between 0.9-9 μM, e.g., between 0.9-8 μM, e.g., between 0.9-7 μM, e.g., between 0.9-6 μM, e.g., between 0.8-5 μM, e.g., between 0.8-4 μM, e.g., between 0.8-3 μM, e.g., between 0.8-2 μM, e.g., between 0.8-1.5 μM, e.g., between 0.9-1.2 μM.

According to some embodiments of the invention, PD184352 is provided at a concentration range from about 0.1 microM (μM) to about 70 μM, e.g., between about 0.1-60 μM, e.g., between about 0.1-50 μM, e.g., between about 0.5-50 μM, e.g., between about 0.5-45 μM, e.g., between about 0.5-40 μM, e.g., between about 0.1-35 μM, e.g., between about 0.5-30 μM, e.g., between about 0.5-25 μM, e.g., between about 0.5-20 μM, e.g., between about 0.5-15 μM, e.g., between about 0.5-10 μM, e.g., between 0.5-9 μM, e.g., between 0.5-8 μM, e.g., between 0.5-7 μM, e.g., between 0.9-6 μM, e.g., between 0.8-5 μM, e.g., between 0.8-4 μM, e.g., between 0.8-3 μM, e.g., about 3 μM. e.g., between 0.8-2 μM, e.g., between 0.8-1.5 μM, e.g., between 0.9-1.2 μM.

According to some embodiments of the invention, Sorafenib is provided at a concentration range from about 0.1 microM (μM) to about 70 μM, e.g., between about 0.1-60 μM, e.g., between about 0.1-50 μM, e.g., between about 0.5-50 μM, e.g., between about 0.5-45 μM, e.g., between about 0.5-40 μM, e.g., between about 0.1-35 μM, e.g., between about 0.5-30 μM, e.g., between about 0.5-25 μM, e.g., between about 0.5-20 μM, e.g., between about 0.5-15 μM, e.g., between about 0.5-10 μM, e.g., between 0.5-9 μM, e.g., between 0.5-8 μM, e.g., between 0.5-7 μM, e.g., between 0.9-6 μM, e.g., between 0.8-5 μM, e.g., about 5 μM, e.g., between 0.8-4 μM, e.g., between 0.8-3 μM, e.g., between 0.8-2 μM, e.g., between 0.8-1.5 μM, e.g., between 0.9-1.2 μM.

As used herein the term "GSK3b" refers to the glycogen synthase kinase 3 beta protein set forth by GenBank Accession Nos. NP_002084.2 (SEQ ID NO: 121) and/or NP_001139628.1 (SEQ ID NO: 122) having the WNT signaling regulatory activity via its kinase activity.

As used herein the term "GSK3b inhibitor" refers to any molecule capable of inhibiting the activity of GSK3b as determined by specifically inhibiting levels of phosphorylated GSK3b (out of total GSK3b present in a cell).

Non-limiting examples of GSK3b inhibitors include CHIR99021 (AXONMEDCHEM – AXON 1386), BIO (AXONMEDCHEM – Axon 1693), and Kenpaullone (TOCRIS – cat no. 1398).

According to some embodiments of the invention, CHIR99021 is provided at a concentration range of between about 0.1-50 μM, e.g., from about 0.2 μM to about 50 μM, e.g., between about 0.2-45 μM, e.g., between about 0.2-50 μM, e.g., between about 0.2-45 μM, e.g., between about 0.2-40 μM, e.g., between about 0.2-35 μM, e.g., between about 0.2-30 μM, e.g., between about 0.2-25 μM, e.g., between about 0.2-20 μM, e.g., between about 0.2-15 μM, e.g., between about 0.2-10 μM, e.g., between about 0.2-10 μM, e.g., between about 0.3-10 μM, e.g., between about 0.4-10 μM, e.g., between about 0.5-10 μM, e.g., between about 0.6-10 μM, e.g., between about 0.7-10 μM, e.g., between 0.8-10 μM, e.g., between 0.9-10 μM, e.g., between 0.9-9 μM, e.g., between 1-8 μM, e.g., between 1-7 μM, e.g., between 1-6 μM, e.g., between 1-5 μM, e.g., between 2-4 μM, e.g., about 3 μM.

According to some embodiments of the invention, BIO is provided at a concentration range of between about 0.1-70 μM, e.g., from about 0.2 μM to about 70 μM, e.g., between about 0.2-60 μM, e.g., between about 0.2-55 μM, e.g., between about 0.2-50 μM, e.g., between about 0.2-45 μM, e.g., between about 0.2-40 μM, e.g., between about 0.2-35 μM, e.g., between about 0.2-30 μM, e.g., between about 0.2-25 μM, e.g., between about 0.2-20 μM, e.g., between about 0.2-15 μM, e.g., between about 0.2-10 μM, e.g., between about 0.3-10 μM, e.g., between about 0.4-10 μM, e.g., between about 0.5-10 μM, e.g., between about 0.6-10 μM, e.g., between about 0.7-10 μM, e.g., between 0.8-10 μM, e.g., between 0.9-10 μM, e.g., between 0.9-9 μM, e.g., between 1-8 μM, e.g., between 1-7 μM, e.g., between 1-6 μM, e.g., between 1-5 μM, e.g., about 5 μM, e.g., between 2-4 μM.

According to some embodiments of the invention, Kenpaullone is provided at a concentration range of between about 0.1-70 μM, e.g., from about 0.2 μM to about 70 μM, e.g., between about 0.2-60 μM, e.g., between about 0.2-55 μM, e.g., between about 0.2-50 μM, e.g., between about 0.2-45 μM, e.g., between about 0.2-40 μM, e.g., between about 0.2-35 μM, e.g., between about 0.2-30 μM, e.g., between about 0.2-25 μM, e.g., between about 0.2-20 μM, e.g., between about 0.2-15 μM, e.g., between about 0.2-10 μM, e.g., between about 0.3-10 μM, e.g., between about 0.4-10 μM, e.g., between about 0.5-10 μM, e.g., between about 0.6-10 μM, e.g., between about 0.7-10 μM, e.g., between 0.8-10 μM, e.g., between 0.9-10 μM, e.g., between 0.9-9 μM, e.g., between 1-8 μM, e.g., between 1-7 μM, e.g., between 1-6 μM, e.g., between 1-5 μM, e.g., between 2-4 μM, e.g., about 5 μM.

As used herein the term "p38" refers to the "p38α (alpha)" mitogen-activated protein kinase 14 (MAPK14), which includes MAPK14 isoform 1 set forth by GenBank Accession No. NP_001306.1 (SEQ ID NO:39), MAPK14 isoform 2 set forth by GenBank Accession No. NP_620581.1 (SEQ ID NO:40), MAPK14 isoform 3 set forth by GenBank Accession No. NP_620582.1 (SEQ ID NO:41) and MAPK14 isoform 4 set forth by GenBank Accession No. NP_620583.1 (SEQ ID NO:42); "p38β (beta)" (MAPK11), which is set forth by GenBank Accession No. NP_002742.3 (SEQ ID NO:43); "p38γ (gamma)" (MAPK12) which is set forth by GenBank Accession No. NP_002960.2 (SEQ ID NO:44); and/or "p38δ (delta)" (MAPK13) which is set forth in

GenBank Accession No. NP_002745.1 (SEQ ID NO:45), all of them having kinase activity and involved in signal transduction.

As used herein the term "p38 inhibitor" refers to any molecule (e.g., small molecules or proteins) capable of inhibiting the activity of p38 family members as determined by Western blot quantification of phosphorylated p38 levels.

Non-limiting examples of p38 inhibitors include SB203580 (AXONMEDCHEM – Axon 1363), and SB 202190 (AXONMEDCHEM – Axon 1364), LY 2228820 (AXONMEDCHEM- Axon 1895), BIRB796 (Axon Medchem 1358) and PD169316 (AXONMEDCHEM – Axon 1365).

As BMP signaling is an activator for p38 signaling, examples of p38 inhibitors also include BMP inhibitors like Dorsomorphin (AXONMEDCHEM – Axon 2150) and LDN193189 (AXON MEDCHEM AXON 1509) or other inhibitors of the BMP pathway such as recombinant NOGGIN protein [GenBank Accession No. NP_005441.1 (SEQ ID NO: 118)] can be used to replace small molecule inhibitors of BMP signaling.

According to some embodiments of the invention, PDSB203580 is provided at a concentration range of between about 0.5-70 μM, e.g., from about 1 μM to about 70 μM, e.g., between about 1-60 μM, e.g., between about 1-55 μM, e.g., between about 1-50 μM, e.g., between about 1-45 μM, e.g., between about 1-40 μM, e.g., between about 1-35 μM, e.g., between about 1-30 μM, e.g., between about 1-25 μM, e.g., between about 1-20 μM, e.g., between about 1-15 μM, e.g., between about 1-10 μM, e.g., between about 2-10 μM, e.g., between about 3-10 μM, e.g., between about 4-10 μM, e.g., between about 4-6 μM, e.g., about 5 μM, e.g., about 10 μM.

According to some embodiments of the invention, SB 202190 is provided at a concentration range of between about 0.1 μM to about 50 μM, e.g., from about 0.5 μM to about 50 μM, e.g., from about 1 μM to about 50 μM, e.g., between about 1-45 μM, e.g., between about 1-40 μM, e.g., between about 1-35 μM, e.g., between about 1-30 μM, e.g., between about 1-25 μM, e.g., between about 1-20 μM, e.g., between about 1-15 μM, e.g., between about 1-10 μM, e.g., between about 1-9 μM, e.g., between about 1-8 μM, e.g., between about 1-7 μM, e.g., between about 2-7 μM, e.g., between about 3-7 μM, e.g., between about 4-7 μM, e.g., between about 4-6 μM, e.g., about 5 μM.

According to some embodiments of the invention, BIRB796 is provided at a concentration range of between about 0.05 to about 30 μM, e.g., from about 0.1 to about 30 μM, e.g., between about 0.2-30 μM, e.g., between about 0.2-25 μM, e.g., between about 0.2-20 μM, e.g., between about 0.2-15 μM, e.g., between about 0.2-10 μM, e.g., between about 0.2-8 μM, e.g., between about 0.2-6 μM, e.g., between about 0.5-6 μM, e.g., between about 0.5-5 μM, e.g., between about 0.5-4 μM, e.g., between about 0.5-3 μM, e.g., between about 0.5-2 μM, e.g., between about 1-3 μM, e.g., between about 1-2.5 μM, e.g., about 2 μM.

As used herein the term "JNK" refers to the mitogen-activated protein kinase 8 (MAPK8) protein set forth by GenBank Accession Nos. NP_620637.1 (isoform alpha2) (SEQ ID NO:46), NP_620635.1 (isoform beta2) (SEQ ID NO:47), NP_620634.1 (isoform beta1) (SEQ ID NO:48), NP_002741.1 (isoform alpha1) (SEQ ID NO:49) which are involved in a wide variety of cellular processes such as proliferation, differentiation, transcription regulation and development.

As used herein the term "JNK inhibitor" refers to any molecule capable of inhibiting the activity of JNK as determined by phosphorylation of JNK family member protein by western blot analysis.

Non-limiting examples of JNK inhibitors include SP600125 (TOCRIS – Cat no. 1496), AEG3482 (AXONMEDCHEM- AXON 1291), and BIRB796 (AXONMEDCHEM – Axon 1358).

According to some embodiments of the invention, SP600125 is provided at a concentration range of between about 0.5-100 μM, e.g., from about 1 μM to about 100 μM, e.g., between about 1-90 μM, e.g., between about 1-80 μM, e.g., between about 1-70 μM, e.g., between about 1-60 μM, e.g., between about 1-55 μM, e.g., between about 1-50 μM, e.g., between about 1-45 μM, e.g., between about 1-40 μM, e.g., between about 1-35 μM, e.g., between about 1-30 μM, e.g., between about 1-25 μM, e.g., between about 1-20 μM, e.g., between about 1-15 μM, e.g., between about 1-10 μM, e.g., between about 2-10 μM, e.g., between about 3-10 μM, e.g., between about 4-10 μM, e.g., between about 4-6 μM, e.g., about 5 μM.

As used herein the term "protein kinase C (PKC)" refers to PKCα (alpha), PKCβ (beta), PKCγ (gamma), PKCδ (delta), PKCζ (zeta) and PKCμ (mu) protein isoforms.

As used herein the term "protein kinase C inhibitor" refers to any molecule capable of inhibiting the activity of protein kinase C as determined by reducing the levels of phosphorylated versus non phosphorylated PKC isoforms.

A non-limiting example of a protein kinase C inhibitor is Go6983 (CAS 133053-19-7), a potent, cell-permeable, reversible, and ATP-competitive inhibitor of protein kinase C (PKC) with a broad spectrum protein kinase C (PKC) inhibitor (IC50 values are 7, 7, 6, 10, 60 and 20000 nM for PKCα, PKCβ, PKCγ, PKCδ, PKCζ and PKCμ respectively). Go6983 is available from various suppliers such as Calbiochem (Catalogue number 365251-500UG), and TOCRIS (Catalogue number 2285).

According to some embodiments of the invention, Go6983 is provided at a concentration range of between about 0.5-100 μM, e.g., from about 1 μM to about 100 μM, e.g., between about 1-90 μM, e.g., between about 1-80 μM, e.g., between about 1-70 μM, e.g., between about 1-60 μM, e.g., between about 1-55 μM, e.g., between about 1-50 μM, e.g., between about 1-45 μM, e.g., between about 1-40 μM, e.g., between about 1-35 μM, e.g., between about 1-30 μM, e.g., between about 1-25 μM, e.g., between about 1-20 μM, e.g., between about 1-15 μM, e.g., between about 1-10 μM, e.g., between about 2-10 μM, e.g., between about 3-10 μM, e.g., between about 4-10 μM, e.g., between about 4-6 μM, e.g., about 5 μM.

As used herein the term "fibroblast growth factor receptor (FGFR)" refers to FGFR1, FGFR2 and FGFR3.

As used herein the term "FGFR inhibitor (or FGFRi)" refers to a molecule capable of inhibiting FGFR expression and/or activity level as determined by levels of phosphorylated FGFR1, 2, and 3.

Non-limiting examples of FGFR inhibitors include PD173074 and SU5401.

According to some embodiments of the invention, the FGFR inhibitor (FGFRi) is PD173074 and is provided in a concentration range between about 0.01-40 μM, e.g., between about 0.02-40 μM, e.g., between about 0.05-40 μM, e.g., between, about 0.1-40 μM, about 0.5-40 μM, about 1-40 μM, e.g., about 2-40 μM, about 5-40 μM, about 10-40 μM, e.g., between about 0.05-5 μM, e.g., about 0.1-5 μM.

According to some embodiments of the invention, the FGFR inhibitor (FGFRi) is SU5401 and is provided at a concentration range of about 0.1-40 μM, e.g., about 0.5-40 μM, about 1-40 μM, e.g., about 2-40 μM, about 5-40 μM, about 10-40 μM.

As used herein the term "transforming growth factor receptor (TGFR)" refers to TGF-β type I receptor ALK5, type I activin/nodal receptor ALK4 and type I nodal receptor ALK7.

As used herein the term "TGFR inhibitor (or TGFRi)" refers to a molecule capable of inhibiting TGFR expression and/or activity level as determined by phosphorylated ALK4, 5 and 7.

Non-limiting examples of TGFR inhibitors include SB431542 and A 83-01 small molecule compound.

According to some embodiments of the invention, the TGFR inhibitor is provided at a concentration range of about 0.1-30 μM, e.g., about 1-30 μM, e.g., 5-25 μM, e.g., 5-10 μM, e.g., 0.1-5 μM, e.g., 0.2-4 μM, e.g., 0.5-3 μM.

According to some embodiments of the invention, the culture medium further comprises a ROCK inhibitor.

As used herein the term "ROCK" refers to the protein set forth by GenBank Accession No. NP_005397.1 (P160ROCK; SEQ ID NO: 50); and NP_004841.2 (ROCK2; SEQ ID NO:51) having the serine/threonine kinase activity, and regulates cytokinesis, smooth muscle contraction, the formation of actin stress fibers and focal adhesions, and the activation of the c-fos serum response element.

As used herein the term "ROCK inhibitor" refers to any molecule capable of inhibiting the activity of ROCK as determined by inhibition of ROCK phosphorylation levels (detected by western blot analysis).

Non-limiting examples of ROCK inhibitors include Y27632 (TOCRIS, Catalogue number 1254).

According to some embodiments of the invention, Y27632 is provided at a concentration range of between about 0.1-100 μM, e.g., from about 0.1 μM to about 90 μM, e.g., between about 0.1-85 μM, e.g., between about 0.1-80 μM, e.g., between about 0.1-70 μM, e.g., between about 0.1-60 μM, e.g., between about 0.1-55 μM, e.g., between about 0.1-50 μM, e.g., between about 0.1-45 μM, e.g., between about 0.1-40 μM, e.g., between about 0.1-35 μM, e.g., between about 0.1-30 μM, e.g., between about

0.1-25 μM, e.g., between about 1-20 μM, e.g., between about 1-15 μM, e.g., between about 1-10 μM, e.g., between about 2-10 μM, e.g., between about 3-10 μM, e.g., between about 4-10 μM, e.g., between about 4-6 μM, e.g., about 5 μM.

According to some embodiments of the invention, the culture medium which comprises leukemia inhibitor factor (LIF), an ERK1/2 inhibitor, a GSK3b inhibitor, a p38 inhibitor, a JNK inhibitor, and a protein kinase C inhibitor, further comprises a ROCK inhibitor.

According to some embodiments of the invention, the culture medium which comprises leukemia inhibitor factor (LIF), an ERK1/2 inhibitor, a GSK3b inhibitor, a p38 inhibitor, a JNK inhibitor, a protein kinase C inhibitor, and a fibroblast growth factor receptor (FGFR) inhibitor (FGFRi) further comprises a ROCK inhibitor.

According to some embodiments of the invention, the culture medium which comprises leukemia inhibitor factor (LIF), an ERK1/2 inhibitor, a GSK3b inhibitor, a p38 inhibitor, a JNK inhibitor, a protein kinase C inhibitor, and a transforming growth factor receptor inhibitor (TGFRi) further comprises a ROCK inhibitor.

According to some embodiments of the invention, the culture medium which comprises leukemia inhibitor factor (LIF), an ERK1/2 inhibitor, a GSK3b inhibitor, a p38 inhibitor, a JNK inhibitor, a protein kinase C inhibitor, a fibroblast growth factor receptor (FGFR) inhibitor (FGFRi) and a transforming growth factor receptor inhibitor (TGFRi) further comprises a ROCK inhibitor.

According some embodiments of the invention, the culture medium which comprises leukemia inhibitor factor (LIF), an ERK1/2 inhibitor, a GSK3b inhibitor, a p38 inhibitor, a JNK inhibitor, TGFβ1 and a protein kinase C inhibitor further comprises a ROCK inhibitor.

According to some embodiments of the invention, the culture medium which comprises leukemia inhibitor factor (LIF), an ERK1/2 inhibitor, a GSK3b inhibitor, a p38 inhibitor, a JNK inhibitor, TGFβ1, a protein kinase C inhibitor and a fibroblast growth factor receptor (FGFR) inhibitor further comprises a ROCK inhibitor.

According to some embodiments of the invention, the culture medium which comprises leukemia inhibitor factor (LIF), an ERK1/2 inhibitor, a GSK3b inhibitor, a p38 inhibitor, a JNK inhibitor, basic fibroblast growth factor (bFGF) and transforming growth factor-beta 1 (TGFβ1) further comprises a ROCK inhibitor.

According to some embodiments of the invention, the culture medium further comprises a protein kinase C inhibitor.

According to some embodiments of the invention, the culture medium which comprises leukemia inhibitor factor (LIF), an ERK1/2 inhibitor, a GSK3b inhibitor, a p38 inhibitor, a JNK inhibitor, basic fibroblast growth factor (bFGF) and transforming growth factor-beta 1 (TGFβ1) further comprises a protein kinase C inhibitor.

According to some embodiments of the invention, the culture medium which comprises leukemia inhibitor factor (LIF), an ERK1/2 inhibitor, a GSK3b inhibitor, a p38 inhibitor, a JNK inhibitor, basic fibroblast growth factor (bFGF), transforming growth factor-beta 1 (TGFβ1) and a ROCK inhibitor further comprises a protein kinase C inhibitor.

According to some embodiments of the invention, the culture medium further comprises a factor selected from the group consisting of: bone morphogenetic protein 4 (BMP4), insulin-like growth factor 1 (IGF1), Forskolin, fibroblast growth factor receptor (FGFR) inhibitor (FGFRi), transforming growth factor receptor inhibitor (TGFRi), Kenpaullone, BayK8644, Bix1294, and stem cell factor (SCF).

According to some embodiments of the invention, the culture medium which comprises leukemia inhibitor factor (LIF), an ERK1/2 inhibitor, a GSK3b inhibitor, a p38 inhibitor, a JNK inhibitor, and a protein kinase C inhibitor further comprises at least one factor selected from the group consisting of bone morphogenetic protein 4 (BMP4), insulin-like growth factor 1 (IGF1), Forskolin, fibroblast growth factor receptor (FGFR) inhibitor (FGFRi), transforming growth factor receptor inhibitor (TGFRi), Kenpaullone, BayK8644, Bix1294, and stem cell factor (SCF).

According to some embodiments of the invention, the culture medium which comprises leukemia inhibitor factor (LIF), an ERK1/2 inhibitor, a GSK3b inhibitor, a p38 inhibitor, a JNK inhibitor, a protein kinase C inhibitor and a fibroblast growth factor receptor (FGFR) inhibitor (FGFRi) further comprises at least one factor selected from the group consisting of bone morphogenetic protein 4 (BMP4), insulin-like growth factor 1 (IGF1), Forskolin, transforming growth factor receptor inhibitor (TGFRi), Kenpaullone, BayK8644, Bix1294, and stem cell factor (SCF).

According to some embodiments of the invention, the culture medium which comprises leukemia inhibitor factor (LIF), an ERK1/2 inhibitor, a GSK3b inhibitor, a

p38 inhibitor, a JNK inhibitor, a protein kinase C inhibitor and a transforming growth factor receptor inhibitor (TGFRi) further comprises at least one factor selected from the group consisting of bone morphogenetic protein 4 (BMP4), insulin-like growth factor 1 (IGF1), Forskolin, fibroblast growth factor receptor (FGFR) inhibitor (FGFRi), Kenpaullone, BayK8644, Bix1294, and stem cell factor (SCF).

According to some embodiments of the invention, the culture medium which comprises leukemia inhibitor factor (LIF), an ERK1/2 inhibitor, a GSK3b inhibitor, a p38 inhibitor, a JNK inhibitor, a protein kinase C inhibitor, a fibroblast growth factor receptor (FGFR) inhibitor (FGFRi) and a transforming growth factor receptor inhibitor (TGFRi) further comprises at least one factor selected from the group consisting of bone morphogenetic protein 4 (BMP4), insulin-like growth factor 1 (IGF1), Forskolin, Kenpaullone, BayK8644, Bix1294, and stem cell factor (SCF).

According to some embodiments of the invention, the culture medium which comprises leukemia inhibitor factor (LIF), an ERK1/2 inhibitor, a GSK3b inhibitor, a p38 inhibitor, a JNK inhibitor, TGFβ1 and a protein kinase C inhibitor further comprises at least one factor selected from the group consisting of bone morphogenetic protein 4 (BMP4), insulin-like growth factor 1 (IGF1), Forskolin, fibroblast growth factor receptor (FGFR) inhibitor (FGFRi), transforming growth factor receptor inhibitor (TGFRi), Kenpaullone, BayK8644, Bix1294, and stem cell factor (SCF).

According to some embodiments of the invention, the culture medium which comprises leukemia inhibitor factor (LIF), an ERK1/2 inhibitor, a GSK3b inhibitor, a p38 inhibitor, a JNK inhibitor, basic fibroblast growth factor (bFGF) and transforming growth factor-beta 1 (TGFβ1) further comprises at least one factor selected from the group consisting of bone morphogenetic protein 4 (BMP4), insulin-like growth factor 1 (IGF1), Forskolin, fibroblast growth factor receptor (FGFR) inhibitor (FGFRi), transforming growth factor receptor inhibitor (TGFRi), Kenpaullone, BayK8644, Bix1294, and stem cell factor (SCF).

According to some embodiments of the invention, the culture medium further comprises ascorbic acid.

As used herein the phrase "ascorbic acid" or "Vitamin C" which is interchangeably used herein, refers to L-ascorbic acid 2-phosphate. Ascorbic acid can be obtained from e.g., Sigma (Catalogue number A8960).

The concentration of ascorbic acid to be used with the medium of some embodiments of the invention can be about 1-300 μg/ml, e.g., about 50 μg/ml.

According to some embodiments of the invention, the culture medium further comprises oleic Acid. It should be noted that oleic Acid can be used instead of ALBUMAX® (Life Technologies) or together with ALBUMAX®.

According to some embodiments of the invention, the culture medium further comprises Linoleic Acid. It should be noted that Linoleic Acid can be used instead of ALBUMAX® (Life Technologies) or together with ALBUMAX®.

According to some embodiments of the invention, the culture medium further comprises Pipecolic Acid. It should be noted that pipecolic acid can be used instead of ALBUMAX® (Life Technologies) or together with ALBUMAX®.

According to some embodiments of the invention, the Oleic Acid (O1257, Sigma Aldrich) can be used at a concentration of about 1-200 μg/ml, e.g., about 10 μg/ml in the culture medium.

According to some embodiments of the invention, the Oleic Acid [O1008 Sigma Aldrich, dissolved in DMSO), can be used at a concentration of 1-200 μg/ml e.g., about 10 μg/ml in the culture medium.

According to some embodiments of the invention, the Pipecolic Acid [P2519 Sigma Aldrich, dissolved in DMSO), can be used at a concentration of 1-200 μg/ml e.g., about 10 μg/ml in the culture medium.

According to some embodiments of the invention, the oleic Acid-Albumin (O3008 Sigma Aldrich) can be used at a concentration of about 1-200 μg/ml, e.g., about 10 μg/ml in the culture medium.

According to some embodiments of the invention, the medium comprises Linoleic/Oleic/Albumin supplement (L9655 Sigma Aldrich) at a concentration of about 1-200 μg/ml, e.g., about 10 μg/ml in the culture medium.

A non-limiting example of a culture medium which can be used to maintain (and induce to naive state) pluripotent stem cells in a naive state include: leukemia inhibitor factor (LIF), an ERK1/2 inhibitor, a GSK3b inhibitor, a p38 inhibitor, a JNK inhibitor, basic fibroblast growth factor (bFGF) and transforming growth factor-beta 1 (TGFβ1), and one or more of the following components:

a) IGFII (range 0.1-100 ng/ml final concentration);

b) IGF1 [insulin-like growth factor 1 (somatomedin C)] (range 0.1-100 ng/ml final concentration);

c) SCF (range 0.1-100 ng/ml final concentration);

d) BMP signaling inhibitor [examples include, but are not limited to: LDN193189 (AXON 1509 - 0.01-20 microM final concentration), K02288 (Axon 2189; 0.1-20 microM final concentration), Dorsomorphin hydrochloride (AXON 2150 0.1-20 microM final concentration);

e) NOTCH signaling inhibitors [examples include, but are not limited to the following gamma secretase inhibitors: DAPT (Axon Medchem 1484 – 0.05-50 microM final concentration), LY2886721 hydrochloride (Axon Medchem 1964 – 0.05-50 microM final concentration)], DBZ (Axon Medchem – Axon 1488- 0.05-50 microM final concentration);

f) Sonic Hedgehog pathway (SHH) inhibitors [examples include, but are not limited to the following: GANT61 (SigmaAldrich – 0.05-50 microM final concentration), RU-SKI 43 (Axon Medchem – Axon 2035 – 0.05-50 microM final concentration)];

g) ERK5 inhibitors (BIX02189 Axon 1809; range 0.1-100 microM final concentration);

h) ROCK inhibitor [Y27632 (AXON 1683) – 0.05-100 microM final];

i) FGF signaling inhibitor: Non-limiting examples of FGFR inhibitors include PD173074 and SU5401; and

j) TGF pathway inhibitor: Non-limiting examples of TGFR inhibitors include SB431542 and A 83-01 small molecule compound (As used herein the term "TGFR inhibitor (or TGFRi)" refers to a molecule capable of inhibiting TGFR expression and/or activity level as determined by phosphorylated ALK4, 5 and 7).

According to some embodiments of the invention, the culture medium of the invention is defined by any one of conditions 1-5, and 7-17 as described in Tables 3-5 in the Examples section which follows.

According to some embodiments of the invention, the culture medium further comprises an MBD3 inhibitor.

As used herein the term "MBD3" refers to the Methyl-CpG-binding domain 3 protein set forth by GenBank Accession No. NP_003917.1 (SEQ ID NO:7) having the co-repressor and chromatin remodeling functional activity.

As used herein the term "MBD3 inhibitor" refers to any agent (e.g., a molecule) capable of downregulating the expression level and/or activity of MBD3, and/or capable of interfering between the interaction of MBD3 with OCT4, and/or MBD3 with SOX2, and/or MBD3 and KLF4 and/or MBD3 and C-Myc, and/or inhibiting the binding of MBD3 to the nucleosome remodeling and deacetylase (NuRD). Downregulation of MBD3 can be effected on the genomic and/or the transcript level using a variety of molecules which interfere with transcription and/or translation [e.g., RNA silencing agents (e.g., antisense, siRNA, shRNA, micro-RNA), Ribozyme and DNAzyme], or on the protein level using e.g., an antibody (e.g., a neutralizing antibody), an antagonist, e.g., small molecules which inhibit MBD3 activity or ability to directly interact with any of the reprogramming factors (Oct4, Sox2, Klf4or c-Myc), enzymes that cleave the polypeptide and the like.

Non-limiting examples of MBD3 inhibitors include siRNA directed against MBD3 mRNA, such as those provided from Invitrogen, mBD3HSS147581(3_RNAI) (Invitrogen): AGGUCAAGGGCAAGCCCGACCUGAA (SEQ ID NO:52); and MBD3HSS147581(3_RNAI) (Invitrogen): UUCAGGUCGGGCUUGCCCUUGACCU (SEQ ID NO:53). Another suitable siRNA directed against MBD3 mRNA which can be used is the commercially available MBD3 Stealth siRNAs that include HSS147580 and HSS147581 components (Life Techniologies™, catalogue number 1299001) that were found efficient for MBD3 knockdown in human cells.

According to some embodiments of the invention, inhibiting the binding of Mbd3 to the NuRD complex is performed using a chromodomain helicase DNA binding protein 4 (CHD4) inhibitor.

Non-limiting examples of CHD4 inhibitors include the human CHD4 siRNA, such as the CHD4 stealth siRNA HSS101850 available from Life technologies™, which was found to efficiently knockdown CHD4 in human cells.

According to some embodiments of the invention, inhibiting the binding of Mbd3 to the NuRD complex is performed using a P66 alpha coiled-coil (P66α-CC) domain.

The peptide of the P66α-CC (SEQ ID NO: 114) can be added to the medium as is, or can be recombinantly expressed from a vector encoding the P66α-CC sequence (e.g., a vector which comprises the nucleotide sequence set forth in SEQ ID NO: 113).

According to some embodiments of the invention, inhibiting Mbd3 expression is performed using a protein kinase C (PKC) inhibitor (e.g., using the agents and molecules as described above).

According to some embodiments of the invention, the medium further comprises an agent which increases expression of endogenous ERAS and/or a recombinant ERAS.

According to some embodiments of the invention, the MBD3 inhibitor is provided in an amount sufficient to downregulate the expression level of the MBD3 RNA and/or protein in the cell by at least about 30%, e.g., at least about 35%, e.g., at least about 40%, e.g., at least about 45%, e.g., at least about 50%, e.g., at least about 55%, e.g., at least about 60%, e.g., at least about 65%, e.g., at least about 70%, e.g., at least about 75%, e.g., at least about 80% as compared to the expression level of the MBD3 RNA and/or protein, respectively, in the same cell when incubated and/or cultured under the same (e.g., identical) conditions yet without the MBD3 inhibitor.

According to some embodiments of the invention, the MBD3 inhibitor is provided in an amount sufficient to downregulate the expression level of the MBD3 RNA and/or protein in the cell by about 30-90%, e.g., about 30-85%, e.g., about 40-85%, e.g., about 50-85%, e.g., about 60-85%, e.g., about 70-85%, e.g., about 80-85%, e.g., about 85% as compared to the expression level of the MBD3 RNA and/or protein, respectively, in the same cell when incubated and/or cultured under the same (e.g., identical) conditions yet without the MBD3 inhibitor.

The expression level of the MBD3 in the cell can be determined by various methods such as real time reverse transcription PCR, Western blot and the like. A non-limiting example for such an assay is provided in the Examples section which follows and in Figures 1I-J, demonstrating about 85% inhibition of MBD3 protein level in cells transformed with the $MBD3^{flox/-}$ construct.

According to some embodiments of the invention, the culture medium is devoid of serum, e.g., devoid of any animal serum.

According to some embodiments of the invention, the culture medium is devoid of any animal contaminants, *i.e.,* animal cells, fluid or pathogens (e.g., viruses infecting animal cells), e.g., being xeno-free.

According to some embodiments of the invention, the culture medium is devoid of human derived serum.

According to some embodiments of the invention, the culture medium further comprises a serum replacement (*i.e.,* a substitute of serum) such as KNOCKOUT™ Serum Replacement (Gibco-Invitrogen Corporation, Grand Island, NY USA), ALBUMAX®II (Gibco®; Life Technologies – Invitrogen, Catalogue No. 11021-029; Lipid-rich bovine serum albumin for cell culture) or a chemically defined lipid concentrate (Gibco®; Invitrogen, Life Technologies – Invitrogen, Catalogue No. 11905-031).

According to some embodiments of the invention, the culture medium further comprises N2 supplement (Gibco®; Life Technologies – Invitrogen, Catalogue No. 17502-048) a chemically defined, serum-free supplement. For a 500 ml of culture medium 5 ml of the N2 mix (Invitrogen) can be added.

Alternatively, the following materials (substitute the N2 supplement) can be added to a 500 ml culture medium: Recombinant Insulin (Sigma I-1882) at a 12.5 microg/ml (μg/ml) final concentration; Apo-Transferrin (Sigma T-1147) at a 500 μg/ml final concentration; Progesterone (Sigma- P8783) at a 0.02 μg/ml final concentration; Putrescine (Sigma- P5780) at a 16 μg/ml final concentration; and 5 microL (μl) of 3 mM stock of Sodium Selenite (Sigma – S5261) are added per 500 ml culture medium (e.g., the WIS-NHSM).

According to some embodiments of the invention, the KNOCKOUT™ Serum Replacement is provided at a concentration of at least 0.5%, e.g., in the range of about 0.5%-25%, e.g., about 5%, about 10%, about 15%, about 20% or about 25%.

According to some embodiments of the invention, the ALBUMAX™ is provided at a concentration of at least 0.01%, e.g., in the range of about 0.01%-10%, e.g., about 0.1%, about 0.2%, about 0.3%, about 0.4%, about 0.5%, about 0.6%, about 0.7%, about 0.8%, about 0.9%, about 1%, about 2%, about 3%, about 4%, about 5%, about 6%, about 7%, about 8%, about 9% or about 10%, e.g., 1%.

According to some embodiments of the invention, the defined lipid concentrate

is provided at a concentration of at least about 0.1%, e.g., in the range of 0.1-5%, e.g., about 0.2%, about 0.3%, about 0.4%, about 0.5%, about 0.6%, about 0.7%, about 0.8%, about 0.9%, about 1%, about 2%, about 3%, about 4%, about 5%, e.g., 1%.

According to some embodiments of the invention, the culture medium comprises the N2 supplement (e.g., 5 ml N2 per 500 ml of culture medium) and the defined lipid concentrate (5 ml defined lipid concentrate per 500 ml medium).

According to some embodiments of the invention, the culture medium comprises the N2 supplement (e.g., 5 ml N2 per 500 ml of culture medium) and ALBUMAX®II (e.g., 1% Albumax®II; Gibco®; Life Technologies – Invitrogen).

According to some embodiments of the invention, the culture medium can further include antibiotics (e.g., PEN-STREP), L-glutamine, NEAA (non-essential amino acids).

According to some embodiments of the invention, the culture medium comprises KO-DMEM with N2 supplement (e.g., about 5 ml N2 per 500 ml of culture medium) with about 5 ml defined lipid concentrate per 500 ml medium, LIF (about 20 ng/ml), bFGF (about 8 ng/ml), TGFβ1 (about 1 ng/ml), ERK1/2i (about 1 μM of PD0325901), GSK3bi (CHIR99021, about 3 μM), p38i (SB203580, about 5 μM), and JNKi (SP600125, about 5-10 μM).

According to some embodiments of the invention, the culture medium comprises KO-DMEM with N2 supplement (e.g., about 5 ml N2 per 500 ml of culture medium) with about 1-2% Albumax®II, LIF (about 20 ng/ml), bFGF (about 8 ng/ml), TGFβ1 (about 1 ng/ml), ERK1/2i (about 1 μM of PD0325901), GSK3bi (CHIR99021, about 3 μM), p38i (SB203580, about 5 μM), and JNKi (SP600125, 5-about 10 μM).

According to some embodiments of the invention, the culture medium comprises KO-DMEM with N2 supplement (e.g., about 5 ml N2 per 500 ml of culture medium) with about 15% Kockout SR (Gibco), LIF (about 20 ng/ml), bFGF (about 8 ng/ml), TGFβ1 (about 1 ng/ml), ERK1/2i (about 1 μM of PD0325901), GSK3bi (CHIR99021, about 3 μM), p38i (SB203580, about 5 μM), JNKi (SP600125, about 5-10 μM).

According to an aspect of some embodiments of the invention, there is provided a cell culture comprising cells and the culture medium of some embodiments of the invention.

According to some embodiments of the invention, the cells can be any cells,

e.g., prokaryotic or eukaryotic cells, e.g., primate cells, e.g., mammalian cells, e.g., human cells.

According to some embodiments of the invention, the cells can be somatic cells, stem cells, primed pluripotent stem cells, and/or naive pluripotent stem cells.

According to some embodiments of the invention, the culture medium is capable of maintaining naive pluripotent stem cell in an undifferentiated state for at least 2 passages, e.g., for at least 5, 10, 20, 30, 40, 50, 60, 70, 80, 90 or 100 passages.

According to an aspect of some embodiments of the invention, there is provided a method of generating a naive pluripotent stem cell (PSC), comprising incubating a non-naive PSC cell under conditions which allow generation of the naive PSC from the non-naive PSC, wherein:

(i) when the naive PSC is a female PSC, then the naive female PSC has two unmethylated alleles of an X-inactive specific transcript (XIST) gene; and

(ii) when the naive PSC is a male PSC, then the naive male PSC has an unmethylated allele of the XIST gene,

thereby generating the naive PSC.

According to some embodiments of the invention, the PSC is a primate (e.g., mammalian, e.g., human) PSC.

According to some embodiments of the invention, the conditions comprise the culture medium of some embodiments of the invention.

According to some embodiments of the invention, the conditions comprise growing the cells in the presence of 1-20% oxygen (O_2) and 5% CO_2.

According to some embodiments of the invention, the conditions comprise hypoxia. Hypoxic conditions (hypoxia) can be induced in the presence of less than 10% O_2 (oxygen) in the growth environment.

The growth environment (e.g., tissue culture incubator) can include about 37°C, 5% CO_2, and hypoxia (less than 10% O_2 in the air).

According to some embodiments of the invention, the conditions comprise a culture medium which comprises an ERK1/2 inhibitor, a GSK3β inhibitor, a p38 inhibitor, a JNK inhibitor, a STAT3 activator and at least one agent selected from the group consisting of: basic fibroblast growth factor (bFGF), transforming growth factor

beta 1 (TGFβ1), a protein kinase C (PKC) inhibitor, a ROCK inhibitor and a NOTCH inhibitor.

According to some embodiments of the invention, the conditions comprise a culture medium which comprises an ERK1/2 inhibitor, a GSK3β inhibitor, a p38 inhibitor, a JNK inhibitor, a STAT3 activator and at least one agent selected from the group consisting of: a transforming growth factor receptor (TGFR) inhibitor, a fibroblast growth factor receptor (FGFR) inhibitor, a protein kinase C (PKC) inhibitor, a ROCK inhibitor and a NOTCH inhibitor.

According to some embodiments of the invention, the STAT3 activator is selected from the group consisting of LIF, IL6 and EGF.

According to some embodiments of the invention, the STAT3 activator is selected from the group consisting of LIF, and IL6.

According to some embodiments of the invention, the STAT3 activator is LIF.

According to some embodiments of the invention, the culture medium further comprising at least one additional agent selected from the group consisting of: insulin-like growth factor 1 (IGF1), insulin-like growth factor II (IGFII), a bone morphogenetic protein (BMP) signaling inhibitor, a Sonic Hedgehog pathway (SHH) inhibitor, an ERK5 inhibitor, Forskolin, Kenpaullone, BayK8644, Bix1294, and stem cell factor (SCF).

According to some embodiments of the invention, the culture medium further comprising at least one additional agent selected from the group consisting of: insulin-like growth factor 1 (IGF1), insulin-like growth factor II (IGFII), bone morphogenetic protein 4 (BMP4), a Sonic Hedgehog pathway (SHH) inhibitor, an ERK5 inhibitor, Forskolin, Kenpaullone, BayK8644, Bix1294, and stem cell factor (SCF).

According to some embodiments of the invention, the STAT3 activator comprises the LIF, and wherein the at least one agent comprises the PKC inhibitor.

According to some embodiments of the invention, the culture medium further comprising FGFR inhibitor.

According to some embodiments of the invention, the culture medium further comprising TGFR inhibitor.

According to some embodiments of the invention, the STAT3 activator comprises the LIF and wherein the at least one agent comprises the TGFβ1 and the protein kinase C inhibitor.

According to some embodiments of the invention, the culture medium further comprising an FGFR inhibitor.

According to some embodiments of the invention, the STAT3 activator comprises the LIF, and wherein the at least one agent comprises the bFGF and the TGFβ1.

According to some embodiments of the invention, the culture medium further comprising a ROCK inhibitor.

According to some embodiments of the invention, the culture medium further comprising a protein kinase C inhibitor.

According to some embodiments of the invention, the STAT3 activator comprises the LIF and wherein the at least one agent comprises the bFGF, the ROCK inhibitor, a bone morphogenetic protein (BMP) inhibitor, the NOTCH inhibitor, and a transforming growth factor receptor (TGFR) inhibitor.

According to some embodiments of the invention, the culture medium further comprising a Sonic Hedgehog pathway (SHH) inhibitor.

According to some embodiments of the invention, the STAT3 activator comprises the LIF and wherein the at least one agent comprises the NOTCH inhibitor, and a fibroblast growth factor receptor (FGFR) inhibitor.

According to some embodiments of the invention, the culture medium further comprises an agent selected from the group consisting of insulin-like growth factor II (IGFII), stem cell factor (SCF) and transforming growth factor beta 1 (TGFβ1).

According to some embodiments of the invention, the conditions comprise a culture medium which comprises LIF, an ERK1/2 inhibitor, a GSK3b inhibitor, a p38 inhibitor, a JNK inhibitor, and a protein kinase C inhibitor.

According to some embodiments of the invention, the culture medium further comprising a FGFR inhibitor (FGFRi).

According to some embodiments of the invention, the culture medium further comprising a TGFR inhibitor (TGFRi).

According to some embodiments of the invention, the conditions comprise a culture medium which comprises LIF, an ERK1/2 inhibitor, a GSK3b inhibitor, a p38 inhibitor, a JNK inhibitor, and a protein kinase C inhibitor, further comprises a FGFR inhibitor (FGFRi).

According to some embodiments of the invention, the conditions comprise a culture medium which comprises LIF, an ERK1/2 inhibitor, a GSK3b inhibitor, a p38 inhibitor, a JNK inhibitor, and a protein kinase C inhibitor, further comprises a TGFRi.

According to some embodiments of the invention, the conditions comprise a culture medium which comprises LIF, an ERK1/2 inhibitor, a GSK3b inhibitor, a p38 inhibitor, a JNK inhibitor, and a protein kinase C inhibitor, further comprises a FGFR inhibitor and a TGFRi.

According to some embodiments of the invention, the conditions comprise a culture medium which comprises LIF, an ERK1/2 inhibitor, a GSK3b inhibitor, a p38 inhibitor, a JNK inhibitor, TGFβ1 and a protein kinase C inhibitor.

According to some embodiments of the invention, the conditions comprise a culture medium which comprises LIF, an ERK1/2 inhibitor, a GSK3b inhibitor, a p38 inhibitor, a JNK inhibitor, TGFβ1 and a protein kinase C inhibitor further comprising FGFR inhibitor (FGFRi).

According to some embodiments of the invention, the conditions comprise a culture medium which comprises LIF, an ERK1/2 inhibitor, a GSK3b inhibitor, a p38 inhibitor, a JNK inhibitor, bFGF and TGFβ1.

According to some embodiments of the invention, the conditions comprise a culture medium which comprises leukemia inhibitor factor (LIF), an ERK1/2 inhibitor, a GSK3b inhibitor, a p38 inhibitor, a JNK inhibitor, and a protein kinase C inhibitor.

According to some embodiments of the invention, the medium further comprises an FGFR inhibitor.

According to some embodiments of the invention, the medium further comprises a TGFR inhibitor.

According to some embodiments of the invention, the conditions comprise a culture medium which comprises leukemia inhibitor factor (LIF), an ERK1/2 inhibitor, a GSK3b inhibitor, a p38 inhibitor, a JNK inhibitor, TGFβ1 and a protein kinase C inhibitor.

According to some embodiments of the invention, the medium further comprises FGFR inhibitor.

According to some embodiments of the invention, the conditions comprise a culture medium which comprises leukemia inhibitor factor (LIF), an ERK1/2 inhibitor, a GSK3b inhibitor, a p38 inhibitor, a JNK inhibitor, basic fibroblast growth factor (bFGF) and transforming growth factor-beta 1 (TGFβ1).

According to some embodiments of the invention, the medium further comprises a ROCK inhibitor.

According to some embodiments of the invention, the medium further comprises a protein kinase C inhibitor.

According to some embodiments of the invention, the medium further comprises a factor selected from the group consisting of: bone morphogenetic protein 4 (BMP4), IGF1, Forskolin, FGFR inhibitor, TGFR inhibitor Kenpaullone, BayK8644, Bix1294, and stem cell factor (SCF).

According to some embodiments of the invention, the medium further comprises an ascorbic acid.

According to some embodiments of the invention, the medium further comprises an oleic Acid.

According to some embodiments of the invention, the medium further comprises a Linoleic Acid.

According to some embodiments of the invention, the culture medium being devoid of animal serum (e.g., devoid of bovine serum, mouse serum, being xeno-free, devoid of animal contaminants).

According to some embodiments of the invention, the culture medium further comprises serum replacement.

According to some embodiments of the invention, the culture medium further comprises an MBD3 inhibitor.

According to some embodiments of the invention, the conditions comprise a culture medium which comprises leukemia inhibitor factor (LIF), an ERK1/2 inhibitor, a GSK3b inhibitor, a p38 inhibitor, a JNK inhibitor, basic fibroblast growth factor (bFGF) and transforming growth factor-beta 1 (TGFβ1).

According to some embodiments of the invention, the culture medium further comprises a ROCK inhibitor.

According to some embodiments of the invention, the culture medium further comprises an MBD3 inhibitor.

According to some embodiments of the invention, the non-naive PSC is selected from the group consisting of a primed PSC, a blastocyst, an induced pluripotent stem cell (a primed iPSC) and a somatic cell.

It should be noted that when the non-naive PSC is a primed PSC (e.g., a blastocyst, an embryonic stem cell, an embryonic germ cell, or an induced pluripotent stem cell) there is no need for exogenous expression of the Oct4, Sox2, Klf4 and c-Myc, nor for the addition of isolated Oct4, Sox2, Klf4 and/or c-Myc factors to the medium.

According to some embodiments of the invention, when the non-naive PSC is a primed PSC, a blastocyst, or an induced pluripotent stem cell (a primed iPSC) the medium does not include the Oct4, Sox2, Klf4 and/or c-Myc factors.

According to some embodiments of the invention, when the non-naive PSC is a primed PSC, a blastocyst, or an induced pluripotent stem cell (a primed iPSC) the cells are not genetically modified to express the Oct4, Sox2, Klf4 and/or c-Myc factors.

According to some embodiments of the invention, wherein when the non-naive PSC comprises a somatic cell then the method further comprising subjecting the somatic cell to de-differentiation conditions, to thereby obtain an induced pluripotent stem cell.

According to some embodiments of the invention, de-differentiation conditions comprise exogenously expressing within the somatic cell at least two growth factors selected from the group consisting of OCT4 [GenBank Accession Nos. NP_002692.2 (SEQ ID NO:54) and NM_002701.4 (SEQ ID NO:55)], SOX2 [GenBank Accession Nos. NP_003097.1 (SEQ ID NO:56) and NM_003106.3 (SEQ ID NO:57)], KLF4 [GenBank Accession Nos. NP_004226.3 (SEQ ID NO:58) and NM_004235.4 (SEQ ID NO:59)] and c-Myc [GenBank Accession Nos. NP_002458.2 (SEQ ID NO:60) and NM_002467.4 (SEQ ID NO:61)].

As used herein the phrase "exogenously expressing" refers to expressing a heterologous nucleic acid sequence which may not be naturally expressed within the cell or which overexpression in the cell is desired. The exogenous polynucleotide may be introduced into the cell in a stable or transient manner, so as to produce a ribonucleic

acid (RNA) molecule and/or a polypeptide molecule. It should be noted that the exogenous polynucleotide may comprise a nucleic acid sequence which is identical or partially homologous to an endogenous nucleic acid sequence of the cell.

The term "endogenous" as used herein refers to any polynucleotide or polypeptide which is present and/or naturally expressed within the cell.

According to some embodiments of the invention, de-differentiation conditions comprise expressing within the somatic cell Klf4 and Oct4.

According to some embodiments of the invention, de-differentiation conditions comprise expressing within the somatic cell Oct4, Sox2 and Klf4.

According to some embodiments of the invention, de-differentiation conditions comprise expressing within the somatic cell Oct4, Klf4 and cMyc.

According to some embodiments of the invention, expressing the growth factors is performed using DNA transfection of the growth factors.

Methods of DNA transfections into mammalian cells are known in the art and include those described for example in Figure 1a and in Reference (Mansour et al. 2012), which is fully incorporated herein by reference in its entirety. Further description of preparation of expression vectors and modes of administering them into cells are provided hereinunder.

According to some embodiments of the invention, expressing the growth factors is performed using RNA transfection of the growth factors.

Methods of RNA transfections into mammalian cells are known in the art and include those described for example in (Warren et al. 2010) which is fully incorporated herein by reference in its entirety.

Once obtained, the cells are cultured in a medium and being serially passaged.

It should be noted that culturing the naive PSC involves replacing the culture medium with a "fresh" medium (of identical composition) every 24-48 hours, and passaging each culture dish (e.g., a plate) to 2 or 3 culture dishes (e.g., plates) every 3-5 days. Thus, when cells in the culture reach about 60-90% confluence the supernatant is discarded, the culture dishes are washed [e.g., with phosphate buffered saline (PBS)] and the cells are subjected to enzymatic dissociation from the culture dish, e.g., using trypsinization (0.25% or 0.05% Try sin + EDTA), e.g., until single cells or cell clumps are separated from each other.

It should be noted that the culture conditions uncovered by the present inventors enables maintenance of human PSCs such as human iPSCs in the naive PSC state without the need of further exogenous expression of the Oct4, Sox2, Klf4 and/or c-Myc factors. This is in sharp contrast to all prior attempts to generate naive human PSCs which required exogenous expression of the Oct4, Sox2, Klf4 and/or c-Myc factors, and which upon withdrawal of these factors the naive PSCs spontaneously differentiated, and could not be maintained in the undifferentiated and pluripotent stem cells (See e.g., Hanna J, 2010b).

According to some embodiments of the invention, exogenous expression of the growth factors is effected for a limited time, such as for no more than 10 days in culture, e.g., for no more than 1 passage.

According to some embodiments of the invention, once the naive iPSCs are generated from the somatic cells, they are further being cultured in the culture medium of some embodiments of the invention (e.g., the WIS-NHSM medium) without exogenous expression of the Oct4, Sox2, Klf4 and/or c-Myc factors by the naive iPSCs, and without addition of the isolated Oct4, Sox2, Klf4 and/or c-Myc factors to the culture medium.

As used herein the phrase "isolated... factors" refers to factors which are recombinantly expressed from an expression vector in a host cell (e.g., a bacteria), being biochemically synthesized, or being isolated from a biological sample (e.g., serum or cells).

The method of some embodiments of the invention can be used to improve generation of iPSCs from somatic cells as compared to generation of iPSC from somatic cells using expression of the Oct4, Sox2, Klf4 and c-Myc factors in somatic cells without further inhibition of the Mbd3 expression.

For example, when human somatic cells are used, the method is effected using a medium which comprises leukemia inhibitor factor (LIF), an ERK1/2 inhibitor, a GSK3b inhibitor, a p38 inhibitor, a JNK inhibitor, basic fibroblast growth factor (bFGF), transforming growth factor-beta 1 (TGFβ1), and an MBD3 inhibitor, and optionally also a ROCK inhibitor. When the somatic cells are subject to de-differentiation using DNA transfection of the growth factors (e.g., at least two of the Oct4, Sox2, Klf4 and c-Myc), then the method results in at least about 30%, e.g., at least about 40%, at least about

50%, e.g., at least about 60%, at least about 70%, e.g., at least about 80%, at least about 90%, e.g., at least about 95%, at least about 99%, e.g., 100% more iPSCs as compared to the yield of the iPSCs obtained when the Oct4, Sox2, Klf4 and c-Myc are expressed using DNA transfection in the somatic cell without further inhibition of the Mbd3 expression.

For example, when human somatic cells are used, the method is effected using a medium which comprises leukemia inhibitor factor (LIF), an ERK1/2 inhibitor, a GSK3b inhibitor, a p38 inhibitor, a JNK inhibitor, basic fibroblast growth factor (bFGF), transforming growth factor-beta 1 (TGFβ1), and an MBD3 inhibitor, and optionally also a ROCK inhibitor. When the somatic cells are subject to de-differentiation using RNA transfection of the growth factors (e.g., at least two of the Oct4, Sox2, Klf4 and c-Myc), then the method results in at least about 5%, e.g., at least about 10%, at least about 20%, e.g., at least about 30%, at least about 40%, e.g., at least about 50%, at least about 60%, e.g., at least about 75%, at least about 99%, e.g., 100% more iPSCs as compared to the yield of the iPSCs obtained when the Oct4, Sox2, Klf4 and c-Myc are expressed using RNA transfection in the somatic cell without further inhibition of the Mbd3 expression. Moreover, while the prior art methods (without MBD3 inhibition and without the medium of some embodiments of the present invention) employ 10-20 rounds of RNA transfection in order to achieve de-differentiation of human somatic cells, the method of some embodiments of the invention employs 1-4 rounds of RNA transfection in order to achieve de-differentiation of human somatic cells, and thus is far more efficient and time consuming.

According to an aspect of some embodiments of the invention, there is provided a method of generating a naive pluripotent stem cell (PSC), comprising incubating a non-naive PSC cell under conditions which allow generation of the naive PSC from the non-naive PSC, the naive PSC comprising:

an unmethylated X-inactive specific transcript (XIST) gene, wherein:

(i) when the naive PSC is a female PSC, then the naive female PSC has two unmethylated alleles of the XIST gene; and

(ii) when the naive PSC is a male PSC, then the naive male PSC has an unmethylated allele of the XIST gene,

and/or

an expression level of transcription factor E3 (TFE3) characterized by a nucleus to cytoplasm expression ratio which is equal to or higher than 1 as determined by an immunostaining assay.

wherein the conditions which comprise a culture medium which comprises KO-DMEM, N2 supplement (Gibco), defined lipid concentrate (Gibco) or Albumax I (Invitrogen), LIF, bFGF, TGFβ1, ERK1/2 inhibitor, GSK3b inhibitor, p38 inhibitor, and JNK inhibitor and a protein kinase C inhibitor,

thereby generating the naive PSC.

According to some embodiments of the invention, the culture medium further comprises FGFR inhibitor.

According to some embodiments of the invention, the culture medium further comprises TGFR inhibitor.

According to an aspect of some embodiments of the invention, there is provided a method of generating a naive pluripotent stem cell (PSC), comprising incubating a non-naive PSC cell under conditions which allow generation of the naive PSC from the non-naive PSC, the naive PSC comprising:

an unmethylated X-inactive specific transcript (XIST) gene, wherein:

(i) when the naive PSC is a female PSC, then the naive female PSC has two unmethylated alleles of the XIST gene; and

(ii) when the naive PSC is a male PSC, then the naive male PSC has an unmethylated allele of the XIST gene,

and/or

an expression level of transcription factor E3 (TFE3) characterized by a nucleus to cytoplasm expression ratio which is equal to or higher than 1 as determined by an immunostaining assay.

wherein the conditions which comprise a culture medium which comprises KO-DMEM, N2 supplement (Gibco), defined lipid concentrate (Gibco) or Albumax I (Invitrogen), LIF, bFGF, TGFβ1, ERK1/2 inhibitor, GSK3b inhibitor, p38 inhibitor, and JNK inhibitor and a protein kinase C inhibitor,

thereby generating the naive PSC.

According to some embodiments of the invention, the culture medium further comprises FGFR inhibitor.

According to an aspect of some embodiments of the invention, there is provided a method of generating a naive pluripotent stem cell (PSC), comprising incubating a non-naive PSC cell under conditions which allow generation of the naive PSC from the non-naive PSC, the naive PSC comprising:

an unmethylated X-inactive specific transcript (XIST) gene, wherein:

(i) when the naive PSC is a female PSC, then the naive female PSC has two unmethylated alleles of the XIST gene; and

(ii) when the naive PSC is a male PSC, then the naive male PSC has an unmethylated allele of the XIST gene,

and/or

an expression level of transcription factor E3 (TFE3) characterized by a nucleus to cytoplasm expression ratio which is equal to or higher than 1 as determined by an immunostaining assay.

wherein the conditions which comprise a culture medium which comprises KO-DMEM, N2 supplement (Gibco), defined lipid concentrate (Gibco) or Albumax I (Invitrogen), LIF, bFGF, TGFβ1, ERK1/2 inhibitor, GSK3b inhibitor, p38 inhibitor, and JNK inhibitor,

thereby generating the naive PSC.

According to an aspect of some embodiments of the invention, there is provided a method of generating a naive pluripotent stem cell (PSC), comprising incubating a non-naive PSC cell under conditions which allow generation of the naive PSC from the non-naive PSC, the naive PSC comprising:

an unmethylated X-inactive specific transcript (XIST) gene, wherein:

(i) when the naive PSC is a female PSC, then the naive female PSC has two unmethylated alleles of the XIST gene; and

(ii) when the naive PSC is a male PSC, then the naive male PSC has an unmethylated allele of the XIST gene,

and/or

an expression level of transcription factor E3 (TFE3) characterized by a nucleus to cytoplasm expression ratio which is equal to or higher than 1 as determined by an immunostaining assay.

wherein the conditions which comprise a culture medium which comprises KO-DMEM, N2 supplement (Gibco), defined lipid concentrate (Gibco), LIF, bFGF, TGFβ1, ERK1/2 inhibitor, GSK3b inhibitor, p38 inhibitor, JNK inhibitor, and an MBD3 inhibitor,

thereby generating the naive PSC.

According to some embodiments of the invention, the method of generating a naive pluripotent stem cell (PSC) comprises incubating a non-naive PSC cell under conditions which comprise a culture medium which comprises KO-DMEM with N2 supplement (e.g., about 5 ml N2 per 500 ml of culture medium) with about 5 ml defined lipid concentrate per 500 ml medium, LIF (about 20 ng/ml), bFGF (about 8 ng/ml), TGFβ1 (about 1 ng/ml), ERK1/2i (about 1 μM of PD0325901), GSK3bi (CHIR99021, about 3 μM), p38i (SB203580, about 5 μM), and JNKi (SP600125, about 5-10 μM), wherein:

(i) when the naive PSC is a female PSC, then the naive female PSC has two unmethylated alleles of an X-inactive specific transcript (XIST) gene; and

(ii) when the naive PSC is a male PSC, then the naive male PSC has an unmethylated allele of the XIST gene,

thereby generating the naive PSC.

According to some embodiments of the invention, the method of generating a naive pluripotent stem cell (PSC) comprises incubating a non-naive PSC cell under conditions which comprise a culture medium which comprises KO-DMEM with N2 supplement (e.g., about 5 ml N2 per 500 ml of culture medium) with about 1-2% Albumax®II, LIF (about 20 ng/ml), bFGF (about 8 ng/ml), TGFβ1 (about 1 ng/ml), ERK1/2i (about 1 μM of PD0325901), GSK3bi (CHIR99021, about 3 μM), p38i (SB203580, about 5 μM), and JNKi (SP600125, about 5-10 μM), wherein:

(i) when the naive PSC is a female PSC, then the naive female PSC has two unmethylated alleles of an X-inactive specific transcript (XIST) gene; and

(ii) when the naive PSC is a male PSC, then the naive male PSC has an unmethylated allele of the XIST gene,

thereby generating the naive PSC.

According to some embodiments of the invention, the method of generating a naive pluripotent stem cell (PSC) comprises incubating a non-naive PSC cell under

conditions which comprise a culture medium which comprises KO-DMEM with N2 supplement (e.g., 5 ml N2 per 500 ml of culture medium) with about 15% Kockout SR (Gibco), LIF (about 20 ng/ml), bFGF (about 8 ng/ml), TGFβ1 (about 1 ng/ml), ERK1/2i (about 1 μM of PD0325901), GSK3bi (CHIR99021, about 3 μM), p38i (SB203580, about 5 μM), JNKi (SP600125, about 5-10 μM), wherein:

(i) when the naive PSC is a female PSC, then the naive female PSC has two unmethylated alleles of an X-inactive specific transcript (XIST) gene; and

(ii) when the naive PSC is a male PSC, then the naive male PSC has an unmethylated allele of the XIST gene,

thereby generating the naive PSC.

According to some embodiments of the invention, the method of generating a naive pluripotent stem cell (PSC) comprises incubating a non-naive PSC cell under conditions which comprise a culture medium which comprises KO-DMEM with N2 supplement (e.g., about 5 ml N2 per 500 ml of culture medium) with about 5 ml defined lipid concentrate per 500 ml medium, LIF (about 20 ng/ml), bFGF (about 8 ng/ml), TGFβ1 (about 1 ng/ml), ERK1/2i (about 1 μM of PD0325901), GSK3bi (CHIR99021, about 3 μM), p38i (SB203580, about 5 μM), JNKi (SP600125, about 5-10 μM) and an MBD3 inhibitor, wherein:

(i) when the naive PSC is a female PSC, then the naive female PSC has two unmethylated alleles of an X-inactive specific transcript (XIST) gene; and

(ii) when the naive PSC is a male PSC, then the naive male PSC has an unmethylated allele of the XIST gene,

thereby generating the naive PSC.

According to some embodiments of the invention, the method of generating a naive pluripotent stem cell (PSC) comprises incubating a non-naive PSC cell under conditions which comprise a culture medium which comprises KO-DMEM with N2 supplement (e.g., about 5 ml N2 per 500 ml of culture medium) with about 1-2% Albumax®II, LIF (about 20 ng/ml), bFGF (about 8 ng/ml), TGFβ1 (about 1 ng/ml), ERK1/2i (about 1 μM of PD0325901), GSK3bi (CHIR99021, about 3 μM), p38i (SB203580, about 5 μM), JNKi (SP600125, about 5-10 μM), and an MBD3 inhibitor, wherein:

(i) when the naive PSC is a female PSC, then the naive female PSC has two unmethylated alleles of an X-inactive specific transcript (XIST) gene; and

(ii) when the naive PSC is a male PSC, then the naive male PSC has an unmethylated allele of the XIST gene,

thereby generating the naive PSC.

According to some embodiments of the invention, the method of generating a naive pluripotent stem cell (PSC) comprises incubating a non-naive PSC cell under conditions which comprise a culture medium which comprises KO-DMEM with N2 supplement (e.g., about 5 ml N2 per 500 ml of culture medium) with about 15% Kockout SR (Gibco), LIF (about 20 ng/ml), bFGF (about 8 ng/ml), TGFβ1 (about 1 ng/ml), ERK1/2i (about 1 μM of PD0325901), GSK3bi (CHIR99021, about 3 μM), p38i (SB203580, about 5 μM), JNKi (SP600125, about 5-10 μM), and an MBD3 inhibitor, wherein:

(i) when the naive PSC is a female PSC, then the naive female PSC has two unmethylated alleles of an X-inactive specific transcript (XIST) gene; and

(ii) when the naive PSC is a male PSC, then the naive male PSC has an unmethylated allele of the XIST gene,

thereby generating the naive PSC.

According to an aspect of some embodiments of the invention, there is provided a method of improving generation of induced pluripotent stem cells (iPSCs) from a somatic cell, comprising:

(a) expressing within the somatic cell at least two growth factors selected from the group consisting of Oct4, Sox2, Klf4 and c-Myc and

(b) inhibiting Mbd3 expression in the somatic cell, and/or inhibiting binding of the Mbd3 to the nucleosome remodeling and deacetylase (NuRD) complex in the somatic cell,

thereby improving generation of the iPSCs from a somatic cell.

According to some embodiments of the invention, inhibiting the binding of the Mbd3 to the NuRD complex is performed using a chromodomain helicase DNA binding protein 4 (CHD4) inhibitor.

According to some embodiments of the invention, inhibiting the binding of the Mbd3 to the NuRD complex is performed using a P66 alpha coiled-coil domain.

According to some embodiments of the invention, inhibiting the Mbd3 expression is performed using a protein kinase C (PKC) inhibitor.

As described in Example 15 of the Examples section which follows, the present inventors have uncovered that overexpression of ERAS or activation of endogenous human *ERAS* in pluripotent stem cells can be used to induce a naive state in pluripotent stem cells.

According to some embodiments of the invention, the method further comprising exogenously expressing ES cell expressed Ras (ERAS) coding sequence (e.g., SEQ ID NO: 109) or activating endogenous expression of the ERAS in the somatic cell.

According to some embodiments of the invention, activating endogenous expression of ERAS is performed by removing the premature poly adenylation sites of the endogenous ERAS gene (SEQ ID NO: 108), e.g., in A-1, A2 or A-3 boxed sequences in Figure 3 by Kameda et al. Stem Cells 2005;23:1535–1540; which is fully incorporated herein by reference in its entirety.

According to some embodiments of the invention, expressing is effected for at least 48 hours such that the inhibiting the Mbd3 is effected to 10-30% of a level of the Mbd3 prior to the expressing.

According to some embodiments of the invention, expressing is effected for about 48 hours and the inhibiting is effected after the about 48 hours.

It should be noted that when inhibition of Mbd3 is performed after 48 hours, the inhibition can be of 100% of the expression level of activity of MBD3.

According to some embodiments of the invention, the iPSC is a murine iPSC.

According to some embodiments of the invention, the method further comprising culturing the murine iPSC in a medium which comprises LIF, an ERK1/2 inhibitor, and a GSK3b inhibitor.

According to some embodiments of the invention, wherein when the iPSC is a human iPSC, the method further comprising:

(c) culturing the human iPSC in a culture medium which comprises LIF, an ERK1/2 inhibitor, a GSK3b inhibitor, a P38 inhibitor, a JNK inhibitor, basic fibroblast growth factor (bFGF) and transforming growth factor-beta 1 (TGFβ1).

According to some embodiments of the invention, step (c) is performed following about 48 hours from the beginning of expression as recited in step (a).

According to some embodiments of the invention, the medium further comprises a ROCK inhibitor.

According to some embodiments of the invention, expressing is performed using DNA transfection of the growth factors.

According to some embodiments of the invention, expressing is performed using RNA transfection of the growth factors.

According to some embodiments of the invention, expressing is performed using protein transfection of the growth factors.

It should be noted that protein transfection into cells and cell nuclei can be performed as described by Hongyan Zhou, Shili Wu, et al. "Generation of Induced Pluripotent Stem Cells Using Recombinant Proteins". Cell Stem Cell - 5 June 2009, Vol. 4, Issue 6, pp. 581; which is incorporated herein by reference in its entirety, essentially by conjugating signal peptides which direct the recombinant factors into the cell or cell nucleus.

According to an aspect of some embodiments of the invention, there is provided an isolated naive pluripotent stem cell obtainable by the method of some embodiments of the invention.

According to some embodiments of the invention, the naive pluripotent stem cell comprising:

an unmethylated X-inactive specific transcript (XIST) gene, wherein:

(i) when the naive PSC is a female PSC, then the naive female PSC has two unmethylated alleles of the XIST gene; and

(ii) when the naive PSC is a male PSC, then the naive male PSC has an unmethylated allele of the XIST gene,

and/or

an expression level of transcription factor E3 (TFE3) characterized by a nucleus to cytoplasm expression ratio which is equal to or higher than 1 as determined by an immunostaining assay.

According to an aspect of some embodiments of the invention there is provided a method of generating differentiated cells, comprising subjecting the naive pluripotent stem cells generated according to the method of some embodiments of the invention to differentiating conditions, thereby generating the differentiated cells.

According to some embodiments of the invention, the naive PSCs of some embodiments of the invention can be used to isolate lineage specific cells.

As used herein, the phrase "isolating lineage specific cells" refers to the enrichment of a mixed population of cells in a culture with cells predominantly displaying at least one characteristic associated with a specific lineage phenotype. It will be appreciated that all cell lineages are derived from the three embryonic germ layers. Thus, for example, hepatocytes and pancreatic cells are derived from the embryonic endoderm, osseous, cartilaginous, elastic, fibrous connective tissues, yachts, myocardial cells, bone marrow cells, vascular cells (namely endothelial and smooth muscle cells), and hematopoietic cells are differentiated from embryonic mesoderm and neural, retina and epidermal cells are derived from the embryonic ectoderm.

Lineage specific cells can be obtained by directly inducing the expanded, undifferentiated naive PSCs to culturing conditions suitable for the differentiation of specific cell lineage.

Following is a non-limiting description of a number of procedures and approaches for inducing differentiation of EBs to lineage specific cells.

Neural precursor cells

To differentiate the EBs of some embodiments of the invention into neural precursors, four-day-old EBs are cultured for 5-12 days in tissue culture dishes including DMEM/F-12 medium with 5 mg/ml insulin, 50 mg/ml transferrin, 30 nM selenium chloride, and 5 mg/ml fibronectin (Its medium, Okabe, S. et al., 1996, Mech. Dev. 59: 89-102). The resultant neural precursors can be further transplanted to generate neural cells *in vivo* (Bristle, O. et al., 1997. *In vitro*-generated neural precursors participate in mammalian brain development. Proc. Natl. Acad. Sci. USA. 94: 14809-14814). It will be appreciated that prior to their transplantation, the neural precursors are trypsinized and triturated to single-cell suspensions in the presence of 0.1 % DNase.

Oligodendrocytes and myelinate cells

EBs of some embodiments of the invention can differentiate to oligodendrocytes and myelinate cells by culturing the cells in modified SATO medium, *i.e.,* DMEM with bovine serum albumin (BSA), pyruvate, progesterone, putrescine, thyroxine, triiodothyronine, insulin, transferrin, sodium selenite, amino acids, neurotrophin 3,

ciliary neurotrophic factor and Hepes (Bottenstein, J. E. & Sato, G. H., 1979, Proc. Natl. Acad. Sci. USA 76, 514-517; Raff, M. C., Miller, R. H., & Noble, M., 1983, Nature 303: 390-396]. Briefly, EBs are dissociated using 0.25 % Trypsin/EDTA (5 min at 37 °C) and triturated to single cell suspensions. Suspended cells are plated in flasks containing SATO medium supplemented with 5 % equine serum and 5 % fetal calf serum (FCS). Following 4 days in culture, the flasks are gently shaken to suspend loosely adhering cells (primarily oligodendrocytes), while astrocytes are remained adhering to the flasks and further producing conditioned medium. Primary oligodendrocytes are transferred to new flasks containing SATO medium for additional two days. Following a total of 6 days in culture, oligospheres are either partially dissociated and resuspended in SATO medium for cell transplantation, or completely dissociated and a plated in an oligosphere-conditioned medium which is derived from the previous shaking step [Liu, S. et al., (2000). Embryonic stem cells differentiate into oligodendrocytes and myelinate in culture and after spinal cord transplantation. Proc. Natl. Acad. Sci. USA. 97: 6126-6131].

Mast cells

For mast cell differentiation, two-week-old EBs of some embodiments of the invention are transferred to tissue culture dishes including DMEM medium supplemented with 10 % FCS, 2 mM L-glutamine, 100 units/ml penicillin, 100 mg/ml streptomycin, 20 % (v/v) WEHI-3 cell-conditioned medium and 50 ng/ml recombinant rat stem cell factor (rrSCF, Tsai, M. et al., 2000. *In vivo* immunological function of mast cells derived from embryonic stem cells: An approach for the rapid analysis of even embryonic lethal mutations in adult mice *in vivo*. Proc Natl Acad Sci USA. 97: 9186-9190). Cultures are expanded weekly by transferring the cells to new flasks and replacing half of the culture medium.

Hemato-lymphoid cells

To generate hemato-lymphoid cells from the EBs of some embodiments of the invention, 2-3 days-old EBs are transferred to gas-permeable culture dishes in the presence of 7.5 % CO_2 and 5 % O_2 using an incubator with adjustable oxygen content. Following 15 days of differentiation, cells are harvested and dissociated by gentle digestion with Collagenase (0.1 unit/mg) and Dispase (0.8 unit/mg), both are available from F. Hoffman-La Roche Ltd, Basel, Switzerland. CD45-positive cells are isolated

using anti-CD45 monoclonal antibody (mAb) M1/9.3.4.HL.2 and paramagnetic microbeads (Miltenyi) conjugated to goat anti-rat immunoglobulin as described in Potocnik, A.J. et al., (Immunology Hemato-lymphoid *in vivo* reconstitution potential of subpopulations derived from *in vitro* differentiated embryonic stem cells. Proc. Natl. Acad. Sci. USA. 1997, 94: 10295-10300). The isolated CD45-positive cells can be further enriched using a single passage over a MACS column (Miltenyi).

It will be appreciated that since EBs are complex structures, differentiation of EBs into specific differentiated cells, tissue or organ may require isolation of lineage specific cells from the EBs.

Such isolation may be effected by sorting of cells of the EBs via fluorescence activated cell sorter (FACS) or mechanical separation of cells, tissues and/or tissue-like structures contained within the EBs.

Methods of isolating EB-derived-differentiated cells via FACS analysis are known in the art. According to one method, EBs are disaggregated using a solution of Trypsin and EDTA (0.025 % and 0.01 %, respectively), washed with 5 % fetal bovine serum (FBS) in phosphate buffered saline (PBS) and incubated for 30 min on ice with fluorescently-labeled antibodies directed against cell surface antigens characteristics to a specific cell lineage. For example, endothelial cells are isolated by attaching an antibody directed against the platelet endothelial cell adhesion molecule-1 (PECAM1) such as the fluorescently-labeled PECAM1 antibodies (30884X) available from PharMingen (PharMingen, Becton Dickinson Bio Sciences, San Jose, CA, USA) as described in Levenberg, S. et al., (Endothelial cells derived from human embryonic stem cells. Proc. Natl. Acad. Sci. USA. 2002. 99: 4391-4396). Hematopoietic cells are isolated using fluorescently-labeled antibodies such as CD34-FITC, CD45-PE, CD31-PE, CD38-PE, CD90-FITC, CD117-PE, CD15-FITC, class I-FITC, all of which IgG1 are available from PharMingen, CD133/1-PE (IgG1) (available from Miltenyi Biotec, Auburn, CA), and glycophorin A-PE (IgG1), available from Immunotech (Miami, FL). Live cells (*i.e.,* without fixation) are analyzed on a FACScan (Becton Dickinson Bio Sciences) by using propidium iodide to exclude dead cells with either the PC-LYSIS or the CELLQUEST software. It will be appreciated that isolated cells can be further enriched using magnetically-labeled second antibodies and magnetic separation columns (MACS, Miltenyi) as described by Kaufman, D.S. et al., (Hematopoietic

colony-forming cells derived from human embryonic stem cells. Proc. Natl. Acad. Sci. USA. 2001, 98: 10716–10721).

An example for mechanical isolation of beating cardiomyocytes from EBs is disclosed in U.S. Pat. Appl. No. 20030022367 to Xu et al. Briefly, four-day-old EBs of some embodiments of the invention are transferred to gelatin-coated plates or chamber slides and are allowed to attach and differentiate. Spontaneously contracting cells, which are observed from day 8 of differentiation, are mechanically separated and collected into a 15-mL tube containing low-calcium medium or PBS. Cells are dissociated using Collagenase B digestion for 60-120 minutes at 37 °C, depending on the Collagenase activity. Dissociated cells are then resuspended in a differentiation KB medium (85 mM KCI, 30 mM K_2HPO_4, 5 mM $MgSO_4$, 1 mM EGTA, 5 mM creatine, 20 mM glucose, 2 mM Na_2ATP, 5 mM pyruvate, and 20 mM taurine, buffered to pH 7.2, Maltsev et al., Circ. Res. 75:233, 1994) and incubated at 37 °C for 15-30 min. Following dissociation cells are seeded into chamber slides and cultured in the differentiation medium to generate single cardiomyocytes capable of beating.

It will be appreciated that the culturing conditions suitable for the differentiation and expansion of the isolated lineage specific cells include various tissue culture medium, growth factors, antibiotic, amino acids and the like and it is within the capability of one skilled in the art to determine which conditions should be applied in order to expand and differentiate particular cell types and/or cell lineages [reviewed in Fijnvandraat AC, et al., Cardiovasc Res. 2003; 58: 303-12; Sachinidis A, et al., Cardiovasc Res. 2003; 58: 278-91; Stavridis MP and Smith AG, 2003; Biochem Soc Trans. 31(Pt 1): 45-9].

In addition to the lineage-specific primary cultures, EBs of the invention can be used to generate lineage-specific cell lines which are capable of unlimited expansion in culture.

Cell lines of some embodiments of the invention can be produced by immortalizing the EB-derived cells by methods known in the art, including, for example, expressing a telomerase gene in the cells (Wei, W. et al., 2003. Mol Cell Biol. 23: 2859–2870) or co-culturing the cells with NIH 3T3 hph-HOX11 retroviral producer cells (Hawley, R.G. et al., 1994. Oncogene 9: 1-12).

Following are non-limiting examples of culturing conditions which are suitable for differentiating and/or expanding lineage specific cells from the naive PSCs of some embodiments of the invention. It should be noted that for inducing differentiation of the naive PSCs into differentiated cells, the medium which was used to maintain the cells in the naive undifferentiated and pluripotent state should be replaced with the appropriate differentiation medium.

Mesenchymal stromal cells which are CD73-positive and SSEA-4-negative can be generated from naive PSCs by mechanically increasing the fraction of fibroblast-like differentiated cells formed in cultures of naive hPSCs, essentially as described in Trivedi P and Hematti P. Exp Hematol. 2008, 36(3):350-9. Briefly, to induce differentiation of hESC the intervals between medium changes are increased to 3-5 days, and the cells at the periphery of the naive PSCs colonies become spindle-shaped fibroblast-looking cells. After 9-10 days under these conditions when about 40-50% of the cells in the culture acquire the fibroblast-looking appearance, the undifferentiated portions of naive PSCs colonies are physically removed and the remaining differentiated cells are passaged to new culture plates under the same conditions.

To induce differentiation of naive hPSCs into dopaminergic (DA) neurons, the cells can be co-cultured with the mouse stromal cell lines PA6 or MS5, or can be cultured with a combination of stromal cell-derived factor 1 (SDF-1/CXCL12), pleiotrophin (PTN), insulin-like growth factor 2 (IGF2) and ephrin B1 (EFNB1) essentially as described in Vazin T, et al., PLoS One. 2009 Aug 12;4(8):e6606; and in Elkabetz Y., et al., Genes Dev. 2008 January 15; 22: 152–165.

To generate mesencephalic dopamine (mesDA) neurons, naive hPSCs can be genetically modified to express the transcription factor Lmx1a (e.g., using a lentiviral vector with the PGK promoter and Lmx1a) essentially as described in Friling S., et al., Proc Natl Acad Sci U S A. 2009, 106: 7613–7618.

To generate lung epithelium (type II pneumocytes) from naive hPSCs, the naive PSCs can be cultured in the presence of a commercially available cell culture medium (Small Airway Growth Medium; Cambrex, College Park, MD), or alternatively, in the presence of a conditioned medium collected from a pneumocyte cell line (e.g., the A549 human lung adenocarcinoma cell line) as described in Rippon HJ., et al., Proc Am Thorac Soc. 2008; 5: 717–722.

To induce differentiation of naive hPSCs cells into neural cells, the pluripotent stem cells can be cultured for about 5 days in the presence of a serum replacement medium supplemented with TGF-b inhibitor (SB431542, Tocris; e.g., 10 nM) and Noggin (R&D; e.g., 500 ng/ml), following which the cells are cultured with increasing amounts (e.g., 25 %, 50 %, 75 %, changed every two days) of N2 medium (Li XJ., et al., Nat Biotechnol. 2005, 23:215-21) in the presence of 500 ng/mL Noggin, essentially as described in Chambers SM., et al., Nat Biotechnol. 2009, 27: 275–280.

The invention, according to some embodiments thereof, contemplates the use of cells, tissues and organs generated from the naive pluripotent stem cells of the invention using any differentiation protocol known in the art.

It will be appreciated that since the lineage-specific cells or cell lines obtained according to the teachings of some embodiments of the invention are developed by differentiation processes similar to those naturally occurring in the human embryo they can be further used for human cell-based therapy and tissue regeneration.

Thus, the invention according to some embodiments thereof envisages the use of the expanded and/or differentiated lineage-specific cells or cell lines of some embodiments of the invention for treating a disorder requiring cell replacement therapy.

For example, diseases presently expected to be treatable by therapeutic transplantation of PSC or PSC-derived cells include Parkinson's disease, cardiac infarcts, juvenile-onset diabetes mellitus, and leukemia (Gearhart J. Science 1998, 282:1061; Rossant and Nagy, Nature Biotech. 1999, 17:23).

For example, oligodendrocyte precursors can be used to treat myelin disorders (Repair of myelin disease: Strategies and progress in animal models. Molecular Medicine Today. 1997. pp. 554-561), chondrocytes or mesenchymal cells can be used in treatment of bone and cartilage defects (U.S. Pat. No. 4,642,120) and cells of the epithelial lineage can be used in skin regeneration of a wound or burn (U.S. Pat. No. 5,716,411).

For certain disorders, such as genetic disorders in which a specific gene product is missing [e.g., lack of the CFTR gene-product in cystic fibrosis patients (Davies JC, 2002. New therapeutic approaches for cystic fibrosis lung disease. J. R. Soc. Med. 95 Suppl 41:58-67)], PSC-derived cells are preferably manipulated to over-express the mutated gene prior to their administration to the individual. It will be appreciated that

for other disorders, the PSC-derived cells should be manipulated to exclude certain genes.

Over-expression or exclusion of genes can be effected using knock-in and/or knock-out constructs [see for example, Fukushige, S. and Ikeda, J. E.: Trapping of mammalian promoters by Cre-lox site-specific recombination. DNA Res 3 (1996) 73-50; Bedell, M. A., Jerkins, N. A. and Copeland, N. G.: Mouse models of human disease. Part I: Techniques and resources for genetic analysis in mice. Genes and Development 11 (1997) 1-11; Bermingham, J. J., Scherer, S. S., O'Connell, S., Arroyo, E., Kalla, K. A., Powell, F. L. and Rosenfeld, M. G.: Tst-1/Oct-6/SCIP regulates a unique step in peripheral myelination and is required for normal respiration. Genes Dev 10 (1996) 1751-62].

In addition to cell replacement therapy, the lineage specific cells of some embodiments of the invention can also be utilized to prepare a cDNA library. mRNA is prepared by standard techniques from the lineage specific cells and is further reverse transcribed to form cDNA. The cDNA preparation can be subtracted with nucleotides from embryonic fibroblasts and other cells of undesired specificity, to produce a subtracted cDNA library by techniques known in the art.

The lineage specific cells of some embodiments of the invention can be used to screen for factors (such as small molecule drugs, peptides, polynucleotides, and the like) or conditions (such as culture conditions or manipulation) that affect the differentiation of lineage precursor to terminally differentiated cells. For example, growth affecting substances, toxins or potential differentiation factors can be tested by their addition to the culture medium.

According to an aspect of some embodiments of the invention, there is provided a method of generating a primordial germ cell, comprising culturing primate naive pluripotent stem cells in a culture medium selected capable of inducing the primate naive pluripotent stem cells into primordial germ cell, wherein the culture medium comprises a Rho kinase (ROCK) inhibitor and bone morphogenetic protein 4 (BMP4), thereby generating the primordial germ cell.

According to some embodiments of the invention, the primate naive pluripotent stem cell comprises:

an unmethylated X-inactive specific transcript (XIST) gene, wherein:

(i) when the naive PSC is a female PSC, then the naive female PSC has two unmethylated alleles of the XIST gene; and

(ii) when the naive PSC is a male PSC, then the naive male PSC has an unmethylated allele of the XIST gene,

and/or

an expression level of transcription factor E3 (TFE3) characterized by a nucleus to cytoplasm expression ratio which is equal to or higher than 1 as determined by an immunostaining assay.

According to some embodiments of the invention, the primordial germ cell is characterized by CD61 (intergrin beta 3) positive expression pattern.

According to some embodiments of the invention, the primordial germ cell is characterized by $CD61^+/SSEA4^+$ expression pattern (expression signature).

According to some embodiments of the invention, the culture medium selected capable of inducing the primate naive pluripotent stem cells into primordial germ cell further comprises at least one agent selected from the group consisting of: leukemia inhibitory factor (LIF), Stem Cell Factor (SCF) and Epidermal Growth Factor (EGF).

According to an aspect of some embodiments of the invention, there is provided an isolated population of primate primordial germ cells comprising primate primordial germ cells generated according to the method of some embodiments of the invention.

According to some embodiments of the invention, the isolated population of primate primordial germ cells comprising at least about 50%, e.g., at least about 60%, e.g., at least about 70%, e.g., at least about 80%, e.g., at least about 90%, e.g., at least about 95%, e.g., at least about 99%, e.g., 100% of primordial germ cells characterized by $CD61^+/SSEA4^+$ expression pattern.

It should be noted that the isolated primordial germ cells (PGCs) of some embodiments of the invention can be injected into adult human testis or ovary to complete their maturation and generate sperm or eggs.

According to an aspect of some embodiments of the invention, there is provided a method of treating a subject in need thereof, comprising administering the primordial germ cells of some embodiments of the invention to a gonad tissue of the subject, thereby treating the subject in need thereof.

The term "subject" refers to a mammal, e.g., a primate, preferably a human being at any age which suffer from the pathology.

The term "treating" refers to inhibiting, preventing or arresting the development of a pathology (disease, disorder or condition) and/or causing the reduction, remission, or regression of a pathology. Those of skill in the art will understand that various methodologies and assays can be used to assess the development of a pathology, and similarly, various methodologies and assays may be used to assess the reduction, remission or regression of a pathology.

According to some embodiments of the invention, the subject suffers from infertility.

According to an aspect of some embodiments of the invention, there is provided a kit comprising the primate primordial germ cells of some embodiments of the invention and a medicament for treating infertility.

The kit may also include appropriate buffers and preservatives for improving the shelf-life of the kit.

The kit may include appropriate instructions for use and labels indicating FDA approval for use in treating a subject, such as treating infertility in the subject.

As shown in Figures 26A-C, 108A-C and 109A-E and described in Examples 8 of the Examples section which follows, the present inventors were capable of using the isolated naïve PSC of some embodiments of the invention for generation of a chimeric human-mouse organism, and to contribute to development of mouse embryo in vivo (Gafni et al. Nature 2013; Dec 12;504(7479):282-6. doi: 10.1038/nature12745. Epub 2013 Oct 30). Thus, 24 hours and later after administration of the human PSC, the injected cells were viable in the developing early mouse embryos. These results indicate that human naive cells grown in the medium of some embodiments of the invention (e.g., WIS-NHSM conditions) can contribute to cross-species chimeric organisms.

Thus, according to an aspect of some embodiments of the invention, there is provided a method of generating a chimeric animal. The method comprising introducing the isolated primate (e.g., human) naive PSC of some embodiments of the invention, or the primordial germ cells of some embodiments of the invention into a pre-implantation embryo of a host animal, thereby generating the chimeric animal.

According to some embodiments of the invention, the method further comprising allowing the chimeric animal to grow *in vivo* or *ex vivo*.

It should be noted that since the isolated naïve pluripotent stem cells or the primordial germ cells are introduced into the pre-implantation embryo they are likely to form a normal embryo.

As used herein, the phrase "chimeric animal" refers to an animal comprising cells of at least two genetically distinct individuals.

As used herein, the term "pre-implantation embryo" refers to an embryo at an 8-cell stage, 16- cell stage embryo, early morula, late morula, early blastocyst, and/or a late blastocyst.

It is noted that the chimeric animal can be composed of cells of two different individuals belonging to two different species, or to the same species.

According to some embodiments of the invention, the isolated naive PSC or the primordial germ cell is allogeneic to the host animal.

As used herein, the term "alloegeneic" refers to at least two genetically different individuals of the same species.

According to some embodiments of the invention, the isolated naive PSC or the primordial germ cell is xenogeneic to the host animal.

As used herein, the term "xenogeneic" refers to at least two individuals of different species.

According to some embodiments of the invention, the host animal is not human.

According to some embodiments of the invention, introducing the cells is performed *in vivo*.

Methods of *in vivo* administration of cells into a morula of an animal are well known in the art, such as in Gafni O, Weinberger L, Mansour AA, Manor YS, Chomsky E, Ben-Yosef D, Kalma Y, Viukov S, Maza I, Zviran A, Rais Y, Shipony Z, Mukamel Z, Krupalnik V, Zerbib M, Geula S, Caspi I, Schneir D, Shwartz T, Gilad S, Amann-Zalcenstein D, Benjamin S, Amit I, Tanay A, Massarwa R, Novershtern N, Hanna JH. Nature. 2013 Dec 12;504(7479):282-6. doi: 10.1038/nature12745. Epub 2013 Oct 30.; and *Manipulating the Mouse Embryo*: A Laboratory Manual, Fourth Edition. By Richard Behringer; Marina Gertsenstein; Kristina Vintersten Nagy; Andras Nagy, each of which is fully incorporated herein by reference.

According to some embodiments of the invention, introducing the cells is performed *in vitro* or *ex vivo* via direct injection or aggregation with the developing host embryo.

According to some embodiments of the invention, the morula comprises at least 4 cells.

According to some embodiments of the invention, the morula comprises no more than 128 cells.

According to some embodiments of the invention, the host animal is a primate, e.g., a mammal.

According to some embodiments of the invention, the host animal is mouse.

According to some embodiments of the invention, the host animal is pig.

According to some embodiments of the invention, the host animal is monkey.

According to some embodiments of the invention, the host animal is chimpanzee.

It should be noted that once the chimeric animal is formed, and allowed to grow, the cells of the chimeric animal can be used for cell therapy. For example, the mature differentiated cells (e.g., hematopoietic stem cells, liver hepatocytes, insulin producing Beta cells) generated in the chimeric animal based on some embodiments of the invention can be used for transplantation in adult humans or for biomedical applications.

Thus, according to an aspect of some embodiments of the invention, there is provided a method of isolating differentiated cells, cell lineages, tissues or organs from the chimeric animal of some embodiments of the invention.

Methods of isolating such differentiated cells, tissues or organs are well known in the art and are also described hereinabove.

Thus, in case the naive PSCs that were used to form the chimeric animal are human cells, these cells can be further isolated from the formed chimeric animal and used for treating a human subject.

According to some embodiments of the invention, the method further comprises isolating human-derived (human-originated) cells or tissues from the chimeric animal.

Non-limiting examples of using such human-originated cells, tissues or organs include cell based therapy, tissue replacement, organ or tissue implantation.

Following is a non-limiting description of expression vectors and modes of administering thereof into cells which can be used to express a polypeptide-of-interest (e.g., any of the proteins described hereinabove, e.g., OCT4, c-MYC, SOX2, KLF4, LIF, bFGF, TGFβ1) in a cell.

To express an exogenous protein in mammalian cells, a polynucleotide sequence encoding the polypeptide-of-interest is preferably ligated into a nucleic acid construct suitable for mammalian cell expression. Such a nucleic acid construct includes a promoter sequence for directing transcription of the polynucleotide sequence in the cell in a constitutive or inducible manner.

The nucleic acid construct (also referred to herein as an "expression vector") of some embodiments of the invention includes additional sequences which render this vector suitable for replication and integration in prokaryotes, eukaryotes, or preferably both (e.g., shuttle vectors). In addition, a typical cloning vectors may also contain a transcription and translation initiation sequence, transcription and translation terminator and a polyadenylation signal. By way of example, such constructs will typically include a 5' LTR, a tRNA binding site, a packaging signal, an origin of second-strand DNA synthesis, and a 3' LTR or a portion thereof.

The nucleic acid construct of some embodiments of the invention typically includes a signal sequence for secretion of the peptide from a host cell in which it is placed. Preferably the signal sequence for this purpose is a mammalian signal sequence or the signal sequence of the polypeptide variants of some embodiments of the invention.

Eukaryotic promoters typically contain two types of recognition sequences, the TATA box and upstream promoter elements. The TATA box, located 25-30 base pairs upstream of the transcription initiation site, is thought to be involved in directing RNA polymerase to begin RNA synthesis. The other upstream promoter elements determine the rate at which transcription is initiated.

Enhancer elements can stimulate transcription up to 1,000 fold from linked homologous or heterologous promoters. Enhancers are active when placed downstream or upstream from the transcription initiation site. Many enhancer elements derived from viruses have a broad host range and are active in a variety of tissues. For example, the SV40 early gene enhancer is suitable for many cell types. Other enhancer/promoter

combinations that are suitable for some embodiments of the invention include those derived from polyoma virus, human or murine cytomegalovirus (CMV), the long term repeat from various retroviruses such as murine leukemia virus, murine or Rous sarcoma virus and HIV. See, Enhancers and Eukaryotic Expression, Cold Spring Harbor Press, Cold Spring Harbor, N.Y. 1983, which is incorporated herein by reference.

In the construction of the expression vector, the promoter is preferably positioned approximately the same distance from the heterologous transcription start site as it is from the transcription start site in its natural setting. As is known in the art, however, some variation in this distance can be accommodated without loss of promoter function.

Polyadenylation sequences can also be added to the expression vector in order to increase the efficiency of mRNA translation. Two distinct sequence elements are required for accurate and efficient polyadenylation: GU or U rich sequences located downstream from the polyadenylation site and a highly conserved sequence of six nucleotides, AAUAAA, located 11-30 nucleotides upstream. Termination and polyadenylation signals that are suitable for some embodiments of the invention include those derived from SV40.

In addition to the elements already described, the expression vector of some embodiments of the invention may typically contain other specialized elements intended to increase the level of expression of cloned nucleic acids or to facilitate the identification of cells that carry the recombinant DNA. For example, a number of animal viruses contain DNA sequences that promote the extra chromosomal replication of the viral genome in permissive cell types. Plasmids bearing these viral replicons are replicated episomally as long as the appropriate factors are provided by genes either carried on the plasmid or with the genome of the host cell.

The vector may or may not include a eukaryotic replicon. If a eukaryotic replicon is present, then the vector is amplifiable in eukaryotic cells using the appropriate selectable marker. If the vector does not comprise a eukaryotic replicon, no episomal amplification is possible. Instead, the recombinant DNA integrates into the genome of the engineered cell, where the promoter directs expression of the desired nucleic acid.

The expression vector of some embodiments of the invention can further include additional polynucleotide sequences that allow, for example, the translation of several

proteins from a single mRNA such as an internal ribosome entry site (IRES) and sequences for genomic integration of the promoter-chimeric polypeptide.

It will be appreciated that the individual elements comprised in the expression vector can be arranged in a variety of configurations. For example, enhancer elements, promoters and the like, and even the polynucleotide sequence(s) encoding a the protein-of-interest can be arranged in a "head-to-tail" configuration, may be present as an inverted complement, or in a complementary configuration, as an anti-parallel strand. While such variety of configuration is more likely to occur with non-coding elements of the expression vector, alternative configurations of the coding sequence within the expression vector are also envisioned.

Examples for mammalian expression vectors include, but are not limited to, pcDNA3, pcDNA3.1(+/-), pGL3, pZeoSV2(+/-), pSecTag2, pDisplay, pEF/myc/cyto, pCMV/myc/cyto, pCR3.1, pSinRep5, DH26S, DHBB, pNMT1, pNMT41, pNMT81, which are available from Invitrogen, pCI which is available from Promega, pMbac, pPbac, pBK-RSV and pBK-CMV which are available from Strategene, pTRES which is available from Clontech, and their derivatives.

Expression vectors containing regulatory elements from eukaryotic viruses such as retroviruses can be also used. SV40 vectors include pSVT7 and pMT2. Vectors derived from bovine papilloma virus include pBV-1MTHA, and vectors derived from Epstein Bar virus include pHEBO, and p2O5. Other exemplary vectors include pMSG, pAV009/A$^+$, pMTO10/A$^+$, pMAMneo-5, baculovirus pDSVE, and any other vector allowing expression of proteins under the direction of the SV-40 early promoter, SV-40 later promoter, metallothionein promoter, murine mammary tumor virus promoter, Rous sarcoma virus promoter, polyhedrin promoter, or other promoters shown effective for expression in eukaryotic cells.

As described above, viruses are very specialized infectious agents that have evolved, in many cases, to elude host defense mechanisms. Typically, viruses infect and propagate in specific cell types. The targeting specificity of viral vectors utilizes its natural specificity to specifically target predetermined cell types and thereby introduce a recombinant gene into the infected cell. Thus, the type of vector used by some embodiments of the invention will depend on the cell type transformed. The ability to select suitable vectors according to the cell type transformed is well within the

capabilities of the ordinary skilled artisan and as such no general description of selection consideration is provided herein. For example, bone marrow cells can be targeted using the human T cell leukemia virus type I (HTLV-I) and kidney cells may be targeted using the heterologous promoter present in the baculovirus Autographa californica nucleopolyhedrovirus (AcMNPV) as described in Liang CY et al., 2004 (Arch Virol. 149: 51-60).

Recombinant viral vectors are useful for *in vivo* expression of the protein-of-interest since they offer advantages such as lateral infection and targeting specificity. Lateral infection is inherent in the life cycle of, for example, retrovirus and is the process by which a single infected cell produces many progeny virions that bud off and infect neighboring cells. The result is that a large area becomes rapidly infected, most of which was not initially infected by the original viral particles. This is in contrast to vertical-type of infection in which the infectious agent spreads only through daughter progeny. Viral vectors can also be produced that are unable to spread laterally. This characteristic can be useful if the desired purpose is to introduce a specified gene into only a localized number of targeted cells.

Various methods can be used to introduce the expression vector of some embodiments of the invention into stem cells. Such methods are generally described in Sambrook et al., Molecular Cloning: A Laboratory Manual, Cold Springs Harbor Laboratory, New York (1989, 1992), in Ausubel et al., Current Protocols in Molecular Biology, John Wiley and Sons, Baltimore, Md. (1989), Chang et al., Somatic Gene Therapy, CRC Press, Ann Arbor, Mich. (1995), Vega et al., Gene Targeting, CRC Press, Ann Arbor Mich. (1995), Vectors: A Survey of Molecular Cloning Vectors and Their Uses, Butterworths, Boston Mass. (1988) and Gilboa et at. [Biotechniques 4 (6): 504-512, 1986] and include, for example, stable or transient transfection, lipofection, electroporation and infection with recombinant viral vectors. In addition, see U.S. Pat. Nos. 5,464,764 and 5,487,992 for positive-negative selection methods.

Introduction of nucleic acids by viral infection offers several advantages over other methods such as lipofection and electroporation, since higher transfection efficiency can be obtained due to the infectious nature of viruses.

Currently preferred *in vivo* nucleic acid transfer techniques include transfection with viral or non-viral constructs, such as adenovirus, lentivirus, Herpes simplex I virus,

or adeno-associated virus (AAV) and lipid-based systems. Useful lipids for lipid-mediated transfer of the gene are, for example, DOTMA, DOPE, and DC-Chol [Tonkinson et al., Cancer Investigation, 14(1): 54-65 (1996)]. The most preferred constructs for use in gene therapy are viruses, most preferably adenoviruses, AAV, lentiviruses, or retroviruses. A viral construct such as a retroviral construct includes at least one transcriptional promoter/enhancer or locus-defining element(s), or other elements that control gene expression by other means such as alternate splicing, nuclear RNA export, or post-translational modification of messenger. Such vector constructs also include a packaging signal, long terminal repeats (LTRs) or portions thereof, and positive and negative strand primer binding sites appropriate to the virus used, unless it is already present in the viral construct. In addition, such a construct typically includes a signal sequence for secretion of the peptide from a host cell in which it is placed. Preferably the signal sequence for this purpose is a mammalian signal sequence or the signal sequence of the polypeptide variants of some embodiments of the invention. Optionally, the construct may also include a signal that directs polyadenylation, as well as one or more restriction sites and a translation termination sequence. By way of example, such constructs will typically include a 5' LTR, a tRNA binding site, a packaging signal, an origin of second-strand DNA synthesis, and a 3' LTR or a portion thereof. Other vectors can be used that are non-viral, such as cationic lipids, polylysine, and dendrimers.

Other than containing the necessary elements for the transcription and translation of the inserted coding sequence, the expression construct of some embodiments of the invention can also include sequences engineered to enhance stability, production, purification, yield or toxicity of the expressed peptide. For example, the expression of a fusion protein or a cleavable fusion protein comprising the polypeptide-of-interest of some embodiments of the invention and a heterologous protein can be engineered. Such a fusion protein can be designed so that the fusion protein can be readily isolated by affinity chromatography; e.g., by immobilization on a column specific for the heterologous protein. Where a cleavage site is engineered between the protein-of-interest and the heterologous protein, the protein-of-interest can be released from the chromatographic column by treatment with an appropriate enzyme or agent that disrupts

the cleavage site [e.g., see Booth et al. (1988) Immunol. Lett. 19:65-70; and Gardella et al., (1990) J. Biol. Chem. 265:15854-15859].

As mentioned hereinabove, a variety of prokaryotic or eukaryotic cells can be used as host-expression systems to express the polypeptides of some embodiments of the invention. These include, but are not limited to, microorganisms, such as bacteria transformed with a recombinant bacteriophage DNA, plasmid DNA or cosmid DNA expression vector containing the coding sequence; yeast transformed with recombinant yeast expression vectors containing the coding sequence; plant cell systems infected with recombinant virus expression vectors (e.g., cauliflower mosaic virus, CaMV; tobacco mosaic virus, TMV) or transformed with recombinant plasmid expression vectors, such as Ti plasmid, containing the coding sequence. Mammalian expression systems can also be used to express the polypeptides of some embodiments of the invention.

Examples of bacterial constructs include the pET series of E. coli expression vectors [Studier et al. (1990) Methods in Enzymol. 185:60-89).

In yeast, a number of vectors containing constitutive or inducible promoters can be used, as disclosed in U.S. Pat. Application No: 5,932,447. Alternatively, vectors can be used which promote integration of foreign DNA sequences into the yeast chromosome.

In cases where plant expression vectors are used, the expression of the coding sequence can be driven by a number of promoters. For example, viral promoters such as the 35S RNA and 19S RNA promoters of CaMV [Brisson et al. (1984) Nature 310:511-514], or the coat protein promoter to TMV [Takamatsu et al. (1987) EMBO J. 6:307-311] can be used. Alternatively, plant promoters such as the small subunit of RUBISCO [Coruzzi et al. (1984) EMBO J. 3:1671-1680 and Brogli et al., (1984) Science 224:838-843] or heat shock promoters, e.g., soybean hsp17.5-E or hsp17.3-B [Gurley et al. (1986) Mol. Cell. Biol. 6:559-565] can be used. These constructs can be introduced into plant cells using Ti plasmid, Ri plasmid, plant viral vectors, direct DNA transformation, microinjection, electroporation and other techniques well known to the skilled artisan. See, for example, Weissbach & Weissbach, 1988, Methods for Plant Molecular Biology, Academic Press, NY, Section VIII, pp 421-463.

Other expression systems such as insects and mammalian host cell systems which are well known in the art and are further described hereinbelow can also be used by some embodiments of the invention.

Transformed cells are cultured under effective conditions, which allow for the expression of high amounts of the recombinant polypeptide-of-interest (e.g., the LIF, TGFβ1, bFGF, OCT4, c-myc, SOX2, KLF-4). Following a predetermined time in culture, recovery of the recombinant polypeptide is effected. The phrase "recovery of the recombinant polypeptide" used herein refers to collecting the whole fermentation medium containing the polypeptide and need not imply additional steps of separation or purification.

Thus, polypeptide-of-interest can be purified using a variety of standard protein purification techniques, such as, but not limited to, affinity chromatography, ion exchange chromatography, filtration, electrophoresis, hydrophobic interaction chromatography, gel filtration chromatography, reverse phase chromatography, concanavalin A chromatography, chromatofocusing and differential solubilization.

The polypeptide-of-interest is preferably retrieved in "substantially pure" form. As used herein, the phrase "substantially pure" refers to a purity that allows for the effective use of the polypeptide-of-interest (e.g., the LIF, TGFβ1, bFGF) in maintaining the human embryonic stem cells in an undifferentiated state while in culture.

As used herein the term “about” refers to ± 10 %.

The terms "comprises", "comprising", "includes", "including", “having” and their conjugates mean "including but not limited to".

The term “consisting of” means “including and limited to”.

The term "consisting essentially of" means that the composition, method or structure may include additional ingredients, steps and/or parts, but only if the additional ingredients, steps and/or parts do not materially alter the basic and novel characteristics of the claimed composition, method or structure.

As used herein, the singular form "a", "an" and "the" include plural references unless the context clearly dictates otherwise. For example, the term "a compound" or "at least one compound" may include a plurality of compounds, including mixtures thereof.

Throughout this application, various embodiments of this invention may be presented in a range format. It should be understood that the description in range format is merely for convenience and brevity and should not be construed as an inflexible limitation on the scope of the invention. Accordingly, the description of a range should be considered to have specifically disclosed all the possible subranges as well as individual numerical values within that range. For example, description of a range such as from 1 to 6 should be considered to have specifically disclosed subranges such as from 1 to 3, from 1 to 4, from 1 to 5, from 2 to 4, from 2 to 6, from 3 to 6 etc., as well as individual numbers within that range, for example, 1, 2, 3, 4, 5, and 6. This applies regardless of the breadth of the range.

Whenever a numerical range is indicated herein, it is meant to include any cited numeral (fractional or integral) within the indicated range. The phrases “ranging/ranges between” a first indicate number and a second indicate number and “ranging/ranges from” a first indicate number “to” a second indicate number are used herein interchangeably and are meant to include the first and second indicated numbers and all the fractional and integral numerals therebetween.

As used herein the term "method" refers to manners, means, techniques and procedures for accomplishing a given task including, but not limited to, those manners, means, techniques and procedures either known to, or readily developed from known manners, means, techniques and procedures by practitioners of the chemical, pharmacological, biological, biochemical and medical arts.

As used herein, the term “treating” includes abrogating, substantially inhibiting, slowing or reversing the progression of a condition, substantially ameliorating clinical or aesthetical symptoms of a condition or substantially preventing the appearance of clinical or aesthetical symptoms of a condition.

It is appreciated that certain features of the invention, which are, for clarity, described in the context of separate embodiments, may also be provided in combination in a single embodiment. Conversely, various features of the invention, which are, for brevity, described in the context of a single embodiment, may also be provided separately or in any suitable subcombination or as suitable in any other described embodiment of the invention. Certain features described in the context of various

embodiments are not to be considered essential features of those embodiments, unless the embodiment is inoperative without those elements.

Various embodiments and aspects of the present invention as delineated hereinabove and as claimed in the claims section below find experimental support in the following examples.

EXAMPLES

Reference is now made to the following examples, which together with the above descriptions illustrate some embodiments of the invention in a non limiting fashion.

Generally, the nomenclature used herein and the laboratory procedures utilized in the present invention include molecular, biochemical, microbiological and recombinant DNA techniques. Such techniques are thoroughly explained in the literature. See, for example, "Molecular Cloning: A laboratory Manual" Sambrook et al., (1989); "Current Protocols in Molecular Biology" Volumes I-III Ausubel, R. M., ed. (1994); Ausubel et al., "Current Protocols in Molecular Biology", John Wiley and Sons, Baltimore, Maryland (1989); Perbal, "A Practical Guide to Molecular Cloning", John Wiley & Sons, New York (1988); Watson et al., "Recombinant DNA", Scientific American Books, New York; Birren et al. (eds) "Genome Analysis: A Laboratory Manual Series", Vols. 1-4, Cold Spring Harbor Laboratory Press, New York (1998); methodologies as set forth in U.S. Pat. Nos. 4,666,828; 4,683,202; 4,801,531; 5,192,659 and 5,272,057; "Cell Biology: A Laboratory Handbook", Volumes I-III Cellis, J. E., ed. (1994); "Current Protocols in Immunology" Volumes I-III Coligan J. E., ed. (1994); Stites et al. (eds), "Basic and Clinical Immunology" (8th Edition), Appleton & Lange, Norwalk, CT (1994); Mishell and Shiigi (eds), "Selected Methods in Cellular Immunology", W. H. Freeman and Co., New York (1980); available immunoassays are extensively described in the patent and scientific literature, see, for example, U.S. Pat. Nos. 3,791,932; 3,839,153; 3,850,752; 3,850,578; 3,853,987; 3,867,517; 3,879,262; 3,901,654; 3,935,074; 3,984,533; 3,996,345; 4,034,074; 4,098,876; 4,879,219; 5,011,771 and 5,281,521; "Oligonucleotide Synthesis" Gait, M. J., ed. (1984); “Nucleic Acid Hybridization" Hames, B. D., and Higgins S. J., eds. (1985); "Transcription and Translation" Hames, B. D., and Higgins S. J., Eds. (1984); "Animal Cell Culture" Freshney, R. I., ed. (1986); "Immobilized Cells and Enzymes" IRL Press, (1986); "A Practical Guide to Molecular Cloning" Perbal, B., (1984) and "Methods in Enzymology"

Vol. 1-317, Academic Press; "PCR Protocols: A Guide To Methods And Applications", Academic Press, San Diego, CA (1990); Marshak et al., "Strategies for Protein Purification and Characterization - A Laboratory Course Manual" CSHL Press (1996); all of which are incorporated by reference as if fully set forth herein. Other general references are provided throughout this document. The procedures therein are believed to be well known in the art and are provided for the convenience of the reader. All the information contained therein is incorporated herein by reference.

GENERAL MATERIALS AND EXPERIMENTAL METHODS

Mouse stem cell lines and cell culture - Reprogramming and maintenance of murine naive pluripotent cells were conducted in serum-free chemically defined N2B27-based media: 240 ml DMEM/F12 (Biological Industries – custom made), 240 ml Neurobasal (Invitrogen; 21103), 5 ml N2 supplement (Invitrogen; 17502048), 5 ml B27 supplement (Invitrogen; 17504044), 15% knockout serum replacement (Invitrogen – 10828), 1 mM glutamine (Invitrogen), 1% nonessential amino acids (Invitrogen), 0.1 mM β-mercaptoethanol (Sigma), penicillin-streptomycin (Invitrogen), 5 mg/ml BSA (Sigma). Naive conditions for murine PSCs included 10 ng/ml recombinant human LIF (Millipore; LIF1005) (5 μg per 500 ml). Where indicated "2i" inhibitors the following agents were added: small-molecule inhibitors CHIR99021 (CH, 3 μM- Axon Medchem) and PD0325901 (PD, 1 μM - TOCRIS). The "2i" was added 48 hours after OSKM induction.

"Primed N2B27 media" for murine cells (EpiSCs) contained 8 ng/ml recombinant human bFGF (Peprotech Asia) and 20 ng/ml recombinant human Activin (Peprotech Asia).

Stem cell lines and mice deficient for Mbd3 and their derived ES lines were obtained as previously described (Kaji et al., 2007) ($Mbd3^{flox/flox}$, $Mbd3^{flox/-}$ and $Mbd3^{+/-}$) (Kaji et al., 2006). For additional gene targeting of mouse pluripotent stem cell lines (Nanog-GFP reporter, pBRY-Mbd3 rescue constructs, Rosa26-CreER) 50 μg DNA of the targeting construct was linearized and electroporated into the indicated pluripotent cell lines, that were then subjected to selection with G418 (300 microg/ml) or Puromycin (1 microg/ml). After 10 days of antibiotic selection, drug resistant clones were analyzed for correct targeting by PCR or Southern blot analysis.

Mbd3Utx$^{+/-}$ males and females for ESC derivation in defined mouse 2i/LIF conditions were mated and E3.5 blastocysts were harvested and explanted for ESC derivation in defined mouse 2i/LIF conditions on MEF coated plates.

NGFP1-Mbd3^{KD} was established by infection and sub cloning of secondary NGFP1 iPSC line with a ShRNA pLKO-Tet-On vector (addgene) as previously described (Hanna, J. et al. Nature 462, 595–601, 2009). V6.5 mouse ESCs harboring a Flag-tagged endogenous Oct4 allele (Figure 60C) were generated by direct gene targeting as previously described (Tsai, H. H., Bourque, G. & Lufkin, T. In silico tandem affinity purification refines an Oct4 interaction list. Stem cell research Ther. 2: 26, 2011). Mycoplasma detection test are weekly conducted, to ensure exclusion of any contaminated cells. Genotyping and functional validation of Mbd3 depletion are presented throughout the study (Examples in Figures 1I-J and Figures 8M-N).

Epigenetic reversion of mouse primed epiblast cells - Male naive V6.5 (Mbd3$^{+/+}$) Nanog-GFP ESCs (Mansour et al., 2012) cells maintained in 2i/LIF conditions, were injected into BDF2 blastocysts and Epiblast. Chimeric embryos were dissected at day E6.5 and explanted on gelatin/vitronectin-coated plates in N2B27 bFGF/Activin conditions supplemented with 1 μg/ml puromycin, allowing the isolation of Nanog-GFP EpiSCs. For epigenetic reversion of murine EpiSCs to naive pluripotency, cells were passaged into N2B27 2i/LIF conditions on vitronectin (1 μg/ml) and gelatin (0.2%) coated plates (without overexpression of exogenous reprogramming factors). When epigenetic reversion assay involved single cell plating, EpiSC growth medium was supplemented with ROCK inhibitor for 24 hours before trypsinization. siRNAs (ON-TARGETplus SMARTpools) and the control siRNA (ON-TARGETplus Non-targeting pool D-001810-10-05) were purchased from Dharmacon. 10 nM siRNA or control was used for each transfection with Lipofectamine RNAiMAX (Invitrogen).

For EG (mouse embryonic germ cells) derivation experiments, Oct4-GFP+ PGC (Primordial Germ Cells) cells were sorted from E8.5 dissected chimeric embryos and single plated in N2B27 15% KSR, LIF (20 ng/ml)/SCF (10 ng/ml) /bFGF (8 ng/ml) medium and 2i (supplemented 48 hours later). Nuclear mCherry labeling of EpiSCs and their derived PGCs was used to allow calculating plating efficiency and calculate reprogramming efficiency (reprogramming efficiency % = Oct4 or Nanog-GFP clones /

mCherry+ clones).

OKSM factors: Oct4 (SEQ ID NO:54 protein), Sox2 (SEQ ID NO:56 protein), c-Myc (SEQ ID NO:60 protein) and Klf4 (SEQ ID NO:58 protein).

Reprogramming of mouse somatic cells and cell infection - Virus-containing supernatants of the different reprogramming viruses (STEMCA-OKSM polycistronic vector (SEQ ID NO:62) (Dox inducible and constitutive expression) (Mansour et al., 2012), STEMCCA-OKS polycistronic vector (DOX inducible and constitutive expression), FUW-tetO-lox-hKLF4, FUW-tetO-lox-hOCT4 and FUW-tetO-lox-hSOX2, FUW-tetO-mKlf4, FUW-tetO-mOct4, FUW-tetO-mSox2, FUW-tetO-c-Myc, FUW-Oct4-2A-Sox2, FUW-Oct4-2A-Klf4, FUW-tetO-lox-SOX2, pMXs-OCT4, pMXs-SOX2, pMXs-KLF4, pMXs-cMYC) was supplemented with the FUW-lox-M2rtTA virus (when necessary) and an equal volume of fresh culture medium for infection. Mouse fibroblast and other somatic cells types were isolated and single cell sorted from secondary transgenic reprogrammable chimeras (Hanna et al., 2009a; Mansour et al., 2012). Secondary transgenic mouse somatic cells carrying DOX inducible OSKM encoding transgene (Hanna et al. Cell 2008, Mansour et al. Nature 2012) were reprogrammed by applying mouse naive ESCs medium + Doxycycline (DOX) (without 2i in the first 48 hours and then adding also 2i until completion of process). Human iPSC reprogramming was applied by lentiviral infection of human differentiated cells with OSKM encoding lentivirus and applying WIS-NHSM conditions starting from 48 hours after infection.

iPSCs reprogramming by using mouse naive ESCs medium 2i/LIF + DOX (1 μg/ml) (without 2i in the first 48 hours) under physiological 5% O_2 conditions. $Mbd3^{-/-}$ MEF (but not pluripotent cells) experience accelerated senescence and proliferation capacity loss, and thus $Mbd3^{-/-}$ cells were reprogrammed by applying tamoxifen on $Mbd3^{flox/-}$ cells after 48 hours of OSKM induction. Similarly, for acute knockdown of Mbd3 in somatic cells with Mbd3 siRNAs in an attempt to boost reprogramming, transfection were conducted at least after 48 hours of OSKM induction. Alternatively, somatic cells with hypomorphic expression (rather than complete ablation) of Mbd3 do not demonstrate proliferation defects or accelerated senescence due to the residual Mbd3 expression levels, yet they retain sufficiently reduced Mbd3 levels that allow deterministic synchronized reprogramming by OSKM (Figure 4B). Thus the following

systems were preferably and predominantly used throughout this study: $Mbd3^{flox/-}$, NGFP1-$Mbd3^{KD}$ or WIBR3-$MBD3^{flox/flox}$ genetic backgrounds. Notably, in the reprogramming conditions used herein, single cell plating of MEFs yielded approximately 70% survival efficiency (with or without DOX). Thus for live imaging, upon plating 150 MEFs per well the present inventors observed formation of 100-120 colonies that were tracked in $Mbd3^{flox/-}$ samples. Importantly, constitutive mCherry allowed controlling for survival after plating to obtain accurate and unbiased reprogramming efficiencies (reprogramming efficiency % = Oct4 or Nanog-GFP clones (cells) / mCherry+ clones (cells)). Equivalent reprogramming efficiencies were obtained on mouse irradiated feeder cells or gelatin, matrigel or gelatin/vitronectin coated plates. Reprogramming on irradiated DR4 MEF cells was preferably used for live imaging and single cell reprogramming experiments in order to enhance cell survival and adherence. Mbd3 Stealth siRNAs mix that includes MSS-237238, MSS-275658 and MSS-275659 components (Invitrogen), and Chd4 Stealth siRNAs mix that includes MSS-200894, MSS-200895 and MSS-200896 (Invitrogen) were used for efficient knockdown in mouse cells. Transfections were conducted with RNAiMAX (Invitrogen) according to manufacturer instructions.

DNA plasmids and TALEN gene editing - The following lentiviral and mammalian constitutive over-expression vectors were used in somatic and pluripotent cells: pBRY-Mbd3-Ires-Zeocin. Constitutively expressed lenti-viruses FUW-Mbd2 and FUW-Mbd3 were generated by insert cloning into EcoRI sites of FUW vector to generate constitutive expression following viral transduction and stable integration in somatic or PSC lines.

Flag-Mbd3 mutations and deletions were done by PCR with Q5 DNA polymerase (NEB). TALEN expressing plasmids were designed with a help of TALEN targeter 2.0 [talent (dot) cac (dot) cornell (dot) edu/] and cloned using GoldenGate TALEN kit 2.0 purchased from Addgene (Bedell, VM, et al. Nature 491: 114-8, 2012) according to the published protocol. For targeting G the present inventors have used NN-type repeat. Donor construct was made with DNA fragments amplified from WIBR3 HUMAN ESC genomic DNA. 10^7 ESCS were electroporated with 30 μg of donor plasmid and 10 μg of each of the TALEN expressing plasmids and grown in the presence of G418 (75 μg/ml) and 0iclovir (1 μM). Resistant clones were isolated and

genomic DNA was extracted for Southern Blot and PCR analysis. For generating OCT4-GFP reporter subcloned cell lines, 10^7 MBD3$^{+/+}$ and MBD3$^{flox/-}$ iPSCs were electroporated with 30 μg of previously described OCT4-GFP-2A-PURO knock-in donor plasmid (Hockemeyer, D. et al. Nat Biotechnol 29, 731–734, 2011; kindly provided by Prof. Jaenisch through Addgene) and 10 μg of each of the TALEN expressing plasmids and grown in the presence of Puromycin (0.4 μg/ml). Resistant clones were isolated and genomic DNA was extracted for Southern Blot and PCR analysis. In vitro differentiated fibroblasts from human ESCs/iPSCs were generated as previously described (Hockemeyer, D. et al. Cell Stem Cell 3, 346–353, 2008).

Reprogramming of human somatic cells and cell infection - Reprogramming was conducted at 5% pO_2 in DOX (1-2 μg/ml) supplemented conditions: 1) First 48 hours cells were incubated in conventional human ES medium (hESM – see below). 2) After 48 hours, cells were transferred until day 7-8 to naive defined growth conditions termed WIS-NHSM (see below) and supplemented with ROCKi (5 mM final concentration). 3) After 8 days DOX was withdrawn and cells were expanded in WIS-NHSM conditions. MBD3 Stealth siRNAs that includes HSS147580, HSS147581 components (Cat. #1299003) were used for efficient MBD3 knockdown in human cells. Transfections were conducted with RNAiMAX (Invitrogen) according to manufacturer instructions.

Conventional human ES conditions (hESM) include: 475 ml Knockout DMEM (Invitrogen 10829), 15% KSR (Invitrogen), 8 ng/ml recombinant bFGF (Peprotech) and 1 ng/ml recombinant TGFβ1 (Peprotech), 1 mM glutamine (Invitrogen), 1% nonessential amino acids (Invitrogen), 0.1 mM β-mercaptoethanol (Sigma), Penicillin-Streptomycin (Invitrogen).

The following serum free defined conditions, termed "WIS-NHSM" (Weizmann Institute of Science Naive human Stem cell Medium) were used to isolate, generate, derive and stabilize naive human pluripotent stem cells (PSCs and ESCs). WIS-NHSM media was generated by including: 475 ml Knockout DMEM (Invitrogen 10829), 15% KSR (Invitrogen) or 5 gr AlbuMAX (Invitrogen 11020-021), 5 ml N2 supplement (Invitrogen 17502048), 10 μg of recombinant human LIF (Peprotech), 8 ng/ml recombinant bFGF (Peprotech), 1 ng/ml recombinant TGFβ1 (Peprotech), 1 mM glutamine (Invitrogen), 1% nonessential amino acids (Invitrogen), 0.1 mM β-

mercaptoethanol (Sigma), Penicillin-Streptomycin (Invitrogen) and small molecule inhibitors: PD0325901 (1 μM, ERK1/2i, AXON MEDCHEM); CHIR99021 (3 μM, GSK3βi, AXON MEDCHEM); SB203580 (5 μM, p38i, TOCRIS); SP600125 (10 μM, JNKi, TOCRIS). Throughout the study Naive hESCs/hiPSCs were grown on 0.2% gelatin + 1 ng/ml vitronectin coated plates for at least 1 hour in 37°C. Cells were passage by single cell trypsinization (0.25% or 0.05% Trysin+EDTA) every 3-4 days. Although not essential, enhanced single cell cloning efficiency can be obtained with WIS-NHSM supplementation with ROCK pathway inhibitor Y-27632 (5 μM, ROCKi Axon Medchem) for 24 hours before and after cell passaging.

Immunofluorescence staining of pre- and post-implantation embryos - For pre-implantation, oocytes and one-cell embryos were collected from the oviducts of hormone-primed B6D2F1 mice, and cultured in KSOM (Millipore) until desired stage. Immunostaining was performed as described previously with modifications (Silva, J. et al. Cell 138, 722–737, 2009). Briefly, The zona pellucida was removed using acid Tyrode's solution (Sigma). Embryos were transferred to watch-glass dish (Genenet), fixed for 15 minutes in 4% PFA in phosphate buffer (PB), rinsed three times in PBS containing 3 mg/ml PVP, permeabilized in PBS/PVP with 1% triton X-100 for 30 minutes, and blocked in blocking solution (2% normal donkey serum, 0.05% BSA, 0.01% Tween in PBS) for 1 hour. Embryos were then incubated overnight at 4°C in primary antibodies diluted in blocking solution, washed three times in blocking solution for 15 minutes each, incubated with secondary antibodies for 1 hour at room temperature, counterstained with DAPI for 15 minutes, washed twice in PBS, and mounted in 96 well glass bottom plates for confocal imaging. Post-implantation embryos were fixed and embedded in paraffin as described previously (Acampora, D., et al. Development. 1997; 124:3639-50) with modification. Embryos in the maternal decidua, were fixed in 4% PFA/PB overnight at 4°C, washed 3 times in PBS for 30 minutes each, dehydrated and embedded in paraffin using standard procedure. Embryonic Paraffin sections (5-7 μm) were rehydrated, treated with antigen retrieval, rinsed in PBS, permeabilized in 0.1% Triton/PBS for 10 minutes, rinsed in PBT (0.02% Tween/PBS), and blocked in blocking solution (5% normal donkey serum, 0.05% BSA, in PBT) for 1 hour. Slides were then incubated in the appropriate primary and secondary antibodies diluted in blocking solution as described above, and processed as described

previously (Mansour, AA, et al. Nature 488, 409–413, 2012). The following antibodies were used: mouse anti-Oct4 (1:100, C-10; Santa Cruz SC-5279), goat anti-Mbd3 (1:50, C-18; Santa Cruz SC- 9402).

Immunoprecipitation and immunoblotting analyses - HEK293T cells were transfected with each cDNA clones in an expression vector using jetPEI (Polyplus transfection) and were lysed 48 hours later in lysis buffer (50 mM Tris-HCl pH 7.4, 150 mM NaCl, 1% Triton, 0.1% NP40 and 1.5 mM EDTA). The following plasmids were used for transfections in different combinations: pCaggs-Mbd3, FUW-Oct4, FUW-Klf4, FUW-Sox2, FUW-c-Myc, FUW-Nanog, pCaggs-Flag-Mbd3, pMSCV-Flag-OCT4, pMSCV-Flag-SOX2, pMSCV-Flag-KLF4, pCaggs-Flag-c-Myc, pCaggs-Flag-Nanog, pcDNA3.1-Flag-HDAC1 (obtained through addgene). 30 µl of anti-FlagM2 Magnetic beads (Sigma) were incubated for 6 hours in cell lysate fractions, for IgG control 6 µg of IgG and 50 µl of protein-G Dynabeads (Invitrogen) were added to the cell lysate for 6 hours. Both fractions (the anti-flag and anti-IgG) were loaded on Invitrogen magnetic separator and the beads were washed six times with lysis buffer. The binding proteins were eluted with 0.5 µg/ml of X3Flag peptide (sigma) buffer for the anti-flagM2 beads or by boiling with sample buffer and analyzed by SDS–polyacrylamide gel electrophoresis and immunoblotting. The immunoblot analyses were performed using the following primary antibodies: anti-Flag (clone M2, F3165, Sigma), anti-Mbd3 (A300-258A, Bethyl), anti-Nanog (A300-397A, Bethyl), anti-OCT4 (sc-9081, H134, Santa Cruz), anti-KLF4 (sc20691,H180, Santa Cruz), anti-SOX2 (#2748s, Cell signaling), anti-c-Myc (#9402s, Cell signaling)

Primordial germ cell (PGC) isolation differentiation - For EG derivation experiments, Oct4-GFP+ cells were sorted from E8.5 dissected chimeric embryos and single plated in N2B27 2i/LIF/SCF (10 ng/ml) /bFGF (8 ng/ml) medium.

RT-PCR analysis - Total RNA was isolated using the RNeasy Kit (Qiagen). Three µg of total RNA was treated with DNase I to remove potential contamination of genomic DNA using a DNA Free RNA kit (Zymo Research). 1 µg of DNase-I-treated RNA was reverse transcribed using a First Strand Synthesis kit (Invitrogen) and ultimately re-suspended in 100 µl of water. Quantitative PCR analysis was performed in triplicate using 1/50 of the reverse transcription reaction in an Viia7 platform (Applied Biosystems). Error bars indicate standard deviation of triplicate measurements for each

measurement.

For single cell RT-PCR analysis, single cells from different samples were single cell sorted, and Ambion® Single Cell-to-CT™ Kit was used for sample processing according to Manufacturer Instructions. TaqMan probe based chemistry and TaqMan Real-Time PCR master mix were used on Viia7 platform for gene expression detection. The following TaqMan (Invitrogen) probes were used: Sall4 Mm00453037_s1, Esrrb Mm00442411_m1, Utf1 Mm00447703_g1; Sox2 (endogenous mouse allele specific) Mm03053810_s1; Nanog Mm02384862_g1; Gapdh Mm99999915_g1. C_T cutoff of 39 cycles was used as threshold for defining transcript detection.

Knock down of human mbd3 by siRNA - The present inventors used for human cells siRNA the "Stealth" from Invitrogen, with the following catalogue numbers: Cat. No/Lot -10620318/168750 F02 "MBD3HSS147581" (3_RNAI) for-AGGUCAAGGGCAAGCCCGACCUGAA (SEQ ID NO:52), and Cat. No/Lot -10620319/168750 F03 "MBD3HSS147581" (3_RNAI) for-UUCAGGUCGGGCUUGCCCUUGACCU (SEQ ID NO:53).

Knock down of mouse mbd3 by shRNA - For mouse cells the present inventors used the pLKO.1 lentiviral or the pLKO-Tet-On systems with the following sequences: "TRCN0000039069 F" - CCG GCT AAG TGG ATT GAG TGC CTT TCT CGA GAA AGG CAC TCA ATC CAC TTA GTT TTT G (SEQ ID NO:63) and the "TRCN0000039069 R" - AAT TCA AAA ACT AAG TGG ATT GAG TGC CTT TCT CGA GAA AGG CAC TCA ATC CAC TTA G (SEQ ID NO:64); or the "TRCN0000039071 Fl - CCG GGC GCT ATG ATT CTT CCA ACC ACT CGA GTG GTT GGA AGA ATC ATA GCG CTT TTT G (SEQ ID NO:65) and the "TRCN0000039071 R" - AAT TCA AAA AGC GCT ATG ATT CTT CCA ACC ACT CGA GTG GTT GGA AGA ATC ATA GCG C (SEQ ID NO:66).

Microscopy image acquisition and analysis - Secondary OKSM inducible $Mbd3^{+/+}$ and $Mbd3^{flox/-}$ MEFs carrying Oct4-GFP pluripotency reporter and constitutively expressed nuclear mCherry marker, were plated in 12-well plates at low densities (150 cells per well) and imaged using AxioObserver Z1 (Zeiss) in %5 O_2, %5 CO_2, 37°C controlled conditions. Plates were taken out at day 3-4 for media replacement (but without passaging/splitting) and put back for the automated live imaging stage. Full well mosaic images were taken every 12 hours for 6 days at 5x

magnification, including phase contrast and two fluorescent wavelength images. In house automated segmentation protocol was developed and implemented in Matlab to analyze time-lapse measurements of full well mosaics with fluorescent mCherry and Oct4-GFP markers.

The challenge in this protocol was to implement fast segmentation of unknown number of colonies in 10^8 pixels mosaic image. Main protocol steps (as shown in Figures 40A-E) include:

Adaptive Detection: Erasing the plate margins with circular filter. Defining detection threshold using median with offset (10% of the dynamic_range), and creating a binary image of detected pixels. These steps were carried out separately for each time-point and each fluorescent wavelength.

Complexity Reduction: For this task the present inventors applied a morphological filter to isolate mCherry colonies using median sliding filter (60[μm]*60[μm]) (Arce, G. R. Nonlinear Signal Processing: A Statistical Approach - Gonzalo R. Arce - Google Books, 2005). This filter retains only dense colonies, erasing noise and single isolated cells (a single nucleus is approximately 6[um]*6[um]), this step is crucial for reducing the dimension of the clustering task.

Colony Segmentation: The segmentation was done using Moving average filter (Low-pass filter) (60[um]*60[um]) (Arce, G. R. Nonlinear Signal Processing: A Statistical Approach - Gonzalo R. Arce - Google Books, 2005) to merge adjacent colony fragments into large connected colonies and then apply connected components clustering, labeling connected objects using 8-connected neighborhood.

Colony Feature Extraction: Extracting the features of each mCherry colony including area, bounding box and centroid. By overlay mCherry colony segmentation on the GFP binary image (detected pixels) the present inventors extract for each colony the GFP^+ indicator (0/1) and the fraction of GFP^+ and $mCherry^+$ pixels out of all $mCherry^+$ pixels.

This segmentation protocol was run over time-lapse mosaics collecting information on colony formation dynamics, colony GFP^+ dynamics and ratios of offspring Oct4-GFP^+ cells. Colony and reprogramming dynamics features were then statistically analyzed using Matlab program, including estimation of the cumulative distribution, density function and box-plot graphical interpretation (Figures 42A-E). The

box-plot analysis characterizes the distribution of intra-colony Oct4-GFP reactivation for all single colonies segmented, representing the distribution of offspring iPS cells within segmented colonies. In addition, movies characterizing the process dynamics were produced using customized Matlab program. The above program was validated by artificial input matrix and by collected ES mosaic image collection. In addition, robustness of detection threshold and filter sizes were measured with varying parameters (data not shown).

Chromatin Immuno-precipitation and Sequencing Library Preparation (for Examples 1-4 hereinbelow) - Chromatin Immuno-precipitation followed by deep sequencing (ChIP-Seq) was measured for the following proteins - H3K4me3, H3K27me3, H3K27ac and Mbd3 – in 4 different time points throughout reprogramming: 0 (MEF), 4 days, 8 days, iPS. The binding of each protein was measured in both $Mbd3^{+/+}$ and $Mbd3^{flox/-}$ conditions, as well as in $Mbd3^{-/-}$ ES cells. Oct4 was measured in all the above conditions, excluding 8 day. Approximately $40*10^6$ cells were cross-linked in formaldehyde (1% final concentration, 10 minutes at room temperature (RT)), and then quenched with glycine (5 minutes at RT). Fixed cells were lysed in 50 mM HEPES KOH pH 7.5, 140 mM NaCl, 1 mM EDTA, 10% Glycerol, 0.5% NP-40 alternative, 0.25% Triton supplemented with protease inhibitor at 4°C (Roche, 04693159001), centrifuged at 950 x g for 10 minutes and re-suspended in 0.2% SDS, 10 mM EDTA, 140 mM NaCl and 10 mM Tris-HCL. Cells were then fragmented with a Branson Sonifier (model S-450D) at -4°C to size ranges between 200 and 800 bp, and precipitated by centrifugation. 10 µg of each antibody was pre-bound by incubating with Protein-G Dynabeads (Invitrogen100-07D) in blocking buffer (PBS supplemented with 0.5% TWEEN and 0.5% BSA) for 2 hours at room temperature. Washed beads were added to the chromatin lysate, and then incubated overnight. Samples were washed 5 times with RIPA buffer, twice with RIPA buffer supplemented with 500 mM NaCl, twice with LiCl buffer (10 mM TE, 250mM LiCl, 0.5% NP-40, 0.5% DOC), once with TE (10 mM Tris-HCl pH 8.0, 1 mM EDTA), and then eluted in 0.5% SDS, 300 mM NaCl, 5 mM EDTA, 10 mM Tris Hcl pH 8.0 at 65°C. Eluate was incubated in 65°C for 8 hours, and then treated sequentially with RNaseA (Roche, 11119915001) for 30 minutes and Proteinase K (NEB, P8102S) for two hours. DNA was purified with The Agencourt AMPure XP system (Beckman Coulter Genomics, A63881). Libraries of

cross reversed ChIP DNA samples were prepared according to a modified version of the Illumina Genomic DNA protocol, as described previously [75] (Blecher-Gonen, R., et al. Nat. Protoc. 2013, 8: 539-54). Briefly, ChIP DNA was ligated to Illumina adaptors and subjected to 14 cycles of PCR amplification. Amplified products between 200 and 800 bp were purified on a 2% agarose gel. Roughly 5 picomoles of DNA library was then applied to each lane of the flow cell and sequenced on Illumina Hiseq2000 sequencer according to standard Illumina protocols. The following antibodies were used for chromatin-IP experiments: Control IgG (ChIP grade, ab46540, Abcam), Anti-Histone H3 tri methyl K4 (ChIP grade, ab8580, Abcam), Anti-Histone H3 acetyl K27 (ChIP grade, ab4729, Abcam), anti-Histone H3 tri methyl K27 (ChIP grade, 07-449, Millipore), anti-Oct4 (sc5729 (C-10), Santa Cruz), anti-Chd4 (ChIP Grade, ab70469, Abcam). For Mbd3 chip 1:1 antibody mix was used: anti-Mbd3 (Bethyl laboratories A302-528\9A) and anti-Mbd3 (ab16057, Abcam).

Alignment and Peak Detection – The present inventors used bowtie software (Langmead, B., Trapnell, C., Pop, M. & Salzberg, S. L. Ultrafast and memory-efficient alignment of short DNA sequences to the human genome. *Genome Biol.* (2009)) version 0.12.5 to align reads to mouse mm9 reference genome (UCSC, July 2007). The present inventors only considered reads that were uniquely aligned to the genome with up to a single mismatch, taking the single best match of each read. The present inventors identified enriched intervals of H3K4me3, H3K27me3, H3K27ac, Mbd3 and Oct4 using MACS version 1.4.1 (Zhang, Y., et al. Genome Biol. 2008, 9(9):R137). The present inventors used sequencing of whole cell extract as control in order to define a background model. Duplicate reads aligned to the exact same location are excluded by MACS default configuration. Enriched intervals were mapped to genes if they overlapped a single Kb symmetric interval around their Transcription Start Sites (Taken from RefSeq known gene table in UCSC genome browser). ChIP-seq data on wild-type samples were highly reproducible in comparison to previous publications (Sridharan, R., et al. Cell 36(2):364-77, 2009; Mikkelsen, T. S. et al. Nature 454, 49–55, 2008) (data not shown).

Motif detection (Figure 63) - Motifs that are enriched in Mbd3 binding regions were detected using SeqPos tool in Cistrome package [cistrome (dot) org/ap/]. Mbd3 peaks in MEF, MEF+DOX and iPSC were run against Cistrome curated motif database

with p-value cutoff 0.001.

Histone mark profiles (Figures C-E) - were calculated using in-house script. Shortly, this script generates a matrix of read densities in given genomic intervals. In this case, the profiles of all 29,952 Entrez genes (mm9, taken from UCSC known gene tables) were calculated between 1kb upstream to TSS and TES. These read densities were then converted to z-score by normalizing each position by the mean and standard deviation of the sample noise ($\hat{X}_j = \frac{X_j - \mu_{Noise}}{\sigma_{Noise}}$). Noise parameters were estimated for each sample from $6*10^7$ random bp across the genome. Finally, to present aligned profiles, the z-score profile of each gene was binned to 20 bins upstream to TSS and another 100 quantiles between TSS to TES. The value of each bin or quantile was selected to be the max value within that interval.

In the histone mark distribution analysis (Figures 65A-E and 66A-J) and in the correlation and clustering of histone marks (Figures 47A-B and Figures 48A-C) each gene and each histone mark is represented with the maximal z-score measured in the profile of that gene, where the profiles were calculated as described above. Clustering of histone marks was carried out on concatenated vectors that include all marks for every gene in tandem.

Annotation Enrichment Analysis - Mbd3 target genes were tested for enrichment of functional gene sets taken from Gene Ontology [GO, geneontology (dot) org]. Protein-DNA binding annotations were taken from various publications (Boyer, L. A., et al. Cell. 2005, 122(6):947-56; Mikkelsen, T. S. et al. Nature 448, 553–560, 2007; Kim, J., et al., Cell 132(6):1049-61, 2008; Loh, YH. et al. Nat Genet 38, 431–440, 2006). Enrichment *P* values were calculated using Fisher exact test (Fisher, S., Genetiker, S., Fisher, R. A. & Genetician, S. Statistical methods for research workers, 1970) and corrected for multiple hypotheses using false discovery rate (FDR) threshold of 0.0001%.

Gene expression data acquisition, processing and analysis - Total RNA was isolated from indicated cell lines. The concentration of RNA was quantified and subjected to quality control on Agilent Bioanalyzer. 250 ng of RNA was simultaneously processed from each sample. cDNA was fragmented, labeled, and hybridized to Affymetrix Mouse Gene 1.0 ST GeneChip (Affymetrix, Santa Clara, CA), which

contain 35,557 probes. Affymetrix arrays were used for analysis of human cell samples. Transcripts levels were processed from image files [from Affymetrix CEL files and CDF file (version V1.r3, which maps probes into 33,252 probe sets)] using RMA method (Irizarry, R. A. et al. Biostatistics, 2003, 4:249-64), which corrects for non-biological sample variation using quantile normalization, implemented by the Affymetrix "Expression Console" software. Data was further filtered to include probes that have at least one call higher than 64 ($=2^6$), resulting in 21,811 probes that are mapped to 15,815 RefSeq transcripts [ncbi (dot) nlm (dot) nih (dot) gov/RefSeq/]. Unique Entrez IDs using current annotations from Affymetrix (NetAffx Annotation Files version 33.1) and NCBI sites. Probes targeting the same gene were collapsed by median resulting in 13,894 genes. Microarray data are available at the National Center for Biotechnology Information Gene Expression Omnibus database under the series accession nos. GSE37822, GSE45352, and GSE46872. Additional human ESC samples data from previously described Affymetrix GeneChip Human Genome U133 Plus 2.0 Arrays which contain 54,675 probe sets (GSE21222;(Hanna, J. *et al. Proc. Natl. Acad. Sci. U.S.A.* 107, 9222–9227, 2010) were passed through the same processing as previously described, resulting in 15,571 genes. The two gene lists were then intersected into one list containing 12,071 genes. The batch effect resulting from two different platforms was corrected by normalizing each data set to a sample of the same genotype (WIBR3, reference samples excluded from further analyses), allowing the two datasets to be united for further analysis. The samples were hierarchically clustered using average linkage and either Spearman or Pearson correlation as a distance matrix as noted, with similar results. In order to compare the samples to Inner-Cell-Mass (ICM)-stage cells, Human pre-implantation data from Vassena et al. (Vassena, R. *et al. Development* 138, 3699–3709, 2011) were included. This data, from Affymetrix HuGene 1.0 st microarrays described before, was passed through the same processing as previously described, resulting in 16,953 genes before and 12,062 genes after intersection with the previous gene list. Batch effect was corrected by normalization of the new data to the mean values of its ESC samples. Differentially Expressed Genes between Naive and Primed samples were found using two-sample two-sided t-test, whose p-values were corrected for multiple hypotheses using the Benjamini–Hochberg false discovery rate (FDR) threshold of 0.05, combined with a two-fold change

expression threshold. Differentially expressed genes were checked for functional enrichment using the online tool GOrilla [cbl-gorilla (dot) cs (dot) technion (dot) ac (dot) il/ (Eden, E., et al. *BMC Bioinformatics* 10, 48, 2009)], with the entire gene list used as background. An FDR-corrected p-value threshold of 0.05 was used. For gene expression statistical analysis, the present inventors used "Cluster" software [rana (dot) lbl (dot) gov/EisenSoftware (dot) htm] to run hierarchical clustering on the samples, using complete linkage centered correlation as a distance metric. The present inventors used Matlab version R2011a and Version R2012b and their Bioinformatics toolbox to run Principle Component Analysis that detects the principle components with the largest variation in the data.

Gene expression analysis - Probes were mapped to Entrez Gene IDs and further filtered to include IDs that have at least one call higher than 32 ($=2^5$), resulting in 16,620 gene IDs. For gene expression analysis, the present inventors used Matlab version R2011b. Gene signatures differentially expressed between MEF samples ($Mbd3^{+/+}$, $Mbd3^{f/-}$, $Mbd3^{-/-}$ MEF samples) and ES samples (ES V6.5, $Mbd3^{-/-}$ ES, $Mbd3^{f/-}$ IPS and $Mbd3^{+/+}$ iPS) were characterize using two-sample t-test and corrected for multiple hypotheses using false discovery rate (FDR) [Benjamini, Y. and Hochberg, Y. Journal of the Royal Statistical Society Series B (Methodological), 57: 289-300, 1995]. Differentially expressed gene signatures include genes that are under FDR threshold of 5%, as well as above 4-fold change, resulting in 1,323 genes. Sample clustering with all 16,620 genes (Figure 8R and Figures 45A-B) and with 1,323 differentially expressed genes (Figure 7), was done in two ways: (1) Hierarchical clustering (Sibson, R. SLINK: An optimally efficient algorithm for the single-link cluster method. The Computer Journal 16, 30–34, 1973) using Spearman correlation as a distance metric and average linkage. (2) Principle component analysis (PCA) that detects the principle components with the largest variation in the data. Single gene progression in reprogramming (Figures 46A-E) were quantified using the following transformation

$$\hat{X}_j(t) = \max\left(\frac{X_j(t) - X_j(MEF_Mbd3^{+/+})}{\overline{X}_j(IPS) - \overline{X}_j(MEF)}, 0\right)$$

Where, Xj(t) denotes gene j expression value at time t (e.g. Xj(4d) or Xj(MEF)) and $\overline{X}_j(IPS), \overline{X}_j(MEF)$ denotes the averaged expression value for IPS and MEF samples,

respectively. The above transformation represents a distance from MEF expression values (set to 0) towards iPS values (set to 1), where genes whose expression changes towards (up/down-regulating) their iPS value show $\ddot{X}_j(t) > 0$. Distribution of gene expression fold-change, relative to MEF, is presented by box plots (Figures 36A-J, and Figures 65A-E, 66A-J). Distribution difference significance was calculated with paired samples t-test.

Preparation and analysis of reduced representation bisulfite sequencing libraries - RRBS libraries were generated as described previously with slight modifications (Smith, Z. D. et al. Nature 484, 339–344, 2012). Briefly, DNA was isolated from snap-frozen cell pellets using the Quick-gDNA mini prep kit (Zymo). Isolated DNA was then subjected to MspI digestion (NEB), followed by end repair using T4 PNK / T4 DNA polymerase mix (NEB), A-tailing using Klenow fragment (3'→5' exo-) (NEB), size selection for fragments shorter than 500-bp using SPRI beads (Beckman Coulter) and ligation into a plasmid using quick T4 DNA ligase (NEB). Plasmids were treated with sodium bisulfite using the EZ DNA Methylation-Gold kit (Zymo) and the product was PCR amplified using GoTaq Hot Start DNA polymerase (Promega). The PCR products were A-taild using Klenow fragment, ligated to indexed Illumina adapters using quick T4 DNA ligase and PCR amplified using GoTaq DNA polymerase. The libraries were then size-selected to 200-500-bp by extended gel electrophoresis using NuSieve 3:1 agarose (Lonza) and gel extraction (Qiagen). Libraries were pooled and sequenced on an Illumina HiSeq 2500 system. The sequencing reads were aligned to the Mouse Genome Build 37 (mm9) using Bismark. Methylation levels were calculated and averaged only for CpGs that were covered by 5 or more distinct sequencing reads across all libraries. The CpG content "experienced" by each CpG site was defined as the number of CpG dinucleotides found within a 500-bp window surrounding the site divided by the window size.

Numerical modeling analysis

Data acquisition for modeling – The present inventors measured reprogramming latencies for multiple systems in order to establish empirical cumulative distributions for reprogramming dynamics. Monoclonal secondary NGFP1 ($Mbd3^{+/+}$) B-cell reprogramming dynamics with or without additional genetic perturbations (scrambled shRNA, Nanog over expression ($Nanog^{OE}$)) were measured weekly using

FACS, as described before (Hanna, J. et al. Nature 462, 595–601, 2009). NGFP1-Mbd3^{KD} iPSC line was established, and Pre-B cells were harvested from chimeric animals and subjected to DOX reprogramming. Monoclonal follow-up measurements were conducted by single cell plating followed by Nanog-GFP detection at day 7 (1 week). Since monoclonal follow-up yielded 100% efficiency in NGFp1-Mbd3KD pre-B cells, the present inventors also conducted polyclonal reprogramming experiments on NGFP1 and NGFP1-Mbd3^{KD} derived pre-B cells and measured Nanog-GFP daily by FACS during the first 8-10 days of OSKM induction (Figures 31A-E). Finally, the monoclonal weekly measurements of NGFP1 and the polyclonal daily measurements of NGFP1-Mbd3^{KD} established latency distributions for the reprogramming dynamics. These latency distributions were fitted to multiple modeling schemes as indicated below.

Implementation of model fit - The fitting for the models (detailed below) were implemented by Matlab program performing nonlinear regression fitting with adjusted R^2 statistic. Definition of the adjusted R^2 is

$$\text{Adjusted } R^2 = 1 - \frac{\sum_{i=1}^{n}(y_i - \hat{y}_i)^2}{n-m} \cdot \frac{n-1}{\sum_{i=1}^{n}(y_i - \bar{y})^2} = 1 - \frac{MSE}{Var(y)}$$

Here, y_i is the measured latency distribution data point, $\hat{y}_i$ is the estimated data point according to the predicted model and $\bar{y}$ is the mean value of the measured latency distribution. In addition, n denotes the number of samples taken and m denotes the number of model parameters used for the model fitting. Some of the models were also fitted using maximum likelihood estimator as will be detailed below.

Fitting to a step-function model - In the deterministic case all cells become pluripotent at the same time following to DOX induction. This behavior is well approximated by step function like dynamics. The present inventors fitted the observed reprogramming latency to a step function, where the deterministic transition time was estimated by optimizing adjusted R^2 statistic. The fitting was done on Matlab using nonlinear regression (Figures 35A-C).

Fitting to Gaussian model - In order to estimate the variability observed in the reprogramming latency measurements, we used fitting to Gaussian distribution and calculated the mean, variance and coefficient of variation (CV=std/mean) for each

sample (Mbd3$^{+/+}$ and Mbd3^{KD}) (Figures 56A-F, Figs. 57A-D). The fitting was done in Matlab using both nonlinear regression and maximum likelihood estimations.

Fitting to Brownian motion model - Biological changes (*e.g.* gene expression) may be described by the chemical Langevin equation (CLE) [Wilkinson, D. J. Stochastic modelling for quantitative description of heterogeneous biological systems. *Nat Rev Genet* 10, 122–133 (2009).

$$dX_t = (\beta - \alpha \cdot X_t)\, dt + \sqrt{\beta + \alpha \cdot X_t} \cdot dW_t$$

Where, X_t is the gene/protein expression as a function of time, β denotes the production rate, α denotes the degradation rate and W_t is a Wiener process (or standard Brownian motion). However, the measured reprogramming duration is one or two orders of magnitude (10d for Mbd3^{KD} and >100d for WT) higher than the production/degradation time scale. Moreover, the time between samples in the measured reprogramming latency is longer than the half-life ($T_{1/2}$) time of the production/degradation process. Therefore, due to the separation of time scales the present inventors assume that the production/degradation process is at quasi-steady state, where the steady state expression (β/α) value changes slowly due to regulatory changes that effect the production rate β, possibly due to epigenetic modifications.

For these slow accumulating changes, we assume a simpler linear diffusion model

$$X_t = X_0 + \nu \cdot t + \sigma \cdot W_t$$

Now, X_t is the quasi-steady state expression as function of time, $\nu \cdot t$ represents the deterministic dynamics where ν is called the process drift, and $\sigma \cdot W_t$ represents the gene expression noise where σ is the standard deviation and *Wt* is a Wiener process.

The present inventors assume that the observed reprogramming dynamics is dominated by the transition of some master regulators (possibly Nanog or Oct4) from their low inactive state to high expression state. For this transition the reprogramming latency corresponds with the *first passage time* distribution (see illustration in Figure 57C), where reprogramming time depends on the first passage time of some fixed expression threshold. Therefore for a fixed (unknown) expression threshold $\alpha > X_0$, we get

$$T = \inf\left\{ t > 0 \middle| X_t = \alpha \right\} \sim IG\left(\alpha/\nu, \alpha^2/\sigma^2\right)$$

$$f_T(x) = \frac{\alpha}{\sigma\sqrt{2\pi \cdot x^3}} \exp\left\{ -\frac{(\alpha - \nu \cdot x)^2}{2\sigma^2 x} \right\}$$

Where T is a random variable representing reprogramming time (or first passage time), $IG(:,:)$ denotes the Inverse Gaussian distribution (or Wald distribution), with the parameters $\mu = \frac{\alpha}{\nu}$ (mean) and $\lambda = \frac{\alpha^2}{\sigma^2}$(shape parameter), and f_T is the density function. The present inventors assume, without loss of generality, that X_0 is zero, elsewhere the present inventors can shift everything including $\alpha' = \alpha - X_0 > 0$.

Thus, the present inventors fit the observed reprogramming latency to Inverse Gaussian distribution using maximum likelihood estimator, finding the best fit parameters (μ, λ) for each sample. Still α is an unknown model parameter, but the present inventors can calculate $\mu/\sqrt{\lambda} = \sigma/\nu$ from the fitting results, this defines the dynamic variability for each sample. This variability is the ratio of the Brownian motion standard deviation (σ) divided by the Brownian motion drift parameter (ν), where $\sigma/\nu > 1$ corresponds to a high variability dynamics. The present inventors show that while the dynamics variability in the Mbd3$^{+/+}$ sample is $\sigma/\nu > 5$, the Mbd3^{KD} and cell cycle measurements show both a dynamic variation of $\sigma/\nu \approx 0.5$ (Figure 57B).

Propagation of error - Fitting Gaussian and inverse Gaussian distributions returns 95% confidence intervals for the parameters. Calculating the ratio for the coefficient of variation and dynamics variability, the present inventors assumed that σ and μ are uncorrelated and used the following equation for the error:

$$\Sigma_{CV} = \sqrt{\Sigma_\sigma^2 \cdot \frac{1}{\mu^2} + \Sigma_\mu^2 \cdot \frac{\sigma^2}{\mu^4}}$$

Where $\sum_{CV}$, $\sum_{\mu}$ and $\sum_{\sigma}$ denotes the errors in the coefficient of variation, mean and standard deviation, respectively.

Modeling cell cycle duration - Doubling time parameters (mean and standard deviation) were measured as previously described in Hanna, J. *et al.* 2009 [*Nature* **462,** 595–601] for the current Mbd3$^{+/+}$ and Mbd3^{KD} cell lines. The present inventors sought to estimate the number of generations according to the reprogramming duration, and fit

the cell cycle time distribution to the observed reprogramming latency. Note that Hanna, J. et al. 2009 (Nature 462, 595–601) showed a dependency between cell cycle duration and reprogramming latency distribution. Without being bound by any theory, the present inventors argue that the reduction in rate–limiting barriers may reduce reprogramming variability to variability explained by cell-cycles alone. Doubling time distribution was previously characterized (Duffy, K. R. et al. Science 335, 338–344, 2012) for B lymphocytes, the present inventors assume for simplicity that the cell cycle duration obeys a Gaussian distribution, this is supported by (Duffy K.R, 2012, Science 335: 338–344, Fig. 3A) and validated by applying Shapiro-Wilk normality test [Shapiro, S. S. and Wilk, M. B. An analysis of variance test for normality (complete samples). Biometrika (1965), 52: 591] on the measured doubling times (P value>0.7). In addition, a model for multiple generation cell cycle distribution should be defined, and the present inventors considered in the analysis two opposing models

Dependent model: Cell cycle duration is inherited between siblings and generations. Therefore each mono-clonal population (each well) represents a single sample of the cell cycle distribution ($\tau_i \sim N(\mu,\sigma)$). Hence, the time for well *i* to achieve *K* divisions is distributed by $T_i^K = K \cdot \tau_i \sim N(K \cdot \mu, K \cdot \sigma)$, where N(:,:) denotes normal distribution.

Independent model: Cell cycle duration is independent between siblings and generations. Therefore for each mono-clonal population (each well) *i* the time to achieve *K* divisions is a random walk process. Hence, $T_i^K = \tau_i^1 + \tau_i^2 + \ldots + \tau_i^K \sim N(K \cdot \mu, \sqrt{K} \cdot \sigma)$, where $\tau_i^j \sim N(\mu,\sigma)$ are iid (independent identically distributed) random variables.

The real biological process probably lies between those two opposing models. Correlation between siblings has been characterized (Duffy K.R, 2012, Science 335: 338–344, Fig.2F) which supports the dependency model, however correlation deteriorates with time, thus supporting the independent behavior of multiple generation processes. Hence, the present inventors decided to check the fitting for both models (dependent and independent) in order to calculate boundaries that allow confidence in the results.

Fitting procedure consists of: 1) Estimating the mean (μ) and standard deviation (σ) of doubling time in each sample ($Mbd3^{+/+}$ and $Mbd3^{KD}$), as previously described in (Hanna, Nature 2009). 2) Fitting the observed reprogramming latency to both models:

$N(K\cdot\mu,K\cdot\sigma)$ for the dependent and $N\left(K\cdot\mu,\sqrt{K}\cdot\sigma\right)$ for the independent model. The mean (μ) and standard deviation (σ) are empirically estimated from each sample. The fitting was done on Matlab using nonlinear regression. 3) Estimating the number of generations (K) required to account for the measured reprogramming duration, by optimizing adjusted R^2 statistic (see above for details on adjusted R^2).

Fitting of the dependent model is given in (Figures 57D-E), where the results of the independent model are very similar to the dependent model, as seen in the following Table 1.

Table 1

	Dependent model	Independent model
$Mbd3^{KD}$	Adj R^2=0.9986	Adj R^2=0.9982
$Mbd3^{+/+}$	Adj R^2=0.73	Adj R^2=0.69

Table 1.

Therefore the fitting results in the dependent and independent models are equivalent and should be valid to realistic cell cycle model (with partial generation dependent correlation).

Inferring structural model (Phase-Type model) - Several papers have suggested that the reprogramming process can be modeled by tandem rate limiting steps [Buganim, Y. et al. Cell 150, 1209–1222 (2012); Polo, J. M. et al. Cell 151, 1617–1632 (2012); Hanna, J. et al. Nature 462, 595–601 (2009); Smith, Z. D., et al. Nat. Biotechnol 28, 521–526 (2010)]. To study how this multiple step process changes following Mbd3 depletion in reprogramming, the present inventors applied a Phase-Type (PH) modeling (Bolch, G., Greiner, S., de Meer, H. & Trivedi, K. S. Queueing networks and Markov chains: modeling and performance evaluation with computer science applications. WILEY, Second Edition, 2006) that is a novel approach used to characterize the dynamics of finite-space continuous-time Markov chain models with a single absorbing phase (in our case iPSC phase). $Mbd3^{KD}$ and $Mbd3^{+/+}$ observed reprogramming latencies were fit to multiple tandem step model, where convergence of estimation efficiency was used in order to select the best fit model (Figures 55C-D, 58D, 59G). Note that for this model the present inventors used the $Mbd3^{KD}$ measurements collected by live microscopy, to allow high temporal resolution on the reprogramming transition period

(sample every 12 hours). Those measurements show equivalent dynamics to $Mbd3^{KD}$ measurements acquired by FACS (Figure 55B).

Without being bound by any theory, the present inventors describe the reprogramming process as a sequential Markov chain model with *M* phases, where the probability of being in phase *i* ($i \in \{1, \ldots, M\}$) at time *t* is denoted by *Pi(t)*. In this model the probability of an induced cell to be a B-cell is $P_1(t)$, the probability of being an iPSC is $P_M(t)$, and there are *M-2* intermediate phases within the path from the B-cell to iPSC phases. It is assumed that transition occurs between the i^{th} and $(i+1)^{th}$ phases with transition rate μ_i, meaning that the current model neglects feedbacks between phases. In addition, in order to allow for a deterministic delay in the model, the present inventors incorporated to the fitting an additional parameter t_0 denoting a deterministic 'shift' in the model dynamics. Therefore an *M* phases model can be characterize by the following equations for all $t > t_0$

$$\begin{cases} \dfrac{dP_1(t-t_0)}{dt} = -\mu_1 \cdot P_1(t-t_0) \quad for \quad i=1; \\ \dfrac{dP_i(t-t_0)}{dt} = \mu_{i-1} \cdot P_{i-1}(t-t_0) - \mu_i \cdot P_i(t-t_0) \quad for \quad i \in \{2,\ldots,M-1\}; \\ \dfrac{dP_M(t-t_0)}{dt} = \mu_{M-1} \cdot P_{M-1}(t-t_0). \quad for \quad i=M. \end{cases}$$

This model can be solved with the following initial conditions: $P_1(t)=1$, $P_i(t)=0$ for all $i>1$ and for all $t \leq t_0$. The solution for the M phases model defines $P_i(t)$ for all $t>0$ as a function of the transition rates (μ_i, $i \in \{1,\ldots,M-1\}$) and t_0, in a physical context $P_i(t)$ describes the time evolution of the ratio of population of cells in phase *i*.

The present inventors constructed a nested fitting procedure for the fitting of $Mbd3^{KD}$ and control $Mbd3^{+/+}$ dynamics to multiple models with *M* varies from 2 to 6. Since the present inventors measured only the distribution of complete reprogramming latency the fit was done between the measured latency distribution of each system and the $P_M(t)$ function calculated for each model, seeking the best fit model for each measured latency distribution. The present inventors applied nonlinear regression fitting for each model with adjusted R^2 statistic for the rejection of over fitted models. Note that over fitting is rejected by the adjusted R^2 since that increased number of model parameters m decreases the adjusted R^2 statistic as long as the sum of squares of residuals converge (estimation efficiency convergence).

The best-fit model defines the number of phases that recapitulate the dynamics of each reprogramming system ($Mbd3^{KD}$ and $Mbd3^{+/+}$), the fitting procedure calculates the optimized transition rates μ_i and the deterministic delay t_0. Consistent with previous reports [Buganim, Y. *et al.* Single-cell expression analyses during cellular reprogramming reveal an early stochastic and a late hierarchic phase. *Cell* 150, 1209–1222 (2012); Polo, J. M. *et al.* A Molecular Roadmap of Reprogramming Somatic Cells into iPS Cells. *Cell* 151, 1617–1632 (2012); Hanna, J. *et al.* Direct cell reprogramming is a stochastic process amenable to acceleration. *Nature* 462, 595–601 (2009); Smith, Z. D., Nachman, I., Regev, A. & Meissner, A. Dynamic single-cell imaging of direct reprogramming reveals an early specifying event. *Nat Biotechnol* 28, 521–526 (2010)], $Mbd3^{+/+}$ dynamics fit a multi-step process consisting 1 or 2 but not 0 intermediate phases (Figures 55C-D, 58A-D). Remarkably, $Mbd3^{KD}$ measured dynamics optimally fit a single step process with no intermediate phases (Figures 55C-D and 58D). In addition, the average rate of the reprogramming process was then estimated using $v_{eff} = 1\Big/\sum_{i=1}^{M-1}\frac{1}{\mu_i}$, for each sample. Fitting results and estimated model parameters were documented (data not shown). Note that the models fit was validated using a second fitting procedure based on weighted nonlinear fit by chi^2 minimization. The results show (Figures 58A-D and Figures 59A-G) that the two fitting procedures gave equivalent results.

The result obtained for the $Mbd3^{KD}$ may infer a reduction in intermediate states and therefore reduction in rate-limiting barriers. It does not directly argue for stochasticity, but there is clearly a connection between the barriers and the process variability. The obtained results also have many experimental observations supporting them, such as previous established intermediate phases in reprogramming that were characterized extensively in previous works (Mikkelsen, T. S. et al. Nature 454, 49–55, 2008). The model prediction that $Mbd3^{KD}$ protocol achieves barrier free reprogramming dynamics is supported by the fact that intermediates (SSEA1 positive with negative Oct4 and Nanog) were detected in the WT (wild type) sample, but none were observed in the $Mbd3^{KD}$ sample (Figure 8S, and Figures 8F-K). Also, previously described (Mikkelsen, T. S. et al. Nature 454, 49–55, 2008) partially reprogrammed (intermediate pre-iPS) cell lines were robustly converted to iPSC upon Mbd3 depletion (Figure 50B).

Altogether those results validate experimentally the model predictions for elimination of the rate limiting barriers in the Mbd3^{KD} reprogramming protocol.

Additional technical notes: First, note that the rates for Mbd3^{KD} and Mbd3$^{+/+}$ are scaled differently due to differences in measurements of polyclonal and monoclonal assays (Figures 55C-D). For the Mbd3$^{+/+}$ monoclonal system, positive detection of iPS cells in clonal populations is defined by FACS threshold of *>0.5%* GFP+ cells per well, for this system the transition and overall rates should be scaled to population-averaged rate by $\mu_i' = \frac{\mu_i}{N_{eff}}$, according to the model previously described (Hanna, J. *et al. Nature* **462,** 595–601, 2009), the reason behind this scaling is that each activation event (well) represent a competition between many iid (identical and independently distributed) exponential variables. On the other hand for the Mbd3^{KD} polyclonal assay, the global fraction of Nanog-GFP+ cells out of the entire population was measured daily, for this single cell measurement the transition rates need not to be scaled to population-average.

Second, note that non-linear effects such as in Hill functions may result a similar dynamics to the observed reprogramming latency, but due to the multi-well mono-clonal (homogeneous population) measurement scheme the present inventors can rule out such effects. Clearly each activation event (each well) is independent and physically isolated from all other wells so cannot be influenced by proximal well activations. In addition the reprogrammed cell lines were secondary systems with homogeneous DOX induction stable constructs. So the S function dynamic must correspond to the reprogramming latency distribution and not to other nonlinear effect.

Finally, the present inventors note that the parameter t_0 used in the model fitting is not the onset of the process. By examining the gene expression and chromatin results one can see that major changes in gene expression and chromatin are already evident in 4d after induction (for Mbd3^{KD}) and 8d (for WT) (see Figures 45A-B, 47A-B). The parameter t_0 is technical for allowing the distributions to move and fit each other, it may represent the minimum deterministic duration needed for the changes required in reprogramming. Note that for the monoclonal Mbd3$^{+/+}$ system, detection delay is due to a threshold obtained in the FACS which can be formulated by $t = T_d \cdot Log_2(N_{FACS} \cdot Thr_{FACS}) \approx 4d$, where T_d is the doubling time (~20 hours), N_{FACS} equal 5000 cells and Thr equal 0.05%. DOX induction delay is approximated by 0.5d.

While that $Mbd3^{KD}$ detection delay is negligible (polyclonal assay). Reduction of those mechanistic delays from the estimated t_0 the present inventors get that both $Mbd3^{+/+}$ and $Mbd3^{KD}$ has approximately 3[days] 'minimum duration' requires for the reprogramming changes to complete.

Non-linear regression assumptions - Most of the above model estimations utilized nonlinear regression as their fitting procedure. For this we assume that: 1) The observational errors, *i.e.* the residuals defined as a difference between observed and model-predicted values, are normally distributed. 2) The errors in observations at successive times are independent. 3) The variance of observation errors (σ^2) is the same for all the state variables and observation times. The present inventors checked the distribution of the residuals for all previous estimation problems using Kolmogorov–Smirnov and Shapiro–Wilk normality tests [Shapiro, S. S. & Wilk, M. B. An analysis of variance test for normality (complete samples). Biometrika (1965), 52: 591; Smirnov, N. JSTOR: The Annals of Mathematical Statistics, Vol. 19, No. 2 (Jun., 1948), pp. 279-281]. The residuals passed the normality tests with the P values reported in Supplementary table 1 in Rais Y, et al. ["Deterministic direct reprogramming of somatic cells to pluripotency", Nature. 2013 Oct 3;502(7469): 65-70. Epub 2013 Sep 18], which is fully incorporated herein by reference in its entirety.

Evolutionary analysis of the NuRD complex and other associated proteins - The present inventors assigned orthologs for 15 human proteins that are either known to be part of the NuRD complex or are related to these proteins (MBD1; Gene ID: 4152; SEQ ID NO: 5), MBD2 (Gene ID: 8932; SEQ ID NO: 6), MBD3 (Gene ID: 53615; SEQ ID NO: 7), MBD4 (Gene ID: 8930; SEQ ID NO: 8), OCT4 (Gene ID: 5460; SEQ ID NO: 9), SOX2 (Gene ID: 6657; SEQ ID NO: 10), CHD4 (Gene ID: 1108; SEQ ID NO: 11), Nanog (Gene ID: 79923; SEQ ID NO: 12), RBBP4 (Gene ID: 5928; SEQ ID NO: 13), RBBP6 (Gene ID: 5930; SEQ ID NO: 14), RBBP7 (Gene ID: 5931; SEQ ID NO: 15), HDAC1 (Gene ID: 3065; SEQ ID NO: 16), HDAC2 (Gene ID: 3066; SEQ ID NO: 17), MTA1 (Gene ID: 9112; SEQ ID NO: 18), MTA2 (Gene ID: 9219; SEQ ID NO: 19), for 15 representative metazoan species (mouse - M.musculus, platypus - O.anatinus, zebra finch - T.guttata, chicken – G.gallus, frog – X. tropicalis, zebrafish – D.rerio, pufferfish - T.nigroviridis, lancelet - B.floridae, sea urchin - S.purpuratus, mosquito - A.gambiae, fruit fly -D. melanogaster, honeybee - A.mellifera, beetle -

T.castaneum, sea anemone - N. vectensis, trichoplax - T. adhaerens), and the yeast S.cerevisiae, as an outgroup. The last metazoan in this list – T. adhaerens, represents a basal group of metazoan, and is used to study the origins of animal multicellularity [Rokas, A. Annual review of genetics, 42: 235-251, 2008; Knoll, A. H. Annu. Rev. Earth Planet. Sci. 39, 217–239, 2011]. Proteins that have an ortholog in T. adhaerens were likely to be present in the basal multicellular animals, while proteins that appear in yeast precede animal multicellularity. The orthologs were retrieved using the COG component (version 9.0) of the STRING database (version 9.0) (Szklarczyk, D. et al. The STRING database in 2011: functional interaction networks of proteins, globally integrated and scored. Nucleic Acids Res. 39, D561–D568, 2010). The present inventors limited the analysis to orthologs that are found in the same cluster of orthologs (COG) as the human proteins (and ignored any other similar proteins, if they are assigned to a different COG). In cases where more than one ortholog (Altschul, S. F., et al. Nucleic Acids Res. 1997, 25:3389-402) for a species were found, the present inventors blasted the various orthologs of that species against the human ortholog to quantify their relative degrees of similarity. The present inventors discarded proteins that are shorter than 50 residues, or that had e-values higher than 0.001. As the closest homolog for the human protein, the present inventors chose the ortholog in the compared species with the lowest e-value from the remaining proteins. The present inventors calculated a normalized similarity score between the two orthologs, by dividing the similarity score in the length of the longer protein of the two orthologs (the human ortholog and the compared species' ortholog).

Capturing naive human pluripotent cells **-** The following serum free defined conditions, termed WIS-NHSM (Weizmann Institute of Science Naive human Stem cell Medium) were used to isolate, generate, derive and stabilize naive human pluripotent stem cells (iPSCs and ESCs) with the unique biological properties described in this study. WIS-NHSM-(i) medium was generated by including: 475 ml Knockout DMEM (Invitrogen 10829), 5 grams AlbuMAX (Invitrogen 11020-021), 5 ml N2 supplement (Invitrogen 17502048), 10 μg (micrograms) of recombinant human LIF (leukemia inhibitory factor) (Peprotech), 8 ng/ml recombinant bFGF (Peprotech) and 1 ng/ml recombinant TGFβ1 (Peprotech), 1 mM glutamine (Invitrogen), 1% nonessential amino acids (Invitrogen), 0.1 mM β-mercaptoethanol (Sigma), Penicillin-Streptomycin

(Invitrogen) and small molecule inhibitors: PD0325901 (1 μM, ERK1/2i, Axon Medchem); CHIR99021 (3 μM, GSK3βi, Axon Medchem); SP600125 (10 μM, JNKi, TOCRIS), SB203580 (5-10 μM, p38i, TOCRIS). After further optimization the present inventors alternatively used SB202190 (5 μM, p38i, Axon Medchem) or BIRB796 (2 μM, P38i Axon Medchem) for enhanced P38 inhibition instead of using SB203580.

Throughout the study Naive hESCs/hiPSCs were grown on 0.2% gelatin + 1 ng/ml vitronectin coated plates for at least 1 hour in 37°C. Notably, 1 ng/ml recombinant vitronectin or laminin (Sigma Aldrich L2020, 1 ng/ml for at least 1 hour at 37°C) can also be used to maintain human naive cells in WIS-NHSM conditions.

Cells were passaged by single cell trypsinization (0.25% or 0.05% Trysin+EDTA) every 3-4 days. Although not essential, enhanced single cell cloning efficiency can be obtained with WIS-NHSM supplementation with ROCK pathway inhibitor Y-27632 (5 μM, ROCKi Axon Medchem) for 24 hours before and after cell passaging. Passage numbers of naive -hiPSC/hESCs indicates number of passages counted after induction or stabilization of the naive state (and do not include previous passages when the cells were established and maintained in conventional/primed ESC conditions). For transfection of mouse and human naive iPSCs/ESCs, cells were harvested with 0.05% trypsin-EDTA solution (Invitrogen), and cells resuspended in PBS were transfected with 75 μg DNA constructs (Gene Pulser Xcell System; Bio- Rad; 500 V, 25 μF, 0.4-cm cuvettes).

While the cells described and analyzed in this study were maintained as described above, the present inventors note that naive hESCs/iPSCs can be expanded on gelatin coated plates together with mitomycin C-inactivated, or gamma irradiated mouse embryonic fibroblast (MEF) feeder cells.

Further, alternative composition of WIS-NHSM is possible by replacing Albumax component with 15-20% knockout serum replacement (KSR; Invitrogen 10828-028) or chemically Defined Lipid Concentrate (GIBCO0 Invitrogen 11905-031) or Oleic Acid-Albumin (O3008 Sigma Aldrich, 10μ/ml final) or Oleic Acid (O1257, Sigma Aldrich, 10μg/ml final concentration) or Linoleic/Oleic/Albumin supplement (L9655 Sigma Aldrich, 10 μg/ml final concentration) or Oleic Acid [O1008 Sigma Aldrich (dissolved in DMSO), 10 μg/ml final concentration].

Instead of adding 5 ml of ready N2 mix, individual components can be added to

500 ml media bottle at the indicated final concentration: 1) Recombinant Human Insulin (Sigma I-1882) – 12.5 µg/ml Final concentration; 2) Apo-Transferrin (Sigma T-1147) – 500 µg/ml Final concentration; 3) Progesterone (Sigma- P8783) – 0.02 µg/ml Final concentration; 4) Putrescine (Sigma- P5780) – 16 µg/ml Final concentration; 5) Sodium Selenite (Sigma – S5261) - add 5 µL of 3 mM stock solution per 500 ml WIS-NHSM media.

Instead of SB203580 (p38i), the WIS-NHSM medium can include SB202190 (5 µM, p38i, TOCRIS) or BIRB796 (2 µM, P38i Axon Medchem) without any change in OCT4-GFP expression in WIS-NHSM conditions.

Supplementation of Vitamin C (L-ascorbic acid 2-phosphate, Sigma, A8960, 50 microg/ml final concentration) and/or Hypoxia growth conditions (5% PO_2), were tested and found accommodating for expanding Oct4-GFP+ naive human ESCs and iPSCs.

Instead of KO-DMEM the following media can also be alternatively used: DMEM-F12 (Biological Industries or Invitrogen), KO-DMEM/F12 (Invitrogen12660-012), GMEM (Invitrogen 11710) or 1:1 DMEM/F12:Neurobasal mix (Invitrogen 21103-049).

Following is a non-limiting example of an alternative WIS-NHSM medium (termed "WIS-NHSM-ii") which was used to culture the naive cells of some embodiments of the invention: 425 ml Knockout DMEM (Invitrogen 10829), 74 ml of knockout serum replacement (Invitrogen 10828-028), 5 ml N2 supplement (Invitrogen 17502048), 10 µg of recombinant human LIF (Millipore, LIF1005), 8 ng/ml recombinant bFGF and 1 ng/ml recombinant TGFβ1 (Peprotech), 1 mM glutamine (Invitrogen), 1% nonessential amino acids (Invitrogen), 0.1 mM β-mercaptoethanol (Sigma), Penicillin-Streptomycin (Invitrogen) and small molecule inhibitors: PD0325901 (1 µM, ERK1/2i, AXONMEDCHEM); CHIR99021 (3 µM, GSK3bi, AXON MEDCHEM); SB203580 (5 µM, p38i, TOCRIS); SP600125 (5 µM, JNKi, TOCRIS) with or without Y-27632 (5 µM, ROCKi Axon Medchem).

Alternative composition of WIS-NHSM medium involved replacing 15% KSR with 1% albumax: 500 ml Knockout DMEM (Invitrogen 10829), 5 gr of AlbuMAX (Invitrogen 11020-021), 5 ml N2 supplement (Invitrogen 17502048), 10 µg of recombinant human LIF (Millipore, LIF1005), 8 ng/ml recombinant bFGF and 1 ng/ml recombinant TGFβ1 (Peprotech), 1 mM glutamine (Invitrogen), 1% nonessential amino

acids (Invitrogen), 0.1 mM β-mercaptoethanol (Sigma), Penicillin-Streptomycin (Invitrogen) and small molecule inhibitors: PD0325901 (1 μM, ERK1/2i, AXONMEDCHEM); CHIR99021 (3 μM, GSK3bi, AXON MEDCHEM); SB203580 (5 μM, p38i, TOCRIS); SP600125 (5 μM, JNKi, TOCRIS) with or without Y-27632 (5 μM, ROCKi Axon Medchem).

Derivation of iPSCs - For derivation of iPSCs directly from fibroblasts (and not from already established iPSC lines), BJ fibroblasts or C1/2 derived secondary fibroblast cells (Hanna, J., et al. 2010. Proc. Natl. Acad. Sci. U.S.A. *107*, 9222–9227) harboring doxycycline (DOX) lentiviral vectors encoding Oct4, Sox2, and Klf4 reprogramming factors (Hanna, J., et al. 2010. Proc. Natl. Acad. Sci. U.S.A. *107*, 9222–9227) and a constitutively active lentivirus encoding the reverse tetracycline transactivator were grown in the presence of DOX in WIS-NHSM conditions (as described above) on vitronectin/gelatin-coated plates until initial PSC colonies were observed and subcloned.

ESC derivation form human blastocysts - The use of human preimplantation embryos for ESC derivation was performed in compliance with protocols approved by a Weizmann Institute ESCRO committee, Lis hospital Institutional review committee and Israeli National Ethics Committee (7/04-043) and following the acceptance of a written informed consent. The couples' participation in the study was voluntary after signing informed consent forms and there was no monetary compensation for their embryo donation. Inner cell masses (ICMs) were isolated mechanically by laser-assisted micromanipulation from spare IVF embryos, at day 6-7 following fertilization [Ben-Yosef, D. *et al.* Female Sex Bias in Human Embryonic Stem Cell Lines. *Stem Cells and Development* **21,** 363–372 (2012)]. The intact ICM clumps were placed on a feeder cell layer of irradiation treated DR4 mouse embryonic fibroblasts and cultured in WIS-NHSM media. Initial outgrowths of proliferating ESCs were evident by day 6, and were trypsinized into single cells, 6-10 days following ICM plating. The newly established cell lines were further propagated by trypsin and then either frozen or used for further analysis.

Small molecule compounds and cytokines - Small molecules and cytokines were purchased from Tocris, Calbiochem, Stemgent, Peprotech or Sigma, and were supplemented as indicated at the following final concentration: JAK inhibitor (420099

JAKi, 0.6 μM – CAL BIOCHEM), Kenopaullone (KP, 5 μM, Sigma Aldrich), PD0325901 (PD, 1 μM, Axon Medchem); CHIR99021 (CH, 3 μM, AXON MEDCHEM), Forskolin (FK, 10 μM, TOCRIS), FGF4-Receptor inhibitors PD173074 (0.1 μM, TOCRIS) and SU5401 (2 μM, TOCRIS); TGFβ/ALK inhibitors A83-01 (1 μM, STEMGENT), PKC inhibitor Go6983 (1 μM,TOCRIS), ALK inhibitor (ALKi: SB431542, 2 μM,TOCRIS); AICAR (0.5 mM); BixO1294 (1 μM); BayK8644 (1 μM, Stemgent); SB203580 (5-10μM, p38i, TOCRIS); SBS202190 (5μM, p38i, TOCRIS), BIRB796 (2μM Axon Medchem), SP600125 (10μM, JNKi, TOCRIS); recombinant human BMP4 (5-10 ng/ml; Peprotech), recombinant human SCF (10 ng/ml, Peprotech), recombinant human IGF1 (10 ng/ml, Peprotech), Media with inhibitors was replaced every 24-48 hours.

Culture of conventional/primed human ESCs and iPSCs - The following already established conventional human ESCs and iPSC lines were used (indicated passage number of the cell line taken for conversion into naive pluripotency is indicated in parentheses): Human induced pluripotent stem cells C1 (P21) and C2 (P9) hiPSC lines (Hanna, J. *et al. Proc. Natl. Acad. Sci. U.S.A.* 107, 9222–9227, 2010) and the human embryonic stem cell (hESC) lines BGO1 (P35) (National Institutes of Health ID code BG01; BresaGen], H1 (P40), H9 (P37), WIBR1 (P13), WIBR2, WIBR3 (P11) hESCs (Lengner, C. J. *et al. Cell* 141, 872–883, 2010) were maintained in 20% pO_2 conditions (unless indicated otherwise) on irradiated mouse embryonic fibroblast (MEF) feeder layers or Gelatin/vitronectin coated plates, in hESC medium: 425 ml Knockout-DMEM – Invitrogen 10829) supplemented with 15% Knockout Serum Replacement (Invitrogen 10828-028), 1 mM glutamine (Invitrogen), 1% nonessential amino acids (Invitrogen), 0.1 mM β-mercaptoethanol (Sigma), 8 ng/mL bFGF (Peprotech) and 1-8 ng/ml (e.g., 1-2 ng/ml) recombinant human TGFβ1 (Peprotech). Cultures were passaged every 5–7 days either manually or, or by trypsinization (24 hour pre and 24 hour after addition of ROCK inhibitor at 5-10 nM concentration). For transfection of hiPSC and hESC lines, cells were cultured in Rho kinase (ROCK) inhibitor (Calbiochem; Y-27632) 24 hours before electroporation. Primed/conventional human ESC and iPSC cells were harvested with 0.05% trypsin-EDTA solution (Invitrogen), and cells resuspended in PBS were transfected with 75 μg DNA constructs (Gene Pulser Xcell System; Bio- Rad; 250 V, 500 μF, 0.4-cm cuvettes). Cells were subsequently plated on

MEF feeder layers (DR4 MEFs for puromycin selection) in hESC medium supplemented with ROCK inhibitor for the first 24 hours, and then antibiotic selection was applied.

Mouse naive and primed stem cell lines and cultivation - Murine naive V6.5 ESCs (C57B6/129sJae) pluripotent cells were maintained and expanded in serum-free chemically defined N2B27-based media: 500 ml KO-DMEM (Invitrogen), 5 ml N2 supplement (Invitrogen; 17502048), 5 ml B27 supplement (Invitrogen; 17504044), 1 mM glutamine (Invitrogen), 1% nonessential amino acids (Invitrogen), 0.1 mM β-mercaptoethanol (Sigma), penicillin-streptomycin (Invitrogen), 5 mg/ml BSA (bovine serum albumin; Sigma). Naive 2i/LIF conditions for murine PSCs included 5 μg recombinant human LIF (Peprotech). Where indicated "2i" the following was added: small-molecule inhibitors CHIR99021 (CH, 3 μM- Axon Medchem) and PD0325901 (PD, 1 μM - TOCRIS). Murine Naive ESCs and iPSCs were expanded on gelatin-coated plates, unless indicated otherwise. Previously described $Eras^{-/Y}$ ESCs were kindly provided by Dr. Shinya Yamanaka [Takahashi, K., Mitsui, K. & Yamanaka, S. *Nature* **423,** 541–545 (2003)]. Primed 129Jae EpiSC line (derived from E6.5 embryos) or C57BL6/129sJae EpiSC line (derived following *in vitro* priming of V6.5 mouse ESCs) were expanded in N2B27 with 8 ng/ml recombinant human bFGF (Peprotech Asia) and 20 ng/ml recombinant human Activin (Peprotech Asia) and 1% KSR (knockout serum replacement). Murine EpiSC were expanded on feeder free Gelatin/Vitronectin or Matrigel coated plates. Cell lines were routinely checked for Mycoplasma contaminations every month (LONZA – MYCOALERT KIT), and all samples analyzed in this study were not contaminated.

Reprogramming of somatic cells and cell infection - Virus-containing supernatants of the different reprogramming viruses: STEMCA-OKSM polycistronic vector (DOX inducible and constitutive expression) [Mansour, A.A. *et al. Nature* 488, 409–413 (2012)] was supplemented with the FUW-lox-M2rtTA virus (when necessary) and an equal volume of fresh culture medium for infection. For derivation of iPSCs directly from fibroblasts (and not from already established iPSC lines), BJ fibroblasts or C1.2 derived secondary fibroblast cells [Hockemeyer, D. *et al. Cell Stem Cell* **3,** 346–353 (2008)] harboring doxycycline (DOX) lentiviral vectors encoding Oct4, Sox2, and Klf4 reprogramming factors and a constitutively active lentivirus encoding the reverse

tetracycline transactivator [Hockemeyer, D. *et al. Cell Stem Cell* **3,** 346–353 (2008)], were grown in the presence of DOX in WIS-NHSM conditions on vitronectin/gelatin-coated plates until initial iPSC colonies were observed and subcloned. Generation of BJ1 hiPSCs form human BJ foreskin fibroblasts was conducted by OSKM and LIN28 mRNA transfection kit (Stemgent) according to manufacturers' instructions, but in WIS-NHSM conditions applied starting from day 2 of the reprogramming process. Fragile X male patient specific fibroblasts were obtained through Coriell repository (GM05131 and GM07071). iPSCs were reprogrammed either in conventional or naive (WIS-NHSM) conditions as indicated in Figures 21A-D and 71A-E. Previously described PCR primers were used for FMR1 gene detection [Urbach, A., et al. *Stem Cell* **6,** 407–411 (2010)]: Forward primer: 5'-CAGGGCTGAAGAGAAGATGG-3' (SEQ ID NO:72), Reverse primer: 5'-ACAGGAGGTGGGAATCTGA-3' (SEQ ID NO:73). Pyro sequencing analysis for methylation at FMR1 locus was performed as previously described [Urbach, A., et al. *Stem Cell* **6,** 407–411 (2010)].

Differentiation Assays of human iPSCs and ESCs - For embryoid body (EB) induced differentiation, naive hESCs/hiPSCs were trypsinized and cultured for 6–8 days in non-adherent suspension culture dishes (Corning) in DMEM supplemented with 15% fetal bovine serum. For teratoma formation and analysis, naive hESCs and iPSCs were harvested by trypsinization before injection. Cells were injected sub-cutaneously (s.c.) into 6-8 week old male NSG mice (Jackson laboratories). Tumors generally developed within 4–6 weeks and animals were sacrificed before tumor size exceeded 1.5 cm in diameter. Naive C1 hiPSCs were infected with a lentivirus harboring a VASA-EGFP reporter construct, selected with neomycin, subcloned, and subsequently used for primordial germ cell (PGC) differentiation protocol (Hanna et al., 2010b). All animal studies were conducted according to the guideline and following approval by the Weizmann Institute IACUC (approval #00960212-3).

Mouse embryo micromanipulation - Pluripotent mouse ESCs or naive human iPSCs (pre-treated with 10 μM ROCKi for 12 hours) were trypsinized and subsequently injected into BDF2 diploid mouse morulas or blastocysts, harvested from hormone primed BDF1 6 week old females. Microinjection into E2.5 morulas or E3.5 blastocysts placed in M16 medium under mineral oil was done by a flat-tip microinjection pipette. Embryos injected with human iPSCs were allowed to recover in KSOM medium

(Invitrogen) supplemented with ROCKi (5 μM) for 3-9 hours before they were transplanted into surrogate pseudo-pregnant mice. A controlled number of 10-12 cells were injected into the blastocyst cavity. After injection, blastocysts were returned to KSOM media (Invitrogen) and placed at 37°C until transferred to recipient females. Ten to fifteen injected blastocysts were transferred to each uterine horn of 2.5 days post coitum pseudo-pregnant females. 4n tetraploid complementation assay was performed by fusing BDF2 embryos at 2 cell stage [Stadtfeld, M. *et al. Nature* **465,** 175–181 (2010)], and subsequently allowing the embryos to develop until the blastocyst stage at day 3.5, and were then utilized for PSC micro-injection. Embryos were allowed to develop into full term. Determining germ-line transmission was performed by mating chimeric animals with C57B/6 females, and continuous checking for agouti colored pups. For teratoma formation and analysis, naive hESCs and hiPSCs were harvested by trypsinization before injection. Cells were injected sub cutaneously into NSG mice (Jackson laboratories). Tumors generally developed within 4–6 weeks and animals were killed before tumor size exceeded 1.5 cm in diameter. All animal studies were conducted according to the guideline and following approval by the Weizmann Institute IACUC (approval #00960212-3). The present inventors have not excluded animals from the analysis, and did not apply randomization by blinding.

BAC recombineering and TALEN gene editing - TALEN expressing plasmids were designed with a help of TALEN targeter 2.0 and cloned using GoldenGate TALEN kit 2.0 purchased from Addgene [Bedell, VM, et al., *Nature* 491:114-8. (2012)] according to the published protocol. For targeting G the present inventors have used NN-type repeat. 10^7 ESCs/iPSCs were electroporated with 30 μg of previously described OCT4-GFP-2A-PURO knock-in donor plasmid [Hockemeyer, D. *et al.*, *Nat Biotechnol* 29, 731–734 (2011)] (kindly provided by R. Jaenisch through Addgene) and 10 μg of each of the TALEN expressing plasmids and grown in the presence of antibiotic selection. Resistant clones were isolated and genomic DNA was extracted for Southern Blot and PCR analysis. OCT4-GFP-2A-PURO, ΔPE-OCT4-GFP-2A-PURO, ΔDE-OCT4-GFP-2APURO constructs were made from BAC clone containing human OCT4 gene locus by using Red/ET recombination (Gene Bridges). Briefly, GFP-2A-puro cassette was inserted into translation start site of OCT4, and then genomic region from 8 kb upstream to 10kb downstream of TSS was subcloned into

pBS vector. Proximal (PE) and distal (DE) elements were determined by homology with respective elements of mouse Oct4 described in [Bao, S. *et al. Nature* 461, 1292–1295 (2009)], and based on results obtained with luciferase test assay (Figure 25A). ΔPE and ΔDE deletions were made in wild type construct by exchanging these regions with kanamycin selection cassette that was subsequently removed by restriction. Targeting vectors were linearized with SspI and electroporated into different primed and naive pluripotent cells lines as indicated. For making mouse ΔPE-Oct4-GFP reporter the present inventors have modified the previously described mGOF18ΔPE construct [Yeom, Y. I. *et al.* Germline regulatory element of Oct-4 specific for the totipotent cycle of embryonal cells. Development. 1996, 122(3):881-94], by pRed/ET recombination. The pgk-gb2-Neo cassette (GeneBridges) was inserted into the 3' end of cloned Oct4 genomic fragment (9.7 kb downstream of Oct4 TSS). The inserted neo cassette has the same orientation as Oct4 gene. The construct was linearized with SspI and electroporated into mouse V6.5 ESCs and used for experiments in Figures 86A-C and Figures 87A-B. For gene targeting of human OCT4 and COL1A loci, targeting vectors design and strategy were implemented as detailed in Figures 71B-C. Homology arms were amplified by PCR from H9 hESC derived genomic DNA. Gene targeting was introduced by using the isogenic vectors after linearization and transduction in naive and primed H9 hESCs. Correctly targeted clones were validated by southern blot screening for correct targeting by both 5' and 3' external probes (Figures 21A-D).

DNA constructs and plasmid cloning - The pCAG-IresPuro or pCAG-flox-DsRed-IRES- Puro vectors [Ficz G, et al. Cell Stem Cell. 2013 Sep 5;13(3):351-9. doi: 10.1016/j.stem.2013.06.004. Epub 2013 Jul 11] encoded the following inserts (which were cloned by either cohesive or blunt-end ligations in XhoI-NotI sites): Stat3-CA mutant (Addgene 13373) (A662C and N664C mutations - by substituting cysteine residues for A662 and N664 of the Stat3 molecule, disulfide bonds may form between Stat3 monomers and render the molecule capable of dimerizing without a phosphate on Y705); Stat3-Y705F (dominant-negative allele – Addgene 8709). Human OCT4 enhancer sequences [the Oct4DE- and Oct4PE-SV40-luciferase (Luc) constructs] were cloned into the pGL3-Promoter Vector (Promega) with the following primers: 5′ hOcCT4PE KpnI: 5′-GGTACCGGATACTCAGGCCAGGCCCAGAAA-3′ (SEQ ID NO:74; 3′ hOCT4PE XhoI: 5′- CTCGAGTCCACAGACCTCTGGCACT-3′ (SEQ ID

NO:75); 5′ hOCT4DE KpnI: 5′-GGTACCCATTGAGTCCAAATCCTCTTTACTAGGTG-3′ (SEQ ID NO:76); 3′ hOCT4DE XhoI: 5′-CTCGAGCTGAGGCTCATGCTGCTGG-3′ (SEQ ID NO:77). Reporter constructs were used to determine the regulation pattern of Oct4 expression and were electroporated into 0.5–3 × 10^6 cells along with the pRL-TK (Renilla) vector for normalization. Assays were performed 48 hours later using the Dual-Glo Luciferase Assay System (Promega). The basal activity of the empty luciferase vector was set as 1.0. Recombinant vitronectin was produced and purified as previously described [Chen, G. *et al.* Chemically defined conditions for human iPSC derivation and culture. *Nat. Methods* 8, 424–429 (2011)] after obtaining express ion construct through Addgene (vector 30225).

RT-PCR analysis (description for Examples 5-9) - Total RNA was isolated using Trizol (Invitrogen). 1 μg of DNase-I-treated RNA was reverse transcribed using a First Strand Synthesis kit (Invitrogen) and ultimately re-suspended in 100 μl of water. Quantitative PCR analysis was performed in triplicate using 1/50 of the reverse transcription reaction in an Viia7 platform (Applied Biosystems). Error bars indicate standard deviation of triplicate measurements for each measurement. RT-PCR primers used herein are: XIST-Forward: 5'-AGGGAGCAGTTTGCC CTACT-3' (SEQ ID NO:78); XIST-Reverse: 5'-CACATGCAGCGTGGTATCTT-3' (SEQ ID NO:79); OCT4-Forward: 5'-AGTGATTCTCCTGCCTCAGC-3' (SEQ ID NO:80); OCT4-Reverse: 5'-CTTCTGCTTCAGGAGCTTGG-3' (SEQ ID NO:81); SOX1-Forward: 5'-GGAATGGGAGGACAGGATTT-3' (SEQ ID NO:82); SOX1-Reverse: 5'-AACAGCCGGAGCAGAAGATA-3' (SEQ ID NO:83); PAX6-Forward: 5'-AAGGATGTTGAACGGGCAGA-3' (SEQ ID NO:84); PAX6-Reverse: 5'-TCCGTTGGAACTGATGGA GT-3' (SEQ ID NO:85); HPRT-Forward: 5'-TGACACTGGCAAAACAATGCA-3' (SEQ ID NO:86); HPRT-Reverse: 5'-GGTCCTTTTCACCAGCAAGCT-3' (SEQ ID NO:87); EOMES-Forward: 5'-CGCCACCAAACTGAGATGAT-3' (SEQ ID NO:88); EOMES-Reverse: 5'-CACATTGTAGTGGGCAGTGG-3' (SEQ ID NO:89); CDX2-Forward: 5'-CAGTCGCTACATCACCATCC-3' (SEQ ID NO:90); CDX2-Reverse: 5'-TTTCCTCTCCTTTGCTCTGC-3' (SEQ ID NO:91); HAND1-Forward: 5'-AACTCAAGAAGGCGGATGG-3' (SEQ ID NO:92); HAND1-Reverse: 5'-

CGGTGCGTCCTTTAATCCT-3' (SEQ ID NO:93); GSC-Forward: 5'-CGCCTCGGCTACAACAACTA-3' (SEQ ID NO:94); GSC-Reverse: 5'-CGCCTCGGC TACAACAACTA-3' (SEQ ID NO:95); ID1-Forward: AAACGTGCTGCTCTACGACA-3' (SEQ ID NO:96); ID1-Reverse: 5'-TAGTCGATGACGTGCTGGAG-3' (SEQ ID NO:97); ID3-Forward: 5'-CTACAGCGCGTCATCGACTA-3' (SEQ ID NO:98); ID3-Reverse: 5'-TCGTTGGAGATGACAAGTTCC-3' (SEQ ID NO:99); ZIC1-Forward: 5'-GCGCTCCGAGAATTTAAAGA-3' (SEQ ID NO:100); ZIC1-Reverse: 5'-GTCGCTGCTGTTAGCGAAG-3' (SEQ ID NO:101); NANOG-Forward: 5'-GATTTGTGGGCCTGAAGAAA-3' (SEQ ID NO:102); NANOG-Reverse: 5'-CAGATCCATGGAGGAAGGAA-3' (SEQ ID NO:103); MIXL1-Forward: 5'-AGCTGCTGGAGCTCGTCTT-3' (SEQ ID NO:104); MIXL1-Reverse: 5'-CGCCTGTTCTGGAACCATAC-3' (SEQ ID NO:105).

Immunofluorescence staining - Cells were grown for two days on glass cover slips (13 mm 1.5H; Marienfeld, 0117530) fixed with 4% paraformaldehyde/phosphate buffer for 15 minutes at room temperature, washed three times with phosphate buffered saline (PBS), and permeabilized in PBS/0.1% Triton for 10 minutes. Cells were blocked with blocking solution (2% normal donkey serum, 0.1% BSA in PBS/0.05% Tween) and incubated with primary antibody diluted in blocking solution overnight at 4°C (Antibodies in this study have all been validated in the literature and by ourselves). Cells were then washed three times with PBS/0.05% Tween, incubated with secondary antibodies for 1 hour at room temperature, washed in PBS/0.05% Tween, counterstained with DAPI (1 μg/ml), mounted with Shandon Immu-Mount (Thermo Scientific, 9990412), and imaged. For staining of H3K27me3 and nuclear proteins, cells were permeabilized in PBS/0.5% Triton for 30 or 10 minutes, respectively, and 0.1% Triton was included in the blocking solution. All comparative experiments were done simultaneously. For MHC class I staining of human cells, anti MHC class I antibody (BE pharmingen) was used and cells were analyzed on FACS ARIA III analyzer and sorter system. The following antibodies were used at the indicated dilutions:

Table 2

Antibody	Manufacturer (or supplier) with Catalogue number	Dilution
Mouse anti-TRA-1-60	Abcam (ab16288)	1:500
Mouse anti-TRA-1-81	Abcam (ab16289)	1:500
Mouse anti-SSEA1 (MC480)	Abcam (ab16285)	1:100
Mouse anti-SSEA4 (MC813)	Abcam (ab16287)	1:50
Rat anti-SSEA3 (MC631)	Abcam (ab16286)	1:50
Rabbit anti-Klf2	Millipore (09-820)	1:500
Rabbit anti-Nanog	Bethyl (A300-397A)	1:400
Rabbit anti-Nanog	Abcam (ab80892)	1:200
Rabbit anti- Oct3/4 (H134 clone)	Santa Cruz (SC9081)	1:400
Mouse anti-Oct4 (C-10 clone)	Santa Cruz (SC5279)	1:200
Rabbit anti-Klf4 (H-180 clone)	Santa Cruz (SC20691)	1:200
Mouse anti-E-cadherin	Abcam (ab1416-500)	1:100
Rabbit anti-N-cadherin	Abcam (ab12221)	1:800
Rabbit anti-Sox2	Millipore AB5603	1:500
Mouse anti-NR3B2 (ESRRB)	R&D Systems (PP-H6705-00)	1:1000
Rabbit anti-TFE3	Sigma (HPA023881)	1:200; 1:500
Rabbit anti-H3K27me3	Millipore (07-449)	1:4000
Donkey anti-Mouse IgG Alexa 488	Jackson Immuno (715-545-150)	1:200
Donkey anti-Mouse IgG RRX	Jackson Immuno (715-295-150)	1:200
Donkey anti-Mouse IgG Alexa 647	Jackson Immuno (715-605-150)	1:200
Donkey anti-Rabbit IgG Alexa 488	Jackson Immuno (711-545-152)	1:200
Donkey anti-Rabbit IgG RRX	Jackson Immuno (711-295-152)	1:200
Donkey anti-Rabbit IgG Alexa 647	Jackson Immuno (711-605-152)	1:200
Donkey anti-Mouse IgM RRX	Jackson Immuno (715-295-020)	1:200
Goat anti-Rat IgM RRX	Jackson Immuno (112-295-075)	1:200

Table 2.

Imaging, quantifications, and statistical analysis - Images were acquired with D1 inverted microscope (Carl Zeiss, Germany) equipped with DP73 camera (Olympus, Japan) or with Zeiss LSM 700 inverted confocal microscope (Carl Zeiss, Germany) equipped with 405 nm, 488 nm, 555 nm and 635 solid state lasers, using a 20x Plan-Apochromat objective (NA 0.8). All images were acquired in sequential mode. For comparative analysis, all parameters during image acquisition were kept constant throughout each experiment. Images were processed with Zen blue 2011 software (Carl Zeiss, Germany), and Adobe Photoshop CS4. X chromosome inactivation was assayed by presence of a condensed H3K27me3 staining focus per individual nucleus and quantified manually using ImageJ software (NIH) using.

Automated and quantitative image analysis for TFE3 localization - Single cell fluorescence intensity was analyzed by profile function in Zen Blue 2011 software. An in house developed automated segmentation protocol segments the cell's nucleus contained in each image. Nucleus was defined by intersection by both DAPI and OCT4 fluorescent illumination. This protocol is described in Rais et al (Rais Y., et al. Nature. 2013 Oct 3;502(7469):65-70. doi: 10.1038/nature12587. Epub 2013 Sep 18) and deposited on the lab website [weizmann (dot) ac (dot) il/molgen/Hanna/Home (dot) html]. The segmented cells are then processed individually in order to estimate the ratio between intra-nucleus TFE3 intensity and cytoplasmic TFE3 intensity. Major steps in the processing: 1) Defining a bounding box containing the segmented nucleus and 10 pixels margin around the nucleus. 2) Estimating the average TFE3 intensity within nucleus mask. 3) Estimating the average TFE3 intensity within the bounding box but outside of the nucleus mask. Data were measured per sample from 200 cells obtained from at least four independent image fields. Distribution of intensity ratios for all cells is presented using box-plot. Box plot centers indicate the median value, and box edges indicate the 25th and 75th percentiles. P-values of distribution differences indicated in the graph were estimated with paired sample t-test.

Protein Western blotting analysis - Whole-cell protein extracts were isolated from human ES cells. Blots were incubated with the following antibodies in 3%BSA/TBST or PBST: pSTAT3 (9318; 1:1,000; Cell Signaling), STAT3 (C-20; 1:1,000; Santa Cruz), pβ-Catenin (9561; 1:750; Cell Signaling), β-Catenin (610153; 1:2,000; BD Biosciences), HSP90α (CA1016; 1:5,000; Calbiochem), pJNK (9251; 1:500; Cell Signaling), JNK (SC-571; 1:100; Santa Cruz), pp38 (9215; 1:100; Cell Signaling), p38 (9212; 1:1,000; Cell Signaling), pERK (E4; 1:100; Santa Cruz), ERK1,2 (C-14; 1:100; Santa Cruz), KLF4 (AF3158; 1:200; R&D), OCT4 (H-134; 1:1,000; Santa Cruz), Nanog (397A; 1:1,000; Bethyl). Secondary antibodies were HRP-linked goat anti-mouse, goat anti-rabbit and rabbit anti-goat (1:10,000; Jackson). Blots were developed using ECL (Thermo).

Cross-species gene expression analysis - was conducted on human arrays described above and previously described mouse ESC and EpiSC gene expression datasets on an Agilent 4 × 44 k array platform (GSE15603; described in [Hanna, J. *et al. Cell Stem Cell* 4, 513–524 (2009)] containing 45,018 probes. Mouse data was

processed as described above, resulting in 17,885 unique genes. Human-mouse orthology was downloaded from MGI [informatics (dot) jax (dot) org] containing 17,772 pairs of orthologous genes. Of these, 9,803 were mapped to the expression data of the present inventors. The expression values from mouse and human were transformed separately into relative abundance values [Liao, B. Y. *Molecular Biology and Evolution* 23, 530–540 (2005)]: For each gene, the relative abundance value is the expression value divided by the mean of expression values within the same gene across samples in the same species. The resulting expression matrix was subjected to hierarchical clustering (Spearman correlation, average linkage), as was the spearman correlation matrix of the samples. Coefficient of variance, a measure for noise defined as the standard deviation divided by the mean, was calculated separately for each of the two species and for the Naive and Primed states. The statistical significance between the distributions of coefficient of variance for the two states was calculated using single-tail t-test. Outliers were not shown in the plot, but were included in the statistical tests.

Chromatin Immuno-precipitation and Sequencing Library Preparation (for Examples 5-9 below) - Chromatin Immuno-precipitation followed by deep sequencing (ChIP-Seq) was measured for the following proteins - H3K4me3, H3K27me3, H3K4me1, H3K27Ac and H3K9me3 – in mouse and human pluripotent cells (ESCs, EpiSCs and/or iPSCs) expanded in fetal bovine free and feeder free naive or primed/conventional growth conditions (FBS and feeder free expansion, on gelatin/vitronectin coated plates). Approximately $40*10^6$ cells were cross-linked in formaldehyde (1% final concentration, 10 minutes at room temperature (RT)), and then quenched with glycine (5 minutes at RT). Fixed cells were lysed in 50 mM HEPES KOH pH 7.5, 140 mM NaCl, 1 mM EDTA, 10% Glycerol, 0.5% NP-40 alternative, 0.25% Triton supplemented with protease inhibitor at 4°C (Roche, 04693159001), centrifuged at 950 x g for 10 minutes and re-suspended in 0.2% SDS, 10 mM EDTA, 140 mM NaCl and 10 mM Tris-HCL. Cells were then fragmented with a Branson Sonifier (model S-450D) at -4°C to size ranges between 200 and 800 bp, and precipitated by centrifugation. 10 μg of each antibody was pre-bound by incubating with Protein-G Dynabeads (Invitrogen100-07D) in blocking buffer (PBS supplemented with 0.5% TWEEN and 0.5% BSA) for 2 hours at room temperature. Washed beads were added to the chromatin lysate, and then incubated overnight. Samples were

washed 5 times with RIPA buffer, twice with RIPA buffer supplemented with 500 mM NaCl, twice with LiCl buffer (10 mM TE, 250 mM LiCl, 0.5% NP-40, 0.5% DOC), once with TE (10 mM Tris-HCl pH 8.0, 1 mM EDTA), and then eluted in 0.5% SDS, 300 mM NaCl, 5 mM EDTA, 10 mM Tris Hcl pH 8.0 at 65°C. Eluate was incubated in 65°C for 8 hours, and then treated sequentially with RNaseA (Roche, 11119915001) for 30 min and Proteinase K (NEB, P8102S) for two hours. DNA was purified with The Agencourt AMPure XP system (Beckman Coulter Genomics, A63881). Libraries of cross reversed ChIP DNA samples were prepared according to a modified version of the Illumina Genomic DNA protocol, as described previously [Blecher-Gonen, R., et al. Nat Protoc. 2013 Mar;8(3):539-54. doi: 10.1038/nprot.2013.023. Epub 2013 Feb 21]. Briefly, ChIP DNA was ligated to Illumina adaptors and subjected to 14 cycles of PCR amplification. Amplified products between 200 and 800 bp were purified on a 2% agarose gel. Roughly 5 picomoles of DNA library was then applied to each lane of the flow cell and sequenced on Illumina Hiseq2000 sequencer according to standard Illumina protocols. The following antibodies were used for chromatin-IP experiments: Control IgG (ChIP grade, ab46540, Abcam), Anti- H3K4me3 (ab8580, Abcam), H3K27me3 (07-449, Millipore).

Chromatin IP Sequencing data analysis - The chromatin markers H3K27me3, H3K4me3, H3K4me1, H3K27Ac and H3K9me3 were measured in 4 different human pluripotent cell lines: C1, WIBR3, LIS2 (naive and primed), BGO1 and WIBR3-MBD3^{mut} (naive). In addition, H3K27me3, H3K4me3, H3K4me1 and H3K27Ac were measured in mouse V6.5 naive and primed EpiSCs. H3K27me3 and H3K4me3 measurements in naive mouse ES were previously published by our group [Mansour, A. A. *et al. Nature* 488, 409–413 (2012)]. Each sample was accompanied by control sequencing experiment of whole cell extract input. We used bowtie software [Langmead, B., et al. Genome Biol. 2009; 10(3):R25] version 1.0.0 to align human reads to human reference genome hg19 (UCSC, Feb 2009) and mouse reads to mouse mm9 reference genome (UCSC, July 2007). The present inventors only considered reads that were uniquely aligned to the genome with up to a single mismatch, taking the single best match of each read. To rule out sequencing depth bias, the aligned sequences were down-sampled such that all samples had the same number of aligned reads. Human samples of the marks H3K4me3, H3K27me3, H3K4me1 and H3K27Ac,

as well as whole-cell extract, were down-sampled to include 3,750,000 aligned reads. H3K9me3 samples were down-sampled to 5,900,000 aligned reads. Mouse samples of the marks H3K4me3, H3K27me3, H3K4me1 and H3K27Ac, were down-sampled to 3,420,000 aligned reads.

Chromatin profiles (Figures 70A-F and Figures 83A-D) were calculated over all RefSeq genes (n=43,463), and over developmental genes in the following way: (i) Read densities were calculated between 3Kb upstream to TSS, and 3Kb downstream to TES. (ii) Each gene was divided to bins of size 100, and the sum of reads in each bin was calculated. (iii) Average profile was calculated over all genes, where the gene body, which is of changing size, was represented by 100 quantiles. Genes of size less than 1Kb were filtered out. (iv) Profiles of human samples represent mean and s.d. (error-bars) of 3 primed samples and 5 naive samples. Lastly, developmental genes were selected if they have a GO annotation that is related to development or differentiation. Using this criterion, the present inventors had 5922 RefSeq human developmental genes, and 420 RefSeq mouse developmental genes. Concrete examples of genes (Figures 71B-D) were processed and visualized using IGV software version 2.0 [Robinson, J. T. *et al. Nat Biotechnol* 29, 24–26 (2011)].

Accumulation of H3K9me3 marker on chromosome X (Figure 76C) was also processed and visualized using IGV[69]. Here, each chromosome is represented by 100 random genes. To measure the distribution of H3K9me3 accumulation in chromosome X genes, RPKM (reads per kilobase per 5.9 million reads) was calculated for each gene (between 1Kb upstream to TSS and TES). P-values between distributions were calculated with one-tail paired-sample t-test.

Enhancers were detected following the guidelines set by Rada-Iglesias et al. [Rada-Iglesias, A. *et al. Nature* 470, 279–283 (2011)]. Shortly, enhancers of type one are genomic intervals that contain H3K4me1 and H3K27Ac marks, do not contain H3K4me3 or H3K27me3 marks and are at least 500 bp away from any TSS. Enhancers of type two are genomic intervals that contain H3K4me1 and H3K27me3 marks, do not contain H3K27Ac mark, and are at least 500 bp away from any TSS. To find those enhancers the present inventors first identified enriched intervals of the marks above using MACS version 1.4.1 [Zhang, Y., *Genome Biol. 2008;9(9):R137*]. The present inventors used sequencing of whole cell extract as control in order to define a

background model. Duplicate reads aligned to the exact same location are excluded by MACS default configuration. Enriched intervals ("peaks") that overlap by at least 1 bp were considered as overlapping, and their union was defined as the enhancer interval, unless at least 10% of it overlapped with any of the excluded marks (e.g. H3K27me3 in the case of type one enhancers) or with TSS. To calculate the number of enhancers in human samples (Figures 84D-E) the present inventors only considered enhancers that are common to 2 primed cell lines C1 and WIBR3, or common to 4 naive cells lines: C1, WIBR3, WIBR3-MBD3^{mut} and BGO1. The expression level of genes associated with enhancers (Figures 84G-F) was calculated by mapping each enhancer to the nearest gene (as long as it is at most 100 Kb away), converting it to Entrez Gene and taking its expression value from the raw gene expression dataset described above.

To detect bivalent genes the present inventors identified enriched intervals of H3K4me3 and H3K27me3 using MACS. Enriched intervals were mapped to genes if they overlapped a 3 kb interval before their Transcription Start Sites and after their Transcription End Site. Genes marked as bivalent if they had both H3K27me3 and H3K4me3. In human samples the present inventors required that the genes are bivalent in at least 2 cell lines. Distribution of H3K27me3 mark in genomic components was calculated by counting the number of H3K27me3 peaks in each component: promoter (6 Kb symmetric interval around TSS), Gene body (between 3 Kb downstream to TSS and TES), and intergenic (outside promoter and gene body). The peaks were divided to bins according to their height, calculated as RPKM.

DNA Constructs inserted into human pluripotent cells. The pCAG-IresPuro or pCAG-flox-DsRed-IRES- Puro vectors (7) encoded the following inserts (which were cloned by either cohesive or blunt-end ligations in XhoI-NotI sites): Stat3-C (A662C and N664C mutations) (8), Stat3-Y705F (dominant-negative allele). Human Oct4 enhancer sequences [the Oct4DE- and Oct4PE-SV40-luciferase (Luc) constructs] were cloned into the pGL3-Promoter Vector (Promega) with the following primers: 5′ hOcCT4PE KpnI: 5′-GGTACCG GATACTCAGGCCAGGCCCAGAAA-3′ (SEQ ID NO:1); 3′ hOCT4PE XhoI: 5′- CTCGAGTCCACAGACCTCTGGCACT-3′ (SEQ ID NO:2); 5′ hOCT4DE KpnI: 5′-GGTACCCATTGAGTCCAAATCCTCTTTACTAGGTG-3′ (SEQ ID NO:3); 3′ hOCT4DE XhoI: 5′-CTCGAGCTGAGGCTCATGCTGCTGG- 3′ (SEQ ID NO:4).

Reporter constructs were used to determine the regulation pattern of Oct4 expression and were electroporated into 0.5–3 × 10^{-6} cells along with the pRL-TK vector for normalization. Assays were performed 48 hours later using the Dual-Glo Luciferase Assay System (Promega). The basal activity of the empty luciferase vector was set as 1.0.

Generation of the NGFP1-Mbd3KD cell line: NGFP1-$Mbd3^{KD}$ was established by infection and sub cloning of secondary NGFP1 iPSC line with a ShRNA pLKO-Tet-On vector (addgene) as previously described (Hanna et al. Nature 2009).

Immunocytochemistry and FACS Analysis - Cells were fixed in 4% paraformaldehyde in PBS and immunostained according to standard protocols using the following primary antibodies: SSEA1, SSEA4 and SSEA3 (Developmental Studies Hybridoma Bank); Tra-1-60 and Tra-1-81 (Millipore); SOX2 (R&D Systems); OCT3/4 (Santa Cruz Biotechnology); human NANOG (goat polyclonal; R&D Systems), mouse Nanog (polyclonal rabbit; Bethyl). Appropriate Alexa Fluor dye-conjugated secondary antibodies (Molecular Probes, Invitrogen) were used. For MHC class I staining of human cells, the present inventors used anti MHC class I antibody (BE pharmingen). For mouse cells, the present inventors used anti-mouse MHC class I H-2Kb and H-2Kd (eBioscience). Human Cells were stained with specific cell surface markers; SSEA4 conjugated APC or TRA-1-60(R) conjugated PE (R&D). Data were collected on BD FACS ARIA III and analyzed with Flowjow software.

DNA Methylation Analysis - DNA was proteinase K-treated and extracted, and 1 μg of DNA was subjected to conversion using the Qiagen EpiTect Bisulfite Kit. Promoter regions of OCT4 and XIST were amplified using previously described primers (Hanna et al., 2010b; Lengner CJ, et al. (2010) Derivation of pre-x inactivation human embryonic stem cell line in physiological oxygen conditions. Cell. 2010 May 28;141(5):872-83; Hockemeyer D, et al. (2008) A drug-inducible system for direct reprogramming of human somatic cells to pluripotency. Cell Stem Cell 3:346–353; and Soldner F, et al. (2009) Parkinson's disease patient-derived induced pluripotent stem cells free of viral reprogramming factors. Cell 136:964–977; each of which is fully incorporated herein by reference in its entirety). XIST forward primer (used on bisulfite treated DNA): 5'-taa att tta aat taa tta aat tat-3' (SEQ ID NO:106); XIST reverse primer (used on bisulfite treated DNA): 5'-tgt ttt aga aag aat ttt aag tgt aga ga-3' (SEQ

ID NO:107). PCR products were cloned using the pCR2.1-TOPO vector and sequenced using the M13 forward primer. Method for LC-MS quantification of relative cytosine methylation: Mass spectrometry measurement of 5-methylcytosine (5mC) content was conducted (on human primed iPSCs/ESCs, and human naive iPSCs/ESCs expanded in a modified WIS-NHSM conditions which included PKCi and which did not include FGF2 and TGFB cytokines, as previously described [Leitch, H. G. *et al.* Naive pluripotency is associated with global DNA hypomethylation. *Nat. Struct. Mol. Biol.* 20, 311–316 (2013)] with a slight modification. Briefly, 250 ng genomic DNA from naive or primed pluripotent cells expanded without MEF feeder cells, was denatured by heating at 100 °C for 3 minutes. Samples were incubated with 1/10 volume of 0.1 M ammonium acetate, pH 5.3, and 2 Units (U) of nuclease P1 for 2 hours at 45 °C. A 1/10 volume of 1 M ammonium bicarbonate and 0.002 units of phosphodiesterase I were added, followed by incubation for 2 hours at 37°C. Finally, samples were incubated for 1 hour at 37°C with 0.5 U alkaline phosphatase. Samples were subsequently diluted in 2 mM ammonium formate, pH 5.5. The nucleosides were separated on an Agilent RRHD Eclipse Plus C18 2.1 × 100 mm 1.8u column by using the HPLC system 1200 (Agilent) and were analyzed by using an Agilent 6490 triple quadruple mass spectrometer. To calculate the concentrations of individual nucleosides within the samples analyzed, standard curves with known amounts of synthetic nucleosides were generated and used to convert the peak-area values to corresponding concentrations.

Reduced representation bisulfite sequencing (RRBS) libraries for genome wide sequencing profile of DNA methylation - RRBS libraries were generated as described previously with slight modifications [Smith, Z. D. *et al. Nature* 484, 339–344 (2012)]. Briefly, DNA was isolated from snap-frozen cell pellets using the Quick-gDNA mini prep kit (Zymo). Isolated DNA was then subjected to MspI digestion (NEB), followed by end repair using T4 PNK / T4 DNA polymerase mix (NEB), A-tailing using Klenow fragment (3'→5' exo-) (NEB), size selection for fragments shorter than 500-bp using SPRI beads (Beckman Coulter) and ligation into a plasmid using quick T4 DNA ligase (NEB). Plasmids were treated with sodium bisulfite using the EZ DNA Methylation-Gold kit (Zymo) and the product was PCR amplified using GoTaq Hot Start DNA polymerase (Promega). The PCR products were A-taild using Klenow fragment, ligated to indexed Illumina adapters using quick T4 DNA ligase and PCR

amplified using GoTaq DNA polymerase. The libraries were then size-selected to 200-500-bp by extended gel electrophoresis using NuSieve 3:1 agarose (Lonza) and gel extraction (Qiagen). Libraries were pooled and sequenced on an Illumina HiSeq 2500 system. The sequencing reads were aligned to the Mouse Genome Build 37 (mm9) using Bismark. Methylation levels were calculated and averaged only for CpGs that were covered by 5 or more distinct sequencing reads across all libraries. The CpG content "experienced" by each CpG site was defined as the number of CpG dinucleotides found within a 500-bp window surrounding the site divided by the window size.

Protocol for injecting human and primate naive pluripotent stem cells:

1. Dissect oviducts of hormone primed and mated B6D2F1 females X B6D2F1 males, and extract zygotes (as routinely done with mouse micro-manipulation).
2. Culture zygotes for 2 days in KSOM medium droplets (Zenith Biotech KSOMaa Evolve cat # ZEKS-050) covered with mineral oil at 37°C, 5%O_2 incubator, until they develop to morula stage.
3. Grow human naive cells to 70-90% confluence in NHSM medium on gelatin/DR4 irradiated MEF coated plates.
4. The day before cell harvesting add 10 µM ROCKi to the cells (in case not continuously used in the NHSM medium).
5. Trypsinize the cells for ~ 5 minutes with 0.05% trypsin, shake and pipette thoroughly to yield one cell suspension. Stop the reaction with DMEM+15% FBS and centrifuge at 1000 RPM for 3 Minutes. Aspirate and discard medium.
6. Resuspend cells in 900 µl NHSM medium, add 100 µl filtered FBS (to reduce stickiness of cells) and 10 µM ROCKi. Keep on ice until and during injections (very important). It is preferable to inject the cells as soon as they are harvested.
7. Inject 15-20 human naive cells to a mouse morula by using of Piezo (as routinely done with mouse ES injections).
8. After injection, incubate for 3-4 hours in KSOM droplets supplemented with 10 µM ROCKi covered with mineral oil.
9. After 3-4 hours transfer the morulas to KSOM droplets (without ROCKi) covered with mineral oil, incubate over night.

10. The next day, most morulas should develop to blastocysts. Transfer 15-20 blastocysts to uterus of pseudo-pregnant B6D2F1 female mice.

EXAMPLE 1

BOOSTING PRIMED STEM CELLS REVERSION TO NAIVE PLURIPOTENCY

The present inventors set out to test whether additional genetic manipulations may enable radically efficient and homogenous reprogramming towards ground state pluripotency. Recent studies have pointed out the importance of chromatin derepression in converting somatic cells into iPSCs (Mansour et al., 2012; Soufi et al., 2012). In addition, the ground state of pluripotency pertains an open chromatin configuration with reduced levels of repressive chromatin marks (Marks et al., 2012). Therefore, the present inventors aimed to conduct a loss of function screen for epigenetic repressor factors in an attempt to dramatically boost the efficiency of reprogramming to ground state pluripotency. The present inventors initially focused on reverting primed epiblast stem cells (EpiSCs) (Mansour et al., 2012), that in the absence of exogenous transcription factor over-expression, can convert within 7 days into naive pluripotent state in naive 2i/LIF (2i= PD0325901 ERK1/2 inhibitor and GSK3β inhibitor CHIR99021) growth conditions. The present inventors utilized an EpiSC line carrying a Nanog-GFP knock-in reporter that is active only in the naive ground state (Mansour et al., 2012), and applied siRNA screening in order to identify boosters of EpiSC reversion into Nanog-GFP+ naive pluripotent cells (Figures 1A-B, and 33A-G). While inhibition of DNA methylation and H3K27me3 by knockdown of Dnmt1 and EED/Suz12 respectively (Mikkelsen et al., 2008), increased epigenetic reversion efficiency, still only a minority of the donor cells turned on the Nanog-GFP reporter (Figure 1A-B). Remarkably, the present inventors noted that Mbd3 inhibition using the Mbd3siRNA [mBD3HSS147581(3_RNAI) Invitrogen:

AGGUCAAGGGCAAGCCCGACCUGAA (SEQ ID NO:52);

MBD3HSS147581(3_RNAI) Invitrogen-UUCAGGUCGGGCUUGCCCUUGACCU; (SEQ ID NO:53)] dramatically increased the EpiSC reversion efficiency, where up to 80% of the transfected cells turned on Nanog-GFP in 2i/LIF conditions (Figures 1A-B) compared to <20% in control EpiSCs (Figures 1A-B). Such a dramatic effect was not

observed with any of the other factors tested, including all other Mbd family members tested (Figures 1A-B).

Methyl-CpG-binding domain 3 (Mbd3; SEQ ID NO:7) is a structural component protein in the Nucleosome remodeling and Deacetylation (NuRD) complex, and together with Mbd 1, 2 and 4, was originally characterized as a protein containing a region with high homology to the methyl-CpG-binding domain (MBD) of MeCP2 (Kaji et al., 2007). Mbd2 and Mbd3 assemble into mutually exclusive distinct NuRD complexes (Le Guezennec, X. et al. Mol. Cell. Biol. 26, 843–851, 2006), which can mediate gene repression through histone deacetylation via histone deacetylase 1 (HDAC1) and 2, and chromatin remodeling ATPase activities through its chromodomain helicase DNA binding protein 3 (CHD3) (Mi2a) and CHD4 (Mi2b) subunits (Zhu et al., 2009).

Mbd3/NuRD preferentially binds and represses actively transcribed genes, and some of its components (e.g. Chd4) have also been implicated in serving as transcriptional activators at certain loci [Reynolds, N., et al., Cell Stem Cell, 2012, 10: 583-594; Günther, K. et al. Nucleic Acids Res. 2013, 41: 3010-3021].

To validate the siRNA screening results, the present inventors used $Mbd3^{+/+}$ and $Mbd3^{flox/-}$ ESCs (Kaji et al., 2007) and introduced Rosa26-CreER and a Nanog-GFP knock-in alleles by gene targeting (Figures 1C and 1H). EpiSCs were established from the latter engineered lines following microinjection into E3.5 blastocysts and rederivation at E6.5 from post-implantation epiblast (Figures 33B-G). In comparison to $Mbd3^{+/+}$ EpiSCs, $Mbd3^{flox/-}$ primed cells reverted with increased efficiency in 2i/LIF + tamoxifen conditions (Figures 1C and 1H), and showed homogenous Nanog-GFP reactivation, consistent with reversion to ground state pluripotency[36] (Figures 1D-L). Single cell clonal analysis for epigenetic reversion of EpiSCs (constitutively labeled with mCherry to control for plating efficiency) demonstrated 95% Nanog-GFP+ single cell reversion efficiency in Mbd3 depleted cells (Figures 1C and 1H). Importantly, $Mbd3^{flox/-}$ EpiSCs, that retain hypomorphic (~20%) Mbd3 protein expression (Figures 1I-J) (Kaji, K. et al. Nat Cell Biol 8, 285–292, 2006), also yielded reverted ESCs with >93% efficiencies (Figures 1C and 1H). Both reverted $Mbd3^{-/-}$ (after transgenic insertion of Mbd3 to rescue their differentiation deficiency (Kaji, K., et al. Development 134, 1123–1132, 2007; Kaji, K. et al. Nat Cell Biol 8, 285–292, 2006) and $Mbd3^{flox/-}$

cells can contribute to adult chimera formation (Figures 1I, J, K, L). Reconstitution of Mbd3 expression in $Mbd3^{-/-}$ and $Mbd3^{flox/-}$ EpiSCs inhibited reversion efficiencies in 2i/LIF down to <20% as typically observed in wild type cells (Figures 1C and 1H). These results directly demonstrate that reduction of Mbd3 protein levels renders nearly complete reversion of murine EpiSCs to ground state pluripotency.

The fact that lack of Mbd3 promotes reversion to pluripotency is seemingly contradictory to previous *in vivo* studies that had suggested that Mbd3 is essential for establishing the ground state of pluripotency after fertilization (Kaji et al., 2006; 2007). This conclusion was based on the fact that while Oct4+ cells could be observed in the inner cell mass of $Mbd3^{-/-}$ E3.5 embryos, $Mbd3^{-/-}$ ESCs could not be derived *in vitro* after explantation in serum/LIF derivation conditions (Kaji et al., 2006; 2007). However, already established ES cells, that can tolerate loss of Mbd3 following gene targeting, show a propensity for trophoblast differentiation in serum containing conditions (Figures 34A-B) (Zhu et al., 2009), which may have also underlied the previous technical inability to derive $Mbd3^{-/-}$ ESC in serum containing conditions. Thus, the present inventors revisited ESC derivation from $Mbd3^{-/-}$ E3.5 embryos in serum free 2i/LIF conditions [Ying, Q.-L. *et al.* The ground state of embryonic stem cell self-renewal. *Nature* 453, 519–523 (2008)], and indeed were able to isolate $Mbd3^{-/-}$ ESCs that expressed all pluripotency markers tested (Figures 34A-C, 2A-O). This indicates that Mbd3 is dispensable for establishing the ground state of pluripotency and mouse ESC derivation. Consistently, nuclear expression of Mbd3 protein is reduced after fertilization throughout pre-implantation development, and becomes readily detected only at the late blastocyst stage and post-implantation epiblast (Figures 1O-T, and Figures 35A-C, 36A-J). Nuclear Mbd3 protein expression is preserved after *in vitro* derivation in both naive and primed mouse pluripotent cells (Figures 36E-H). These results indicate that pre-implantation *in vivo* reprogramming and development are accompanied by depletion of Mbd3 expression, which gets re-expressed once pluripotency is established, consistent with a critical role for Mbd3 in allowing differentiation and exit from naive pluripotency [Reynolds, N., Strouboulis, J., Behrens, A., Bertone, P. & Hendrich, B. NuRD suppresses pluripotency gene expression to promote transcriptional heterogeneity and lineage commitment. *Cell Stem Cell,* 2012, 10: 583-594]. Finally, the present inventors aimed to test the influence of reducing

Mbd3 expression in reprogramming Oct4+ primordial germ cells into ES-like pluripotent embryonic germ (EG) cells. Typically, these cells are derived from E8.5 PGCs following explantation in ES growth conditions [Durcova-Hills, G., Tang, F., Doody, G., Tooze, R. & Surani, M. A. Reprogramming primordial germ cells into pluripotent stem cells. *PLoS ONE* 3, e3531 (2008); Leitch, H. G. *et al.* Embryonic germ cells from mice and rats exhibit properties consistent with a generic pluripotent ground state. *Development* 137, 2279–2287 (2010)]. Single cell sorted $Mbd3^{flox/-}$ Oct4-GFP+ E8.5 PGCs from chimeric animals, were proficient in forming EG cell colonies and lines (>95% efficiency), while PGCs isolated from chimeras generate from $Mbd3^{+/+}$ or $Mbd3^{flox/-}$ cells carrying an exogenous Mbd3 expressing transgene reprogrammed at less than 10% efficiency (Figures 1N-M). Collectively, these findings show that neutralizing Mbd3 expression facilitates access to ground state pluripotency from early embryonic Oct4 expressing cells.

EXAMPLE 2

ALLEVIATING MBD3 INHIBITION FACILITATES SOMATIC CELL REPROGRAMMING

The present inventors tested whether Mbd3 inhibition in somatic cells, that lack expression of endogenous pluripotency markers like Oct4 and are more developmentally restricted in comparison to EpiSCs and PGCs, facilitates their direct conversion to ground state pluripotency at efficiencies nearing 100%. $Mbd3^{+/+}$, $Mbd3^{flox/-}$ and $Mbd3^{-/-}$ fibroblasts carrying Oct4-GFP reporter were directly infected with O, K, S, M encoding moloney viruses, and Oct4-GFP reactivation was evaluated by flow cytometry. While Mbd3 depleted cells reprogrammed more efficiently in comparison to wild type cells, only 15% Oct4-GFP cells were obtained from $Mbd3^{flox/-}$ and $Mbd3^{-/-}$ depleted samples (Figure 37A). This is consistent with a recent study reporting a modest up to 1.5% iPSC formation efficiency following Mbd3 knockdown [Luo, M. *et al.* NuRD Blocks ReprogAramming of Mouse Somatic Cells into Pluripotent Stem Cells. *Stem Cells* (2013)]. Infection with OKSM polycistronic vector [Sommer, C. A. *et al.* Induced pluripotent stem cell generation using a single lentiviral stem cell cassette. *Stem Cells* 27, 543–549 (2009)] dramatically increased $Mbd3^{flox/-}$ iPSC reprogramming towards 45%, likely due to enhanced transgene delivery per

individual somatic cell (Figure 37B). Given that Mbd3 depleted ESCs require serum free 2i/LIF growth conditions to optimally maintain their pluripotency (Figures 34A-B), the present inventors next tested whether the supplementation of a variety of exogenous factors that promote naive stem cell growth can attain maximal efficiency (Figure 37C). Remarkably, by supplementing ES medium with 2i starting at 48 hours after transgene induction, and applying physiologic oxygen conditions, a dramatic reprogramming enhancement was obtained. Under these conditions, 95% of $Mbd3^{flox/-}$ and $Mbd3^{-/-}$ cells were Oct4-GFP positive at day 10, while only levels up to 18% were observed in control $Mbd3^{+/+}$ fibroblasts reprogrammed under identical growth and reprogramming conditions (Figure 4A). To accurately evaluate reprogramming kinetics and efficiencies, the present inventors established "secondary reprogrammable" (Hanna et al., 2009b; Wernig et al., 2008) $Mbd3^{+/+}$ and $Mbd3^{flox/-}$ transgenic cell lines harboring a DOX inducible OKSM polycistronic cassette [Sommer, C. A. *et al.* Induced pluripotent stem cell generation using a single lentiviral stem cell cassette. *Stem Cells* 27, 543–549 (2009)], a constitutive nuclear mCherry marker (to allow their tracking as individual cells and control for plating efficiency), and an Oct4-GFP specific reporter (Boiani, M., Kehler, J. & Schöler, H. R. in METHODS IN MOLECULAR BIOLOGY, 2004, 254: 001–034) (Figures 3A-D and 3G). The latter cells were injected into host blastocyst and secondary reprogrammable MEFs were derived and utilized for reprogramming quantifications (Hanna et al., 2009b). Single cell sorting of mCherry+ $Mbd3^{flox/-}$ MEFs and subsequent reprogramming in 2i-LIF+DOX and 5% O_2 conditions reproducibly yielded 100% iPSC derivation efficiency by day 8. In wild type cells reprogrammed under identical conditions, no more than 20% of clones reactivated Oct4-GFP, while the majority of mCherry secondary fibroblasts cells had neither reactivated Oct4-GFP marker nor acquired ES-like morphology (Figure 4B). Mbd3 depleted somatic cells had similar growth rates on DOX, and background viability levels compared to control wild type cells upon OSKM induction, thus excluding cell proliferation and apoptosis as potential factors underlying the observed differences in iPSC derivation efficiencies (Figures 5A-F). Radically high single cell reprogramming efficiency rates were obtained with multiple $Mbd3^{flox/-}$ secondary lines established harboring different OKSM integrations (Figure 4B) and from a variety of adult progenitor and terminally differentiated cells obtained from NGFP1 iPSC line (Hanna, J. *et al. Nature* 462, 595–

601, 2009) containing a DOX inducible Mbd3 specific shRNA (Mbd3-KD) allele and a Nanog-GFP knock in reporter (Figures 31A-E and 38A-B). All randomly tested clones stained positive for alkaline phosphatase (AP), Oct4 and Nanog pluripotency markers (Figures 4C-G). Mature teratomas and high contribution chimeras, some of which were germ-line transmission competent, were obtained from multiple iPSC clones (Figures 4C-G, and 39A-D), consistent with adequate reprogramming to ground state pluripotency.

The present inventors analyzed the reprogramming dynamics of "secondary" $Mbd3^{flox/-}$ and control $Mbd3^{+/+}$ fibroblasts by applying microscopic live imaging (Smith et al., 2010) (Figures 40A-E). Time-lapse measurements showed a dramatic increase in ES-like colony formation in $Mbd3^{flox/-}$ fibroblasts (Figures 4H-I). An in house developed algorithm that allows segmentation of single mCherry colonies and tracking of Oct4-GFP reactivation dynamics during reprogramming on clonal populations was applied (Figures 40A-E, 4H-I, 41A-D, 42A-E). By day 6 following DOX induction, >98% of $Mbd3^{flox/-}$ clonal populations reactivated the Oct4-GFP pluripotency marker, while only up to 15% efficiency was detected in control samples reprogrammed in identical growth conditions (including 2i/LIF and 5% pO2) (Figures 4J-O, 4Q, 4R). By day 6, approximately 85% of cells within each individual $Mbd3^{flox/-}$ clonal population became Oct4-GFP^{+} cells, while <2% of cells within successfully reprogrammed $Mbd3^{+/+}$ clones turned on the Oct4-GFP marker (Figure 4R). The latter unbiased quantitative analysis demonstrated a dramatically intra- and interclonal synchronized reactivation of Oct4-GFP occurring during a narrow window in $Mbd3^{flox/-}$ clonal populations at days 4.5-5.5 (Figures 4Q-R, and Figures 42A-E), and highlights a dramatic increase in reprogramming synchrony and efficiency following Mbd3 depletion in OSKM transduced somatic cells. Detection of Oct4-GFP by flow cytometry on polyclonal populations demonstrated similar kinetics for iPSC reprogramming (Figures 43A-B). Re-infection with lentiviruses encoding Mbd3, but not Mbd2, before day 5 of reprogramming had a profound inhibitory effect on iPSC generation from $Mbd3^{flox/-}$ MEFs, while reinfection after day 5 had a diminished effect (Figures 44A-B). The above kinetic analysis suggests that Mbd3 can inhibit reprogramming when introduced before final stages of reprogramming coinciding with endogenous Oct4/Nanog reactivation (Silva, J. et al. Cell 138, 722–737, 2009). However, once

pluripotency is reestablished, Mbd3 presence is tolerated and does not compromise the maintenance of ground state pluripotency.

To evaluate the molecular extent of reprogramming in OSKM transduced $Mbd3^{flox/-}$ and $Mbd3^{+/+}$ somatic cells, the present inventors conducted global gene expression analysis on donor MEFs and at days 0, 4 and 8 following DOX induction without cell passaging, and compared them to iPSC and ESC lines. Only $Mbd3^{flox/-}$ somatic cells clustered separately from donor fibroblasts already at day 4 following DOX. Amazingly, by Day 8 they were transcriptionally indistinguishable from multiple ESC and subcloned established iPSC lines (Figures 8R, Figures 45A-B, Figure 7, and Figures 46A-E). Single cell RT-PCR analysis confirmed that only in $Mbd3^{flox/-}$ reprogrammed samples 100% (12/12) of single cells tested expressed all pluripotency markers recently shown to indicate successfully reprogrammed cells (Buganim, Y. et al. Cell 150, 1209–1222, 2012) (Sall4, Utf1, Esrrb, Sox2 and Nanog) (Figures 46D-E). Genome wide chromatin mapping for H3K27me3 (K27me3), H3K4me3 (K4me3) and H3K27acetyl (K27ac) by Chromatin Immunoprecipitation followed by sequencing analysis (Chip-Seq), also confirmed that by day 8, only $Mbd3^{flox/-}$ transduced MEFs had assumed ES-like chromatin profile (Figures 47A-B, 48A-C). Genome wide DNA methylation mapping by Reduced Representation Bisulfite Sequencing (RRBS) confirmed that iPSC-like methylation pattern can be seen in $Mbd3^{flox/-}$ polyclonal population sample only after 8 days of DOX treatment, but not in $Mbd3^{+/+}$ cells, consistent with results indicating CpG methylation loss predominantly occurring in later stages of successful reprogramming (Polo, J. M. et al. Cell 151, 1617–1632, 2012) (Figures 49A-B). Collectively, the above results indicate that Mbd3 depletion following OSKM induction in 2i/LIF conditions yields authentic molecular reestablishment of the ground state of pluripotency in the entire population of donor somatic cells and their progeny.

Following the depletion of Mbd3 expression, the present inventors were not able to isolate stable partially reprogrammed cells that did not reactivate Oct4/Nanog-GFP and could be stably expanded *in vitro* as typically can be obtained from OSKM transduced wild-type somatic cells (Figure 8S, 8A-D, 8E) [Sridharan, R., et al., Cell 36(2):364-77 (2009); Mikkelsen, T. S. et al. Nature 454, 49–55 (2008); Costa Y., et al. NANOG-dependent function of TET1 and TET2 in establishment of pluripotency.

Nature 495, 370–374 (21 March 2013]. The residual 1-15% Oct4-GFP negative cells seen at day 6 in $Mbd3^{flox/-}$ cells (Figures 4Q and 4R), rapidly become GFP+ within 1-2 days of continued reprogramming (Figures 43A-B). The present inventors took 3 independent $Mbd3^{+/+}$ OSKM transduced partially reprogrammed lines derived by different reprogramming methods from either fibroblasts or B cells, and attempted to complete their reprogramming by Mbd3 inhibition. Remarkably, by introducing Mbd3 siRNA

[mBD3HSS147581(3_RNAI) Invitrogen: 5'-

AGGUCAAGGGCAAGCCCGACCUGAA (SEQ ID NO:52);

MBD3HSS147581(3_RNAI) Invitrogen- 5'-

UCAGGUCGGGCUUGCCCUUGACCU; (SEQ ID NO:53)], all 3 clones dramatically turned on Oct4-GFP or Nanog-GFP pluripotency markers following continued OSKM expression in 2i/LIF (Figures 8F-K and 50A-B). Finally, the expression of Mbd3 either in somatic epigenome or in pluripotent cells specifically prohibited the reprogramming of murine somatic cells to pluripotency via cell fusion (Figure 51) (Tada, M., et al. Current Biology, 11: 1553–1558, 2001). These results indicate that depleting Mbd3 expression opens a "gateway" to the ground state of pluripotency.

Phylogenetic analysis of Mbd3 and other NuRD complex proteins across 16 metazoan which span the entire clade (from mammals to the simplest multicellular animal T. adhaerens) showed that Mbd3 and other NuRD complex proteins were found to have an ortholog in T.adhaerens, but not in yeast, which might imply on their appearance in the first multicellular animals alongside with Oct4 and developmental pluripotency (Figure 9).

To functionally validate a conserved inhibitory role for MBD3 in human iPSC reprogramming (Figure 9), the present inventors generated $MBD3^{flox/-}$ hESCs by gene editing with TALE nuclease effectors (Figure 8L, and Figures 52A-C) (Hockemeyer, D. *et al. Nat Biotechnol* 29, 731–734, 2011), and validated hypomorphic MBD3 protein expression in a correctly engineered clone (Figures 8M-N). Fibroblasts were *in vitro* differentiated from $MBD3^{+/+}$ and $MBD3^{flox/-}$ hESCs and reprogrammed by OSKM transduction in recently described human naive pluripotency promoting conditions (WIS-NHSM conditions - that contain 2i/LIF+bFGF), and dramatically yielded >90% iPSC efficiency only from MBD3 depleted samples, as determined by SSEA4 and

TRA1-60 staining at day 8 (Figure 8O). Single cell reprogramming efficiency was tested following introducing OCT4-GFP knock-in reporter and a constitutive mCherry in MBD3$^{+/+}$ and MBD3$^{flox/-}$ hiPSC harboring DOX inducible OSKM factors. *In vitro* differentiated secondary fibroblasts from Mbd3$^{flox/-}$ cells reprogrammed at near 100% efficiency, while secondary fibroblasts differentiated and reprogrammed by same methods did not exhibit reprogramming efficiencies higher than 2% in WIS-NHSM conditions (Figure 8O, Figures 53A-E). MBD3$^{flox/-}$ iPSCs were evident only after DOX induction, and this effect was inhibited by Mbd3 overexpression, thus ruling out contamination with residual primary iPSCs as a source for the high reprogramming efficiencies observed (Figure 8O). Furthermore, dramatically increased human iPSC formation was obtained by applying *MBD3* siRNA [mBD3HSS147581(3_RNAI) Invitrogen: AGGUCAAGGGCAAGCCCGACCUGAA (SEQ ID NO:52); MBD3HSS147581(3_RNAI) Invitrogen-UUCAGGUCGGGCUUGCCCUUGACCU; (SEQ ID NO:53)] at days 2 and 4 following DOX induction in MBD3$^{+/+}$ OSKM transgenic secondary fibroblasts (Figures 10A-D). *MBD3* siRNA treatment allowed reproducible generation of human iPSCs from adult human patient specific fibroblasts only after 2-3 rounds of OSKM + LIN28 mRNA transfection [Warren, L. *et al.* Highly Efficient Reprogramming to Pluripotency and Directed Differentiation of Human Cells with Synthetic Modified mRNA. *Cell Stem Cell* (2010)] and subsequent colony detection and isolation at day 8 (Figures 54A-G). Taken together, these results demonstrate that inhibiting MBD3 alleviates predominant roadblocks for direct human somatic cell reprogramming to pluripotency by OSKM, and thus inhibition of MBD3 can be used in a new technology platform for boosting iPSC formation. Importantly, MBD depleted human pluripotent stem cells have a dramatic round mouse-ESC like morphology and grow homogenously (Figures 8P-Q). These results indicate that Mbd3 inhibition might further improve WIS-NHSM naive growth conditions (described herein).

EXAMPLE 3

NUMERICAL DESCRIPTION OF OSKM REPROGRAMMING FOLLOWING MBD3 DEPLETION

The present inventors next sought to quantitatively characterize the

reprogramming latency distribution for both $Mbd3^{+/+}$ and $Mbd3^{KD}$ samples, and compare it to known deterministic behavior. To do so, the present inventors applied a previously described approach for monoclonal murine Pre-B cell weekly follow-up for reactivation of Nanog-GFP (Figure 31A) (Hanna, J. et al. Nature 462, 595–601, 2009). A secondary OSKM transgenic NGFP1-iPSC line was rendered transgenic for a DOX inducible Mbd3 knockdown (NGFP1-$Mbd3^{KD}$) (Figures 5B, 5C and 5D). Indeed, only NGFP1-$Mbd3^{KD}$ derived monoclonal B cell populations converted into Nanog-GFP+ iPSCs at day 7 at 100% efficiency (Figures 31B-C). Subsequently, during the first 10 days of reprogramming the present inventors conducted daily Nanog-GFP detection on polyclonal NGFP1-control and NGFP1-$Mbd3^{KD}$ B cell populations. The latter cells showed a dramatic increase in reprogramming and followed similar kinetics to those measured in $Mbd3^{flox/-}$ MEFs, as measured by microscopic live imaging (Figures 55A-B). The present inventors next tested whether $Mbd3^{KD}$ cell reprogramming behaves like a deterministic function. In this case, the present inventors expect all cells to become pluripotent at the same time following DOX induction. Such deterministic behavior is well approximated by a step function with 0% reprogramming before a fixed deterministic time and 100% iPS formation afterwards. Fitting the clonal cells reprogramming dynamics to such deterministic step-function revealed a tight fit (R^2>0.9, Chi^2=52) of $Mbd3^{KD}$ cells, but not of control $Mbd3^{+/+}$ cells (R^2=0.55, Chi^2=405) (Figures 31D-E). Despite the observed similarity to a deterministic behavior, variability was still evident in the $Mbd3^{KD}$ sample under the optimized condition devised herein. Thus, the present inventors sought to quantify and compare the variability detected in the reprogramming latency measurements in both $Mbd3^{+/+}$ and $Mbd3^{KD}$ samples, and further compare it to the inherent measured cell cycle variability (Hanna, J. et al. Nature 462, 595–601, 2009). For this purpose the present inventors used two modeling schemes. First, the present inventors fitted the observed reprogramming latency to Gaussian distribution: The present inventors estimated the coefficient of variation (CV=std/mean) of each sample, and found that while the coefficient of variation in the $Mbd3^{+/+}$ sample is 0.5, the $Mbd3^{KD}$ coefficient of variation was reduced to 0.09, tightly proximal to the cell cycle estimated coefficient of variation (0.08) (Figures 56A-F and 57A). Second, the present inventors sought to use a dynamic stochastic model to estimate reprogramming variability. The present inventors used a

Brownian motion (BM) model (Figure 57C) and found that indeed $Mbd3^{KD}$ and cell cycle measurements showed the same dynamic variation, while $Mbd3^{+/+}$ samples showed higher variability (Figure 57B and general materials and experimental methods above). To further support reduction in rate-limiting barrier(s) upon Mbd3 depletion, the present inventors modeled the dynamics of the OSKM reprogramming process using multi-step Markov chain model (Phase-Type (PH) modeling (Bolch, G., Greiner, S., de Meer, H. & Trivedi, K. S. Queueing networks and Markov chains: modeling and performance evaluation with computer science applications. WILEY, Second Edition, 2006) (Figures 55C-D, 58A-D, 59A-G). Finally, without being bound by any theory, the present inventors hypothesized that the reduction in rate–limiting barriers in $Mbd3^{KD}$ samples may reduce reprogramming variability to variability explained by cell cycle alone. For this purpose the present inventors fitted the observed reprogramming latency to a cell cycle model that captures the required reprogramming duration (General materials and experimental methods above and data not shown) (Hanna, J. et al. Nature 462, 595–601, 2009; Duffy, K. R. *et al.* Activation-Induced B Cell Fates Are Selected by Intracellular Stochastic Competition. *Science* 335, 338–344, 2012). Specifically, the present inventors estimated the number of generations according to the reprogramming duration, and fit the cell cycle time distribution to the observed reprogramming latency. By applying this method, the present inventors obtained a profound fit (R^2=0.999) between the $Mbd3^{KD}$ dynamic and cell cycle model, but not in the control $Mbd3^{+/+}$ dynamics (R^2=0.73) (Figures 57D-E). Altogether these results consistently show a reduction in reprogramming variability and proximity to deterministic dynamic behavior upon Mbd3 depletion, where the remaining variability can be accounted for by the inherent cell cycle variability. Importantly, these findings do not exclude the existence of alternative pathways that can further accelerate or improve the deterministic reprogramming dynamics observed in Mbd3 depleted cells following OSKM induction and/or enable deterministic induction of pluripotency without manipulating Mbd3 expression or activity (Maekawa, M. et al. Nature 474, 225–229, 2011). Further, these results show a deterministic trajectory for successfully obtaining iPSCs based on measuring reactivation of endogenous pluripotency genes as a final outcome.

EXAMPLE 4

MECHANISMS FOR MBD3 INHIBITION OF IPSC REPROGRAMMING BY OSKM

Recent work has shown that the pluripotency factor Zfp281 directly recruits Mbd3/NuRD to Nanog promoter and repress its expression (Fidalgo et al., 2012), and that inhibition of Zfp5281 led to a modest 2-fold increase in iPSC formation efficiency (Fidalgo et al., 2012). Given that Mbd3 inhibition conducted here led to a much more pronounced effect, in comparison to Zfp281 depletion, this has raised the hypothesis that Mbd3 may be acting more globally in pluripotency regulation by directly interacting with many other pluripotency promoting factors. The present inventors show that Flag-Tagged Oct4, Klf4, and Sox2 specifically co-immunoprecipitated with Mbd3 following overexpression in 293HEK cells (Figures 11A-D, and Figures 11I-L). Importantly, Mbd2 did not directly interact with all other pluripotency factors tested (Figures 11E-H, and Figures 11M-P). The above could explain the distinct influence of Mbd2 and Mbd3 on reprogramming to ground state pluripotency (Figures 1A-B). Collectively, these results support a critical role for pluripotency factor and Mbd3 direct interaction in inhibiting iPSC formation by OSKM.

Mbd3 inhibition was a key and dominant contributor to the radically efficient progression towards pluripotency reported herein. Thus the present inventors aimed to define the mechanisms of Mbd3 inhibition of iPSC reprogramming. Inhibiting Mbd3 expression was not sufficient to induce iPSC formation in the absence of exogenous OSKM overexpression in somatic cells (even in NPCs that can be reprogrammed with Oct4 expression alone) (Kim, J. B. et al. Nature 461, 649–653, 2009) (Figure 38A). Mbd3 did not replace exogenous OSK expression to give rise to iPSCs (Figure 38B). The presence of exogenous c-Myc was essential to obtain iPSCs at 100% efficiency following factor transduction (Figure 38B). Mbd3 depletion without OSKM expression does not independently lead to endogenous reactivation of bona fide pluripotency genes (Figure 38A). Further, Mbd3 inhibitory effect on pluripotency could not be predominantly attributed to its ability to repress endogenous Nanog directly or indirectly [Luo, M. *et al.* NuRD Blocks ReprogAramming of Mouse Somatic Cells into Pluripotent Stem Cells. *Stem Cells* (2013); Fidalgo, M. *et al.* Zfp281 mediates Nanog autorepression through recruitment of the NuRD complex and inhibits somatic cell

reprogramming. *Proc. Natl. Acad. Sci. U.S.A.* 109, 16202–16207 (2012)], since ectopic Nanog overexpression together with OSKM resulted in modest enhancement in iPSC formation and the process remained to follow a stochastic course (Hanna, J. *et al. Nature* 462, 595–601, 2009) (Figure 31A and Figure 8E). Recent work has shown that the pluripotency factor Zfp281 directly recruits Mbd3/NuRD to repress Nanog promoter activity, and that inhibition of Zfp281 led to a modest 2 fold increase in iPSC formation efficiency (Fidalgo, M. et al. Proc. Natl. Acad. Sci. U.S.A. 109, 16202–16207, 2012). Given that, in comparison to Zfp281 depletion or Nanog over-expression (Fidalgo, M. et al. Proc. Natl. Acad. Sci. U.S.A. 109, 16202–16207, 2012), Mbd3 inhibition led to a radically more pronounced effect, raised the hypothesis that Mbd3 may be acting more globally in reprogramming regulation by directly interacting with other critical pluripotency promoting factors. The present inventors established that Flag-Tagged Oct4, Klf4, Sox2 and c-Myc specifically co-immunoprecipitated with Mbd3 following exogenous overexpression in HEK293 cells (Figures 32A-B). Reciprocal experiments showed that Flag-tagged Mbd3 specifically co-immunoprecipitated with Oct4, Sox2, Klf4 and c-Myc, but not Nanog (Figures 60A-B). OSKM specifically co-immunoprecipitated with Mbd3/NuRD components in MEF cells undergoing reprogramming following 3 days of OSKM induction (Figure 60C). $Mbd3^{-/-}$ ESCs expressing Flag-tagged Mbd3 transgene validated direct interaction of Mbd3 with Sall4 reprogramming factor, that is known to get reactivated later in the reprogramming process and cooperate with OSKM in finalizing the reprogramming process (Figure 61A) (Buganim, Y. *et al. Cell* 150, 1209–1222, 2012; Mansour, A. A. *et al. Nature* 488, 409–413, 2012). These interactions were mediated via MBD domain of Mbd3, and defined deletions introduced in MBD domain abrogated co-immunoprecipitation of Mbd3 with OSKM reprogramming factors (Figures 62A-C). As previously seen in a variety of somatic and cancer cell lines (Le Guezennec, X. et al. Mol. Cell. Biol. 26, 843–851, 2006), Mbd2 and Mbd3 do not co-localize to the same NuRD complexes as validated by co-immunoprecipitation experiments (Figures 61A-C). The above explains, at least in part, the lack of dramatic influence for perturbing Mbd2 expression on reprogramming to ground state pluripotency (Figures 1A-B, 1A and 44A-B).

Consistent with the direct protein interactions for Mbd3/NuRD complex with OSKM reported above, genome wide ChIP-seq analysis of Mbd3 binding in DOX

induced wild type MEFs, identified a global increase in Mbd3 recruitment and binding following OSKM induction (1177 binding regions in MEF compared to 8657 following OSKM induction). Only after DOX induction, Mbd3 bound genes are enriched for targets of Klf4, Oct4, Sox2 and Esrrb ($p<10^{-22}$) as well for genes with H3K4me3 active chromatin mark in ES cells ($p < 10^{-38}$) (Figures 32C-D). Motif search analysis in Mbd3 binding locations identified 30 motifs ($p<0.001$), where the motifs of Klf4, Sox2, and Oct4 are among the top six ($p<10^{-30}$) (Figure 63). Importantly, in somatic MEFs prior to OSKM induction, Mbd3 is not localized to pluripotency factor target genes (Figures 32C-D). NuRD component Chd4 was similarly recruited to downstream targets only after DOX induction, indicating NuRD recruitment with Mbd3 after DOX induction (Figures 32C-D). Chd4 localization to downstream targets of OKSM was diminished in Mbd3 depleted cells and its knockdown in $Mbd3^{+/+}$ MEFs undergoing reprogramming significantly enhanced iPSC formation (up to 50% Oct4-GFP+ cell on day 8 – (Figure 63), thus supporting the notion that Mbd3 exerts its inhibitory function on reprogramming predominantly through NuRD complex dependent functions. Notably, inhibition of Chd4 had a relatively milder effect on boosting iPSC reprogramming, in comparison to Mbd3 depletion, possibly because Chd4 (also known as Mi2b) is also found in other protein complexes whose influence on pluripotency remains to be defined (e.g. Ep300 activator complex (Reynolds, N., Development 140, 505–512, 2013). However, without being bound by any theory, the present inventors cannot exclude additional NuRD independent inhibition for Mbd3 on reprogramming.

Transcription level of Mbd3 target genes following 4 days of DOX was significantly upregulated following DOX in Mbd3 depleted samples (Figure 32E), consistent with predominant function of Mbd3/NuRD complex as a repressor of pluripotency gene network during reprogramming. Chromatin of Mbd3 direct targets was significantly more active and open in Mbd3 depleted samples during reprogramming, including statistically significant higher levels of H3K4me3 and H3K27ac, and reduced H3K27me3 repressive chromatin mark (Figure 32F). Further, Mbd3 depletion allowed enhanced exogenous Oct4 binding to targets of Mbd3 at day 4 following DOX ($p<10^{-16}$, Figure 32F). Known OSKM target genes that get reactivated during iPSC formation were found to be significantly upregulated at 4 days in Mbd3 depleted cells, and retained an open chromatin confirmation in comparison to control

Mbd3$^{+/+}$ cells (Figures 65A-E). Similar gene expression and chromatin pattern were observed with the shared targets of Mbd3 and the reprogramming factors (OSKM) (Figures 66A-J). Mbd3 mutants with compromised ability to directly interact with OSKM reprogramming factors were deficient in reducing reprogramming efficiency of Mbd3$^{flox/-}$ somatic cells, supporting the notion that direct OSKM-Mbd3 interactions are important for inhibiting iPSC formation (Figure 32G). Importantly, the present inventors noted that a minimum 5-day exogenous transgene (DOX) induction was similarly required to obtain iPSCs from Mbd3$^{+/+}$ and Mbd3$^{flox/-}$ cells (Figures 67A-D), and that the expression of OSK interacting partners that positively propel reprogramming to pluripotency (like Utx and Wdr5) is also essential for iPSC formation in Mbd3 depleted cells (Figures 67B-D). Collectively, these results establish a paradigm where exogenous OSKM interact with multiple epigenetic complexes that de-repress pluripotency promoting gene networks (e.g. Wdr5 or Utx containing complexes) (Ang, Y.-S. et al. Cell 145, 183–197, 2011; Mansour, A. A. *et al. Nature* 488, 409–413, 2012), they also directly assemble with the Mbd3/NuRD repressor complex. As a result, Mbd3/NuRD is directly recruited to downstream OSKM target genes that are essential for propelling the reprogramming process, and potently counteracts their robust reactivation (Han, J. et al. Nature 463, 1096–1100, 2010; Doege, C. A. et al. Nature 488, 652–655, 2012; Chia, N.-Y. et al. Nature 468, 316–320, 2010). In the absence of Mbd3 inhibitory effect, OSKM interactions with pluripotency promoting epigenetic regulators predominates functionally, and drive uninterrupted progression of direct reprogramming to pluripotency.

Analysis and discussion

Mbd3 And Deterministic Reprogramming To Ground State Naive Pluripotency

Here the present inventors identify the specific of Mbd3/NuRD repressor complex as major barrier preventing epigenetic reversion of EpiSCs, PGCs and somatic cells to ground state pluripotency by defined signaling and transcriptional input. This complex is evolutionary conserved since the emergence of multicellularity and counteracts the reprogramming potential of a variety of pluripotency factors that cooperatively establish the ground state of pluripotency. Mbd3 repression is tolerated

once pluripotency is established, however when trying to enter this state the inhibitory function become dramatically rate limiting and preventing majority of cells assume the pluripotent state. Collectively, these findings show that direct reprogramming to pluripotency need not be stochastic, and that OSKM and other reprogramming methods applied thus far are reductionist. It would be interesting to investigate whether there are alternative pathways that can enable deterministic induction of pluripotency and/or further accelerate the deterministic reprogramming dynamics observed in Mbd3 depleted cells following OSKM induction. It will also be of great interest to determine whether and how is Mbd3 neutralized *in vivo* during pre-implantation and germ-line reprogramming.

The ability to directly reprogram somatic cells into iPSCs has boosted the scientific interest to comprehend the dynamics of epigenetic reprogramming at high resolution, and to accurately define the temporal regulation between transcription factors and chromatin remodelers throughout the entire process of iPSC formation. Despite of the great progress achieved in the field, the present inventors are still highly limited in comprehending the molecular mechanisms, dynamics and interdependence between different layers of chromatin regulation, and how they lead to the establishment of distinct pluripotent states. The latter directly results from the inefficiency and stochasticity of currently devised reprogramming methods together with the difficulty to prospectively isolate the rare cells that correctly and rapidly reprogram into iPSCs. While the study of intermediate populations has provided important insights into mechanisms of pluripotency reprogramming, such cells overly great molecular heterogeneity and retain randomness in progressive towards pluripotency. The near deterministic reprogramming strategies reported herein can allow dissection of authentic molecular events accompanying a more synchronized and non-saltatory progression pattern towards iPSCs, which is critical for molecular deciphering of the black box of reprogramming.

The present inventors show that the stochastic and a-synchronized trajectory of direct reprogramming by OSKM (Hanna, J. H., et al., *Cell,* 143**,** 508–525, 2010) can be coaxed to become radically efficient and deterministic with modified reprogramming approaches. The present inventors highlight Mbd3/NuRD repressor complex, which is naturally depleted during normal pre-implantation development (Figures 1O-T), as a

predominant barrier preventing epigenetic reversion of EpiSCs, PGCs and somatic cells to ground state pluripotency by defined signaling and transcriptional input. A variety of critical reprogramming factors directly interact and recruit Mbd3/NuRD complex, and thus form a highly potent negative regulatory complex that restrains pluripotency gene reactivation throughout the process. Alleviating this inhibitory pathway facilitates direct and synchronized conversion into iPSCs by defined transcriptional and signaling input (Figure 32H). It will be of great interest to explore whether direct reprogramming in the absence of Mbd3 repression improves the quality of reprogrammed cells and reduces the frequency of obtaining aberrantly reprogrammed iPSCs (Zwaka, T. P. Stem cells: Troublesome memories. Nature. 2010, 467: 280-1). Finally, the inefficiency and stochasticity of currently devised reprogramming methods together with the difficulty to prospectively isolate the rare cells that correctly and rapidly reprogram into iPSCs, have restricted the ability to characterize the temporal regulation between transcription factors and chromatin remodelers throughout the entire process of iPSC formation (Buganim, Y. *et al. Cell* 150, 1209–1222, 2012). While the study of intermediate populations (Hanna, J. et al. Nature 462, 595–601, 2009) has provided important insights into mechanisms of pluripotency reprogramming, such cells overly great molecular heterogeneity and retain randomness in progressing towards pluripotency (Polo, J. M. et al. Cell 151, 1617–1632, 2012). The deterministic reprogramming strategy reported herein may allow dissection of authentic molecular events accompanying a more synchronized and non-saltatory progression pattern towards iPSCs, which is critical for biochemical and functional deciphering of the black box of reprogramming.

EXAMPLE 5

CHEMICALLY DEFINED GROWTH CONDITIONS FOR DERIVING TRANSGENE INDEPENDENT AND INDEFINITELY STABLE HUMAN NAIVE PLURIPOTENT CELLS

The recent isolation of naive pluripotent stem cells from non-obese diabetic (NOD) mouse strains and rats (Hanna et al., 2009a), previously considered "non-permissive" for ESC derivation, has been achieved by supplementation with small molecules or growth factors that alleviate inhibitory differentiation cues and/or

reinforce key signaling pathways that stabilize core transcriptional circuitry of naive pluripotency (Hanna et al., 2010b).

Defining human naive pluripotency growth conditions

To define conditions for expanding human naive pluripotent cells that are independent of ERK1/2 signaling, the present inventors first utilized a previously described "secondary" human female C1.2 iPSC line containing Doxycycline (DOX) inducible lentiviral transgenes encoding OCT4 (SEQ ID NO:54 protein), SOX2 (SEQ ID NO:56 protein) and KLF4 (SEQ ID NO:58 protein) reprogramming factors (Hanna, J. *et al. Proc. Natl. Acad. Sci. U.S.A.* 107, 9222–9227, 2010; Chia, N.-Y. *et al. Nature* 468, 316–320 (2010); Lengner, C. J. *et al. Cell* 141, 872–883 (2010); Tomoda, K. *et al. Cell Stem Cell* 11, 91–99 (2012); Bernstein, B. E. *et al. Cell* 125, 315–326 (2006); Guenther, M. G. *et al. Cell Stem Cell* 7, 249–257 (2010)], and a constitutively active lentivirus encoding the reverse tetracycline transactivator (FUW-M2rtTA) (Figures 12A-C). This clone was targeted with an OCT4-GFP-2A-PURO knock-in reporter construct [Takahashi, K. & Yamanaka, S. *Cell* 126, 663–676 (2006); Hockemeyer, D. *et al. Nat Biotechnol* 29, 731–734 (2011)] to track their pluripotency maintenance (Figures 12A-C). As previously established [Nichols, J. & Smith, A. *Cell Stem Cell* 4, 487–492 (2009); Hanna, J. *et al. Proc. Natl. Acad. Sci. U.S.A.* 107, 9222–9227, 2010] exogenous expression of reprogramming factors transgenes by DOX supplementation, allows maintaining cells that are morphologically similar to mESCs, while retaining approximately 60% OCT4-GFP+ cell fraction in 2i/LIF conditions (Figure 12D). Notably, SOX1 neural marker was highly expressed, indicating that these previously described cells are aberrantly stabilized and retain a propensity for differentiation in 2i/LIF+DOX (Figure 72A). The DOX-dependent C1.2 hiPSC line was utilized to screen for additional compounds and/or growth factors [Ying, Q.-L. et al. Nature 453, 519–523 (2008); Hanna, J. et al. Proc. Natl. Acad. Sci. U.S.A. 107, 9222–9227, 2010; Tiwari, VK. et al. Nat Genet 2011, 44(1):94-100; De Los Angeles A., et al. Curr. Opin. Genet. Dev. 22, 272–282 (2012); Li, W. et al. Cell Stem Cell 4, 16–19 (2009)] that, upon DOX withdrawal, could stabilize C1.2 hiPSCs in 2i/LIF indefinitely with homogenous OCT4-GFP expression (in nearly 100% of the cells) (Figures 12A-C).

While C1.2 cells rapidly differentiated in 2i/LIF only conditions, the combined action of 16 factor conditions (16F– divided into Pool 1 and Pool 2 subgroups)

attenuated the differentiation propensity and allowed retaining 32% of OCT4-GFP+ cells as measured at day 14 after DOX withdrawal (Figure 12D). This indicated that the 16F combination contains factors that cooperatively promote human pluripotency maintenance in 2i/LIF conditions. When Pool 2 components were removed (Figure 12D), OCT4-GFP+ cell fraction significantly increased relative to 16F combination, suggesting that Pool 2 contained factors that were negatively influencing GFP+ cell maintenance (Figure 12D). Without being bound by any theory, the present inventors hypothesized that FGF and TGFβ pathway inhibition was detrimental to growing human pluripotent cells in 2i/LIF conditions. FGF2 and TGFβ have an evolutionary divergent function in promoting pluripotency in humans by inducing KLF4 and NANOG expression in hESCs [Hanna, J. *et al. Proc. Natl. Acad. Sci. U.S.A.* 107, 9222–9227, 2010; De Los Angeles, A., et al. Dev. 22, 272–282 (2012); Li, W. et al. Cell Stem Cell 4, 16–19 (2009); Pribluda, A. et al. Nat Biotechnol 30, 247–249 (2012); Nichols, J. & Smith, A. Pluripotency in the embryo and in culture. Cold Spring Harb Perspect Biol 4, a008128 (2012); Roode, M. et al. Dev. Biol. 361, 358–363 (2012); Rad, R., et al., Proc Natl Acad Sci U S A. 2011, 108(45):18283-8; Xu, Y. et al. Proc. Natl. Acad. Sci. U.S.A. 107, 8129–8134 (2010); Buecker, C. et al. Cell Stem Cell 6, 535–546 (2010)], but not in mEpiSCs, where they play an opposite role and promote murine pluripotency priming. Further, applying FGF receptor inhibition on human developing blastocysts did not prevent ICM differentiation, further suggesting a divergent role for FGF signaling in influencing pluripotency in humans (Roode, M. *et al. Dev. Biol.* 361, 358–363 (2012); Hanna, J. *et al. Proc. Natl. Acad. Sci. U.S.A.* 107, 9222–9227, 2010). Indeed, removing both TGFβ and FGF receptor inhibitors recapitulated the phenotype obtained when removing DOX and Pool 2 components (Figure 12D), and further suggesting that Pool 2 components were not required to promote the maintenance of GFP+ cells in 2i/LIF containing conditions. Moreover, Pool 1 components supplemented with exogenous FGF2 and TGFβ cytokines resulted in homogenous OCT4-GFP in >95% of cells independent of DOX in 2i/LIF containing conditions (Figure 12D). The present inventors then tested which of the Pool 1 components were essential to maintain OCT4-GFP+ DOX independent C1.2 hiPSCs, and found that 2i/LIF, p38i, JNKi together with FGF2 and TGFβ1 cytokine supplementation were essential to maintain exogenous transgene-independent GFP+ C1.2 clones on feeder

free gelatin/vitronectin coated plates (Figure 12S). Secondary optimization identified Rho-associated coiled-coil kinases (ROCK)(Watanabe, K. *et al.* A ROCK inhibitor permits survival of dissociated human embryonic stem cells. *Nat Biotechnol* 25, 681–686 (2007)) and Protein Kinase C (PKC) (Rajendran, G. *et al.* Inhibition of protein kinase C signaling maintains rat embryonic stem cell pluripotency. *Journal of Biological Chemistry* 288, 24351–24362 (2013)) inhibitors as optional boosters of cell viability, and resulted in optimized chemically defined conditions termed *WIS-NHSM* (Weizmann Institute of Science- Naïve Human Stem cell Medium) (Figure 12U). This optimized chemically defined conditions, termed *"WIS-NHSM"* (Figures 12G, 12T, 72B, 72C and 72D), enabled expansion of karyotypically normal and GFP+ C1.2 hiPSCs for over 50 passages (Figures 12J-K, 12V). Remarkably, human pluripotent cells grown in WIS-NHSM medium have domed-shaped colonies resembling murine naive cells, thus the present inventors refer to the selected cells as naive human iPSCs and ESCs, as the present inventors systematically validate below the molecular evidence for this claim.

EXAMPLE 6

DERIVATION OF GROUND STATE NAIVE HUMAN ESCS

New human embryo derived naive ESCs **-** The present inventors next examined whether WIS-NHSM conditions allow derivation of new hESC lines from the ICM of human blastocysts [Lengner, C. J. *et al. Cell* 141, 872–883 (2010); Roode, M. *et al. Dev. Biol.* 361, 358–363 (2012)]. In contrast to the lack of derivation of any cell lines from blastocysts explanted in 2i/LIF/FGF2 conditions (0% efficiency, n=82), human blastocysts plated on mouse embryonic fibroblast (MEF) coated plates and WIS-NHSM medium successfully generated domed cell outgrowths following only 6-8 days of plating (Figures 13N-O). ICM derived outgrowths were then trypsinized and passaged and the present inventors were able to establish and characterize 4 newly derived stem cell lines termed LIS1, LIS2, WIS1 and WIS2 hESCs in naive condition at 36% efficiency (n=11 embryos) versus 9.5% efficiency in conventional/primed conditions as previously published [Hanna, J. et al. Cell Stem Cell 4, 513–524 (2009); Nichols, J. & Smith, A. Cell Stem Cell 4, 487–492 (2009); Ben-Yosef, D. et al. Stem Cells and Development 21, 363–372 (2012)] (Figures 13N-O 14A-B). The outcome of growing

already established conventional hESC lines in WIS-NHSM conditions was also evaluated. Multiple primed/conventional hESC lines (H1, H9, BGO1, WIBR1, WIBR3) and hiPSC lines (C1 and C2) were plated on gelatin/vitronectin-coated dishes in WIS-NHSM medium (Figures 13A-E). After 4-8 days of applying this protocol, dome-shaped colonies with packed round cell morphology, typical of mESCs, could be readily isolated and further expanded (Figures 13A-E and 68A-B). Human BJ fibroblast cells were reprogrammed to hiPSCs in WIS-NHSM conditions following either lentiviral transduction with DOX inducible OKSM factors or by transient transfection with OSKM and Lin28 mRNA (Figures 13V-W). Domed iPSC colonies appeared 10 days following reprogramming factor transductions in WIS-NHSM medium (Figure 13V), which were subsequently picked, trypsinized and expanded for further follow up and characterization (Figures 14A-D). All polyclonal and subcloned hESC and iPSC lines expanded in WIS-NHSM conditions were uniformly positive for pluripotent markers (representative images in Figures 68A-B, 15N-O, 18A-F, 16A-H, and 73A-F), adequately differentiated *in vitro* upon cultivation as embryonic bodies (Figures 19A-I, and 19J-O) and formed mature teratomas *in vivo* (Figures 68C-H, 20A-L and 20M-T).

Naive hESCs and hiPSC lines were expanded in defined growth conditions independent of feeders or fetal bovine serum on vitronectin/gelatin coated plates, and passaged following trypsinization into single cells. Human naive pluripotent lines maintained normal karyotype after extended passaging (Figures 15H-M). The average doubling time for naive hESCs in WIS-NHSM was significantly reduced from 26 hours for primed hESCs to 14 hours for naive hESCs/hiPSCs (Figure 74A). Human naive iPSCs/ESCs displayed 35% single cell cloning efficiency after trypsinization and sorting (without the use of ROCK inhibitors), while conventional genetically matched primed hESCs and hiPSCs did not survive single cell cloning (Figure 74B) (Hanna, J. *et al. Proc. Natl. Acad. Sci. U.S.A.* 107, 9222–9227, 2010). In the presence of ROCK inhibitor, naive hPSCs had single cell cloning efficient up to 88%, while primed cell single cell cloning increased only up to 22% (Figure 74B). However, the relative reduced single cell cloning efficiency in human naive PSCs is not attributed to limitation of WIS-NHSM conditions, but rather due to the fact that humans, unlike rodents, do not express mouse naive pluripotency specific protein ERAS as a result of an upstream premature poly-adenylation signal that results in a truncated non-coding

transcript [Kameda, T. & Thomson, J. *Stem Cells* 23, 1535–1540 (2005)]. Remarkably, naive Eras$^{-/Y}$ mESCs had single cell plating levels nearing 45%, similarly to those obtained in naive hESCs and hiPSCs without the use of ROCK inhibitor (Figure 74C). Transgenic reconstitution of ERAS in naive hESC/hiPSC conditions enabled single cell cloning efficiency comparable to those seen in mESCs (Figure 74C). The present inventors note that Eras null mESC derivation efficiency is also reduced in comparison to wild type (WT) embryos in 2i/LIF (Figure 74D). Collectively, these results indicate that naive hESCs have distinct growth properties from primed hESCs, and are comparable to mESCs, particularly when taking into account the divergence in functional ERAS gene presence between the two species.

The naive hESC/hiPSCs described herein are stably pluripotent in vitro - All cell lines stained uniformly positive for Oct4, Sox2, Nanog, SSEA3, SSEA4, TRA1-60 and TRA1-81 pluripotency markers (representative images in Figures. 13F-H, Figures. 16A-H, Figures. 17A-H and Figures. 18A-F). To determine the differentiation ability of naive hiPSCs and hESCs *in vitro*, the present inventors used floating cultivation to form embryoid bodies (EBs). After 6 days in suspension culture, ball-shaped structures were readily formed from all cell lines tested (Figures. 19A-F).

The naive hESC/hiPSCs described herein are stably pluripotent in vivo - To test pluripotency *in vivo*, the present inventors transplanted naive hESC/hiPSCs subcutaneously into immunodeficient (SCID) mice and 3-5 weeks after injection, teratomas were extracted for histological examination that showed that the tumor contained various tissues, including gut-like epithelial tissues (endoderm), striated muscle (mesoderm), cartilage (mesoderm), neural tissues (ectoderm) (Figures. 20A-U).

Together these results indicate that naive hESC/hiPSC lines established from previously isolated primed hESCs/iPSCs have the functional properties and developmental potency of pluripotent ESCs and iPSCs. .

The WIS-NHSM medium can be used to generate naive PSC from a human inner cell mass (ICM) - The present inventors examined the ability to expand human ICM derived cells (Lengner et al., 2010) in WIS-NHSM conditions. A human blastocyst was plated on mouse embryonic fibroblast (MEF) cells in WIS-NHSM medium (Figures. 13N-O). Outgrowth was evident at day 8, and was trypsinized and passaged. A

pluripotent cell line was established and termed WIS1 hESC line (Figure 13O). The line exhibited a normal karyotype 46XX, stained positive for all pluripotent markers tested, and differentiated *in vivo* into teratomas (Figures. 13P-U). This indicates that WIS-NHSM supports derivation of human ESC lines directly from human embryos.

EXAMPLE 7

EPIGENETIC FEATURES OF HUMAN NAIVE PLURIPOTENCY

The present inventors next moved to characterize epigenetic features in naive hiPSCs and genetically unmodified hESCs established in WIS-NHSM conditions. The evolutionary conserved distal (DE) and proximal enhancer (PE) regions of Oct4 gene are reciprocally regulated in the pre- and post-implantation mouse embryo, and thus the Oct4 distal enhancer is predominantly utilized in naive mESCs (Hanna, J. *et al. Proc. Natl. Acad. Sci. U.S.A.* 107, 9222–9227, 2010), while the proximal enhancer element is preferentially active in primed mEpiSCs. Primed and naive hESC/hiPSCs were transfected with a luciferase reporter construct under the control of either the human distal or the proximal enhancer sequences that control expression of the OCT4 gene (Figure 25A). Consistent with previous reports, primed hESCs showed preferential activation of the proximal OCT4 enhancer element as typically seen in mEpiSCs [Hanna, J. *et al. Proc. Natl. Acad. Sci.* U.S.A. 107, 9222–9227, 2010;Chia, N.-Y. et al. A genome-wide RNAi screen reveals determinants of human embryonic stem cell identity. Nature 468, 316–320 (2010)]. Remarkably, predominant utilization of the OCT4 distal enhancer was detected in naive hESCs and hiPSCs, indicating that the gene expression program active in naive hESCs favors utilization of the distal OCT4 enhancer as typically observed in mESCs (Figure 25A). To further substantiate the latter findings, WIBR3 hESCs were stably transfected with full-length OCT4-GFP-2A-PURO, ΔPE-OCT4-GFP-2A-PURO or ΔDE-OCT4-GFP-2A-PURO engineered BAC reporter constructs (Figure 75A). The wild-type OCT4-GFP reporter was specifically active in both naive and primed conditions, and not detected upon differentiation (Figure 25A). ΔPE-OCT4-GFP reporter was predominantly active in naive growth conditions while the ΔDE-OCT4-GFP reporter was more active in primed pluripotent cells (Figure 25A and Figures 75A-I). Collectively these finding indicate that hESCs/hiPSCs captured in WIS-NHSM conditions utilize a distinct epigenetic

regulation of OCT4 expression from conventional/primed hESCs and hiPSCs.

As a minority of human primed PSC lines can maintain a pre-X inactivation state [Mekhoubad, S. et al. Cell Stem Cell 10, 595–609 (2012); Papp, B. & Plath, K. Cell 152, 1324–1343 (2013)], X chromosome epigenetic status may not be a single reliable marker to unequivocally distinguish between naive and primed state. However, the present inventors aimed to analyze the frequency and properties of X inactivation state in multiple naive hESC/hiPSC lines.

Human ICM (inner cell mass) cells of late stage blastocysts display a unique pre-X inactivation state in females, where despite XIST gene is weakly transcribed (even in male embryos), both X chromosomes are in a pre X-inactivation state and do not demonstrate H3K27me3 and XIST chromosome coating until differentiation [Okamoto, I. *et al.* Nature. 2011; 472(7343):370-4].

The present inventors characterized X-chromosome inactivation state in naive-hESCs/hiPSCs. Primed/conventional WIBR3 hESCs demonstrate X inactivation as evident by ~50% methylation of XIST gene, very high transcription of XIST transcript consistent with initiation of X chromosome inactivation (Figures. 23A-D). Remarkably, all naive hESC and IPSC clones expanded in WIS-NHSM and tested demonstrated a unique pre-X inactivation status similar to that described in human ICM. The cells displayed the near complete absence of H3K27me3/polycomb foci on the X-chromosome alleles (Figure 23C), which was upregulated upon EB differentiation (Figure 23D).

Close monitoring of X chromosome dynamics in primed female hESC lines during *in vitro* derivation in conventional bFGF/TGFβ only conditions, demonstrated that the cells have a great tendency to undergo X chromosome inactivation as a part of an *in vitro* adaptation process [Lengner, C. J. *et al. Cell* 141, 872–883 (2010); Papp, B. & Plath, K. *Cell* 152, 1324–1343 (2013); O'Leary, T. *et al. Nat Biotechnol* 30, 278–282 (2012)]. Indeed, naive pluripotent cells captured in WIS-NHSM uniformly maintain a pre-inactivated X chromosome as evident by nearly complete lack of H3K27me3 nuclear foci and down regulation of XIST expression (Figures 68I-K and Figures 76A-B). The majority of primed/conventional hESCs and hiPSCs demonstrate X inactivation as evident by the presence of H3K27me3 nuclear foci, methylation of one of the XIST gene alleles and very high transcription of XIST transcript consistent with initiation of

X chromosome inactivation (Figures 68I-K and 76A-B). Consistently, genome wide mapping of H3K9me3 by Chromatin Immuno-precipitation followed by deep sequencing (ChIP-Seq) in female and male naive and primed human pluripotent cells, indicated a significant increase ($p < 2.1^{-10}$) in this mark in female cell lines on X chromosome, but not on autosomal chromosome 1, and only in female primed pluripotent cells (Figure 76C). Importantly, as observed in human ICM cells, XIST is transcribed at low levels in human naive pluripotency, even in male cell lines (Figure 76B). XIST promoter alleles are entirely demethylated in male and female naive ESCs (Figure 23A). Upon EB differentiation of female naive hESCs/hiPSCs, inactivation of one of the X chromosomes alleles becomes evident and the cells demonstrate H3K27me3 clouds, upregulation of XIST transcription simultaneously with methylation of one of the XIST promoter regions (Figures 68I-K, Figures 76B and Figures 23A). Collectively, these results indicate that hESCs/hiPSCs expanded in WIS-NHSM uniformly maintain a unique pre-X inactivation state akin to that described in human and primate ICMs [Okamoto, I. *et al.* Nature. 2011, 472(7343):370-4; Masterson, KR., et al. Dev Biol. 2012, 371(2):146-55], and can adequately initiate X chromosome inactivation upon differentiation.

EXAMPLE 8

TRANSCRIPTIONAL AND CHROMATIN STATE OF HUMAN NAIVE PLURIPOTENCY

The present inventors compared global gene expression patterns between naive and primed hESCs and hiPSCs, many of which were genetically matched. Unbiased clustering of genome-wide expression profiles demonstrated that naive hESC and hiPSCs possess a distinct gene expression pattern and clustered separately from conventional/primed hESCs and hiPSCs (Figure 69A and Figures 24A). Gene expression analysis indicated that while OCT4 and KLF4 were similarly transcribed in naive and primed cells, other transcripts associated with naive pluripotency were significantly upregulated in naive cells. The later included NANOG and DUSP family member genes, that has been shown to maintain ERK de-phosphorylation in rodent naive ESCs (Figures 77A-B) [Chappell, J., et al. *Genes Dev.* 27, 725–733 (2013)]. Importantly, naive pluripotent cells had profoundly down regulated transcripts

associated with lineage commitment genes including ZIC1, SOX6 and SOX11 that are expressed at low, but appreciable, levels in primed hESCs (Figures 77A-B). Functional annotation analysis of differentially expressed genes with Gene Ontology (GO) revealed that genes down regulated genes in naive pluripotency were significantly enriched for GO terms linked to developmental processes, particularly ectoderm and neural germ cell specification (Figure 69A, and Figure 78). Furthermore, hierarchical clustering and Principal Component Analysis (PCA) showed that human ICM samples are transcriptionally more similar to Naïve hESCs, than to primed cells (Figures 69H-I). Nearly all of these terms were also found to be significantly down regulated in mouse naive pluripotent cells, in comparison to mEpiSCs (Figure 69A), and are consistent with transcriptional changes associate with pluripotency priming reported in mice [Marks, H. *et al.* The transcriptional and epigenomic foundations of ground state pluripotency. *Cell* 149, 590–604 (2012)]. Furthermore, while ICM cells are known to undergo major transcriptional changes after in vitro derivation [Chu, L.-F., et al. *Curr. Biol.* 21, 1759–1765 (2011)], hierarchical clustering and Principal Component Analysis (PCA) showed that human ICM samples transcriptionally cluster closer to Naive hESCs, than to primed cells (Figure 79). Analogous to expression pattern differences between mouse naive and primed stem cells, primed hESCs demonstrate intermediate expression levels of MHC class I antigen in comparison to somatic cells, while naive hESC/hiPSC express trace levels of MHC class I surface antigen (Figures 24B-C). Moreover, while E-CADHERIN is expressed in primed hESCs, the surface expression pattern becomes more prominent and evenly distributed on the cell surface membrane of naive hESC colonies (Figures 81A-D). The present inventors next conducted an unbiased cross-species hierarchical clustering of globally measured transcriptome to evaluate whether the human primed/conventional and naive pluripotent cells described herein globally correspond to those established in mice (Hanna, J. *et al. Proc. Natl. Acad. Sci. U.S.A.* 107, 9222–9227, 2010). Using a previously established method for cross-species gene expression analysis on all 9,803 mouse-human orthologous genes found in our gene expression datasets (Hanna, J. et al. Proc. Natl. Acad. Sci. U.S.A. 107, 9222–9227, 2010; Hanna, J. et al. Cell Stem Cell 4, 513–524 (2009)], the present inventors found that while primed/conventional hESCs and hiPSC clustered with mEpiSCs, all naive hESCs/hiPSCs clustered with mESCs and miPSCs independent of the genetic

background or naive growth conditions used (Figures 69B and 82A). Further, primed mouse and human pluripotent cells expression patterns were significantly more heterogeneous in comparison to naive counterparts, as reflected by the noise distribution of the two groups in both species (Figures 69C-D). The latter conclusions are consistent with findings reported in serum primed mESCs [Marks, H. *et al. Cell* 149, 590–604 (2012)] and apply when looking at transcriptional heterogeneity of previously highlighted [Oakley, D. H., *Cell* 144, 439–452 (2011)] markers know to highly vary between human iPSCs/ESCs (Figure 82B). Finally, nuclear localization of the transcription factor TFE3 was recently shown to be enhanced in naive mESCs, and compromised upon pluripotency priming [Betschinger, J. *et al. Cell* 153, 335–347 (2013)]. Remarkably, a similar nuclear enrichment pattern for TFE3 was evident in naive hESCs, and relative enrichment was compromised in primed/conventional hESCs (Figures 69E, 69F and 69G, and Figures 80A-D). Collectively, these data demonstrates that WIS-NHSM endows human pluripotent cells with defining features of pluripotency gene expression patterns typically seen in ground state naive mESCs [Marks, H. *et al. Cell* 149, 590–604 (2012)].

The present inventors next tested whether a difference between human naive and primed cells is also apparent at the chromatin level, as priming of murine naive ESCs induced by 2i withdrawal and providing serum is associated with accumulation of H3K27me3 mark and formation of bivalent domains (gene promoter marked by H3K27me3 and H3K4me3) on developmental regulatory genes [Marks, H. *et al. Cell* 149, 590–604 (2012)]. The present inventors mapped H3K4me3 and H3K27me3 chromatin marks by using ChIP-Seq in mouse and human naive ESCs and primed EpiSCs (both expanded in serum free conditions). Indeed, while distribution of both epigenetic markers over all genes showed a significant ($p<2e^{-37}$) decrease in H3K27me3 (Figures 83A-D), an even more dramatic decrease of both marks in developmental genes was observed in mESCs in 2i/LIF conditions in comparison to mEpiSCs ($p<2.5e^{-50}$, Figure 70B). Remarkably, while total levels of H3K27me3 were not altered, there was a dramatic ($p<8.6e^{-61}$) redistribution and reduction of H3K27me3 in promoter and gene body region over developmental genes (n=5922) in human naive cells compared to primed (Figures 70A-B and 70E-F), equivalent to that observed in rodent cells. Notably, together with the reduction of H3K27me3 in naive cells, there is a mild ($p<1.4e^{-9}$)

reduction of H3K4me3 in the promoters of developmental genes in naive cells (Figures 70A-B). The reduction of H3K27me3 mark to nearly background levels in human naive cells is also reflected in the number of bivalent genes, which is more than 13-fold higher in primed (3013) compared to naive cells (226). Pluripotent genes (e.g. OCT4, SOX2, SALL4) showed consistent active chromatin in both naive and primed conditions in human and mouse, while TBX3 pluripotency regulator acquired repressive H3K27me3 marks in primed human and mouse samples (Figures 70C-D).

The present inventors tested whether the WIS-NHSM naive human conditions have an effect also in other genomic components such as enhancers. For this, the present inventors first measured the distribution of H3K27me3 in three genomic components: promoters, genes body and intergenic regions. Consistent with what was observed in mouse cells [Marks, H. *et al. Cell* 149, 590–604 (2012)], the present inventors found that in naive cell state, H3K27me3 peaks are depleted more from promoters and gene-bodies, than from intergenic regions (Figures 84A-B). The present inventors then globally mapped enhancers of class I and class II in the two-pluripotency states. Class I enhancers [Rada-Iglesias, A. *et al. Nature* 470, 279–283 (2011)] are characterized by the presence of H3K4me1 and H3K27ac, and the absence of H3K4me3 and H3K27me3 marks, and are associated with active expression of nearby genes. Class II enhancers on the other hand, are characterized by the presence of H3K4me1 and H3K27me3, and the absence of H3K27ac mark, and are associated with being poised for activation [Rada-Iglesias, A. *et al. Nature* 470, 279–283 (2011)]. Consistent with the reduction of lineage priming molecular features in naive pluripotency, the present inventors observed (Figures 84D-E) a major reduction in the annotated Class II enhancers in naive cell state, in both human (5.8-fold) and mouse (62.5-fold). Although Class II associated genes lose their H3K27me3 mark in naive state, they do not become more actively transcribed (Figures 84F-G) (as was observed previously in mouse [Marks, H. *et al. Cell* 149, 590–604 (2012)]. Collectively, these findings indicate the naive ground state of pluripotency largely lacks features associated with pre-marking of repressed developmental genes and rendering them poised for activation.

Rodent ground state naive pluripotency is associated with global DNA hypomethylation, while maintaining epigenetic imprinting signatures. This effect is mediated by 2i-mediated down regulation of de novo methyltransferase enzymes, and

maintaining expression of TET hydroxylases and Dnmt1 enzyme. Remarkably, human naive ESC sand IPSCs expanded in WIS-NHSM conditions demonstrated a dramatic down-regulation of DNMT3a, DNMT3b and DNMT3L methyl-transferase enzymes, but not of DNMT1 and TET1/2 enzymes (Figure 71D). The present inventors then analyzed human naive and primed pluripotent cells for global levels of 5-methylcytosine (5mC) by LC-MS) [Leitch, H. G. et al. Embryonic germ cells from mice and rats exhibit properties consistent with a generic pluripotent ground state. Development 137, 2279–2287 (2010); Meissner, A. et al. Genome-scale DNA methylation maps of pluripotent and differentiated cells. Nature 454, 766–770 (2008)]. A striking drop in global 5mC content was observed in under WIS-NHSM conditions, equivalent to those measured in naive mESC in 2i/LIF conditions or mouse ICM (Figure 71E). Collectively, these results highlight that human naive pluripotent cells captured herein, recapitulate defining epigenetic characteristics of rodent naive pluripotency: global reduction of DNA methylation and H3K27me3 modification on lineage commitment affiliated gene promoter and enhancers.

ICM-like pre-x inactivation state in naive human PSCs

The highly conserved distal and proximal enhancer regions of Oct4 genes are reciprocally regulated in the pre and post implantation mouse embryo, and thus the Oct4 distal enhancer is predominantly utilized in mouse naive ESCs (Hanna et al., 2010b). Primed and naive hESC/hiPSCs were transfected with a luciferase reporter construct under the control of either the human distal or the proximal enhancers sequences that control expression of the Oct4 gene (Figure 25A). Predominant utilization of the Oct4 distal enhancer was observed in rev-hESCs and human-iPSCs indicating that the gene expression program active in rev-hESCs favors utilization of the distal Oct4 enhancer as typically observed in mouse ESCs (Figure 25A). To further substantiate the latter findings, WIBR3 hESCs were targeted with Oct4-GFP-2A-PURO or deltaPE-Oct4-GFP-2A-PURO (Figures 25B-M). The complete Oct4 GFP reporter was specifically active in both naive and primed conditions (and lost upon differentiation). DeltaPE-Oct4-GFp-2A-PURO reporter was specifically active in naive, but not conventional/primed, pluripotent growth conditions (Figures 25B-M). Collectively these finding indicate that ESCs/iPSCs expanded in WIS-NHSM conditions carry a distinct molecular and epigenetic state.

Naive human iPSCs can contribute to mouse development in vivo - Human naive C2 iPSCs were constitutively labeled with GFP and BCL-2 overexpression vector. Cells were aggregated with developing mouse embryo morulas, and 24 hours GFP cells were viable in developing early mouse embryos (Figures. 26A-C). These results indicate that human naive cells grown in WIS-NHSM conditions can contribute to cross-species chimeric organisms.

EXAMPLE 9

FUNCTIONAL AND SIGNALING PROPERTIES OF HUMAN NAIVE PSCS

The above results indicate that while both human naive and primed growth conditions that contain bFGF and TGFβ cytokines, the supplementation of the naive conditions with 2i/LIF, p38 and JNK inhibitors reconfigures the molecular and epigenetic properties of human pluripotent cells. Thus, the present inventors next characterized the signaling dependence and response patterns of naive and primed human pluripotent cells to different signaling stimuli or inhibitors, in comparison to their rodent counterparts. The pluripotency of mESCs is stabilized upon inhibition of RAF-ERK1/2 pathway, while in hESCs and mEpiSCs (Hanna, J. *et al. Proc. Natl. Acad. Sci. U.S.A.* 107, 9222–9227, 2010), ERK and RAF inhibition with either one out of four different small molecules leads to their differentiation (Figures 21A-F, and Figures 15A-M). However, as similarly observed with naive mESCs, the stability of naive hESCs/iPSCs was dependent on the continuous presence of ERK1/2 inhibition (Figures 12S, 86A-C, 87A). Supplementation of TGFβ is necessary to inhibit the pro-neural differentiation effect of ERK inhibition in naive WIS-NHSM conditions (Figure 86B). When testing p38 and JNK pathways signaling requirements, primed hESCs and mEpiSC tend to differentiate upon inhibition of these pathways (Figures Fig 21A-D, 15A-M, and 86C). Murine ESCs maintain their naive pluripotent state identity as measure by ΔPE-Oct4-GFP expression and "all-ESC" mouse formation ability by tetraploid embryo complementation assay, upon inhibition of either one of p38, JNK or ERK pathways (Figures 88A-J and 89A-D). In human naive cells, simultaneous inhibition of these pathways is essentially required to maintain naive pluripotency, and their withdrawal resulted in differentiation and upregulation of lineage commitment

genes (Figures 21A-L, 15A-M, 86A-C, and 87A-B). Supplementation of TGFβ is necessary to inhibit the pro-neural differentiation effect of ERK inhibition in naive WIS-NHSM conditions. Naïve hESCs stably transfected with a dominant-negative Stat3 encoding transgenes rapidly differentiated and could not be maintained in vitro with WIS-NHSM conditions, while cells transgenic for a constitutively active Stat3 mutant (Stat3-CA) could be propagated *in vitro* in the absence of exogenous LIF (Figure 108B). These findings highlight that several signaling pathways distinctly regulate the two human pluripotent states, in a manner similar to that observed in mic e (Marks, H. et al. The transcriptional and epigenomic foundations of ground state pluripotency. Cell 149, 590–604 (2012); Hanna, J. et al. Human embryonic stem cells with biological and epigenetic characteristics similar to those of mouse ESCs. Proc. Natl. Acad. Sci. U.S.A. 107, 9222–9227 (2010)].

LIF/Stat3 signaling is an important pathway in promoting the rodent ground state of naive pluripotency, and in 2i/LIF conditions, mESCs are dependent on LIF signaling and readily differentiate when exposed to JAK inhibitor (JAKi) that blocks Stat3 phosphorylation (Figures 21A-D) [Niwa, H., et al. *Nature* 460, 118–122 (2009)]. Traditional hESCs maintained low levels of phosphorylated STAT3 (pSTAT3), which was increased in response to LIF addition, however the cells were resistant to addition of JAK1 inhibitor (Figures 15A-M and 90). Alternatively, naive hESCs/hiPSCs had high levels of pSTAT3 (Figures 15A-M) and differentiated upon pharmacological inhibition of JAK/STAT3, as similarly observed with mESCs (Figures 21A-D). Naive hESCs stably transfected with a dominant-negative Stat3 encoding transgenes rapidly differentiated and could not be maintained in vitro with WIS-NHSM conditions, while cells transgenic for a constitutively active Stat3 mutant (Stat3-CA) could be propagated *in vitro* in the absence of exogenous recombinant LIF and generated teratomas (Figure 71A, Figures 22G-L). Finally, BMP4 cytokine and Forskolin, a PKA agonist, led to differentiation of primed but not naive human or mouse pluripotent cells (Figures 21A-D, Figures 22A-F and Figures 91A-C), indicating that several pathways are differentially regulated between the two human pluripotent cell states in a similar manner to that observed between mESCs and mEpiSCs.

The present inventors next characterized functional difference between human

naive and primed pluripotent cells. Naive human pluripotent cells were reproducibly more amenable to gene targeting by homologous recombination with isogenic targeting vectors directed at the endogenous OCT4 and COL1A loci, in comparison to their genetically matched primed cells (Figures 71B, C). Further, given that naive pluripotency promoting conditions have been shown to be important for deterministic induction of pluripotency by OSKM upon Mbd3 depletion in mice, WIS-NHSM are analogously critical for obtaining near 100% naive ground state iPSC formation levels from Mbd3 depleted human fibroblasts following OSKM induction (Figure 71D). Consistent with global reduction of DNA methylation levels in naive human pluripotency conditions, iPSC from fragile X patient specific fibroblasts [Urbach, A., Bar-Nur, O., Daley, G. Q. & Benvenisty, N. Brief Report. Stem Cell 6, 407–411 (2010)] are able to undergo FMR1 gene reactivation and demethylation following reprogramming under naive, but not primed, pluripotency conditions (Figures 71E-G). Finally, consistent with robust E-cadherin expression and enhanced single cell survival, microinjection of human naive iPSCs into mouse morulas shows robust integration in mouse ICM at E3.5 (Figures 26D-K) and microinjection of human GFP labeled naïve iPSCs into mouse E2.5 morulas showed robust integration in mouse *in vitro* developed ICMs at E3.5, and higher than that of primed pluripotent cells (Figures 109A-C). The latter results (with respect to primed iPSCs in Figure 109B) are consistent with previously reported near absence of integration and chimerism following embryo micro-injection of primate primed ESCs (James, D., Noggle, S. A., Swigut, T. & Brivanlou, A. H. Contribution of human embryonic stem cells to mouse blastocysts. *Dev. Biol.* 295, 90–102 (2006); Tachibana, M., Sparman, M., Ramsey, C., Ma, H. & Lee, H. S. Generation of Chimeric Rhesus Monkeys. *Cell* 148, 285-295 (2012)]. Mouse blastocysts obtained after microinjection with human naïve iPSCs were implanted in pseudo-pregnant female mice and allowed to develop for 7 additional days *in vivo*, after which they were dissected and imaged *in toto* under confocal microscopy for GFP+ cell detection. Remarkably, the present inventors were able to obtain multiple mouse embryos (n=4), corresponding to E8.5-E10.5 developmental stages, that showed chimerism with naïve human iPSC derived GFP+ cells integrated at different locations, including craniofacial tissues and embryonic neural folds (Figure 108C; Figure 109D). In depth functional and developmental analysis of the *in vivo* integrating human naïve

iPSC derived cells is of great future scientific interest. Collectively, the above indicate that the altered biological features of human naive PSCs directly endows them with unique functional properties.

Notably however, naive human ESC/iPSCs generated herein are distinct from murine naive cells, in the way that they are still dependent on bFGF and TGF signaling, and inhibition of these pathways leads to their naive cells state loss and differentiation.

Collectively these findings indicate that the naive ground state of pluripotency requires a unique combination of growth factors and cytokines. Human cells are more stringent from mouse, thus they need simultaneous inhibition of different MAPK pathways (ERK and JNK and p38 simultaneous inhibition) together with LIF and WNT stimulation (by CHIR99021). Also, bFGF and TGF have diverged between mouse and humans, and in humans they are also essential to promote naive pluripotency and contribute to the unique molecular and epigenetic configuration of naive pluripotency described herein.

These findings substantiate the concept of naive ground state in human pluripotent cells, and indicate that its maintenance requires a unique combination of growth factors and cytokines. Human pluripotent cells are more stringent relative to their mouse counterparts, as they need simultaneous inhibition of different MAPK pathways (ERK, JNK and P38 MAPK simultaneous inhibition) together with LIF and WNT stimulation (by CHIR99021). FGF2 and TGFβ signaling are divergent between mice and humans [Greber, B. et al. Cell Stem Cell 6, 215–226 (2010); Roode, M. et al. Dev. Biol. 361, 358–363 (2012)], as in humans they are also essential to promote naive pluripotency and contribute to the unique molecular and epigenetic configuration of naive pluripotency described herein. These results suggest that epigenetic priming of human pluripotent cells is predominantly caused by withdrawal of LIF and inhibitors of MAPK signaling [Pribluda, A. & Hanna, J. H. Nat Biotechnol 30, 247–249 (2012)]. These findings are consistent with the notion that different genetic backgrounds assume distinct states of pluripotency *in vitro*, the stability of which is regulated by endogenous genetic determinants and can be modified by defined exogenous factors that support the naive ground state of pluripotency. The stringency in requirement for these factors appears to be different among distinct species, as exemplified by the requirement for simultaneous inhibition of multiple MAPK kinase pathways in human naive cells

[Hanna, J. et al. Cell Stem Cell 4, 513–524 (2009); Hanna, J. H., et al., Cell 143, 508–525 (2010); Hanna, J. et al. Proc. Natl. Acad. Sci. U.S.A. 107, 9222–9227, 2010]. It would be of interest to explore whether the naive ground state of pluripotency in humans could be captured merely by signaling pathway inhibition [Ying, Q.-L. *et al. Nature* 453, 519–523 (2008)]. The epigenetic changes induced by naive pluripotency conditions indicate that naive conditions might influence previously described phenotypes of epigenetic memory and aberrant reprogramming in human iPSCs.

Without being bound by any theory, these data do not claim that naive and primed pluripotent states are identical between humans and mice, and in fact differences may still exist between naive mESCs and the naive human pluripotent cells described in this work. Without being bound by any theory, the present inventors cannot exclude that alternative growth conditions may be devised to capture human naive pluripotent cells with features similar to those described herein, or that WIS-NHSM conditions might be modified for improving the extent of naive features in human pluripotent cells. Further molecular characterization of human ICM cells will help improve and understand the relevance of naive pluripotency *in vitro* characteristics described herein [Smith, Z. D. et al. Nature 484, 339–344 (2012); Okamoto, I. et al. Nature. 2011, 472(7343):370-4; Niakan KK, et al. Dev. Biol. 375, 54–64 (2013)]. Finally, defining a novel naive pluripotent state in humans that is stable and does not require any genetic modifications might be relevant for the molecular study of early lineage commitment *in vitro,* and for expanding the capabilities for utilizing hESCs and hiPSCs in regenerative medicine research and disease modeling in vitro and *in vivo* [Dimos JT, et al. Science 321, 1218–1221 (2008); Sandoe, J. et al. Nature Publishing Group 16, 780–789 (2013)].

The results described herein demonstrate that naive hESC/iPSCs grown in WIS-NHSM are distinct from previously isolated hESCs/hiPSCs and extensively recapitulate growth characteristics, signaling dependence, epigenetic and transcriptional properties that define naive mouse ESCs, rather than the mouse post-implantation epiblast and EpiSCs. Further, they capture molecular features of human ICM that are not present in rodent/mouse ICM. These findings supports the notion that different genetic backgrounds assume distinct states of pluripotency *in vitro*, the stability of which is regulated by endogenous genetic determinants and can be modified by defined

exogenous factors that support the naive pluripotent state. The threshold and requirement for these factors is different among different species where in the "permissive" 129 mouse strain LIF/Stat3 signaling can stabilize mouse ESCs, while on the NOD genetic background promotion of Wnt signaling and inhibition of ERK1 or providing small molecules that promote Klf2/4 expression (KP or FK) stabilize NOD ESCs. The human genetic background seems to be further non-permissive, as it required modulation of additional signaling pathways to stabilize the naive state *in vitro*. Evolutionary divergence has contributed to the findings that in humans, and possibly other species, as bFGF and TGF signaling contribute to human naive pluripotency maintenance. Finally, defining a novel naive pluripotent state in humans that is indefinitely stable and does not require any genetic modifications might be relevant for the molecular study of early lineage commitment *in vitro* and for expanding the capabilities for utilizing human ESCs and iPSCs in regenerative medicine research and disease modeling *in vitro* and *in vivo*.

Framing these challenges by WIS-NHSM conditions and/or Mbd3 inhibition, may prove to be key not only for understanding early human development, but also for dissecting the core-transcriptional circuitry in human naive pluripotent cells in the absence of exogenous transgenes, as it allows more authentic analysis of this state. Most importantly, Human primed ESCs display great level of heterogeneity in gene expression, including differential expression of lineage commitment genes and X chromosome activation status. Moreover, substantial differences among cell lines in gene expression are not evident in the undifferentiated state but appear when cells differentiate in same growth conditions. Careful comparative analysis for directed differentiation into specific lineages uncovered dramatic heterogeneity that was evident by marked differences in differentiation propensity among human embryonic stem cell line. It is possible that this properties are direct result of the cells used correspond to EpiSC stage, where the cells become highly sensitive to exogenous differentiating cues and initiate lineage commitment. Naive human ESCs/iPSCs are homogenous functionally and molecularly when expanded in WIS-NHSM conditions. Without being bound by any theory is seems that the naive pluripotent cells are inherently resistant to differentiation signals by the presence that promote naive pluripotency, and thus may prove to display reduced heterogeneity upon differentiation.

In addition to heterogeneity in differentiation propensity, naive human pluripotent state might facilitate adaptation of differentiation protocols that have only been successful with naive mouse ESCs. A prominent example is the generation of engraftment competent hematopoietic progenitors with mouse ESC capable of long-term *in vivo* re-population and secondary engraftment, while the success with conventional human ESC has been rudimentary. It remains to be seen whether human naive pluripotent cells will be more useful and more efficient in generating Disease-Relevant Phenotypes with Human-Animal Chimeras (as shown here in Figures. 26A-C). Lastly, achieving homologous recombination has been highly inefficient in primed/conventional human embryonic stem cells. The use of zinc finger exo-nuclease has been very successful however this method is complex, expensive, and could introduce non-specific genetic alterations in the manipulated cells that are hard to identify. Comparative analysis for susceptibility to homologous recombination between WIS-NHSM naive and primed pluripotent states in mice and humans might provide conclusive answer to whether the naive cells are significantly more amenable to homologous recombination.

EXAMPLE 10

P66 ALPHA COILED-COIL DOMAIN AS A DOMINANT NEGATIVE INHIBITOR OF MBD3/NURD AND AS A FACILITATOR FOR DETERMINISTIC IPSC REPROGRAMMING

Following the studies described hereinabove concerning the effect of Mbd3 upon the reprogramming process, the present inventors aimed to screen for an Mbd3 inhibitor, in order to neutralize the function of the MBD3\NuRD complex.

Since the inhibitory effect of Mbd3 is probably mediated by the recruitment of the NuRD complex, one of the approaches that were taken by the present inventors was to try and prevent the binding of MBD3 to the complex.

Gnanapragasam et al. (Gnanapragasam et al. 2011. "*p66α-MBD2 coiled-coil interaction and recruitment of Mi-2 are critical for globin gene silencing by the MBD2-NuRD complex*". Proc. Natl. Acad. Sci. 108:7487-7492) describe a unique coiled-coil interaction between MBD2 and p66α, another component of the NuRD complex, mediated by two coiled-coil regions in these proteins.

The MBD2 coiled coil region is highly conserved between the MBD2 homologs (including MBD3), and interspecies.

Gnanapragasam et al. 2011 (Supra) show that overexpression of p66α coiled-coil region competes with the wild type p66α, and inhibits the binding of MBD2 to Mi-2(α or β). Moreover, they show that the p66α-CC also binds to MBD3 in the same region, and creates a similar structure [Nuclear magnetic resonance (NMR) structure of MBD2 binding to the p66α-CC is found under the Protein Data Bank (PDB) ID – 2L2L; An Information Portal to Biological Macromolecular Structures]. This interaction between the p66α-CC and the MBD2 inhibits the ability of MBD2 to repress its downstream target gene expression, probably mediated through the binding to CHD4 (chromodomain helicase DNA binding protein 4).

Another paper that was recently published by Walavalkar et al. (Walavalkar et el. 2013. "*Unique features of the anti-parallel, heterodimeric coiled-coil interaction between methyl-cytosine-binding domain 2 (MBD2) homologues and GATA zinc finger domain containing 2A (GATAD2A\P66α)*". J. Biol. Chem. 288: 3419-3427) shows that the p66α coiled-coil domain interacts with Mbd3, mbd3l1, mbd3l2 in different efficiency; MBD2 and MBD3 binds approximately in the same efficiency to p66α. Therefore, without being bound by any theory, the present inventors envisage that the p66α coiled-coil domain can interfere with the NuRD complex assembly, and inhibit the recruitment of Chd4, a critical component.

As mentioned, p66α is a component of the NuRD complex. It has been shown that P66α null (loss of function) mice die during early development (day 10), and that p66 is not required for blastocyst formation (Marino et al. 2007. "*Mutants in the mouse NuRD/Mi2 component p66 are embryonic lethal*". PLoS ONE 2(6): e519. doi:10.1371/journal.pone.0000519).

As a proof of concept the present inventors cloned p66α coiled-coil domain into the pCAG-HA vector, in order to check its effect upon the NuRD complex assembly.

The present inventors overexpressed MBD3-WT (SEQ ID NO: 112) and the HA-tagged p66α-CC in 293T cells, and further show in a co-immunoprecipitation for anti-Mbd3 pulldown, that the presence of p66α inhibits MBD3 binding and recruitment to CHD4 (Figure 93).

In addition, Figures 92A-C show that knockdown of Mbd3 or Chd4 increases the efficiency of reprogramming efficiency of MEFs (Figures 92A-D).

Following are the MBD3 and CHD4 siRNAs used by the present inventors:

For mouse:

Mbd3 Stealth siRNA mix that includes MSS-237238, MSS-275658 andMSS-275659 components (Invitrogen);

Chd4 Stealth siRNA mix that includes MSS-200894, MSS-200895 and MSS-200896 (Invitrogen), were used for efficient knockdown in mouse cells.

For human:

MBD3 Stealth siRNAs that include HSS147580 and HSS147581 components (catalogue number 1299003) were used for efficient MBD3 knockdown in human cells.

Human CHD4 stealth siRNA - Life technologies HSS101850 was used to efficiently knockdown CHD4 in human.

Since the present inventors have proved in previous experiments that MBD3 inhibitory effect is probably mediated mainly by Chd4, without being bound by any theory it is assumed that a peptide which can inhibit Chd4 binding to Mbd3 can serve as a potent inhibitor to MBD3.

Further biochemical investigation of MBD3 loss of function as a result of P66aCC over expression (examining the interactions with the OSKM and the NuRD complex other members Mta2, Hdac1, 2) are ongoing. The coding sequence of the P66 alpha coiled-coil domain was amplified using the primers depicted in SEQ ID NOs: 115 and 116. The resulting P66 alpha coiled-coil domain coding sequence is set forth in SEQ ID NO: 113, and the encoded P66 alpha coiled-coil domain amino acid sequence is set forth in SEQ ID NO: 114. The P66 alpha coiled-coil domain (SEQ ID NO:114) can be used as an inhibitor of MBD3.

Functional assays, including reprogramming (following chip-seq with and without p66aCC treatment) are ongoing.

Deep structural analysis of the predicted NMR in order to find or design compounds which can bind this region of MBD3 is ongoing.

Synthesizing a peptide of the p66alpha CC region (with TAT-NLS- signal) for functional test is ongoing.

EXAMPLE 11

IPSC REPROGRAMMING FROM HUMAN ADULT SOMATIC CELLS VIA OKSM AND ERAS OVER EXPRESSION, TOGETHER WITH MBD3 DEPLETION

Human BJ fibroblasts were infected with TRIPZ MBD3 shRNA lentiviruses (3.1, 3.2, 3.3 indicate three different hairpin constructs targeting MBD3). Real time PCR expression for MBD3 was conducted after 72 hours with or without DOX induction. The results presented in Figure 99A validate down-regulation of MBD3 in human fibroblasts in a DOX dependent manner. ShRNA hairpin numbers 1 and 3 were used for further analysis as a combination.

Human primary fibroblast cell lines #13 and 14# (obtained from adult healthy dermal biopsy) were infected with lentiviruses encoding OKSM, RtTa, ERAS (SEQ ID NO:109) (for overexpression of OKSM, RtTa, and ERAS) and with a lentivirus encoding MBD3 shRNAs (for downregulation of MBD3).

RtTa (also known as M2rtTA) is the element that allows responding to Doxyccycline. Any DOX inducible system requires introducing RtTA element, so the present inventors used a Lentiviral plasmid expressing the reverse tetracycline transactivator (M2rtTA) [vector from addgene, Catalogue Number: 20342; SEQ ID NO:110).

The following DOX inducible MBD3 knockdown lentiviral clones were used: TRIPZ Human MBD3 shRNA Clone ID: V3THS_392206 (#1) and V3THS_392210 (#3) – Thermo Scientific). Clonal populations with ES-like morphology appeared 6-10 days after DOX induction (Figures 99B-C). Red fluorescent protein (RFP) fluorescence is driven by TetO promoter (DOX responsive) of the TRIPZ-MBD3 shRNA constructs. More examples of colonies observed at day 5 or 11 are shown in Figures 99D-G.

Figures 100A-I show staining for OCT4 and SSEA4 pluripotency markers on cells reprogramming in NHSM conditions following 10 days of OKSM, RtTa, ERAS and MBD3 shRNA DOX induction. It is noted that the MBD3-shRNA induction reporter (ShMBD3 vector activity marked by red fluorescence reporter activation that is also encoded on the TRIPZ-MBD3 vector under DOX inducible TetO promoter, Figure 100I) co-localizes with OCT4 expression and SSEA4 pluripotency markers.

Figures 100J-N show staining for OCT4 and TRA1-60 staining pluripotency markers on cells reprogramming in NHSM conditions following 10 days of OKSM,

RtTa, ERAS and MBD3 shRNA DOX induction. It is noted that the MBD3-shRNA induction reporter (ShMBD3, Figure 100I) co-localizes with OCT4 expression and TRA1-60 pluripotency markers.

Figures 100O-S show staining for OCT4 and TRA1-81 staining pluripotency markers on cells reprogramming in NHSM conditions following 10 days of OKSM, RtTa, ERAS and MBD3 shRNA DOX induction. It is noted that the MBD3-shRNA induction reporter (ShMBD3, Figure 100I) co-localizes with OCT4 expression and TRA1-81 pluripotency markers.

Primary females adult dermal fibroblast cells (line #13) were transduced with RtTa, OSKM and ERAS vectors in WIS-NHSM conditions, with or without TRIPZ-MBD3 shRNAs 1+3 mix (to knockdown human MBD3). iPSC colony numbers were counted at day 10 by staining for NANOG and TRA1-60 markers (Figure 100T). Note the dramatic increase in iPSC formation from primary human somatic cells when MBD3 inhibition is introduced.

EXAMPLE 12

HUMAN NAIVE IPSCS AND ESCS CAN DIFFERENTIATE INTO PRIMORDIAL GERM CELLS PRECURSORS

Primordial germ cell (PGC)-like cells (PGCLC) derived from human naive iPSCs/ESCs can be injected in human/primate or mouse testis and give rise to functional sperm. Alternatively, they may be used for oocyte generation.

Materials and media:

N2-KSR medium - 250 ml Neurobasal medium (Invitrogen - #21103-049), 250 ml DMEM-F12, N2 supplement (Invitrogen, #17502-048), 1% KSR (knockout serum replacement, Invitrogen, # 10828028) medium] with 8 ng/ml bFGF (Peprotech), 1 ng/ml TGF-β1 (Peprotech) and ROCKi (10 μM).

PGC medium is comprised of GMEM (Invitrogen, # 21710082), 15% KSR, 1% NNEA (Biological industries, 01-340-1B), Penicillin-Streptomycin, 1 mM L-Glutamine, 5 μM ROCKi (Y-27632, Axon Medchem) and the following cytokines: 500 ng/ml BMP4 (bone morphogenetic protein 4; R&D Systems Inc.), 20 ng/ml LIF (leukemia inhibitory factor; PeproTech), 100 ng/ml SCF (Stem Cell Factor; PeproTech), 50 ng/ml EGF (Epidermal Growth Factor; Peprotech).

Experimental Methods:

Generation of mCherry knock in reporter allele in NANOS3 locus – In order to create mCherry reporter expression driven by endogenous human NANOS3 locus, the present inventors have chosen to knock in p2a-mCherry coding sequence in frame with the last exon of the NANOS3 gene. The present inventors have generated plasmids encoding TALEN molecules specific to the region covering NANOS3 stop codon. TALEN constructs were generated using GoldenGate TALEN kit2.0 (addgene cat#1000000024).

Targeting construct for 2A-mCherry knock in was designed as shown in Figure 94A. WIS1 naive human ESCs (carrying also deltaPE-OCT4-GFP reporter) were electroporated with pair of TALEN coding plasmids and donor targeting construct. After selection with G418 (150 μg/ml) and ganciclovir (2 μM), the present inventors used PCR to analyze 96 of surviving individual clones. One of the correctly targeted clones (based on PCR and Southern Blot analysis) was transfected with a plasmid encoding flippase enzyme with subsequent subcloning. Neo cassette deletion was confirmed by PCR. In addition to this the whole targeted locus was sequenced, and karyotype analysis was performed for one of correctly targeted clones. Both sequencing and karyotyping did not revealed any abnormalities, and thus the cells were used for further functional validation.

Inducement of epiblast state - Naive human ESCs, either genetically modified cells with the NANOS3-mCherry construct or unmodified cells, were grown on irradiated mouse embryonic fibroblasts (MEFs) or 0.2% Gelatin or vitronectin\gelatin coated plates, in WIS-NHSM medium supplemented with 5 μM ROCKi (Y-27632, Axon Medchem). The cells were trypsinized with 0.05% Trypsin + EDTA, and 50,000 cells/ 6-well were plated on 1 ng/ml Fibronectin (F1141, Sigma) covered plates in N2-KSR medium, which induces epiblast like (EpiLC) state.

After two days in the N2-KSR medium the EpiLC cells were trypsinized and moved to low-cell-binding 96-well plates (145399, NUNC), at a density of 2500 cells/well, in 120 μl PGC medium.

Fifty microliters (50 μl) of fresh PGC medium were added to each well after two days. Four or six days after the cells were moved to the PGC medium, they were

separated using TripLE select (10x) (Invitrogen) for flow-cytometry or molecular analysis.

Experimental Results

Generation of mCherry knock in reporter allele in Nanos3 locus - As shown in Figures 94A-B, human naive cells (WIS1) were targeted to a genetic engineering process via the TALENs in order to prepare cells in which expression of NANOS3 is visible by expression of the reporter gene mCherry. NANOS3 is a gene specifically expressed in PGCs already from early stages of their development (Julaton et al. Hum Mol Genet. 2011 Jun 1;20(11):2238-50.)

Naive ESCs were induced to the epiblasts state by plating the cells on fibronectin covered plates and incubation in the presence of N2-KSR medium for 2 days. Following, the cells were removed by trypsinization from the plates and were transferred to low-cell binding plates in the presence of the PGC medium. Four to six days later, the cells were separated from the plates using TripLE select agent and were subjected to flow cytometry and molecular analysis. Figure 95 shows representative images of the cells during the differentiation process.

BMP4 induces expression of NANOS3-mCherry reporter gene - Cells that were subjected to the differentiation process described herein, using the N2-KSR and PGC media were examined by FACS for the expression of the NANOS3-mCherry reporter gene which indicates that the cells are in the PGC-like state. Thus, as shown in Figures 96A and 96B, while naive ESCs (Figure 96BA) and primed EpiLC (Figure 96C) cells did not express the NANOS3-mCherry reporter, following 4 days in the PGC medium (after being for 2 days in the N2-KSR medium), and in the presence of BMP4 in the PGC medium, a significant fraction of the cells expressed the mCherry reporter gene, indicating expression of NANOS3 (17.7%; Figure 96E). On the other hand, under the same conditions but without the BMP4 in the PGC medium, only minimal expression of mCherry reporter was seen (0.45% of the cells; Figure 96H), suggesting that BMP4 is important for differentiation of the human naive cells into PGC-like cells (PGCLCs).

Evaluation of PGC markers in the PGCLC cells induced from the naive ESCs demonstrates generation of PGC from naive pluripotent stem cells – The PGCLC cells generated by the method described herein were further evaluated for expression of PGC makers. Thus, as shown in Figures 97A-H, PGCLC markers are induced in protocol

applied on human naive ESCs, including STELLA (Figure 97D), INTEGRINB3 (Figure 97G), BLIMP1 (Figure 97B) and VASA (Figure 97H).

Primed ESCs, that were genetically modified with the NANOS3-mCherry knock in vector, were subjected to the same differentiation protocol described herein. However, they failed to form PGCLC. Thus, as shown in Figures 98A-B, FACS analyses of conventional/primed human ESCs that were subjected to either incubation in the PGC medium alone (Figure 98A) or in the EpiLC medium followed by the PGC medium (Figure 98B) did not result in expression of the NANOS3-mCherry reporter gene, thus demonstrating lack of differentiation into the primordial germ cells. These results show that conventional/primed human ESCs subjected to BMP4 including PGCLC induction protocol do not successfully turn on NANOS3 mCherry reporter.

Further FACS analyses (Figures 106A-D) show that NANOS3 mcherry+ cells specifically upregulate CD61 surface marker (IntergrinB3). The NANOS3-mCherry+ cells also express SSEA4 surface markers (Figures 107A-B). This analysis indicates that CD61+ cells marker or CD61+/SSEA4+ cell surface combination can be used to sort out and isolate human PGCLCs derived from human naive pluripotent cells (without the need for NANOs3 knockin reporter genetic engineering). Results indicate the importance of using human naive pluripotent cells as a starting material for human PGCLC induction.

EXAMPLE 13

INHIBITION OF PROTEIN KINASE C RESUTLS IN REDUCED MBD3 PROTEIN LEVLES OF EMBRYONIC STEM CELLS

The present inventors tested various factors, small molecules and agents for the ability to reduce MBD3 protein expression levels in embryonic stem cells.

V6.5 mouse ES cells were expanded for 4 days in various conditions in order to identify combination of factors which result in reduced MBD3 protein levels. As shown in Figures 101A-B, while treatment with the "2i/LIF" conditions with or without DMSO, or addition of a TGFβ inhibitor did not affect MBD3 levels, the use of the "2i/LIF" conditions with a PKC inhibitor resulted in a significant reduction in MBD3 protein levels. The results show that inhibition of PKC leads to down regulation in MBD3 expression in mouse embryonic stem cells. These results suggest the use of PKC

inhibitors as agents which deplete or downregulate MBD3 expression and as boosters of deterministic iPSC reprogramming.

EXAMPLE 14

ADJUSTMENT OF THE WIS-NHSM MEDIA

The present inventors have devised various modifications of the basic WIS-NHSM medium in order to test the effect of inhibitors and growth factors on naive pluripotent stem cells. Table 3 hereinbelow and Figures 102-105 describe the effect of various factors and inhibitors on maintenance of naive pluripotent state.

Table 3
WIS-NHSM media

Condition No. / agents	***1***	***2***	***3***	***4***	***5***	***6***
LIF	20 ng/ml	20 ng/ml	20 ng/ml	20 ng/ml	20 ng/ml	20 ng/ml
ERK1/2i (PD0325901)	1 μM	1 μM	1μM	1 μM	1 μM	1 μM
GSK3βi (CHIR99021)	3 μM	3 μM	3 μM	3 μM	3 μM	3 μM
JNKi (SP600125)	5 μM	5 μM	5 μM	5 μM	5 μM	5 μM
P38i (BIRB796)	2 μM	2 μM	2 μM	2 μM	2 μM	-
FGF2	16 ng/ml	16 ng/ml	16 ng/ml	16 ng/ml	16 ng/ml	16 ng/ml
TGFβ1	2 ng/ml	2 ng/ml	2 ng/ml	2 ng/ml	2 ng/ml	2 ng/ml
ROCKi (Y27632)	5 μM	5 μM	5 μM	5 μM	5 μM	5 μM
IGFII	-	20 ng/ml	20 ng/ml	20 ng/ml	-	-
SCF	-	-	10 ng/ml	10 ng/ml	-	-
BMPi (LDN-193189)	-	-	-	0.5 μM	0.5 μM	0.5 μM

Table 3: Provided are the agents (factors, inhibitors) included in various modifications of the basic WIS-NHSM medium. LIF – leukemia inhibitory factor; FGF2 = fibroblast growth factor 2 (also termed "basic FGF"); TGFβ1 = transforming growth factor beta 1; SCF = stem cell factor; BMPi = bone morphogenetic protein inhibitor; IGFII = insulin-like growth factor 2 (somatomedin A). Note that condition No. 6 is devoid of the p38i.

Figures 102-105 show the effect of the various modifications of the WIS-NHSM media on methylation of DNA (% of total methylated cytosine levels (5 mdC) normalized to dG; Figure 102), relative DNMT3L mRNA expression (normalized to

primed cells; Figure 103), relative DNMT3B mRNA expression (normalized to primed cells; Figure 104), and percentage (%) of $OCT4^+$ WIBR3 cells after 9 passages on 0.2% gelatin plates (Figure 105). These experiments show that inclusion of p38i is essential to maintain naive pluripotency features associated with downregulation of de novo DNA methyltransferase genes DNMT3b and DNMT3L and leads to loss in global DNA methylation levels. Omission of p38i and addition of BMPi instead (combination 6, Table 3 above), did not result in such effect which is the hallmark of human naive pluripotency. BMPi can be added together with p38i, and does not compromise naive pluripotency when used in combination (combinations 4 or 5, Table 3 above).

Similarly, Tables 4 and 5 below and Figures 85A-C show the effect of the various compositions of the medium on the naive state of pluripotent stem cells. WIBR3 hESCs were cultured in the WIS-NHSM conditions 1 and 7-17 and the cells were tested for percentage of pluripotent stem cells (by OCT4 positive cells; Figure 85B) and percentage of total methylated cytosine (5mdC; Figure 85C).

Table 4
WIS-NHSM media (Conditions 1 and 7-11)

Condition No. / agents	***1***	***7***	***8***	***9***	***10***	***11***
LIF	20 ng/ml	20 ng/ml	20 ng/ml	20 ng/ml	20 ng/ml	20 ng/ml
ERK1/2i (PD0325901)	1 μM	1 μM	1 μM	1 μM	1 μM	1 μM
GSK3βi (CHIR99021)	3 μM	3 μM	3 μM	3 μM	3 μM	3 μM
JNKi (SP600125)	5 μM	5 μM	5 μM	5 μM	5 μM	5 μM
P38i (BIRB796)	2 μM	2 μM	2 μM	2 μM	2 μM	2
FGF2	16 ng/ml	16 ng/ml	16 ng/ml	16 ng/ml	16 ng/ml	16 ng/ml
TGFβ1	2 ng/ml	2 ng/ml	2 ng/ml	2 ng/ml	2 ng/ml	2 ng/ml
ROCKi (Y27632)	5 μM	5 μM	5 μM	5 μM	5 μM	5 μM
IGFII	-	-	-	-	20 ng/ml	-
SCF	-	-	-	-	-	-
BMPi (LDN-193189)	-	0.5 μM	-	0.5 μM	0.5 μM	0.5 μM
NOTCHi (DBZ)	-	-	2 μM	2 μM	2 μM	2 μM
SHHi (RU-SKI-43)	-	-	-	-	-	5 μM

Table 4: Provided are the agents (factors, inhibitors) included in the WIS-NHSM medium. LIF – leukemia inhibitory factor; FGF2 = fibroblast growth factor 2 (also termed "basic FGF"; TGFβ1 = transforming growth factor bet 1; SCF = stem cell factor; BMPi = bone morphogenetic protein inhibitor; IGFII = insulin-like growth factor 2 (somatomedin A). NOTCHi = NOTCH inhibitor; SHHi = Sonic Hedgehog pathway (SHH) inhibitor; TGFRi = transforming growth factor receptor inhibitor; FGFRi = fibroblast growth factor receptor inhibitor.

Table 5
WIS-NHSM media (Conditions 12-17)

Condition No. / agents	***12***	***13***	***14***	***15***	***16***	***17***
LIF	20 ng/ml	20 ng/ml	20 ng/ml	20 ng/ml	20 ng/ml	20 ng/ml
ERK1/2i (PD0325901)	1 μM	1 μM	1 μM	1 μM	1 μM	1 μM
GSK3βi (CHIR99021)	3 μM	3 μM	3 μM	3 μM	3 μM	3 μM
JNKi (SP600125)	5 μM	5 μM	5 μM	5 μM	5 μM	5 μM
P38i (BIRB796)	2 μM	2 μM	2 μM	2 μM	2 μM	2
FGF2	16 ng/ml	16 ng/ml	-	16 ng/ml	-	-
TGFβ1	-	2 ng/ml	-	-	2 ng/ml	-
ROCKi (Y27632)	5 μM	5 μM	5 μM	5 μM	5 μM	5 μM
IGFII	-	20 ng/ml	20 ng/ml	-	20 ng/ml	20 ng/ml
SCF	-	10 ng/ml	10 ng/ml	-	10 ng/ml	10 ng/ml
BMPi (LDN-193189)	0.5 μM	0.5 μM	0.5 μM	0.5 μM	0.5 μM	0.5 μM
NOTCHi (DBZ)	2 μM	2 μM	2 μM	2 μM	2 μM	2 μM
SHHi (RU-SKI-43)	-	-	-	5 μM	5 μM	5 μM
TGFRi (SB432541)	2 μM	-	2 μM	2 μM		2 μM
FGFRi (PD173471)		-	0.1 μM	-	0.1 μM	0.1 μM

Table 5: Provided are the agents (factors, inhibitors) included in the WIS-NHSM medium. LIF – leukemia inhibitory factor; FGF2 = fibroblast growth factor 2 (also termed "basic FGF"; TGFβ1 = transforming growth factor bet 1; SCF = stem cell factor; BMPi = bone morphogenetic protein inhibitor; IGFII = insulin-like growth factor 2 (somatomedin A). NOTCHi = NOTCH inhibitor; SHHi = Sonic Hedgehog pathway (SHH) inhibitor; TGFRi = transforming growth factor receptor inhibitor; FGFRi = fibroblast growth factor receptor inhibitor.

As shown in Figures 85A-C, all of conditions 1 and 7-17 were capable of maintaining the naive state of the pluripotent stem cells, with the notable reduced percentage of total methylated cytosine.

It is noted that in conditions 12 and 15 (Table 5 above), when NOTCHi is used, TGFRi can then be used (and recombinant TGFB1 can be omitted) to maintain naive pluripotency with reduced DNA methylation levels.

In addition, in condition 16, when NOTCHi is used, FGFRi can then be used (and recombinant FGF2 can be omitted) to maintain naive pluripotency with reduced DNA methylation levels. Recombinant IGFII and SCF are used in these conditions to boost human naive cells proliferation in the absence of FGF2 signaling.

In addition, in conditions 14 and 17, when NOTCHi is used, FGFRi and TGRFi can then be used (and recombinant FGF2 and TGFB1 can be omitted) to maintain naive pluripotency with reduced DNA methylation levels. Recombinant IGFII and SCF are used in these conditions to boost human naive cells proliferation in the absence of FGF2 signaling.

It should be noted that WIS-NHSM condition 15 medium (Table 5 above) is excellent for culturing human pluripotent stem cells in the naive state as is evidenced by the domed colony morphology and lack of defined borders between individual cells in each colony (data not shown).

It should be noted that the above WIS-NHSM conditions can be used to maintain the naive state of non-human primates pluripotent stem cells.

In summary, the following modifications of the medium for establishing a naive pluripotent state can be used:

P38i: Inhibitors for P38 include upstream blockers for pathways that activate p38 signaling: including BMP signaling inhibitors/

STAT3 activation: Activators for STAT3 signaling can be used to replace LIF including IL-6.

TGFB1 – Activators of TGF/ACTIVIN pathway including ACTIVIN A (also known as Inhibin beta A, Gene ID: 3624 can be sued to replace TGFB1).

BMPi: protein inhibitors of BMP pathway like recombinant NOGGIN protein, can be used to replace small molecule inhibitors of BMP signaling.

A non-limiting example of a culture medium which can be used to maintain (and induce to naive state) pluripotent stem cells in a naive state include: A culture medium comprising leukemia inhibitor factor (LIF), an ERK1/2 inhibitor, a GSK3b inhibitor, a p38 inhibitor, a JNK inhibitor, basic fibroblast growth factor (bFGF) and transforming growth factor-beta 1 (TGFβ1), and one or more of the following components:

a) IGFII (range 0.1-100 ng/ml final concentration);

b) IGF1 [insulin-like growth factor 1 (somatomedin C)] (range 0.1-100 ng/ml final concentration);

c) SCF (range 0.1-100 ng/ml final concentration);

d) BMP signaling inhibitor [examples include, but are not limited to: LDN193189 (AXON 1509 - 0.01-20 microM final concentration), K02288 (Axon 2189; 0.1-20 microM final concentration), Dorsomorphin hydrochloride (AXON 2150 0.1-20 microM final concentration);

e) NOTCH signaling inhibitors [examples include, but are not limited to the following gamma secretase inhibitors: DAPT (Axon Medchem 1484 – 0.05-50 microM final concentration), LY2886721 hydrochloride (Axon Medchem 1964 – 0.05-50 microM final concentration)], DBZ (Axon Medchem – Axon 1488- 0.05-50 microM final concentration).

f) Sonic Hedgehog pathway (SHH) inhibitors [examples include, but are not limited to the following: GANT61 (SigmaAldrich – 0.05-50 microM final concentration), RU-SKI 43 (Axon Medchem – Axon 2035 – 0.05-50 microM final concentration)].

g) ERK5 inhibitors (BIX02189 Axon 1809; range 0.1-100 microM final concentration)

h) ROCK inhibitor [Y27632 (AXON 1683) – 0.05-100 microM final].

i) FGF signaling inhibitor: Non-limiting examples of FGFR inhibitors include PD173074 and SU5401.

j) TGF pathway inhibitor: Non-limiting examples of TGFR inhibitors include SB431542 and A 83-01 small molecule compound (As used herein the term "TGFR inhibitor (or TGFRi)" refers to a molecule capable of inhibiting TGFR expression and/or activity level as determined by phosphorylated ALK4, 5 and 7).

EXAMPLE 15

ACTIVATION OF ERAS FOR INDUCING AND MAINTENECE OF NAIVE PLURIPOTENT STATE

Human ES Ras (ERAS) gene (Gene ID: 3266) has an upstream premature polyadenylation signal that results in a truncated, noncoding transcript (Kameda T, and Thomson JA, Stem Cells 2005, 23:1535-40).

The present inventors have further envisaged that overexpression of *ERas* or activation of endogenous human *ERas* in pluripotent stem cells can be used to induce a naive state in pluripotent stem cells. Thus, genetically modified pluripotent stem cells in which *ERas* is either over expressed or endogenously activated exhibit a naive state of the pluripotent stem cells.

Overexpression of ERas in pluripotent stem cells - human pluripotent stem cells are transformed with a nucleic acid construct designed for constitutive or transient expression of *ERas* (SEQ ID NO: 109).

Activation of endogenous ERAS expression in human pluripotent stem cells – In human cells, the ERAS gene is not expressed due to the presence of viral sequences that integrated into the human genome and block ERAS expression. Activation of endogenous human ERAS expression is achieved by removing the combinations of polyadenylation sites (Marked as "pre-mature polyadenylation sites" in SEQ ID NO: 108 in the sequence listing; also defined as "poly-A signal" in A-1, A2 or A-3 boxed sequences in Figure 3 by Kameda et al. Stem Cells 2005;23:1535–1540; which is fully incorporated herein by reference in its entirety). The latter modification can be either achieved with homologous recombination, CRISPR [as described in Ryan M. Walsh and Konrad Hochedlinger, Proc Natl Acad Sci U S A. 2013 Sep 24;110(39):15514-5; and Yang Hui et al., Cell 154: 1370–1379, September 12, 2013; each of which is fully incorporated herein by reference in its entirety], or TALENs [Hockemeyer D, et al., Nat Biotechnol. 2011 Jul 7;29(8):731-4, which is fully incorporated herein by reference in its entirety], either alone or in combination.

Human ERAS gene expression/reactivation may be used in combination with any of the media described herein for naive pluripotent stem cells to boost human naive pluripotent cells proliferation.

Although the invention has been described in conjunction with specific embodiments thereof, it is evident that many alternatives, modifications and variations will be apparent to those skilled in the art. Accordingly, it is intended to embrace all such alternatives, modifications and variations that fall within the spirit and broad scope of the appended claims.

All publications, patents and patent applications mentioned in this specification are herein incorporated in their entirety by reference into the specification, to the same extent as if each individual publication, patent or patent application was specifically and individually indicated to be incorporated herein by reference. In addition, citation or identification of any reference in this application shall not be construed as an admission that such reference is available as prior art to the present invention. To the extent that section headings are used, they should not be construed as necessarily limiting.

REFERENCES

(Additional references are cited in text)

Ang, Y.-S., Tsai, S.-Y., Lee, D.-F., Monk, J., Su, J., Ratnakumar, K., Ding, J., Ge, Y., Darr, H., Chang, B., et al. (2011). Wdr5 mediates self-renewal and reprogramming via the embryonic stem cell core transcriptional network. Cell *145*, 183–197.

De Los Angeles, A., Loh, Y.-H., Tesar, P.J., and Daley, G.Q. (2012). Accessing naive human pluripotency. Curr. Opin. Genet. Dev. *22*, 272–282.

Durcova-Hills, G., Tang, F., Doody, G., Tooze, R., and Surani, M.A. (2008). Reprogramming primordial germ cells into pluripotent stem cells. PLoS ONE *3*, e3531.

Fidalgo, M., Faiola, F., Pereira, C.-F., Ding, J., Saunders, A., Gingold, J., Schaniel, C., Lemischka, I.R., Silva, J.C.R., and Wang, J. (2012). Zfp281 mediates Nanog autorepression through recruitment of the NuRD complex and inhibits somatic cell reprogramming. Proc. Natl. Acad. Sci. U.S.a. *109*, 16202–16207.

Hanna, J.H. (2010). The STATs on naive iPSC reprogramming. Cell Stem Cell *7*, 274–276.

Hanna, J.H., Saha, K., and Jaenisch, R. (2010a). Pluripotency and cellular reprogramming: facts, hypotheses, unresolved issues. Cell *143*, 508–525.

Hanna, J., Cheng, A.W., Saha, K., Kim, J., Lengner, C.J., Soldner, F., Cassady, J.P., Muffat, J., Carey, B.W., and Jaenisch, R. (2010b). Human embryonic stem cells with biological and epigenetic characteristics similar to those of mouse ESCs. Proc. Natl. Acad. Sci. U.S.a. *107*, 9222–9227.

Hanna, J., Markoulaki, S., Mitalipova, M., Cheng, A.W., Cassady, J.P., Staerk, J., Carey, B.W., Lengner, C.J., Foreman, R., Love, J., et al. (2009a). Metastable pluripotent states in NOD-mouse-derived ESCs. Cell Stem Cell *4*, 513–524.

Hanna, J., Saha, K., Pando, B., van Zon, J., Lengner, C.J., Creyghton, M.P., van Oudenaarden, A., and Jaenisch, R. (2009b). Direct cell reprogramming is a stochastic process amenable to acceleration. Nature *462*, 595–601.

Hockemeyer, D., Wang, H., Kiani, S., Lai, C.S., Gao, Q., Cassady, J.P., Cost, G.J., Zhang, L., Santiago, Y., Miller, J.C., et al. (2011). Genetic engineering of human pluripotent cells using TALE nucleases. Nat Biotechnol *29*, 731–734.

Kaji, K., Caballero, I.M., MacLeod, R., Nichols, J., Wilson, V.A., and Hendrich, B. (2006). The NuRD component Mbd3 is required for pluripotency of embryonic stem cells. Nat Cell Biol *8*, 285–292.

Kaji, K., Nichols, J., and Hendrich, B. (2007). Mbd3, a component of the NuRD co-repressor complex, is required for development of pluripotent cells. Development *134*, 1123–1132.

Lengner, C.J., Gimelbrant, A.A., Erwin, J.A., Cheng, A.W., Guenther, M.G., Welstead, G.G., Alagappan, R., Frampton, G.M., Xu, P., Muffat, J., et al. (2010). Derivation of pre-X inactivation human embryonic stem cells under physiological oxygen concentrations. Cell *141*, 872–883.

Li, W., Wei, W., Zhu, S., Zhu, J., Shi, Y., Lin, T., Hao, E., Hayek, A., Deng, H., and Ding, S. (2009). Generation of rat and human induced pluripotent stem cells by combining genetic reprogramming and chemical inhibitors. Cell Stem Cell *4*, 16–19.

Mansour, A.A., Gafni, O., Weinberger, L., Zviran, A., Ayyash, M., Rais, Y., Krupalnik, V., Zerbib, M., Amann-Zalcenstein, D., Maza, I., et al. (2012). The H3K27 demethylase Utx regulates somatic and germ cell epigenetic reprogramming. Nature *488*, 409–413.

Marks, H., Kalkan, T., Menafra, R., Denissov, S., Jones, K., Hofemeister, H., Nichols,

J., Kranz, A., Francis Stewart, A., Smith, A., et al. (2012). The transcriptional and epigenomic foundations of ground state pluripotency. Cell *149*, 590–604.
Mikkelsen, T.S., Hanna, J., Zhang, X., Ku, M., Wernig, M., Schorderet, P., Bernstein, B.E., Jaenisch, R., Lander, E.S., and Meissner, A. (2008). Dissecting direct reprogramming through integrative genomic analysis. Nature *454*, 49–55.
Nichols, J., and Smith, A. (2012). Pluripotency in the embryo and in culture. Cold Spring Harb Perspect Biol *4*, a008128.
Okamoto, I., Patrat, C., Thépot, D., Peynot, N., Fauque, P., Daniel, N., Diabangouaya, P., Wolf, J.-P., Renard, J.-P., Duranthon, V., et al. (2011). Eutherian mammals use diverse strategies to initiate X-chromosome inactivation during development. Nature 1–7.
Onder, T.T., Kara, N., Cherry, A., Sinha, A.U., Zhu, N., Bernt, K.M., Cahan, P., Marcarci, B.O., Unternaehrer, J., Gupta, P.B., et al. (2012). Chromatin-modifying enzymes as modulators of reprogramming. Nature *483*, 598–602.
Orkin, S.H., and Hochedlinger, K. (2011). Chromatin Connections to Pluripotency and Cellular Reprogramming. Cell *145*, 835–850.
Polo, J.M., Anderssen, E., Walsh, R.M., Schwarz, B.A., Nefzger, C.M., Lim, S.M., Borkent, M., Apostolou, E., Alaei, S., Cloutier, J., et al. (2012). A Molecular Roadmap of Reprogramming Somatic Cells into iPS Cells. Cell *151*, 1617–1632.
Pribluda, A., and Hanna, J.H. (2012). Tracing the genesis of human embryonic stem cells. Nat Biotechnol *30*, 247–249.
Roode, M., Blair, K., Snell, P., Elder, K., Marchant, S., Smith, A., and Nichols, J. (2012). Human hypoblast formation is not dependent on FGF signalling. Dev. Biol. *361*, 358–363.
Silva, J., Nichols, J., Theunissen, T.W., Guo, G., van Oosten, A.L., Barrandon, O., Wray, J., Yamanaka, S., Chambers, I., and Smith, A. (2009). Nanog is the gateway to the pluripotent ground state. Cell *138*, 722–737.
Smith, Z.D., Nachman, I., Regev, A., and Meissner, A. (2010). Dynamic single-cell imaging of direct reprogramming reveals an early specifying event. Nat Biotechnol *28*, 521–526.
Soufi, A., Donahue, G., and Zaret, K.S. (2012). Facilitators and Impediments of the Pluripotency Reprogramming Factors' Initial Engagement with the Genome. Cell 1–11.
Sridharan, R., Tchieu, J., Mason, M.J., and Yachechko, R. (2009). ScienceDirect.com - Cell - Role of the Murine Reprogramming Factors in the Induction of Pluripotency. Cell.
Takahashi, K., and Yamanaka, S. (2006). Induction of pluripotent stem cells from mouse embryonic and adult fibroblast cultures by defined factors. Cell *126*, 663–676.
Tesar, P.J., Chenoweth, J.G., Brook, F.A., Davies, T.J., Evans, E.P., Mack, D.L., Gardner, R.L., and McKay, R.D.G. (2007). New cell lines from mouse epiblast share defining features with human embryonic stem cells. Nature *448*, 196–199.
Tiwari, V.K., Stadler, M.B., Wirbelauer, C., Paro, R., Schübeler, D., and Beisel, C. (2011). A chromatin-modifying function of JNK during stem cell differentiation. Nat Genet.
Tomoda, K., Takahashi, K., Leung, K., Okada, A., Narita, M., Yamada, N.A., Eilertson, K.E., Tsang, P., Baba, S., White, M.P., et al. (2012). Derivation conditions impact x-inactivation status in female human induced pluripotent stem cells. Cell Stem Cell *11*, 91–99.
Warren, L., Ebina, W., Mandal, P.K., Smith, Z.D., Meissner, A., and Daley, G.Q.

(2010). ScienceDirect.com - Cell Stem Cell - Highly Efficient Reprogramming to Pluripotency and Directed Differentiation of Human Cells with Synthetic Modified mRNA. Cell Stem Cell.

Wernig, M., Lengner, C.J., Hanna, J., Lodato, M.A., Steine, E., Foreman, R., Staerk, J., Markoulaki, S., and Jaenisch, R. (2008). A drug-inducible transgenic system for direct reprogramming of multiple somatic cell types. Nat Biotechnol *26*, 916–924.

Ying, Q.-L., Wray, J., Nichols, J., Batlle-Morera, L., Doble, B., Woodgett, J., Cohen, P., and Smith, A. (2008). The ground state of embryonic stem cell self-renewal. Nature *453*, 519–523.

Zhu, D., Fang, J., Li, Y., and Zhang, J. (2009). Mbd3, a Component of NuRD/Mi-2 Complex, Helps Maintain Pluripotency of Mouse Embryonic Stem Cells by Repressing Trophectoderm Differentiation. PLoS ONE *4*, e7684.

WHAT IS CLAIMED IS:

1. An isolated human naive pluripotent stem cell (PSC), comprising:

an unmethylated X-inactive specific transcript (XIST) gene, wherein:

(i) when the naive PSC is a female PSC, then said naive female PSC has two unmethylated alleles of said XIST gene; and

(ii) when said naive PSC is a male PSC, then said naive male PSC has an unmethylated allele of said XIST gene;

and/or

an expression level of transcription factor E3 (TFE3) is characterized by a nucleus to cytoplasm expression ratio which is equal to or higher than 1 as determined by an immunostaining assay.

2. The isolated human naive PSC of claim 1, wherein when the isolated naive PSC is incubated in the presence of an agent selected from the group consisting of Bone morphogenetic protein 4 (BMP4), JNK inhibitor, and P38 inhibitor, the naive PSC maintains a pluripotent phenotype.

3. The isolated human naive PSC of claim 1 or 2, wherein said human naive PSC is characterized by reduced methylation of CpG islands as compared to a level of methylation of said CpG islands in a human primed PSC.

4. An isolated population of naive PSCs comprising at least 10% of the isolated human naive PSC cells of claim 1, 2 or 3.

5. A cell culture comprising the isolated naive PSC of claim 1, 2 or 3, or the isolated population of naive PSCs of claim 4 and a culture medium.

6. The cell culture of claim 5, wherein said culture medium is capable of maintaining the naive PSC in an undifferentiated and pluripotent state for at least 10 passages.

7. A culture medium comprising an ERK1/2 inhibitor, a GSK3β inhibitor, a p38 inhibitor, a JNK inhibitor, a STAT3 activator and at least one agent selected from the group consisting of: basic fibroblast growth factor (bFGF), transforming growth factor beta 1 (TGFβ1), a protein kinase C (PKC) inhibitor, a ROCK inhibitor and a NOTCH inhibitor.

8. A culture medium comprising an ERK1/2 inhibitor, a GSK3β inhibitor, a p38 inhibitor, a JNK inhibitor, a STAT3 activator and at least one agent selected from the group consisting of: a transforming growth factor receptor (TGFR) inhibitor, a fibroblast growth factor receptor (FGFR) inhibitor, a protein kinase C (PKC) inhibitor, a ROCK inhibitor and a NOTCH inhibitor.

9. The culture medium of claim 7 or 8, wherein said STAT3 activator is selected from the group consisting of leukemia inhibitory factor (LIF) and interleukin 6 (IL6).

10. The culture medium of claim 7, 8 or 9, further comprising at least one additional agent selected from the group consisting of: insulin-like growth factor 1 (IGF1), insulin-like growth factor II (IGFII), a bone morphogenetic protein (BMP) signaling inhibitor, a Sonic Hedgehog pathway (SHH) inhibitor, an ERK5 inhibitor, Forskolin, Kenpaullone, BayK8644, Bix1294, and stem cell factor (SCF).

11. The culture medium of claim 7, 8 or 9, further comprising at least one additional agent selected from the group consisting of: insulin-like growth factor 1 (IGF1), insulin-like growth factor II (IGFII), bone morphogenetic protein 4 (BMP4), a Sonic Hedgehog pathway (SHH) inhibitor, an ERK5 inhibitor, Forskolin, Kenpaullone, BayK8644, Bix1294, and stem cell factor (SCF).

12. The culture medium of claim 7, 8, 9, 10 or 11, wherein said STAT3 activator comprises said LIF, and wherein said at least one agent comprises said PKC inhibitor.

13. The culture medium of claim 12, further comprising FGFR inhibitor.

14. The culture medium of claim 12 or 13, further comprising TGFR inhibitor.

15. The culture medium of claim 7, 9, 10 or 11, wherein said STAT3 activator comprises said LIF and wherein said at least one agent comprises said TGFβ1 and said protein kinase C inhibitor.

16. The culture medium of claim 15, further comprising an FGFR inhibitor.

17. The culture medium of claim 7, 9, 10 or 11, wherein said STAT3 activator comprises said LIF, and wherein said at least one agent comprises said bFGF and said TGFβ1.

18. The culture medium of claim 17, further comprising a ROCK inhibitor.

19. The culture medium of claim 17 or 18, further comprising a protein kinase C inhibitor.

20. The culture medium of claim 7, 9 or 10, wherein said STAT3 activator comprises said LIF and wherein said at least one agent comprises said bFGF, said ROCK inhibitor, a bone morphogenetic protein (BMP) inhibitor, said NOTCH inhibitor, and a transforming growth factor receptor (TGFR) inhibitor.

21. The culture medium of claim 20, further comprising a Sonic Hedgehog pathway (SHH) inhibitor.

22. The culture medium of claim 8, 9, 10 or 11, wherein said STAT3 activator comprises said LIF and wherein said at least one agent comprises said NOTCH inhibitor, and a fibroblast growth factor receptor (FGFR) inhibitor.

23. The culture medium of claim 22, further comprising an agent selected from the group consisting of insulin-like growth factor II (IGFII), stem cell factor (SCF) and transforming growth factor beta 1 (TGFβ1).

24. The culture medium of any of claims 7-23, further comprising ascorbic acid.

25. The culture medium of any of claims 7-24, further comprising oleic Acid.

26. The culture medium of any of claims 7-25, further comprising Linoleic Acid and/or pipecolic acid.

27. The culture medium of any of claims 7-26, being devoid of animal serum.

28. The culture medium of any of claims 7-27, further comprises serum replacement.

29. A cell culture comprising cells and the culture medium of any of claims 7-28.

30. The cell culture of claim 29, wherein said medium is capable of maintaining naive pluripotent stem cell in an undifferentiated state for at least 2 passages.

31. A method of generating a naive pluripotent stem cell (PSC), comprising:

incubating a non-naive PSC cell under conditions which allow generation of the naive PSC from said non-naive PSC, wherein:

(i) when said naive PSC is a female PSC, then said naive female PSC has two unmethylated alleles of an X-inactive specific transcript (XIST) gene; and

(ii) when said naive PSC is a male PSC, then said naive male PSC has an unmethylated allele of said XIST gene,

and/or

an expression level of transcription factor E3 (TFE3) in said naive PSC is characterized by a nucleus to cytoplasm expression ratio which is equal to or higher than 1 as determined by an immunostaining assay,

thereby generating the naive PSC.

32. The method of claim 31, wherein said conditions comprise the culture medium of any of claims 7-28.

33. The method of claim 31 or 32, wherein said conditions comprise hypoxia.

34. The method of any of claims 31-33, wherein said culture medium further comprises an MBD3 inhibitor.

35. The method of any of claims 31-34, wherein said culture medium further comprises a chromodomain helicase DNA binding protein 4 (CHD4) inhibitor.

36. The method of any of claims 31-35, wherein said culture medium further comprises P66 alpha coiled-coil domain.

37. The method of any of claims 31-36, wherein said non-naive PSC is selected from the group consisting of a primed PSC, a blastocyst, an induced pluripotent stem cell (iPSC) and a somatic cell.

38. The method of any of claims 31-37, wherein when said non-naive PSC comprises a somatic cell then the method further comprises subjecting said somatic cell to de-differentiation conditions, to thereby obtain an induced pluripotent stem cell.

39. The method of claim 38, wherein said de-differentiation conditions comprise expressing within said somatic cell at least two growth factors selected from the group consisting of Oct4, Sox2, Klf4 and c-Myc.

40. A method of improving generation of induced pluripotent stem cells (iPSCs) from a somatic cell, comprising:

(a) expressing within the somatic cell at least two growth factors selected from the group consisting of Oct4, Sox2, Klf4 and c-Myc, and

(b) inhibiting Mbd3 expression and/or activity in the somatic cell,

thereby improving generation of the iPSCs from a somatic cell.

41. The method of claim 40, wherein said inhibiting said Mbd3 activity is performed by inhibiting binding of said Mbd3 to the nucleosome remodeling and deacetylase (NuRD) complex.

42. The method of claim 41, wherein said inhibiting said binding of said Mbd3 to the NuRD complex is performed using a chromodomain helicase DNA binding protein 4 (CHD4) inhibitor.

43. The method of claim 41, wherein said inhibiting said binding of said Mbd3 to the NuRD complex is performed using a P66 alpha coiled-coil domain.

44. The method of claim 41, wherein said inhibiting said Mbd3 expression is performed using a protein kinase C (PKC) inhibitor.

45. The method of any of claims 40-44, further comprising exogenously expressing ES cell expressed Ras (ERAS) coding sequence or activating endogenous expression of said ERAS in said somatic cell.

46. The method of claim 40, wherein said expressing is effected for at least 48 h such that said inhibiting said Mbd3 is effected to 10-30% of a level of said Mbd3 prior to said expressing.

47. The method of claim 40, wherein said expressing is effected for about 48 hours and said inhibiting is effected after said about 48 hours.

48. The method of any of claims 40-47, wherein said iPSC is a murine iPSC.

49. The method of claim 48, further comprising culturing said murine iPSC in a medium which comprises LIF, an ERK1/2 inhibitor, and a GSK3b inhibitor.

50. The method of any of claims 40-47, wherein when said iPSC is a human iPSC, the method further comprising

(c). culturing said human iPSC in a culture medium which comprises LIF, an ERK1/2 inhibitor, a GSK3b inhibitor, a P38 inhibitor, a JNK inhibitor, basic fibroblast growth factor (bFGF) and transforming growth factor-beta 1 (TGFβ1).

51. The method of claim 50, wherein said medium further comprises a ROCK inhibitor.

52. The method of claim 50 or 51, wherein step (c) is performed following about 48 hours from said expressing of step (a).

53. The method of any of claims 39-52, wherein said expressing is performed using DNA transfection of said growth factors.

54. The method of any of claims 39-52, wherein said expressing is performed using RNA transfection of said growth factors.

55. The method of any of claims 39-52, wherein said expressing is performed using protein transfection of said growth factors.

56. The isolated naive PSC of claim 1, 2 or 3, the isolated population of naive PSCs of claim 4, the cell culture of claim 5 or 6, or the method of any of claims 31-39, wherein said PSC is selected from the group consisting of embryonic stem cell (ESC), induced pluripotent stem cells (iPSCs), and embryonic germ cell (EGC).

57. The isolated naive PSC of claim 1, 2 or 3, the isolated population of naive PSCs of claim 4, the cell culture of claim 5 or 6, or the method of any of claims 31-39, wherein said naive PSC expresses XIST.

58. The isolated naive PSC of claim 1, 2 or 3, the isolated population of naive PSCs of claim 4, the cell culture of claim 5 or 6, or the method of any of claims 31-39,wherein said naive PSC is devoid of XIST bodies.

59. The isolated naive PSC of claim 1, 2 or 3, the isolated population of naive PSCs of claim 4, the cell culture of claim 5 or 6, or the method of any of claims 31-39, wherein the naive ESC is capable of X-inactivation when induced to differentiate.

60. The isolated naive PSC of claim 1, 2 or 3, the isolated population of naive PSCs of claim 4, the cell culture of claim 5 or 6, or the method of any of claims 31-39, wherein said naive PSC is capable to differentiate into the endodermal, mesodermal and ectodermal embryonic germ layers.

61. The isolated naive PSC of 1, 2 or 3, the isolated population of naive PSCs of claim 4, the cell culture of claim 5 or 6, or the method of any of claims 31-39, wherein said naive PSC is capable of being maintained in said undifferentiated and pluripotent state for more than 20 passages in culture.

62. The isolated naive PSC of claim 1, 2 or 3, the isolated population of naive PSCs of claim 4, the cell culture of claim 5 or 6, or the method of any of claims 31-39, wherein said naive PSC expresses a lower level of MHC class I as compared to a primed PSC under identical detection assay conditions, and wherein said primed PSC exhibits one methylated and one unmethylated allele of XIST, expresses XIST, exhibits XIST bodies and exhibits a H3K27me3/polycomb focus.

63. The isolated naive PSC of claim 1, 2 or 3, the isolated population of naive PSCs of claim 4, the cell culture of claim 5 or 6, or the method of any of claims 31-39, wherein said naive PSC is characterized by at least 10 % more RNA polymerase II

pausing on chromosomes as compared to a primed PSC under identical assay conditions, and wherein said primed PSC exhibits one methylated and one unmethylated allele of XIST, expresses XIST, exhibits XIST bodies and exhibits a H3K27me3/polycomb focus.

64. The isolated naive PSC of claim 1, 2 or 3, the isolated population of naive PSCs of claim 4, the cell culture of claim 5 or 6, or the method of any of claims 31-39, having an inhibited p38 pathway as compared to a primed PSC.

65. The isolated naive PSC of claim 1, 2 or 3, the isolated population of naive PSCs of claim 4, the cell culture of claim 5 or 6, or the method of any of claims 31-39, having an inhibited JNK pathway as compared to a primed PSC.

66. The isolated naive PSC of claim 1, 2 or 3, the isolated population of naive PSCs of claim 4, the cell culture of claim 5 or 6, or the method of any of claims 31-39, having an inhibited ROCK pathway as compared to a primed PSC.

67. A method of generating a naive pluripotent stem cell (PSC), comprising incubating a non-naive PSC cell under conditions which allow generation of the naive PSC from said non-naive PSC, said naive PSC comprising:

an unmethylated X-inactive specific transcript (XIST) gene, wherein:

(i) when said naive PSC is a female PSC, then said naive female PSC has two unmethylated alleles of said XIST gene; and

(ii) when said naive PSC is a male PSC, then said naive male PSC has an unmethylated allele of said XIST gene,

and/or

an expression level of transcription factor E3 (TFE3) characterized by a nucleus to cytoplasm expression ratio which is equal to or higher than 1 as determined by an immunostaining assay,

wherein said conditions which comprise a culture medium which comprises KO-DMEM, N2 supplement (Gibco), Albumax I, LIF, ERK1/2 inhibitor, GSK3b inhibitor, p38 inhibitor, JNK inhibitor and a protein kinase C inhibitor,

thereby generating the naive PSC.

68. The method of claim 67, wherein said culture medium further comprises FGFR inhibitor.

69. The method of claim 67 or 68, wherein said culture medium further comprises TGFR inhibitor.

70. A method of generating a naive pluripotent stem cell (PSC), comprising incubating a non-naive PSC cell under conditions which allow generation of the naive PSC from said non-naive PSC, said naive PSC comprising:

an unmethylated X-inactive specific transcript (XIST) gene, wherein:

(i) when said naive PSC is a female PSC, then said naive female PSC has two unmethylated alleles of said XIST gene; and

(ii) when said naive PSC is a male PSC, then said naive male PSC has an unmethylated allele of said XIST gene,

and/or

an expression level of transcription factor E3 (TFE3) characterized by a nucleus to cytoplasm expression ratio which is equal to or higher than 1 as determined by an immunostaining assay,

wherein said conditions which comprise a culture medium which comprises KO-DMEM, N2 supplement (Gibco), Albumax I (Invitrogen), LIF, TGFβ1, ERK1/2 inhibitor, GSK3b inhibitor, p38 inhibitor, JNK inhibitor and a protein kinase C inhibitor,

thereby generating the naive PSC.

71. The method of claim 70, wherein said culture medium further comprises FGFR inhibitor.

72. A method of generating a naive pluripotent stem cell (PSC), comprising incubating a non-naive PSC cell under conditions which allow generation of the naive PSC from said non-naive PSC, said naive PSC comprising:

an unmethylated X-inactive specific transcript (XIST) gene, wherein:

(i) when said naive PSC is a female PSC, then said naive female PSC has two unmethylated alleles of said XIST gene; and

(ii) when said naive PSC is a male PSC, then said naive male PSC has an unmethylated allele of said XIST gene,

and/or

an expression level of transcription factor E3 (TFE3) characterized by a nucleus to cytoplasm expression ratio which is equal to or higher than 1 as determined by an immunostaining assay,

wherein said conditions which comprise a culture medium which comprises KO-DMEM, N2 supplement (Gibco), Albumax I (Invitrogen), LIF, bFGF, TGFβ1, ERK1/2 inhibitor, GSK3b inhibitor, p38 inhibitor, and JNK inhibitor,

thereby generating the naive PSC.

73. A method of generating a naive pluripotent stem cell (PSC), comprising incubating a non-naive PSC cell under conditions which allow generation of the naive PSC from said non-naive PSC, said naive PSC comprising:

an unmethylated X-inactive specific transcript (XIST) gene, wherein:

(i) when said naive PSC is a female PSC, then said naive female PSC has two unmethylated alleles of said XIST gene; and

(ii) when said naive PSC is a male PSC, then said naive male PSC has an unmethylated allele of said XIST gene,

and/or

an expression level of transcription factor E3 (TFE3) characterized by a nucleus to cytoplasm expression ratio which is equal to or higher than 1 as determined by an immunostaining assay,

wherein said conditions which comprise a culture medium which comprises KO-DMEM, N2 supplement (Gibco), defined lipid concentrate (Gibco), LIF, bFGF, TGFβ1, ERK1/2 inhibitor, GSK3b inhibitor, p38 inhibitor, JNK inhibitor, and an MBD3 inhibitor,

thereby generating the naive PSC.

74. An isolated naive pluripotent stem cell obtainable by the method of any of claims 31-39 and 67-73.

75. The isolated naive pluripotent stem cell of claim 74, wherein said naive pluripotent stem cell comprising:

an unmethylated X-inactive specific transcript (XIST) gene, wherein:

(i) when said naive PSC is a female PSC, then said naive female PSC has two unmethylated alleles of said XIST gene; and

(ii) when said naive PSC is a male PSC, then said naive male PSC has an unmethylated allele of said XIST gene,

and/or

an expression level of transcription factor E3 (TFE3) characterized by a nucleus to cytoplasm expression ratio which is equal to or higher than 1 as determined by an immunostaining assay.

76. A method of generating differentiated cells, comprising subjecting the naive pluripotent stem cells generated according to the method of any one of claims 31-39 and 67-73, the isolated naive pluripotent stem cells of any of claims 1-3, 56-66 and 74, or the isolated population of naive PSCs of any of claims 4 and 56-66 to differentiation conditions, thereby generating differentiated cells.

77. A method of generating a primordial germ cell, comprising culturing primate naive pluripotent stem cells in a culture medium selected capable of inducing the primate naive pluripotent stem cells into primordial germ cell, wherein said culture medium comprises a Rho kinase (ROCK) inhibitor and bone morphogenetic protein 4 (BMP4), thereby generating the primordial germ cell.

78. The method of claim 77, wherein said primate naive pluripotent stem cell comprises:

an unmethylated X-inactive specific transcript (XIST) gene, wherein:

(i) when said naive PSC is a female PSC, then said naive female PSC has two unmethylated alleles of said XIST gene; and

(ii) when said naive PSC is a male PSC, then said naive male PSC has an unmethylated allele of said XIST gene,

and/or

an expression level of transcription factor E3 (TFE3) characterized by a nucleus to cytoplasm expression ratio which is equal to or higher than 1 as determined by an immunostaining assay.

79. The method of claim 77, wherein the primordial germ cell is characterized by CD61 (intergrin beta 3) expression pattern.

80. The method of claim 79, wherein the primordial germ cell is characterized by $CD61^{+}/SSEA4^{+}$ expression pattern.

81. The method of any of claims 77-80, wherein said culture medium further comprises at least one agent selected from the group consisting of: leukemia inhibitory factor (LIF), Stem Cell Factor (SCF) and Epidermal Growth Factor (EGF).

82. The method of any of claims 77-81, wherein said primate is human.

83. An isolated population of primate primordial germ cells comprising primate primordial germ cells generated according to the method of any of claims 77-82.

84. The isolated population of primate primordial germ cells of claim 83, comprising at least 50% of primordial germ cells characterized by $CD61^{+}/SSEA4^{+}$ expression pattern.

85. A method of treating a subject in need thereof, comprising administering the primordial germ cells of claim 83 or 84 to a gonad of the subject, thereby treating the subject in need thereof.

86. The method of claim 85, wherein the subject suffers from infertility.

87. A kit comprising the primate primordial germ cells of claim 83 or 84 and a medicament for treating infertility.

88. A method of generating a chimeric animal, comprising introducing the isolated naive human PSC of claim 1, or the primordial germ cells of claim 83 or 84 into a pre-implantation embryo of a host animal, thereby generating the chimeric animal.

89. The method of claim 88, further comprising allowing said pre-implantation embryo to grow *ex vivo* or *in vivo*.

90. The method of claim 88, wherein said introducing is performed *in vivo*.

91. The method of claim 88, wherein said introducing is performed *in vitro* or *ex vivo*.

92. The method of any of claims 88-91, wherein said pre-implantation embryo comprises at least 4 cells.

93. The method of any of claims 88-91, wherein said pre-implantation embryo comprises no more than 128 cells.

94. The method of any of claims 88-93, wherein said host animal is a mouse.

95. The method of any of claims 88-93, wherein the isolated naïve PSC or the primordial germ cell is allogeneic to said host animal.

96. The method of any of claims 88-93, wherein the isolated naïve PSC or the primordial germ cell is xenogeneic to said host animal.

FIG. 1A

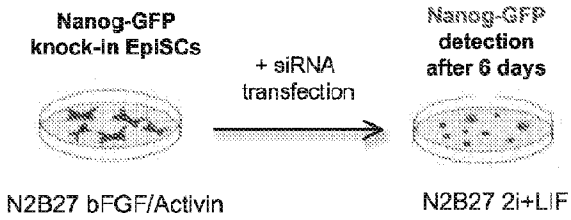


FIG. 1B

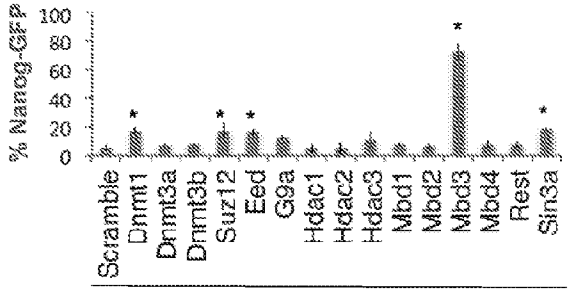
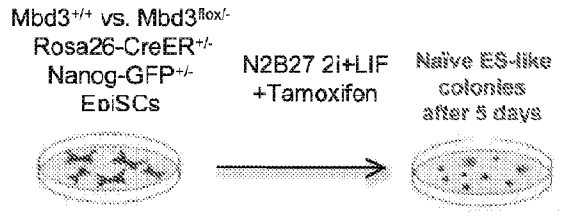


FIG. 1C



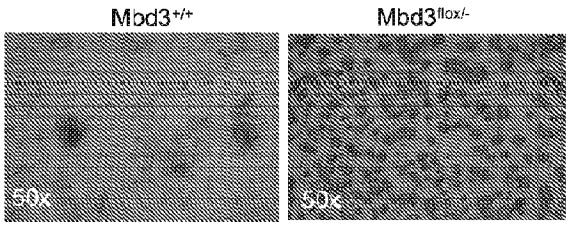


FIG. 1D FIG. 1E

Mbd3flox/- Rosa26-CreER+/- Nanog-GFP+/-

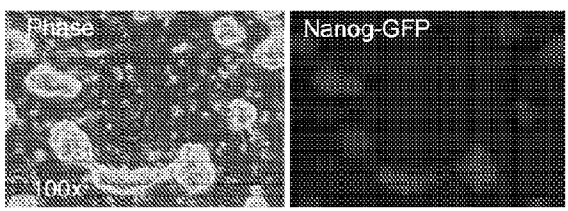
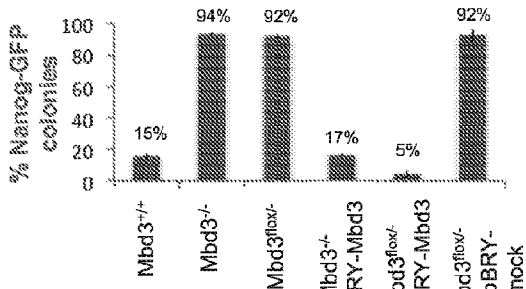


FIG. 1F FIG. 1G

FIG. 1H



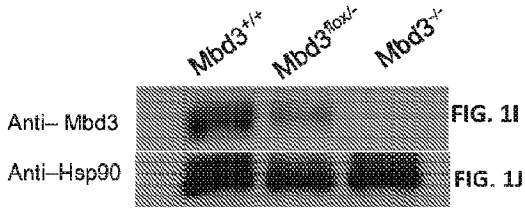


FIG. 1I FIG. 1J

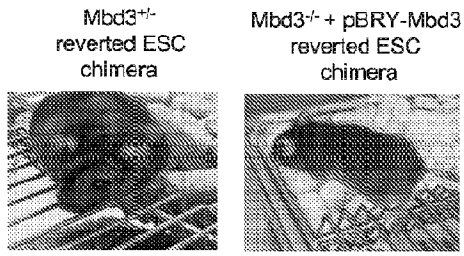


FIG. 1K FIG. 1L

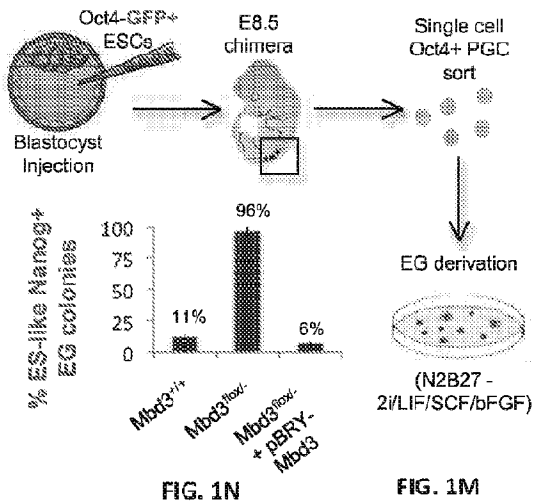


FIG. 1N FIG. 1M

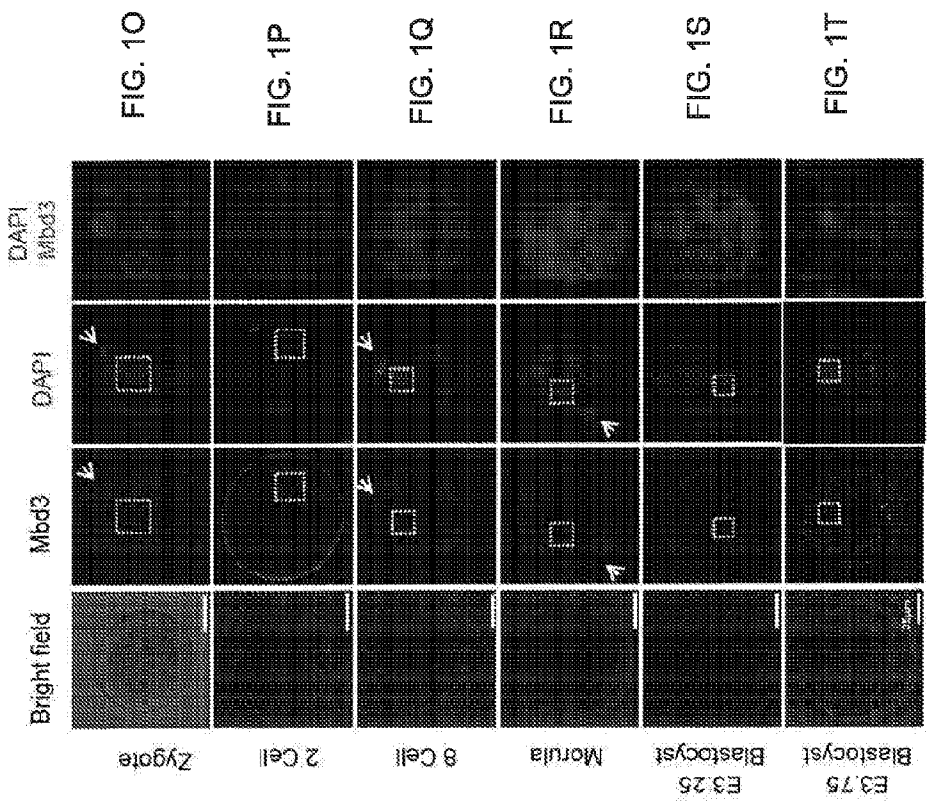
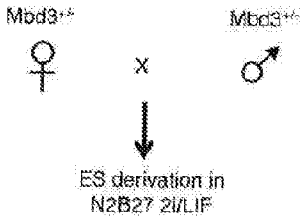

FIG. 1O
FIG. 1P
FIG. 1Q
FIG. 1R
FIG. 1S
FIG. 1T
DAPI Mbd3
DAPI
Mbd3
Bright field
Zygote
2 Cell
8 Cell
Morula
E3.25 Blastocyst
E3.75 Blastocyst

FIG. 2A



	# Mbd3+/+ ESCs derived	# Mbd3+/- ESCs derived	# Mbd3-/- ESCs derived
18 blastocysts in 2i/LIF **Total of 15 ESC lines obtained**	4	7	4

FIG. 2B

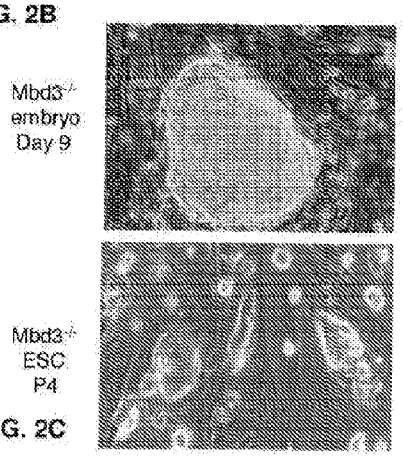


FIG. 2C

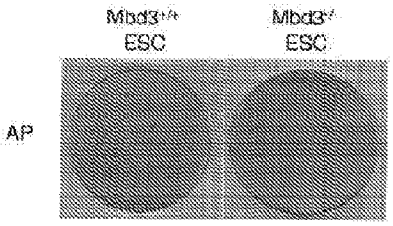


FIG. 2D FIG. 2E

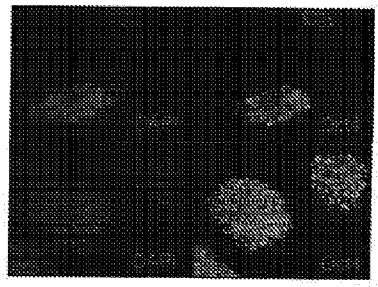


FIG. 2F

FIG. 2G

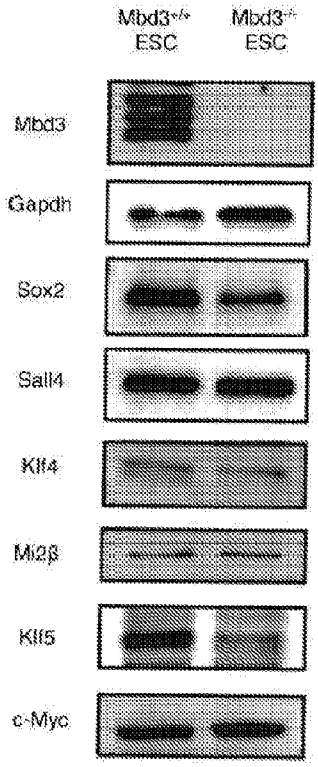


FIG. 2H

FIG. 2I

FIG. 2J

FIG. 2K

FIG. 2L

FIG. 2M

FIG. 2N

FIG. 2O

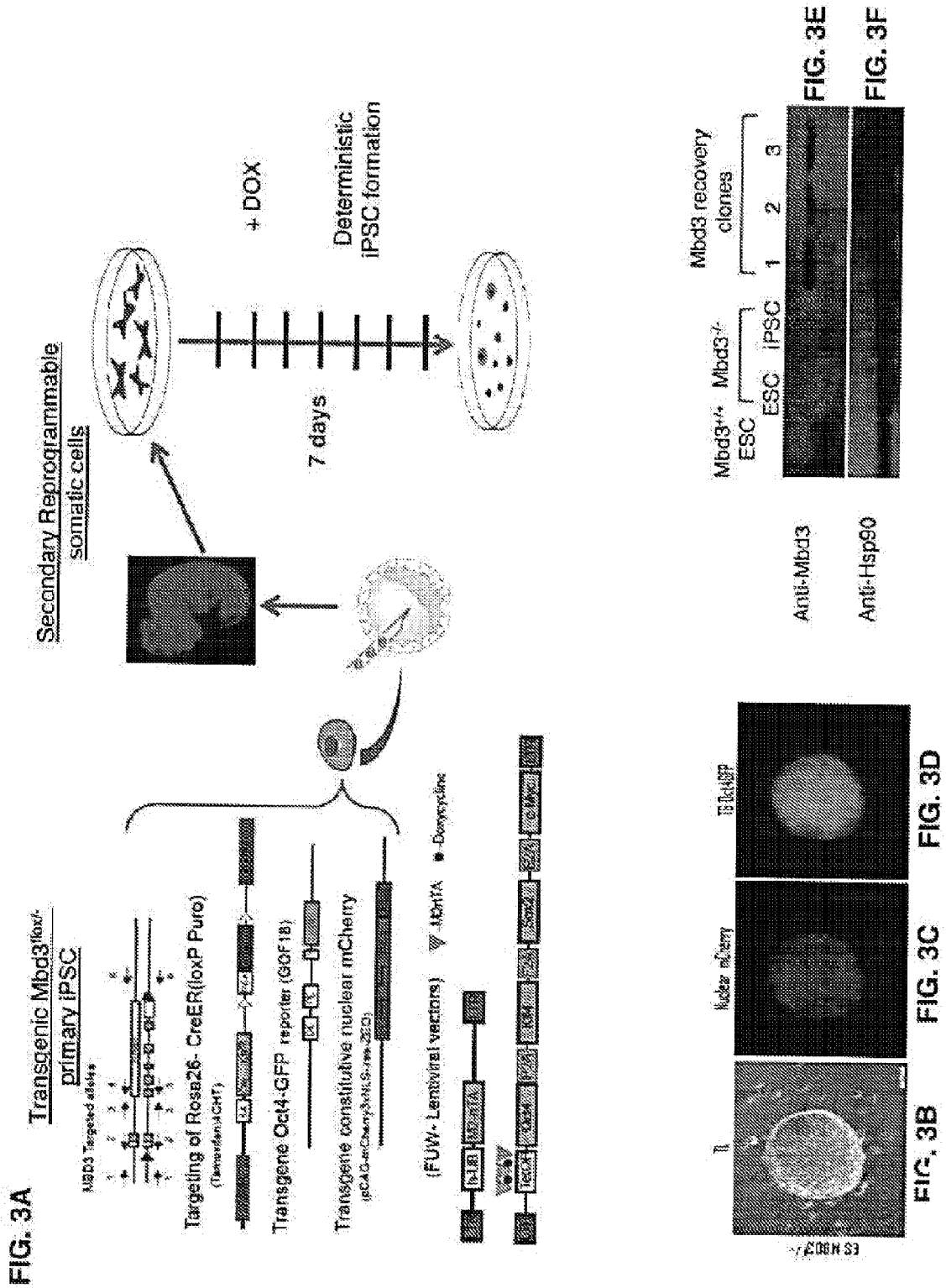


FIG. 3A FIG. 3B FIG. 3C FIG. 3D FIG. 3E FIG. 3F

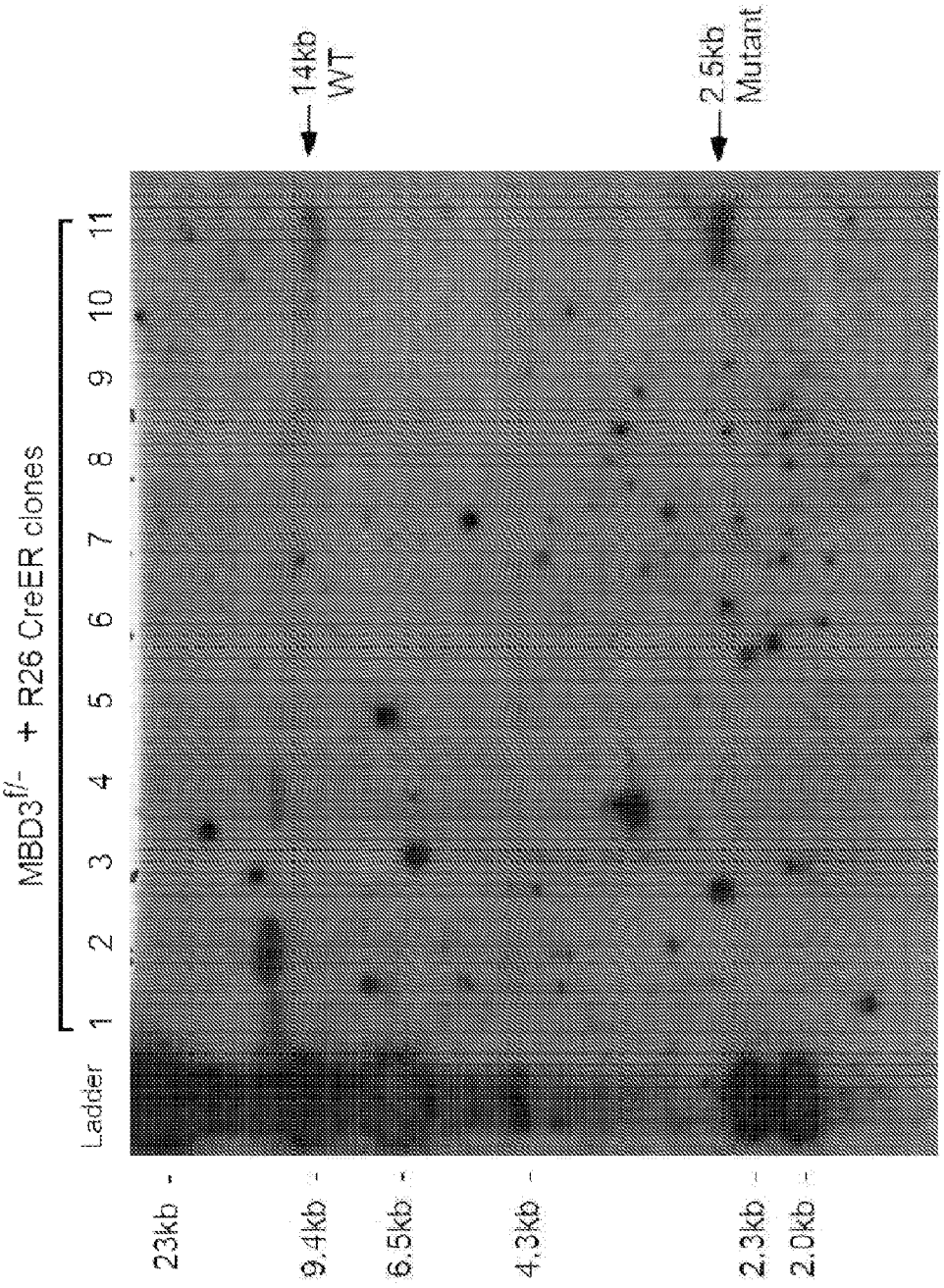
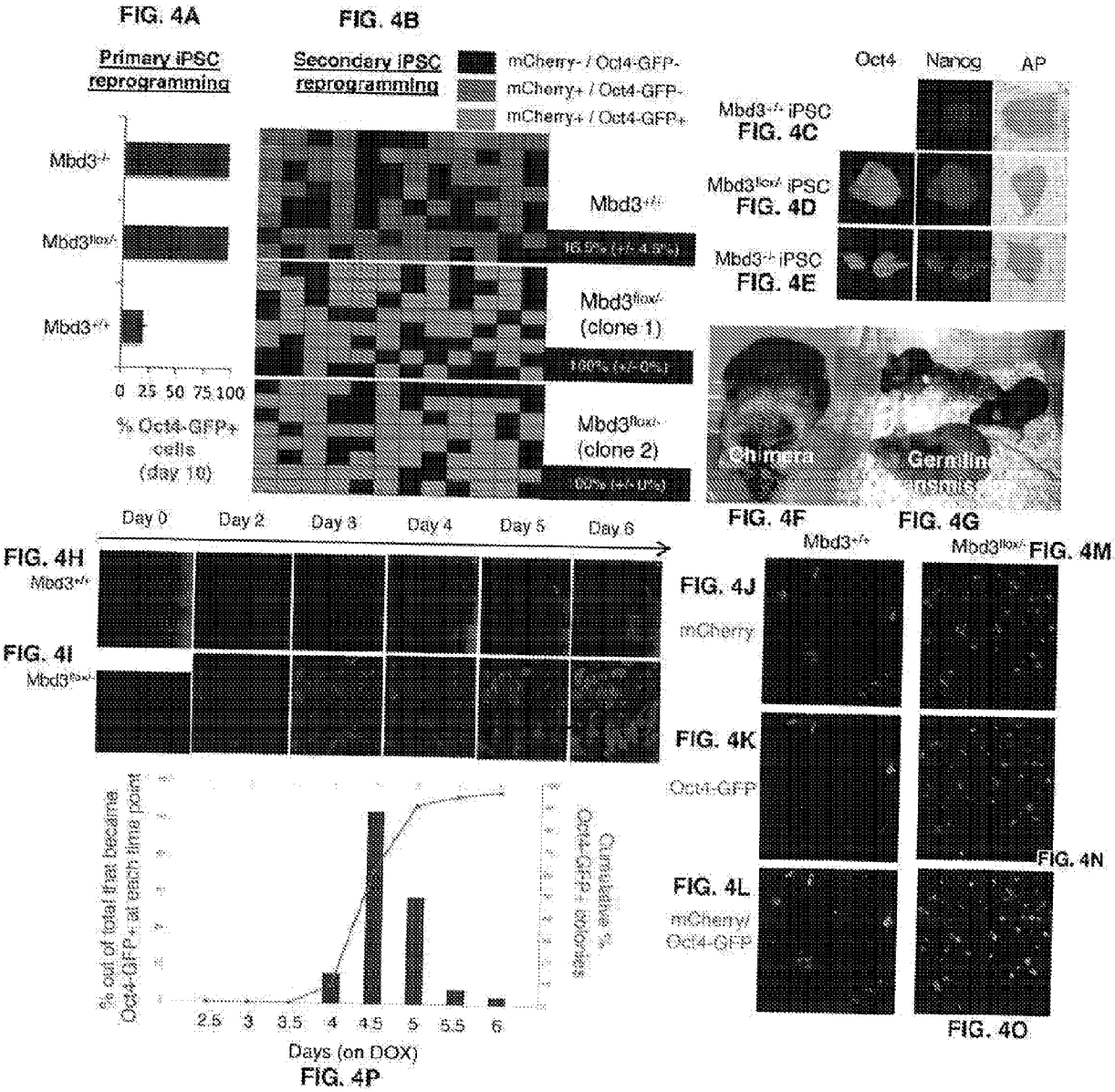

14kb
WT
2.5kb
Mutant
MBD3f/- + R26 CreER clones
Ladder
1
2
3
4
5
6
7
8
9
10
11
23kb
9.4kb
6.5kb
4.3kb
2.3kb
2.0kb

FIG. 3G


FIG. 4A
Primary iPSC reprogramming
Mbd3+/-
Mbd3flox/-
Mbd3+/+
0 25 50 75 100
% Oct4-GFP+ cells (day 10)
FIG. 4B
Secondary iPSC reprogramming
mCherry- / Oct4-GFP-
mCherry+ / Oct4-GFP-
mCherry+ / Oct4-GFP+
Mbd3+/+
Mbd3flox/- (clone 1)
Mbd3flox/- (clone 2)
FIG. 4C
Mbd3-/- iPSC
FIG. 4D
Mbd3flox/- iPSC
FIG. 4E
Mbd3-/- iPSC
Oct4
Nanog
AP
Chimera
Germline transmission
FIG. 4F
FIG. 4G
Day 0
Day 2
Day 3
Day 4
Day 5
Day 6
FIG. 4H
Mbd3+/+
FIG. 4I
Mbd3flox/-
% out of total that became Oct4-GFP+ at each time point
Cumulative % Oct4-GFP+ colonies
2.5 3 3.5 4 4.5 5 5.5 6
Days (on DOX)
FIG. 4P
FIG. 4J
mCherry
FIG. 4K
Oct4-GFP
FIG. 4L
mCherry/ Oct4-GFP
Mbd3+/+
Mbd3flox/-
FIG. 4M
FIG. 4N
FIG. 4O

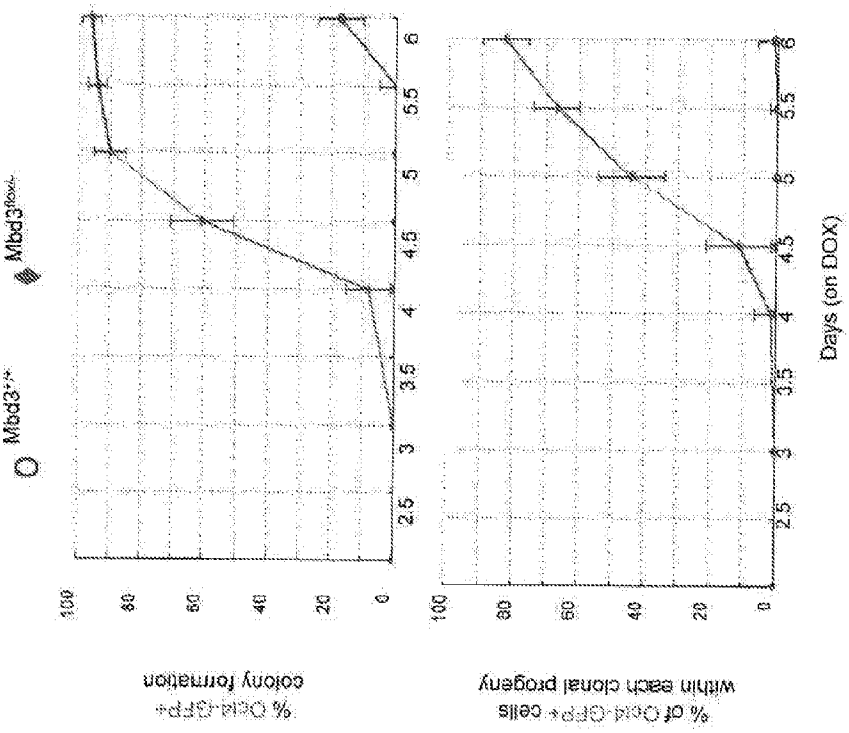
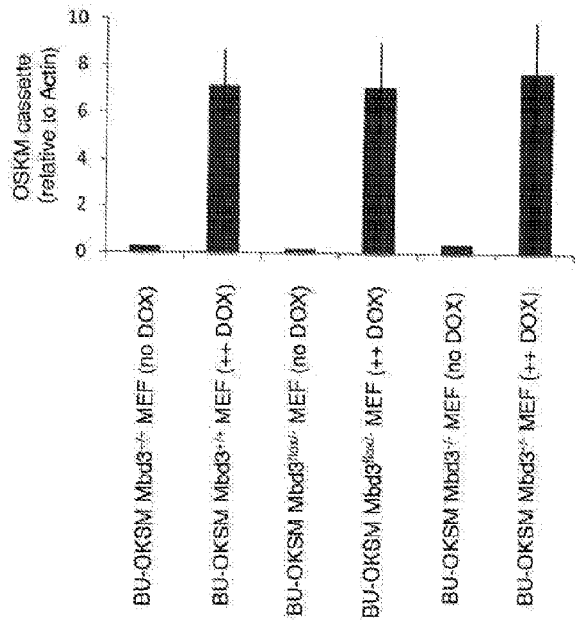

Mbd3+/+
Mbd3flox/-
% Oct4-GFP+ colony formation
% of Oct4-GFP+ cells within each clonal progeny
Days (on DOX)
100
80
60
40
20
0
2.5
3
3.5
4
4.5
5
5.5
6

FIG. 4Q

FIG. 4R

FIG. 5A



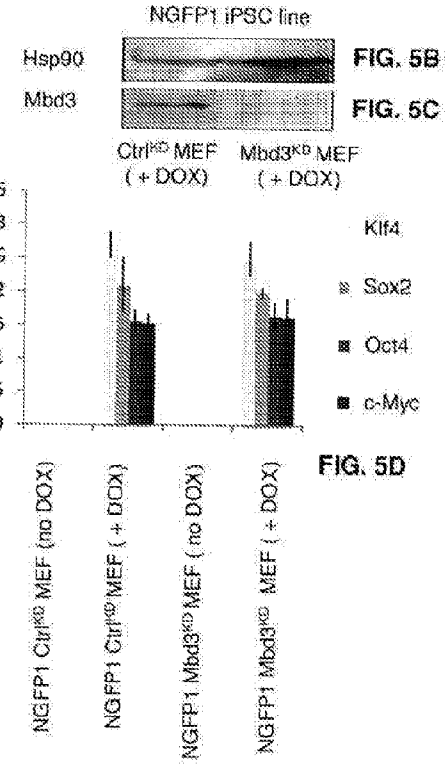


FIG. 5D

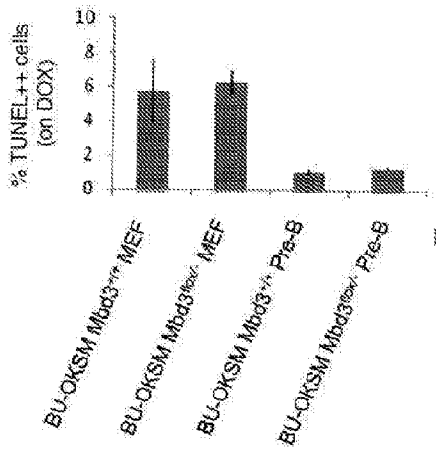


FIG. 5E

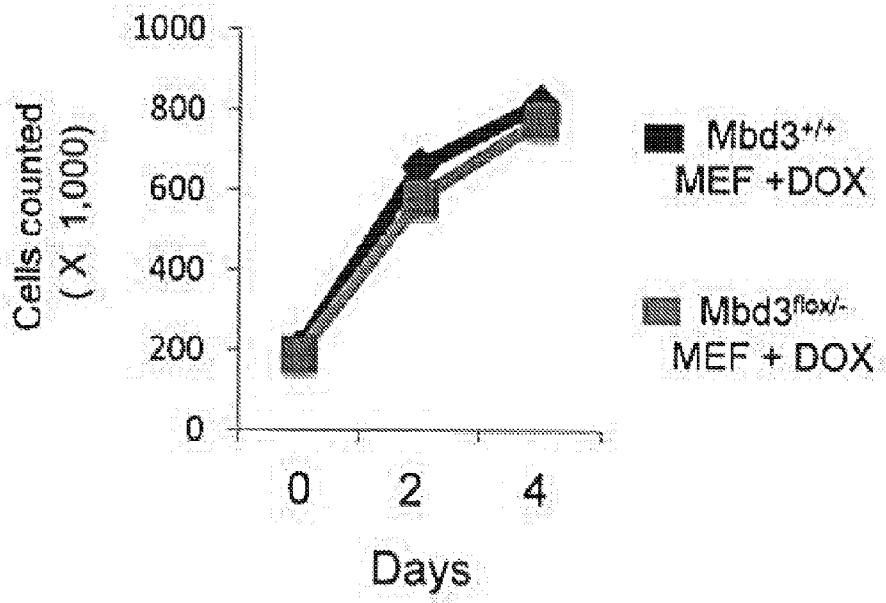

1000
800
600
400
200
0
Cells counted
(X 1,000)
0
2
4
Days
Mbd3+/+
MEF +DOX
Mbd3flox/-
MEF + DOX

FIG. 5F

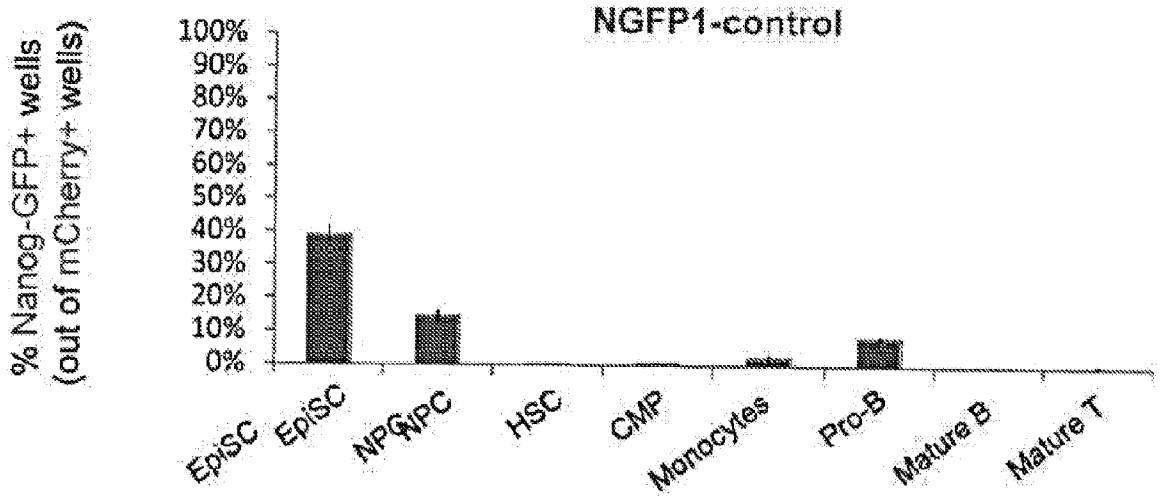

NGFP1-control
% Nanog-GFP+ wells
(out of mCherry+ wells)
100%
90%
80%
70%
60%
50%
40%
30%
20%
10%
0%
EpiSC
EpiSC
NPC
NPC
HSC
CMP
Monocytes
Pro-B
Mature B
Mature T

FIG. 6A

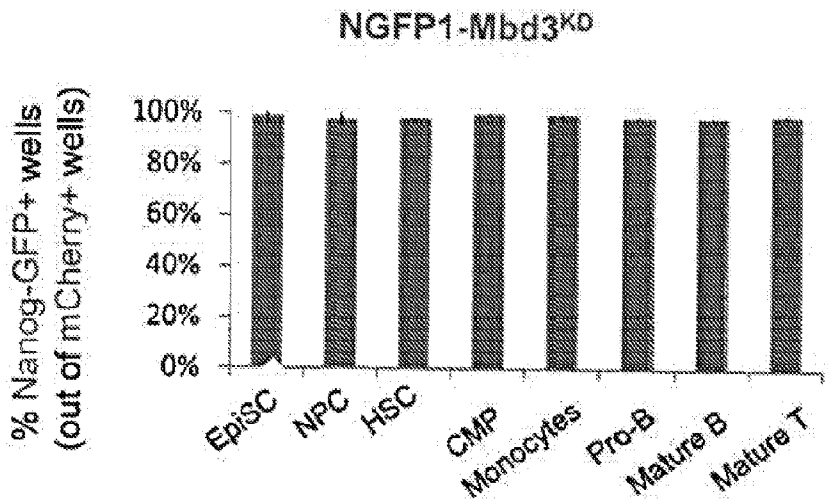

NGFP1-Mbd3KD
% Nanog-GFP+ wells
(out of mCherry+ wells)
100%
80%
60%
40%
20%
0%
EpiSC
NPC
HSC
CMP
Monocytes
Pro-B
Mature B
Mature T

FIG. 6B

FIG. 7

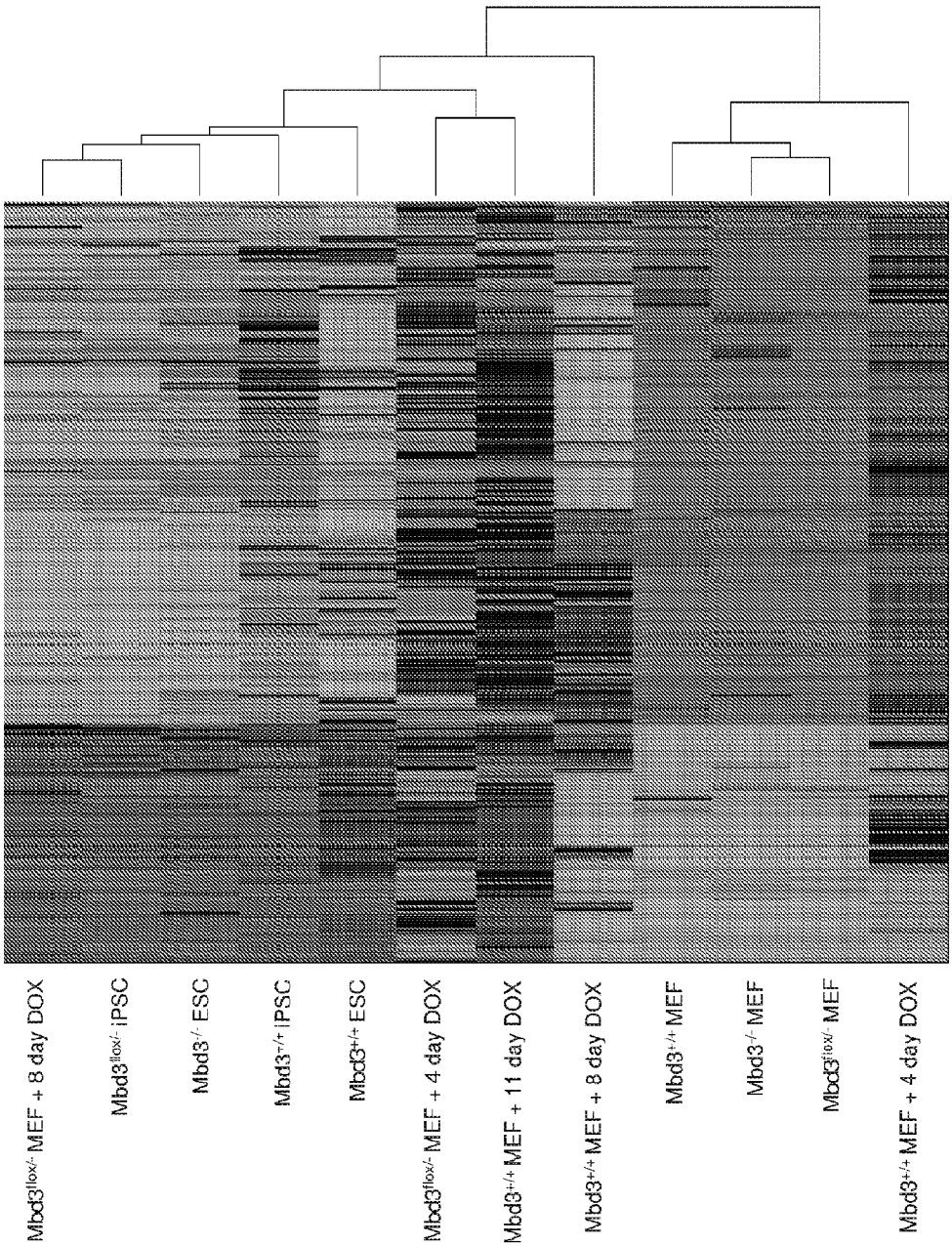

Mbd3flox/- MEF + 8 day DOX
Mbd3flox/- iPSC
Mbd3-/- ESC
Mbd3+/+ iPSC
Mbd3+/+ ESC
Mbd3flox/- MEF + 4 day DOX
Mbd3+/+ MEF + 11 day DOX
Mbd3+/+ MEF + 8 day DOX
Mbd3+/+ MEF
Mbd3-/- MEF
Mbd3flox/- MEF
Mbd3+/+ MEF + 4 day DOX

FIG. 8E

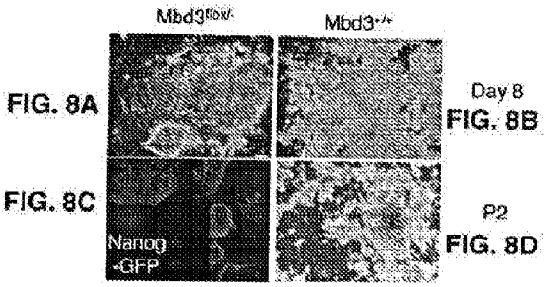


FIG. 8A

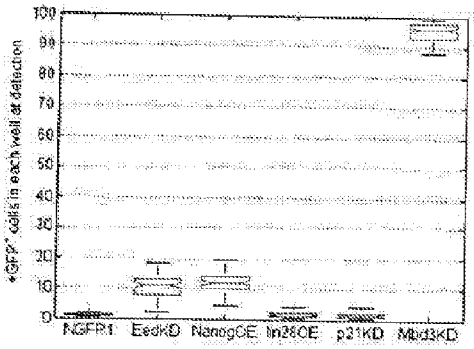
Day 8

FIG. 8B

FIG. 8C

P2

FIG. 8D



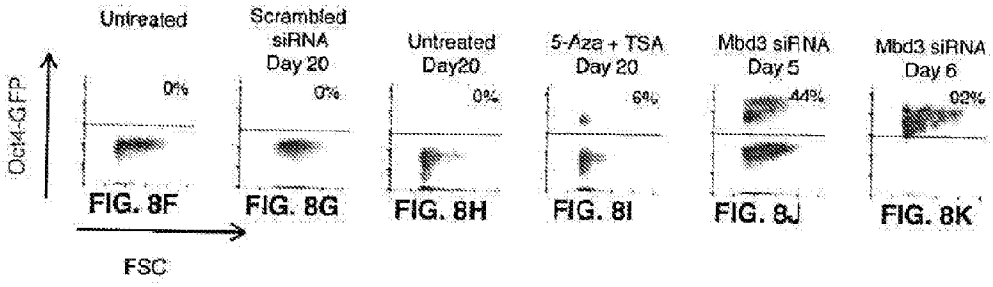
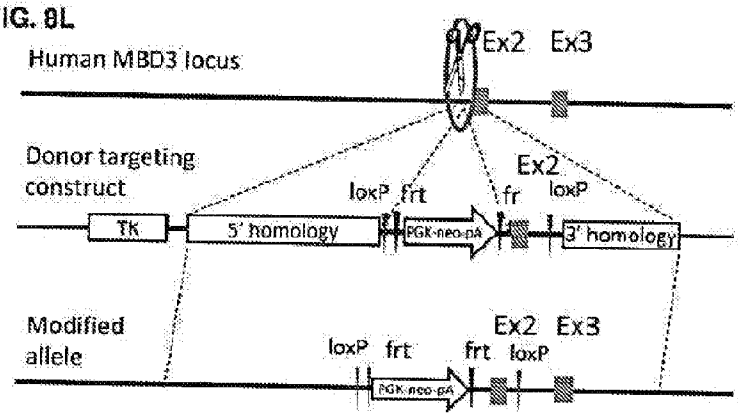


FIG. 8F FIG. 8G FIG. 8H FIG. 8I FIG. 8J FIG. 8K

FIG. 8L



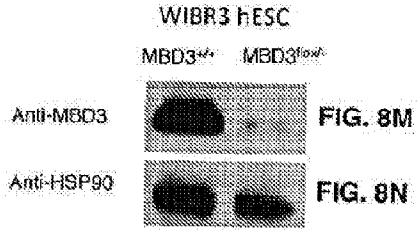


FIG. 8M

FIG. 8N

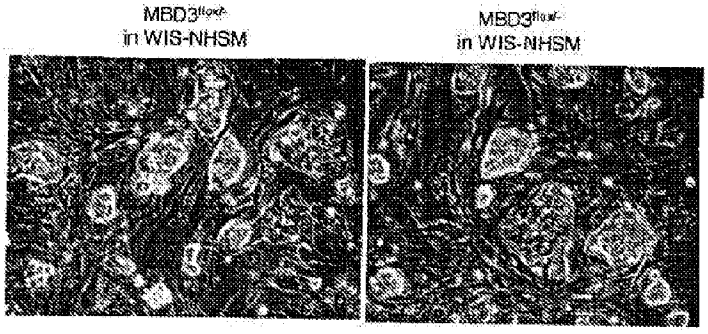


FIG. 8P FIG. 8Q

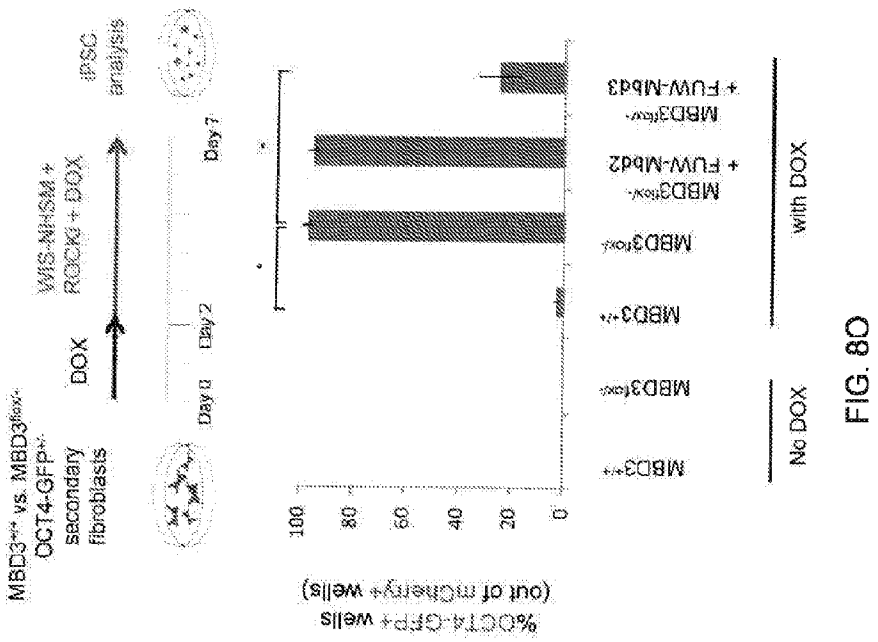

MBD3+/+ vs. MBD3flox/-
OCT4-GFP+/-
secondary fibroblasts
DOX
VitS-NHSM + ROCKi + DOX
iPSC analysis
Day 0
Day 2
Day 7
%OCT4-GFP+ wells
(out of mCherry+ wells)
100
80
60
40
20
0
MBD3+/+
MBD3flox/-
MBD3+/+
MBD3flox/-
+ FUW-Mb42
MBD3flox/-
+ FUW-Mb43
No DOX
with DOX

FIG. 8O

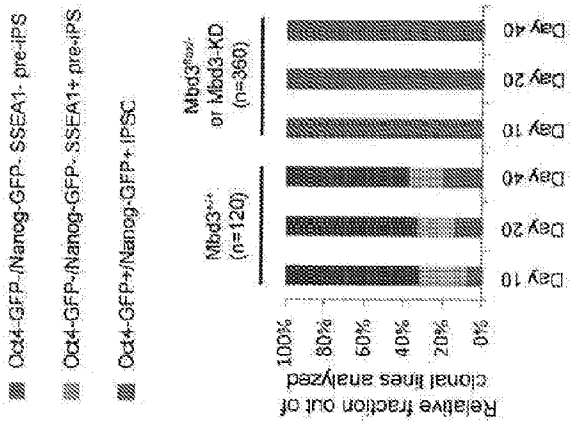

Oct4-GFP-/Nanog-GFP- SSEA1- pre-iPS
Oct4-GFP-/Nanog-GFP- SSEA1+ pre-iPS
Oct4-GFP+/Nanog-GFP+ iPSC
Mbd3+/+ (n=120)
Mbd3flox/- or Mbd3-KD (n=360)
Day 10
Day 20
Day 40
Day 10
Day 20
Day 40
100%
80%
60%
40%
20%
0%
Relative fraction out of clonal lines analyzed

FIG. 8S

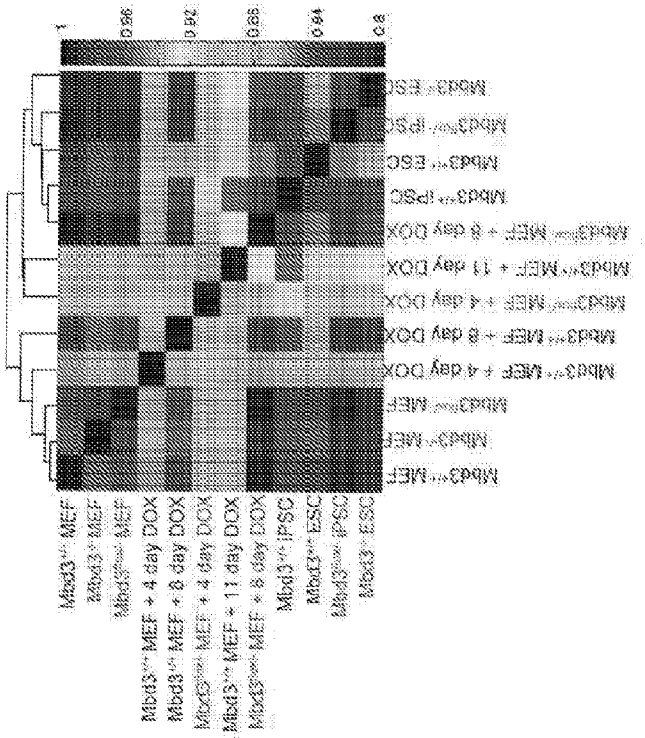

1
0.96
0.92
0.88
0.84
0.8
Mbd3+/+ MEF
Mbd3flox/- MEF
Mbd3-/- MEF
Mbd3+/+ MEF + 4 day DOX
Mbd3+/+ MEF + 8 day DOX
Mbd3flox/- MEF + 4 day DOX
Mbd3+/+ MEF + 11 day DOX
Mbd3flox/- MEF + 8 day DOX
Mbd3+/+ iPSC
Mbd3+/+ ESC
Mbd3flox/- iPSC
Mbd3-/- ESC
Mbd3-/- MEF
Mbd3+/+ MEF
Mbd3flox/- MEF
Mbd3-/- MEF + 4 day DOX
Mbd3-/- MEF + 8 day DOX
Mbd3flox/- MEF + 4 day DOX
Mbd3-/- MEF + 11 day DOX
Mbd3flox/- MEF + 8 day DOX
Mbd3-/- iPSC
Mbd3-/- ESC
Mbd3flox/- iPSC
Mbd3+/+ ESC

FIG. 8R

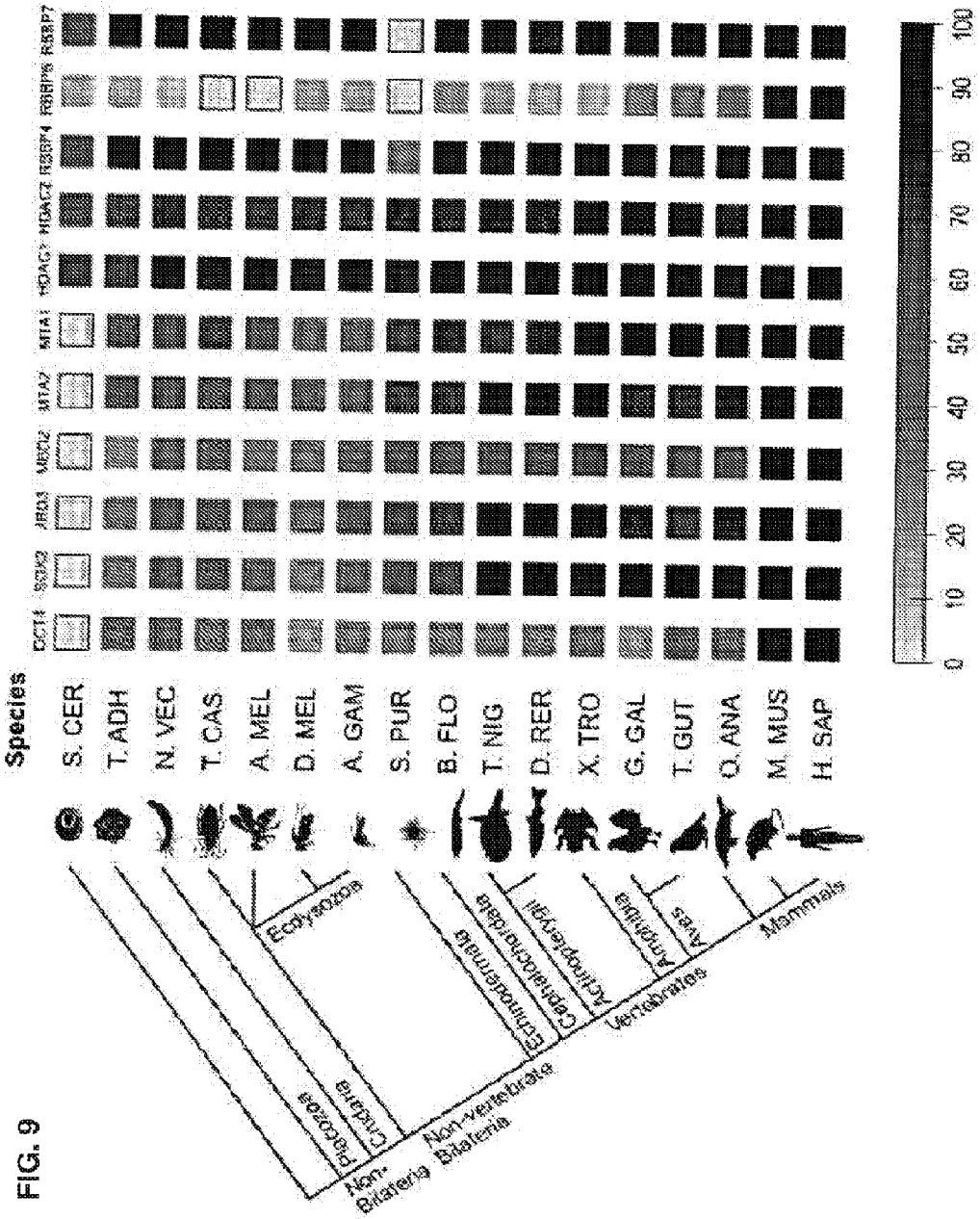

RBBP7
RBBP4
HDAC2
HDAC1
MTA2
MTA1
MBD2
JARID1
SOX2
OCT4
Species
S. CER
T. ADH
N. VEC
T. CAS
A. MEL
D. MEL
A. GAM
S. PUR
B. FLO
T. NIG
D. RER
X. TRO
G. GAL
T. GUT
O. ANA
M. MUS
H. SAP
0
10
20
30
40
50
60
70
80
90
100
Ecdysozoa
Echinodermata
Chordata
Cephalochordata
Actinopterygii
Amphibia
Aves
Mammals
Protozoa
Non-Bilateria
Non-vertebrate Bilateria
Vertebrates

FIG. 9

FIG. 10A

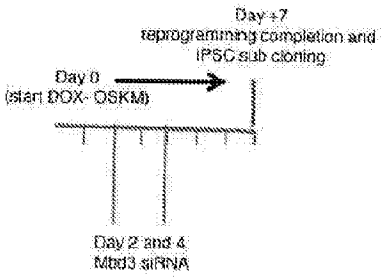
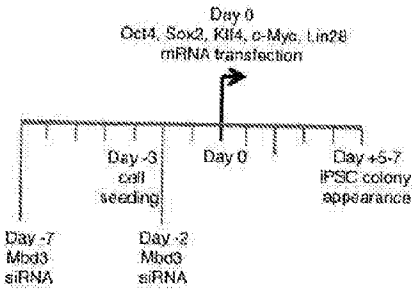


FIG. 10E



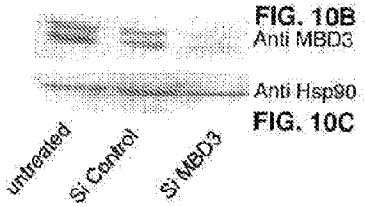


FIG. 10B

FIG. 10C

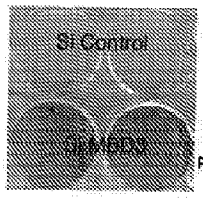
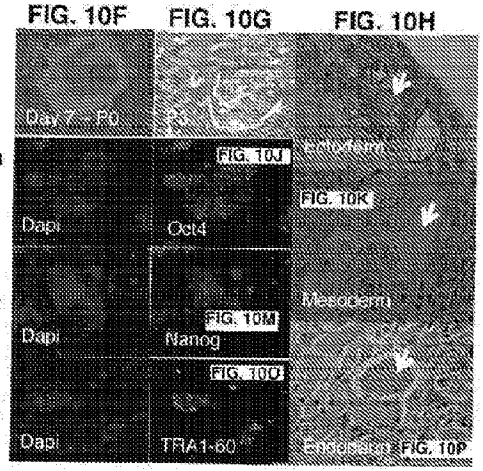


FIG. 10D

FIG. 10F FIG. 10G FIG. 10H



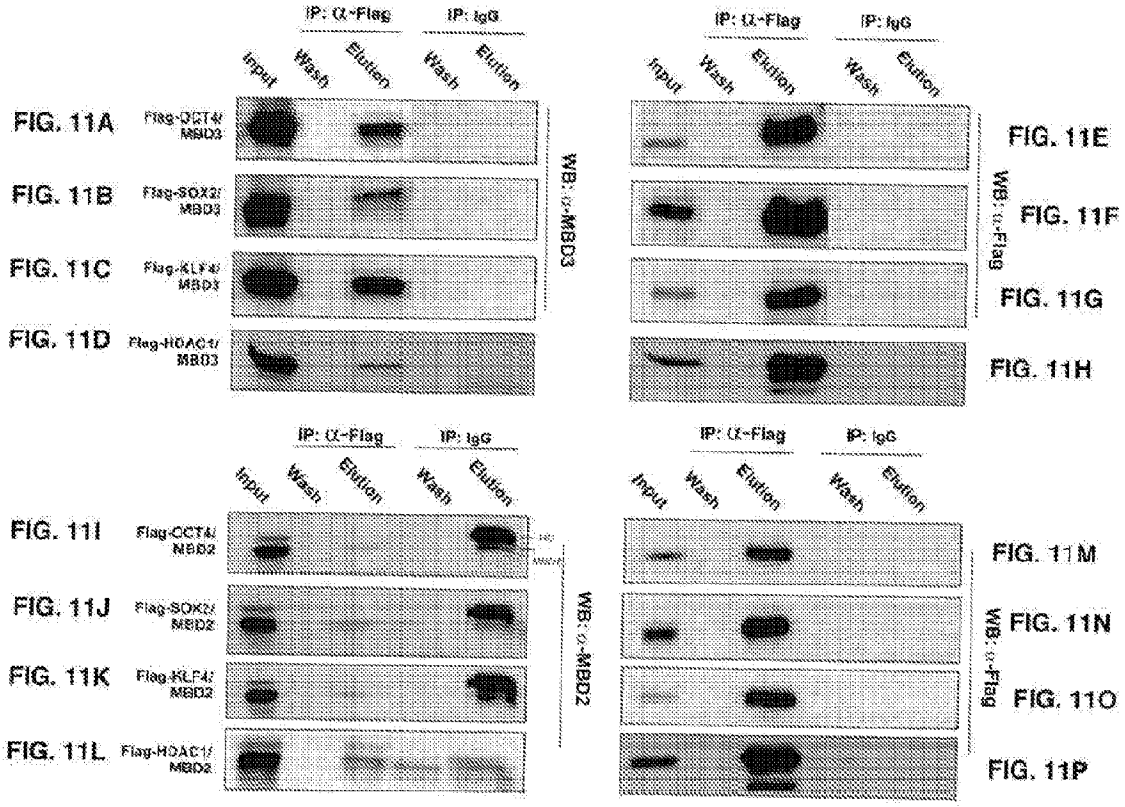

IP: α-Flag
IP: IgG
Input
Wash
Elution
Wash
Elution
FIG. 11A
Flag-OCT4/ MBD3
FIG. 11B
Flag-SOX2/ MBD3
FIG. 11C
Flag-KLF4/ MBD3
FIG. 11D
Flag-HDAC1/ MBD3
WB: α-MBD3
FIG. 11E
FIG. 11F
FIG. 11G
FIG. 11H
WB: α-Flag
FIG. 11I
Flag-OCT4/ MBD2
FIG. 11J
Flag-SOX2/ MBD2
FIG. 11K
Flag-KLF4/ MBD2
FIG. 11L
Flag-HDAC1/ MBD2
WB: α-MBD2
FIG. 11M
FIG. 11N
FIG. 11O
FIG. 11P
WB: α-Flag

FIG. 12A

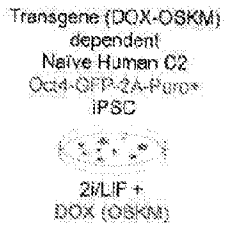


FIG. 12B FIG. 12C

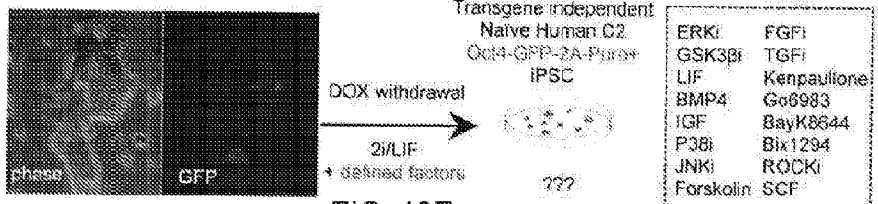


FIG. 12E

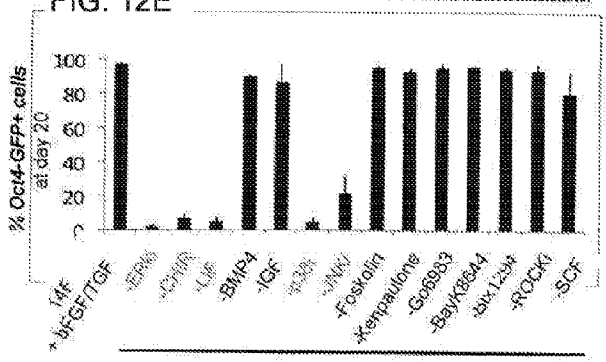


FIG. 12F

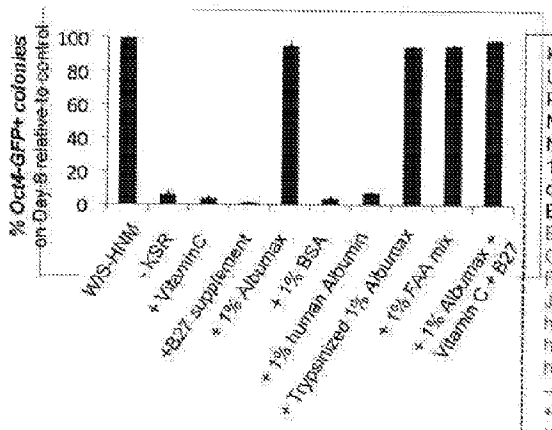


FIG. 12G

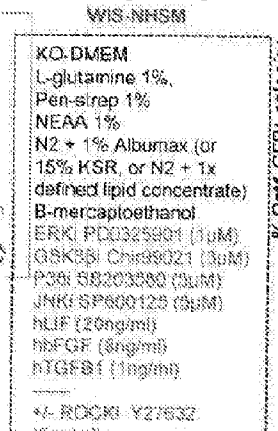


FIG. 12H

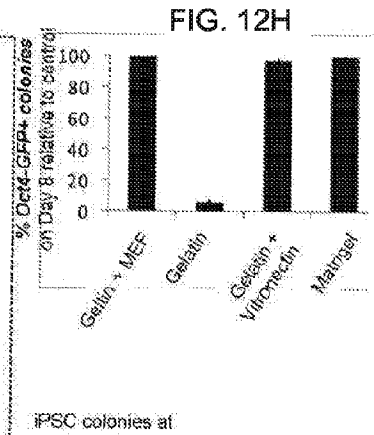


FIG. 12I

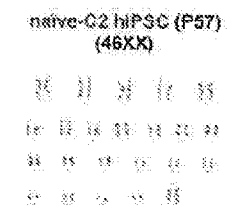


FIG. 12J FIG. 12L

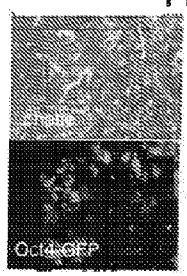


FIG. 12K

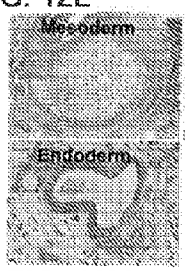


FIG. 12M

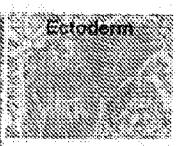


FIG. 12N

iPSC colonies at day 6 DOX In WIS-NHSMP3

FIG. 12O FIG. 12Q

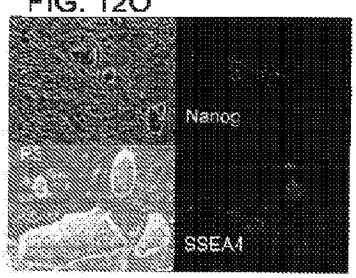


FIG. 12P FIG. 12R

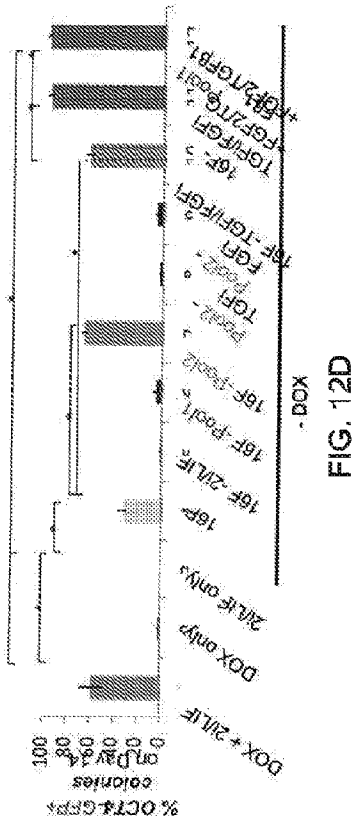


FIG. 12D

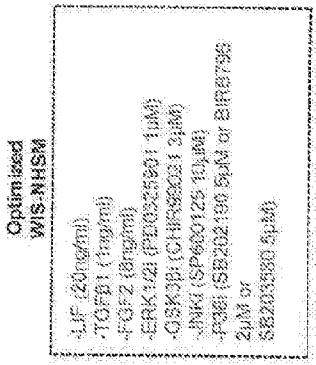


FIG. 12T

FIG. 12S

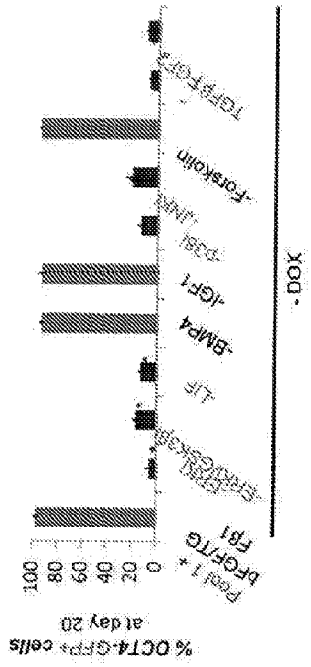


FIG. 12U

WIS-NHSM

Essential components:
LIF (20ng/ml)
TGFβ1 (1ng/ml)
FGF2 (8ng/ml)
ERK1/2i (PD0325901 1μM)
GSK3βi (CHIR99021 3μM)
JNKi (SP600125 10μM)
P38i (SB203580 10μM)

Optimizing components:
ROCKi (Y-27632 5μM)
PKCi (Go6983 5μM)

FIG. 12V

C1.2 hiPSC (P51 in WIS-NHSM conditions

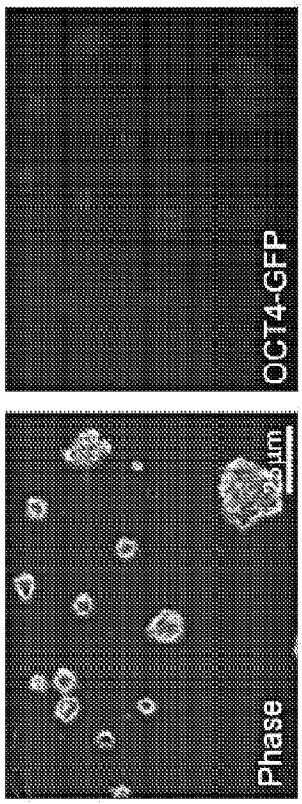


FIG. 13A

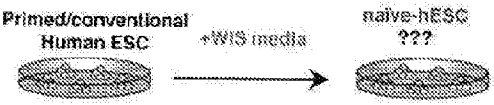


FIG. 13B

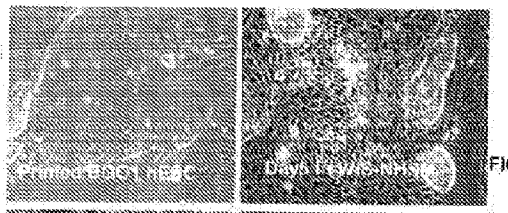


FIG. 13D

FIG. 13C

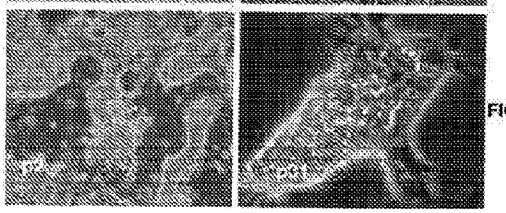


FIG. 13E

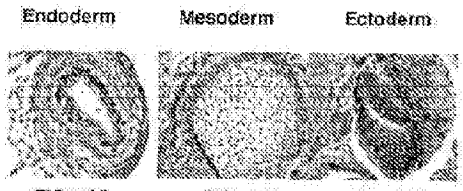


FIG. 13S FIG. 13T FIG. 13U

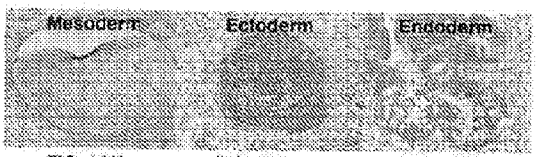
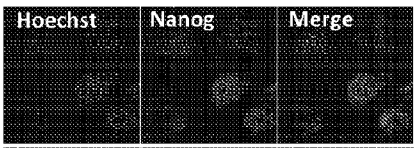


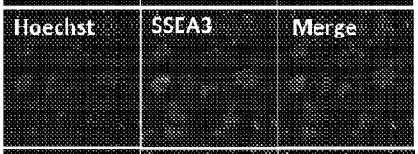
FIG. 13K FIG. 13L FIG. 13M

FIG. 13F



naïve-BGO1 hESC

FIG. 13G



Pasage 41 (46XY)

FIG. 13H

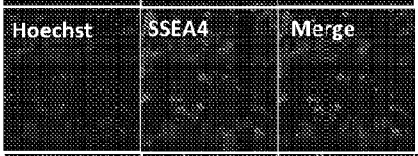


FIG. 13I

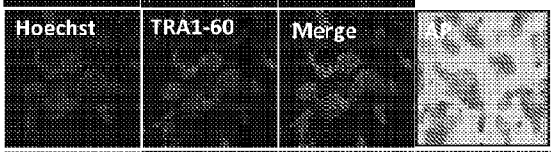
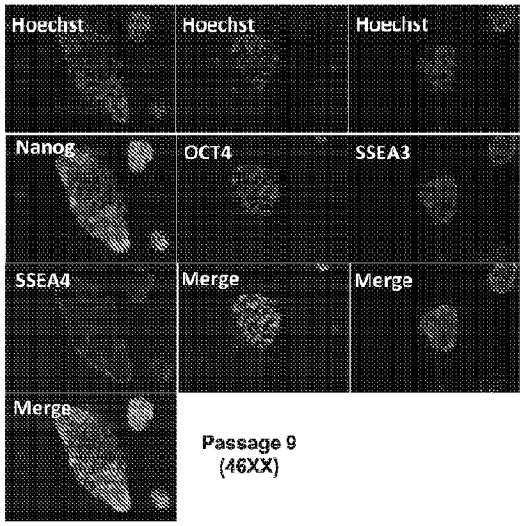


FIG. 13J



naïve-WIS1 hESC

FIG. 13P FIG. 13Q FIG. 13R



Passage 9 (46XX)

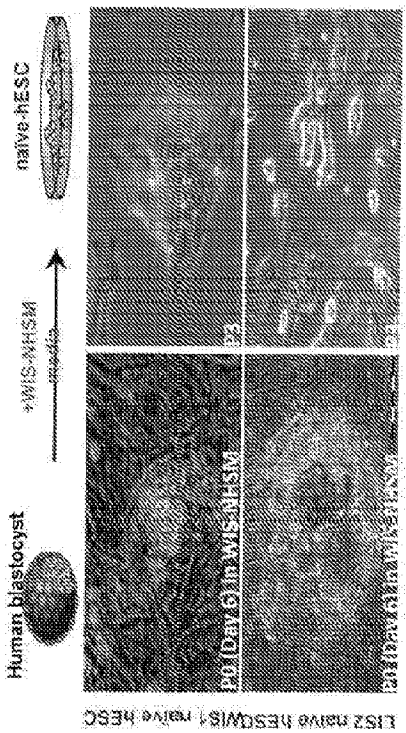


FIG. 13N

FIG. 13O

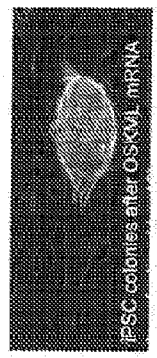


FIG. 13V

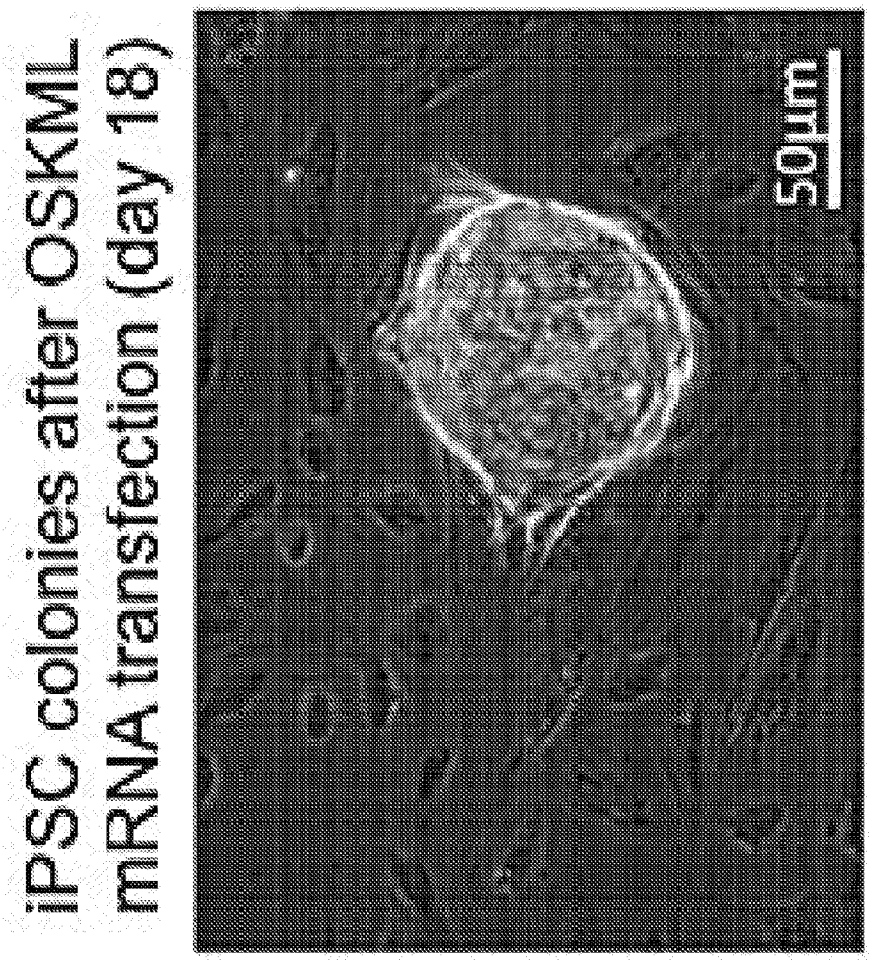


FIG. 13W

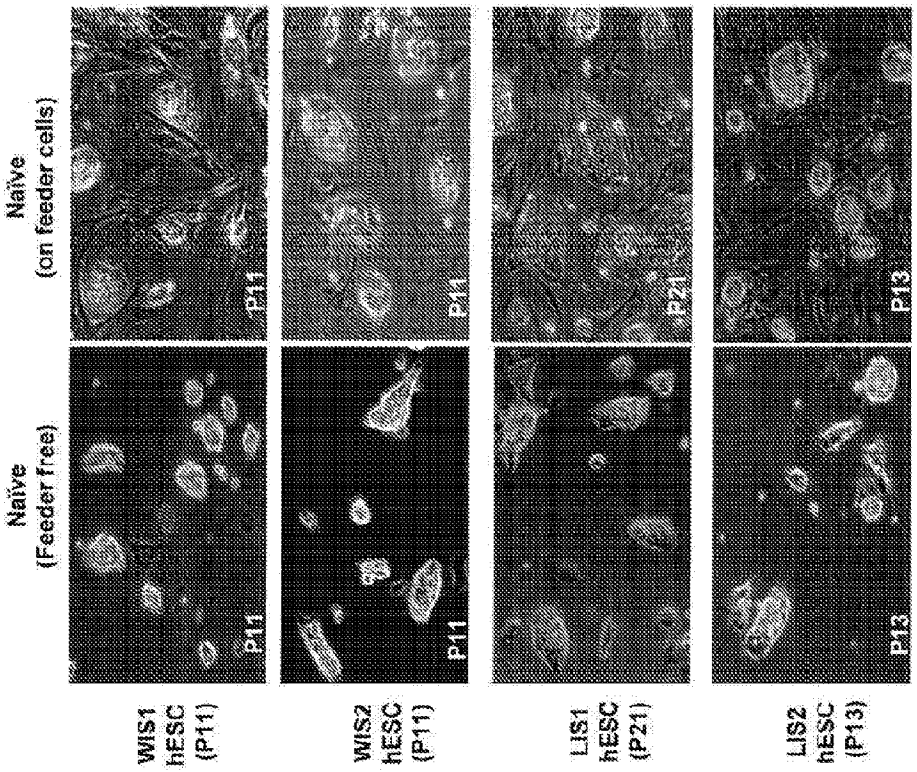


FIG. 14A FIG. 14B

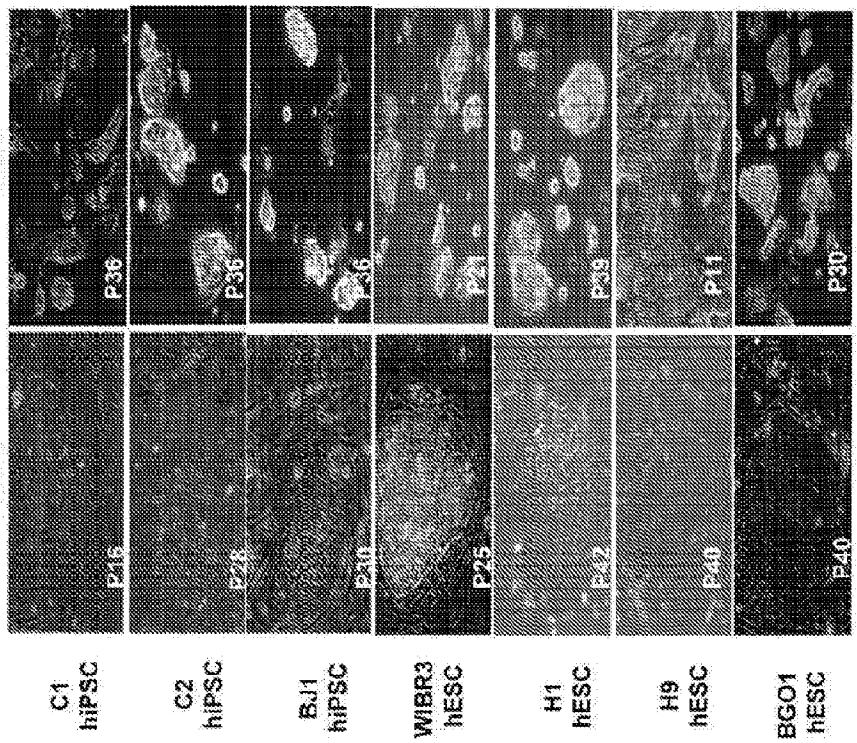


FIG. 14C FIG. 14D

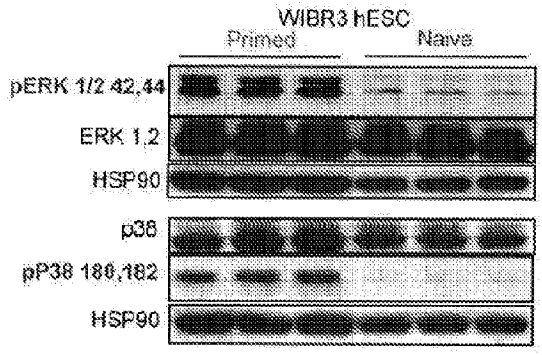


FIG. 15A
FIG. 15B
FIG. 15C
FIG. 15D
FIG. 15E
FIG. 15F

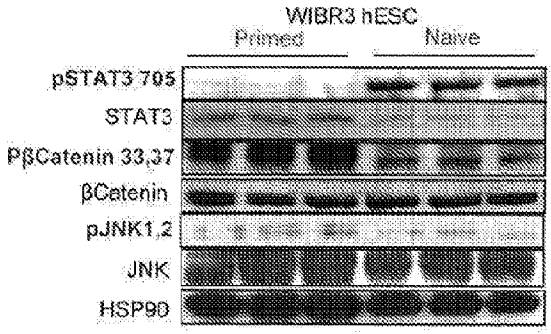


FIG. 15G
FIG. 15H
FIG. 15I
FIG. 15J
FIG. 15K
FIG. 15L
FIG. 15M

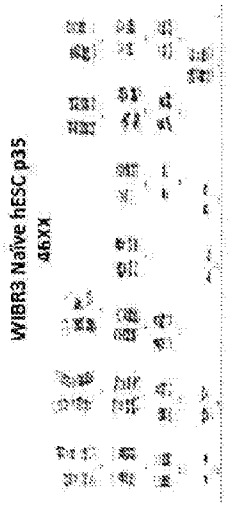


FIG. 15N



FIG. 15O

FIG. 15P



FIG. 15Q

FIG. 15R

FIG. 15S

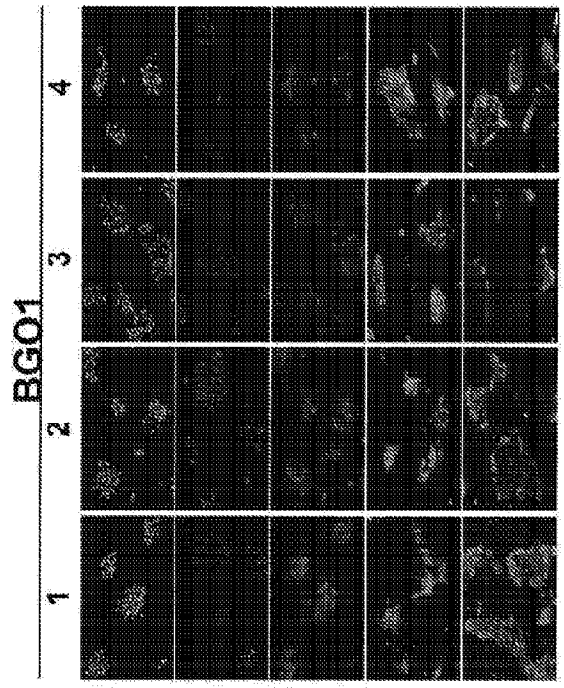


FIG. 15U

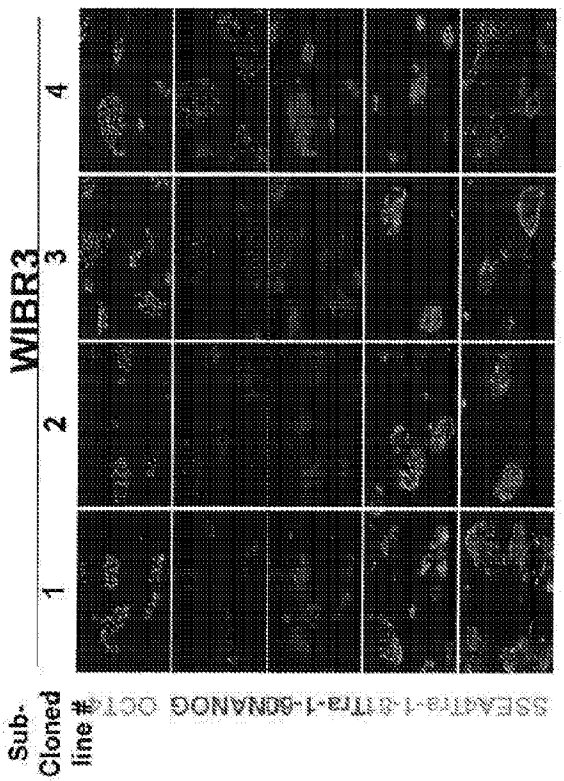
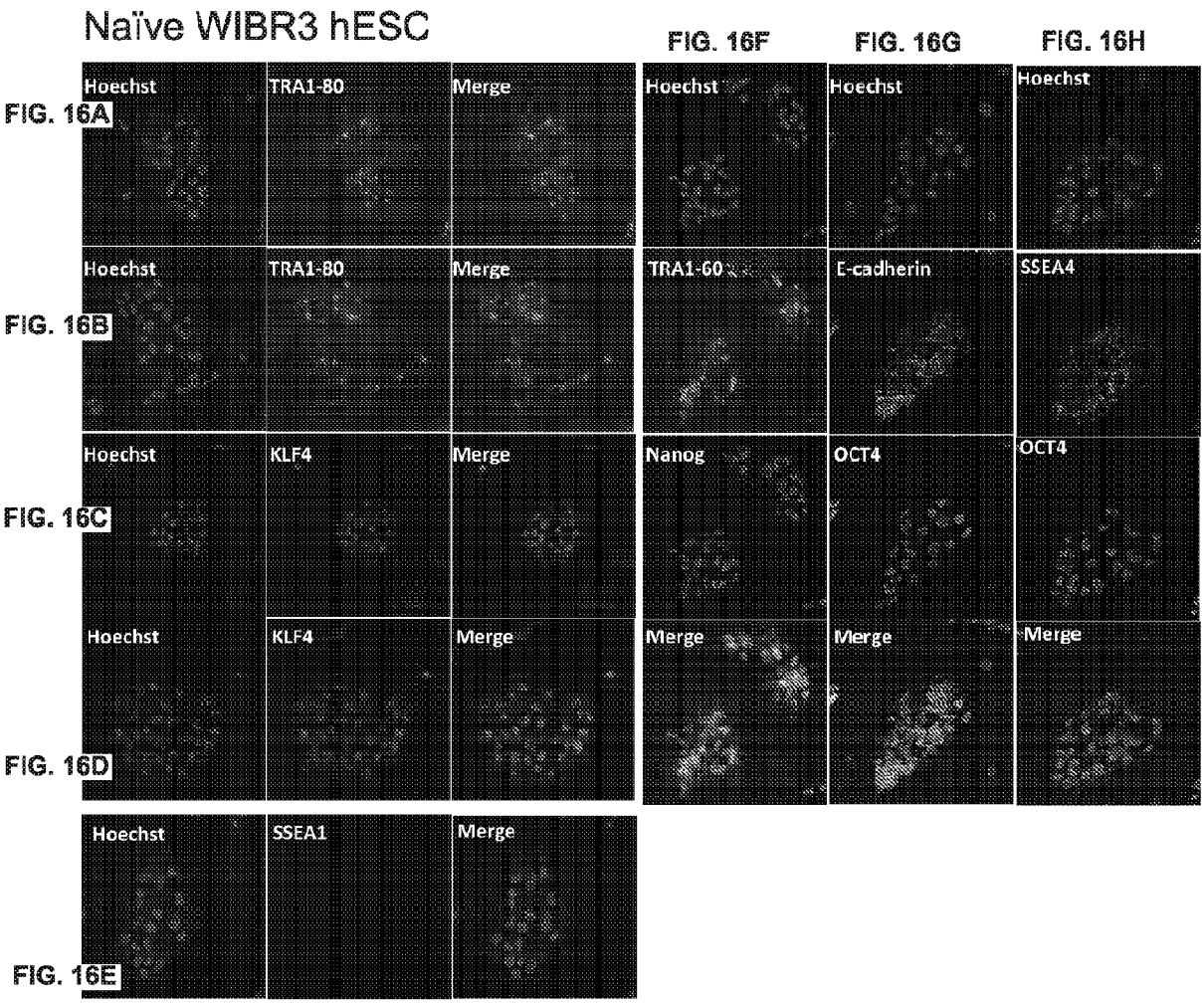
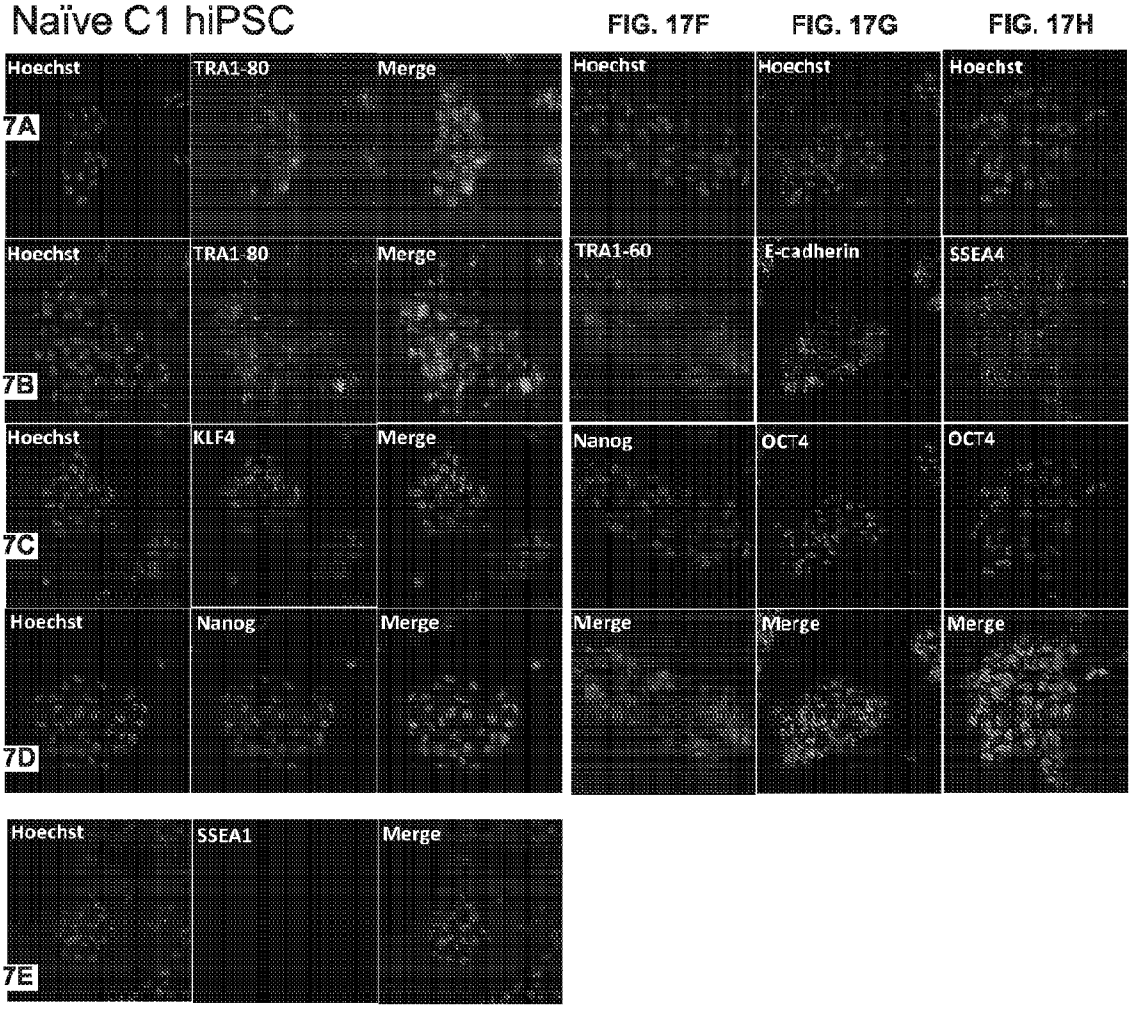


FIG. 15T


Naïve WIBR3 hESC
FIG. 16A
Hoechst
TRA1-80
Merge
FIG. 16B
Hoechst
TRA1-80
Merge
FIG. 16C
Hoechst
KLF4
Merge
FIG. 16D
Hoechst
KLF4
Merge
FIG. 16E
Hoechst
SSEA1
Merge
FIG. 16F
Hoechst
TRA1-60
Nanog
Merge
FIG. 16G
Hoechst
E-cadherin
OCT4
Merge
FIG. 16H
Hoechst
SSEA4
OCT4
Merge


Naïve C1 hiPSC
FIG. 17F
FIG. 17G
FIG. 17H
FIG. 17A
Hoechst
TRA1-80
Merge
Hoechst
Hoechst
Hoechst
FIG. 17B
Hoechst
TRA1-80
Merge
TRA1-60
E-cadherin
SSEA4
FIG. 17C
Hoechst
KLF4
Merge
Nanog
OCT4
OCT4
FIG. 17D
Hoechst
Nanog
Merge
Merge
Merge
Merge
FIG. 17E
Hoechst
SSEA1
Merge

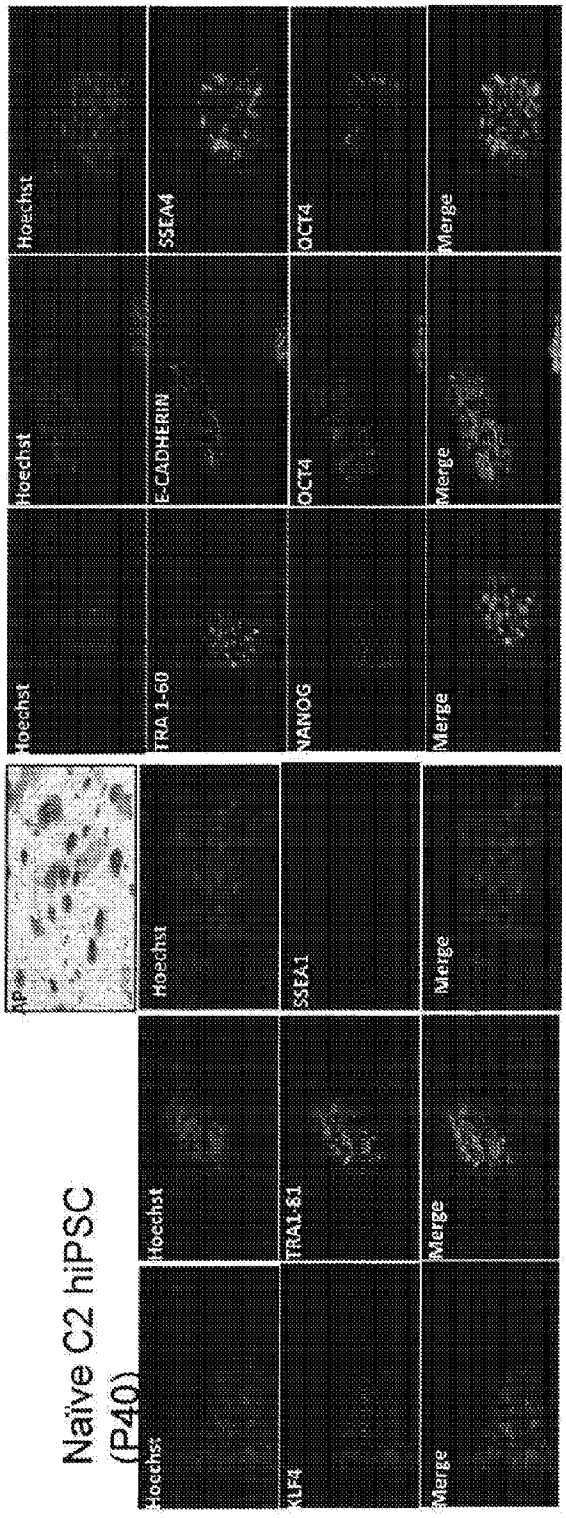
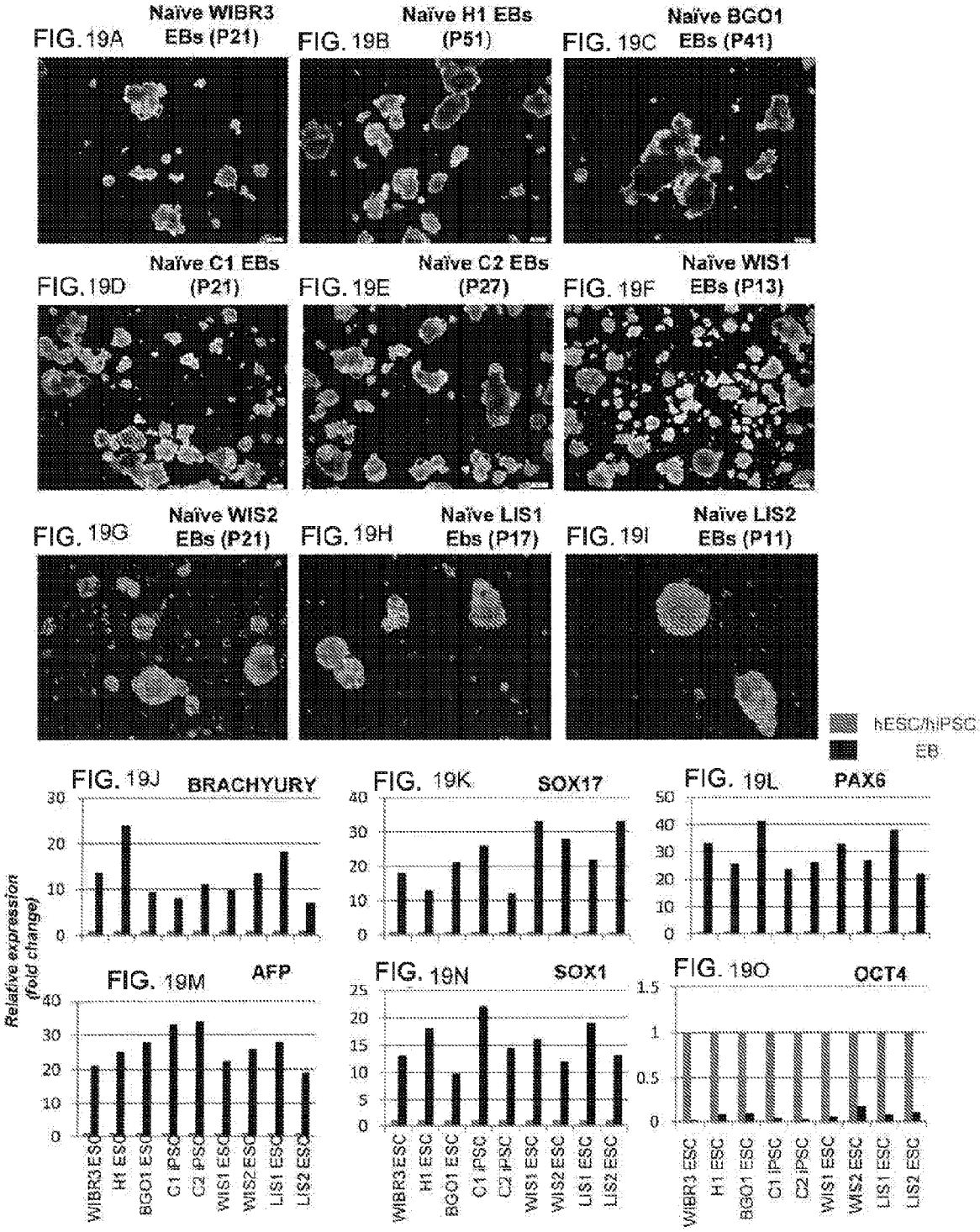


FIG. 18A FIG. 18B FIG. 18C FIG. 18D FIG. 18E FIG. 18F


FIG. 19A
Naïve WIBR3 EBs (P21)
FIG. 19B
Naïve H1 EBs (P51)
FIG. 19C
Naïve BGO1 EBs (P41)
FIG. 19D
Naïve C1 EBs (P21)
FIG. 19E
Naïve C2 EBs (P27)
FIG. 19F
Naïve WIS1 EBs (P13)
FIG. 19G
Naïve WIS2 EBs (P21)
FIG. 19H
Naïve LIS1 Ebs (P17)
FIG. 19I
Naïve LIS2 EBs (P11)
hESC/hiPSC
EB
FIG. 19J BRACHYURY
FIG. 19K SOX17
FIG. 19L PAX6
FIG. 19M AFP
FIG. 19N SOX1
FIG. 19O OCT4
Relative expression (fold change)
WIBR3 ESC
H1 ESC
BGO1 ESC
C1 iPSC
C2 iPSC
WIS1 ESC
WIS2 ESC
LIS1 ESC
LIS2 ESC

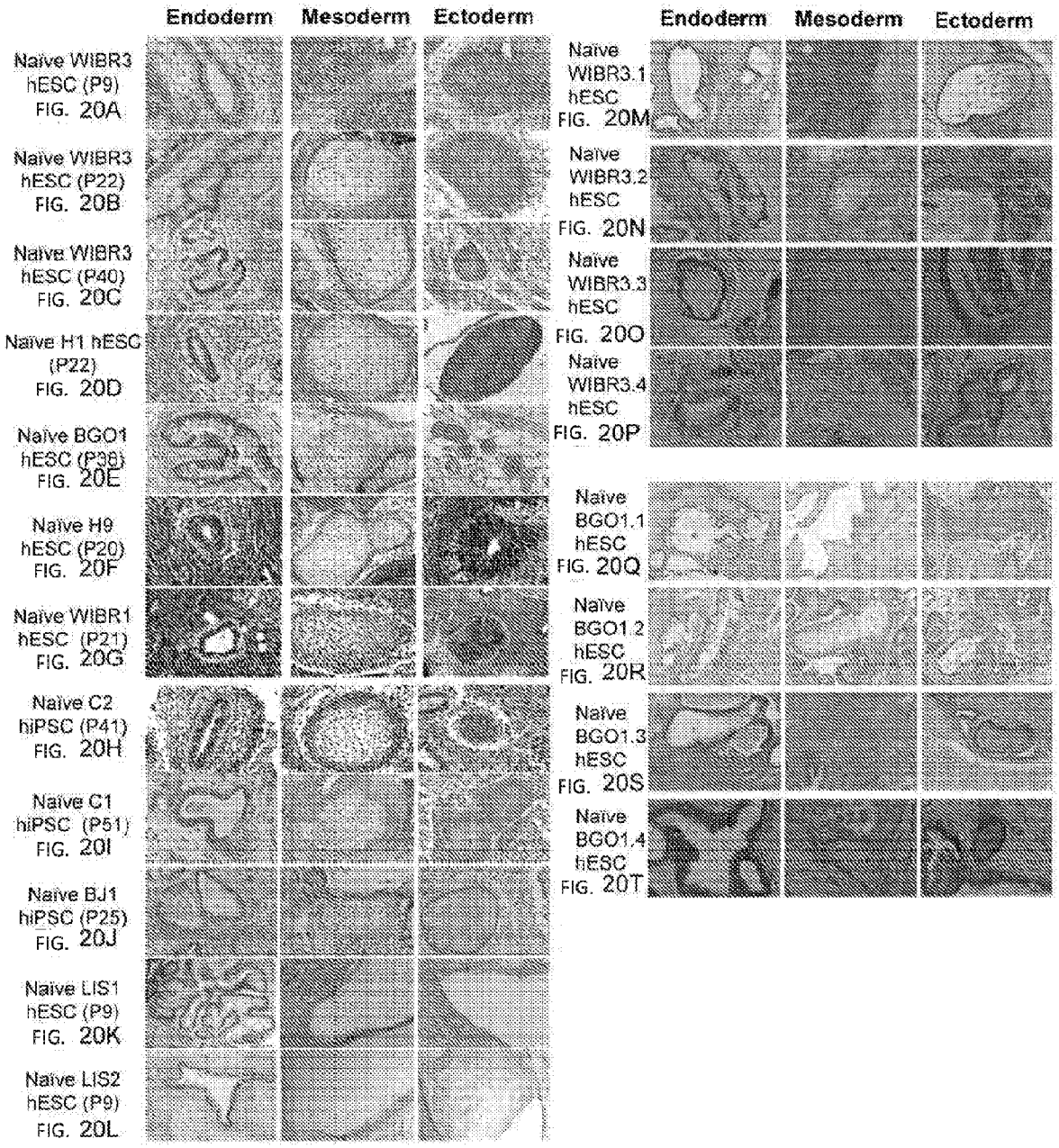

Endoderm
Mesoderm
Ectoderm
Naive WIBR3 hESC (P9) FIG. 20A
Naive WIBR3 hESC (P22) FIG. 20B
Naive WIBR3 hESC (P40) FIG. 20C
Naive H1 hESC (P22) FIG. 20D
Naive BGO1 hESC (P36) FIG. 20E
Naive H9 hESC (P20) FIG. 20F
Naive WIBR1 hESC (P21) FIG. 20G
Naive C2 hiPSC (P41) FIG. 20H
Naive C1 hiPSC (P51) FIG. 20I
Naive BJ1 hiPSC (P25) FIG. 20J
Naive LIS1 hESC (P9) FIG. 20K
Naive LIS2 hESC (P9) FIG. 20L
Endoderm
Mesoderm
Ectoderm
Naive WIBR3.1 hESC FIG. 20M
Naive WIBR3.2 hESC FIG. 20N
Naive WIBR3.3 hESC FIG. 20O
Naive WIBR3.4 hESC FIG. 20P
Naive BGO1.1 hESC FIG. 20Q
Naive BGO1.2 hESC FIG. 20R
Naive BGO1.3 hESC FIG. 20S
Naive BGO1.4 hESC FIG. 20T

FIG. 21A

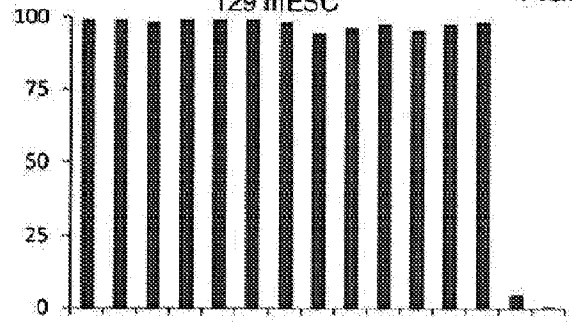


FIG. 21B

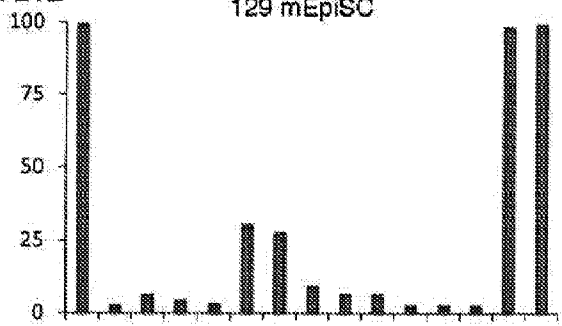


FIG. 21C

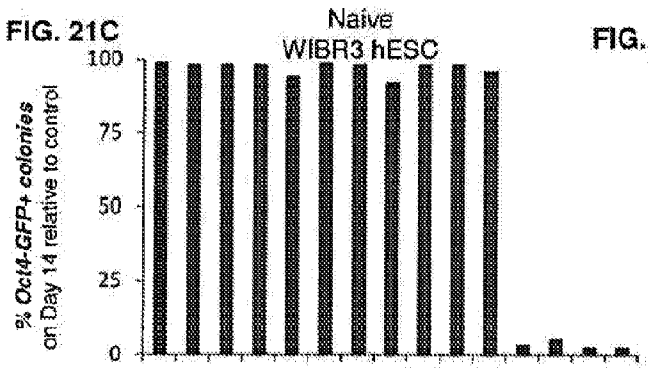


FIG. 21D

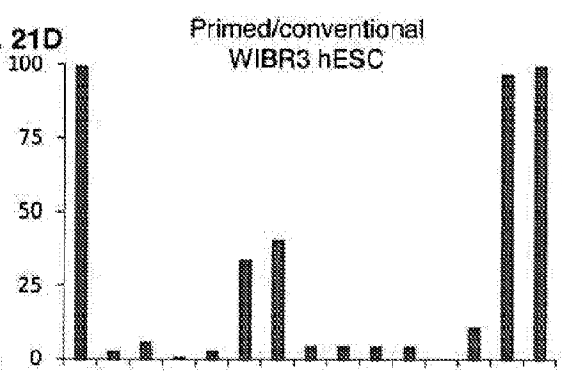


FIG. 21E

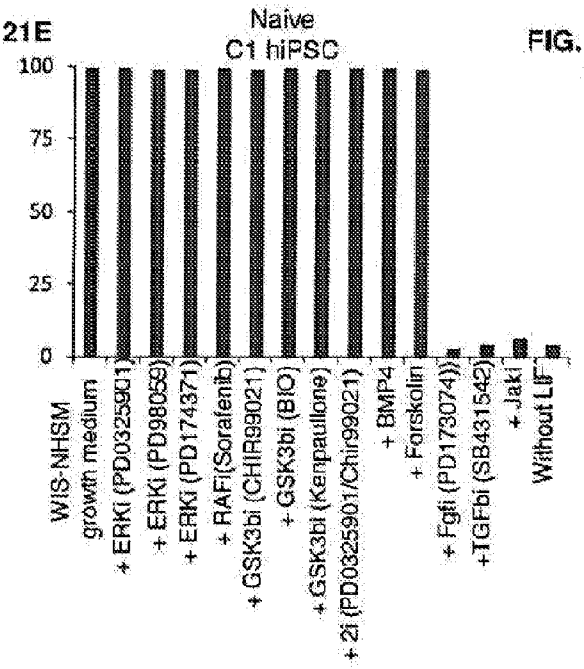


FIG. 21F

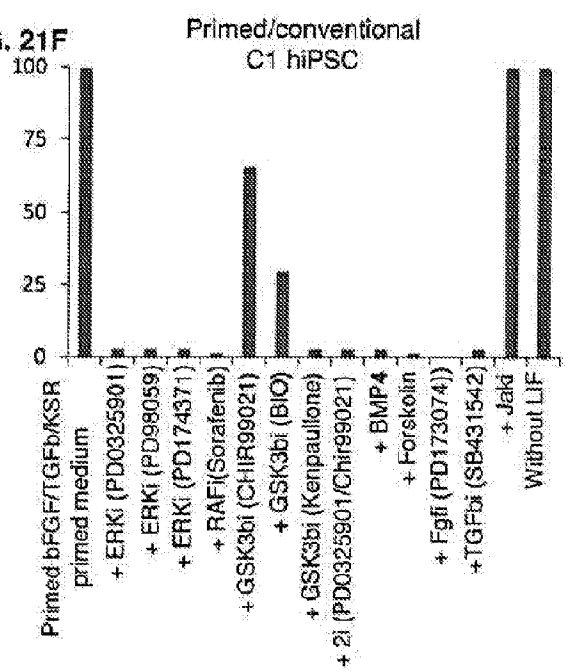


FIG. 21G

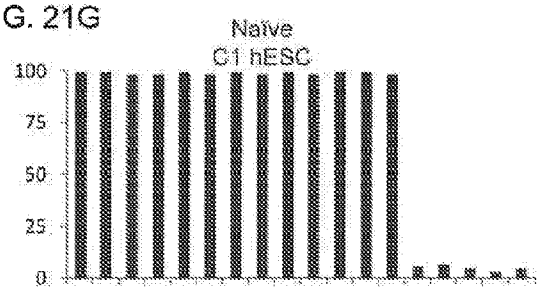


FIG. 21H

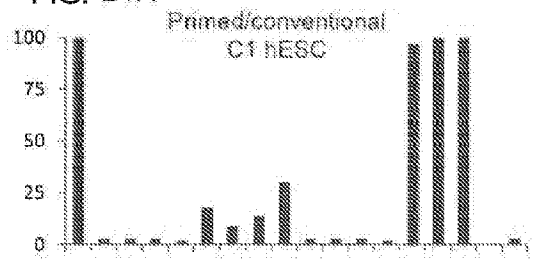


FIG. 21I

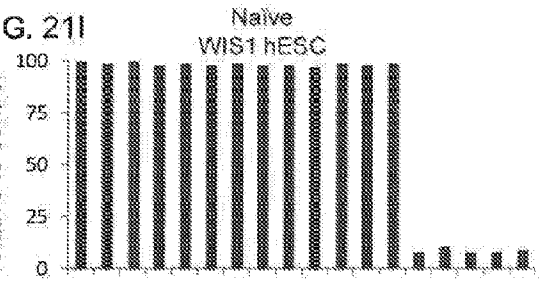


FIG. 21J

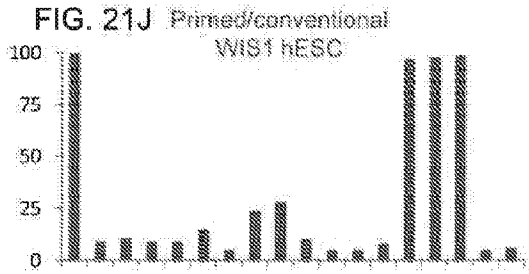


FIG. 21K

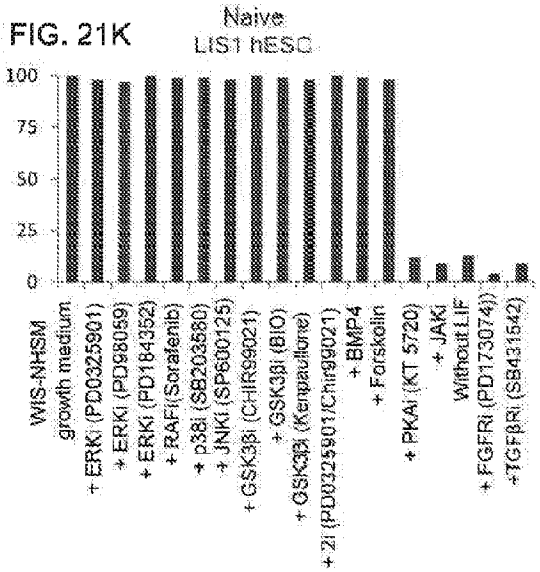
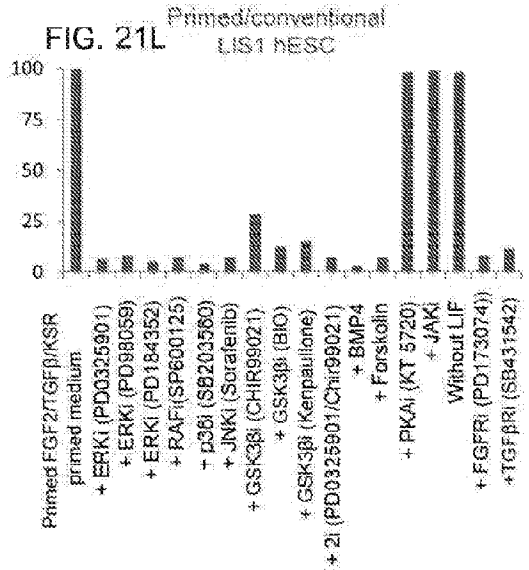


FIG. 21L



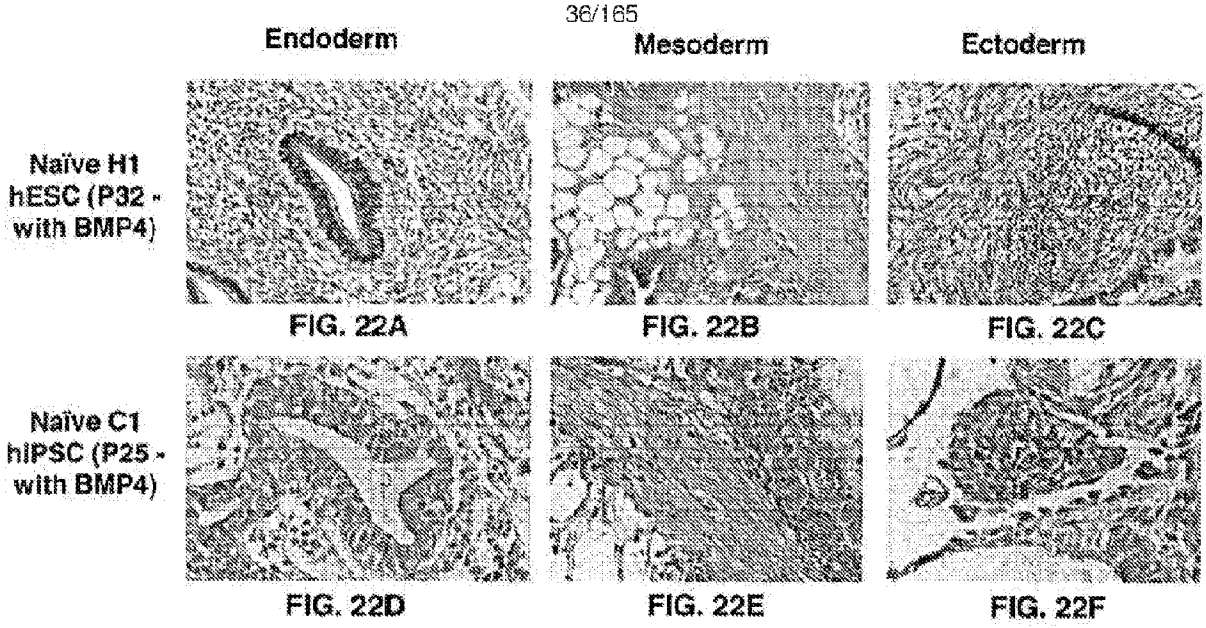


FIG. 22A FIG. 22B FIG. 22C

FIG. 22D FIG. 22E FIG. 22F

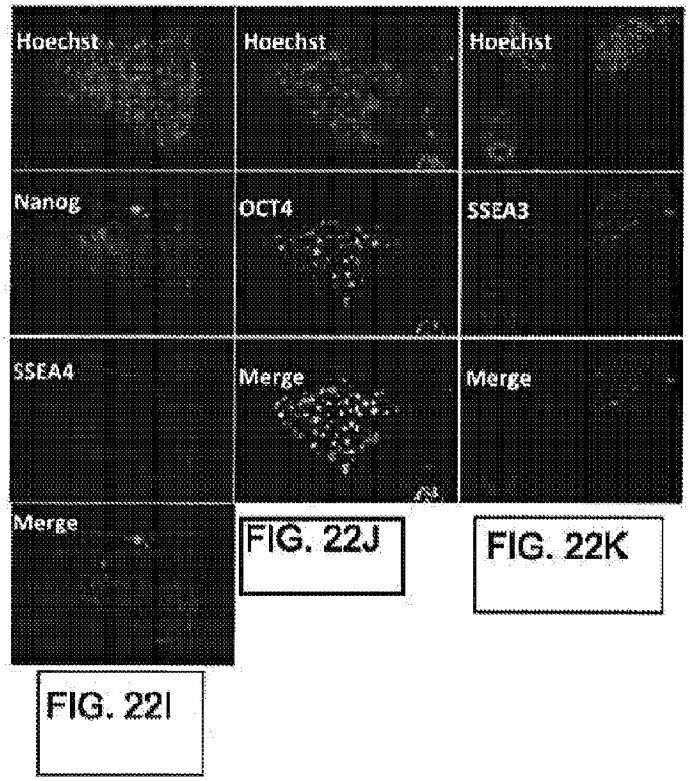
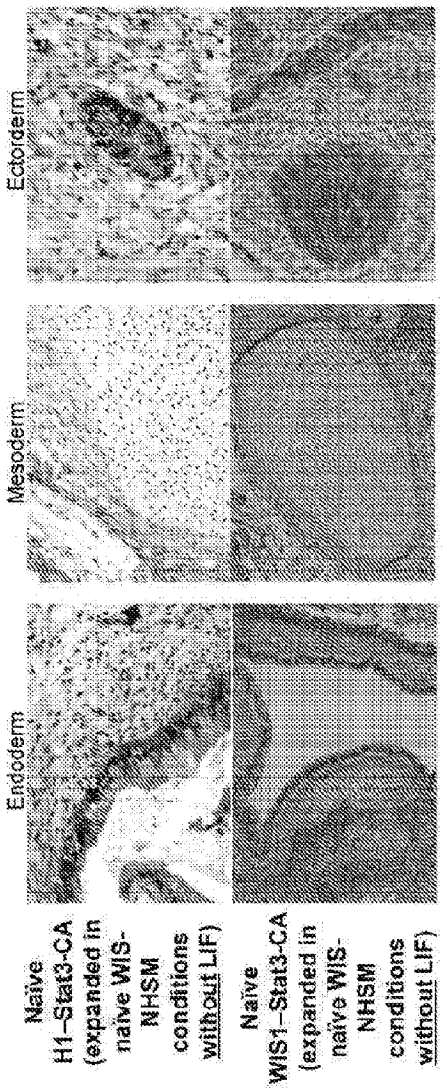


FIG. 22J

FIG. 22K

FIG. 22I

FIG. 22G FIG. 22H



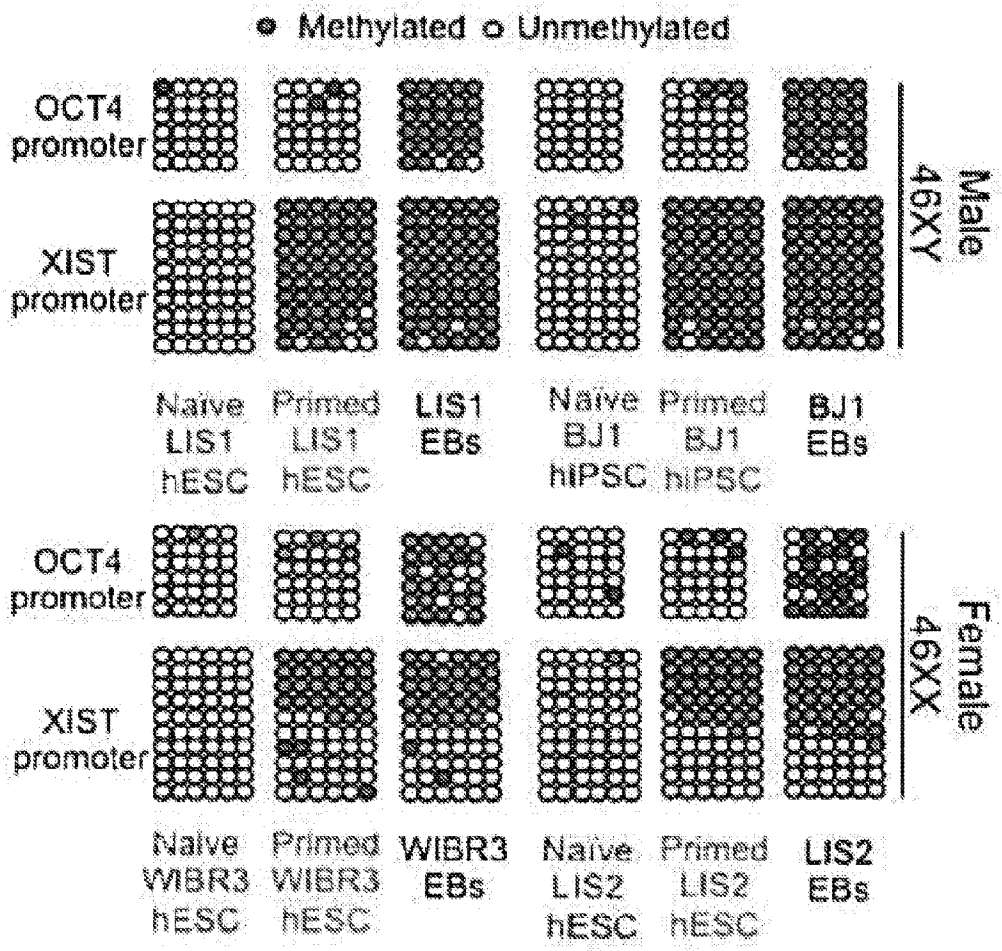
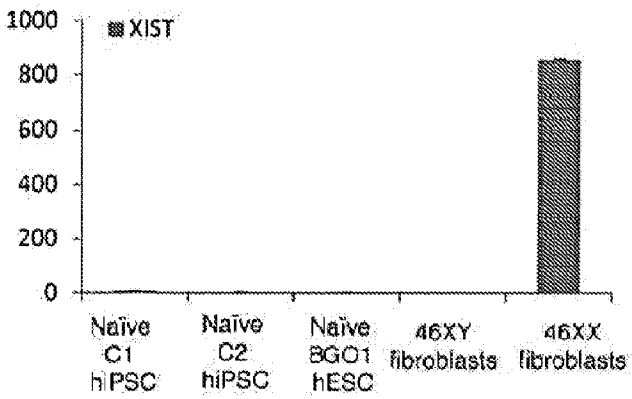

Methylated
Unmethylated
OCT4 promoter
XIST promoter
Male 46XY
Naive LIS1 hESC
Primed LIS1 hESC
LIS1 EBs
Naive BJ1 hiPSC
Primed BJ1 hiPSC
BJ1 EBs
OCT4 promoter
XIST promoter
Female 46XX
Naive WIBR3 hESC
Primed WIBR3 hESC
WIBR3 EBs
Naive LIS2 hESC
Primed LIS2 hESC
LIS2 EBs

FIG. 23A

FIG. 23B



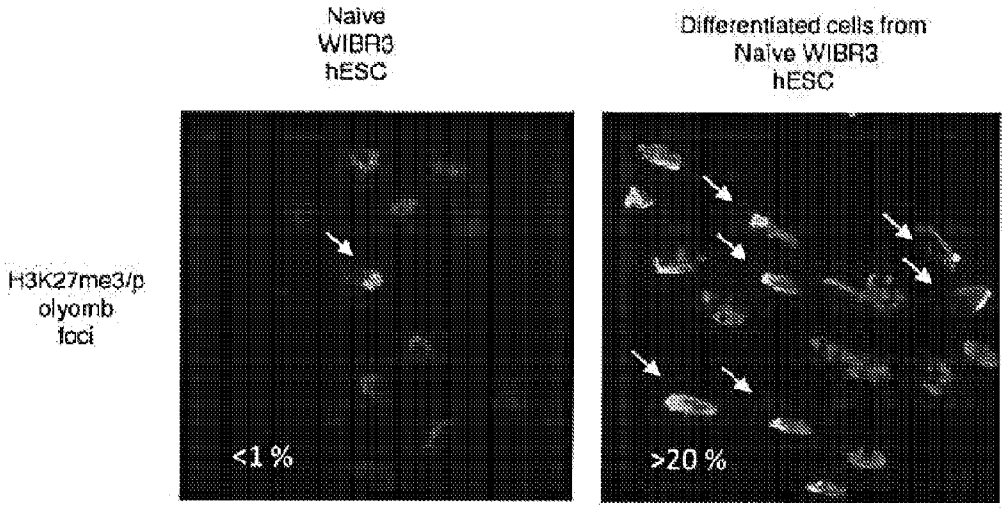
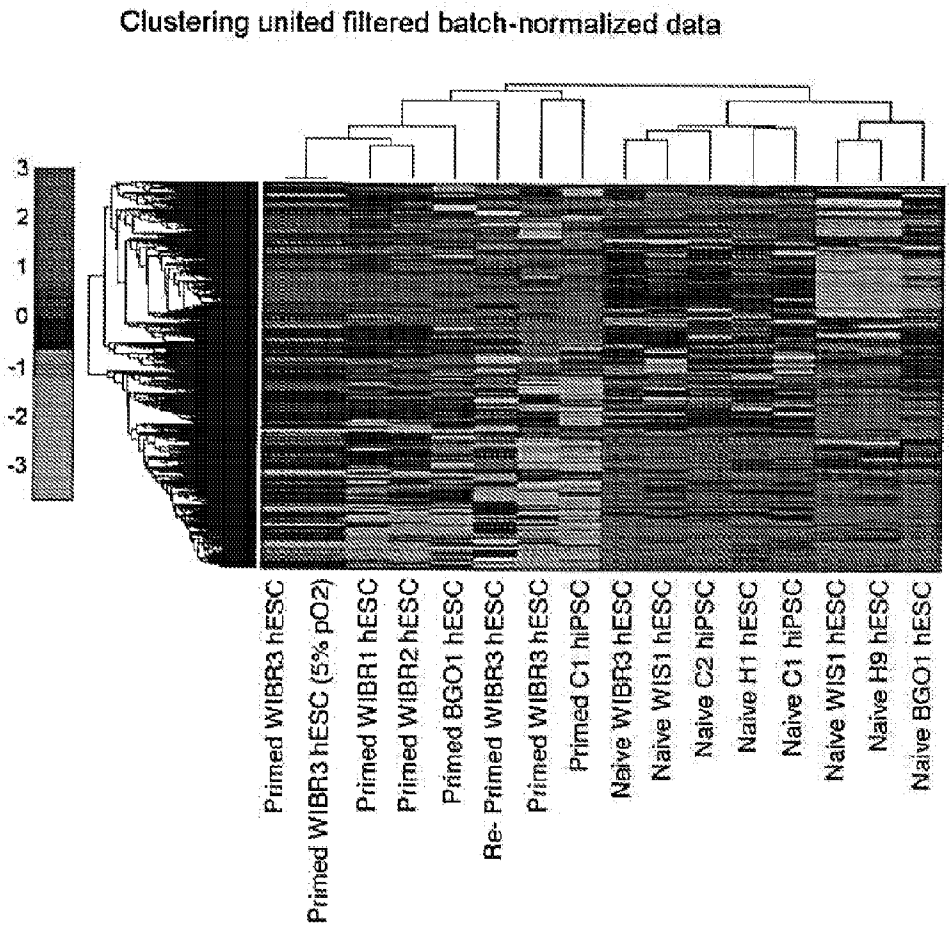


FIG. 23C

FIG. 23D

FIG. 24A



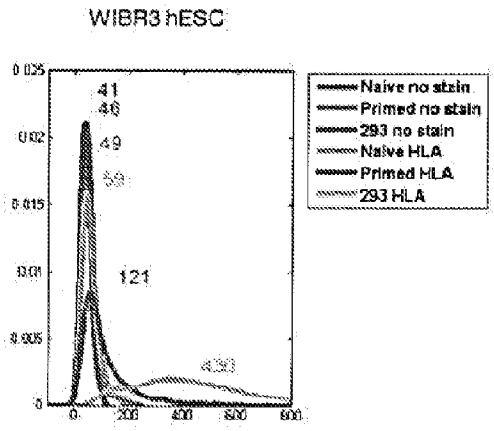


FIG. 24B

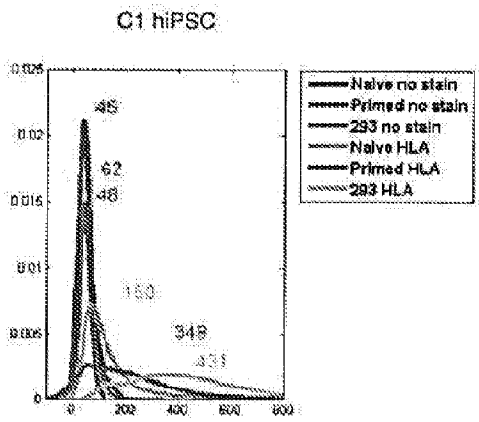
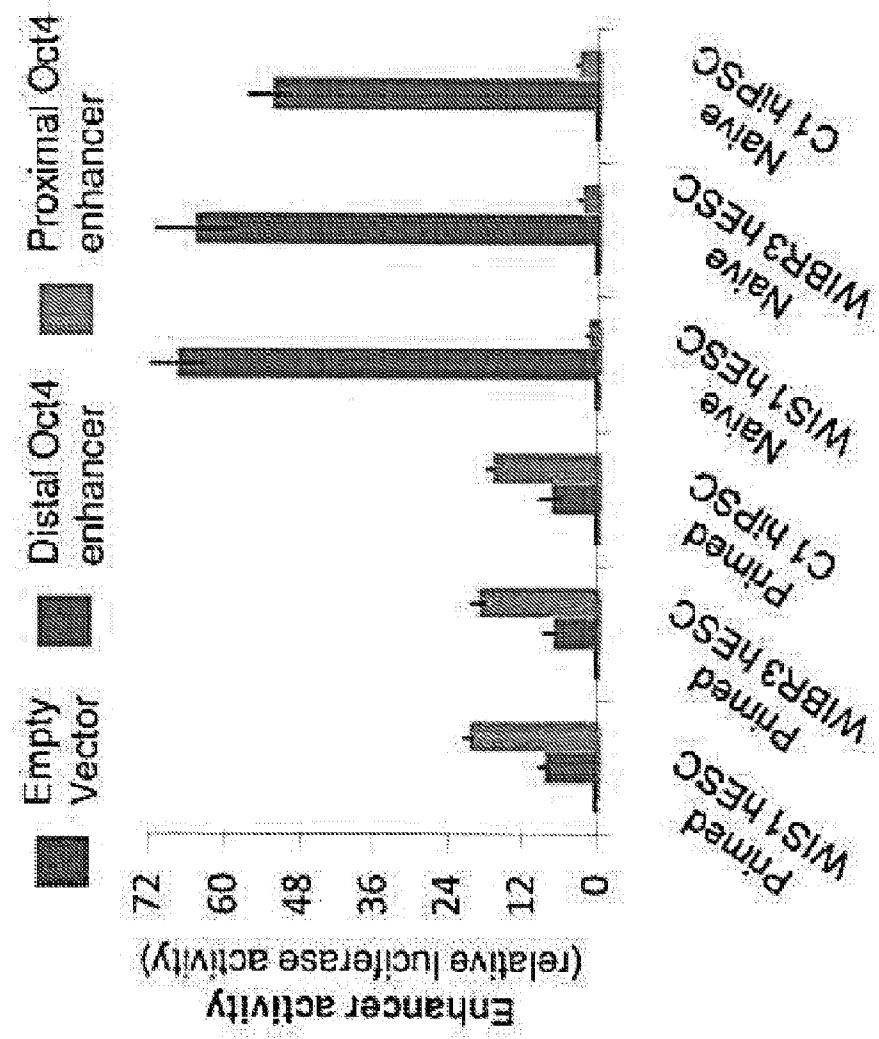


FIG. 24C

FIG. 25A


Empty Vector
Distal Oct4 enhancer
Proximal Oct4 enhancer
Enhancer activity
(relative luciferase activity)
72
60
48
36
24
12
0
Primed WIS1 hESC
Primed WIBR3 hESC
Primed C1 hiPSC
Naive WIS1 hESC
Naive WIBR3 hESC
Naive C1 hiPSC

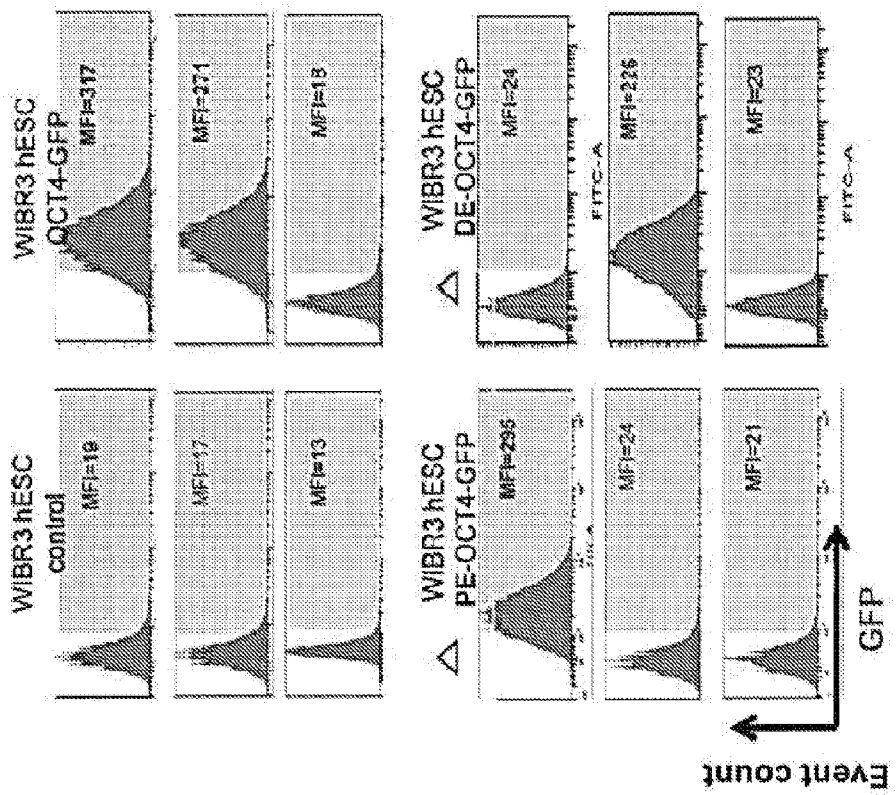


FIG. 25B FIG. 25C

FIG. 25D FIG. 25E

FIG. 25F FIG. 25G

FIG. 25H FIG. 25I

FIG. 25J FIG. 25K

FIG. 25L FIG. 25M

FIG. 26A

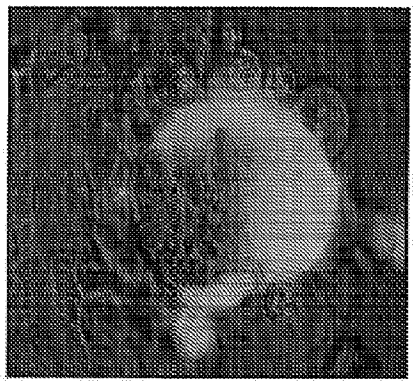
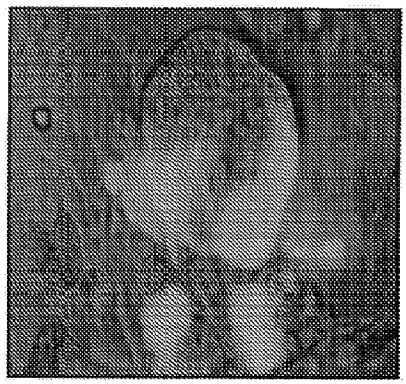


FIG. 26B



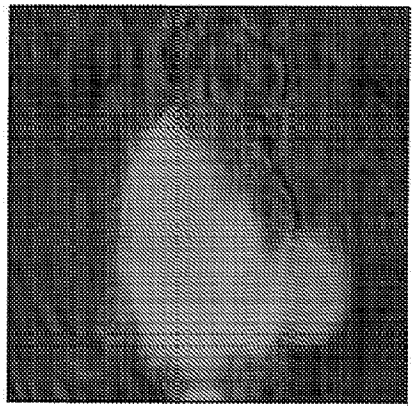


FIG. 26C

Loading human naïve GFP+ iPSC cells

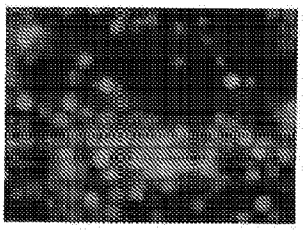


FIG. 26D

Injection into mouse morula

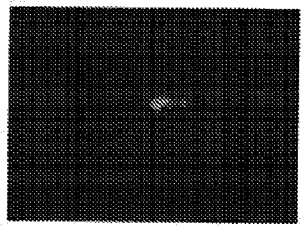


FIG. 26E

Bright field

EGFP

Merge

Day of Inj.

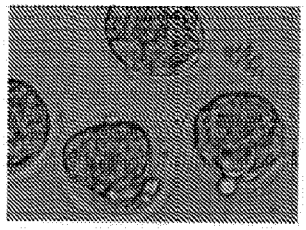


FIG. 26F

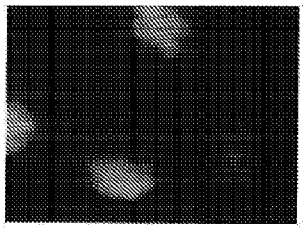


FIG. 26G

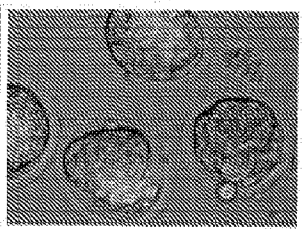


FIG. 26H

1 day after Inj.

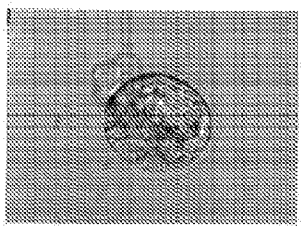


FIG. 26I

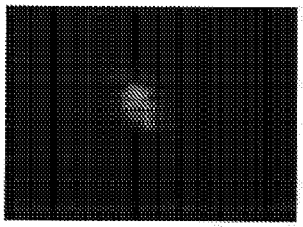


FIG. 26J

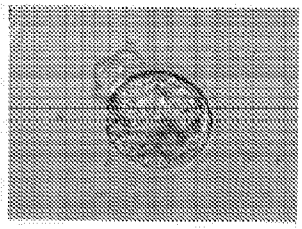


FIG. 26K

XIST promoter CpG islands

GGGTAAATTTTGAACCAACCAAATCACAAAGATGTCCGGCTTTCAATCTTCTAGG
CCACGCCTCTTATGCTCTCTCCGCCCTCAGCCCCCCCTTCAGTTCTTAAAGCGCTG
CAATTCGCTGCTGCAGCCATATTTCTTACTCTCTCGGGGCTGGAAGCTTCCTGACT
GAAGATCTGTTCTAGAAAGAACCCCAAGTGCAGAGA (SEQ ID NO:70)

FIG. 27

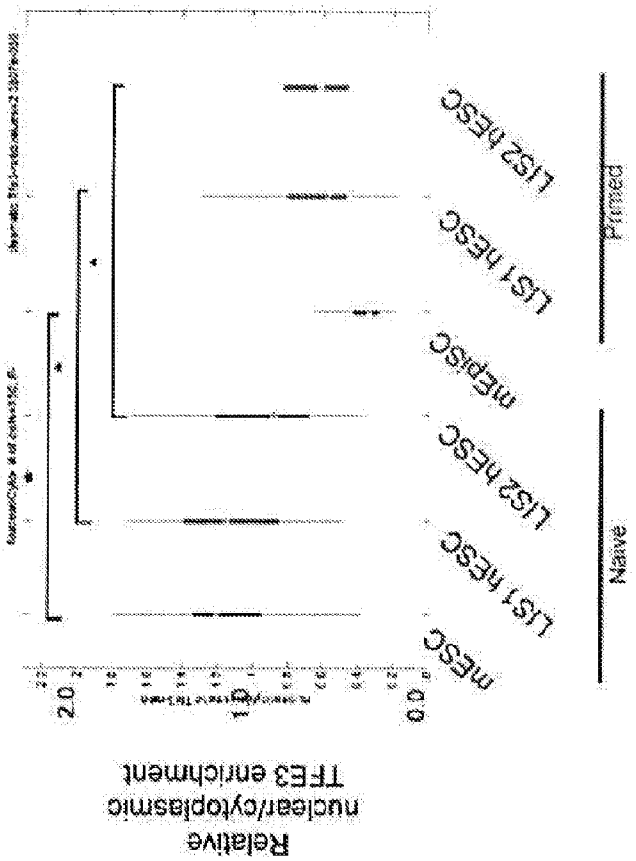


FIG. 28C

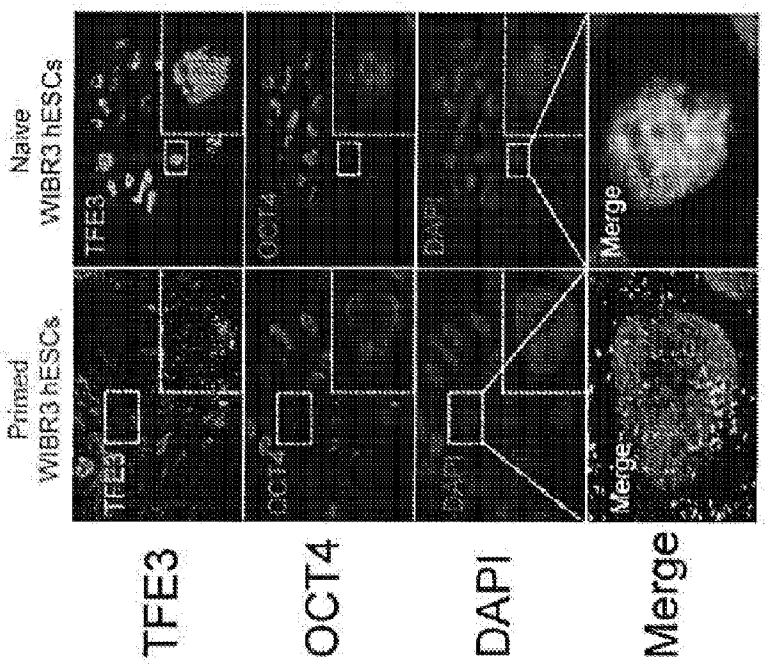


FIG. 28A FIG. 28B

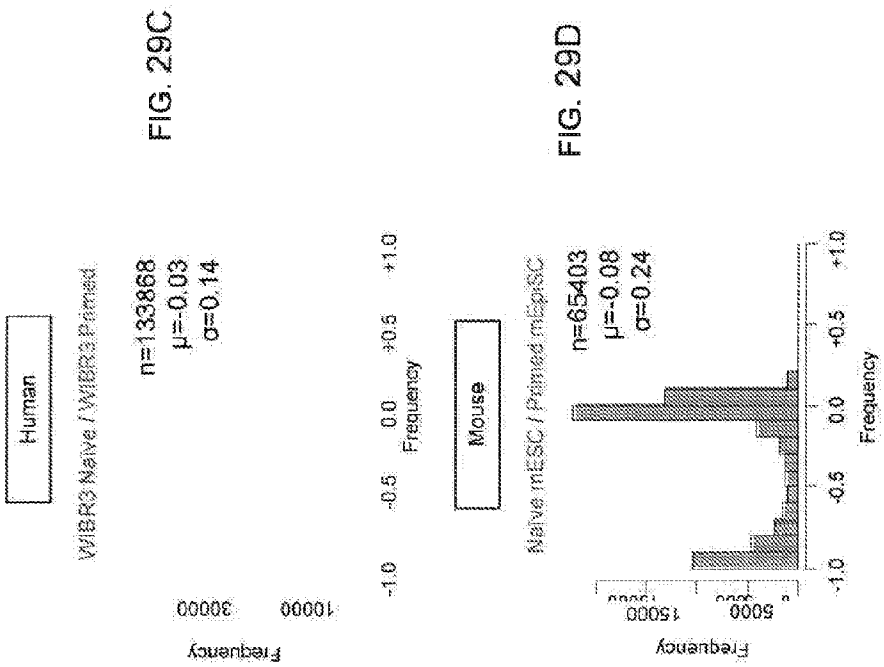


FIG. 29C

FIG. 29D

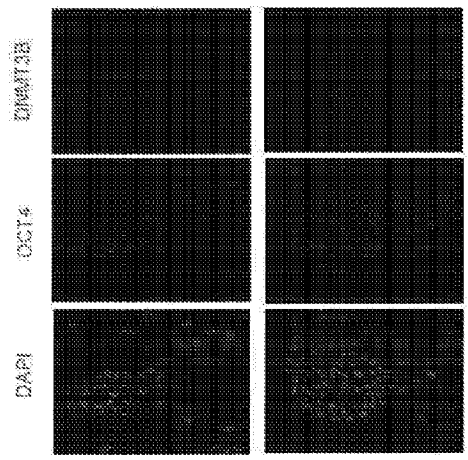
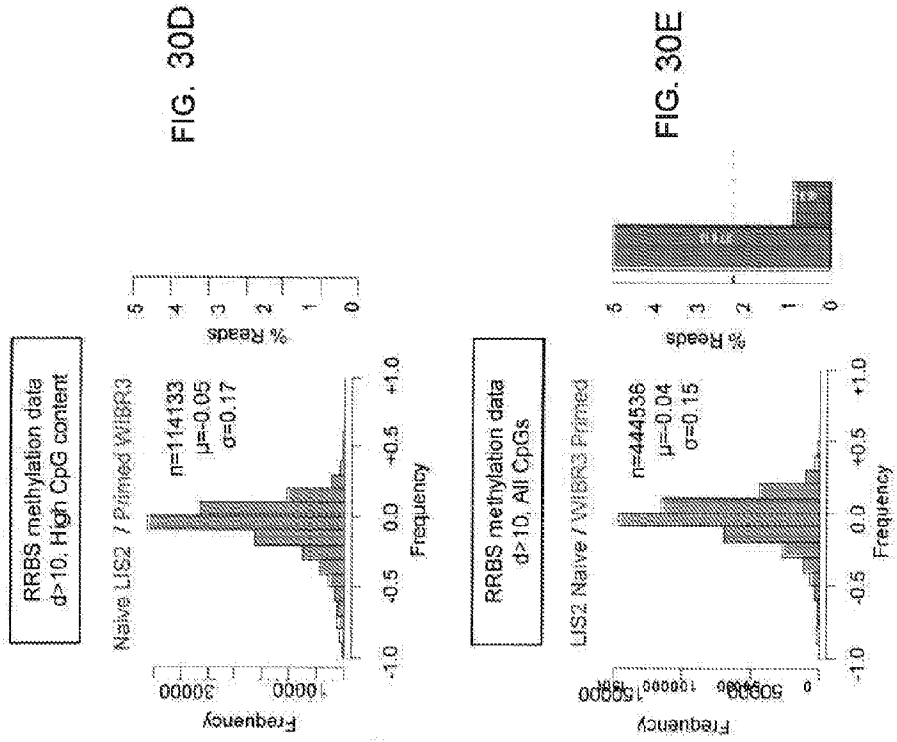


FIG. 29A

FIG. 29B


FIG. 30D
RRBS methylation data
d>10, High CpG content
Naive LIS2 / Primed WIBR3
n=114133
μ=-0.05
σ=0.17
% Reads
Frequency
-1.0
-0.5
0.0
+0.5
+1.0
FIG. 30E
RRBS methylation data
d>10, All CpGs
LIS2 Naive / WIBR3 Primed
n=444536
μ=-0.04
σ=0.15

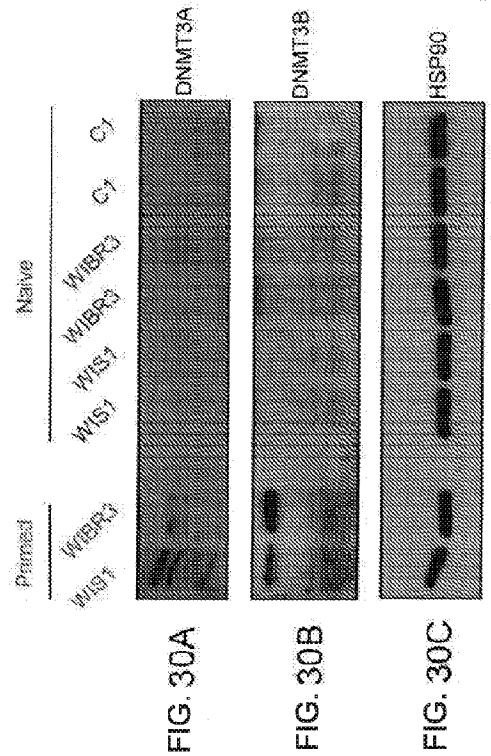

Primed
WIBR3
WIS1
Naive
WIS1
WIS1
WIBR3
WIBR3
C1
C1
DNMT3A
DNMT3B
HSP90
FIG. 30A
FIG. 30B
FIG. 30C

FIG. 30F

Optimized WIS-NHSM
(FGF2 free option)

LIF (20ng/ml)
ERK1/2i (PD0325901 1μM)
GSK3βi (CHIR99021 3μM)
JNKi (SP600125 10μM)
P38i (BIRB796 2μM)
FGFRi (PD173074 0.2μM)
TGFβ1 (8 ng/ml))

+/- ROCKi (Y27632 2μM)

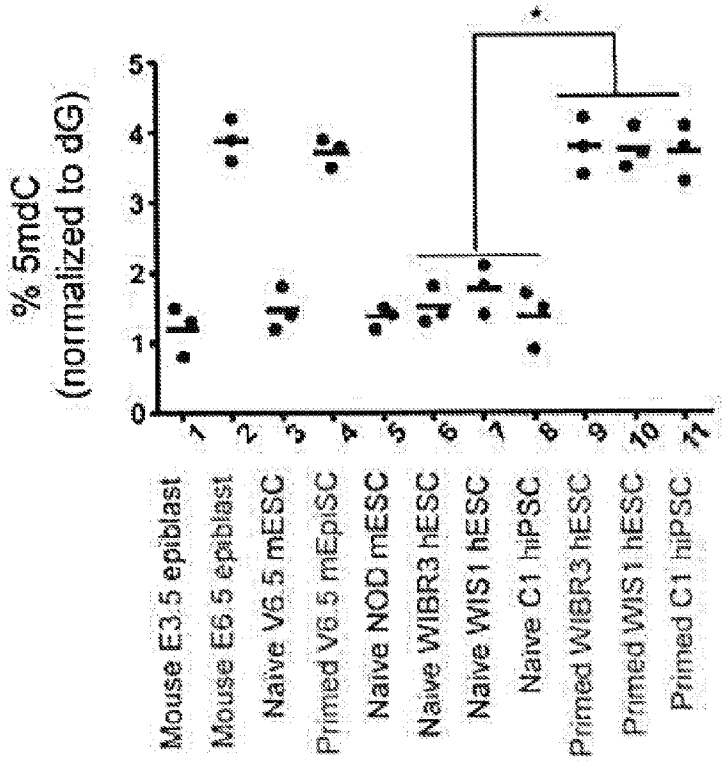


FIG. 30G

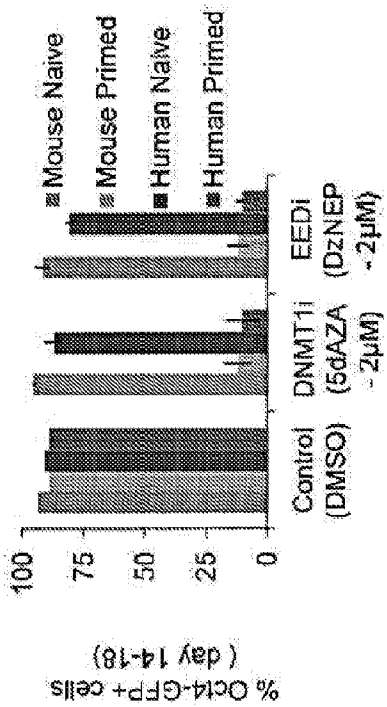


FIG. 30H

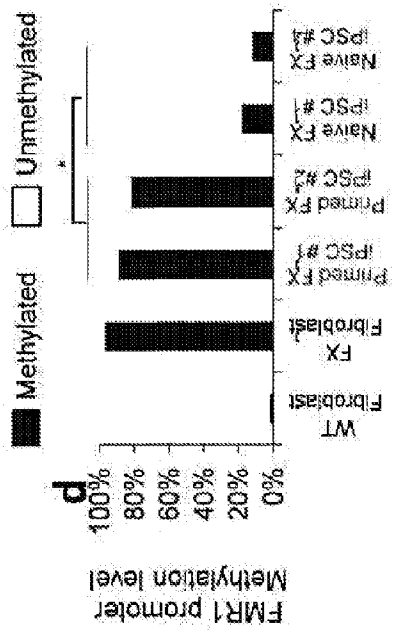


FIG. 30I

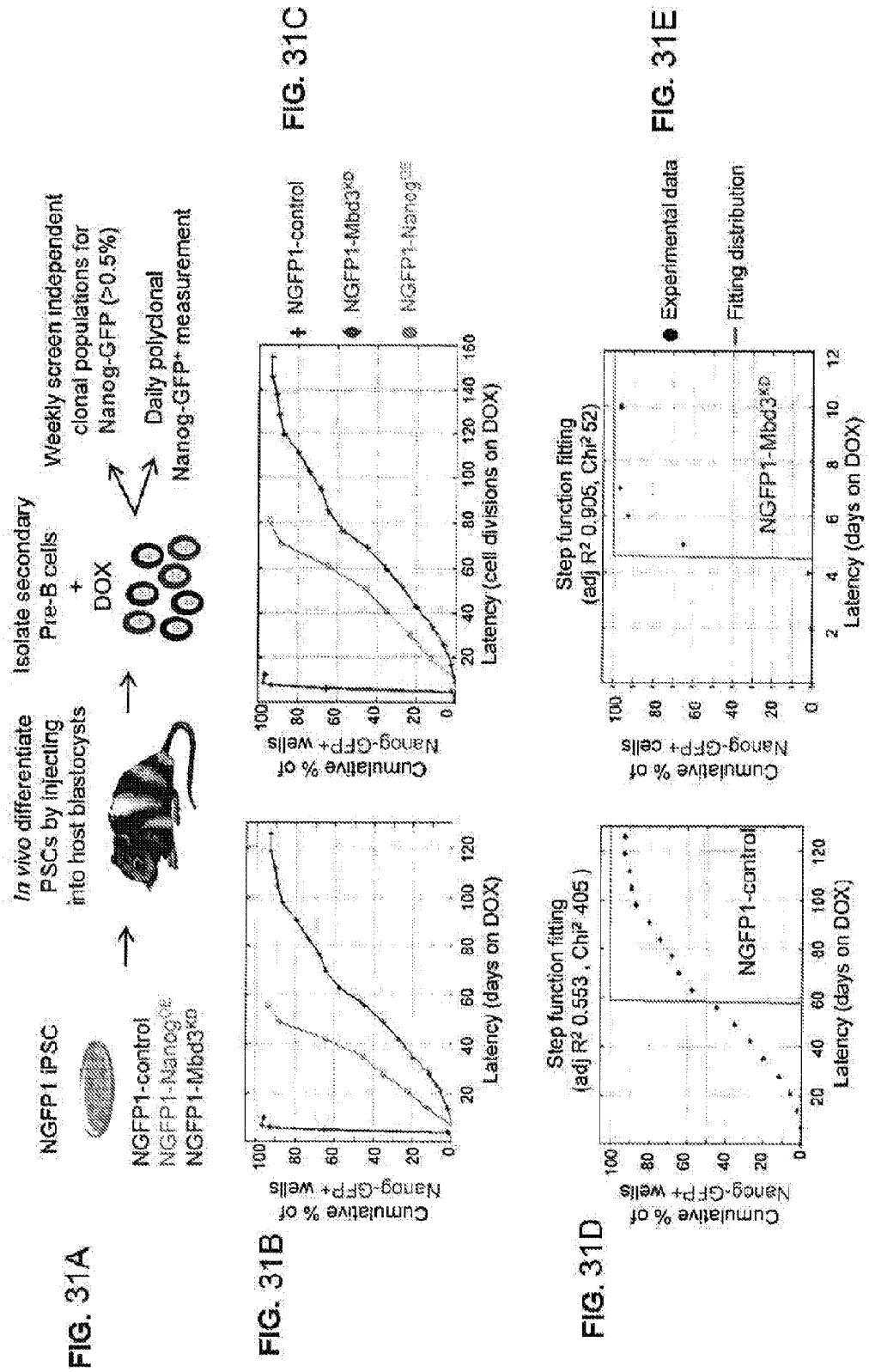


FIG. 31A

FIG. 31B

FIG. 31C

FIG. 31D

FIG. 31E

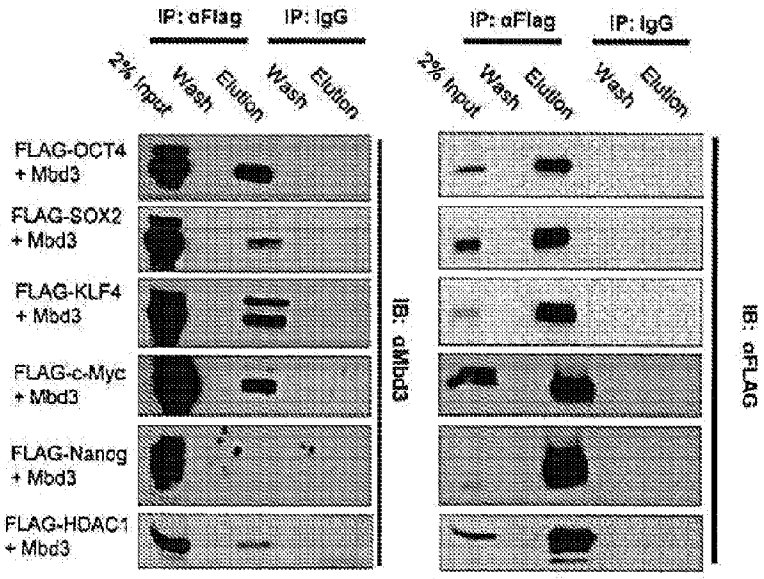


FIG. 32A

FIG. 32B

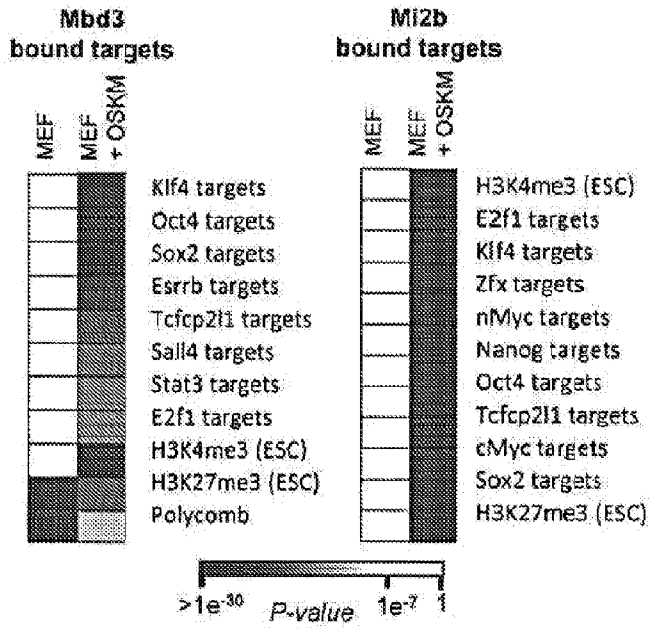


FIG. 32C

FIG. 32D

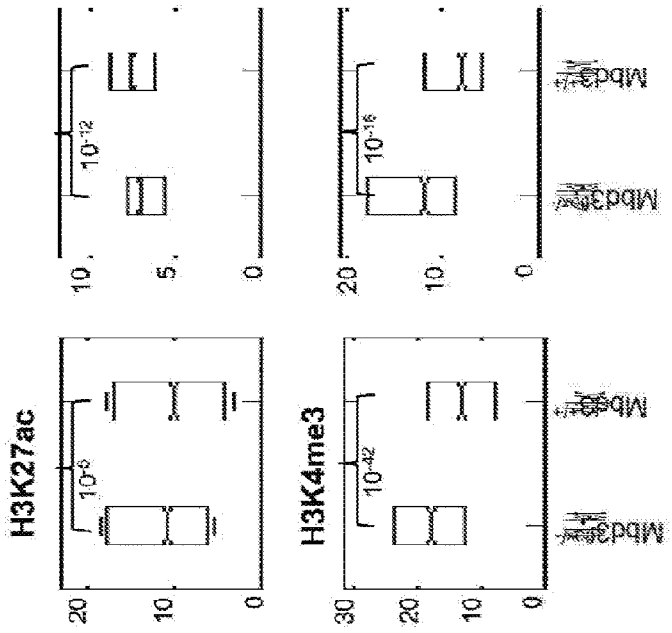


FIG. 32F

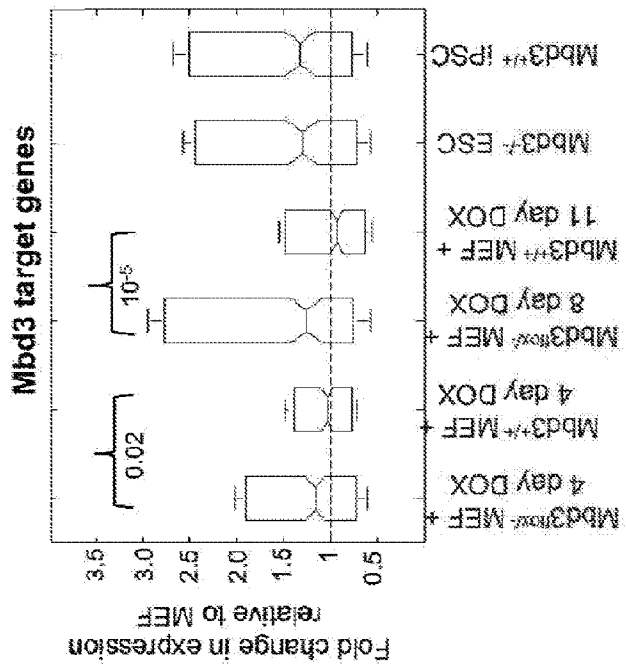


FIG. 32E

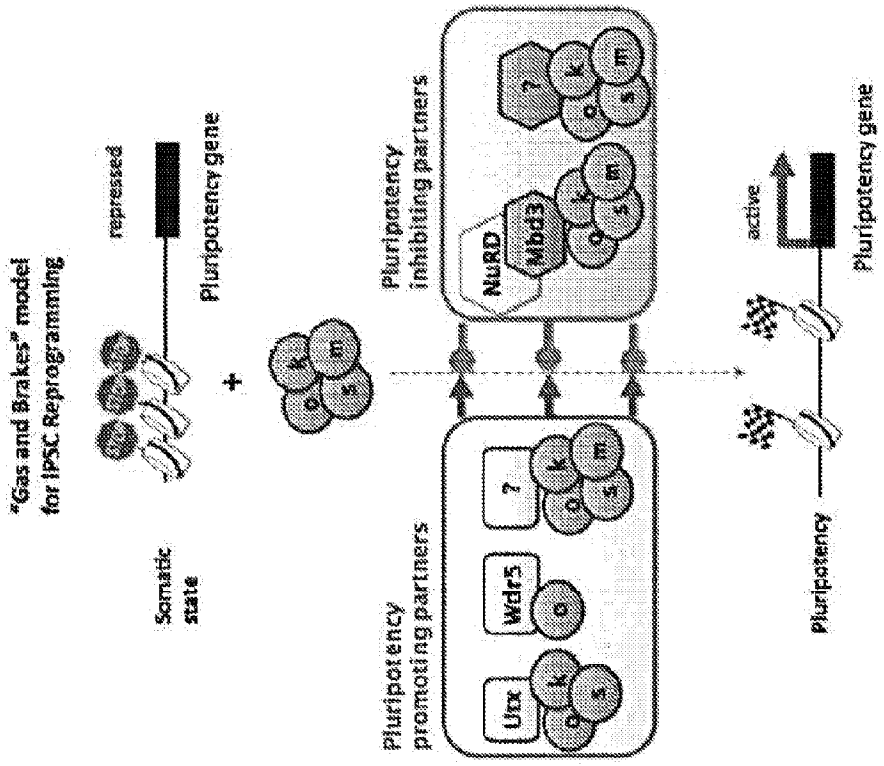


FIG. 32H

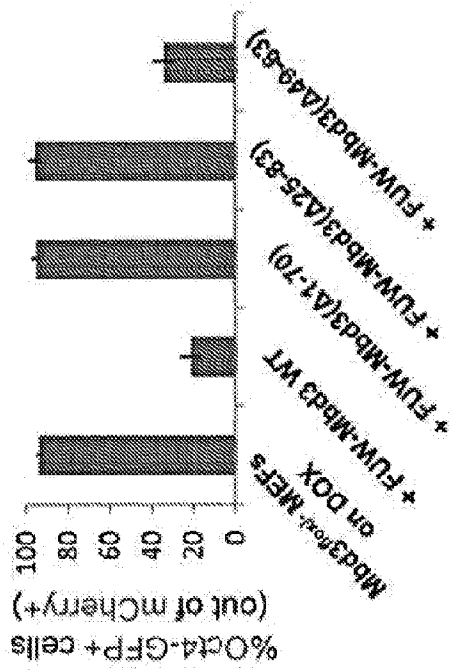


FIG. 32G

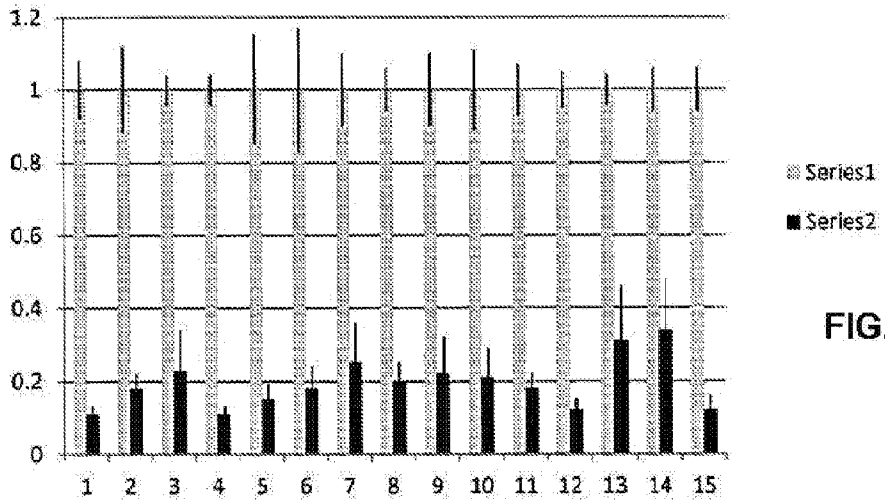


FIG. 33A

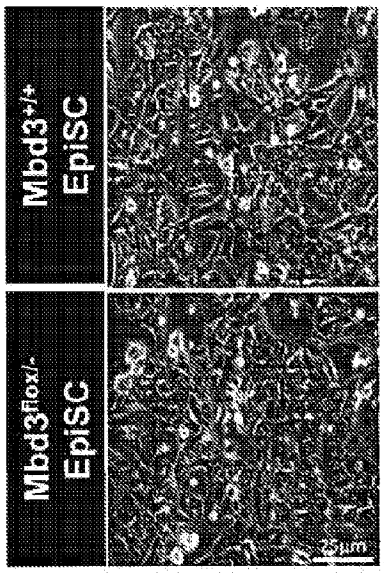


FIG. 33B

FIG. 33C

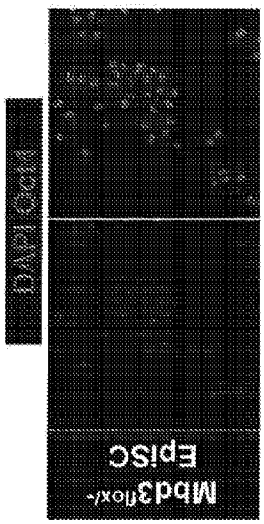


FIG. 33D

FIG. 33E

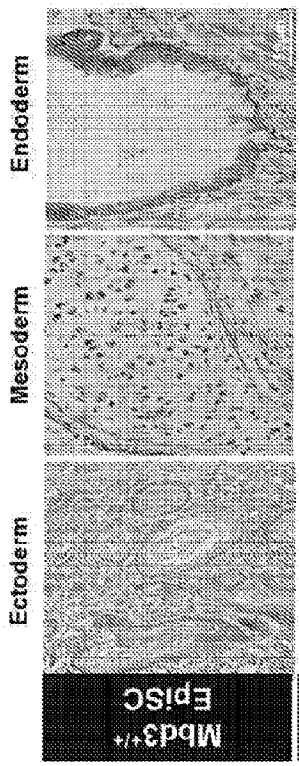


FIG. 33F

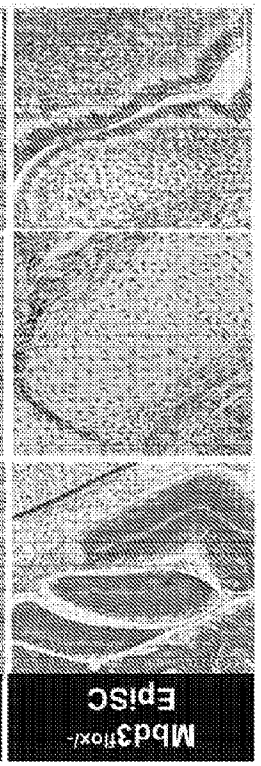


FIG. 33G

FIG. 34A

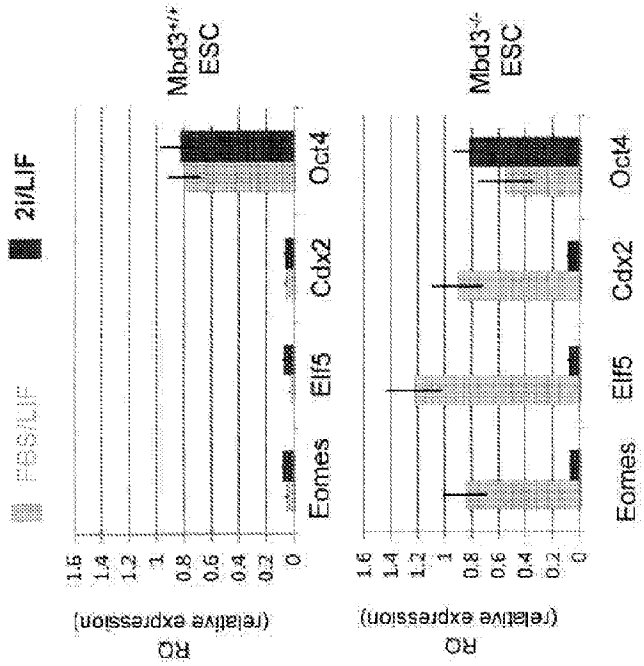
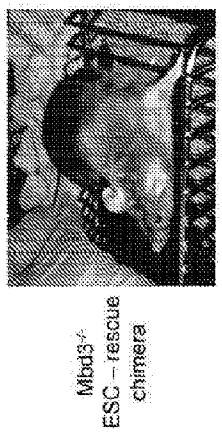


FIG. 34B

FIG. 34C



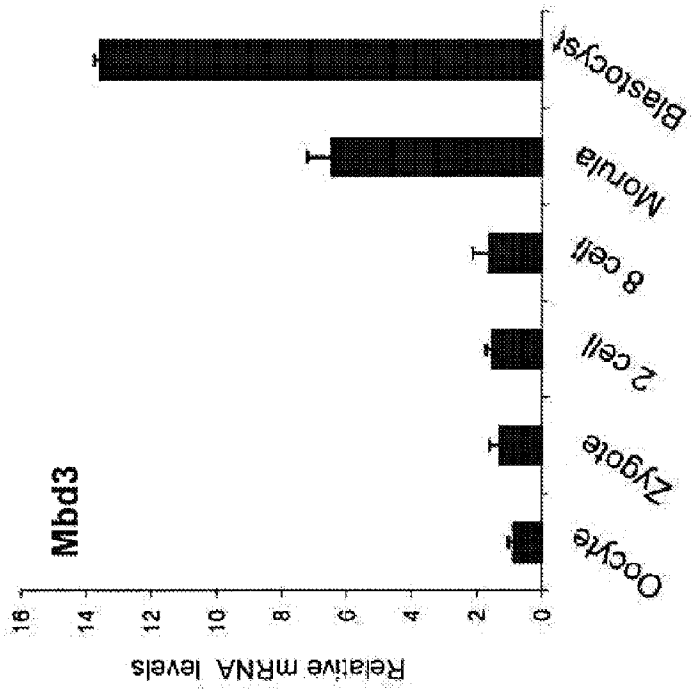


FIG. 35B

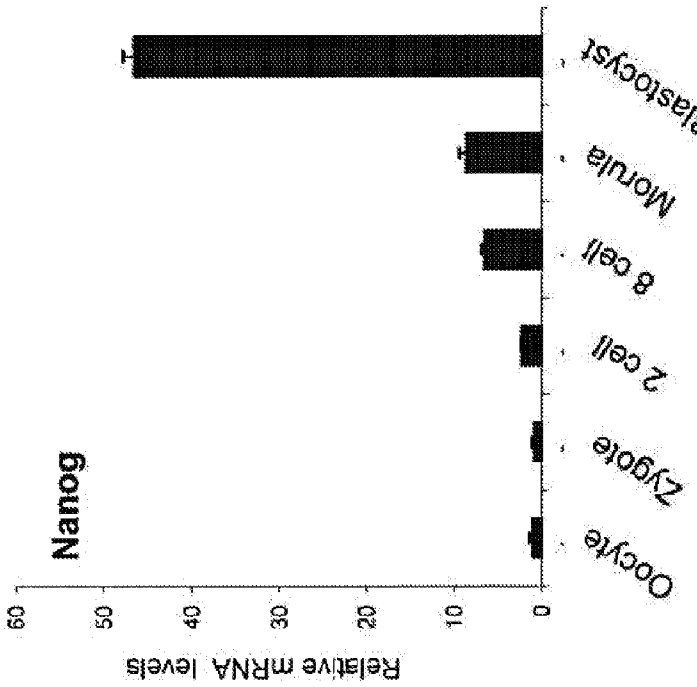


FIG. 35A

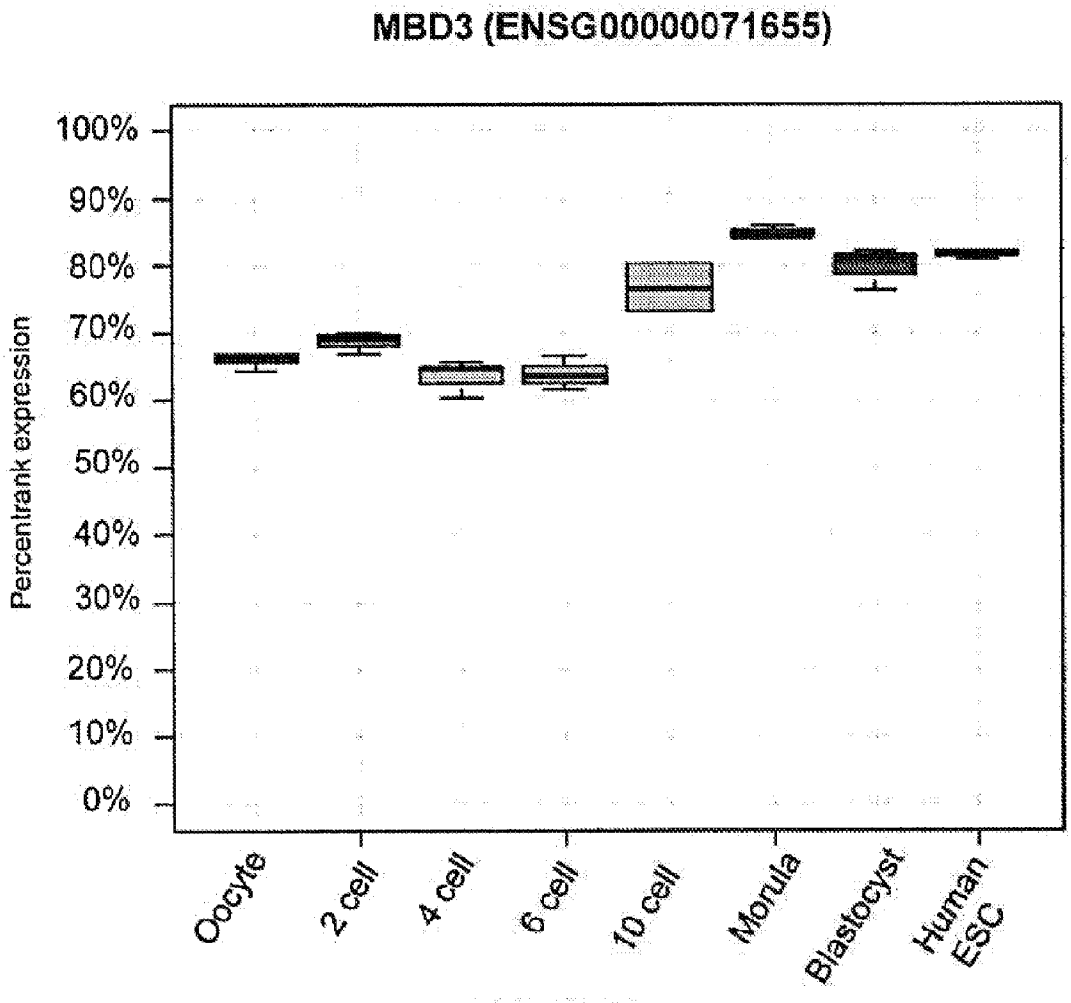

MBD3 (ENSG00000071655)
Percentrank expression
100%
90%
80%
70%
60%
50%
40%
30%
20%
10%
0%
Oocyte
2 cell
4 cell
6 cell
10 cell
Morula
Blastocyst
Human ESC

FIG. 35C

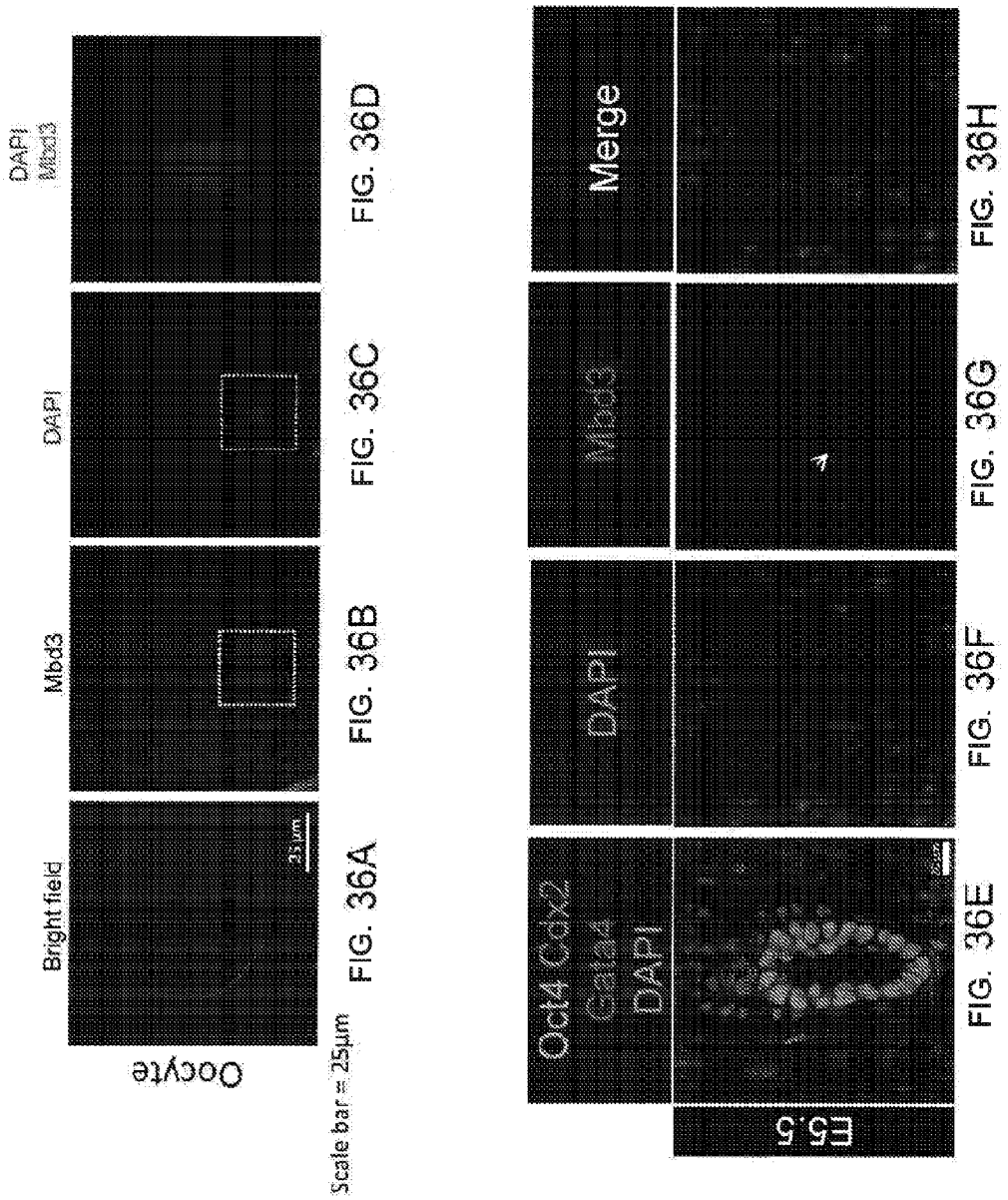


FIG. 36A FIG. 36B FIG. 36C FIG. 36D

FIG. 36E FIG. 36F FIG. 36G FIG. 36H

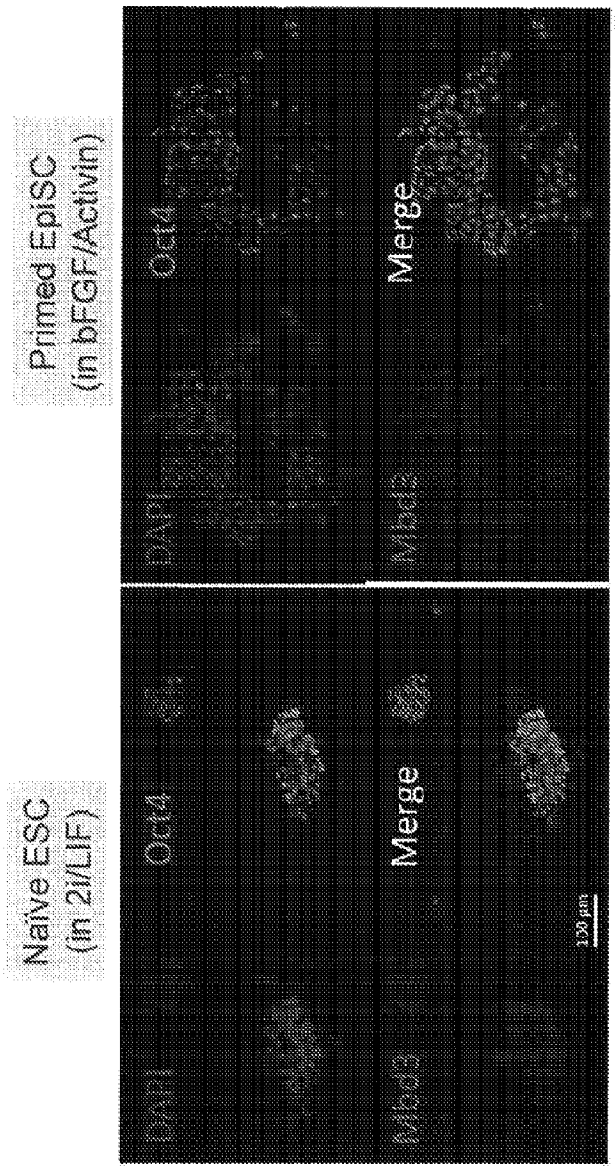


FIG. 36J

FIG. 36I

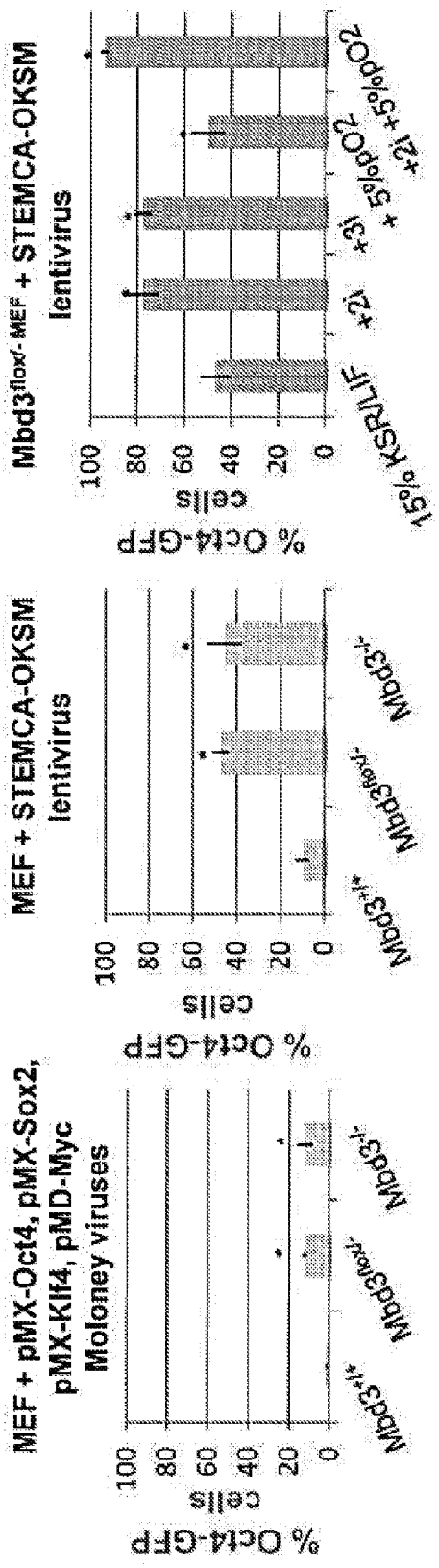


FIG. 37A

FIG. 37B

FIG. 37C

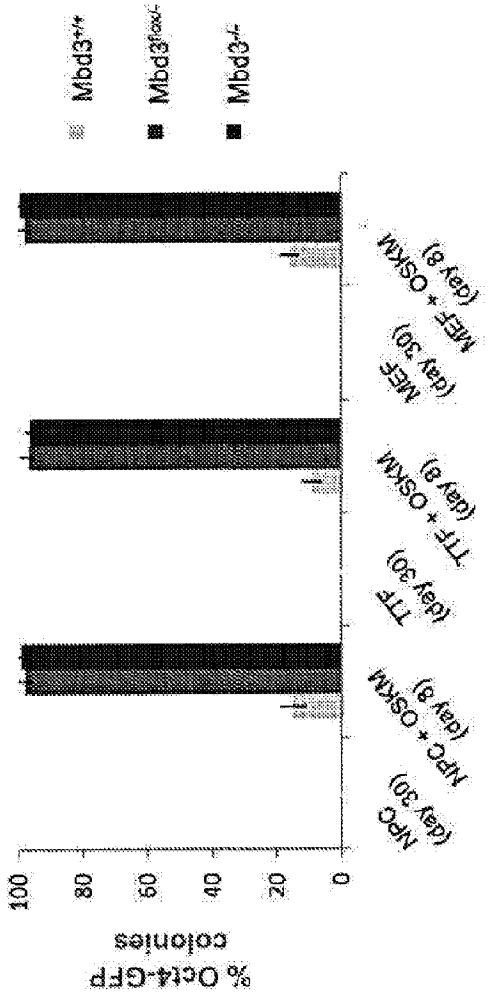


FIG. 38A

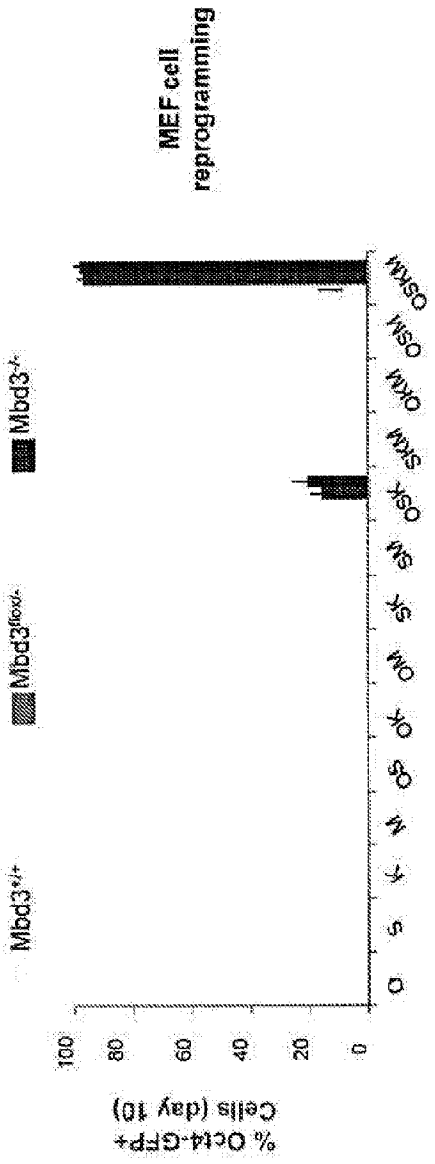


FIG. 38B

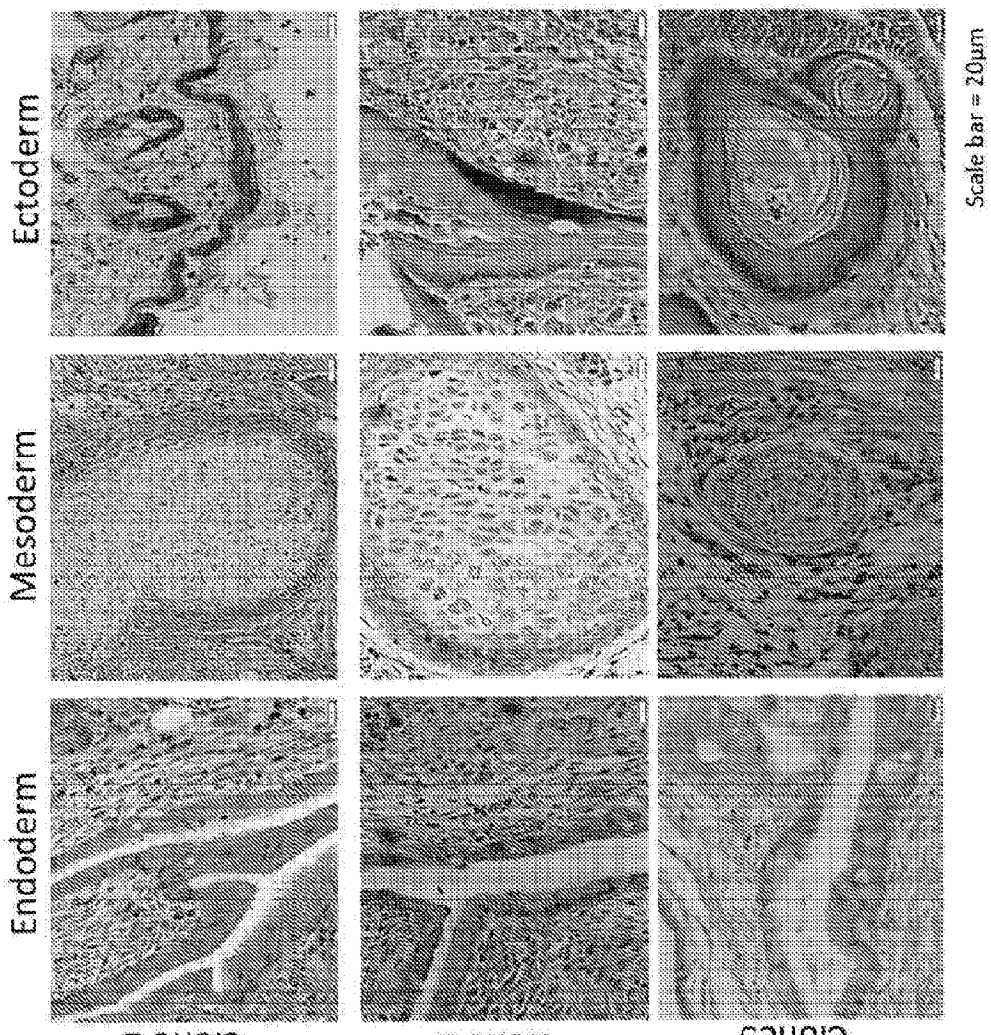


FIG. 39A

FIG. 39B

FIG. 39C

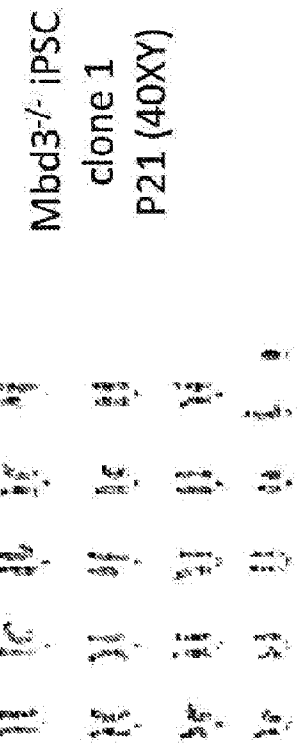


FIG. 39D

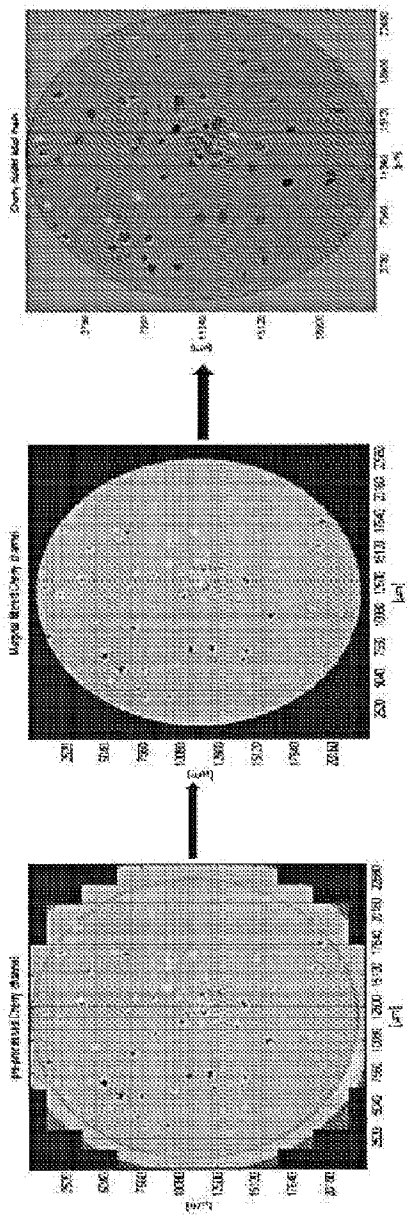
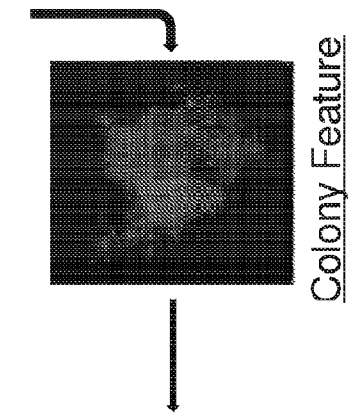


FIG. 40A FIG. 40B FIG. 40C

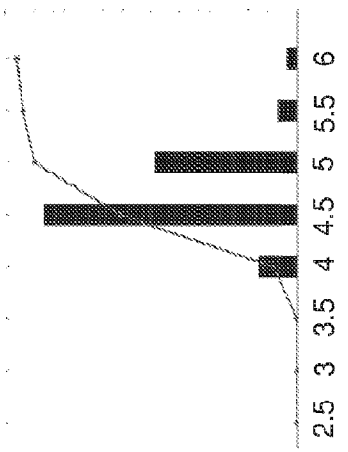


Colony Feature Extraction

- Area
- Bounding Box
- Centroid
- GFP+ flag
- GFP+ area

FIG. 40D

Cumulative % Oct4-GFP+ colonies



% out of total that became Oct4-GFP+ at each time point

Statistical Time-Lapse Analysis

FIG. 40E

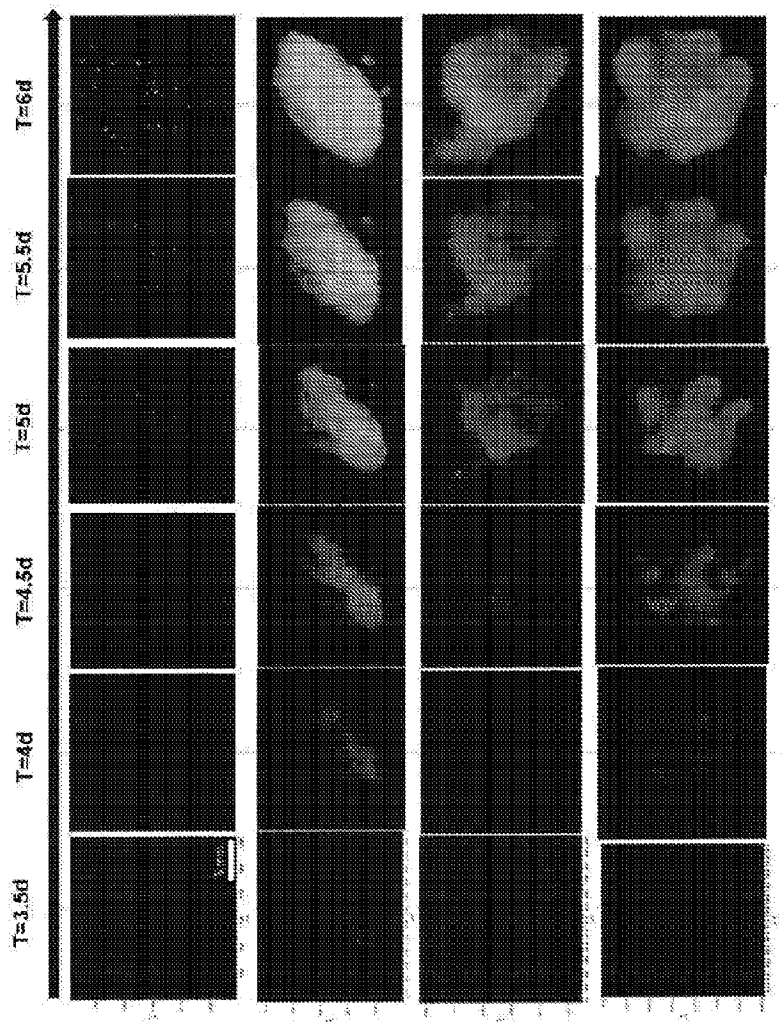


FIG. 41A

FIG. 41B

FIG. 41C

FIG. 41D

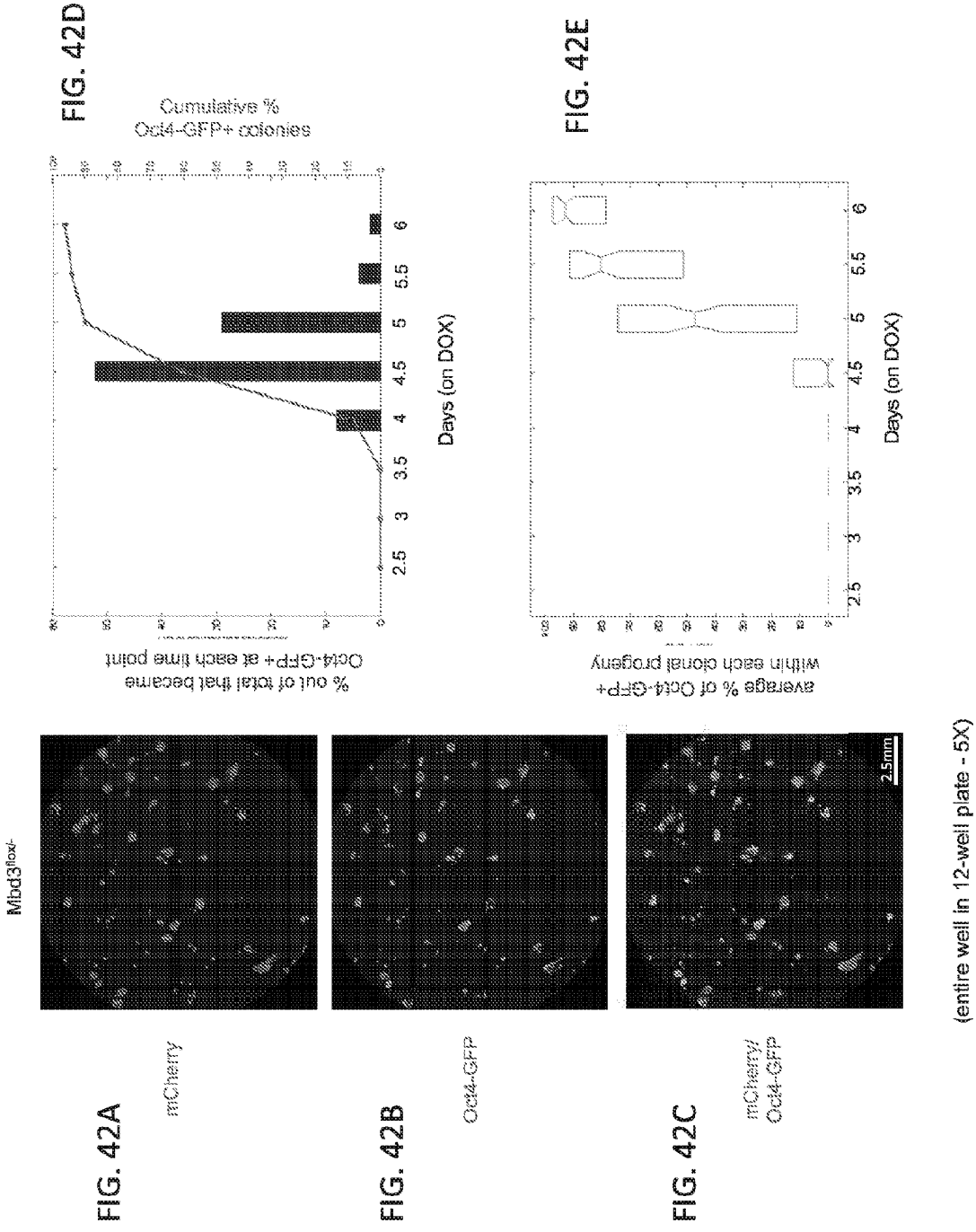
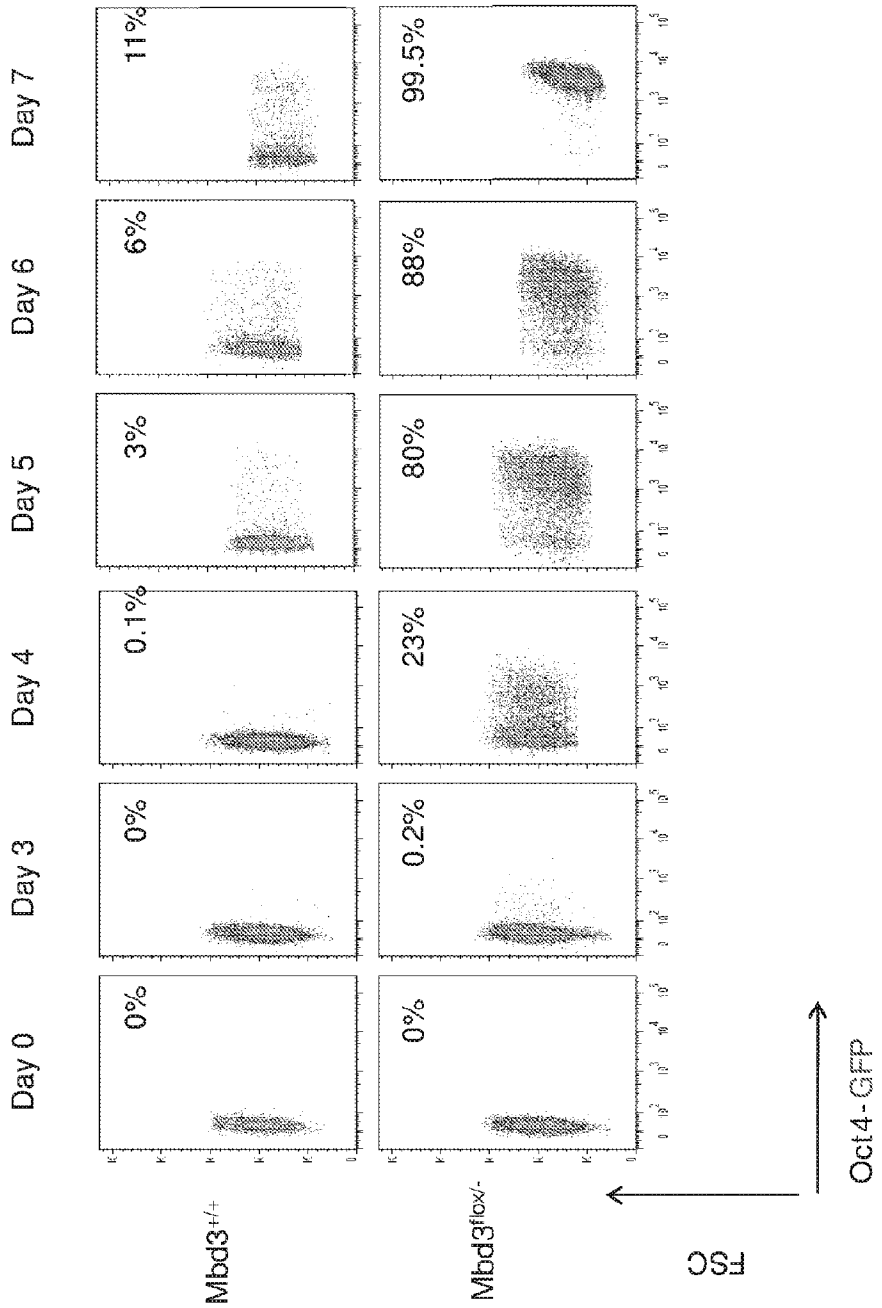

Mbd3flox/-
mCherry
Oct4-GFP
mCherry/ Oct4-GFP
2.5mm
(entire well in 12-well plate - 5X)
FIG. 42A
FIG. 42B
FIG. 42C
FIG. 42D
Cumulative % Oct4-GFP+ colonies
Days (on DOX)
% out of total that became Oct4-GFP+ at each time point
FIG. 42E
average % of Oct4-GFP+ within each clonal progeny
Days (on DOX)

FIG. 43A

FIG. 43B



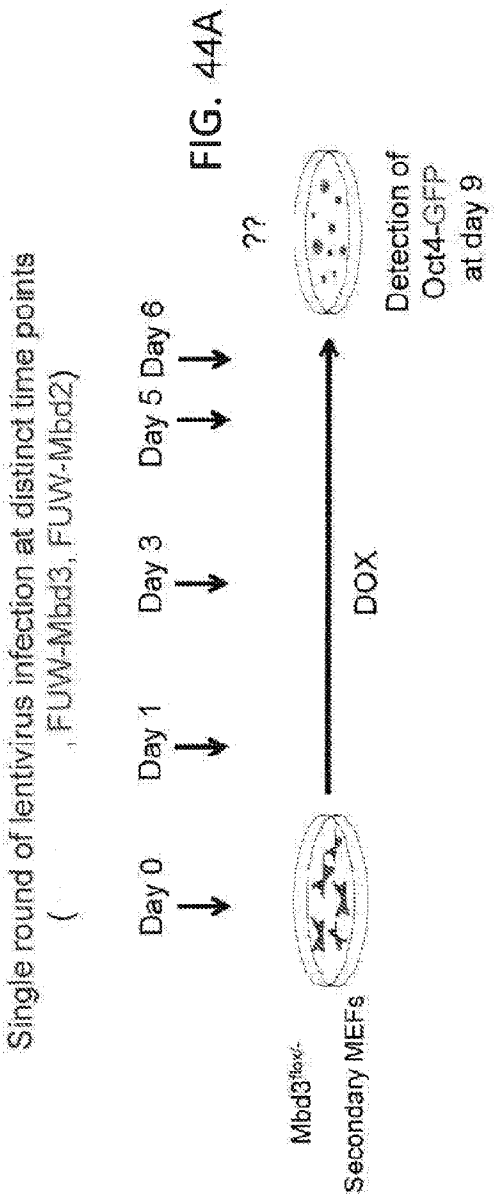


FIG. 44A

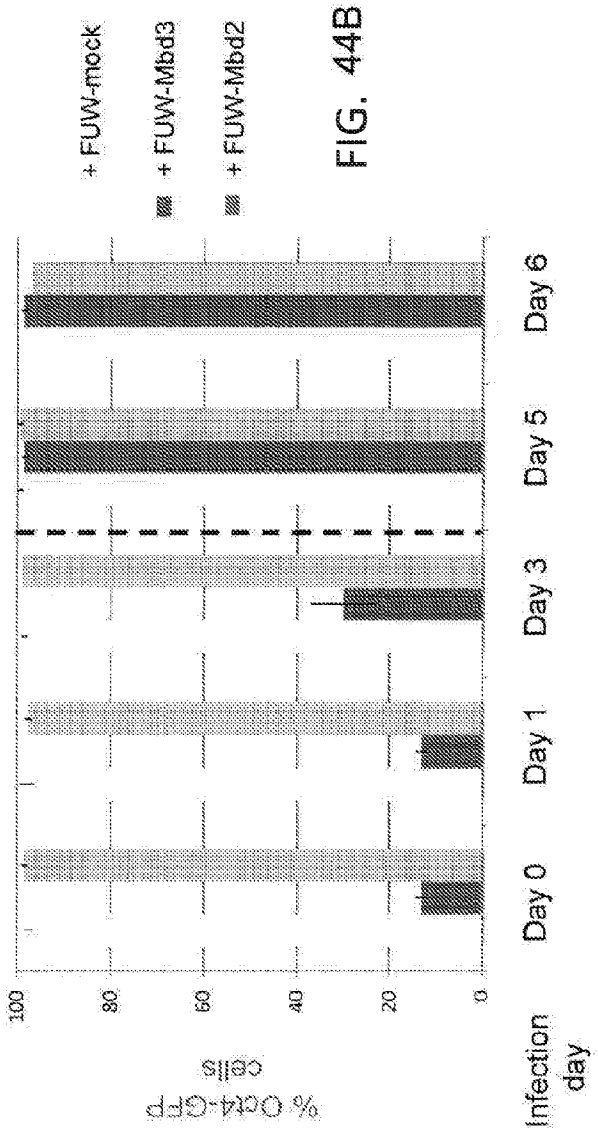


FIG. 44B

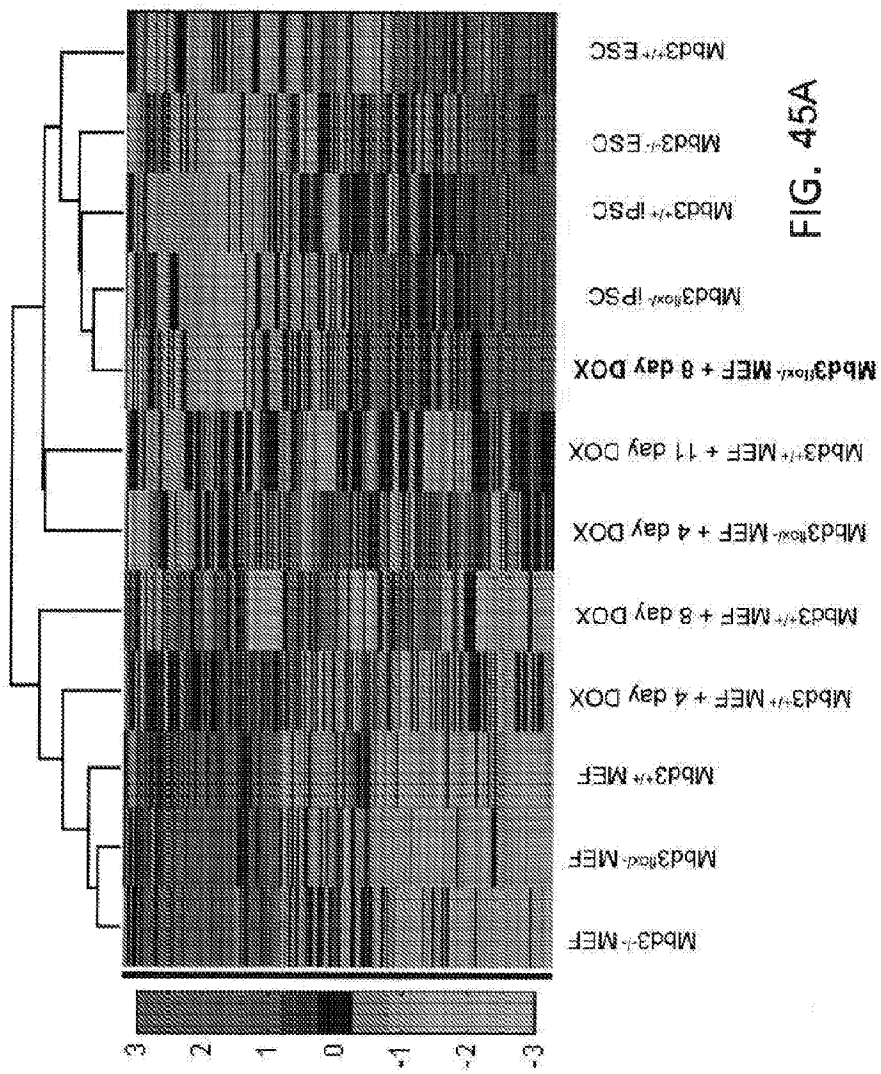

Mbd3-/- MEF
Mbd3flox/- MEF
Mbd3+/+ MEF
Mbd3+/+ MEF + 4 day DOX
Mbd3+/+ MEF + 8 day DOX
Mbd3flox/- MEF + 4 day DOX
Mbd3+/+ MEF + 11 day DOX
Mbd3flox/- MEF + 8 day DOX
Mbd3flox/- iPSC
Mbd3+/+ iPSC
Mbd3-/- ESC
Mbd3+/+ ESC
3
2
1
0
-1
-2
-3

FIG. 45A

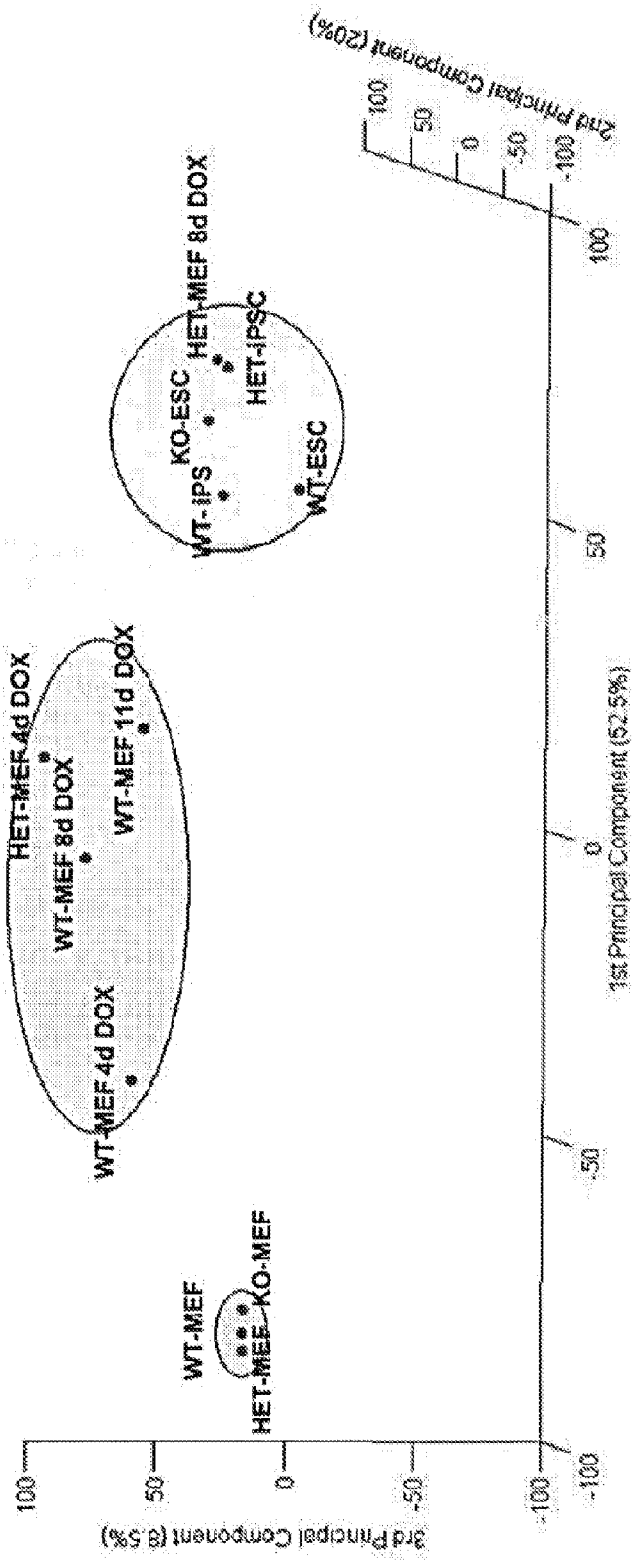

2nd Principal Component (20%)
100
50
0
-50
-100
HET-MEF 8d DOX
HET-iPSC
KO-ESC
WT-iPS
WT-ESC
HET-MEF 4d DOX
WT-MEF 8d DOX
WT-MEF 11d DOX
WT-MEF 4d DOX
WT-MEF
HET-MEF
KO-MEF
1st Principal Component (52.5%)
3rd Principal Component (8.5%)

FIG. 45B

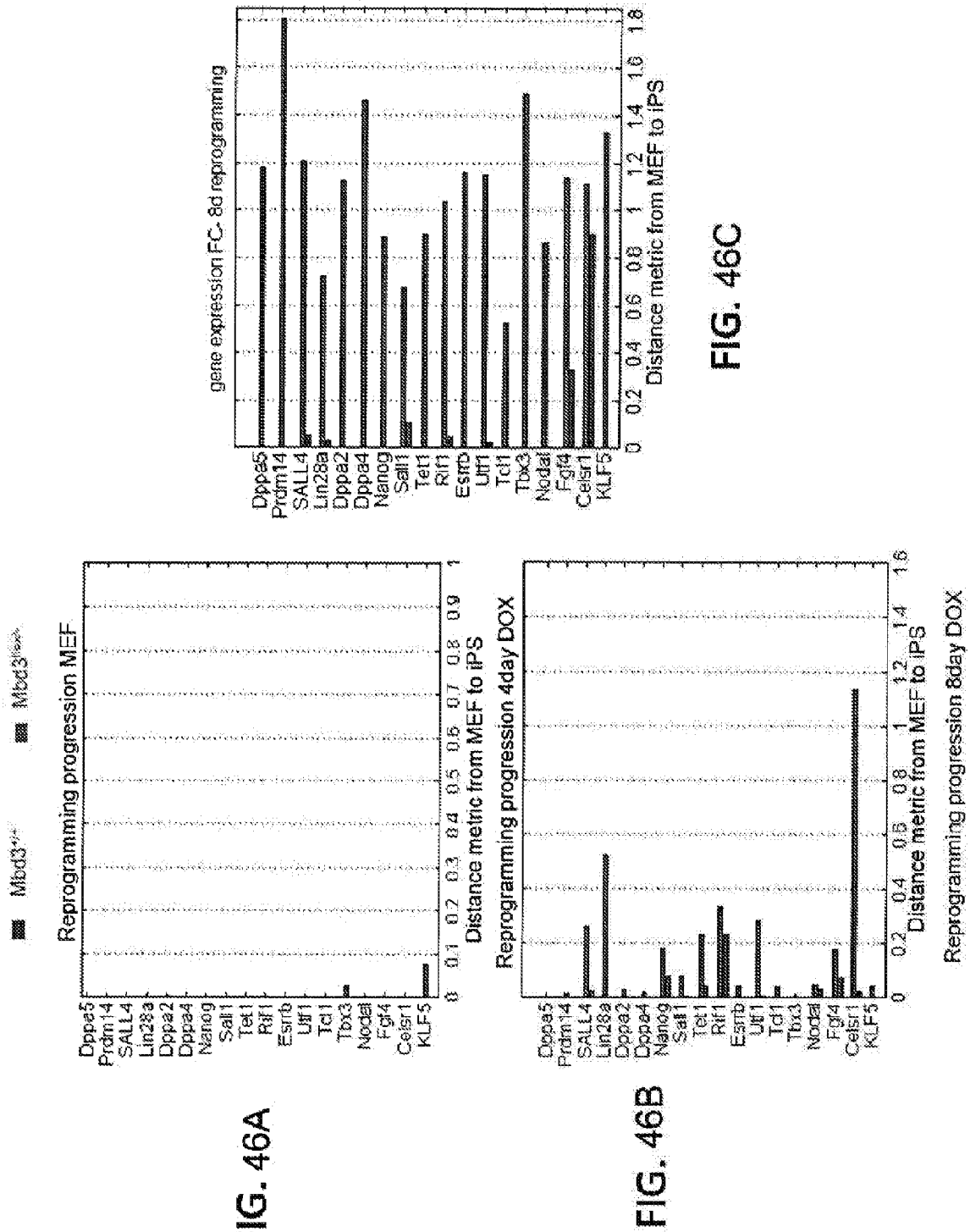


FIG. 46A

FIG. 46B

FIG. 46C

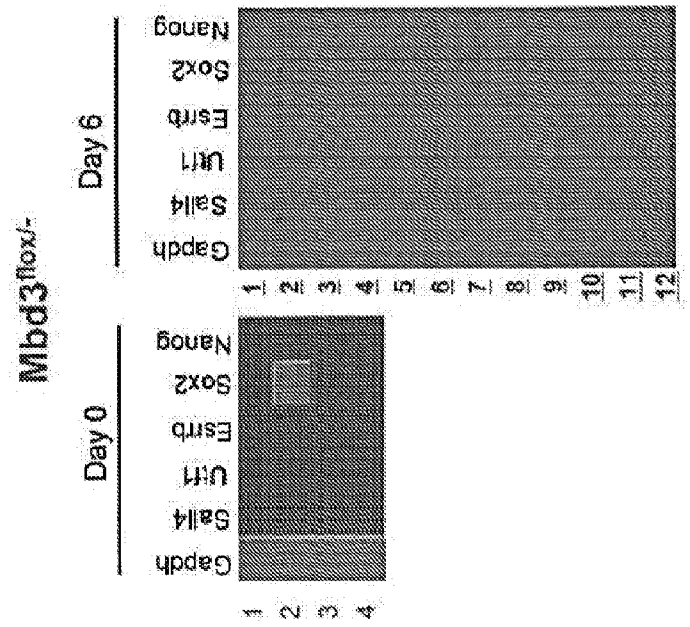


FIG. 46E

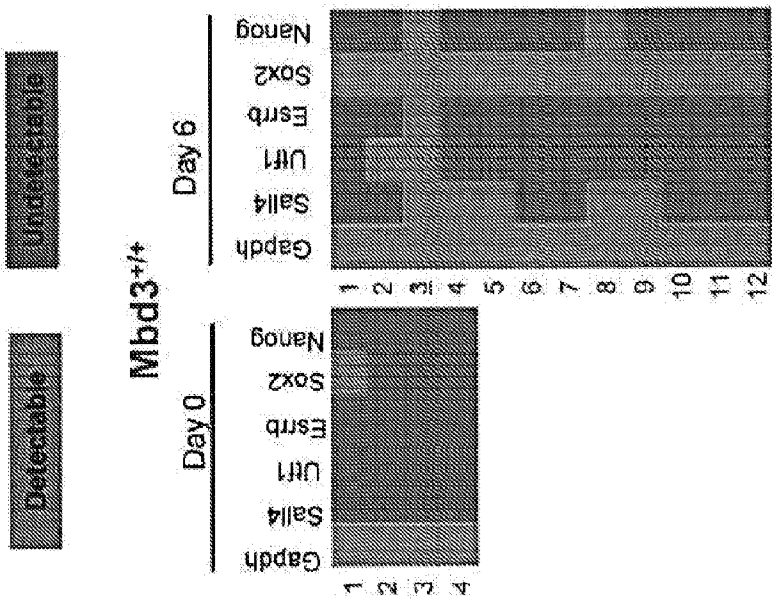


FIG. 46D

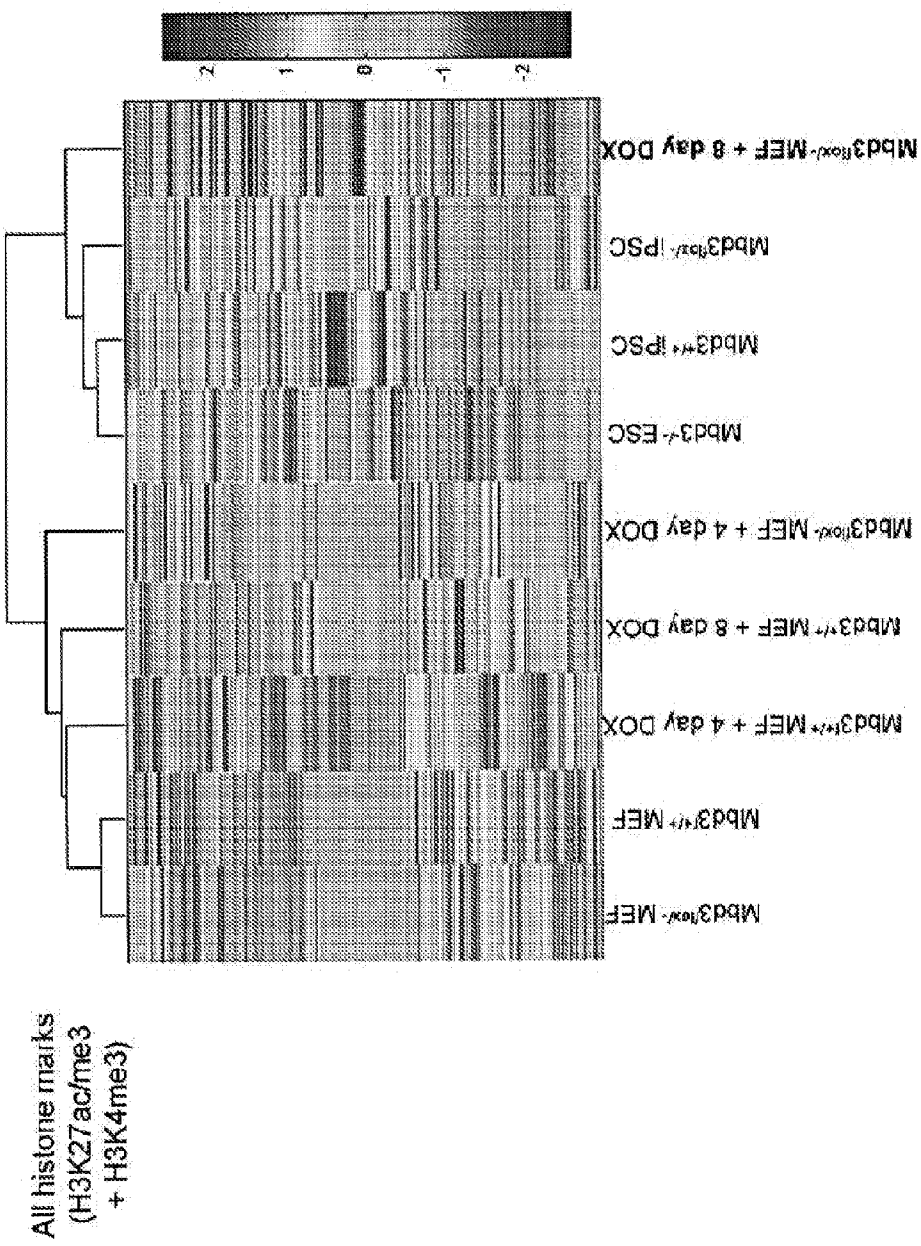

2
1
0
-1
-2
Mbd3flox/- MEF
Mbd3+/+ MEF
Mbd3+/+ MEF + 4 day DOX
Mbd3+/+ MEF + 8 day DOX
Mbd3flox/- MEF + 4 day DOX
Mbd3-/- ESC
Mbd3+/+ iPSC
Mbd3flox/- iPSC
Mbd3flox/- MEF + 8 day DOX
All histone marks
(H3K27ac/me3
+ H3K4me3)

FIG. 47A

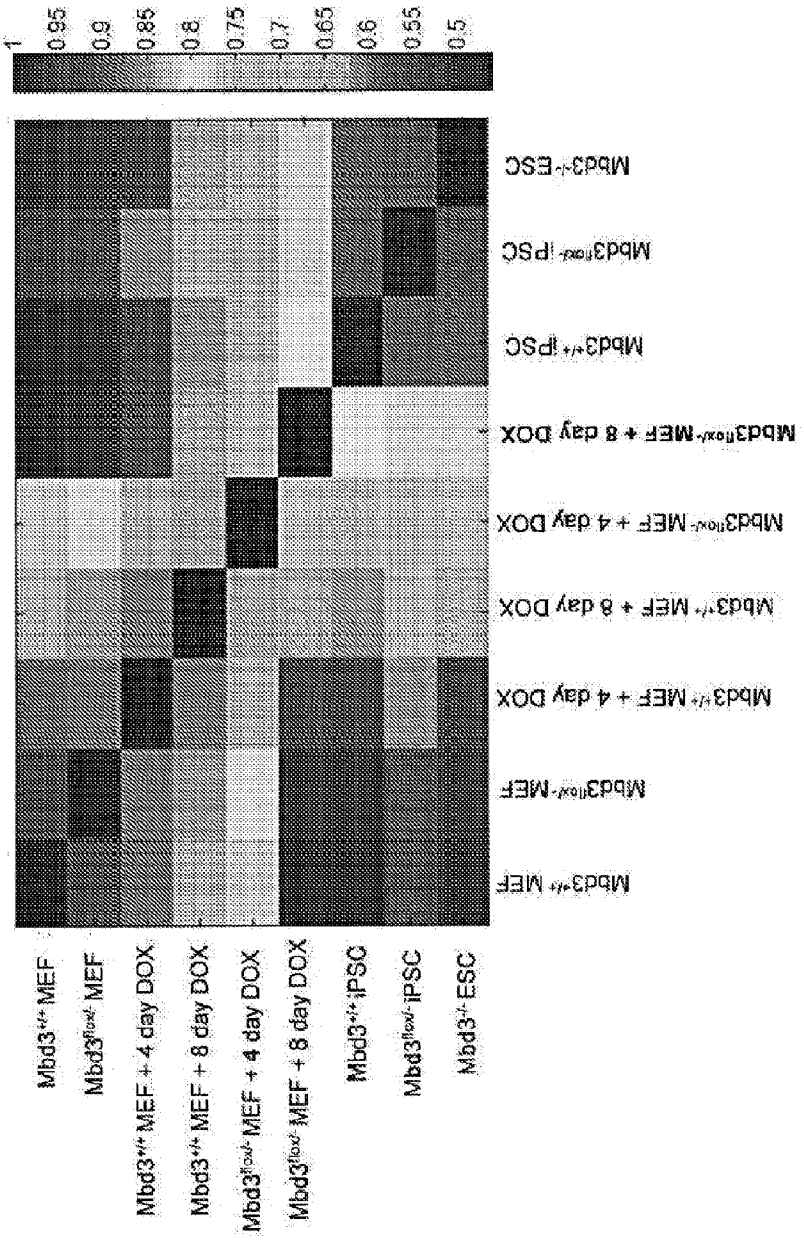

1
0.95
0.9
0.85
0.8
0.75
0.7
0.65
0.6
0.55
0.5
Mbd3+/+ MEF
Mbd3flox/- MEF
Mbd3+/+ MEF + 4 day DOX
Mbd3+/+ MEF + 8 day DOX
Mbd3flox/- MEF + 4 day DOX
Mbd3flox/- MEF + 8 day DOX
Mbd3+/+ iPSC
Mbd3flox/- iPSC
Mbd3-/- ESC
Mbd3+/+ MEF
Mbd3flox/- MEF
Mbd3+/+ MEF + 4 day DOX
Mbd3+/+ MEF + 8 day DOX
Mbd3flox/- MEF + 4 day DOX
Mbd3flox/- MEF + 8 day DOX
Mbd3+/+ iPSC
Mbd3flox/- iPSC
Mbd3-/- ESC

FIG. 47B

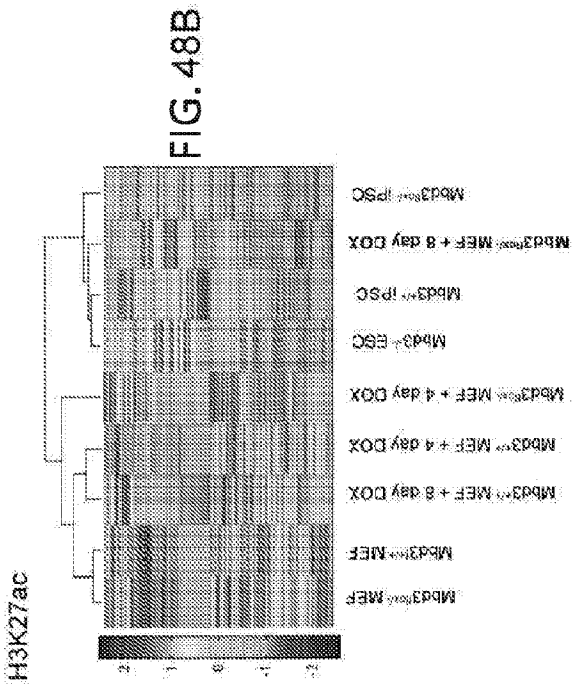


FIG. 48B

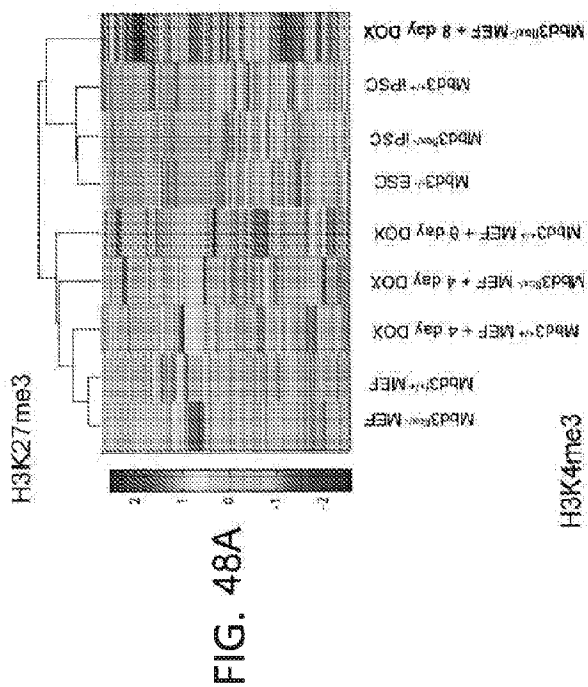


FIG. 48A

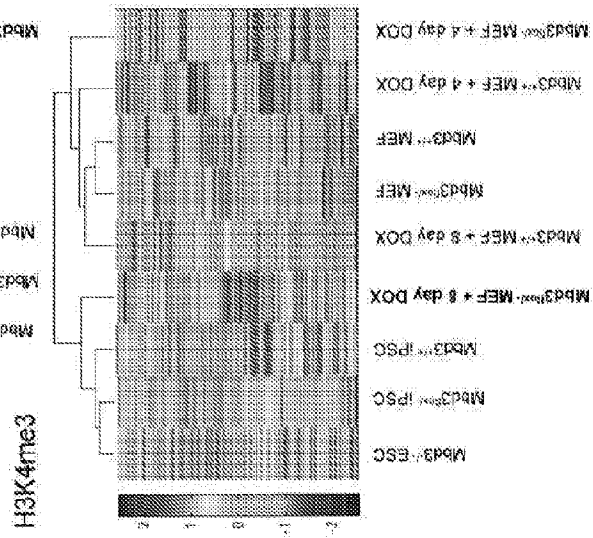


FIG. 48C

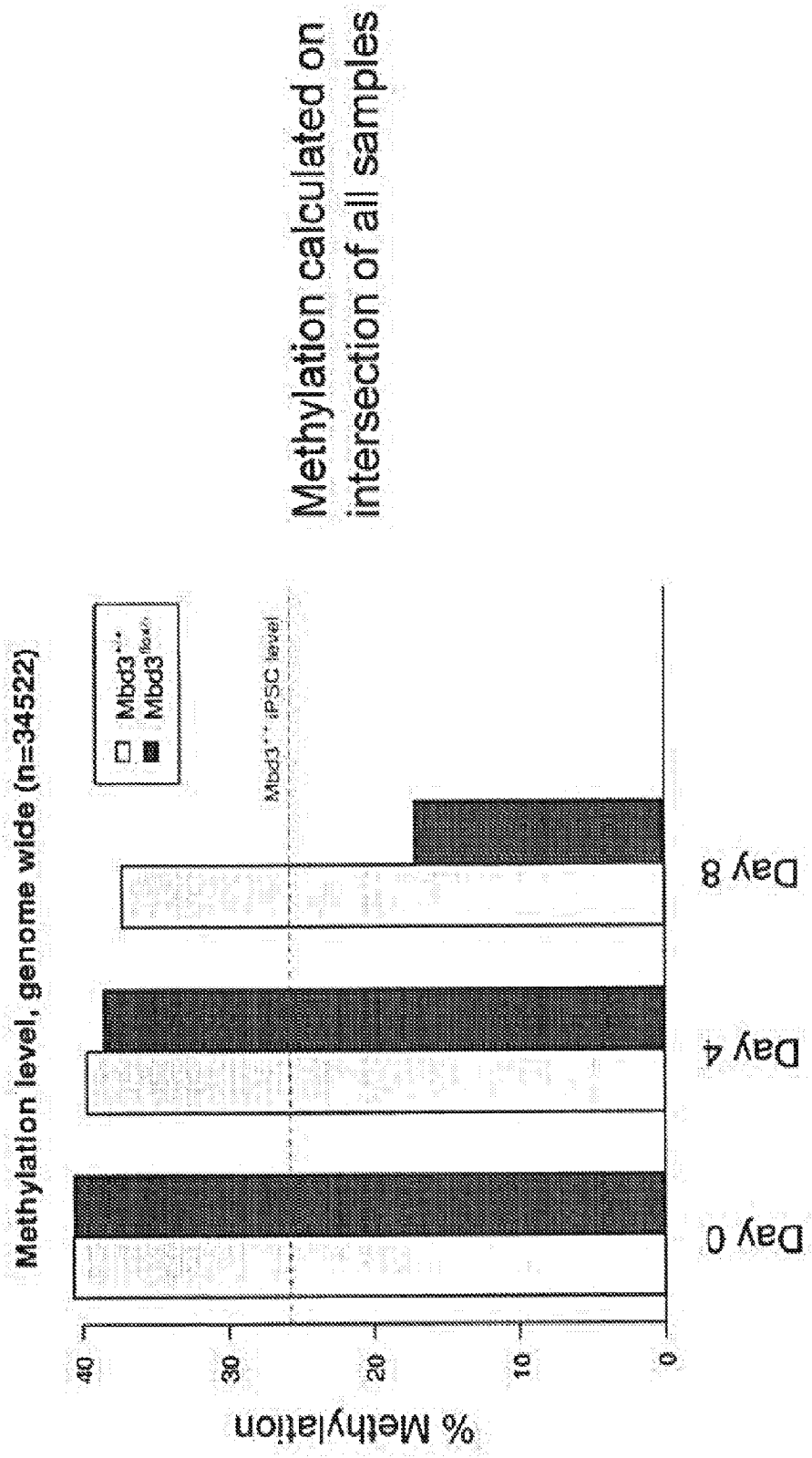

Methylation calculated on intersection of all samples
Methylation level, genome wide (n=34522)
Mbd3+/+
Mbd3fl/fl
Mbd3+/+ iPSC level
% Methylation
40
30
20
10
0
Day 0
Day 4
Day 8

FIG. 49A

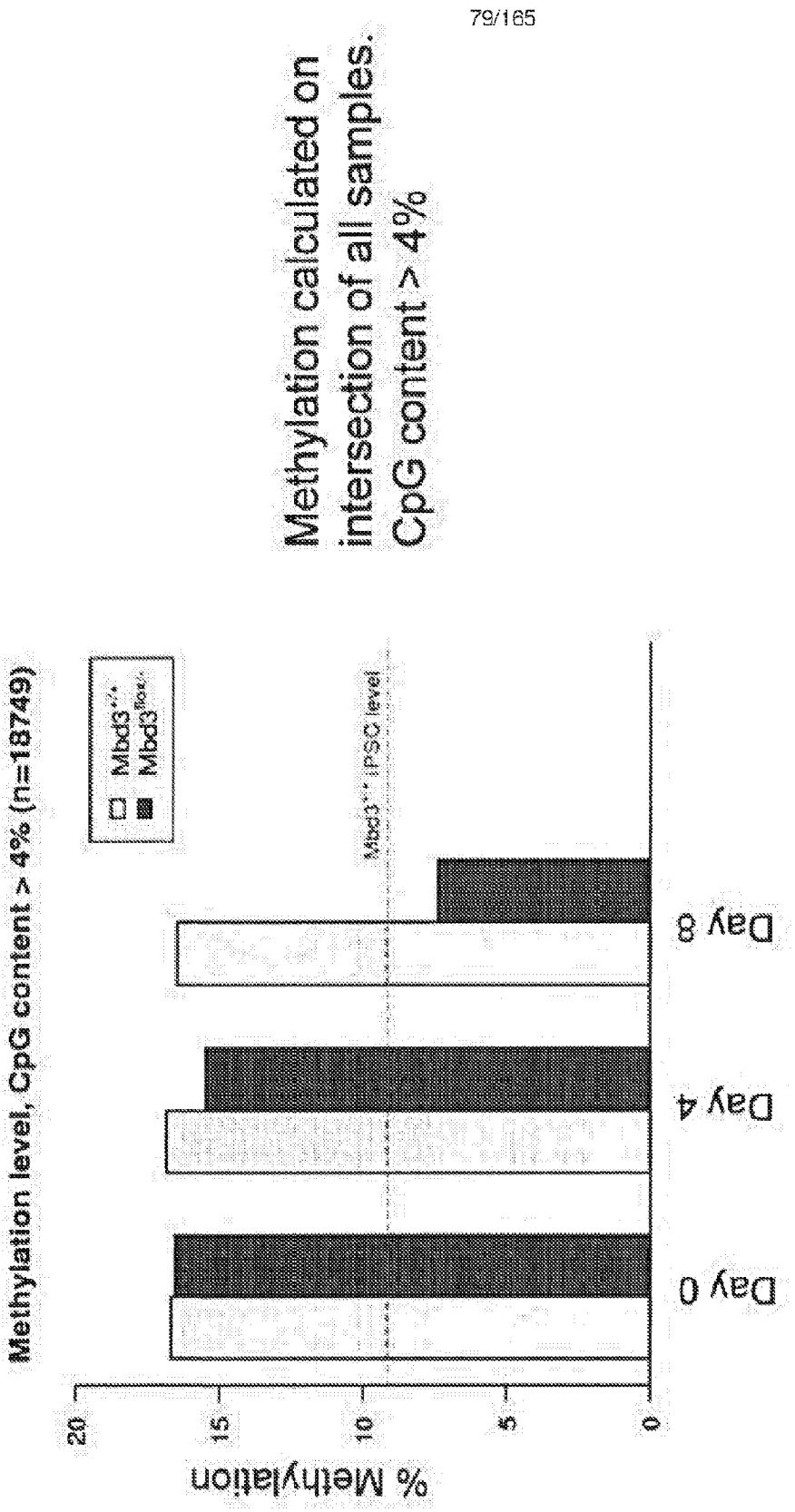

Methylation calculated on intersection of all samples. CpG content > 4%
Methylation level, CpG content > 4% (n=18749)
Mbd3+/+
Mbd3flox/-
Mbd3+/+ iPSC level
% Methylation
0
5
10
15
20
Day 0
Day 4
Day 8

FIG. 49B

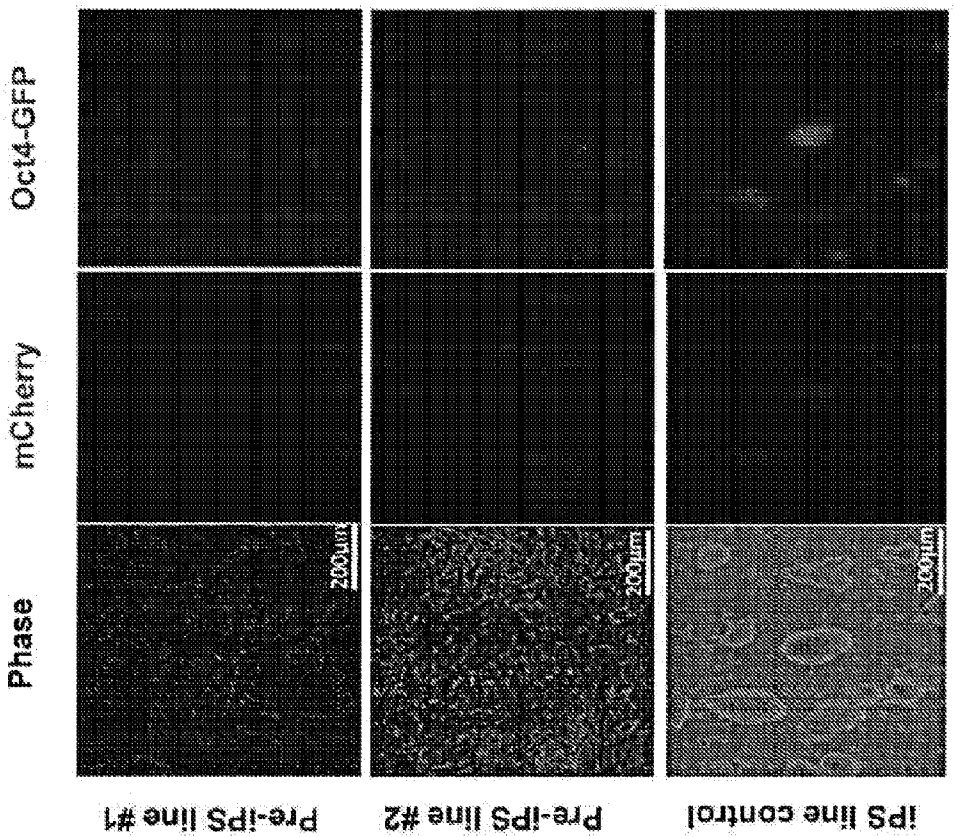


FIG. 50A

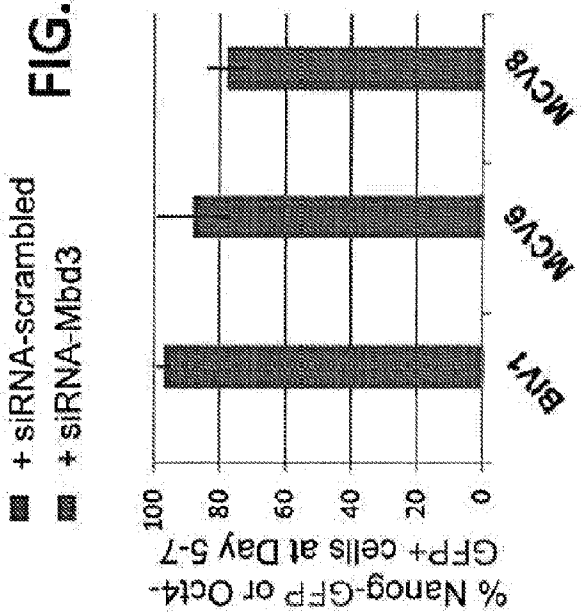


FIG. 50B

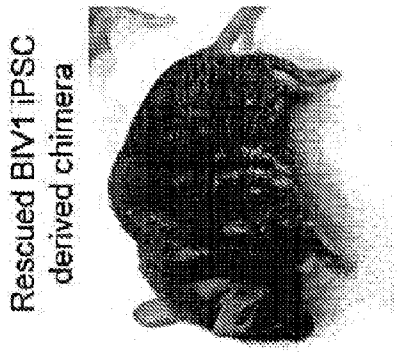


FIG. 50C

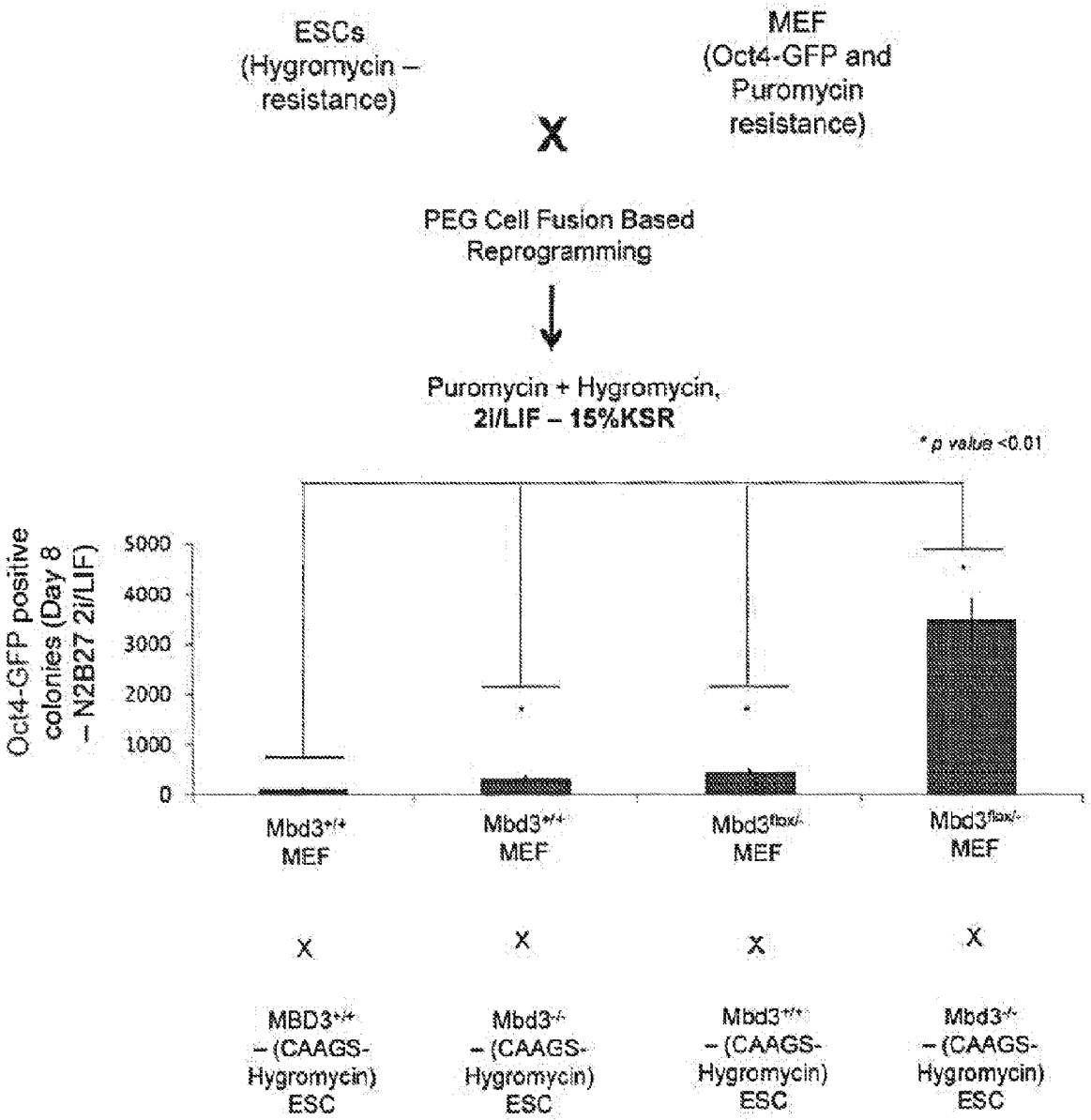

ESCs
(Hygromycin –
resistance)
X
MEF
(Oct4-GFP and
Puromycin
resistance)
PEG Cell Fusion Based
Reprogramming
Puromycin + Hygromycin,
2i/LIF – 15%KSR
* p value <0.01
Oct4-GFP positive
colonies (Day 8
– N2B27 2i/LIF)
5000
4000
3000
2000
1000
0
Mbd3+/+
MEF
Mbd3+/+
MEF
Mbd3flox/-
MEF
Mbd3flox/-
MEF
X
X
X
X
MBD3+/+
– (CAAGS-
Hygromycin)
ESC
Mbd3-/-
– (CAAGS-
Hygromycin)
ESC
Mbd3+/+
– (CAAGS-
Hygromycin)
ESC
Mbd3-/-
– (CAAGS-
Hygromycin)
ESC

FIG. 51

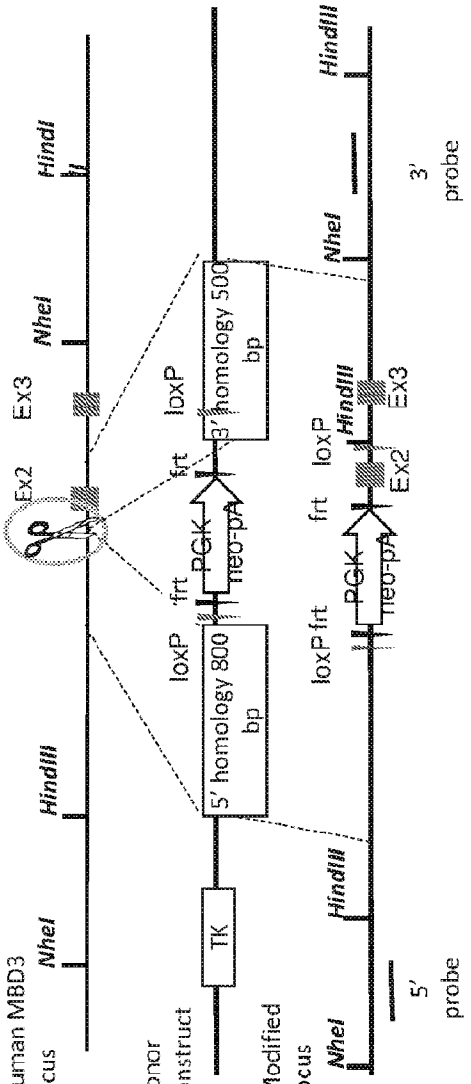


FIG. 52A

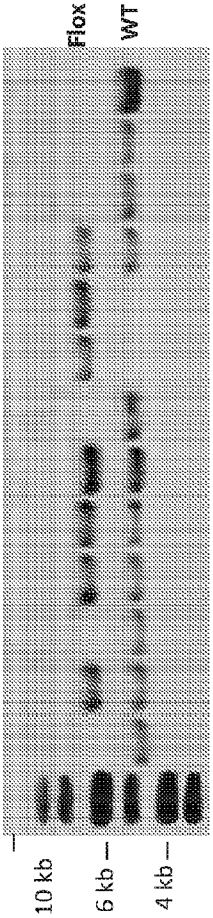


FIG. 52B

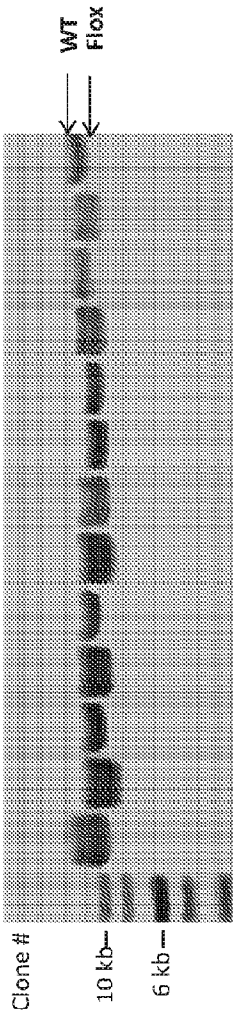


FIG. 52C

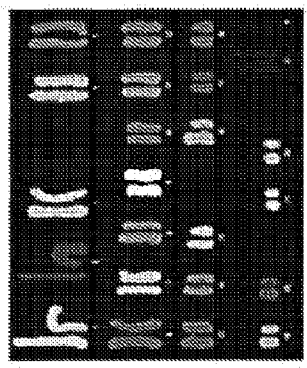


FIG. 53B

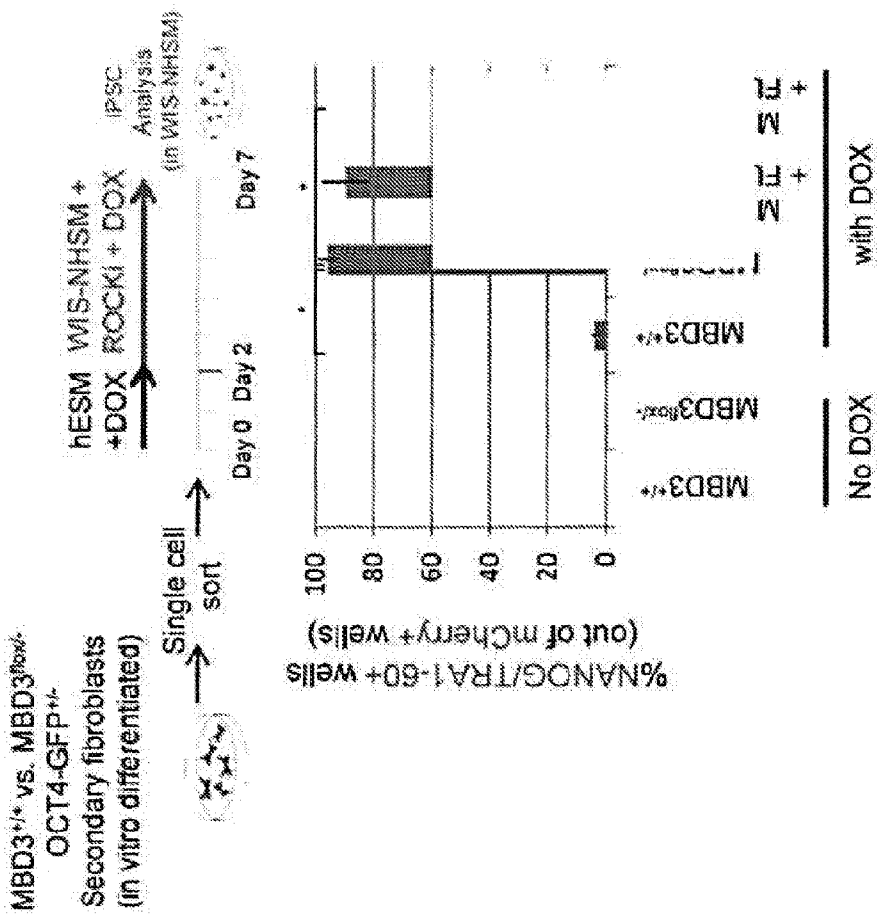


FIG. 53A

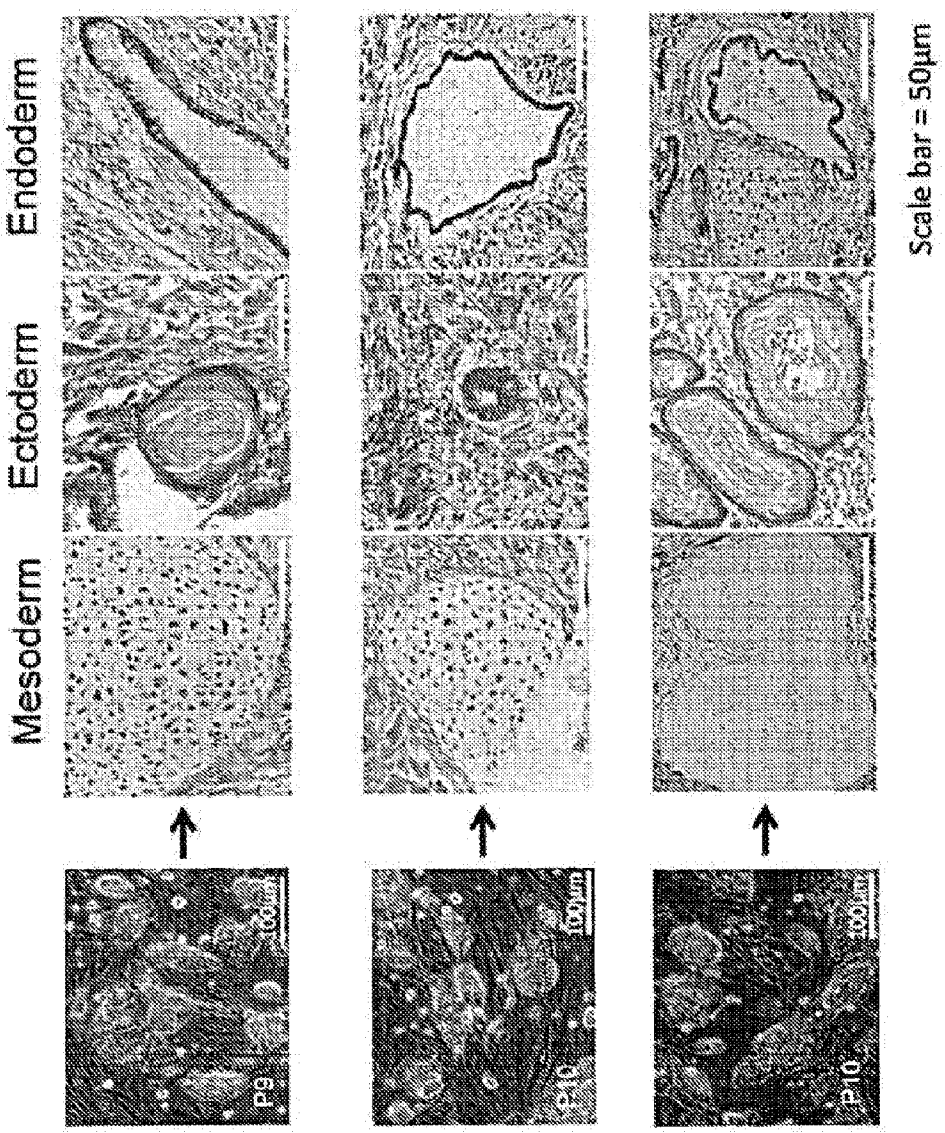


FIG. 53C MBD3$^{flox/-}$ iPSC clone #1

FIG. 53D MBD3$^{flox/-}$ iPSC clone #2

FIG. 53E MBD3$^{flox/-}$ iPSC clone #3

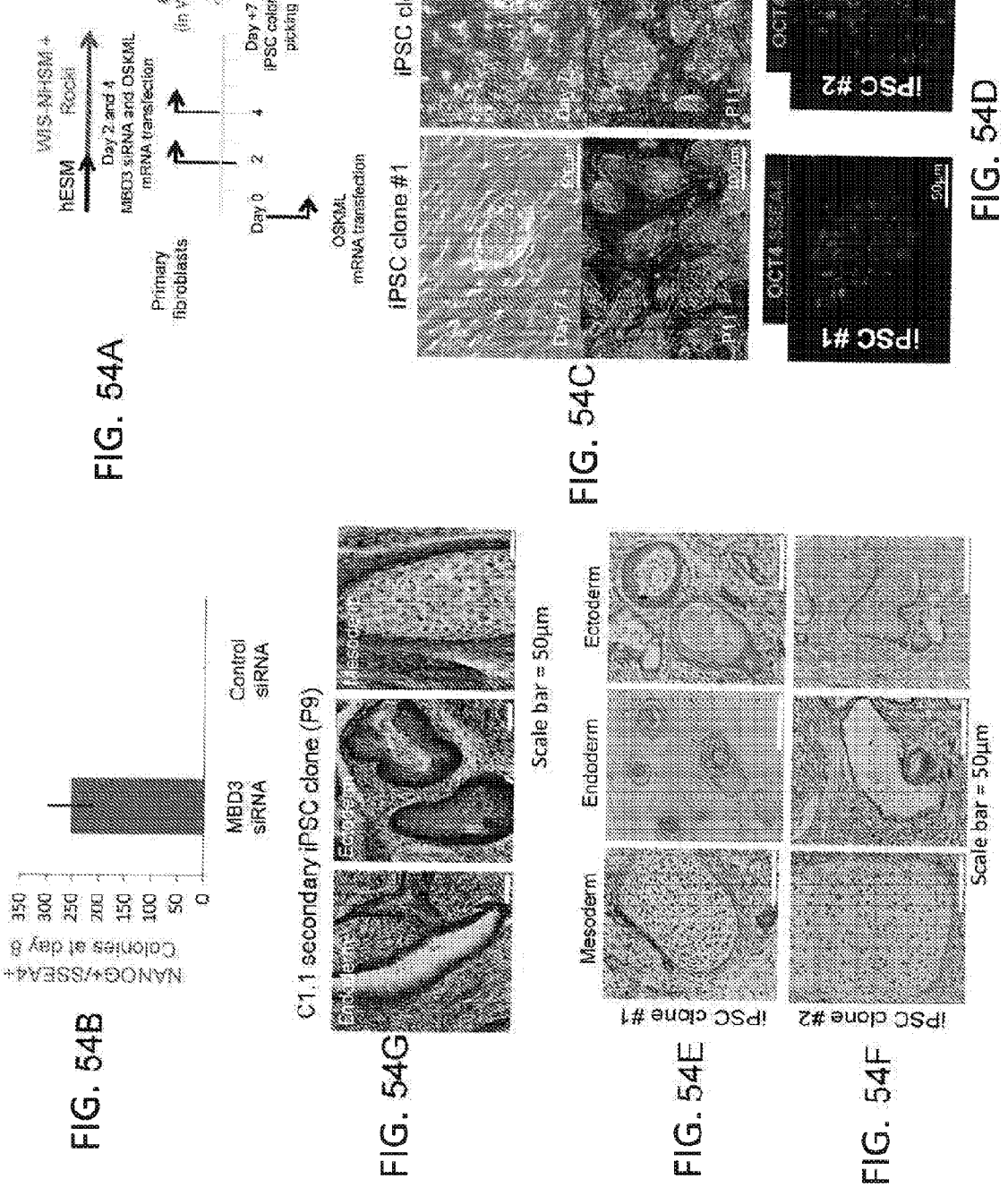


FIG. 54B

FIG. 54A

FIG. 54C

FIG. 54D

FIG. 54G

FIG. 54E

FIG. 54F

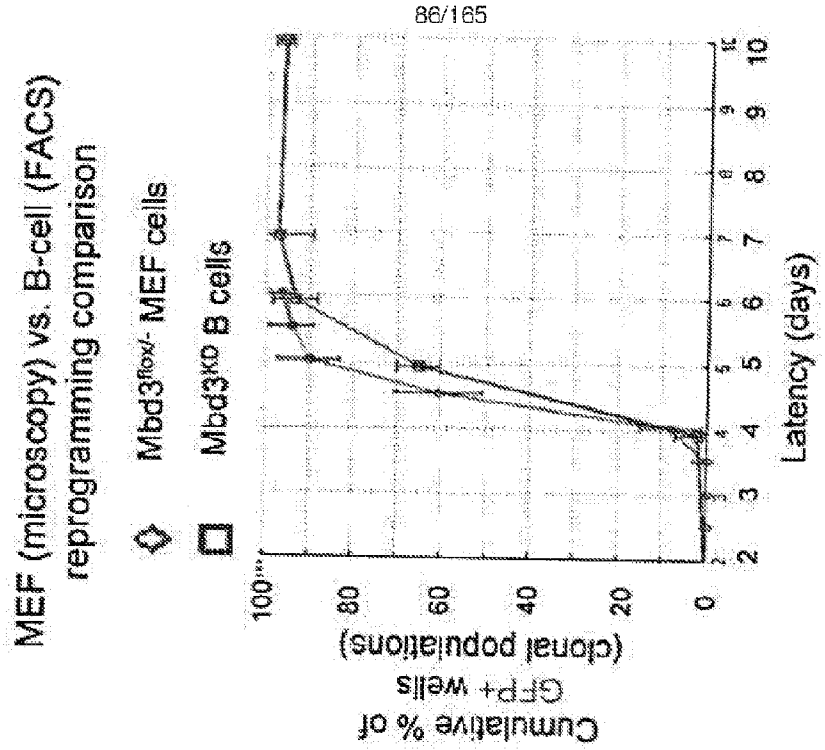


FIG. 55B

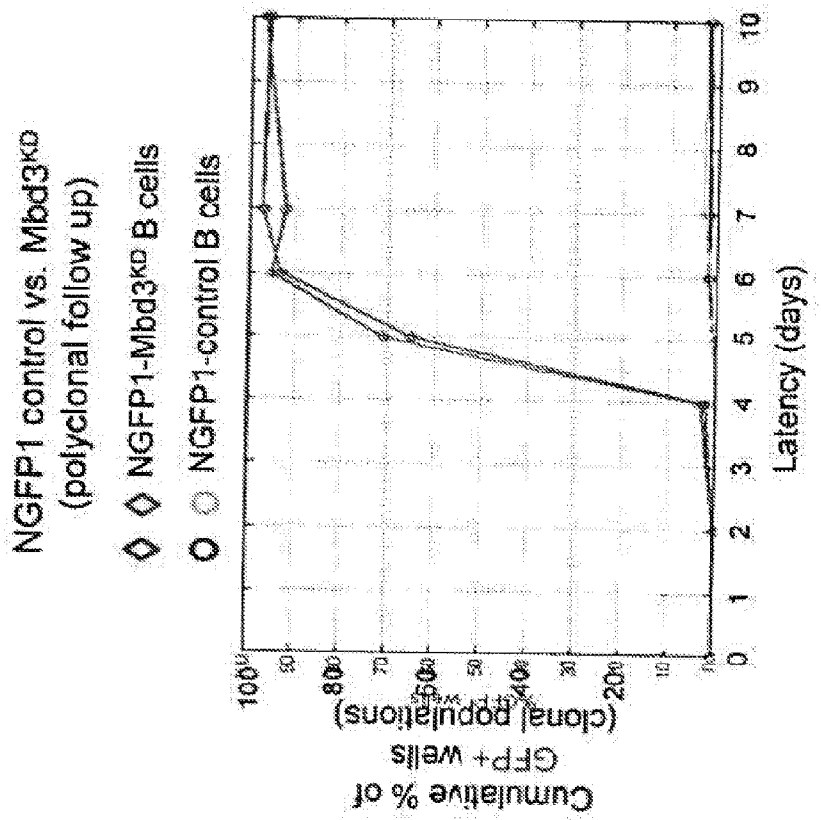
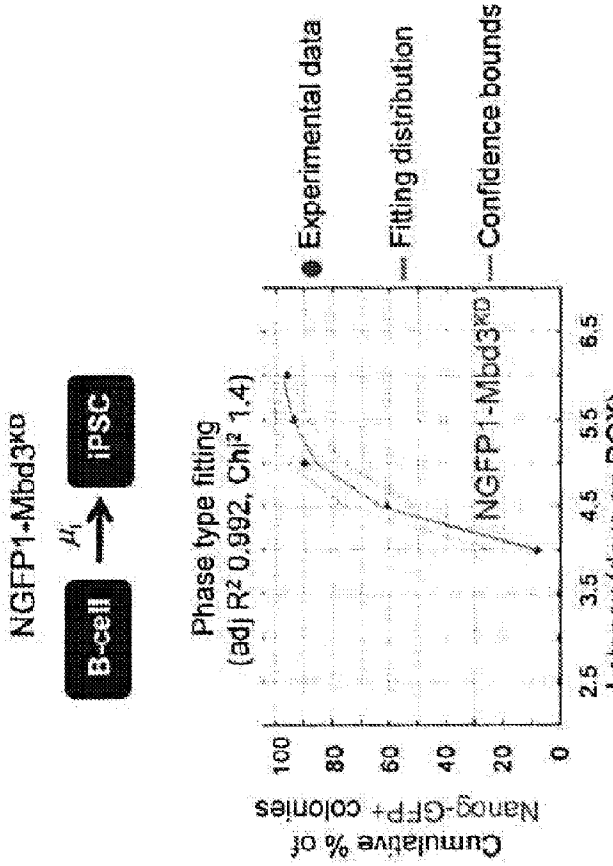
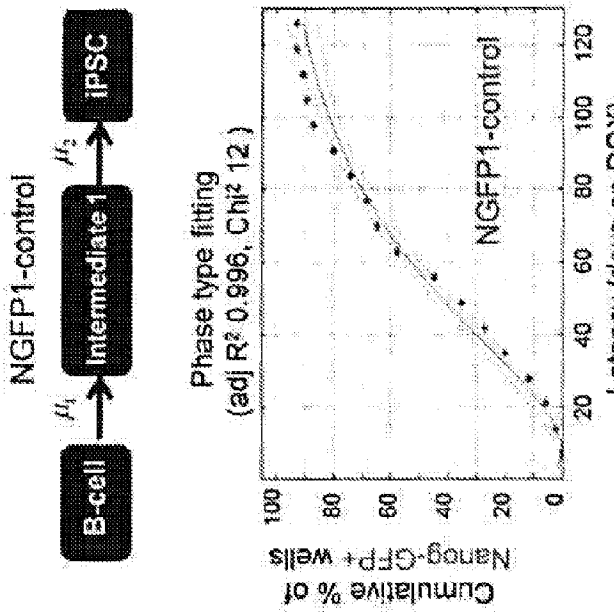


FIG. 55A



Mbd3KD	V_eff1/(days)]
1 exp	1.85

FIG. 55D



Control	V_eff1/(days*Neff)]
2 exp	5.4E-09

FIG. 55C

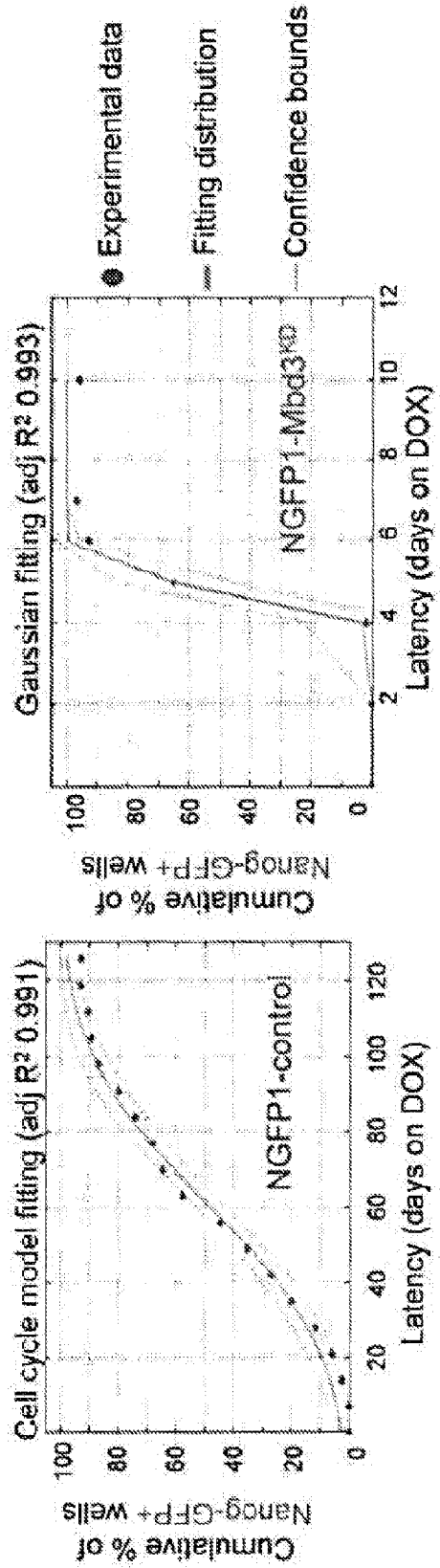


FIG. 56A

FIG. 56B

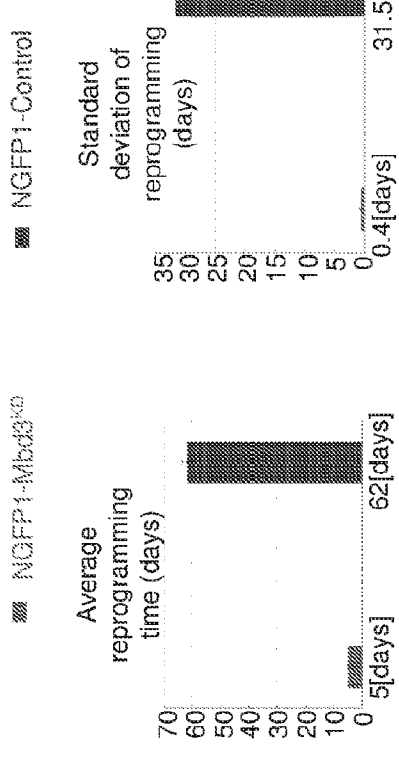


FIG. 56C

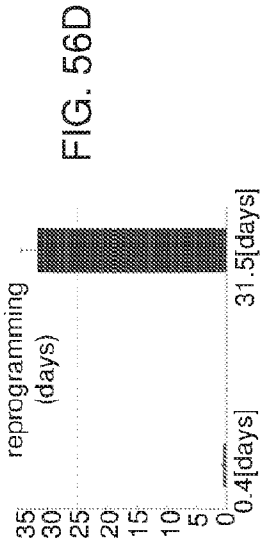


FIG. 56D

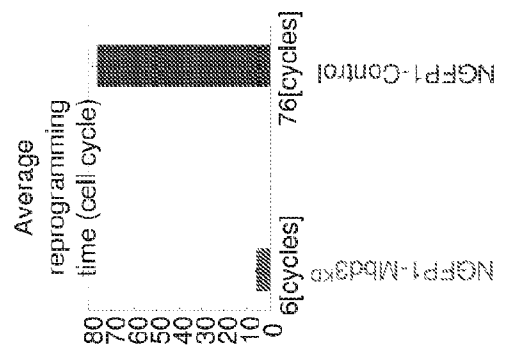


FIG. 56E

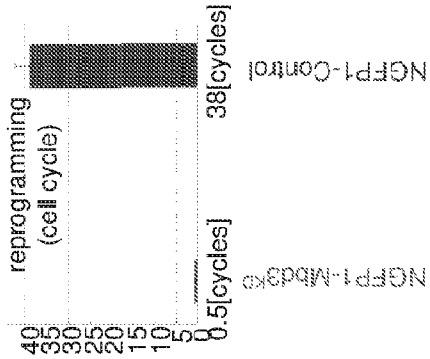


FIG. 56F

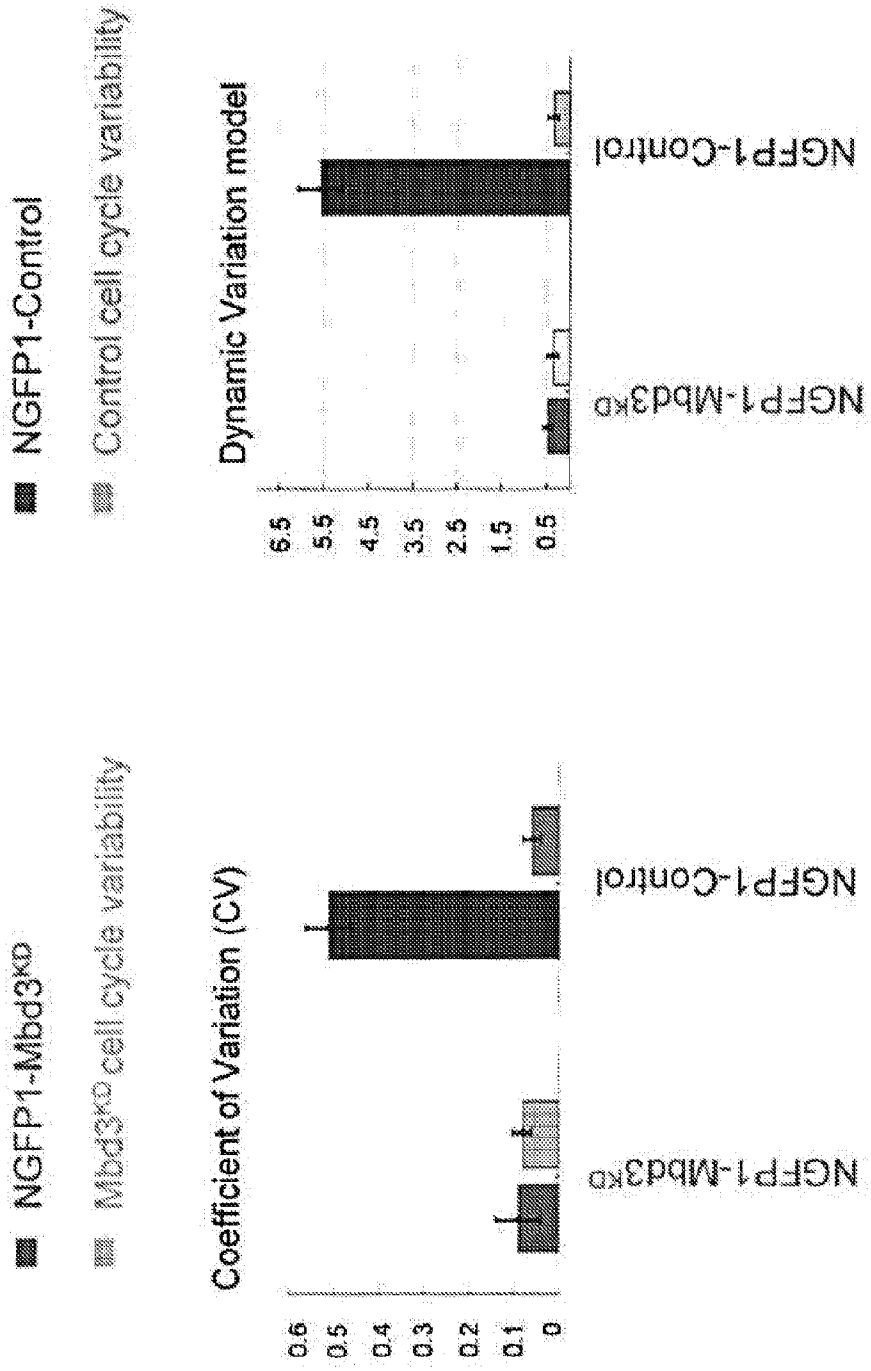


FIG. 57A

FIG. 57B

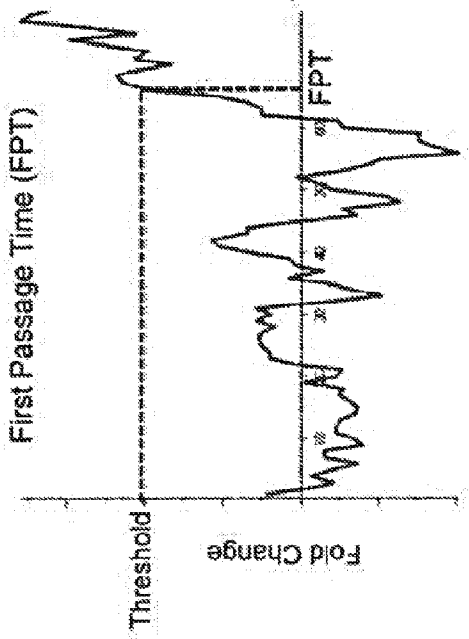


FIG. 57C

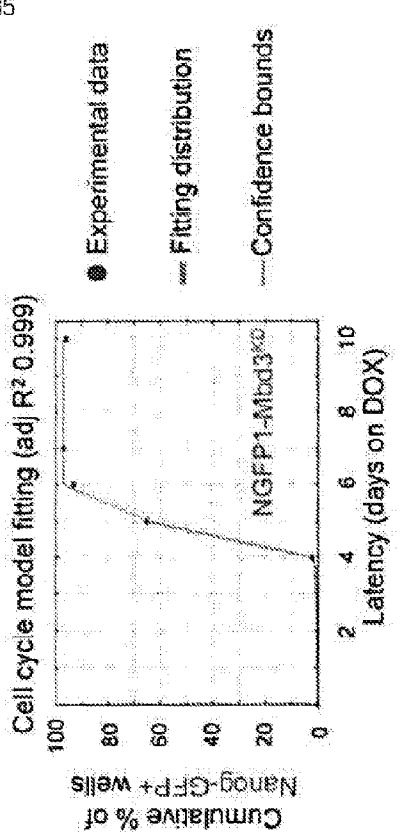


FIG. 57E

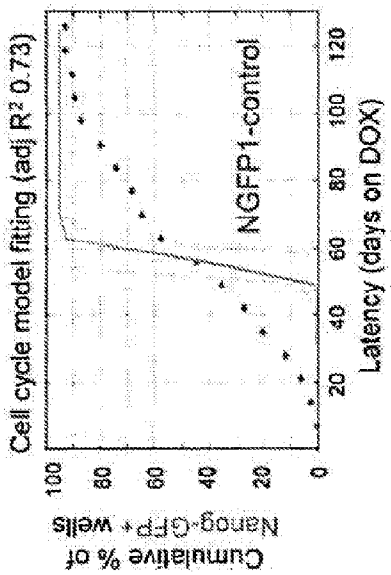


FIG. 57D

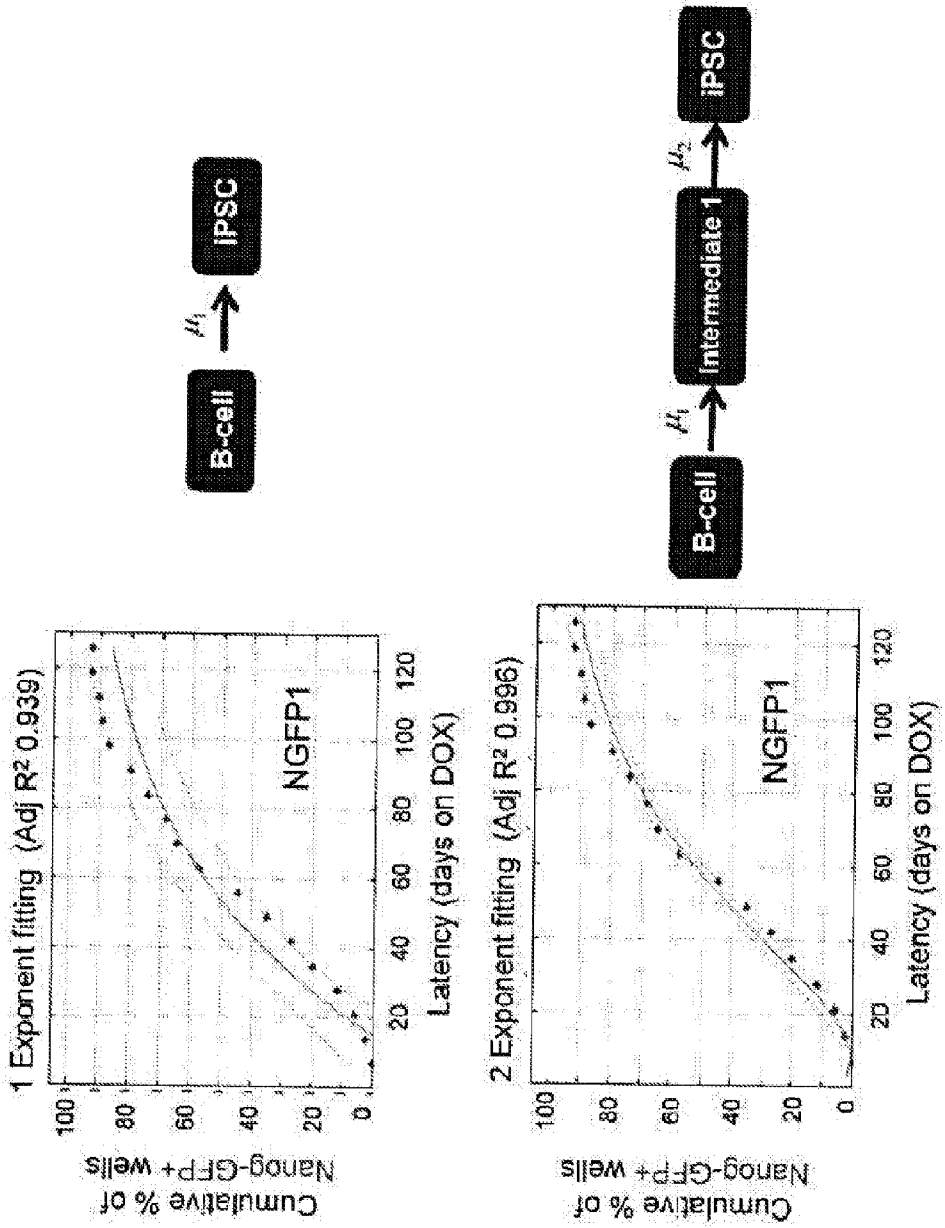


FIG. 58A

FIG. 58B

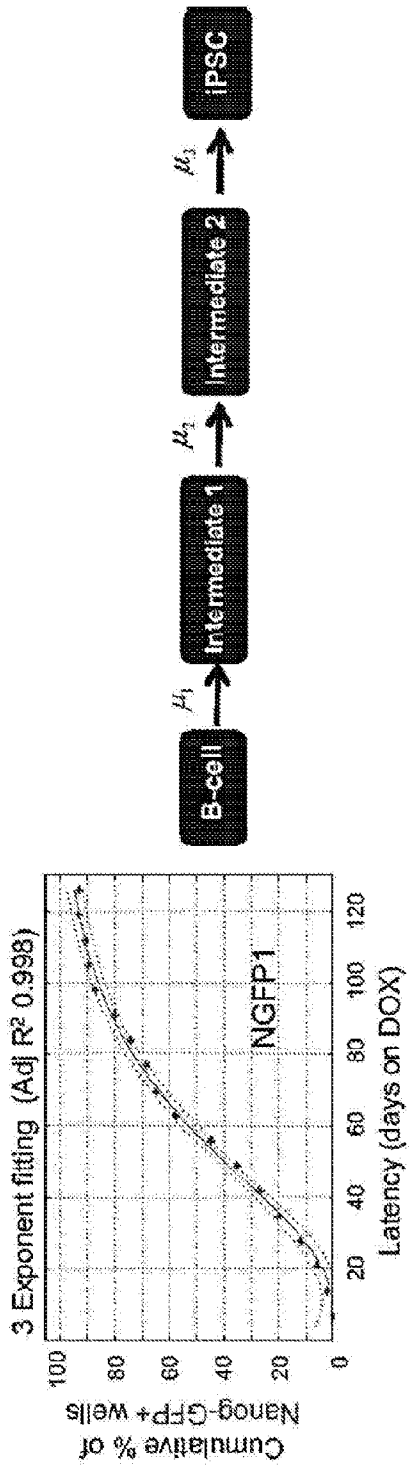


FIG. 58C

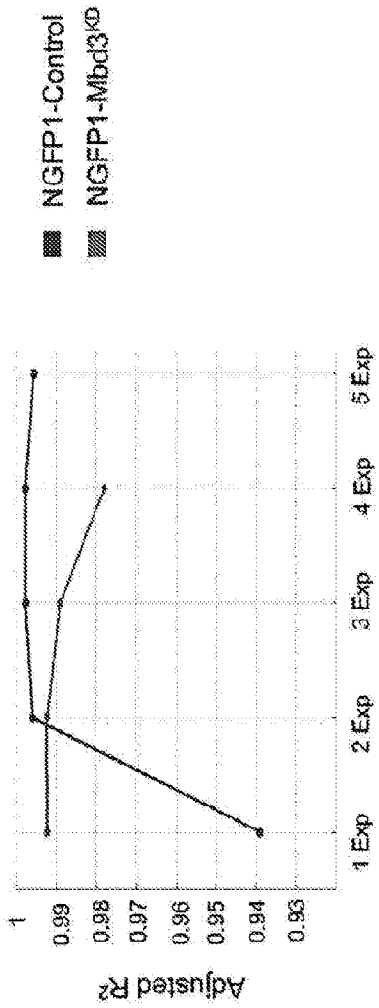


FIG. 58D

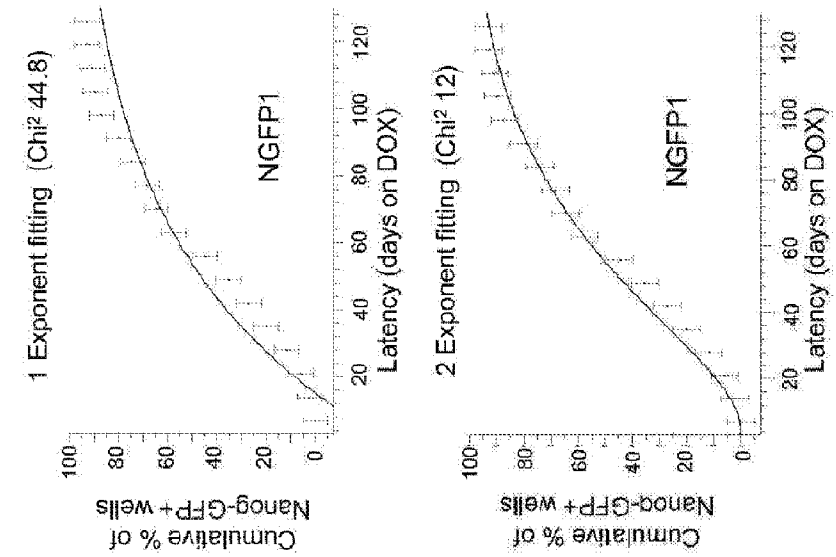


FIG. 59A

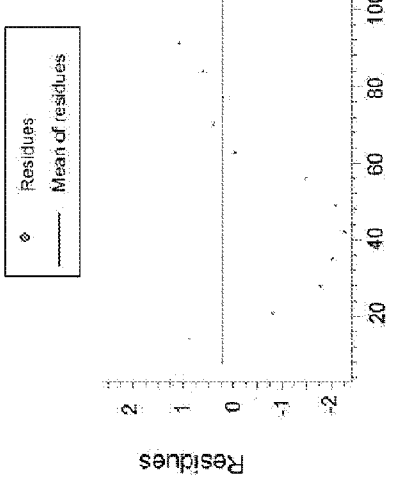


FIG. 59B

FIG. 59C

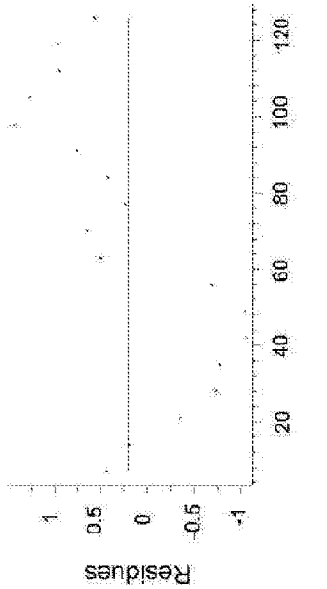


FIG. 59D

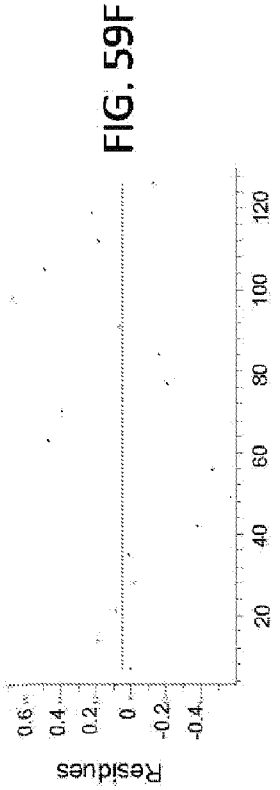


FIG. 59F

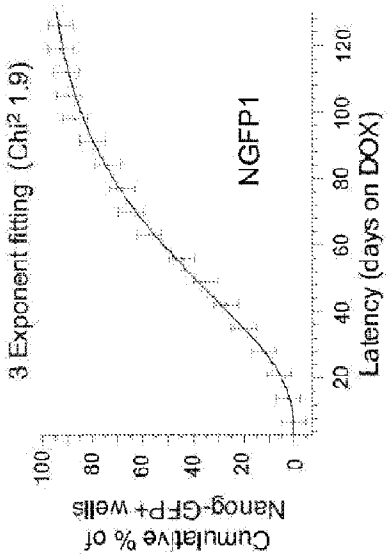


FIG. 59E

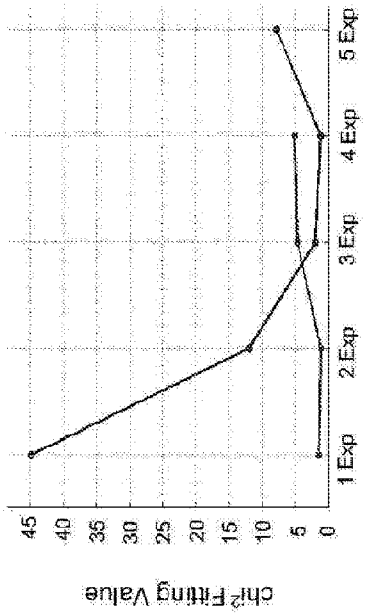


FIG. 59G

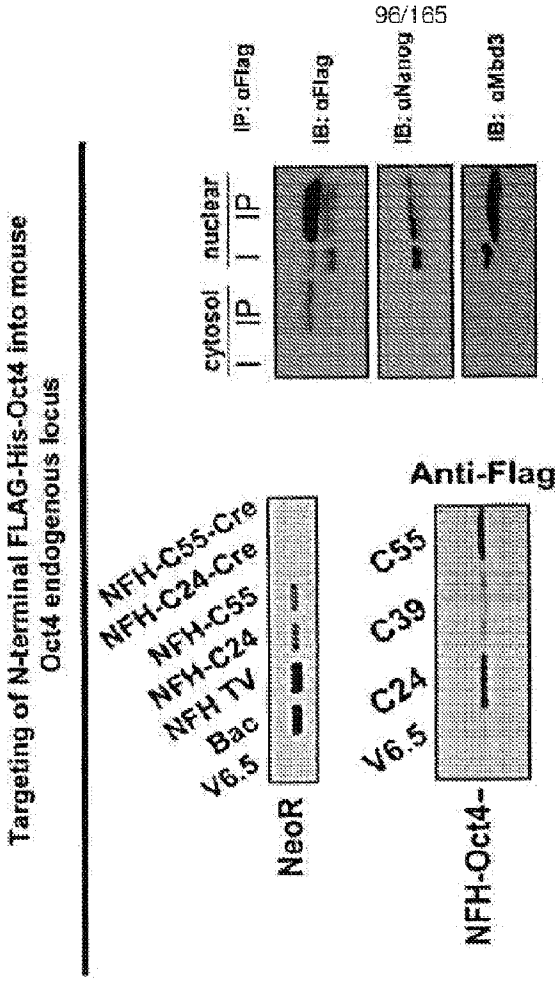


FIG. 60B

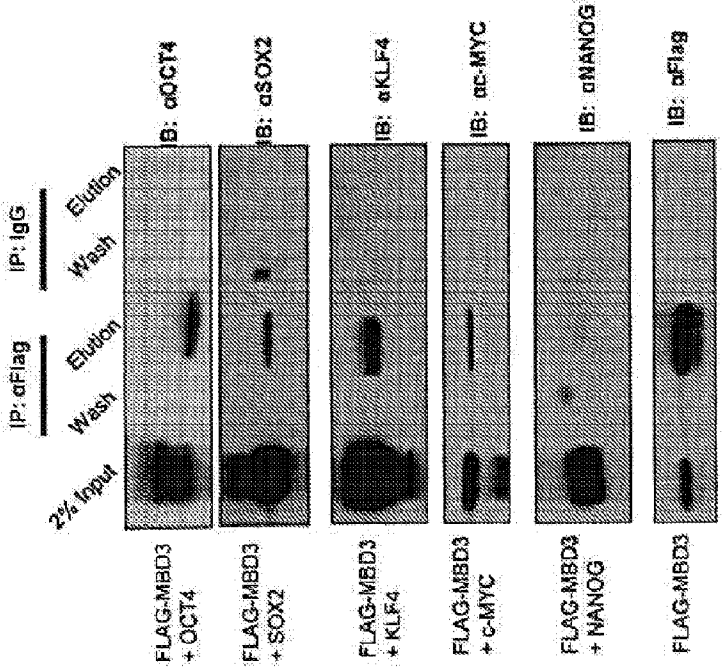


FIG. 60A

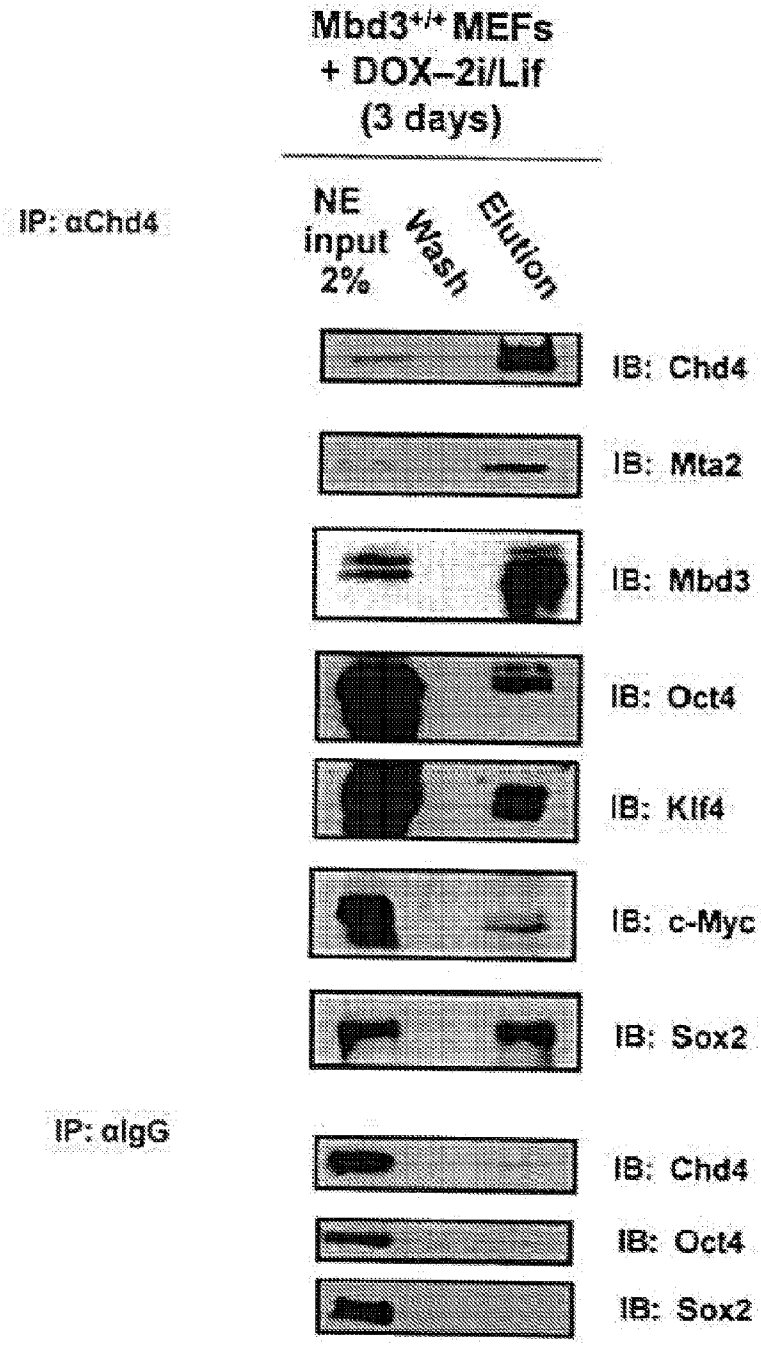

Mbd3+/+ MEFs
+ DOX–2i/Lif
(3 days)
IP: αChd4
NE input 2%
Wash
Elution
IB: Chd4
IB: Mta2
IB: Mbd3
IB: Oct4
IB: Klf4
IB: c-Myc
IB: Sox2
IP: αIgG
IB: Chd4
IB: Oct4
IB: Sox2

FIG. 60C

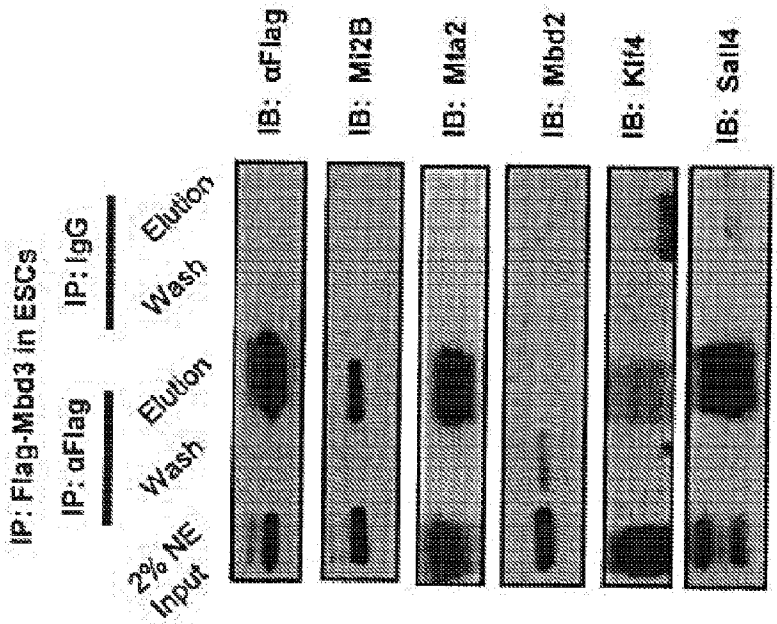


FIG. 61A

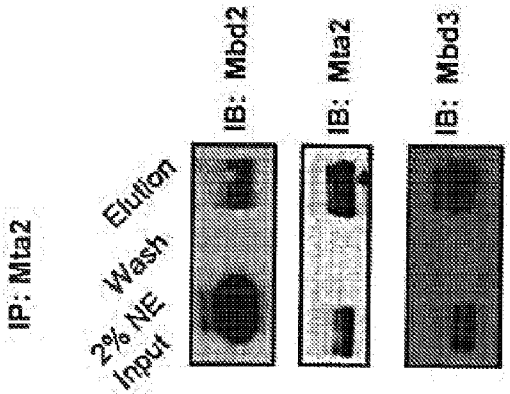


FIG. 61B

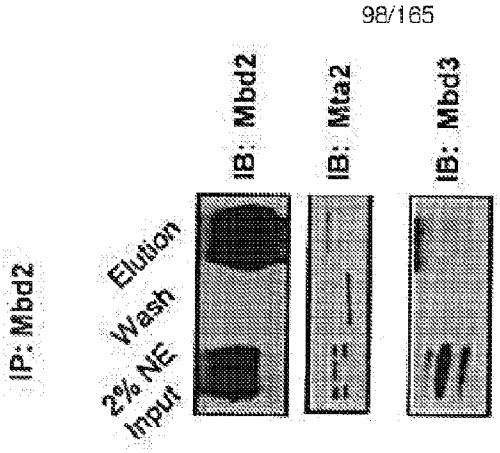


FIG. 61C

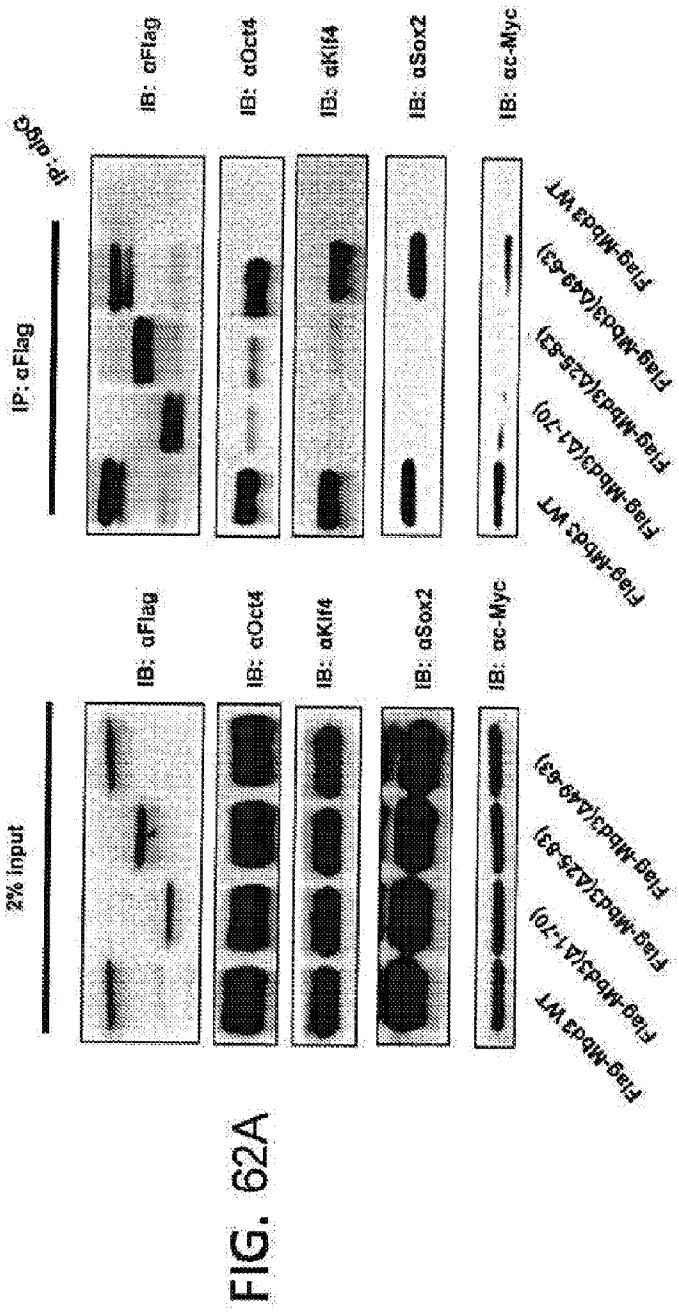


FIG. 62A

FIG. 62B

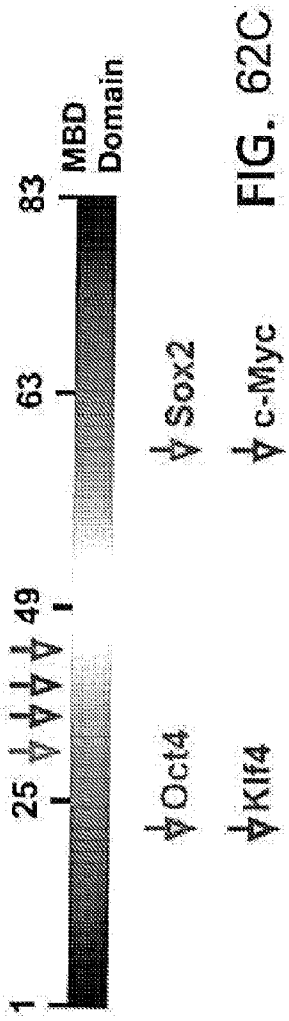


FIG. 62C

Motifs in Mbd3 bound regions following OSKM induction

Factor	Z score	P-value
Smad2/3	-20.7289	1.00E-30
Pou5f1	-20.646	1.00E-30
Klf1	-18.7681	1.00E-30
Sox2	-18.1417	1.00E-30
Klf4	-18.0815	1.00E-30
Klf7	-14.6281	1.00E-30
Rxra	-8.8792	3.37E-19
Zfp281	-7.90E+00	1.35E-15
Nr2f2	-7.6746	8.30E-15
Rara	-7.2955	1.49E-13
Sox11	-7.1281	5.09E-13
Nr5a2	-6.7859	5.77E-12
Nr1d2	-6.6024	2.02E-11
Sox30	-5.1197	1.53E-07
Rela	-4.7827	8.65E-07
Ctcf	-4.7463	0.000001036
Zic3	-4.6215	1.9045E-06
Zfp423	-4.6082	2.0304E-06
LMO2,Lmo2	-4.03E+00	0.000028302
Egr2	-3.8483	0.000059459
Sox15	-3.7769	0.000079394
Zfp740	-3.7689	0.000081987
Tcfap2a	-3.7374	0.000092951
Tcfap2c	-3.5205	0.00021537
Ppara	-3.39E+00	0.00034913
Sox12	-3.2536	0.00056986
Tcfap2b	-3.2505	0.00057604
Zfp161	-5.6591	7.61E-09
Zscan10	-3.6055	0.00015575
Zfp161	-3.1773	0.00074322

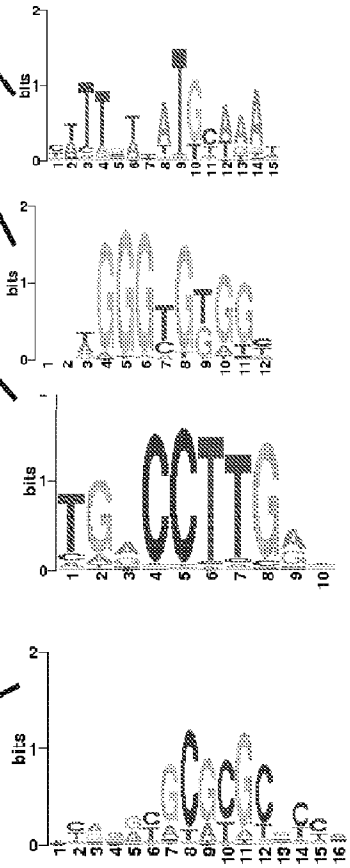


FIG. 63

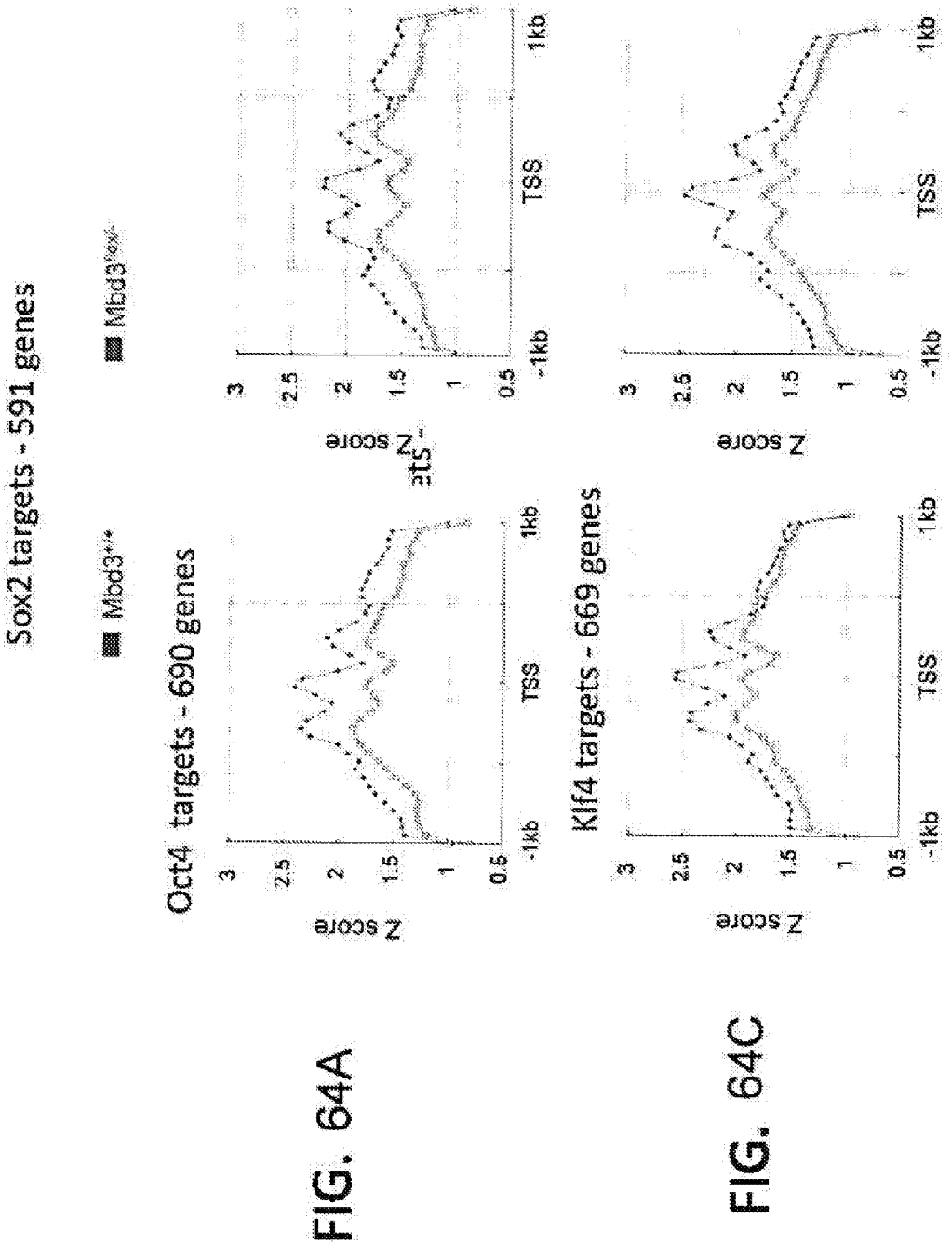


FIG. 64A

FIG. 64B

FIG. 64C

FIG. 64D

FIG. 64G

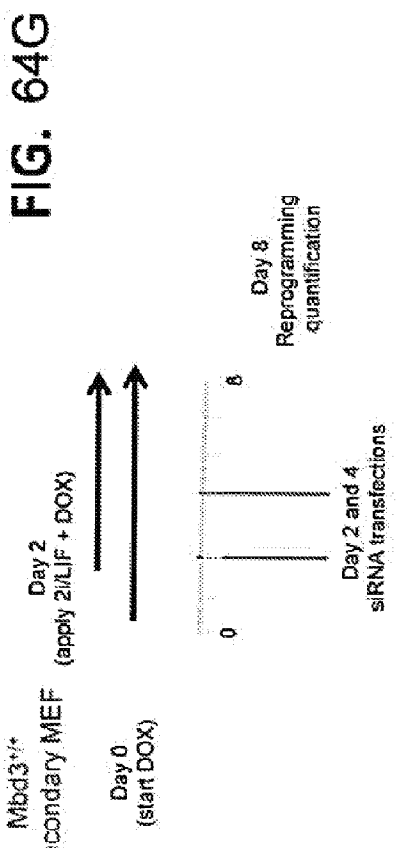


FIG. 64H

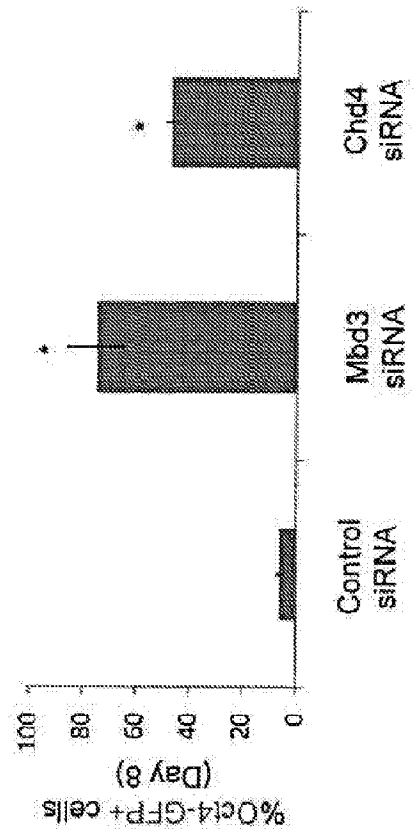


FIG. 64E

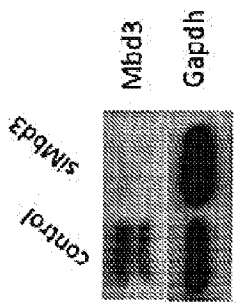
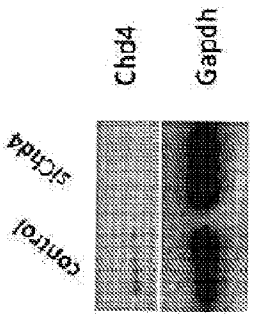


FIG. 64F



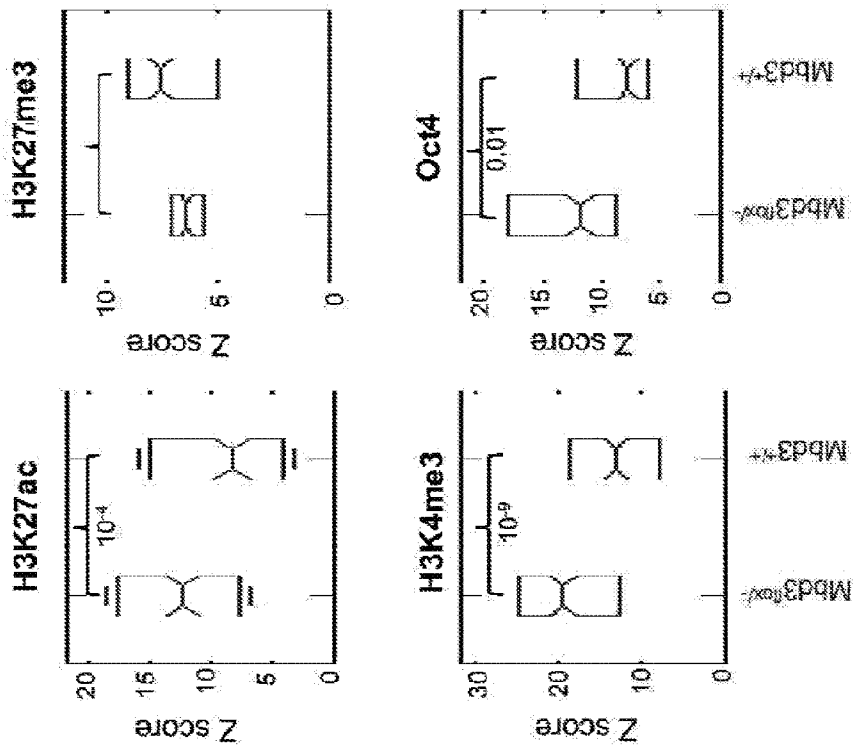


FIG. 65B

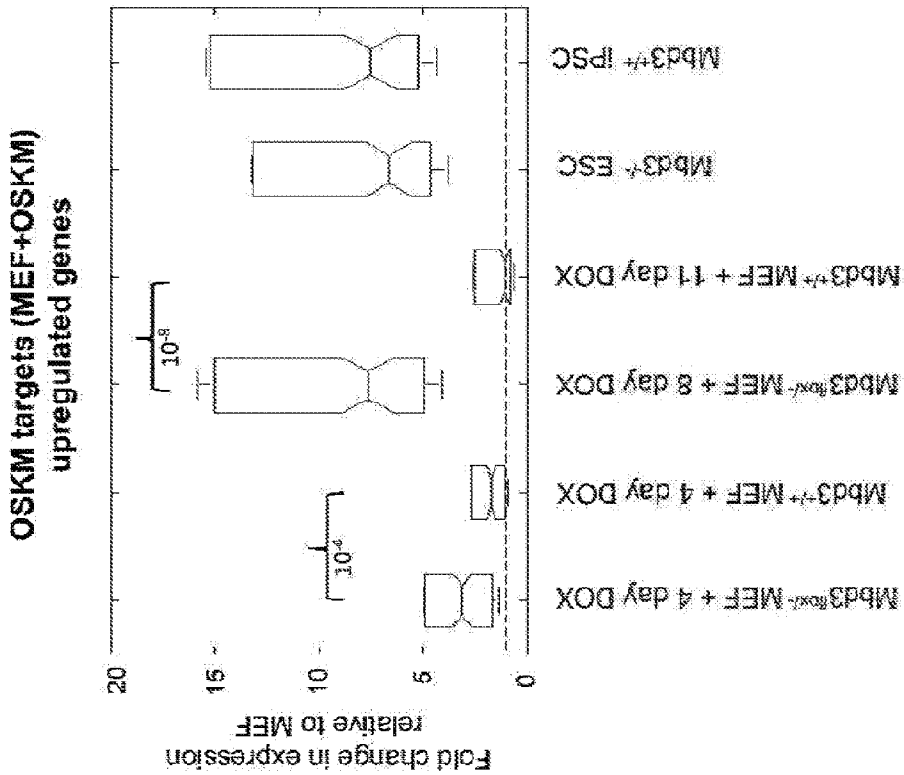


FIG. 65A

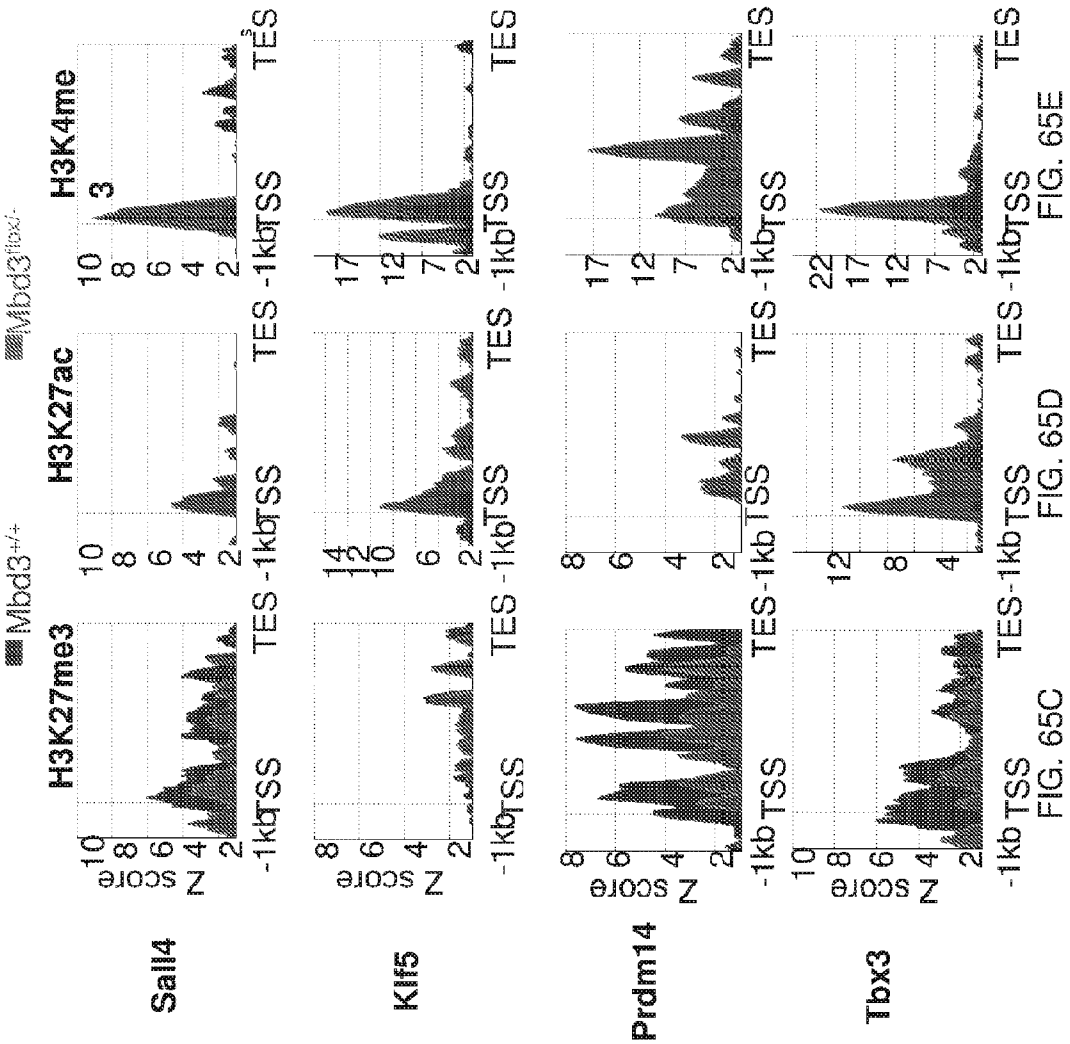


FIG. 65C
FIG. 65D
FIG. 65E

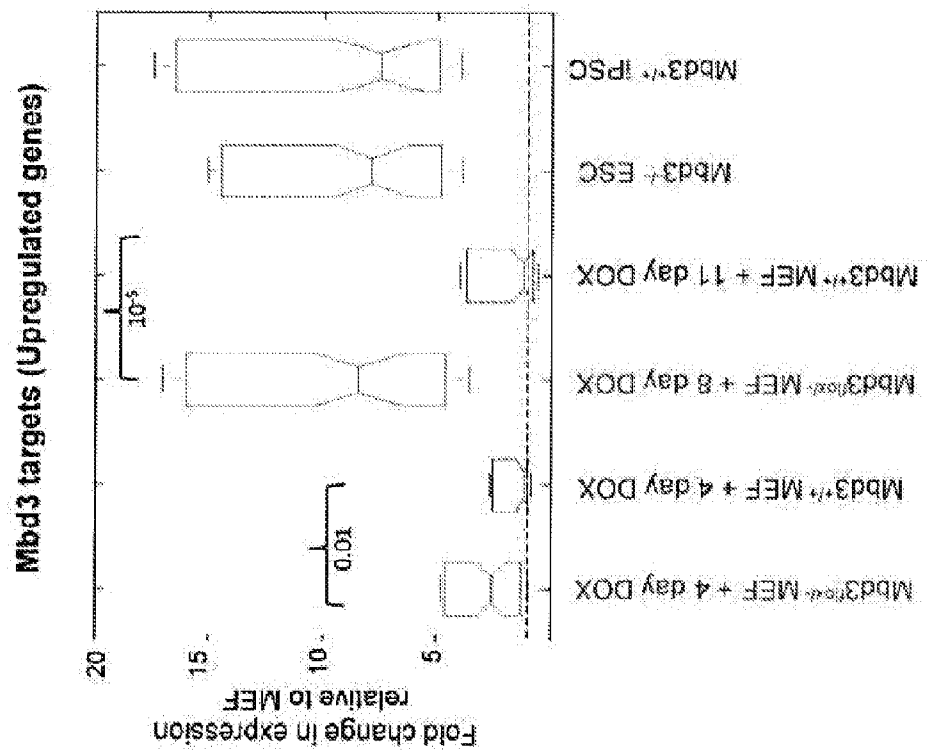


FIG. 66B

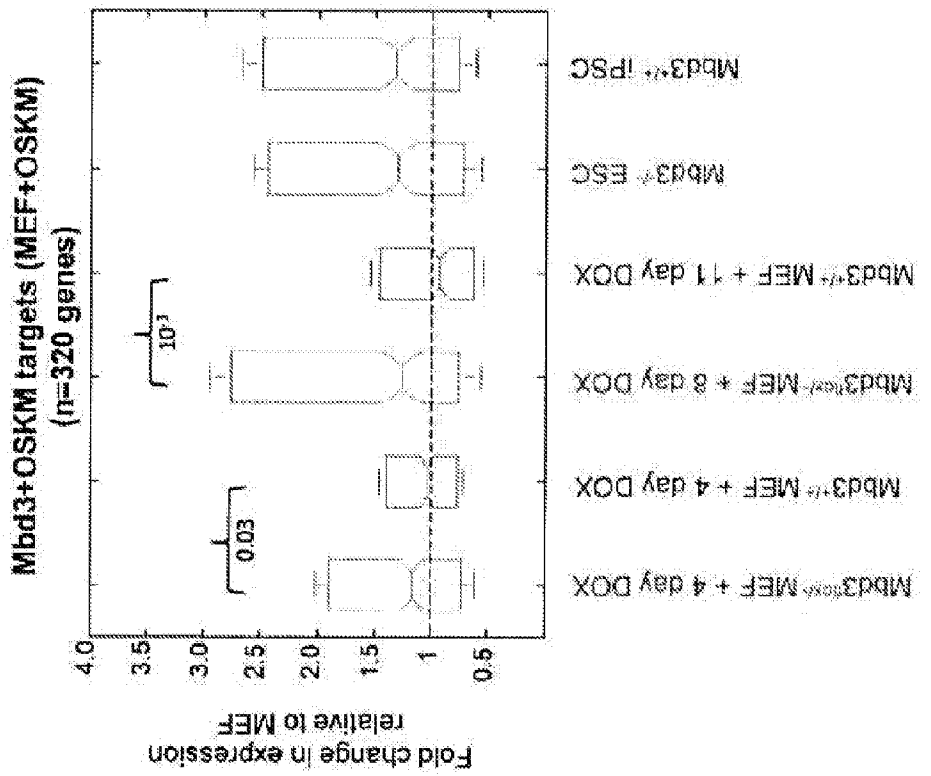


FIG. 66A

FIG. 66C

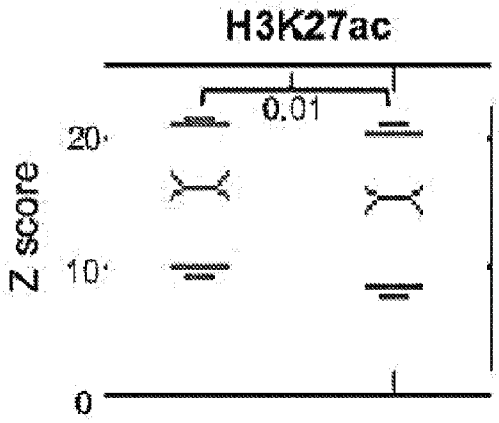
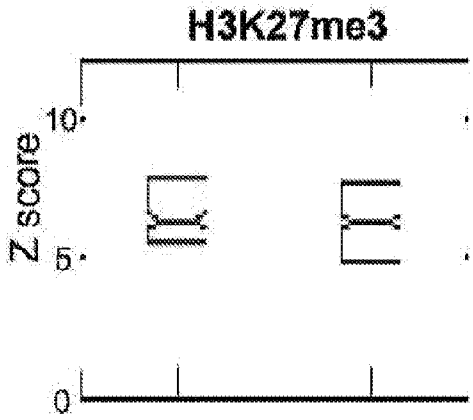


FIG. 66D



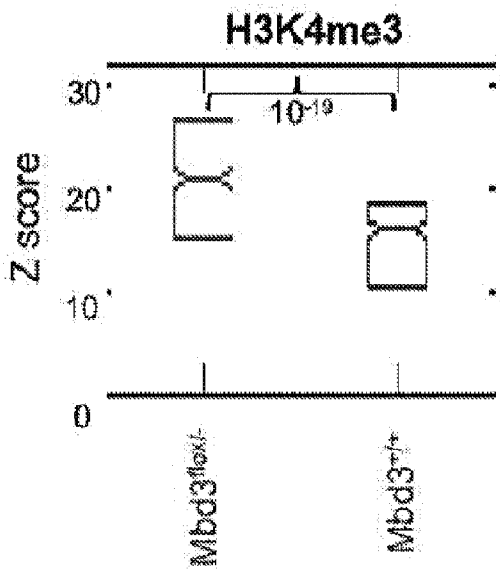


FIG. 66E

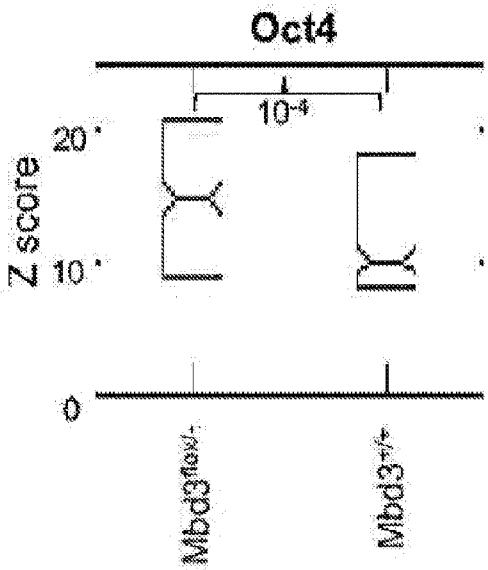
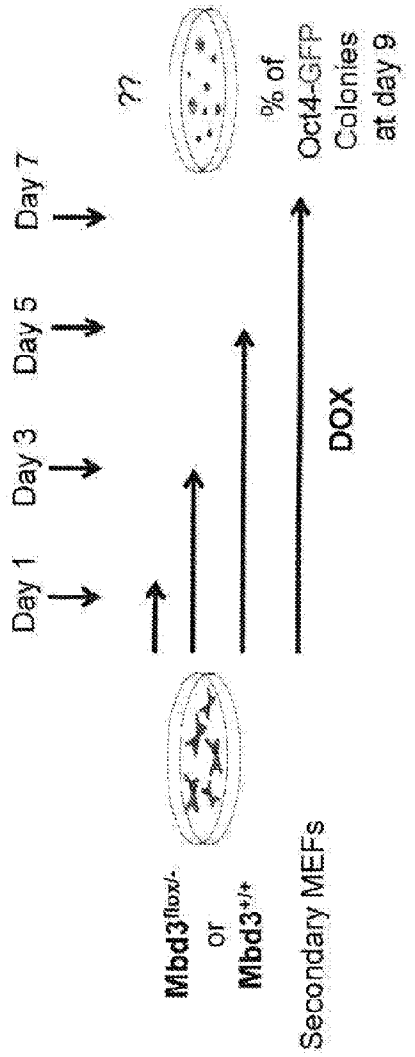


FIG. 66F



DOX stopped at:	Day 1	Day 3	Day 5	Day 7
Mbd3flox/-	0%	0-4%	100%	100%
Mbd3+/+	0%	0-2%	6%	7%

FIG. 67A

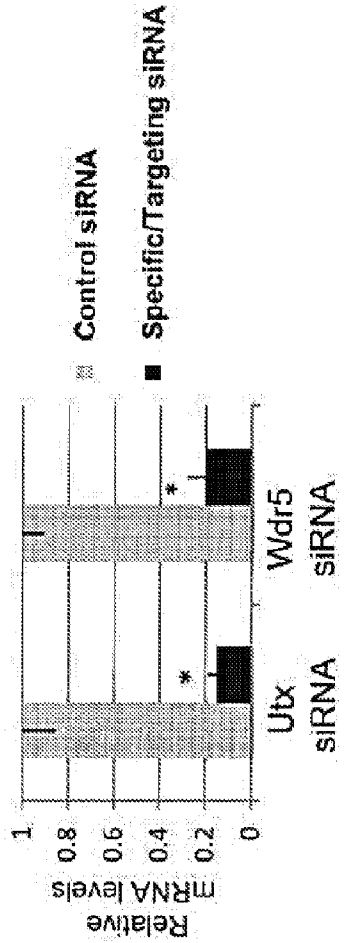


FIG. 67B

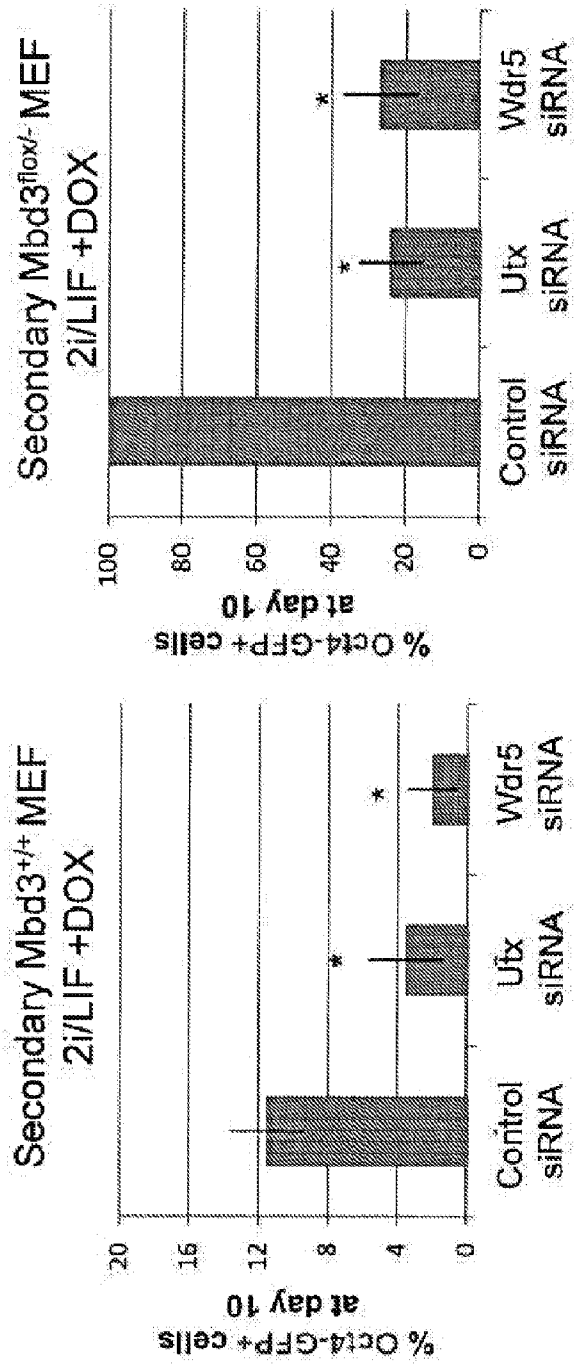


FIG. 67C

FIG. 67D

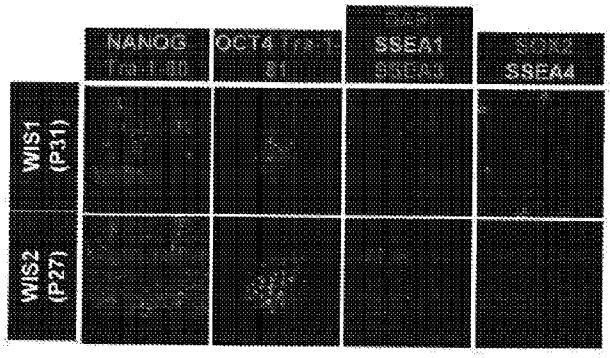


FIG. 68A

FIG. 68B

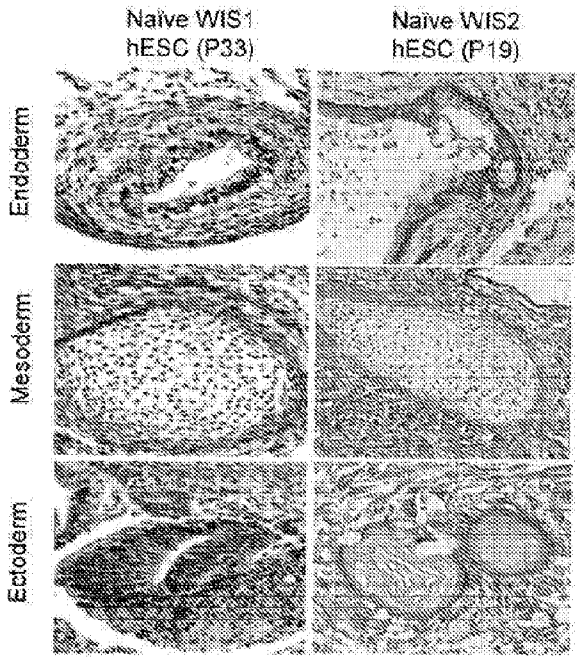


FIG. 68C

FIG. 68D

FIG. 68E

FIG. 68F

FIG. 68G

FIG. 68H

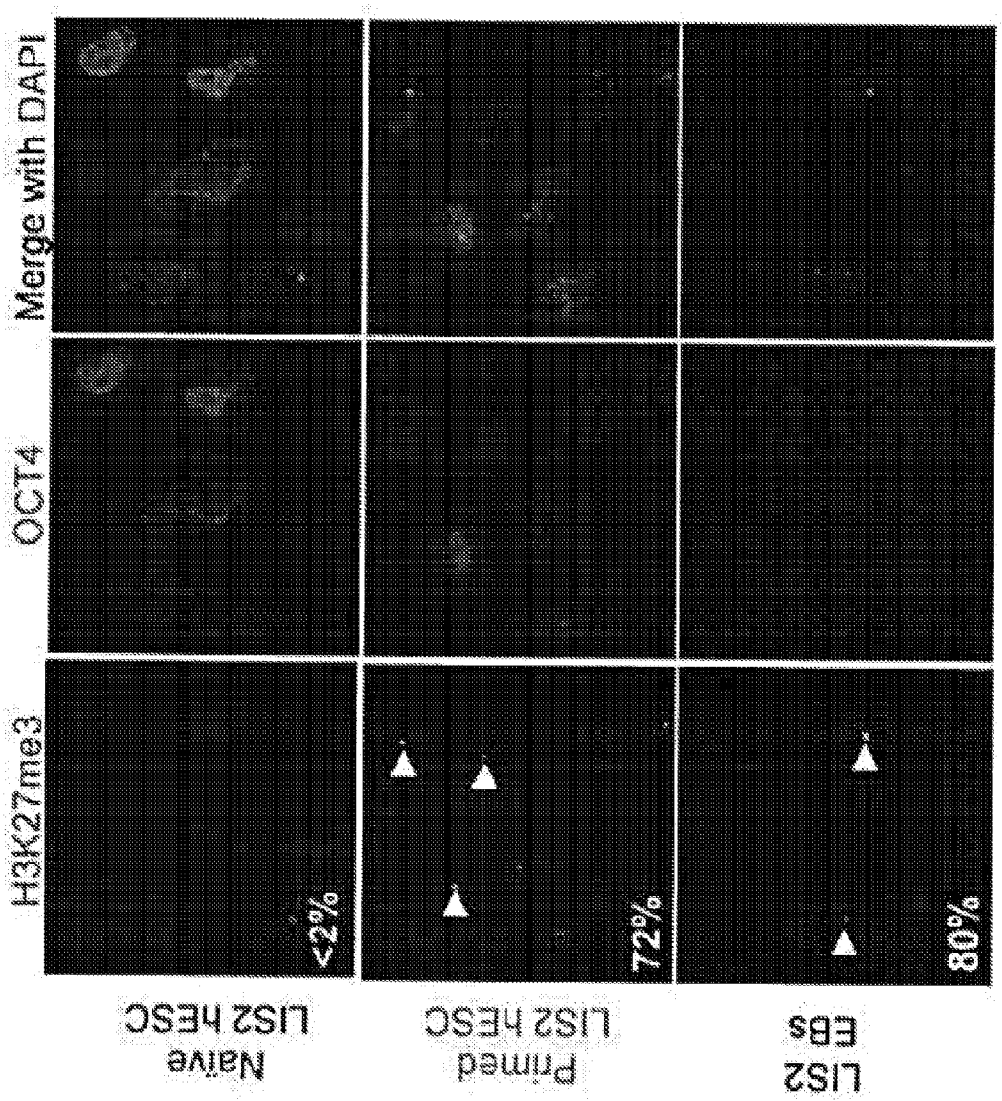


FIG. 68I

FIG. 68J

FIG. 68K

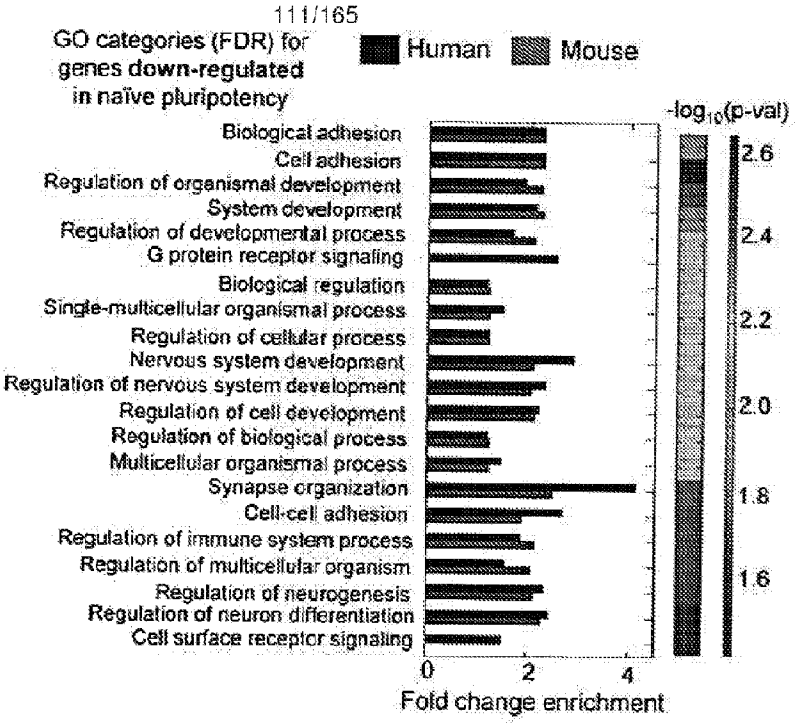


FIG. 69A

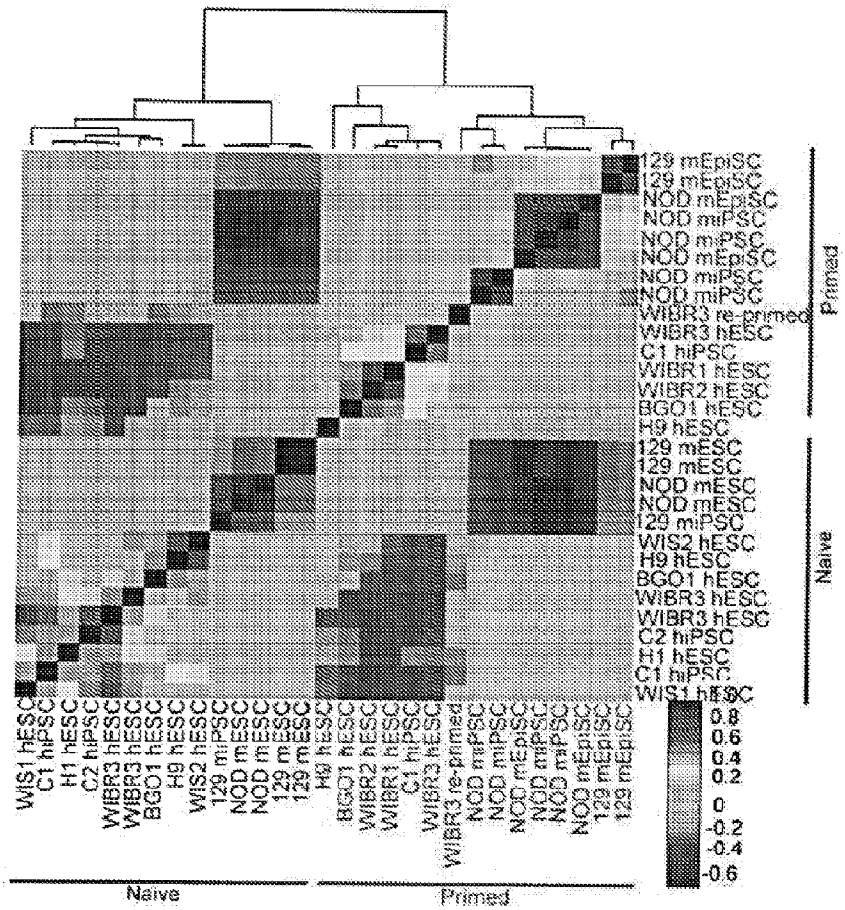


FIG. 69B

FIG. 69C

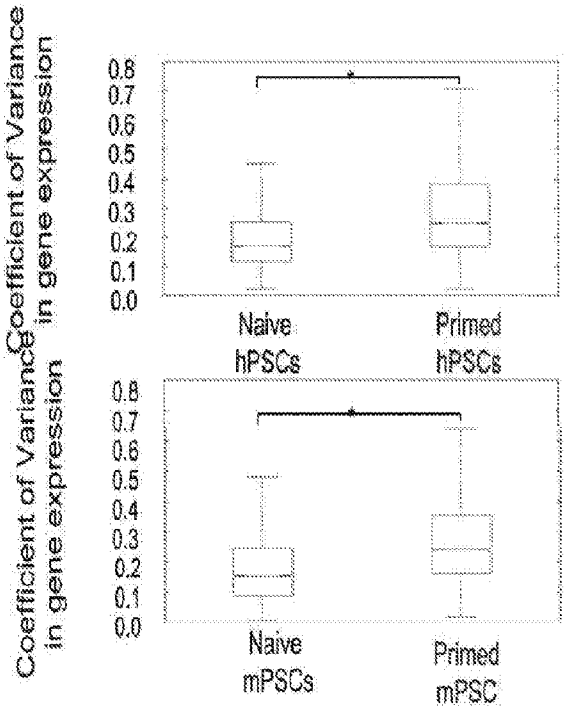


FIG. 69D

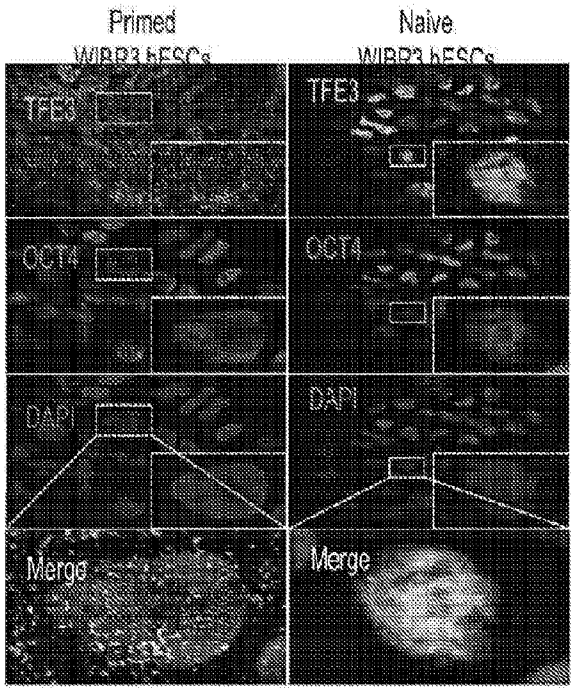


FIG. 69E FIG. 69F

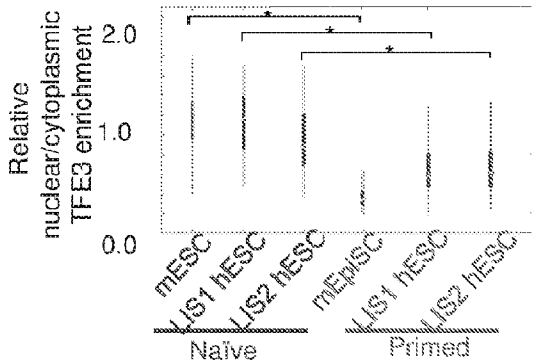


FIG. 69G

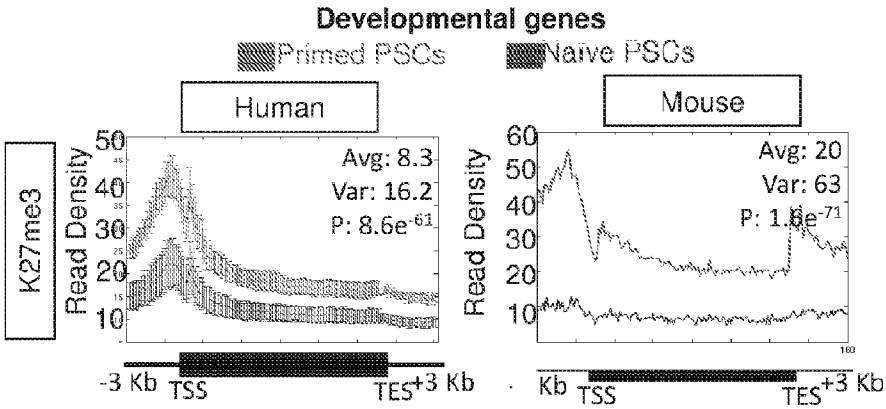


FIG. 70A

FIG. 70B

FIG. 69H

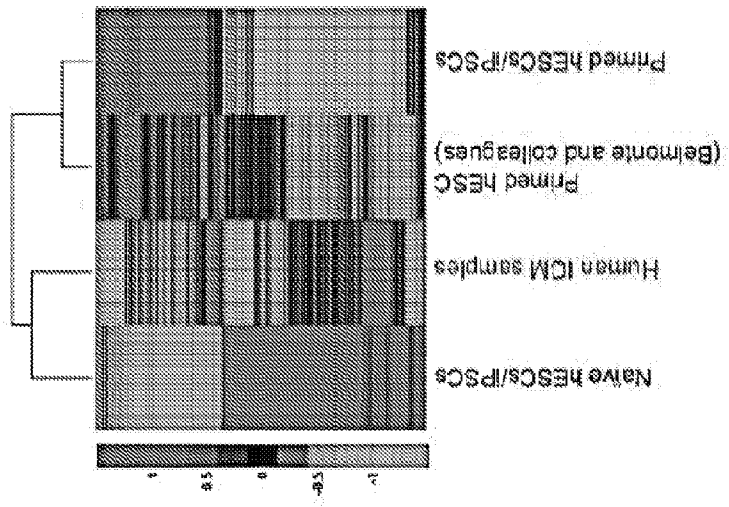
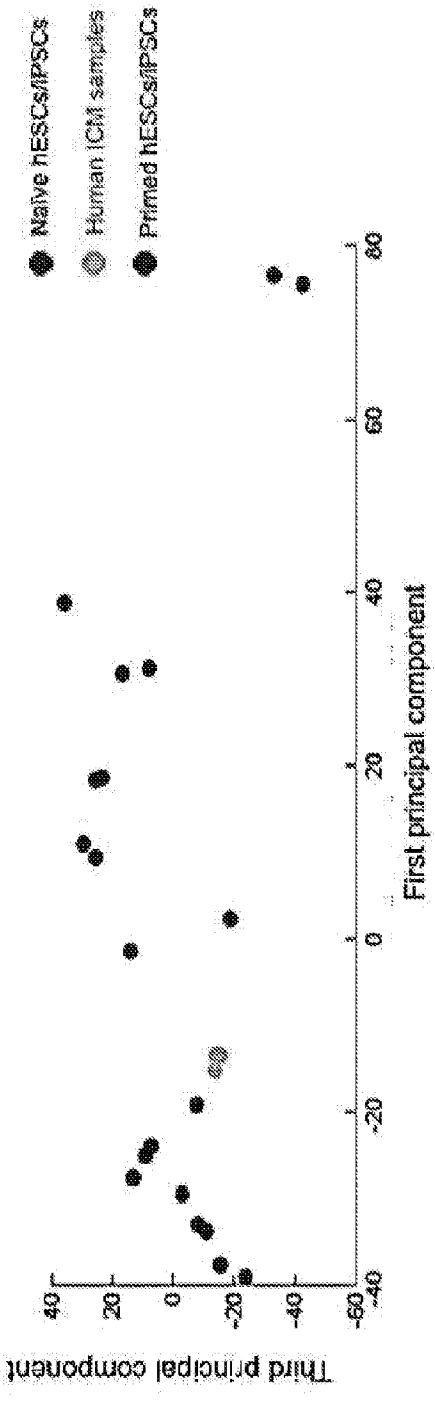


FIG. 69I



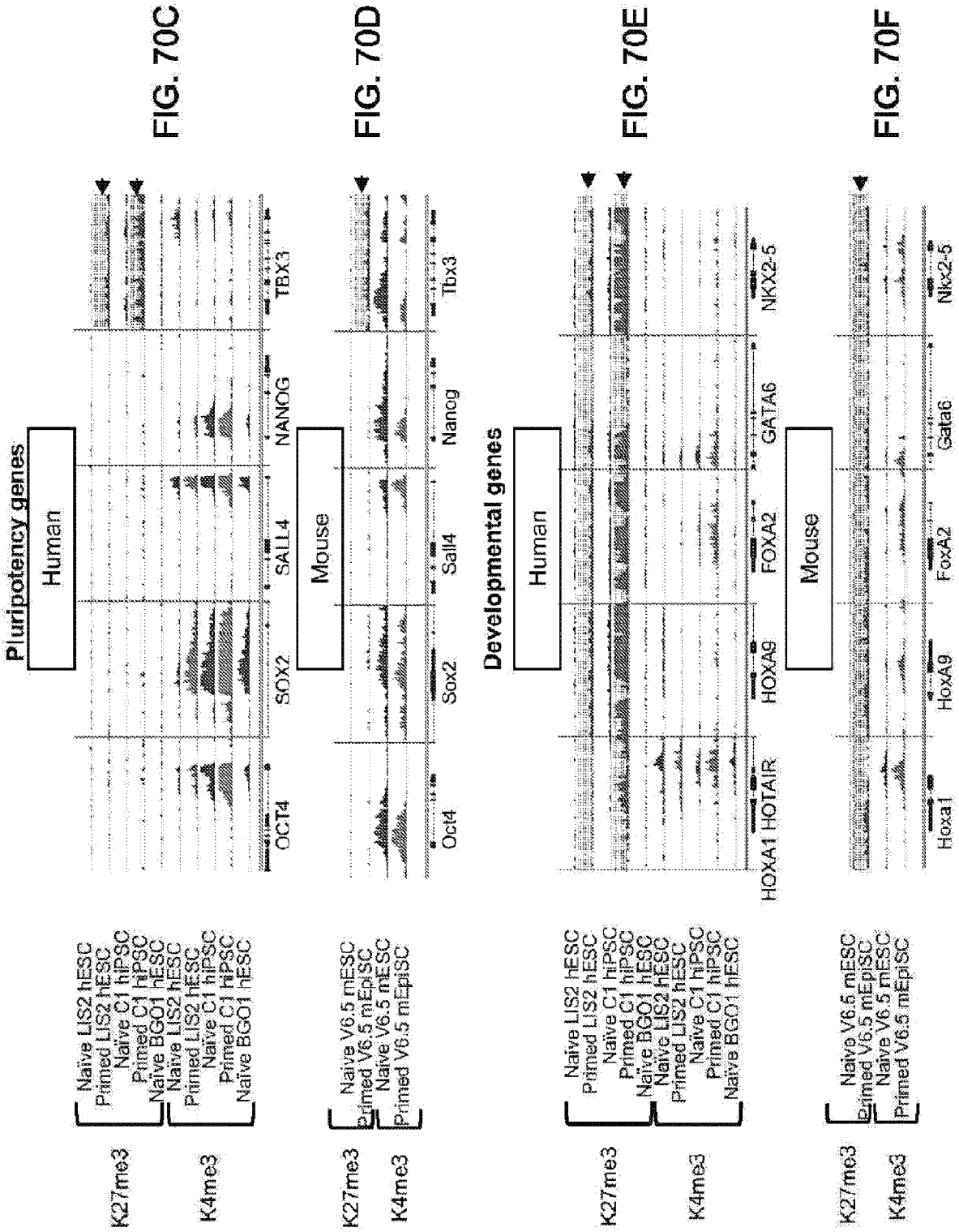


FIG. 70C

FIG. 70D

FIG. 70E

FIG. 70F

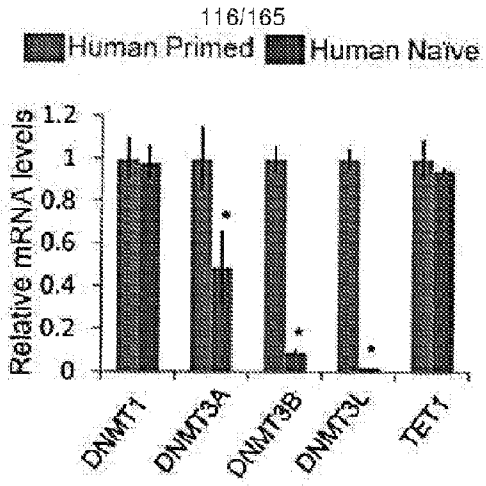


FIG. 70G

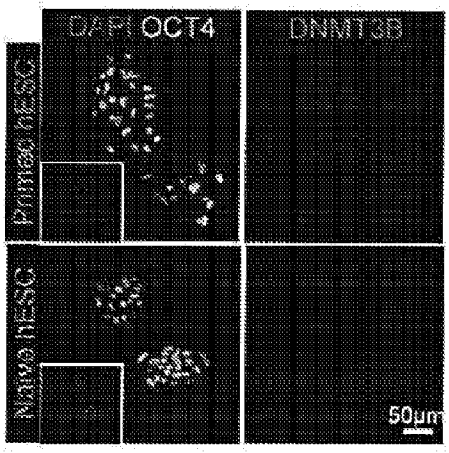


FIG. 70H

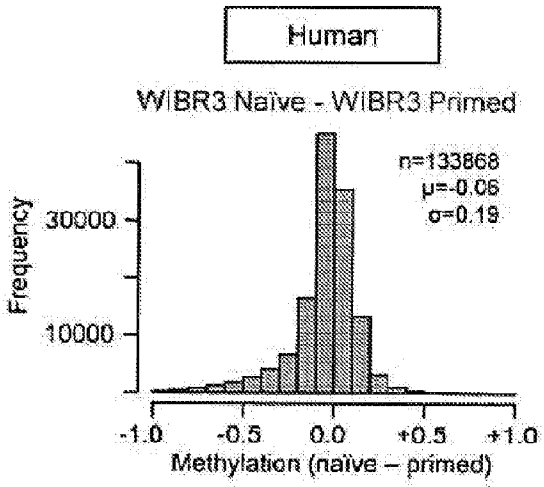


FIG. 70I

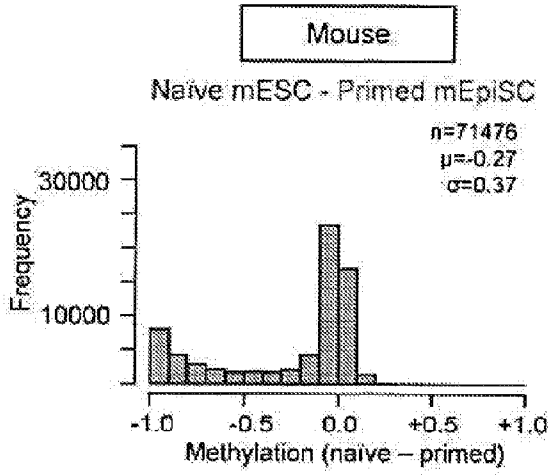
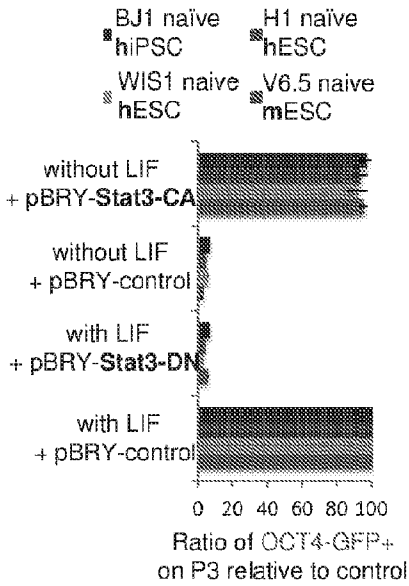
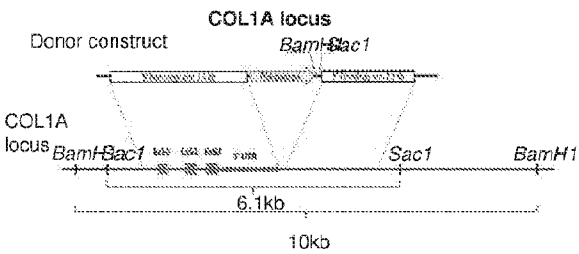


FIG. 70J

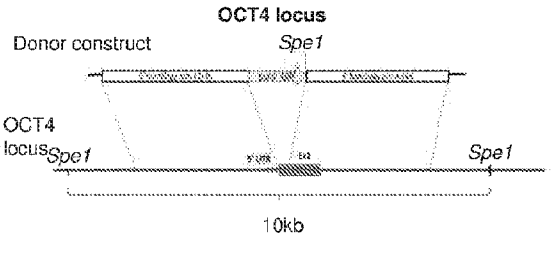
FIG. 71A





Cell Line targeted	Colonies analyzed	Correctly targeted clones	Targeting Efficiency
Primed H9 hESC	120	0	0%
Primed H9 hESC	172	0	0%
Naive H9 hESC	48	8	16%
Naive H9 hESC	24	3	12.5%

FIG. 71B



Cell Line targeted	Colonies analyzed	Correctly targeted clones	Targeting Efficiency
Primed H9 hESC	130	1	0.4%
Primed H9 hESC	140	0	0%
Naive H9 hESC	84	7	8.3%
Naive H9 hESC	22	3	13.6%

FIG. 71C

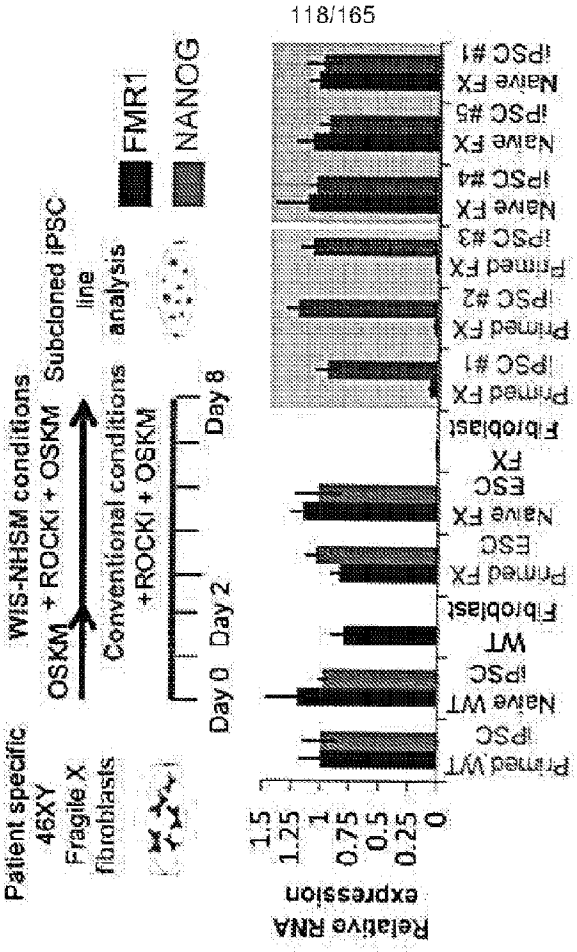


FIG. 71E

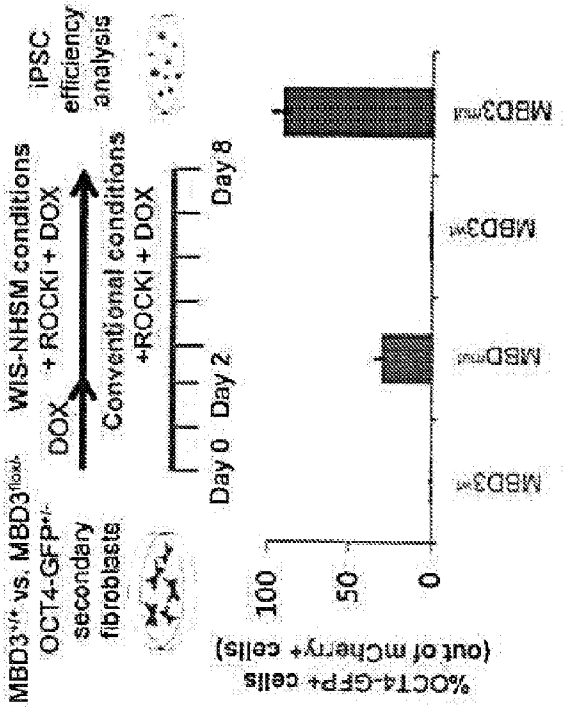


FIG. 71D

FIG. 71G

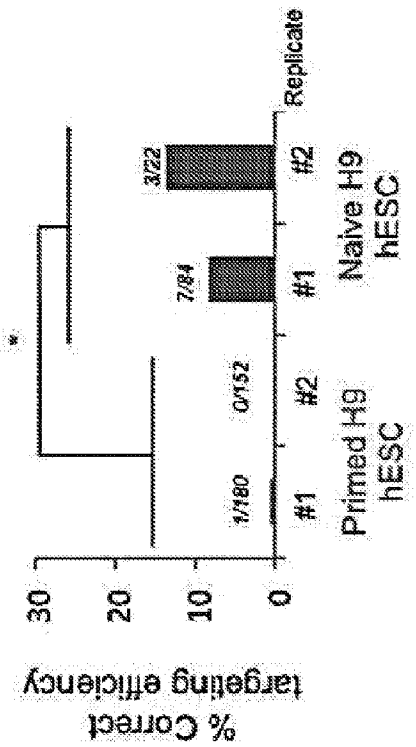
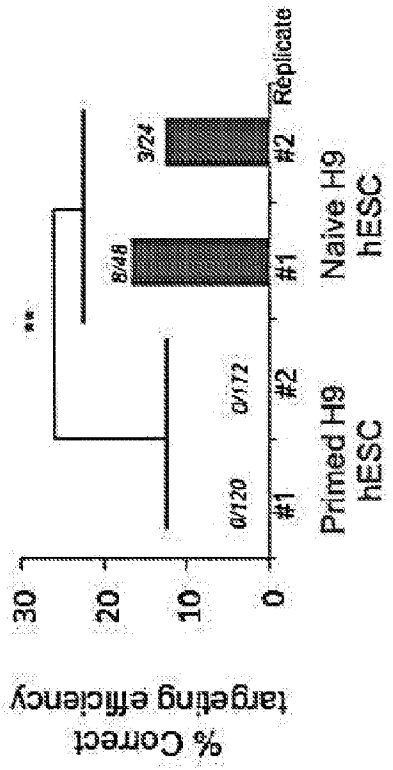


FIG. 71F



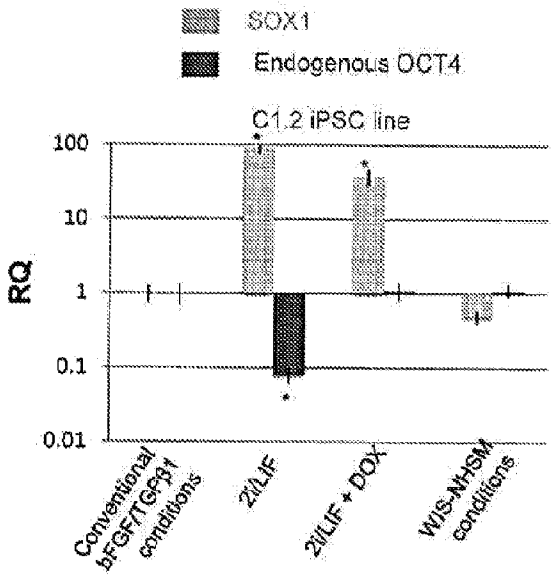


FIG. 72A

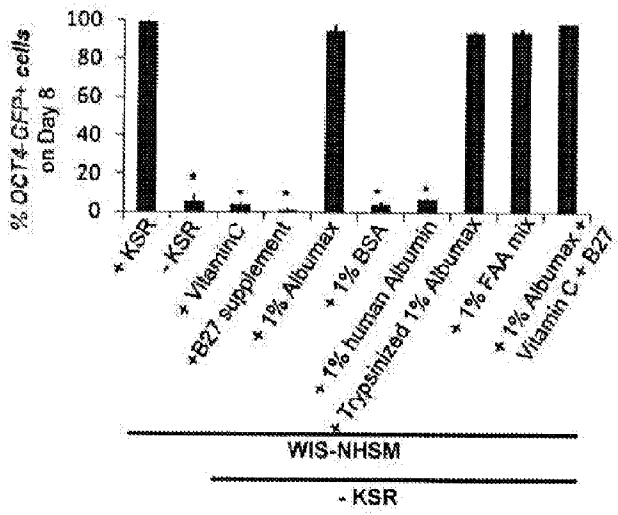


FIG. 72C

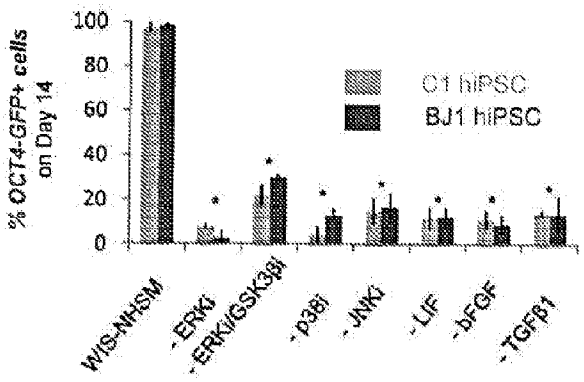


FIG. 72B

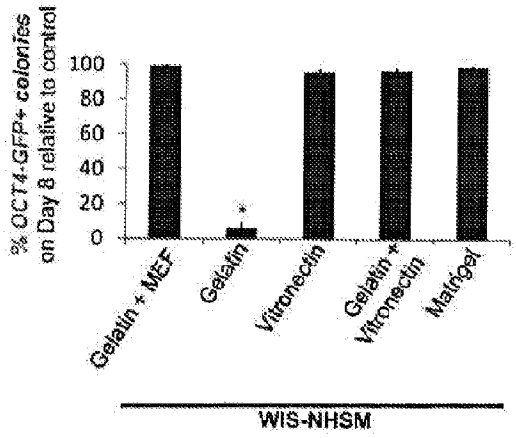


FIG. 72D

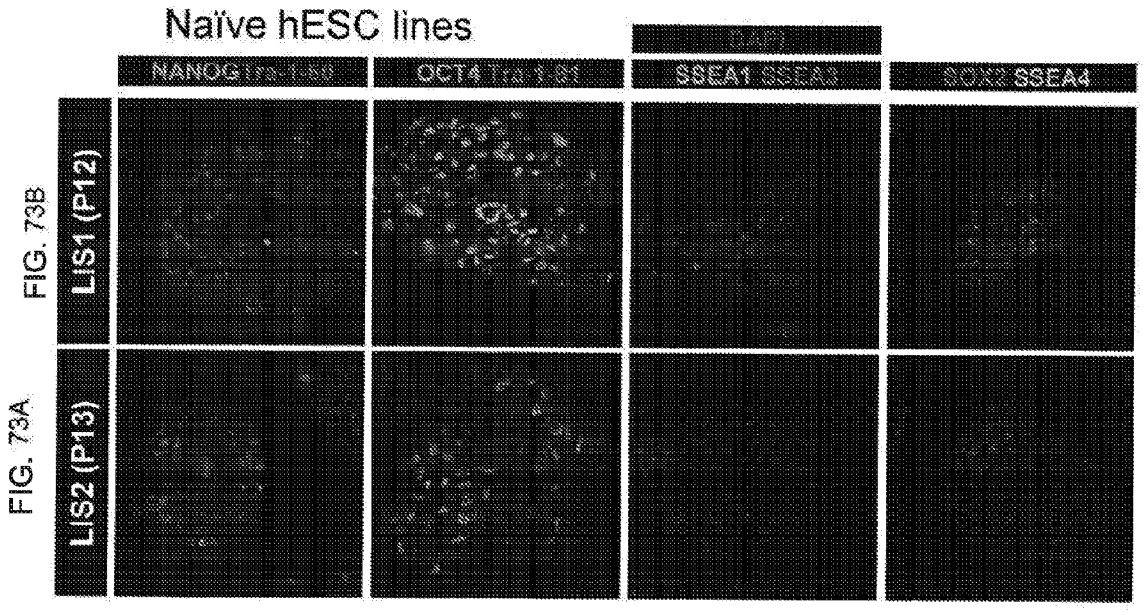


FIG. 73A

FIG. 73B

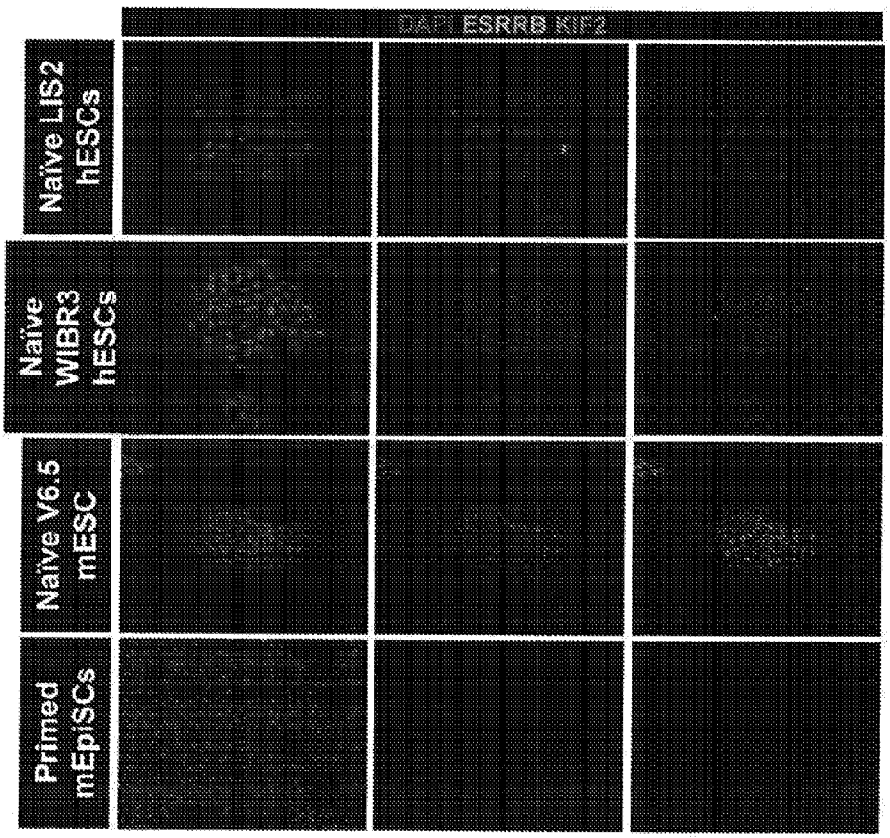


FIG. 73C

FIG. 73D

FIG. 73E

FIG. 73F

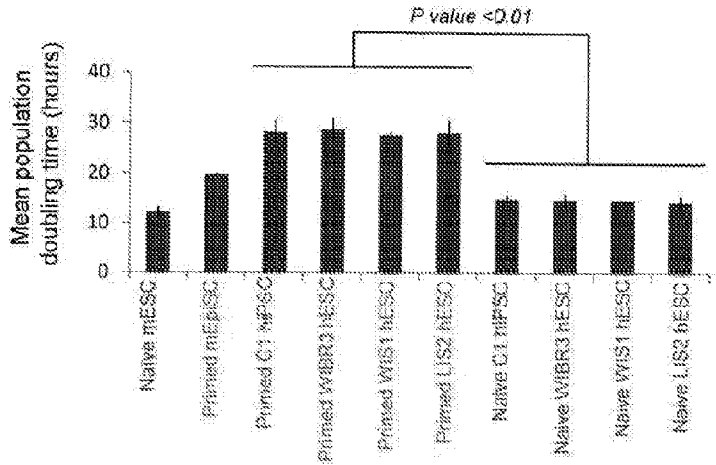


FIG. 74A

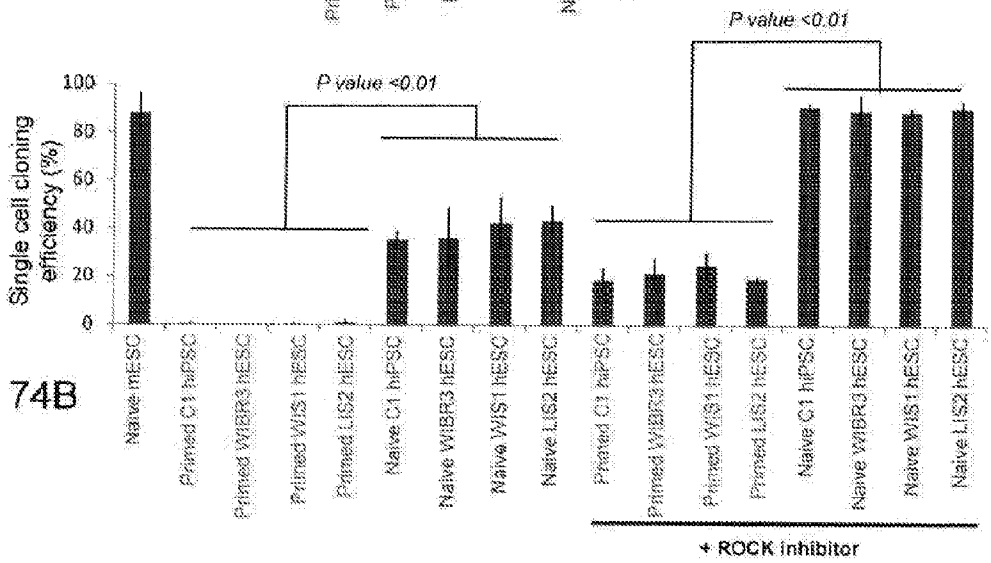


FIG. 74B

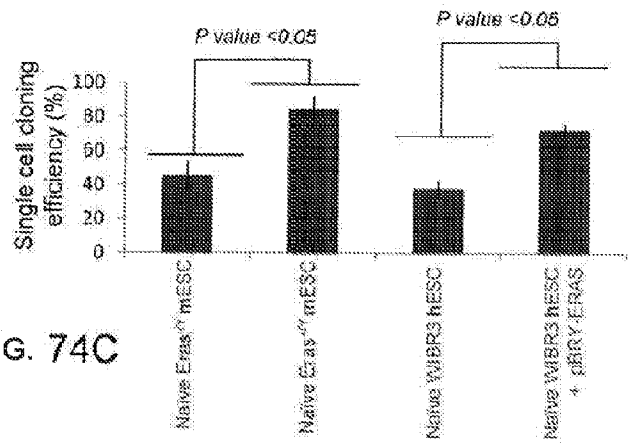


FIG. 74C

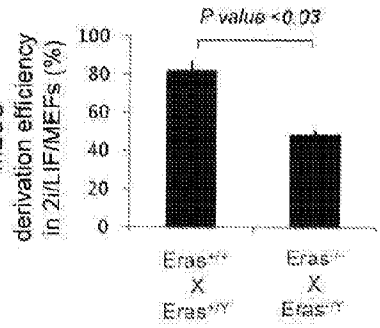
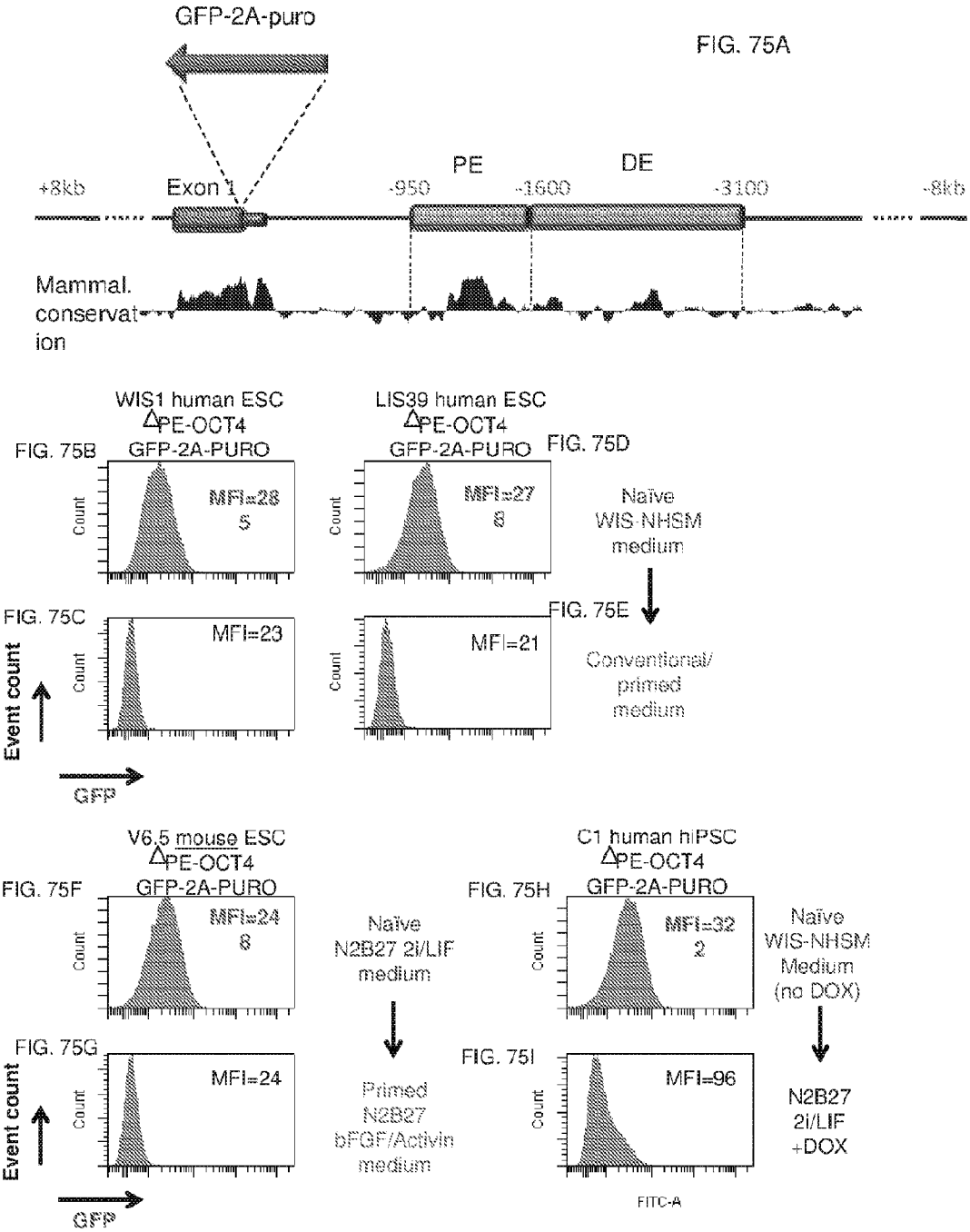


FIG. 74D


GFP-2A-puro
FIG. 75A
PE
DE
+8kb
Exon 1
-950
-1600
-3100
-8kb
Mammal. conservation
WIS1 human ESC
ΔPE-OCT4
GFP-2A-PURO
FIG. 75B
MFI=285
FIG. 75C
MFI=23
Count
Event count
GFP
LIS39 human ESC
ΔPE-OCT4
GFP-2A-PURO
FIG. 75D
MFI=278
MFI=21
Naïve
WIS-NHSM
medium
FIG. 75E
Conventional/
primed
medium
V6.5 mouse ESC
ΔPE-OCT4
GFP-2A-PURO
FIG. 75F
MFI=248
FIG. 75G
MFI=24
Naïve
N2B27 2i/LIF
medium
Primed
N2B27
bFGF/Activin
medium
C1 human hiPSC
ΔPE-OCT4
GFP-2A-PURO
FIG. 75H
MFI=322
FIG. 75I
MFI=96
Naïve
WIS-NHSM
Medium
(no DOX)
N2B27
2i/LIF
+DOX
FITC-A

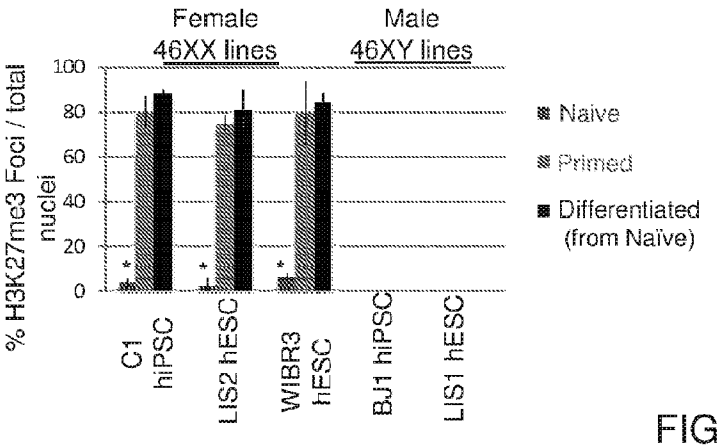


FIG. 76A

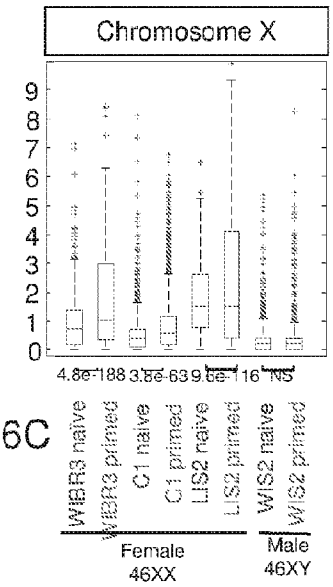


FIG. 76C

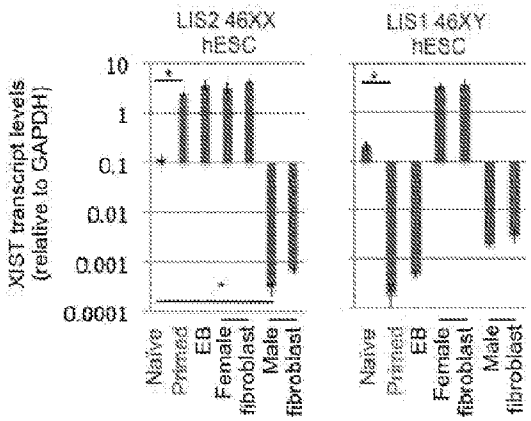


FIG. 76B

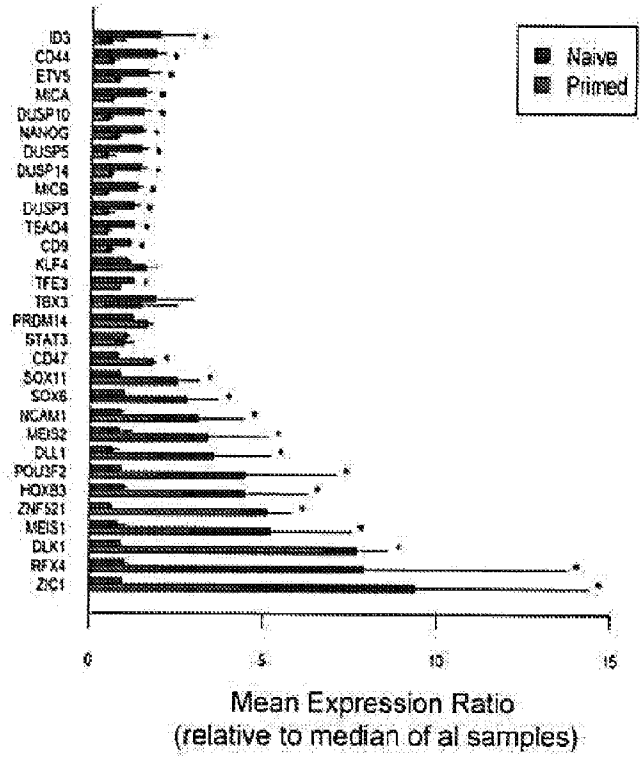


FIG. 77A

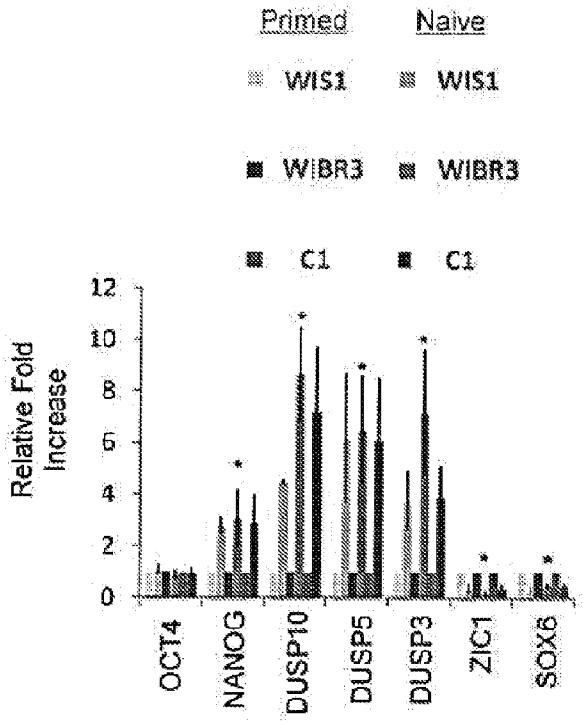


FIG. 77B

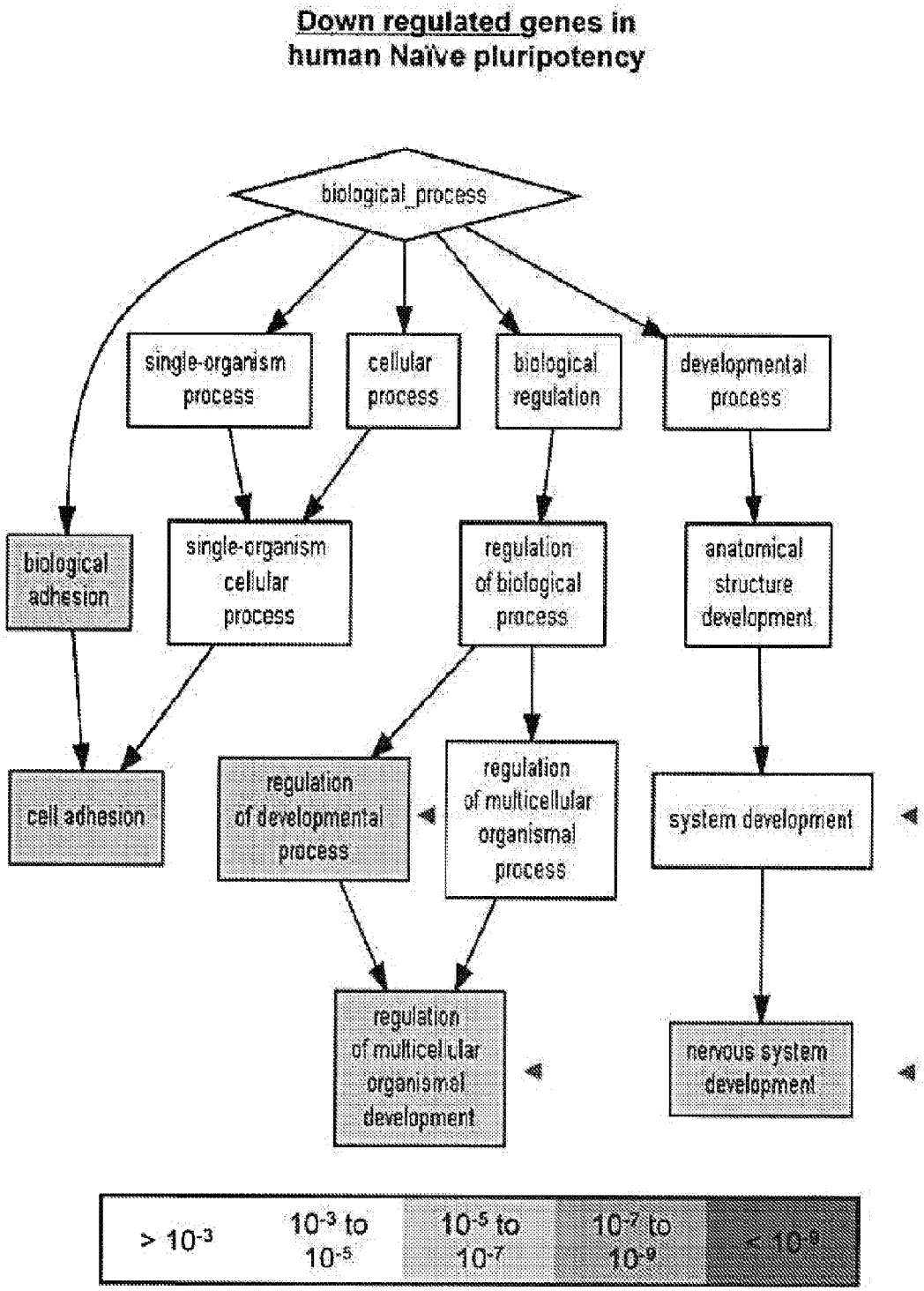

Down regulated genes in human Naïve pluripotency
biological_process
single-organism process
cellular process
biological regulation
developmental process
biological adhesion
single-organism cellular process
regulation of biological process
anatomical structure development
cell adhesion
regulation of developmental process
regulation of multicellular organismal process
system development
regulation of multicellular organismal development
nervous system development
> 10-3
10-3 to 10-5
10-5 to 10-7
10-7 to 10-9
< 10-9

FIG. 78

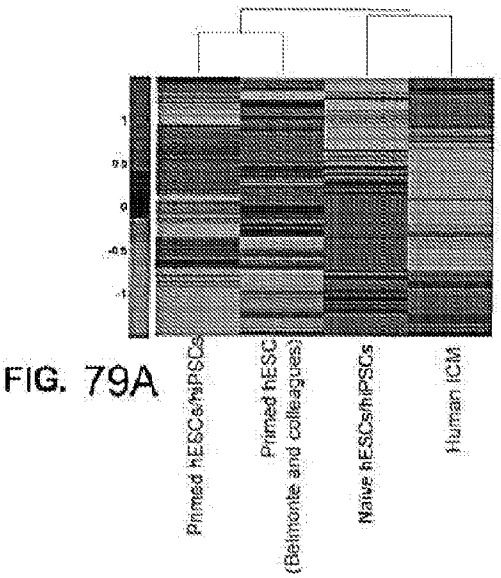


FIG. 79A

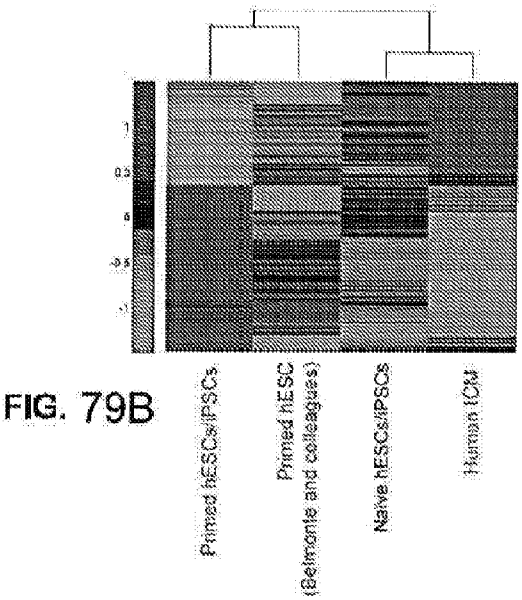


FIG. 79B

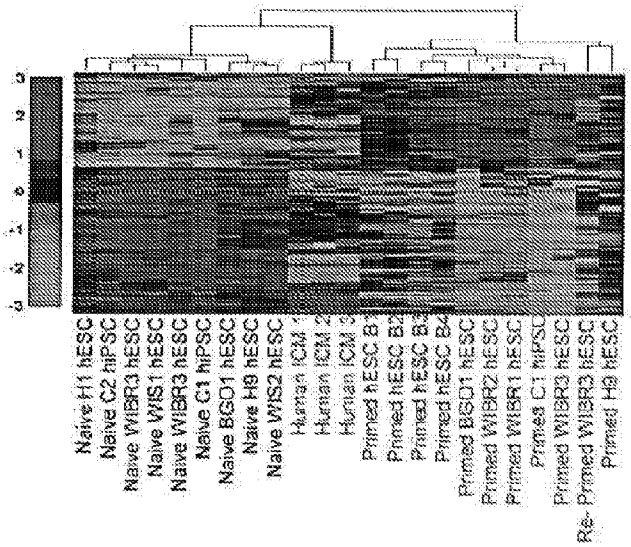


FIG. 79C

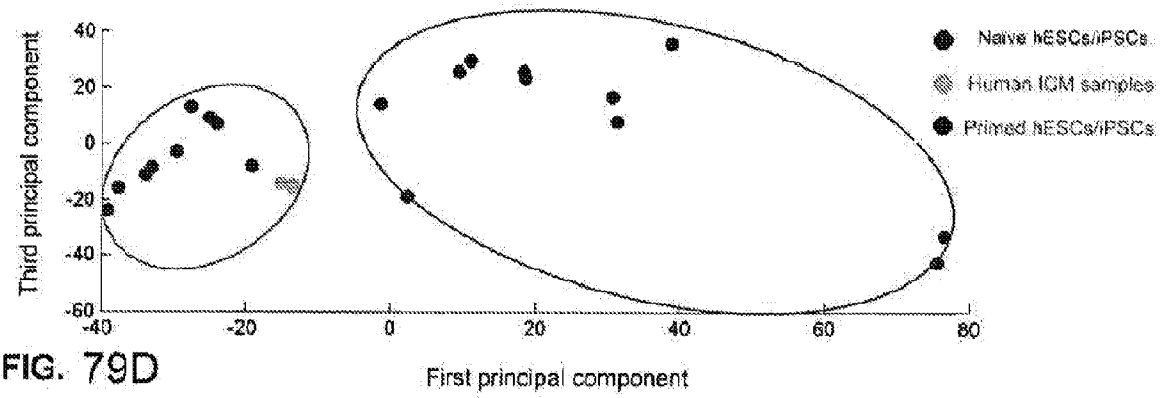


FIG. 79D

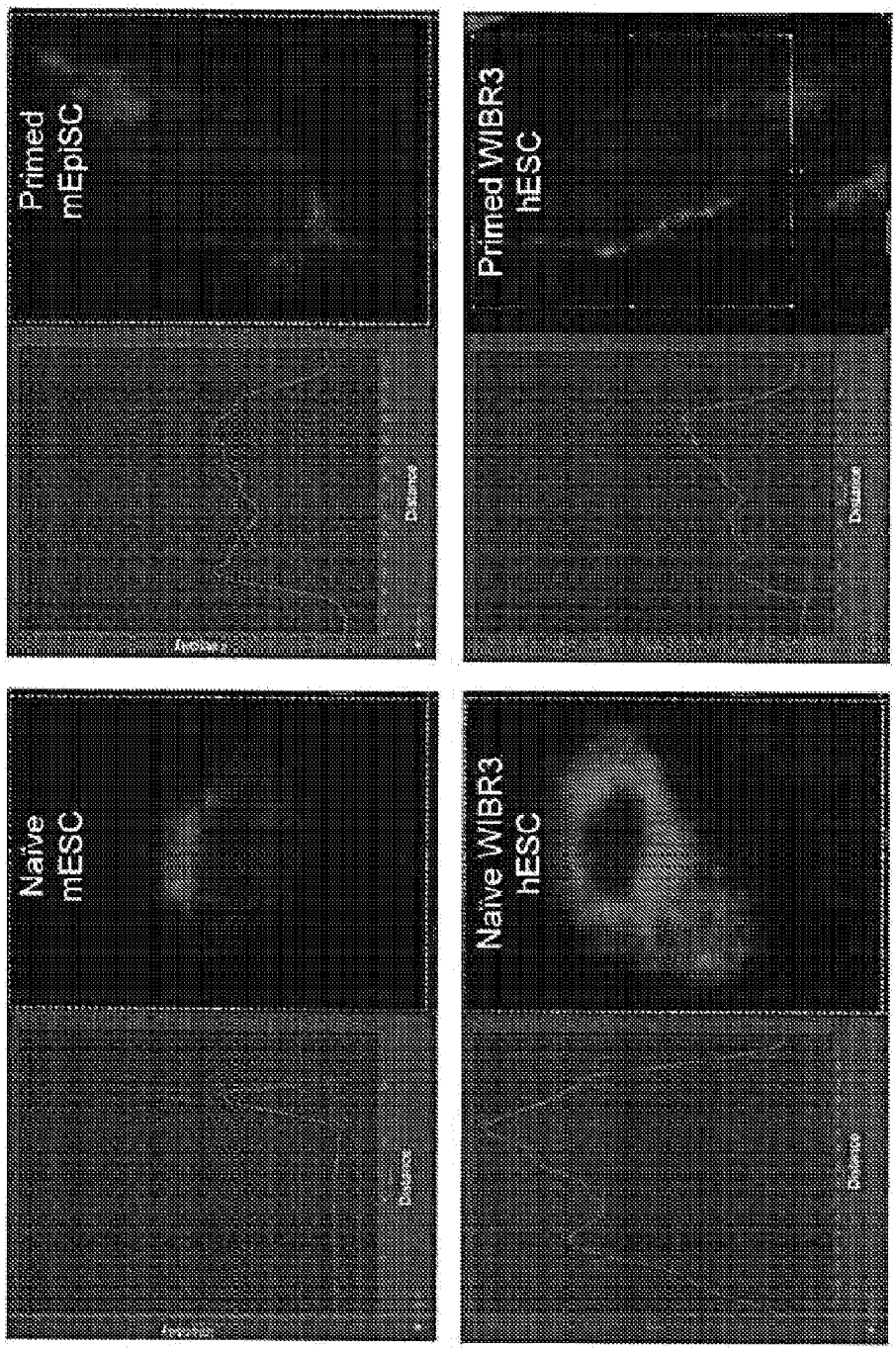


FIG. 80A

FIG. 80C

FIG. 80B

FIG. 80D

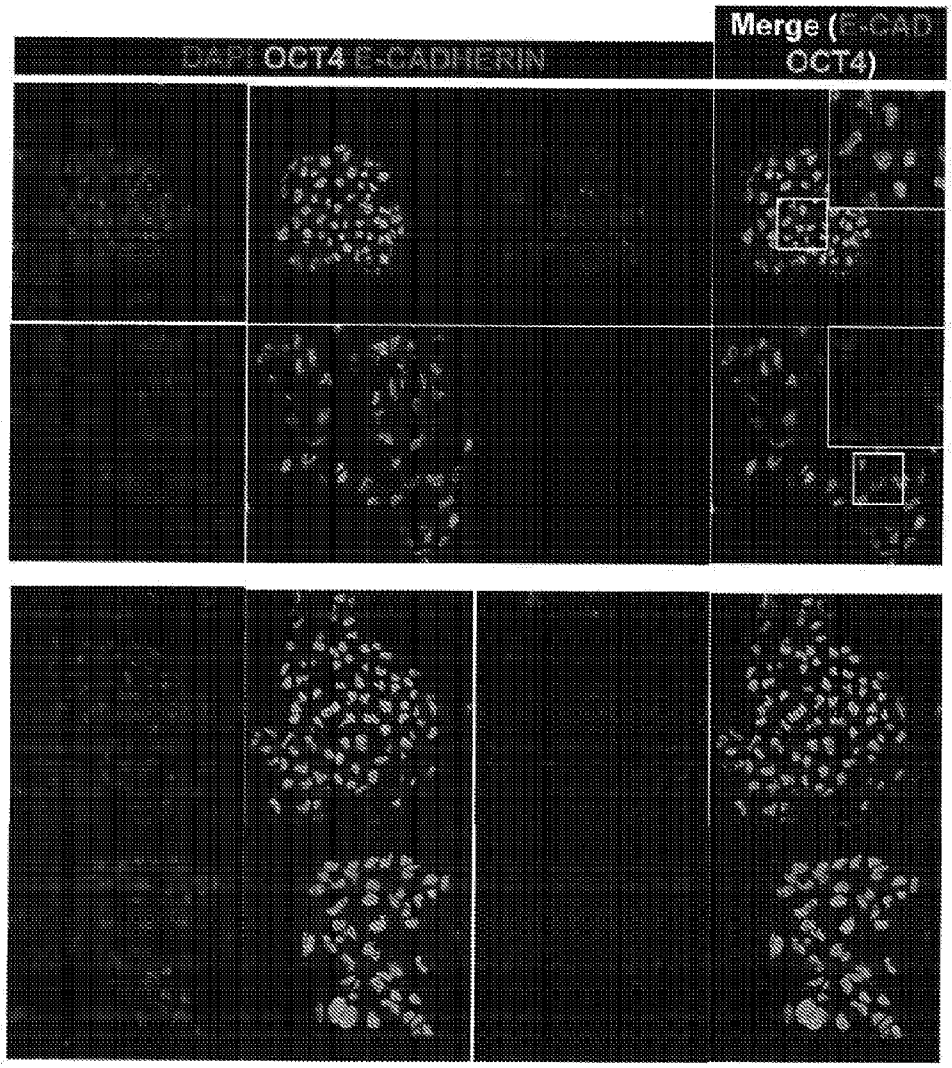


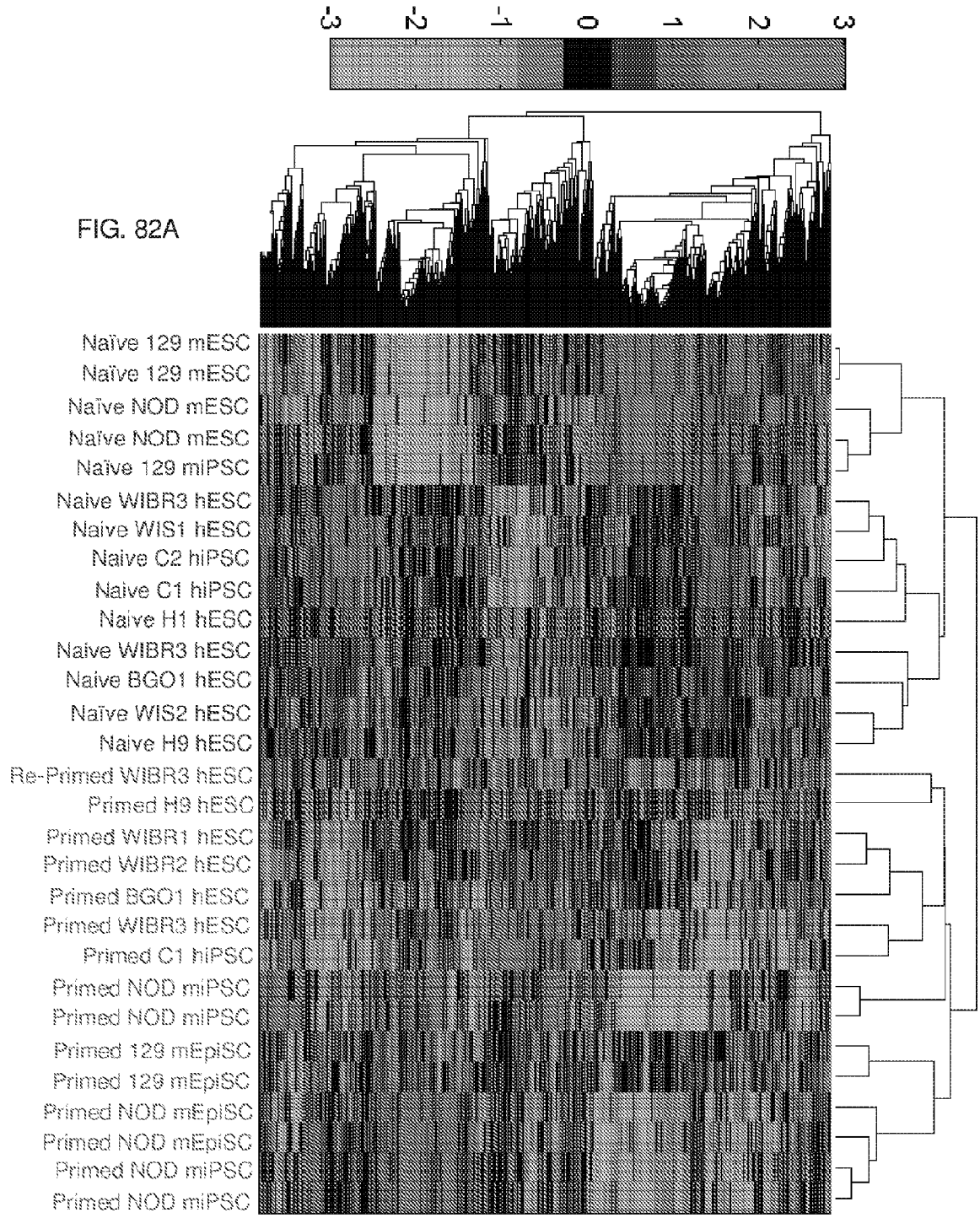
FIG. 81A

FIG. 81B

FIG. 81C

FIG. 81D

FIG. 82A


-3
-2
-1
0
1
2
3
Naïve 129 mESC
Naïve 129 mESC
Naïve NOD mESC
Naïve NOD mESC
Naïve 129 miPSC
Naïve WIBR3 hESC
Naïve WIS1 hESC
Naïve C2 hiPSC
Naïve C1 hiPSC
Naïve H1 hESC
Naïve WIBR3 hESC
Naïve BGO1 hESC
Naïve WIS2 hESC
Naïve H9 hESC
Re-Primed WIBR3 hESC
Primed H9 hESC
Primed WIBR1 hESC
Primed WIBR2 hESC
Primed BGO1 hESC
Primed WIBR3 hESC
Primed C1 hiPSC
Primed NOD miPSC
Primed NOD miPSC
Primed 129 mEpiSC
Primed 129 mEpiSC
Primed NOD mEpiSC
Primed NOD mEpiSC
Primed NOD miPSC
Primed NOD miPSC

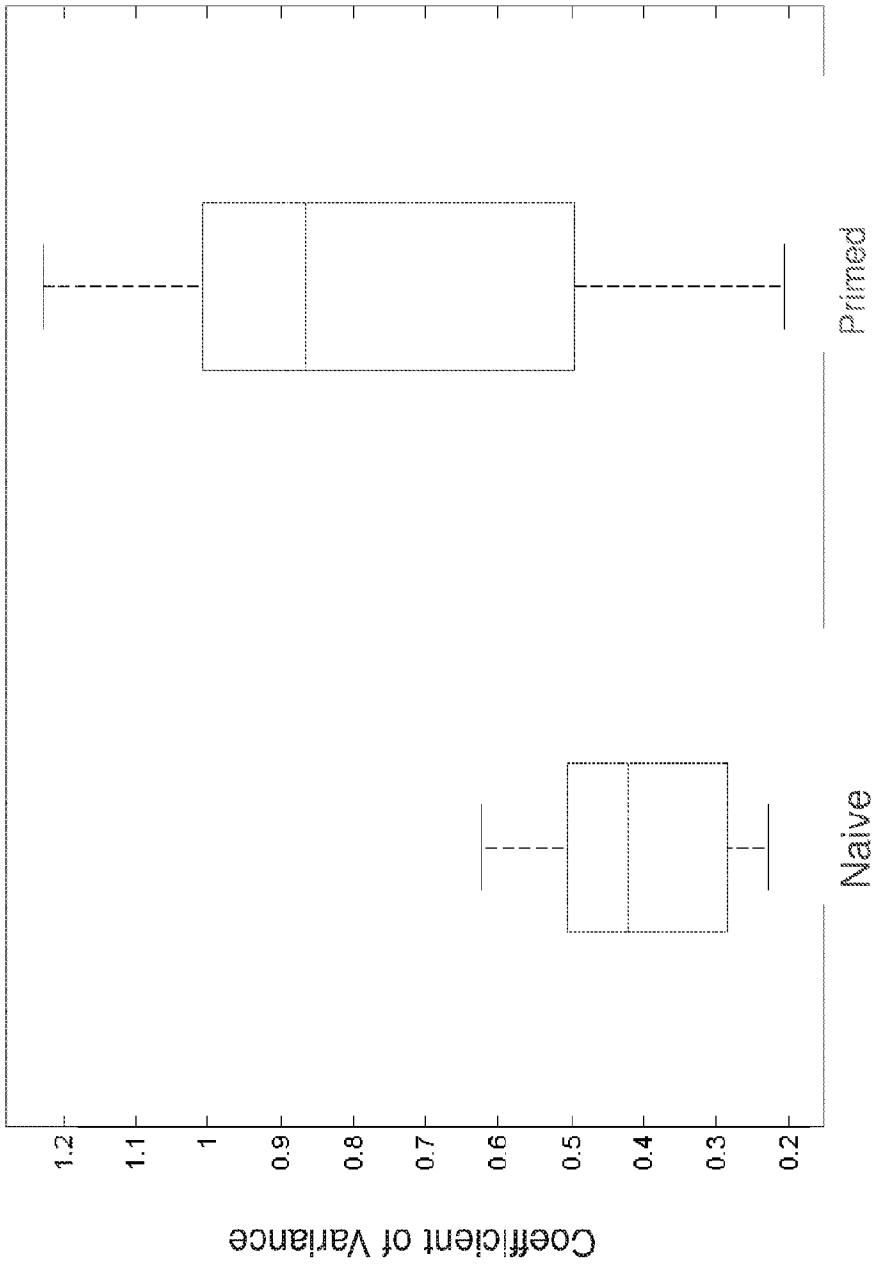

Coefficient of Variance
1.2
1.1
1
0.9
0.8
0.7
0.6
0.5
0.4
0.3
0.2
Naive
Primed

FIG. 82B

FIG. 83A

FIG. 83B

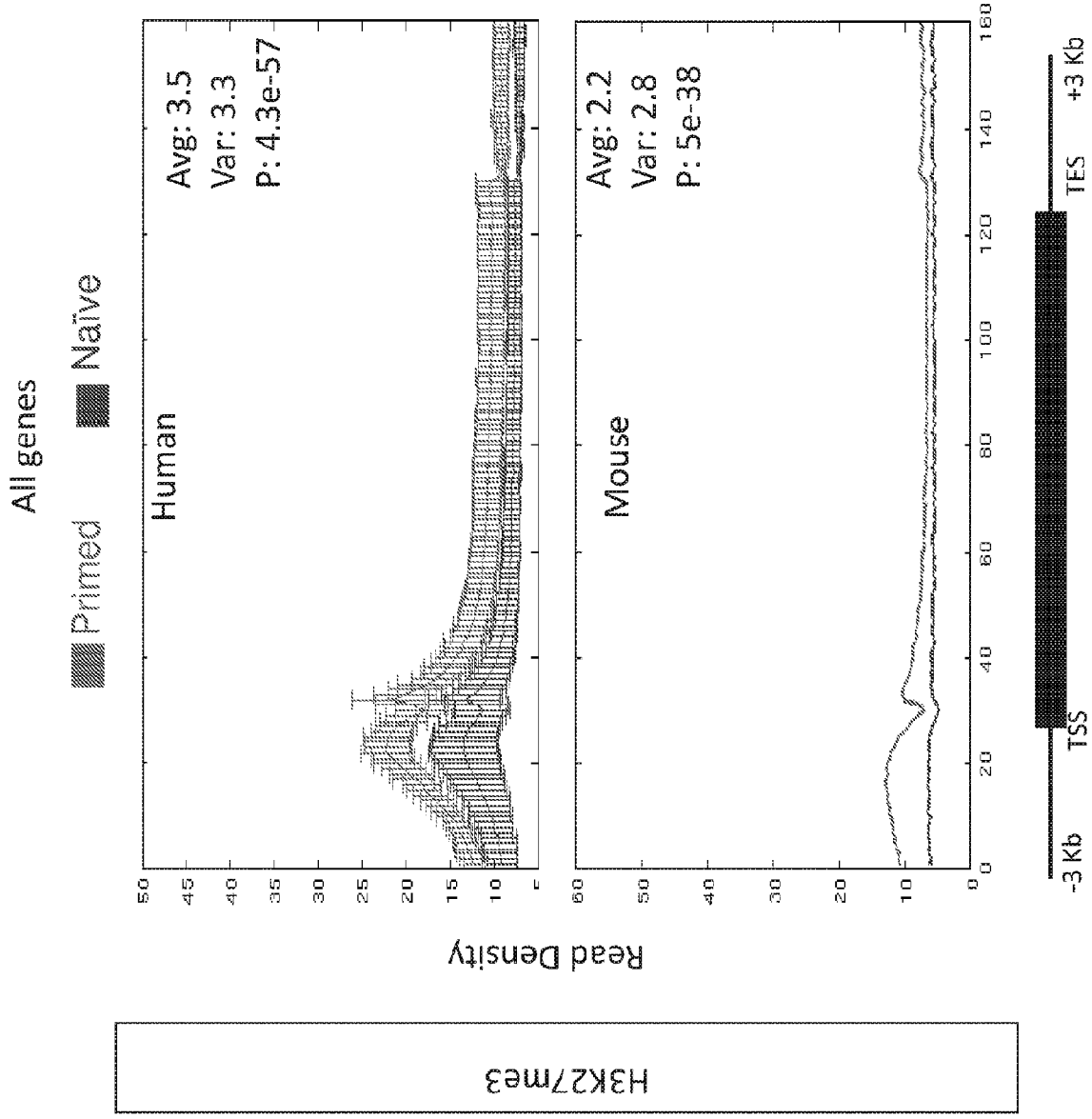


FIG. 83C

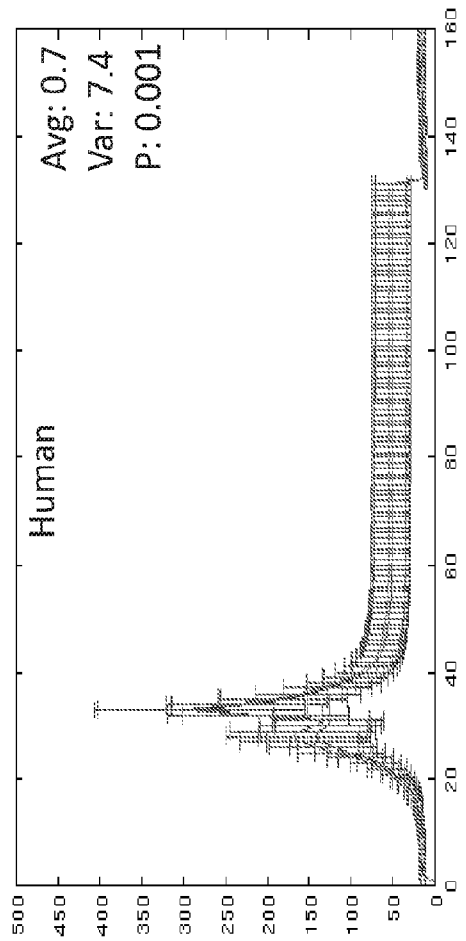
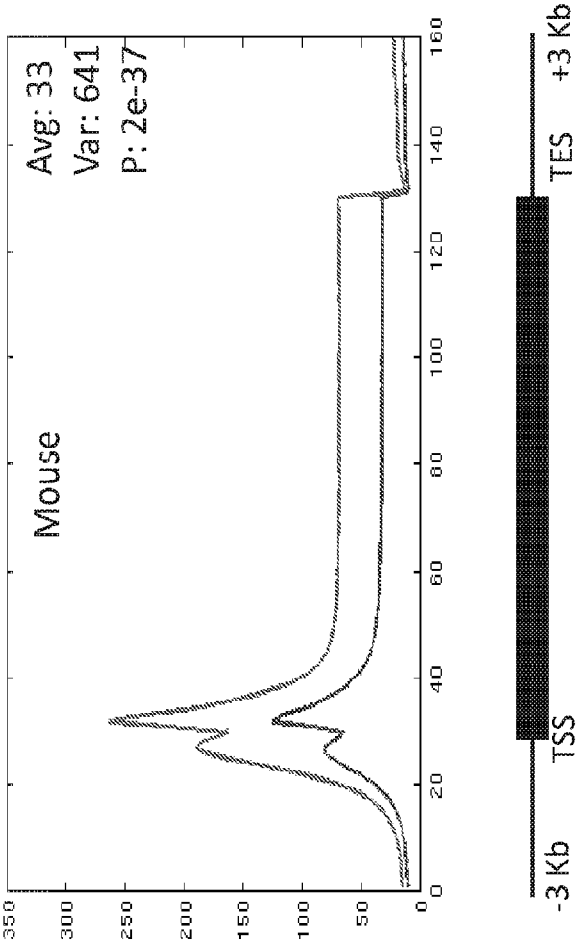


FIG. 83D



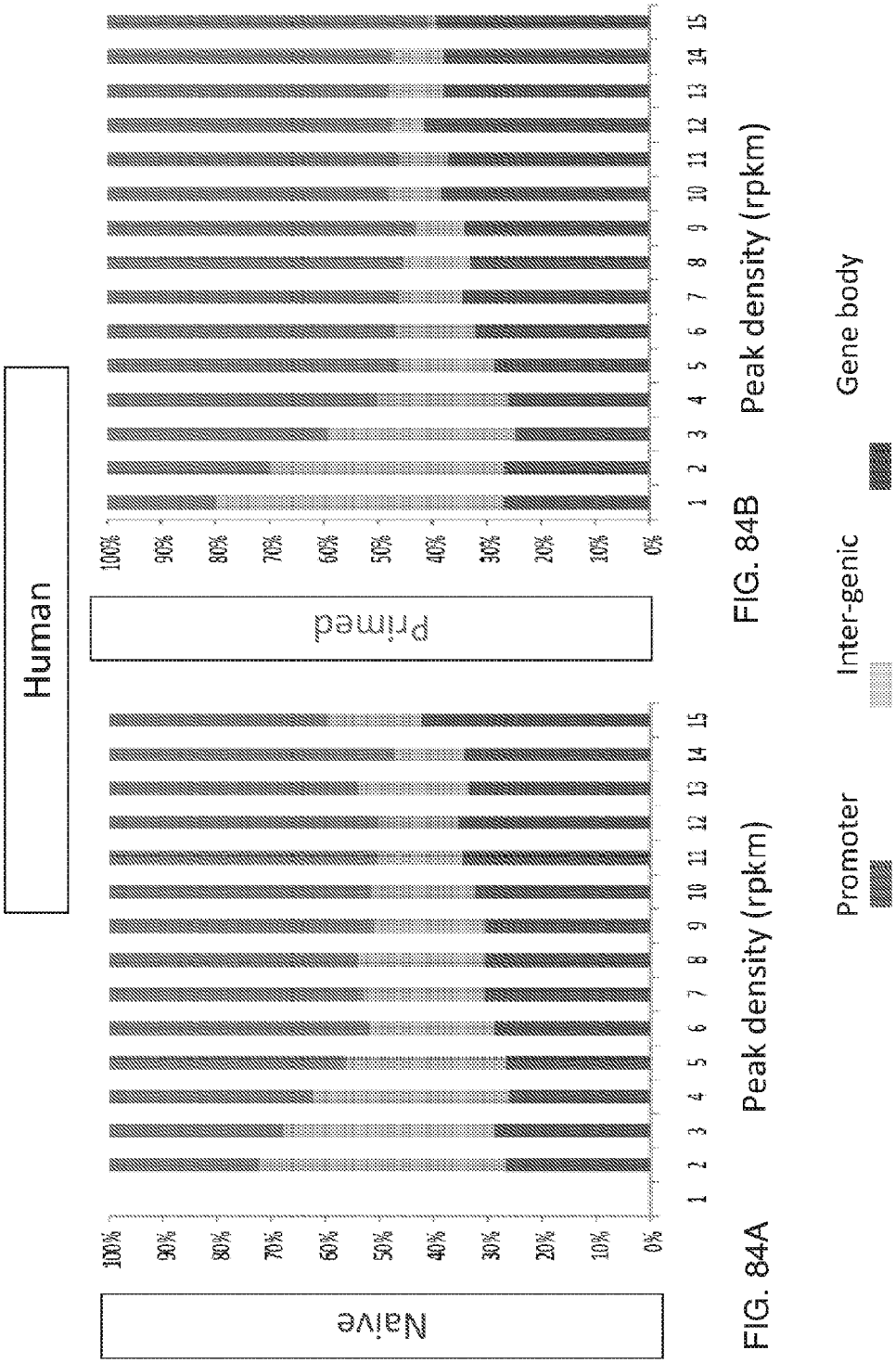


FIG. 84A FIG. 84B

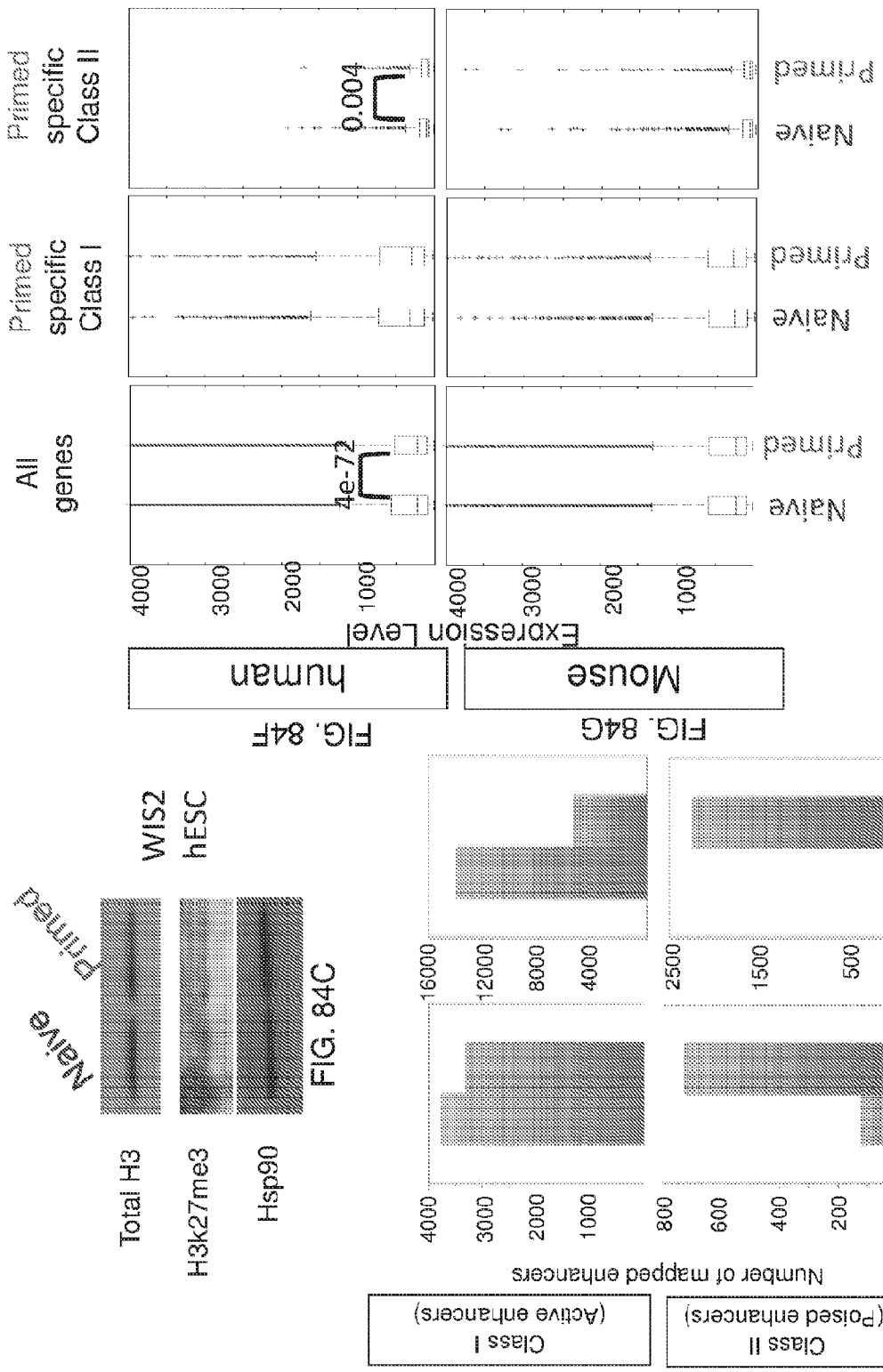

Naive
Primed
WIS2
hESC
Total H3
H3k27me3
Hsp90
FIG. 84C
Class II
(Poised enhancers)
Class I
(Active enhancers)
Number of mapped enhancers
Human
mouse
FIG. 84D
Mouse
human
FIG. 84G
FIG. 84F
All genes
Primed specific Class I
Primed specific Class II
4e-72
0.004
Expression Level
Naive
Primed

FIG. 85A

Condition 1: WIS-NHSM

LIF (20ng/ml)
ERK1/2i (PD0325901 1μM)
GSK3βi (CHIR99021 3μM)
JNKi (SP600125 5μM)
P38i (BIRB796 2μM)
FGF2 (16 ng/ml)
TGFβ1 (2 ng/ml)
ROCKi (Y27632 5μM)

Condition 7: WIS-NHSM

LIF (20ng/ml)
ERK1/2i (PD0325901 1μM)
GSK3βi (CHIR99021 3μM)
JNKi (SP600125 5μM)
P38i (BIRB796 2μM)
FGF2 (16 ng/ml)
TGFβ1 (2 ng/ml)
ROCKi (Y27632 5μM)
+BMPi (LDN-193189 0.5μM)

Condition 8: WIS-NHSM

LIF (20ng/ml)
ERK1/2i (PD0325901 1μM)
GSK3βi (CHIR99021 3μM)
JNKi (SP600125 5μM)
P38i (BIRB796 2μM)
FGF2 (16 ng/ml)
TGFβ1 (2 ng/ml)
ROCKi (Y27632 5μM)
+NOTCHi (DBZ 2μM)

Condition 9: WIS-NHSM

LIF (20ng/ml)
ERK1/2i (PD0325901 1μM)
GSK3βi (CHIR99021 3μM)
JNKi (SP600125 5μM)
P38i (BIRB796 2μM)
FGF2 (16 ng/ml)
TGFβ1 (2 ng/ml)
ROCKi (Y27632 5μM)
+BMPi (LDN-193189 0.5μM)
+NOTCHi (DBZ 2μM)

Condition 10: WIS-NHSM

LIF (20ng/ml)
ERK1/2i (PD0325901 1μM)
GSK3βi (CHIR99021 3μM)
JNKi (SP600125 5μM)
P38i (BIRB796 2μM)
FGF2 (16 ng/ml)
TGFβ1 (2 ng/ml)
ROCKi (Y27632 5μM)
+ BMPi (LDN-193189 0.5μM)
+ NOTCHi (DBZ 2μM)
+ IGFIi (20ng/ml)

Condition 11: WIS-NHSM

LIF (20ng/ml)
ERK1/2i (PD0325901 1μM)
GSK3βi (CHIR99021 3μM)
JNKi (SP600125 5μM)
P38i (BIRB796 2μM)
FGF2 (16 ng/ml)
TGFβ1 (2 ng/ml)
ROCKi (Y27632 5μM)
+ BMPi (LDN-193189 0.5μM)
+ NOTCHi (DBZ 2μM)
+ SHHi (RU-SKI-43 5μM)

Condition 12: WIS-NHSM (TGFR pathway inhibition)

LIF (20ng/ml)
ERK1/2i (PD0325901 1μM)
GSK3βi (CHIR99021 3μM)
JNKi (SP600125 5μM)
P38i (BIRB796 2μM)
FGF2 (16 ng/ml)
TGFRi (SB432541 2μM)
ROCKi (Y27632 5μM)
+ BMPi (LDN-193189 0.5μM)
+ NOTCHi (DBZ 2μM)

Condition 13: WIS-NHSM (FGFR pathway inhibition)

LIF (20ng/ml)
ERK1/2i (PD0325901 1μM)
GSK3βi (CHIR99021 3μM)
JNKi (SP600125 5μM)
P38i (BIRB796 2μM)
FGF2 (16 ng/ml)
TGFβ1 (2 ng/ml)
FGFRi (PD173471 0.1μM)
ROCKi (Y27632 5μM)
+ BMPi (LDN-193189 0.5μM)
+ NOTCHi (DBZ 2μM)
+ IGFIi (20ng/ml)
+ SCF 10ng/ml

Condition 14: WIS-NHSM (TGFR+FGFR pathway inhibition)

LIF (20ng/ml)
ERK1/2i (PD0325901 1μM)
GSK3βi (CHIR99021 3μM)
JNKi (SP600125 5μM)
P38i (BIRB796 2μM)
FGFRi (PD173471 0.1μM)
TGFRi (SB432541 2μM)
ROCKi (Y27632 5μM)
+ BMPi (LDN-193189 0.5μM)
+ NOTCHi (DBZ 2μM)
+ IGFIi (20ng/ml)
+ SCF 10ng/ml

Condition 15: WIS-NHSM (TGFR pathway inhibition)

LIF (20ng/ml)
ERK1/2i (PD0325901 1μM)
GSK3βi (CHIR99021 3μM)
JNKi (SP600125 5μM)
P38i (BIRB796 2μM)
FGF2 (16 ng/ml)
TGFRi (SB432541 2μM)
ROCKi (Y27632 5μM)
+ BMPi (LDN-193189 0.5μM)
+ NOTCHi (DBZ 2μM)
+ SHHi (RU-SKI-43 5μM)

Condition 16: WIS-NHSM (FGFR pathway inhibition)

LIF (20ng/ml)
ERK1/2i (PD0325901 1μM)
GSK3βi (CHIR99021 3μM)
JNKi (SP600125 5μM)
P38i (BIRB796 2μM)
TGFβ1 (2 ng/ml)
FGFRi (PD173471 0.1μM)
ROCKi (Y27632 5μM)
+ BMPi (LDN-193189 0.5μM)
+ NOTCHi (DBZ 2μM)
+ IGFIi (20ng/ml)
+ SCF 10ng/ml
+ SHHi (RU-SKI-43 5μM)

Condition 17: WIS-NHSM (TGFR+FGFR pathway inhibition)

LIF (20ng/ml)
ERK1/2i (PD0325901 1μM)
GSK3βi (CHIR99021 3μM)
JNKi (SP600125 5μM)
P38i (BIRB796 2μM)
FGFRi (PD173471 0.1μM)
TGFRi (SB432541 2μM)
ROCKi (Y27632 5μM)
+ BMPi (LDN-193189 0.5μM)
+ NOTCHi (DBZ 2μM)
+ IGFIi (20ng/ml)
+ SCF 10ng/ml
+ SHHi (RU-SKI-43 5μM)

FIG. 85B

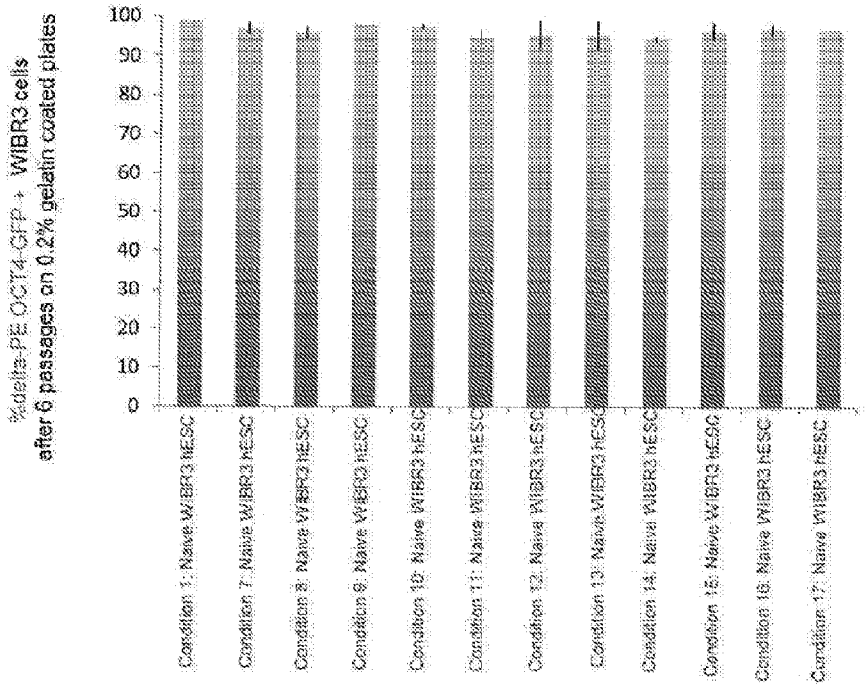


FIG. 85C

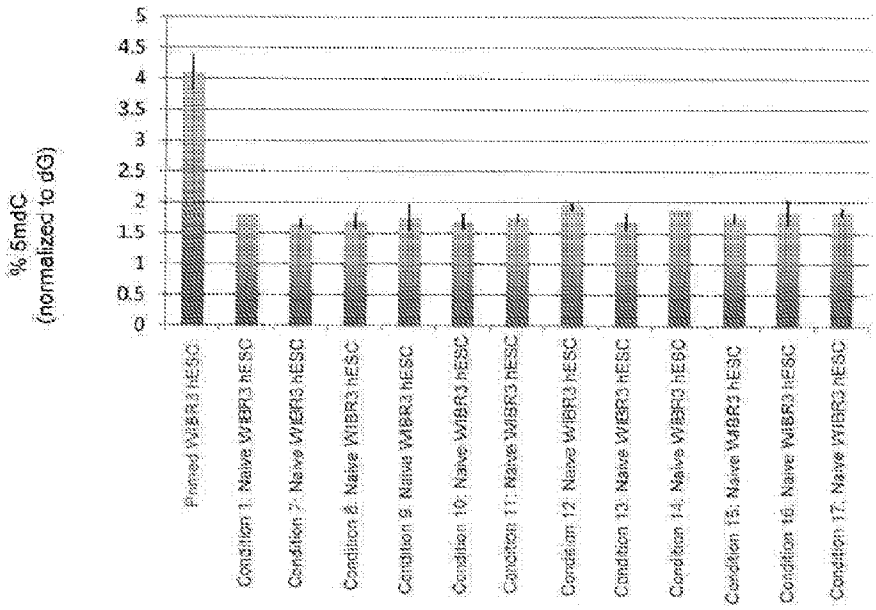


FIG. 86A

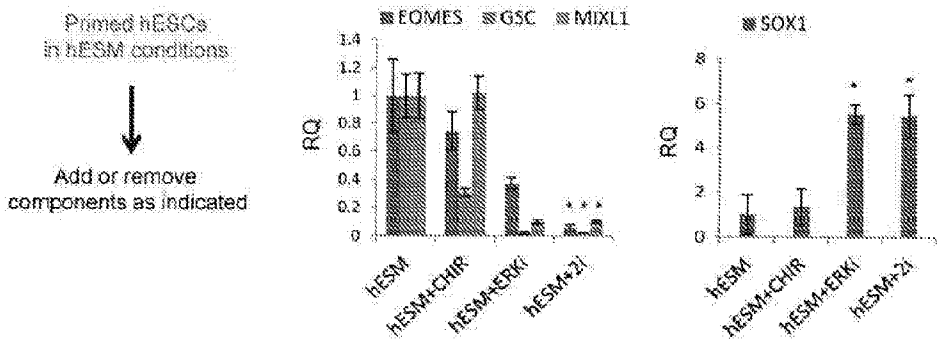


FIG. 86B

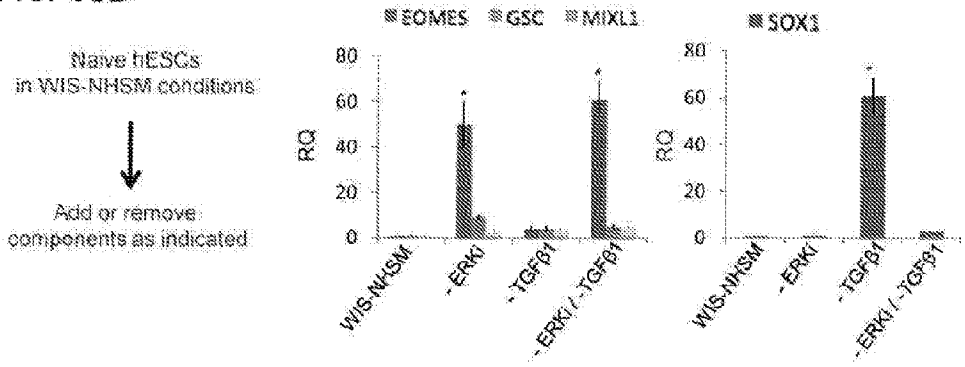


FIG. 86C

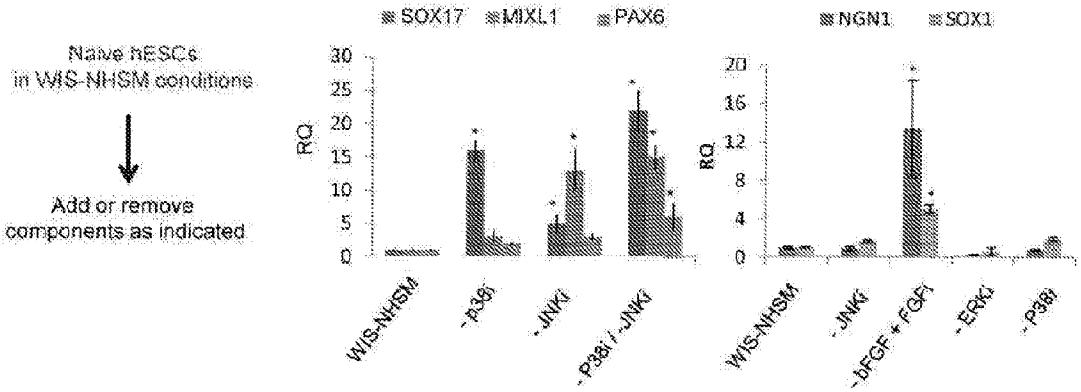


FIG. 87A

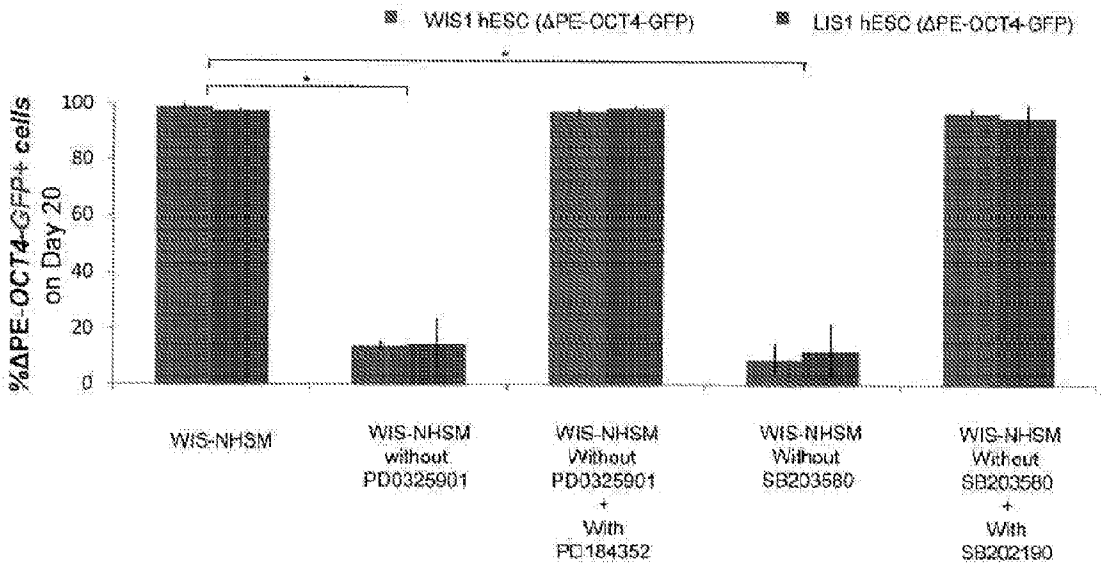
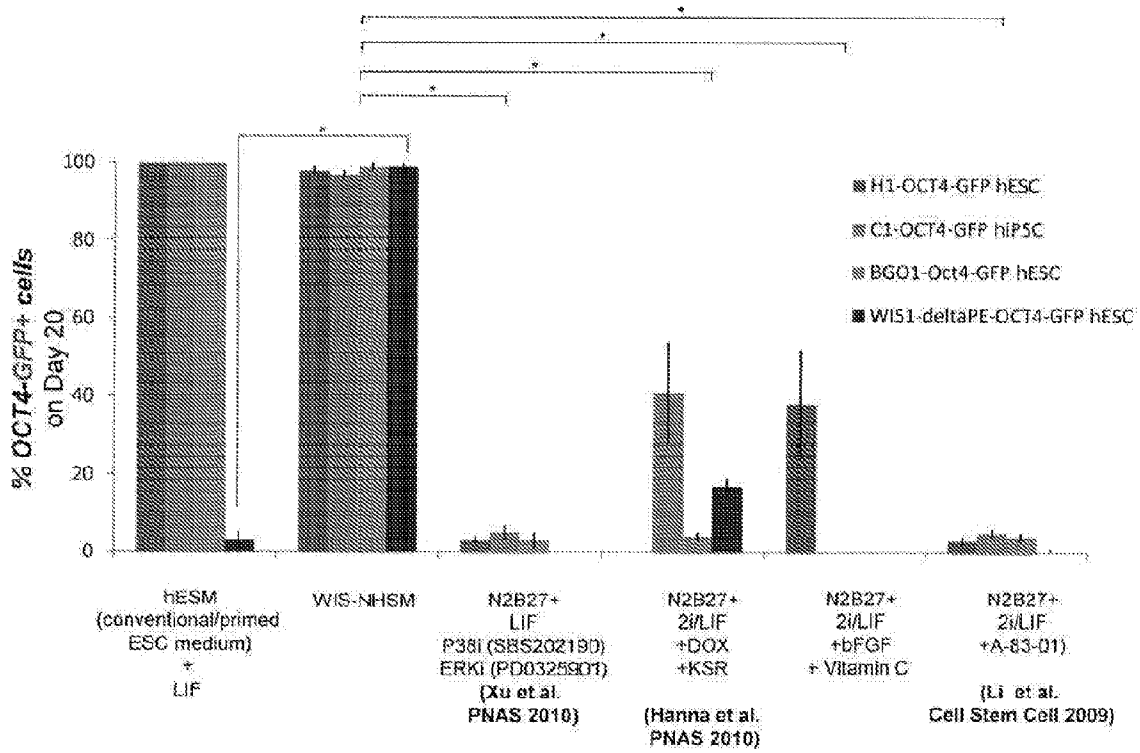


FIG. 87B



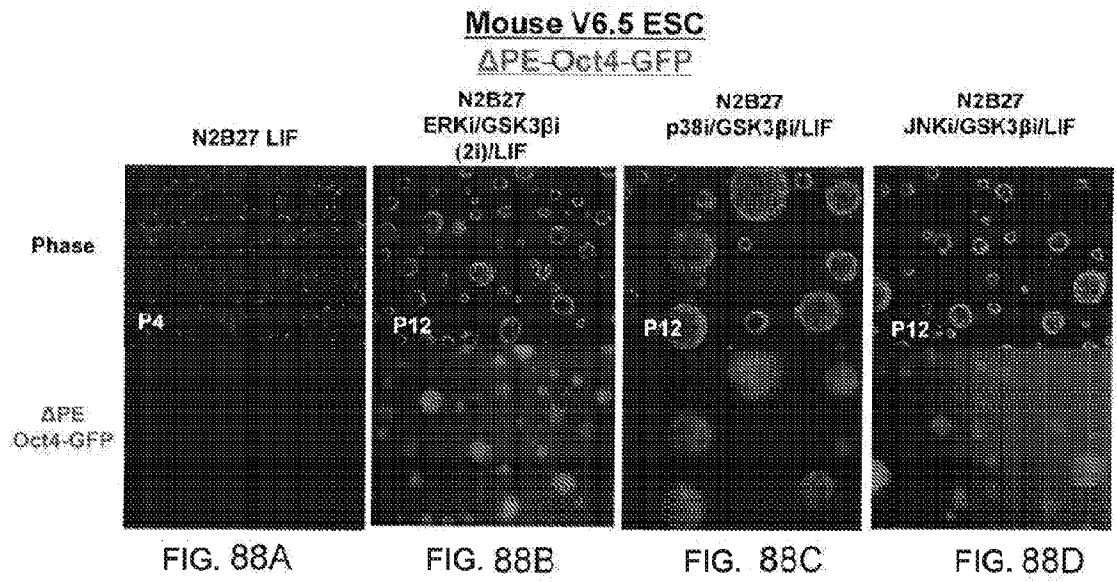


FIG. 88A FIG. 88B FIG. 88C FIG. 88D

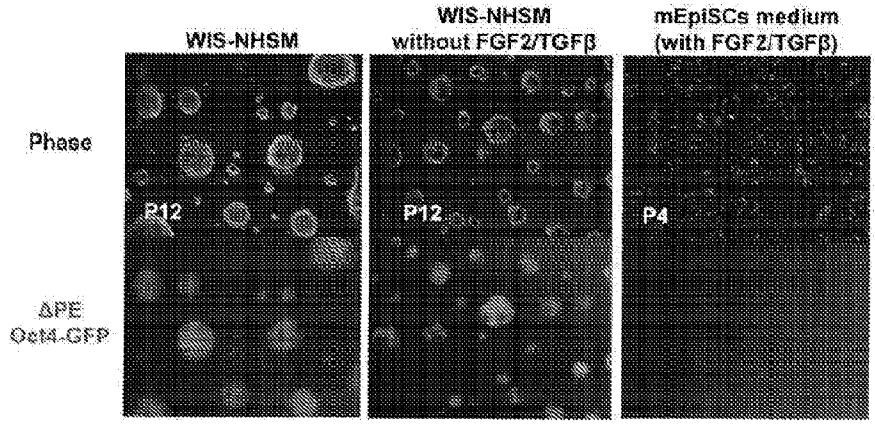


FIG. 88E FIG. 88F FIG. 88G

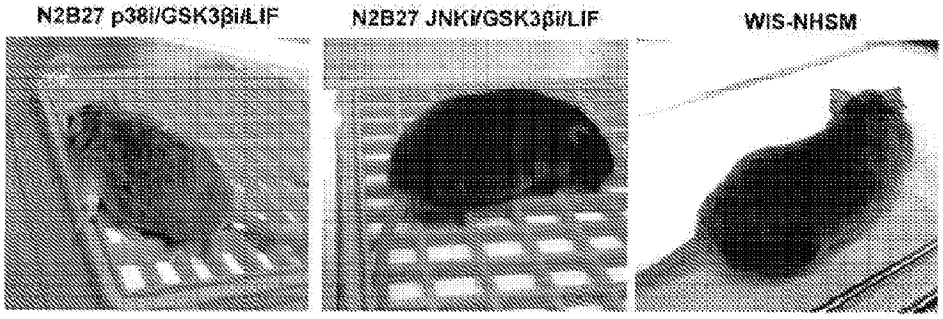


FIG. 88H FIG. 88I FIG. 88J

FIG. 89A

Medium	Injected embryos	Recipient females	Dead fetuses and pups	Pups born alive	Fostered pups
N2B27 2i/LIF	150	7	1	9	7
N2B27 p38i/GSK3βi, LIF	160	8	3	6	4
N2B27 JNKi/GSK3βi, LIF	145	7	1	10	6
WIS-NHSM	150	7	2	12	7
WIS-NHSM (without FGF2/TGFβ)	135	6	3	8	4

V6.5 ESC in WIS-NHSM

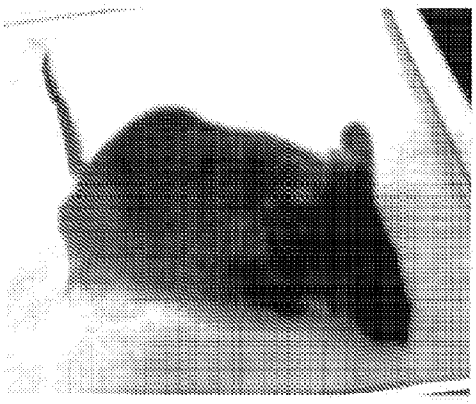


FIG. 89B

V6.5 ESC in WIS-NHSM (without FGF2/TGFβ)



FIG. 89C

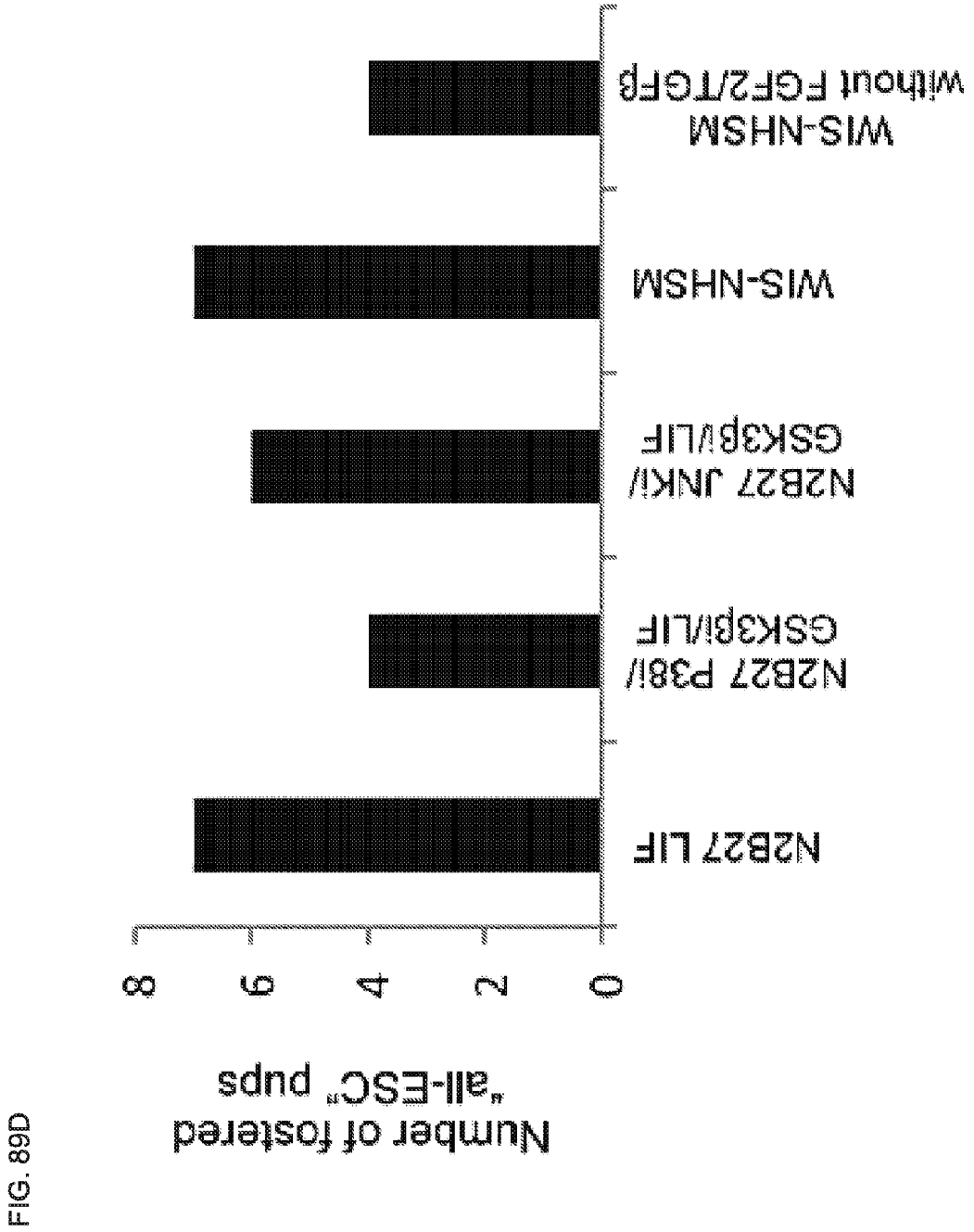
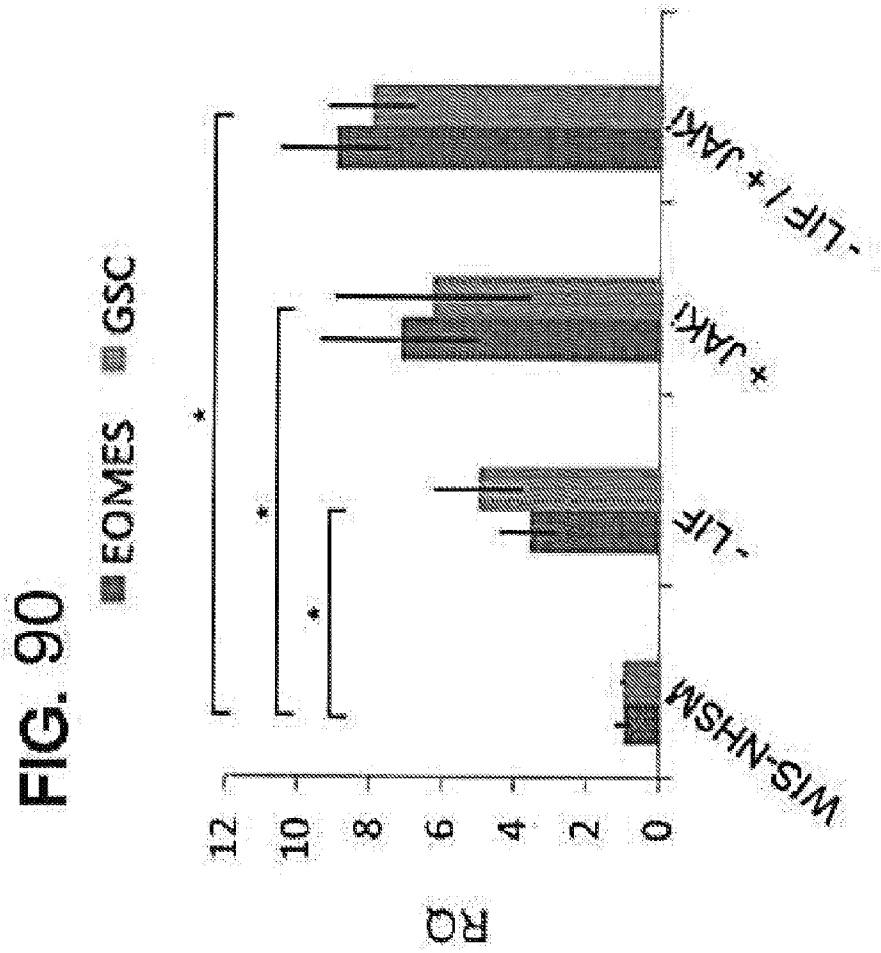

Number of fostered "all-ESC" pups
0
2
4
6
8
N2B27 LIF
N2B27 P38i/ GSK3βi/LIF
N2B27 JNKi/ GSK3βi/LIF
WIS-NHSM
WIS-NHSM without FGF2/TGFβ

FIG. 89D

FIG. 90



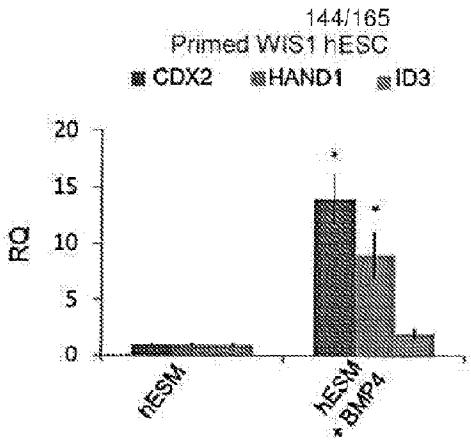


FIG. 91A

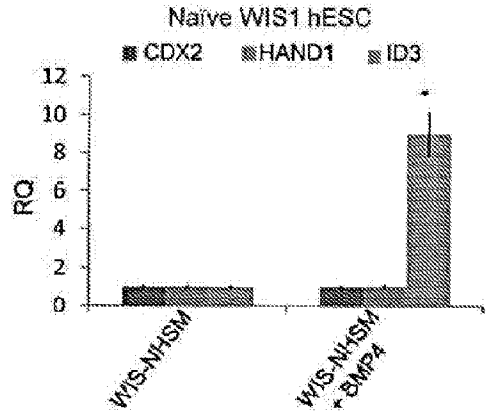


FIG. 91B

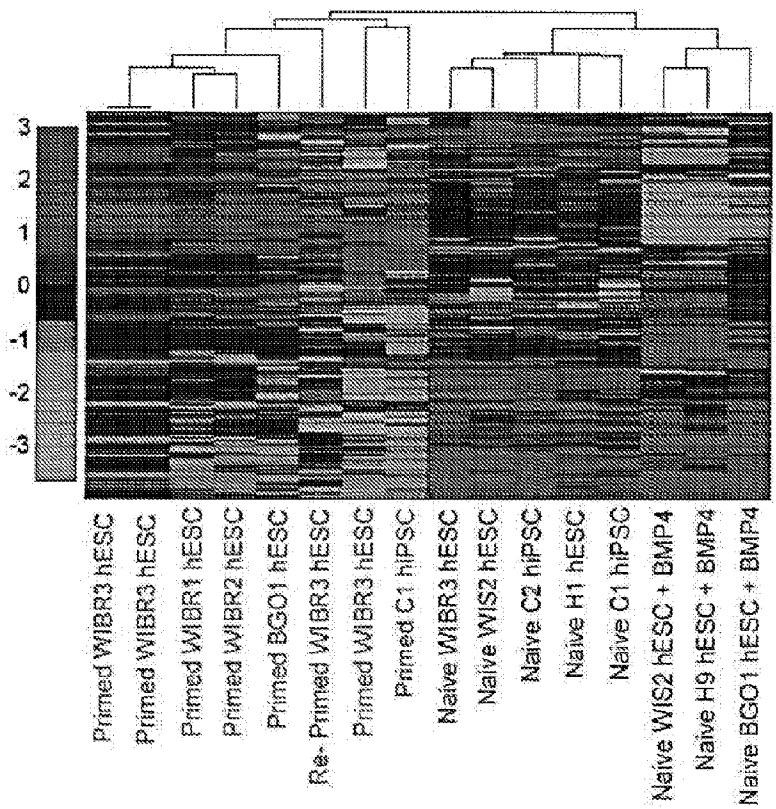


FIG. 91C

FIG. 92A

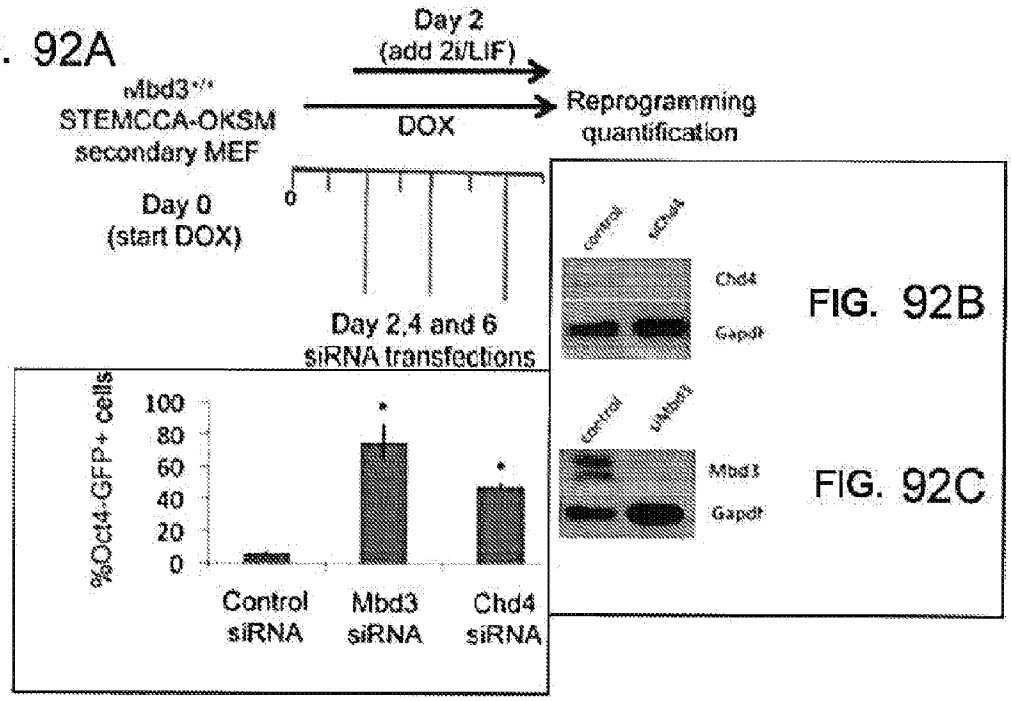
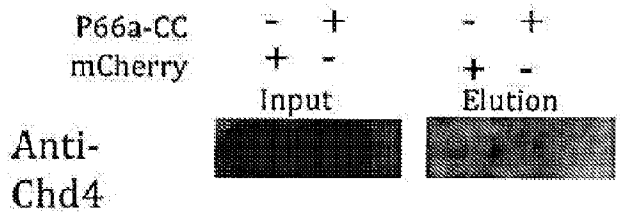


FIG. 92B

FIG. 92C

FIG. 92D

FIG. 93



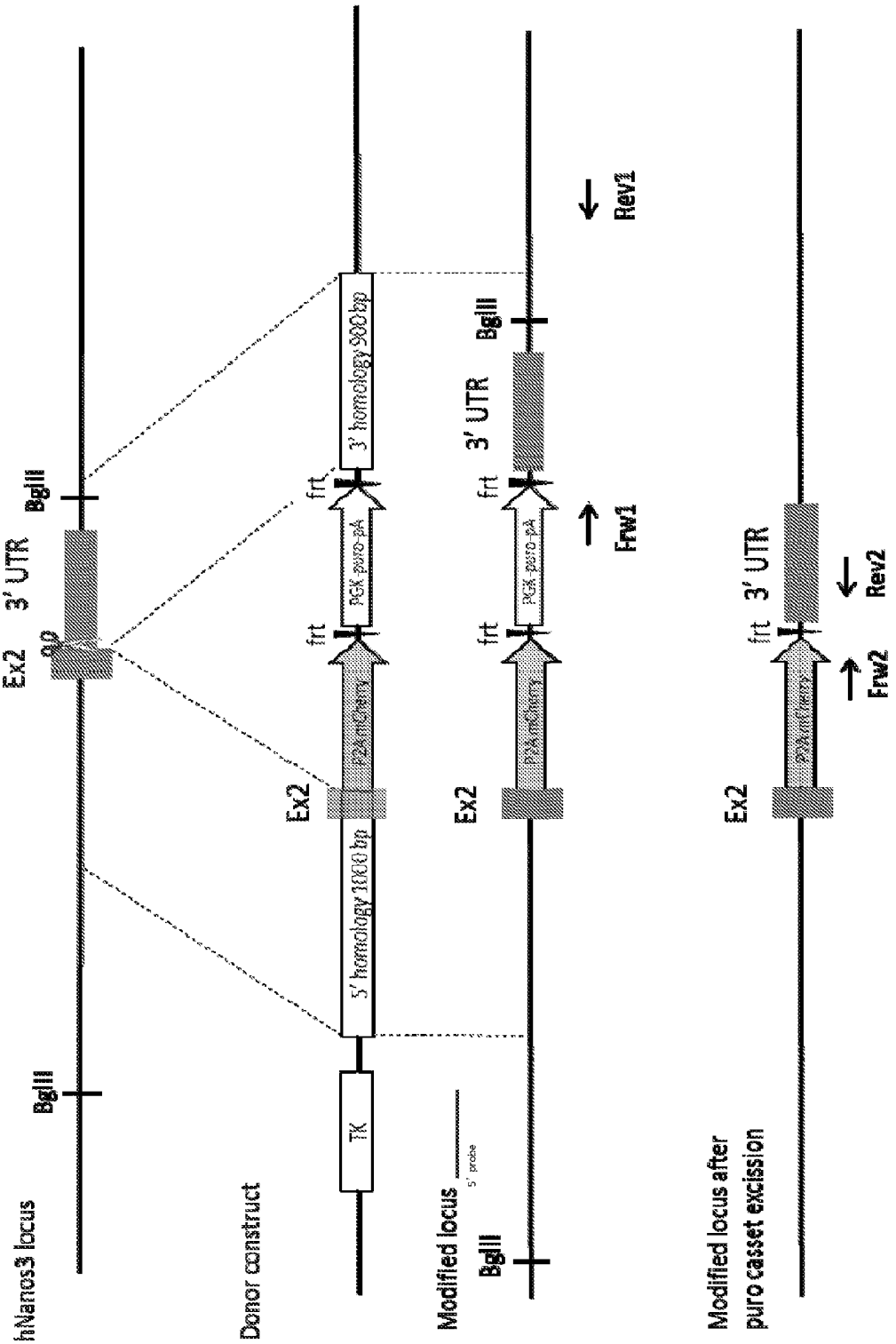

hNanos3 locus
BglII
3' UTR
Ex2
BglII
Donor construct
TK
5' homology 1000 bp
Ex2
frt
PGK puro-pA
frt
3' homology 900 bp
Modified locus
5' probe
BglII
Ex2
frt
PGK puro-pA
frt
3' UTR
BglII
Rev1
Frw1
Modified locus after
puro casset excision
Ex2
frt
3' UTR
Rev2
Frw2

FIG. 94A

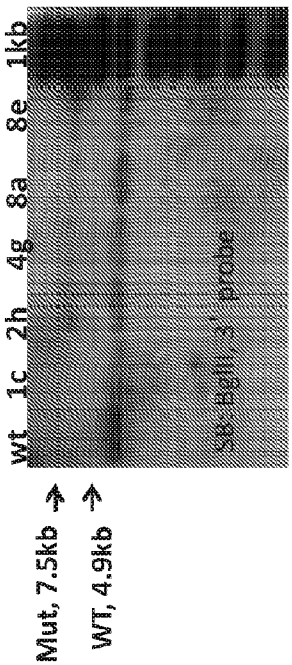


FIG. 94B

FIG. 95

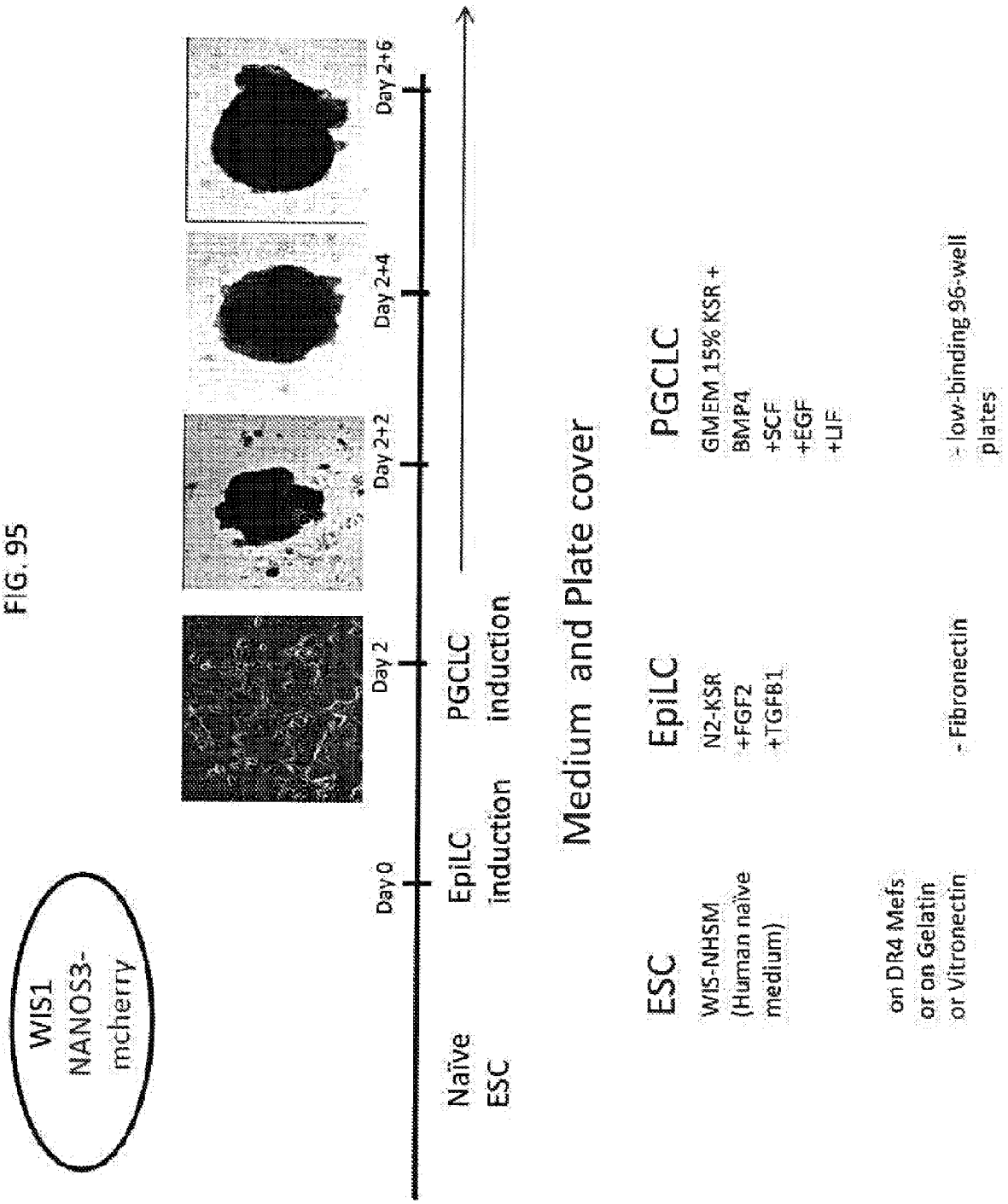

WIS1
NANOS3-
mcherry
Naïve
ESC
Day 0
EpiLC
induction
Day 2
PGCLC
induction
Day 2+2
Day 2+4
Day 2+6
Medium and Plate cover
ESC
WIS-NHSM
(Human naïve
medium)
on DR4 Mefs
or on Gelatin
or Vitronectin
EpiLC
N2-KSR
+FGF2
+TGFB1
- Fibronectin
PGCLC
GMEM 15% KSR +
BMP4
+SCF
+EGF
+LIF
- low-binding 96-well
plates

FIG. 96A

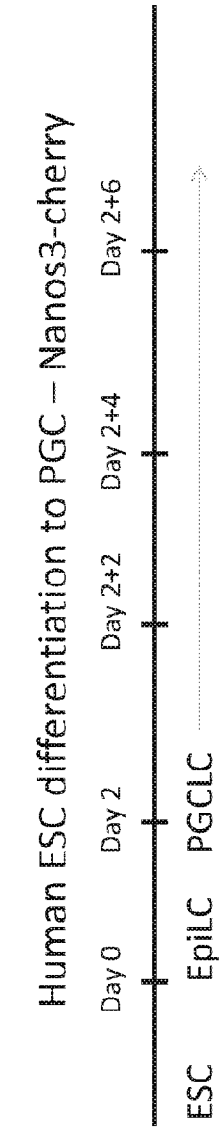


FIG. 96B

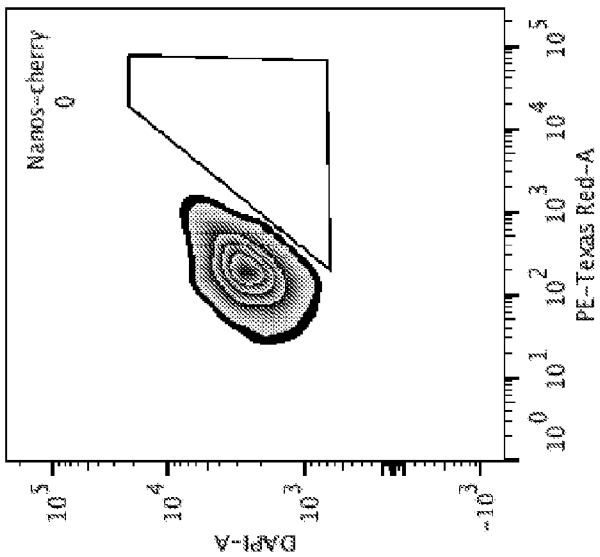
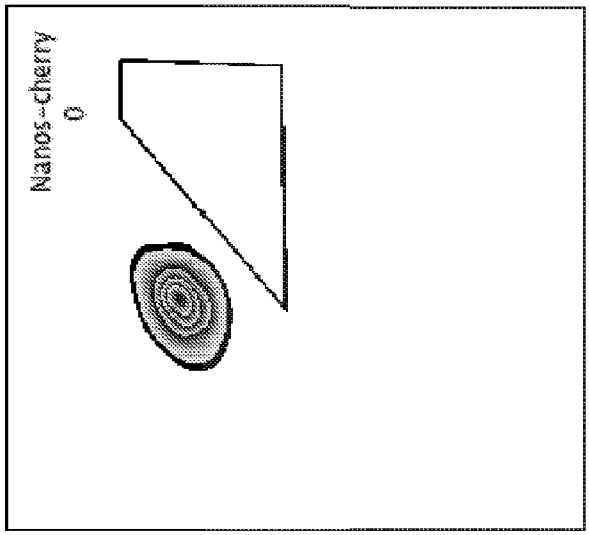
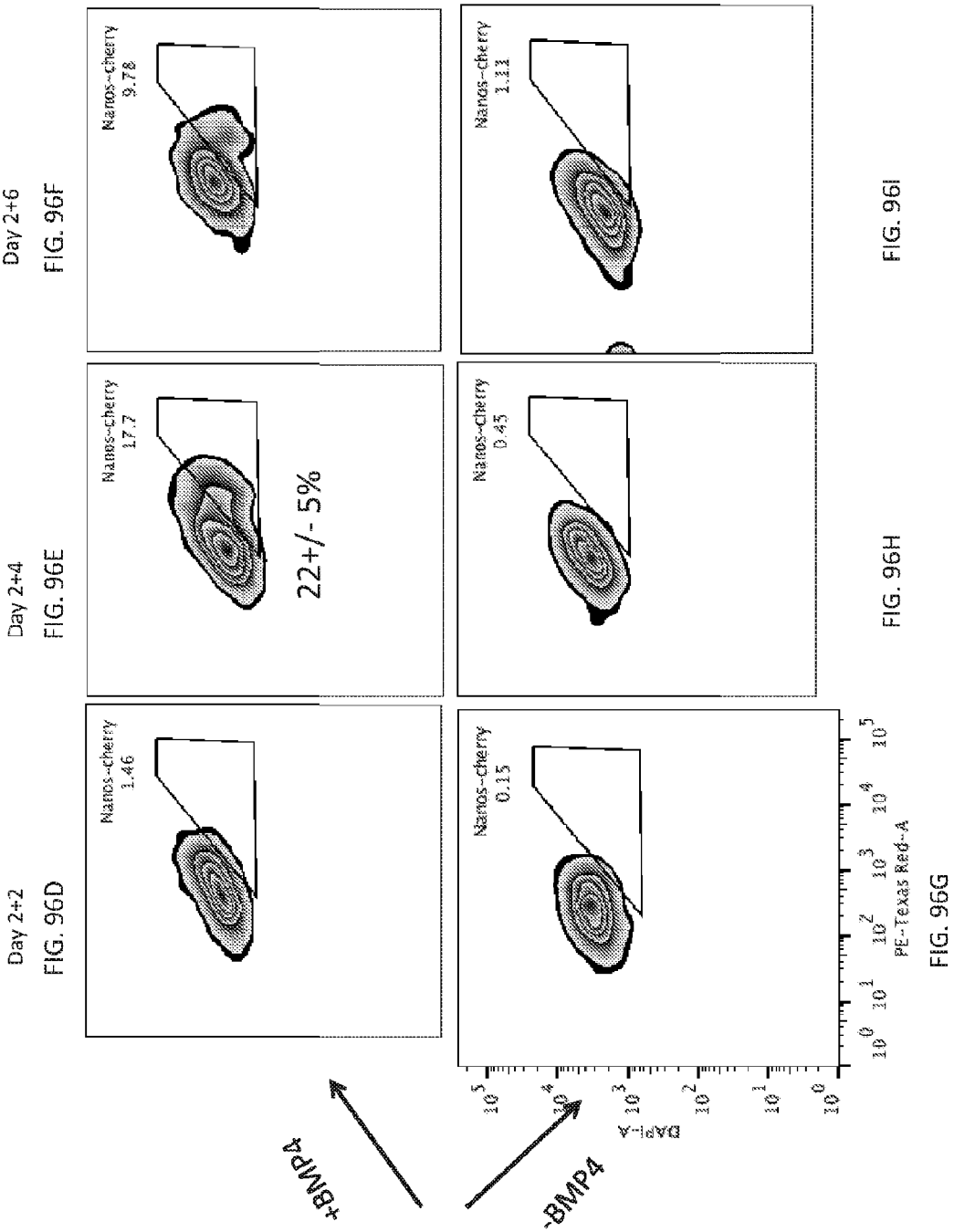


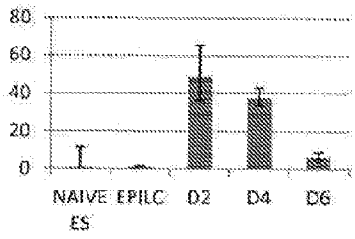
FIG. 96C



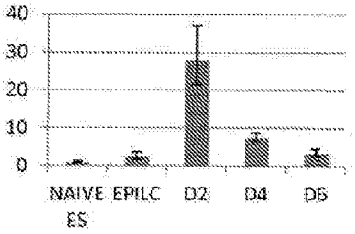

Day 2+2
FIG. 96D
Day 2+4
FIG. 96E
Day 2+6
FIG. 96F
Nanos-cherry
1.46
Nanos-cherry
17.7
Nanos-cherry
9.78
22+/- 5%
Nanos-cherry
0.15
Nanos-cherry
0.45
Nanos-cherry
1.11
+BMP4
-BMP4
DAPI-A
PE-Texas Red-A
FIG. 96G
FIG. 96H
FIG. 96I

Early

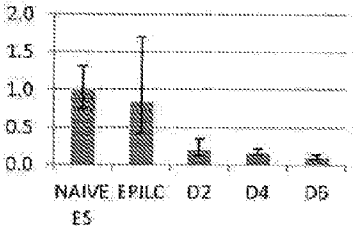
AP2G FIG. 97A



BLIMP1 FIG. 97B

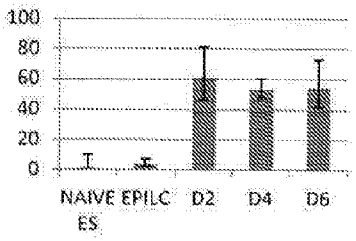


PRDM14 FIG. 97C

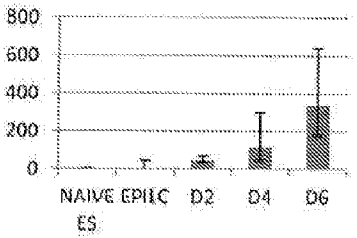


Intermediate

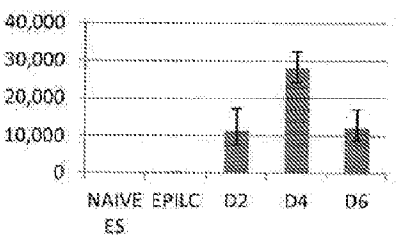
STELLA FIG. 97D



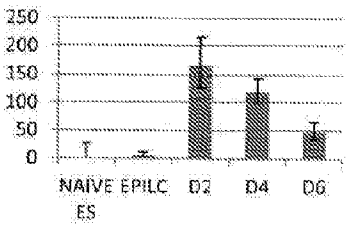
DND1 FIG. 97E



NANOS3 FIG. 97F

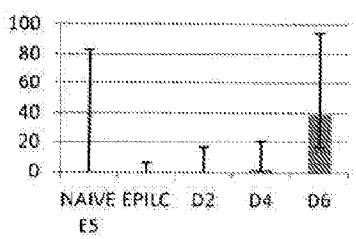


INTEGRIN B3 FIG. 97G



Late

VASA FIG. 97H



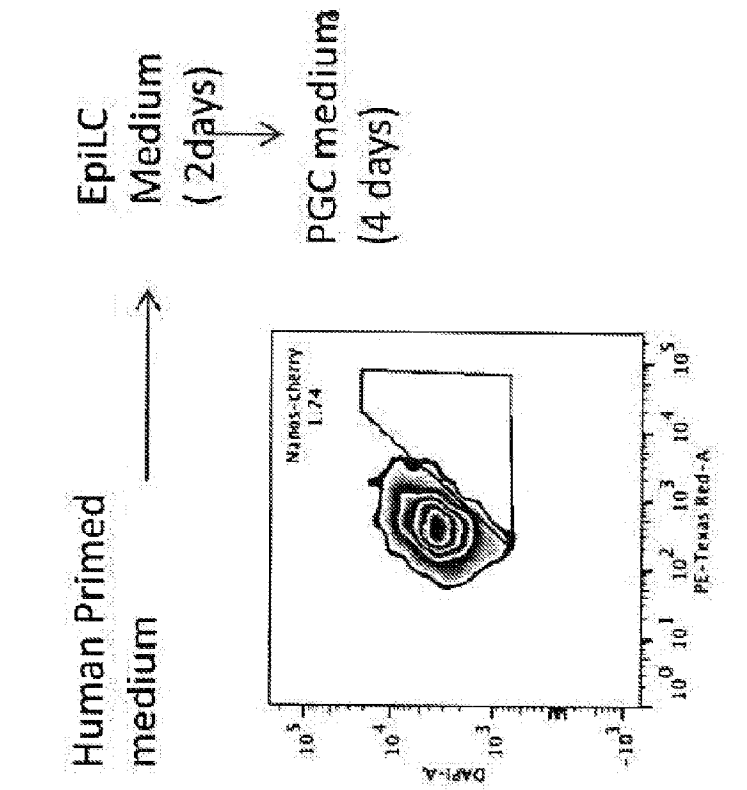


FIG. 98B

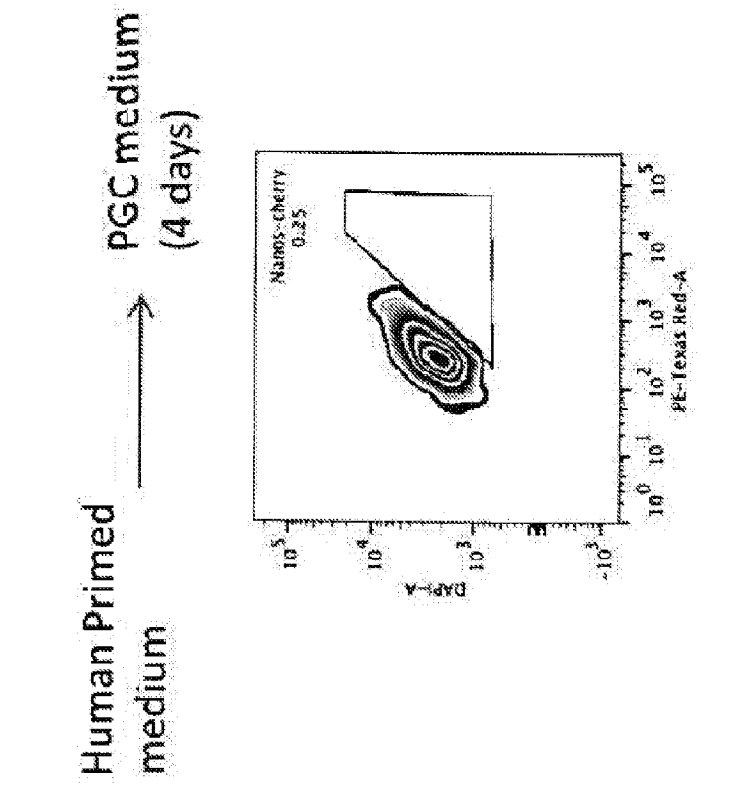


FIG. 98A

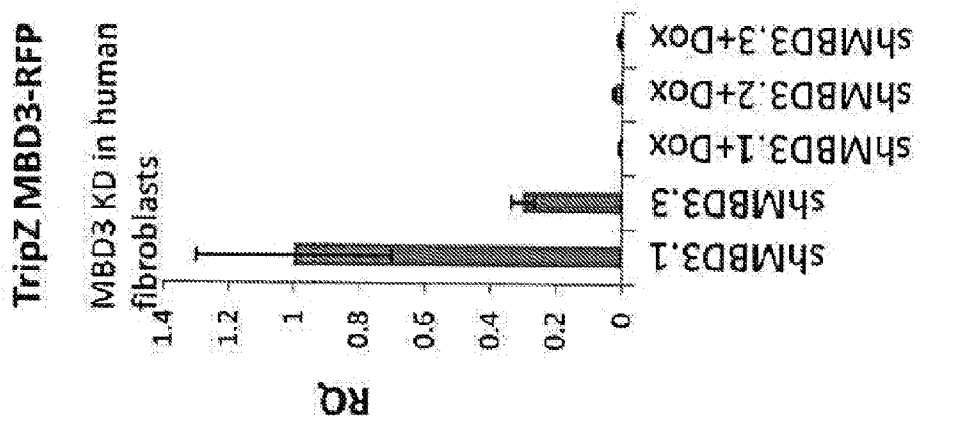


FIG. 99A

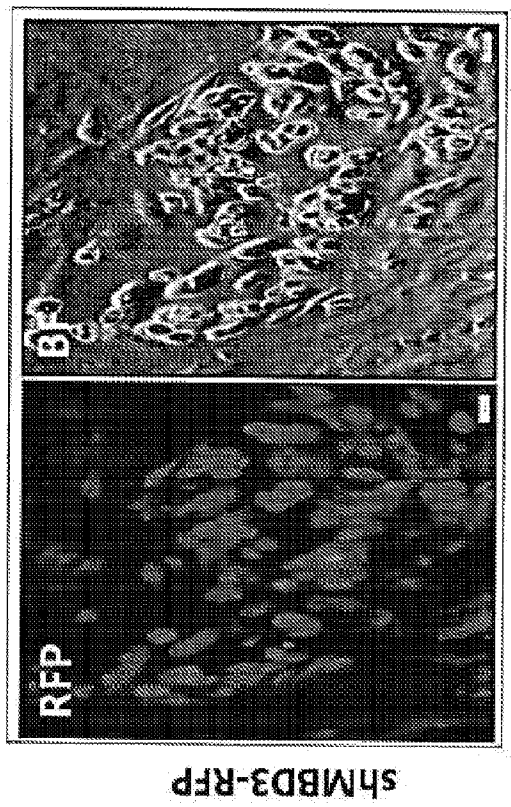


FIG. 99B FIG. 99C

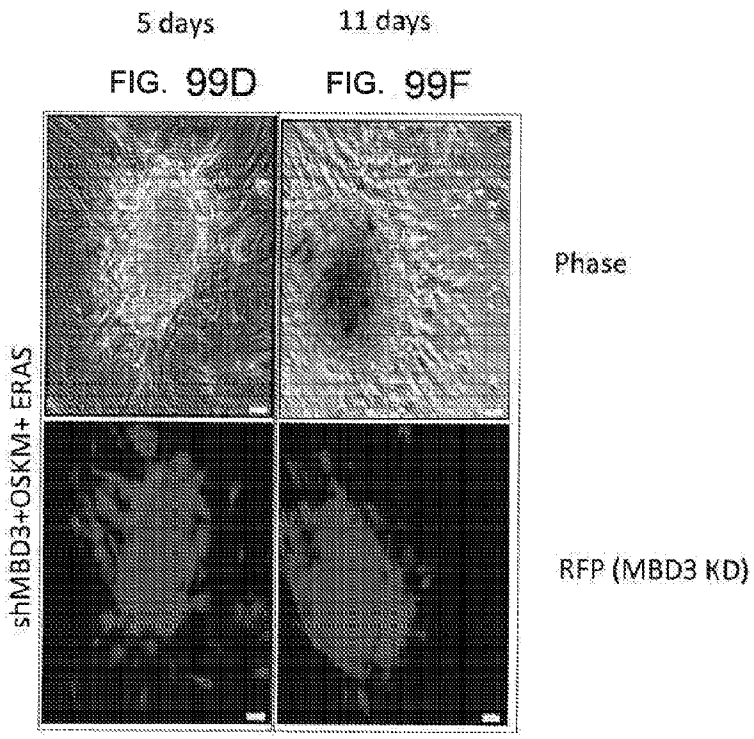


FIG. 99D FIG. 99F

FIG. 99E FIG. 99G

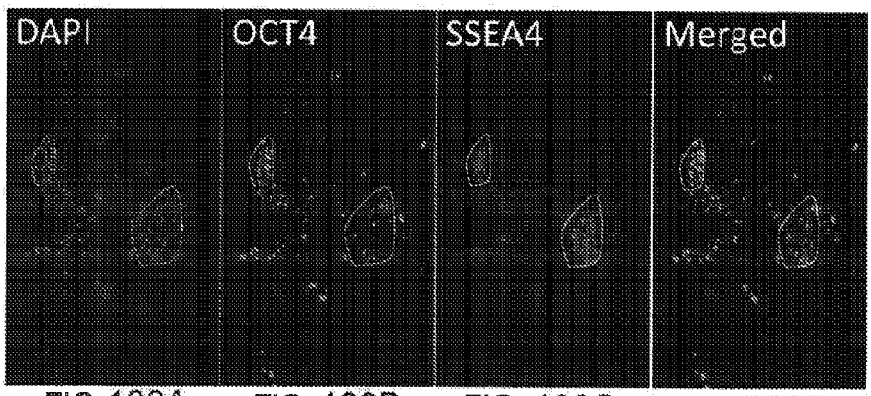


FIG. 100A FIG. 100B FIG. 100C FIG. 100D

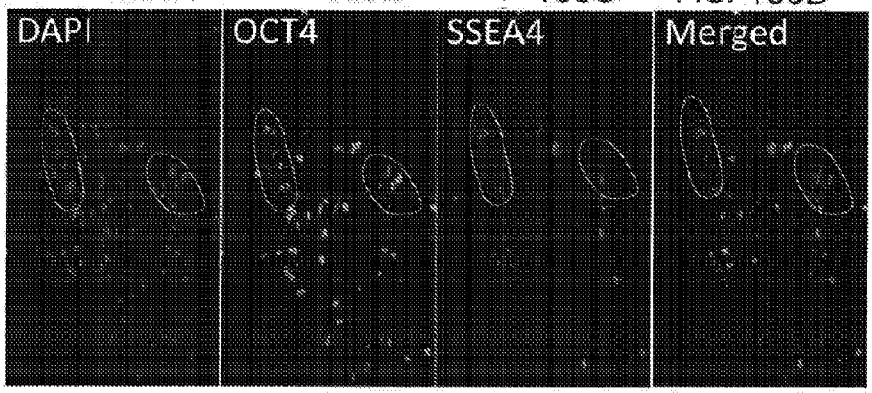


FIG. 100E FIG. 100F FIG. 100G FIG. 100H

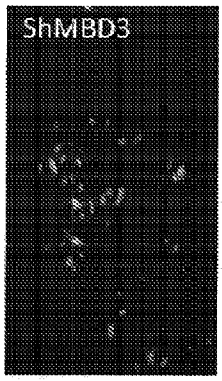


FIG. 100I

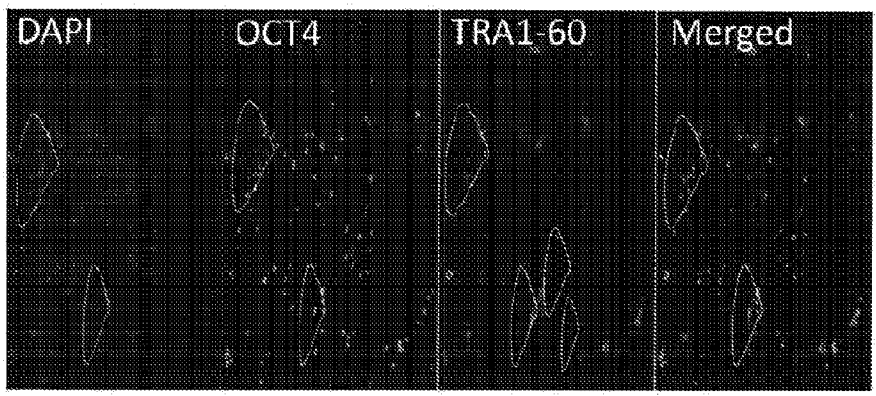


FIG. 100J FIG. 100K FIG. 100L FIG. 100M

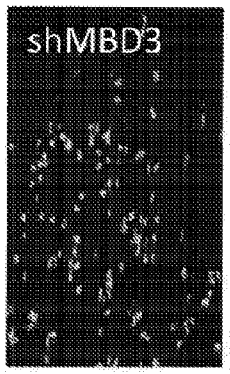


FIG. 100N

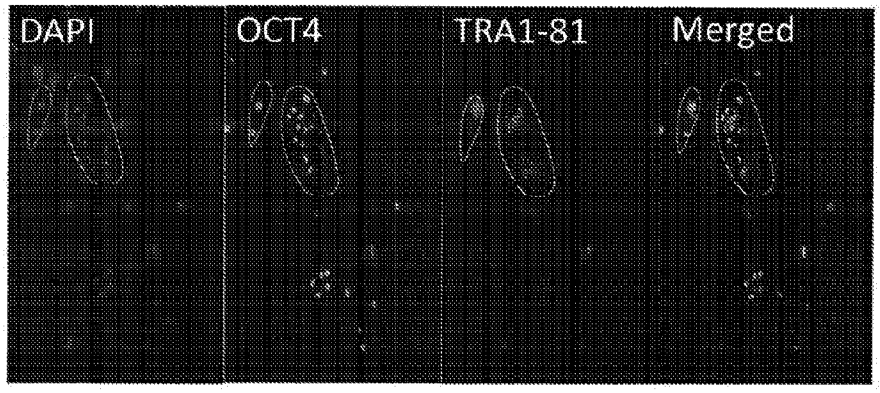


FIG. 100O FIG. 100P FIG. 100Q FIG. 100R

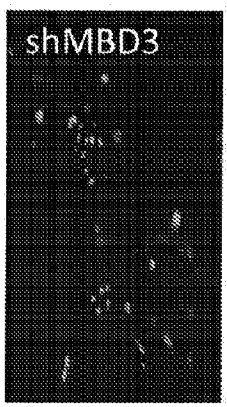


FIG. 100S

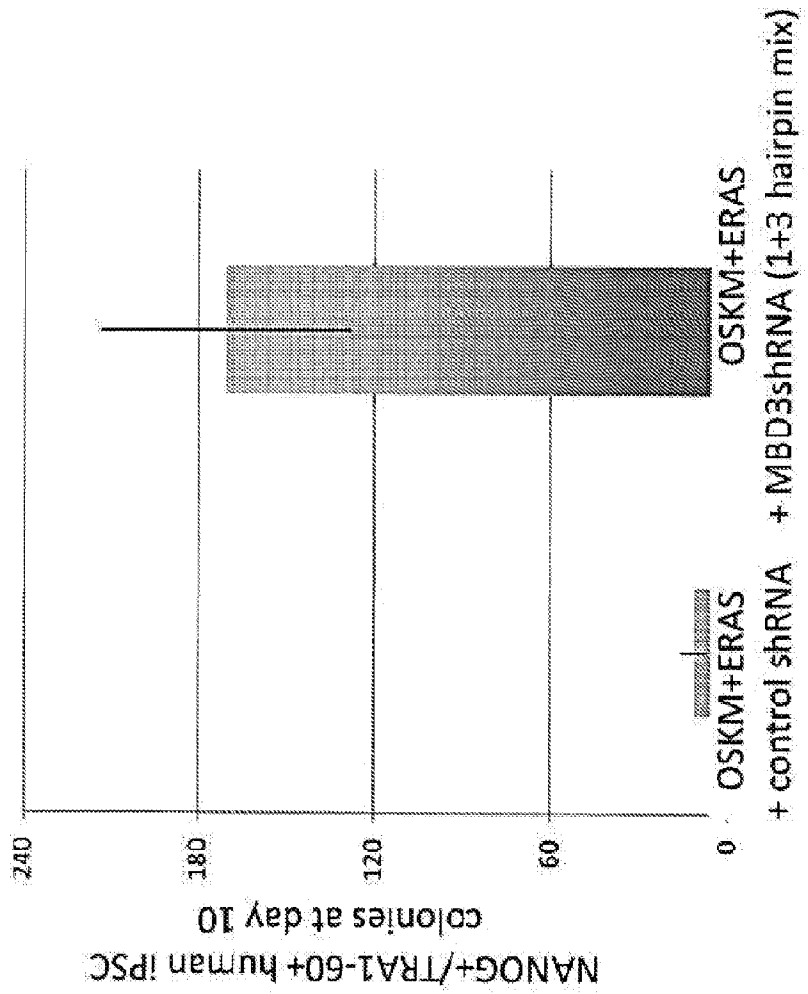

NANOG+/TRA1-60+ human iPSC colonies at day 10
240
180
120
60
0
OSKM+ERAS
+ control shRNA
OSKM+ERAS
+ MBD3shRNA (1+3 hairpin mix)

FIG. 100T

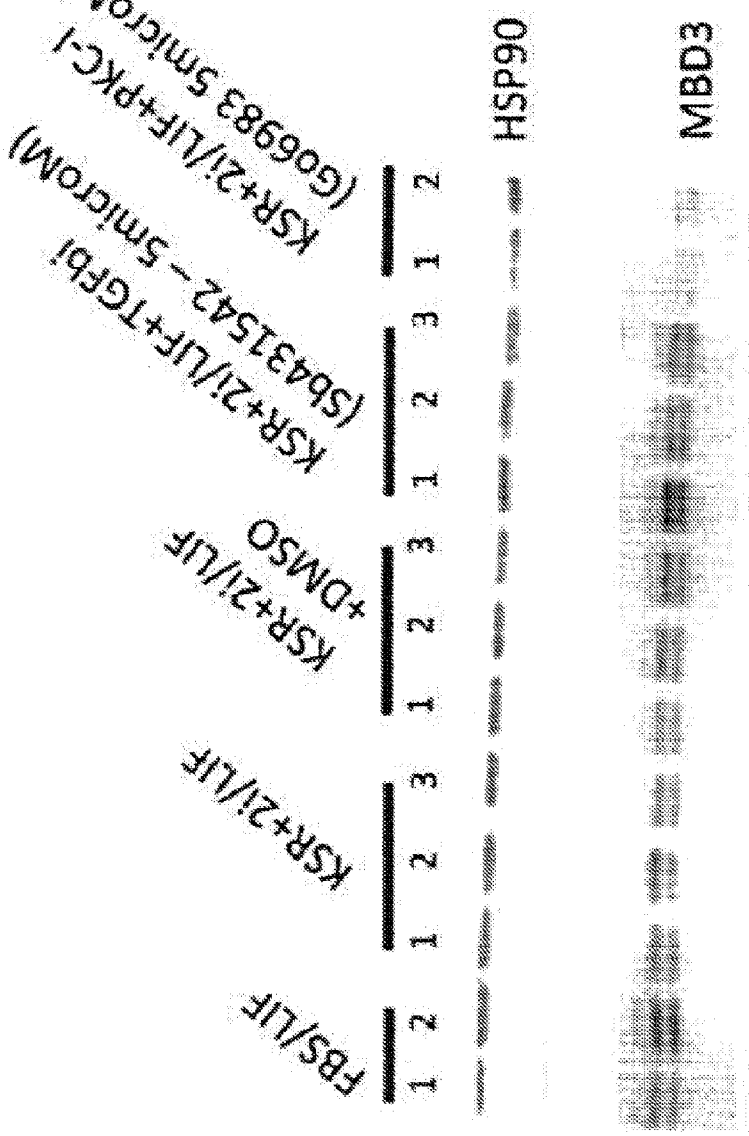


FIG. 101A

FIG. 101B

FIG. 102

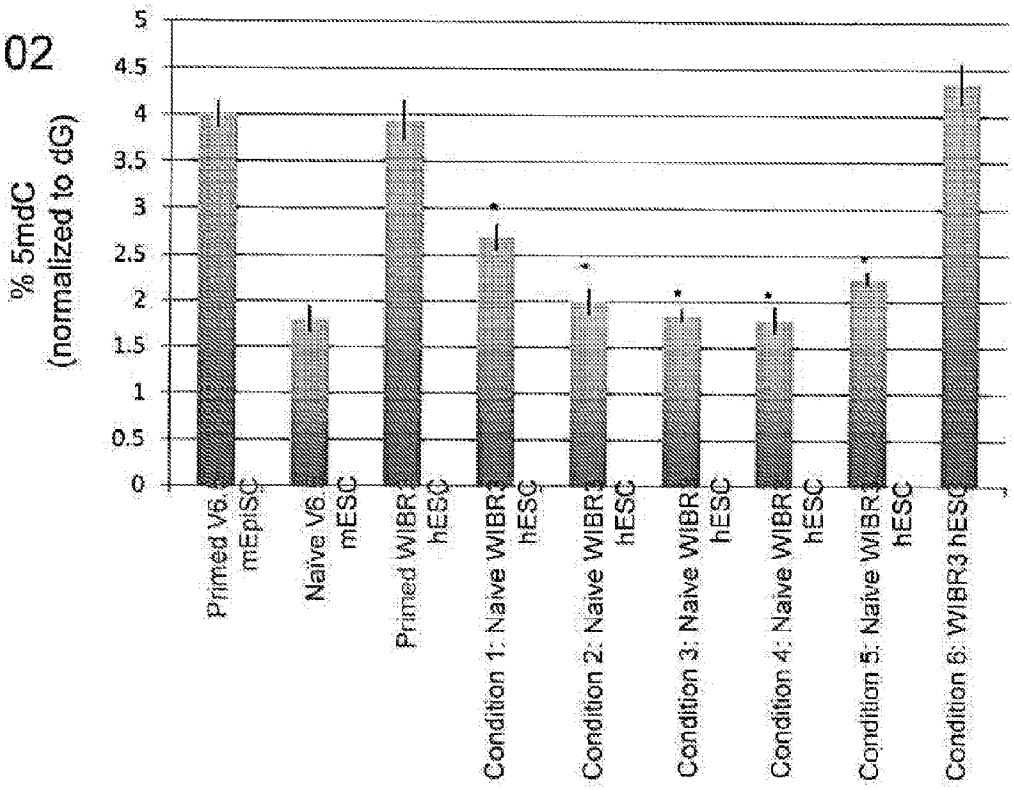


FIG. 103

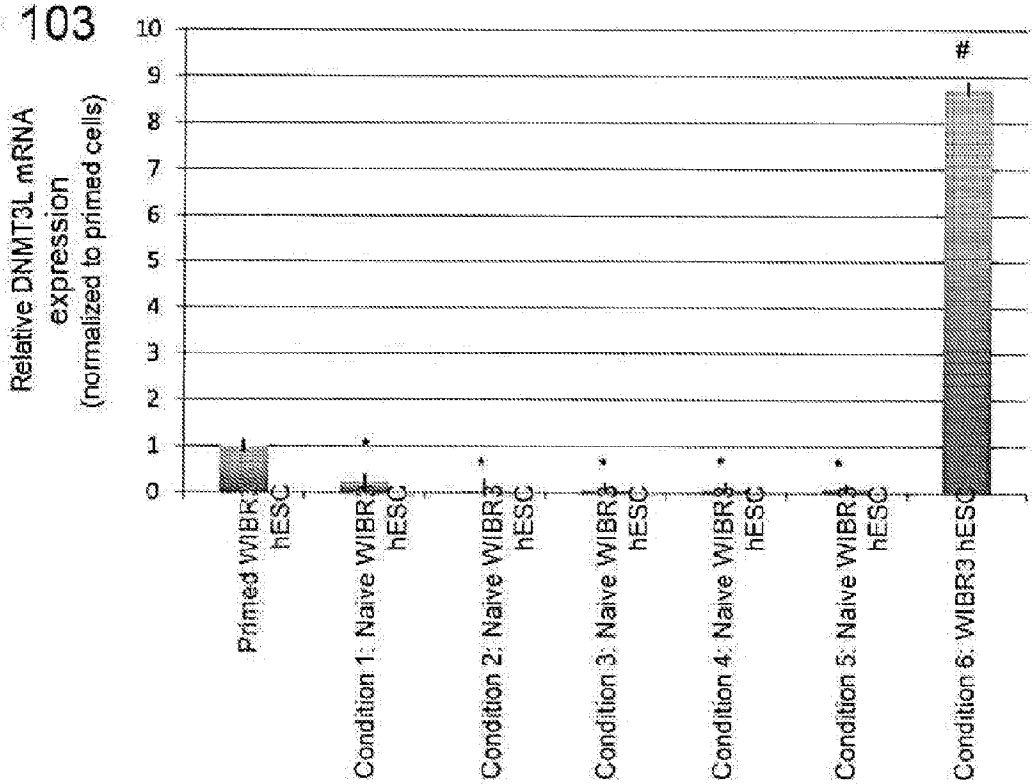


FIG. 104

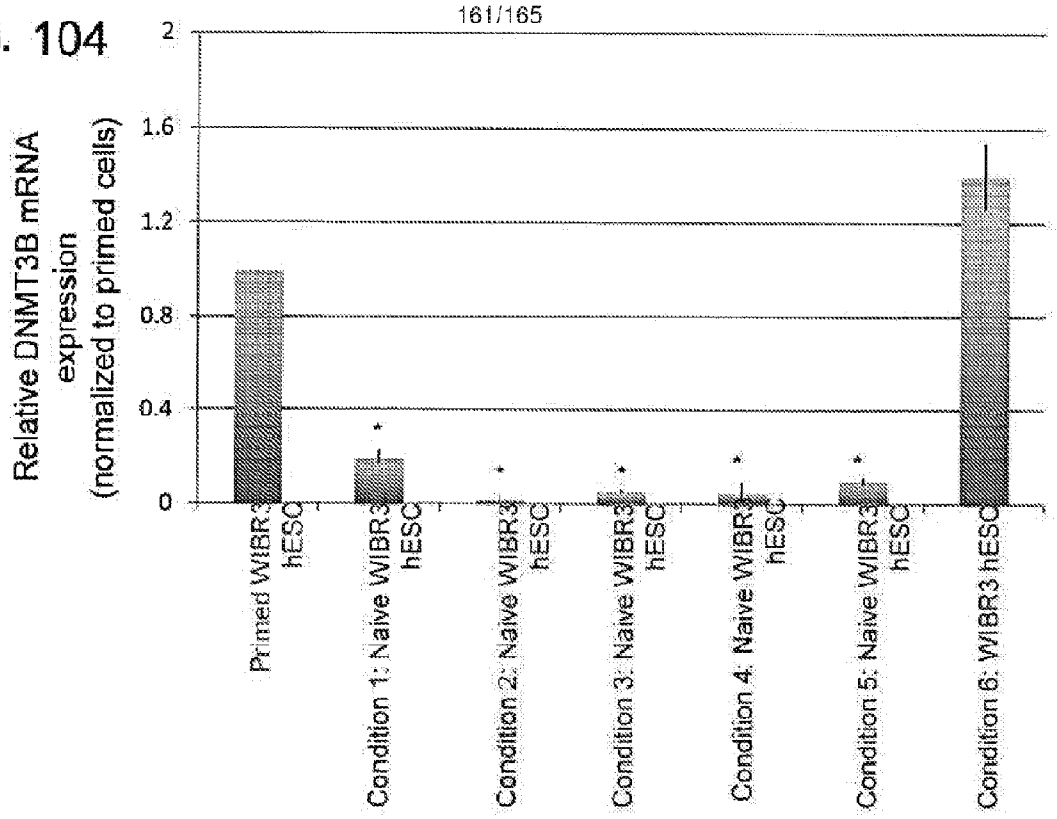
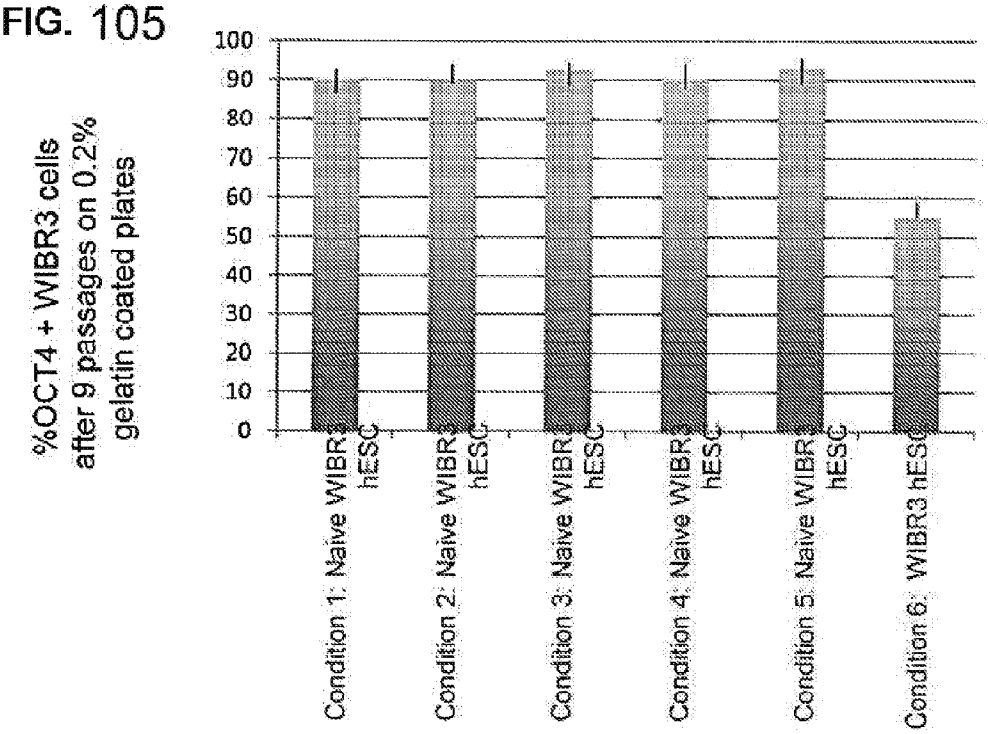


FIG. 105



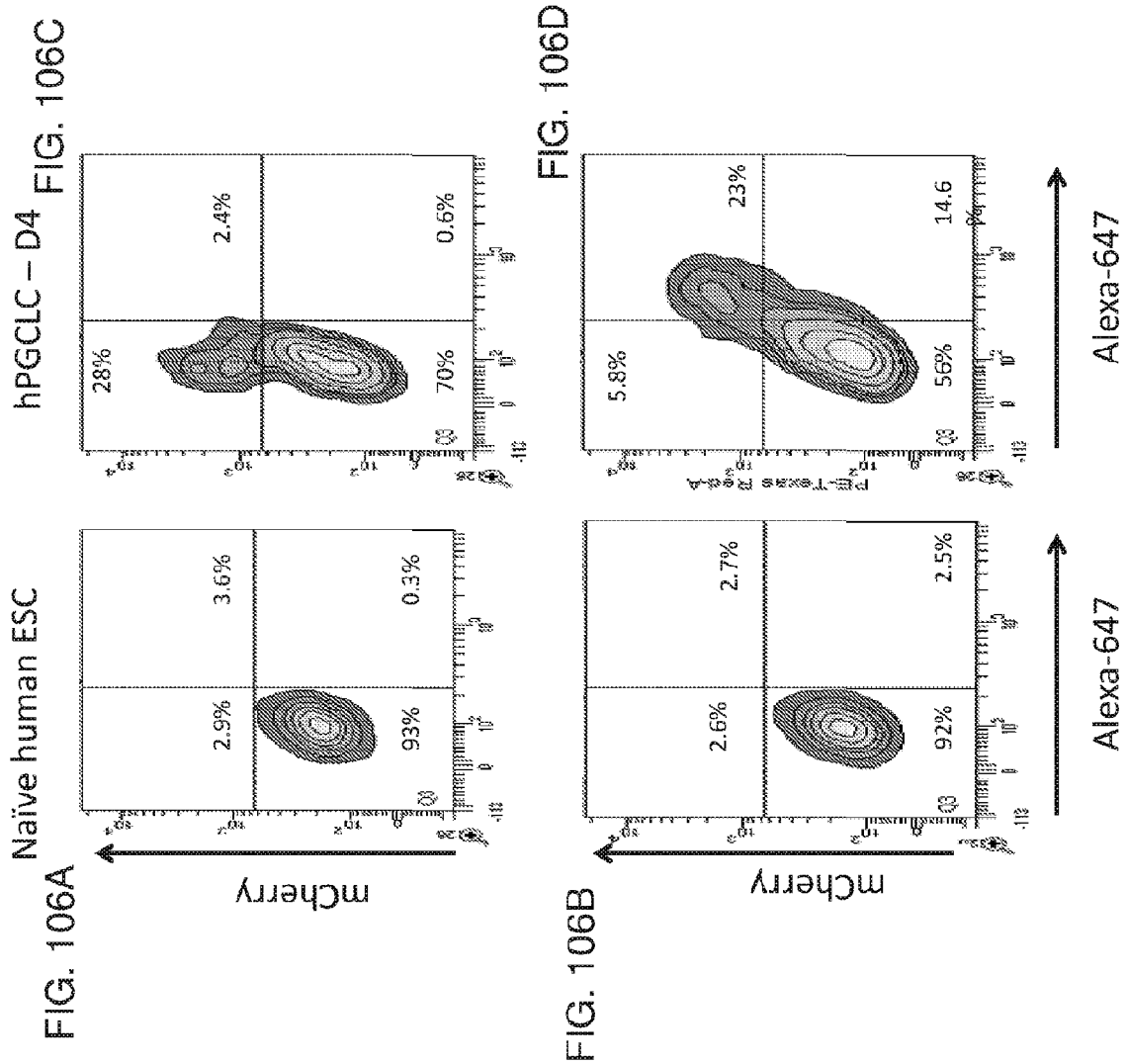


FIG. 106A FIG. 106B FIG. 106C FIG. 106D

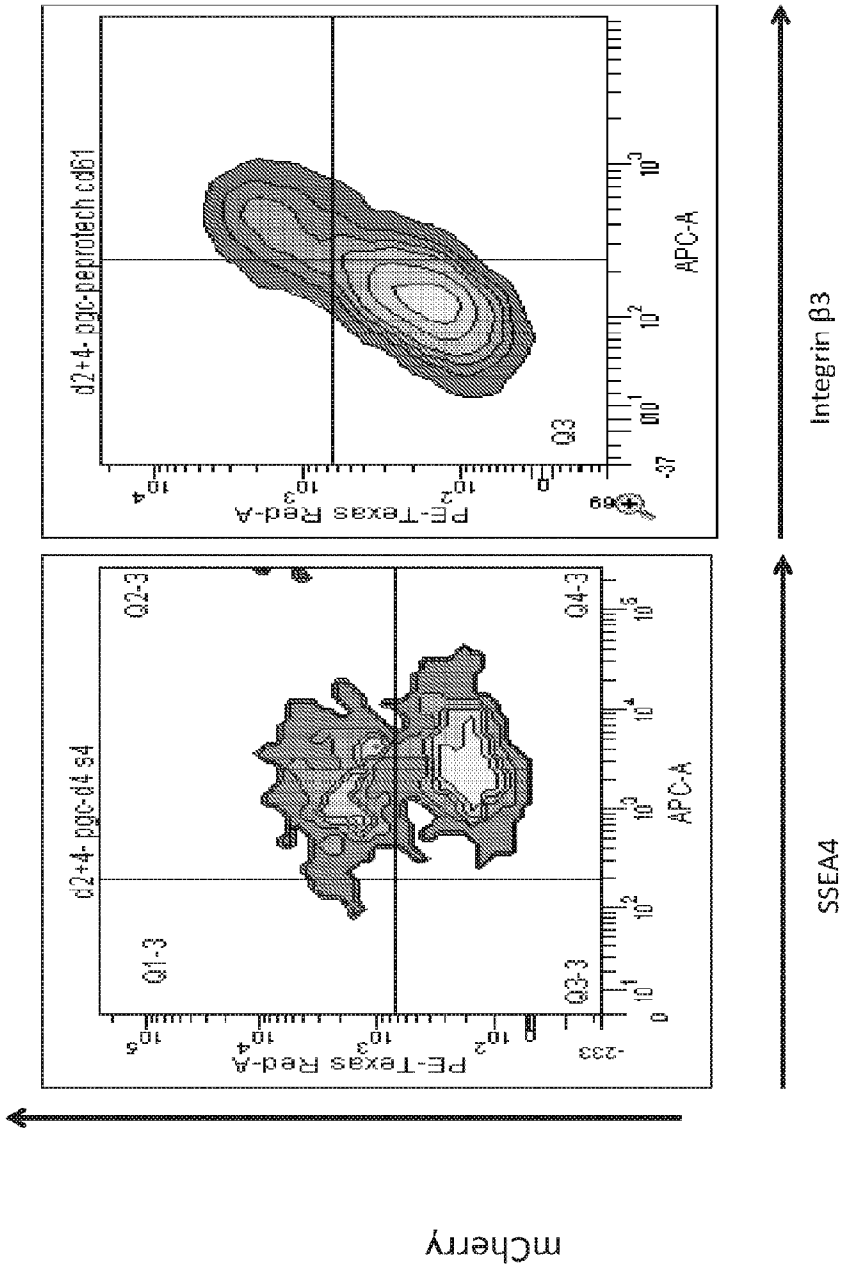

FIG. 107A
FIG. 107B
d2+4- pgc-d4 s4
Q1-3
Q2-3
Q3-3
Q4-3
PE-Texas Red-A
APC-A
SSEA4
d2+4- pgc-peprotech cd61
Q3
PE-Texas Red-A
APC-A
Integrin β3
mCherry

FIG. 108A

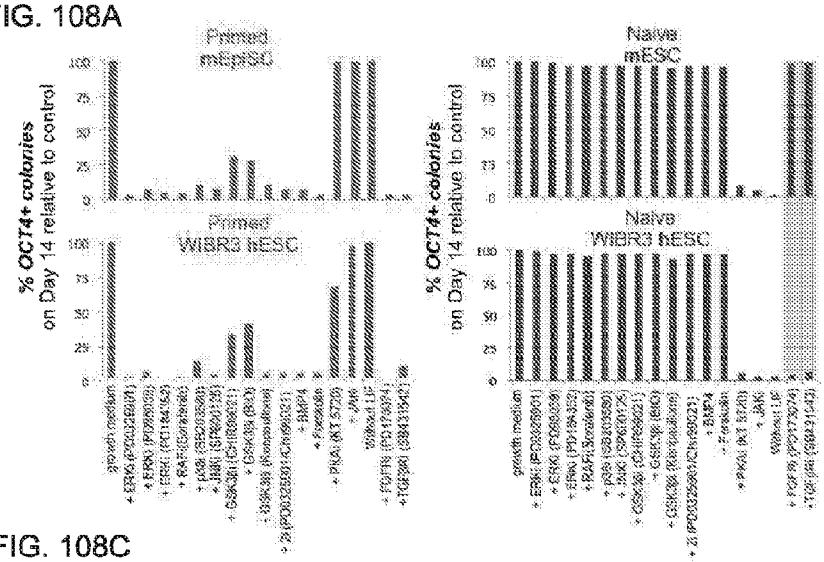


FIG. 108B

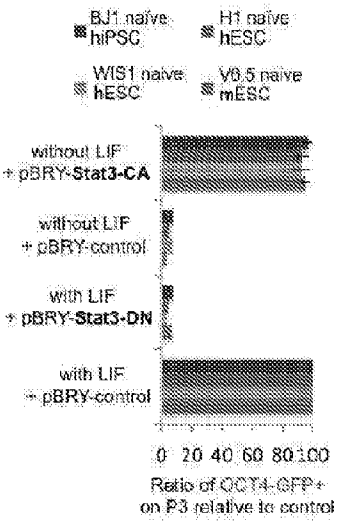


FIG. 108C

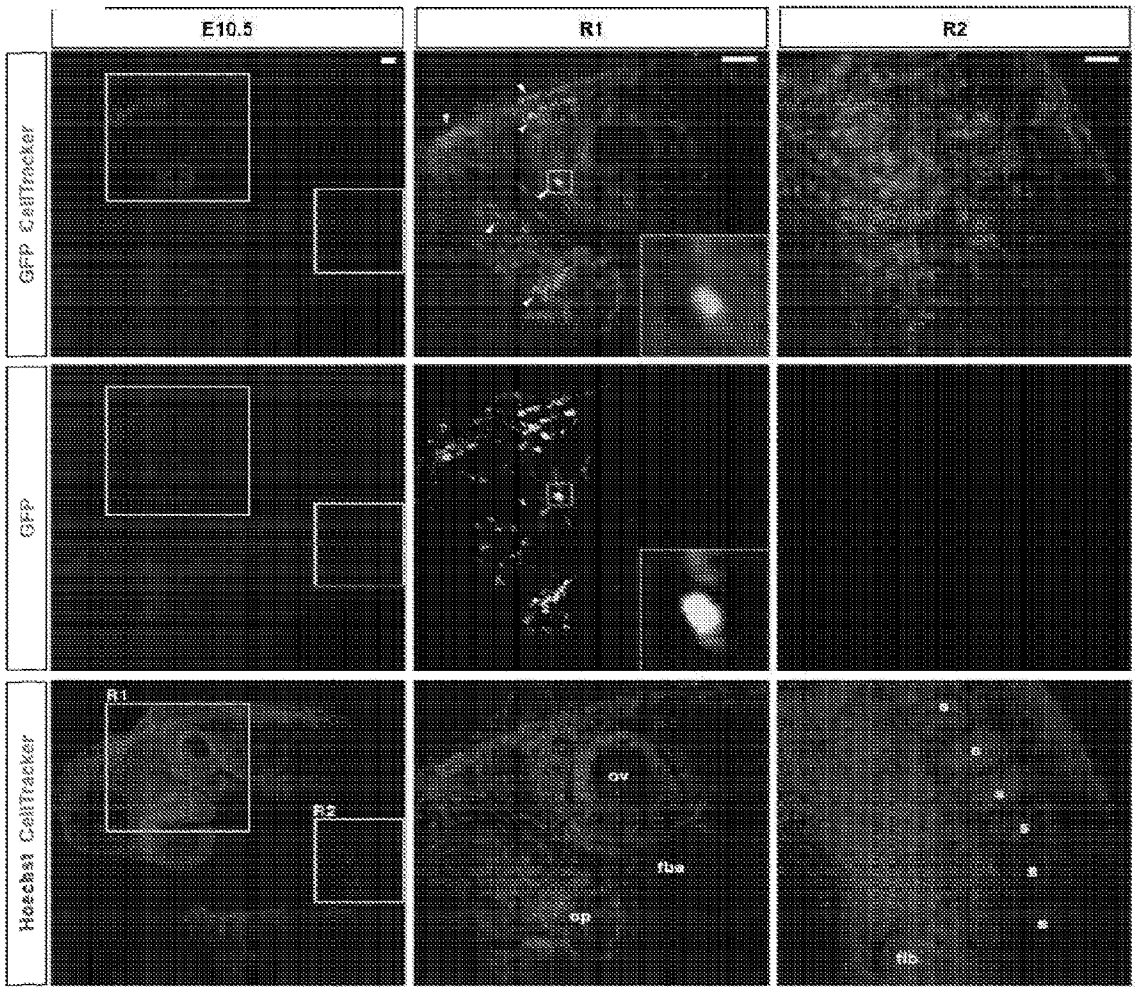


FIG. 109A

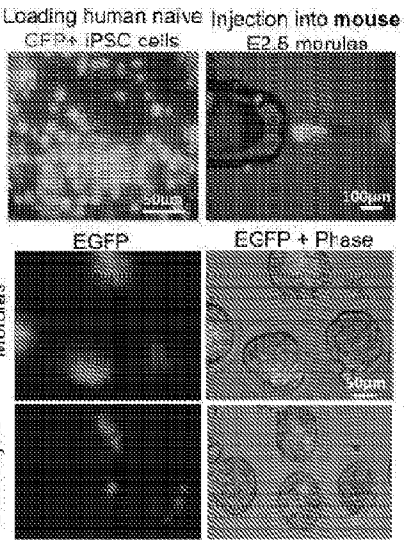


FIG. 109B

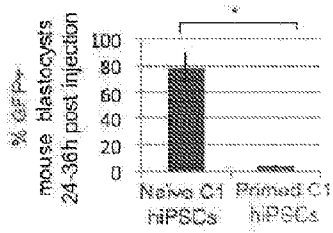


FIG. 109C



FIG. 109D

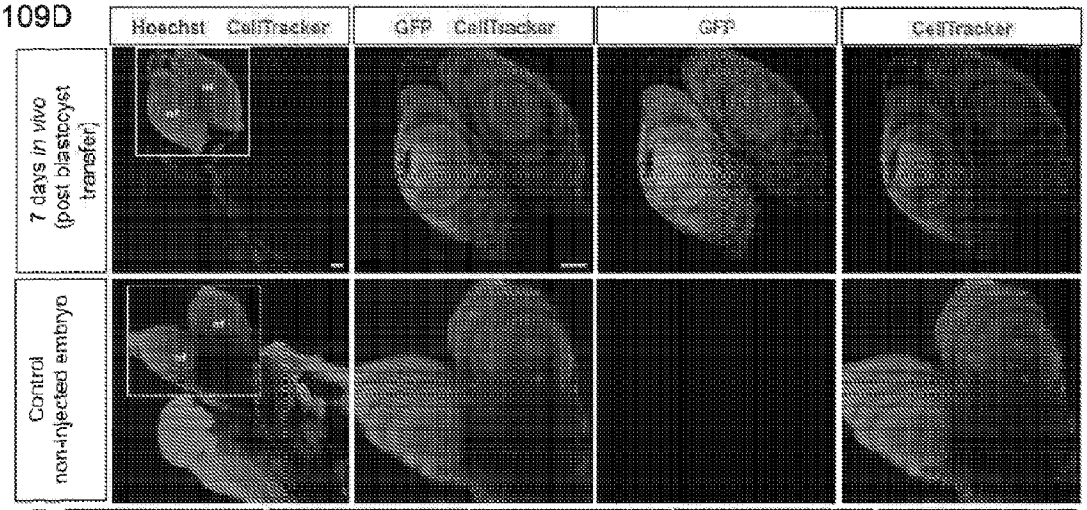
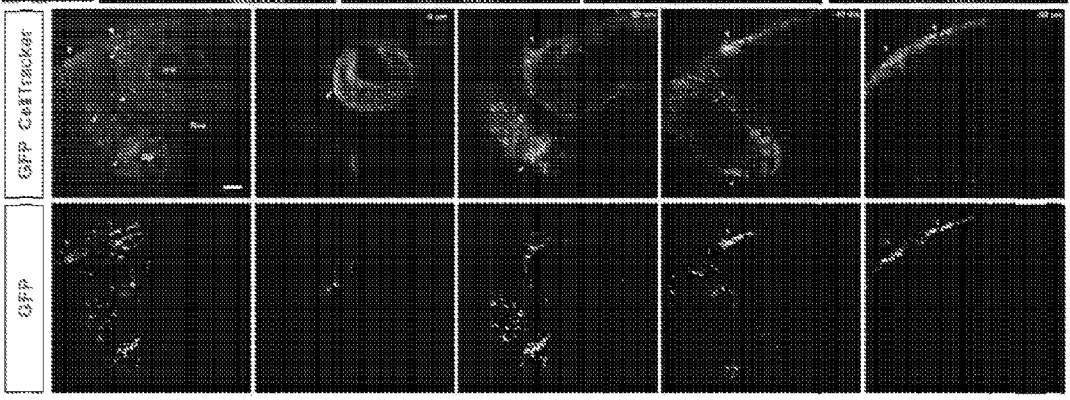


FIG. 109E



INTERNATIONAL SEARCH REPORT

International application No
PCT/IB2014/060954

A. CLASSIFICATION OF SUBJECT MATTER
INV. C12N5/0735 C12N5/074
ADD.

According to International Patent Classification (IPC) or to both national classification and IPC

B. FIELDS SEARCHED

Minimum documentation searched (classification system followed by classification symbols)
C12N

Documentation searched other than minimum documentation to the extent that such documents are included in the fields searched

Electronic data base consulted during the international search (name of data base and, where practicable, search terms used)

EPO-Internal, WPI Data, BIOSIS

C. DOCUMENTS CONSIDERED TO BE RELEVANT

Category*	Citation of document, with indication, where appropriate, of the relevant passages	Relevant to claim No.
X	J. HANNA ET AL: "Human embryonic stem cells with biological and epigenetic characteristics similar to those of mouse ESCs", PROCEEDINGS OF THE NATIONAL ACADEMY OF SCIENCES, vol. 107, no. 20, 18 May 2010 (2010-05-18) , pages 9222-9227, XP055054545, ISSN: 0027-8424, DOI: 10.1073/pnas.1004584107 page 9224 - page 9225 ----- -/--	1-6,31, 38,39, 56-66, 74-76, 88-96

[X] Further documents are listed in the continuation of Box C.

[X] See patent family annex.

* Special categories of cited documents :

"A" document defining the general state of the art which is not considered to be of particular relevance

"E" earlier application or patent but published on or after the international filing date

"L" document which may throw doubts on priority claim(s) or which is cited to establish the publication date of another citation or other special reason (as specified)

"O" document referring to an oral disclosure, use, exhibition or other means

"P" document published prior to the international filing date but later than the priority date claimed

"T" later document published after the international filing date or priority date and not in conflict with the application but cited to understand the principle or theory underlying the invention

"X" document of particular relevance; the claimed invention cannot be considered novel or cannot be considered to involve an inventive step when the document is taken alone

"Y" document of particular relevance; the claimed invention cannot be considered to involve an inventive step when the document is combined with one or more other such documents, such combination being obvious to a person skilled in the art

"&" document member of the same patent family

Date of the actual completion of the international search	Date of mailing of the international search report
23 September 2014	07/10/2014

Name and mailing address of the ISA/	Authorized officer
European Patent Office, P.B. 5818 Patentlaan 2 NL - 2280 HV Rijswijk Tel. (+31-70) 340-2040, Fax: (+31-70) 340-3016	Trommsdorff, Marion

2

Form PCT/ISA/210 (second sheet) (April 2005)

C(Continuation). DOCUMENTS CONSIDERED TO BE RELEVANT

Category*	Citation of document, with indication, where appropriate, of the relevant passages	Relevant to claim No.
X	CHRISTOPHER J. LENGNER ET AL: "Derivation of Pre-X Inactivation Human Embryonic Stem Cells under Physiological Oxygen Concentrations", CELL, vol. 141, no. 5, 1 May 2010 (2010-05-01), pages 872-883, XP055075377, ISSN: 0092-8674, DOI: 10.1016/j.cell.2010.04.010 figures 2, 3	1-6,31, 33,37, 56-66
X	WO 2010/077955 A1 (SCRIPPS RESEARCH INST [US]; LI WENLIN [US]; ZHOU HONGYAN [US]; DING SH) 8 July 2010 (2010-07-08) page 17; example 1	7-11,27, 28
X,P	OHAD GAFNI ET AL: "Derivation of novel human ground state naive pluripotent stem cells", NATURE, vol. 504, no. 7479, 30 October 2013 (2013-10-30), pages 282-286, XP055128176, ISSN: 0028-0836, DOI: 10.1038/nature12745 the whole document	1-39, 56-76, 88-96
A	PABLO BERMEJO-ALVAREZ ET AL: "Solving the "X" in Embryos and Stem Cells", STEM CELLS AND DEVELOPMENT, vol. 21, no. 8, 20 May 2012 (2012-05-20), pages 1215-1224, XP055128368, ISSN: 1547-3287, DOI: 10.1089/scd.2011.0685 the whole document	1-39, 56-76, 88-96
A	Y. ZHANG ET AL: "Small molecules, big roles - the chemical manipulation of stem cell fate and somatic cell reprogramming", JOURNAL OF CELL SCIENCE, vol. 125, no. 23, 1 December 2012 (2012-12-01), pages 5609-5620, XP055112620, ISSN: 0021-9533, DOI: 10.1242/jcs.096032 the whole document	1-39, 56-76, 88-96
A	JACOB H. HANNA ET AL: "Pluripotency and Cellular Reprogramming: Facts, Hypotheses, Unresolved Issues", CELL, vol. 143, no. 4, 1 November 2010 (2010-11-01), pages 508-525, XP055074652, ISSN: 0092-8674, DOI: 10.1016/j.cell.2010.10.008 the whole document	1-39, 56-76, 88-96

2 -/--

C(Continuation). DOCUMENTS CONSIDERED TO BE RELEVANT

Category*	Citation of document, with indication, where appropriate, of the relevant passages	Relevant to claim No.
A	ALEJANDRO DE LOS ANGELES ET AL: "Accessing nave human pluripotency", CURRENT OPINION IN GENETICS & DEVELOPMENT, vol. 22, no. 3, 29 March 2012 (2012-03-29) , pages 272-282, XP028493568, ISSN: 0959-437X, DOI: 10.1016/J.GDE.2012.03.001 [retrieved on 2012-03-06] the whole document	1-39, 56-76, 88-96
T	WARE CAROL B ET AL: "Derivation of naive human embryonic stem cells", PROCEEDINGS OF THE NATIONAL ACADEMY OF SCIENCES OF THE UNITED STATES OF AMERICA, vol. 111, no. 12, March 2014 (2014-03), pages 4484-4489, XP002727154, ISSN: 0027-8424 the whole document	
A	KATSUHIKO HAYASHI ET AL: "Reconstitution of the Mouse Germ Cell Specification Pathway in Culture by Pluripotent Stem Cells", CELL, CELL PRESS, US, vol. 146, no. 4, 28 June 2011 (2011-06-28) , pages 519-532, XP028383021, ISSN: 0092-8674, DOI: 10.1016/J.CELL.2011.06.052 [retrieved on 2011-07-16] page 531; figure 6	77-96
X	WO 98/43679 A1 (UNIV JOHNS HOPKINS MED [US]; GEARHART JOHN D [US]; SHAMBLOTT MICHAEL J) 8 October 1998 (1998-10-08) examples 1-4	83-96
X	US 6 090 622 A (GEARHART JOHN D [US] ET AL) 18 July 2000 (2000-07-18) cited in the application examples 1-4	83-96
X	EGUIZABAL C ET AL: "Generation of primordial germ cells from pluripotent stem cells", DIFFERENTIATION, SPRINGER VERLAG, DE, vol. 78, no. 2-3, 1 September 2009 (2009-09-01), pages 116-123, XP026601254, ISSN: 0301-4681, DOI: 10.1016/J.DIFF.2009.07.001 [retrieved on 2009-08-15] figures 1, 2	83,84,87

-/--

2

C(Continuation). DOCUMENTS CONSIDERED TO BE RELEVANT

Category*	Citation of document, with indication, where appropriate, of the relevant passages	Relevant to claim No.
X	AHN K S ET AL: "Production of human CD59-transgenic pigs by embryonic germ cell nuclear transfer", BIOCHEMICAL AND BIOPHYSICAL RESEARCH COMMUNICATIONS, ACADEMIC PRESS INC. ORLANDO, FL, US, vol. 400, no. 4, 1 October 2010 (2010-10-01), pages 667-672, XP027356570, ISSN: 0006-291X, DOI: 10.1016/J.BBRC.2010.08.125 [retrieved on 2010-09-08] the whole document	88-96
X	PARK TAE SUB ET AL: "Derivation of Primordial Germ Cells from Human Embryonic and Induced Pluripotent Stem Cells Is Significantly Improved by Coculture with Human Fetal Gonadal Cells", STEM CELLS (MIAMISBURG), vol. 27, no. 4, 2009, pages 783-795, XP002730074, ISSN: 1066-5099 the whole document	83-87
A	YING YING ET AL: "Induction of primordial germ cells from pluripotent epiblast", THE SCIENTIFIC WORLD, THE SCIENTIFICWORLD LTD, GB, vol. 2, 26 March 2002 (2002-03-26), pages 801-810, XP009097195, ISSN: 1532-2246 the whole document	77-87

2

INTERNATIONAL SEARCH REPORT

Information on patent family members

International application No
PCT/IB2014/060954

Patent document cited in search report	Publication date	Patent family member(s)	Publication date
WO 2010077955 A1	08-07-2010	AU 2009333259 A1	11-08-2011
		CA 2747398 A1	08-07-2010
		CN 102317442 A	11-01-2012
		EP 2373784 A1	12-10-2011
		JP 2012511935 A	31-05-2012
		KR 20110094348 A	23-08-2011
		SG 172160 A1	28-07-2011
		US 2012028351 A1	02-02-2012
		WO 2010077955 A1	08-07-2010
WO 9843679 A1	08-10-1998	AU 745976 B2	11-04-2002
		AU 6947798 A	22-10-1998
		CA 2285274 A1	08-10-1998
		EP 1023085 A1	02-08-2000
		JP 2001521380 A	06-11-2001
		US 6245566 B1	12-06-2001
		US 6331406 B1	18-12-2001
		US 6562619 B1	13-05-2003
		US 2003148514 A1	07-08-2003
		WO 9843679 A1	08-10-1998
US 6090622 A	18-07-2000	NONE	

INTERNATIONAL SEARCH REPORT

International application No.
PCT/IB2014/060954

Box No. II Observations where certain claims were found unsearchable (Continuation of item 2 of first sheet)

This international search report has not been established in respect of certain claims under Article 17(2)(a) for the following reasons:

1. ☐ Claims Nos.:
because they relate to subject matter not required to be searched by this Authority, namely:

2. ☐ Claims Nos.:
because they relate to parts of the international application that do not comply with the prescribed requirements to such an extent that no meaningful international search can be carried out, specifically:

3. ☐ Claims Nos.:
because they are dependent claims and are not drafted in accordance with the second and third sentences of Rule 6.4(a).

Box No. III Observations where unity of invention is lacking (Continuation of item 3 of first sheet)

This International Searching Authority found multiple inventions in this international application, as follows:

see additional sheet

1. ☐ As all required additional search fees were timely paid by the applicant, this international search report covers all searchable claims.

2. ☐ As all searchable claims could be searched without effort justifying an additional fees, this Authority did not invite payment of additional fees.

3. ☒ As only some of the required additional search fees were timely paid by the applicant, this international search report covers only those claims for which fees were paid, specifically claims Nos.:

1-39, 56-96

4. ☐ No required additional search fees were timely paid by the applicant. Consequently, this international search report is restricted to the invention first mentioned in the claims; it is covered by claims Nos.:

Remark on Protest

☐ The additional search fees were accompanied by the applicant's protest and, where applicable, the payment of a protest fee.

☐ The additional search fees were accompanied by the applicant's protest but the applicable protest fee was not paid within the time limit specified in the invitation.

☒ No protest accompanied the payment of additional search fees.

FURTHER INFORMATION CONTINUED FROM PCT/ISA/ 210

This International Searching Authority found multiple (groups of) inventions in this international application, as follows:

1. claims: 1-39, 56-76(completely); 88-96(partially)

   An isolated human naive pluripotent stem cell having the characteristics of claim 1, a population comprising such a cell, a cell culture, a culture medium suitable for obtaining said naive pluripotent stem cell, methods for generating these cells, methods of generating a chimeric animal using these cells.

   ---

2. claims: 40-55

   A method for improving generation of induced pluripotent stem cells from a somatic cell.

   ---

3. claims: 77-87(completely); 88-96(partially)

   A method for generating a primordial germ cell, an isolated population of primate primordial germ cells, methods of treatment using these cells, methods of generating a chimeric animal using these cells.
